

VALORIZATION OF LIGNOCELLULOSIC BIOMASS IN A BIOREFINERY

From Logistics to
Environmental and
Performance Impact

RAJEEV KUMAR
SEEMA SINGH
VENKATESH BALAN
EDITORS

Biochemistry
Research Trends

Complimentary Contributor Copy

BIOCHEMISTRY RESEARCH TRENDS

**VALORIZATION OF LIGNOCELLULOSIC
BIOMASS IN A BIOREFINERY
FROM LOGISTICS TO ENVIRONMENTAL
AND PERFORMANCE IMPACT**

No part of this digital document may be reproduced, stored in a retrieval system or transmitted in any form or by any means. The publisher has taken reasonable care in the preparation of this digital document, but makes no expressed or implied warranty of any kind and assumes no responsibility for any errors or omissions. No liability is assumed for incidental or consequential damages in connection with or arising out of information contained herein. This digital document is sold with the clear understanding that the publisher is not engaged in rendering legal, medical or any other professional services.

Complimentary Contributor Copy

BIOCHEMISTRY RESEARCH TRENDS

Additional books in this series can be found on Nova's website under the Series tab.

Additional e-books in this series can be found on Nova's website under the e-books tab.

BIOCHEMISTRY RESEARCH TRENDS

**VALORIZATION OF LIGNOCELLULOSIC
BIOMASS IN A BIOREFINERY**

**FROM LOGISTICS TO ENVIRONMENTAL
AND PERFORMANCE IMPACT**

**RAJEEV KUMAR
SEEMA SINGH
AND
VENKATESH BALAN
EDITORS**



Complimentary Contributor Copy

Copyright © 2016 by Nova Science Publishers, Inc.

All rights reserved. No part of this book may be reproduced, stored in a retrieval system or transmitted in any form or by any means: electronic, electrostatic, magnetic, tape, mechanical photocopying, recording or otherwise without the written permission of the Publisher.

We have partnered with Copyright Clearance Center to make it easy for you to obtain permissions to reuse content from this publication. Simply navigate to this publication's page on Nova's website and locate the "Get Permission" button below the title description. This button is linked directly to the title's permission page on copyright.com. Alternatively, you can visit copyright.com and search by title, ISBN, or ISSN.

For further questions about using the service on copyright.com, please contact:

Copyright Clearance Center

Phone: +1-(978) 750-8400 Fax: +1-(978) 750-4470 E-mail: info@copyright.com.

NOTICE TO THE READER

The Publisher has taken reasonable care in the preparation of this book, but makes no expressed or implied warranty of any kind and assumes no responsibility for any errors or omissions. No liability is assumed for incidental or consequential damages in connection with or arising out of information contained in this book. The Publisher shall not be liable for any special, consequential, or exemplary damages resulting, in whole or in part, from the readers' use of, or reliance upon, this material. Any parts of this book based on government reports are so indicated and copyright is claimed for those parts to the extent applicable to compilations of such works.

Independent verification should be sought for any data, advice or recommendations contained in this book. In addition, no responsibility is assumed by the publisher for any injury and/or damage to persons or property arising from any methods, products, instructions, ideas or otherwise contained in this publication.

This publication is designed to provide accurate and authoritative information with regard to the subject matter covered herein. It is sold with the clear understanding that the Publisher is not engaged in rendering legal or any other professional services. If legal or any other expert assistance is required, the services of a competent person should be sought. FROM A DECLARATION OF PARTICIPANTS JOINTLY ADOPTED BY A COMMITTEE OF THE AMERICAN BAR ASSOCIATION AND A COMMITTEE OF PUBLISHERS.

Additional color graphics may be available in the e-book version of this book.

Library of Congress Cataloging-in-Publication Data

ISBN: ; 9: /3/856: 7/: 65/6 (eBook)

Published by Nova Science Publishers, Inc. † New York

Complimentary Contributor Copy

CONTENTS

Preface		vii
Chapter 1	Impact of Feedstock Supply Systems Unit Operations on Feedstock Cost and Quality for Bioenergy Applications <i>Jaya Shankar Tumuluru, Erin Searcy, Kevin L. Kenney, William A. Smith, Garold L. Gresham and Neal A Yancey</i>	1
Chapter 2	Analytical Methods for Biomass Characterization During Pretreatment and Bioconversion <i>Yunqiao Pu, Xianzhi Meng, Chang Geun Yoo, Mi Li and Arthur J. Ragauskas</i>	37
Chapter 3	Biochemical Conversion of Biomass to Biofuels <i>Ximing Zhang, Arun Athmanathan and Nathan S. Mosier</i>	79
Chapter 4	Optimization of Biogas Production by Anaerobic Co-Digestion <i>Raphael M. Jingura and Reckson Kamusoko</i>	143
Chapter 5	Current Developments in Thermochemical Conversion of Biomass to Fuels and Chemicals <i>Chan Seung Park and Arun S. K. Raju</i>	171
Chapter 6	Hydrothermal Liquefaction of Biomass for Biofuel <i>Florin G. Barla and Sandeep Kumar</i>	185
Chapter 7	Application of Heterogeneous Catalysts for the Production of Fuel and Fuel Additives from Lignocellulosic Biomass <i>Małgorzata Wąchala, Agnieszka M. Ruppert, Olga Sneka-Platek and Jacek Grams</i>	201
Chapter 8	Lignin Conversion to Fuels and Chemicals <i>Yu Gao, Merima Beganovic and Marcus B. Foston</i>	245
Chapter 9	Nanocelluloses from Lignocellulosic Biomass <i>G. Siqueira and V. Arantes</i>	293

Chapter 10	Towards Economically Sustainable Lignocellulosic Biorefineries <i>N. V. S. N. Murthy Konda, Dominique Loqué and Corinne D. Scown</i>	321
Chapter 11	Environmental and Performance Impacts of Alternative Fuels in Transportation Applications <i>Thomas D. Durbin, Georgios Karavalakis and Kent C. Johnson</i>	339
Index		447

PREFACE

Human kind will soon face energy crisis in the light of dwindling fossil fuel resources and climate change due to global warming caused by burning fossil fuel that emits greenhouse gases. To overcome these crisis, utilization of abundant and low cost lignocellulosic biomass to produce renewable energy, bio-chemicals, and bio-based materials is the only sustainable way. Biomass utilization to meet human needs is not new as wood and other biomass resources are being used for heating, cooking, and house construction for centuries. However, the industrial economy warrants their efficient utilization to derive the maximum value. For example, as envisioned and practiced in a typical biochemical conversion platform, it may not be economical in the long run to convert only the carbohydrate fraction of biomass to fuels and chemicals and burn lignin to meet the biorefinery energy demand and/or selling (excess) electricity to the grid. In fact, it would be necessary to valorize the whole biomass including lignin to fuels, chemicals, and materials to make the lignocellulosic biorefinery profitable and our planet sustainable.

This book is intended to provide readers the updates on various biomass valorization routes to make fuels, chemicals, and materials. In addition, it covers the past and current developments on biomass logistics, analytical tools applied to characterize lignocellulosic biomass, environmental aspects and engine performance of various fuels, and techno-economical aspects of lignocellulosic biomass refinery. Overall, the book contains eleven chapters. *Chapter 1* is focused on biomass logistics and their impacts on bioenergy applications. *Chapter 2* provides details on analytical tools applied to characterize biomass during pretreatment and bioconversion. *Chapter 3* deals with the past and current developments on biochemical conversion of lignocellulosic biomass to ethanol. *Chapter 4* gives in-depth overview of anaerobic digestion of biomass to biogas and its impacts on energy quality. *Chapter 5* presents the overview of developments in thermochemical conversion of biomass to fuels and chemicals including gasification, pyrolysis, and hydrothermal treatment. *Chapter 6* covers hydrothermal liquefaction of biomass and its life cycle and techno-economical aspects. *Chapter 7* provides a thorough review on heterogeneous catalysts application in low to high temperature conversions of biomass to fuels and chemicals. *Chapter 8* provides details on lignin valorization to fuels and chemicals including lignin structure, its isolation and characterization methods, and the conversion routes. *Chapter 9* deals with the production methods and the physicochemical properties of nanomaterials such as nanocelluloses that are believed to play a major role in the future bio-economy. *Chapter 10* applies techno-economics analysis (TEA) to show the impact of co-

production of muconic acid- a precursor for adipic acid and terephthalic acid- on ethanol price for engineered sweet sorghum. Finally, *Chapter 11* examines the environmental impacts and engine performances of various lignocellulosic biomass derived fuels such as ethanol, butanol, and drop-in fuels as well as bio-diesel.

As covered in this book, several routes of valorizing biomass including biochemical, thermochemical, thermo-catalytic, and combination of these have been proposed and developed. However, due to capital costs, end products selectivity and yields, and the process flexibility for the feedstock and/or end products, one route or process may look attractive over another. Continued research is vital to make these processes more energy efficient and carbon neutral. The future research efforts should also be directed to develop novel conversion routes that use less chemicals, water and energy and are feedstock flexible as well as environmentally sustainable.

We would like to thank all the authors for their expert contributions and valuable time and reviewers for their invaluable feedbacks. We would like to take a chance to thank the Nova Science Publishers for inviting us to put this book together and publishing it. The editors would like to thank the BioEnergy Science Center (BESC, Oak Ridge National Laboratory), Great Lakes Bioenergy Research Center (GLBRC, University of Wisconsin-Madison and Michigan State University), and Joint BioEnergy Institute (JBEI, Lawrence Berkeley National Laboratory), which are U.S. Department of Energy Bioenergy Research Centers supported by the Office of Biological and Environmental Research in the DOE Office of Science as well as the U.S. Department of Energy Office of the Biomass Program (OBP), for funding support.

It is our sincere intention that the book would be of great interest to students and researchers working in biofuels area.

Rajeev Kumar, University of California Riverside, Riverside,

CA and BioEnergy Science Center (BESC)

Venkatesh Balan, Michigan State University and Great Lakes Bioenergy

Research Center (GLBRC)

Seema Singh, Sandia National Laboratories and Joint Bioenergy Institute (JBEI)

Chapter 1

IMPACT OF FEEDSTOCK SUPPLY SYSTEMS UNIT OPERATIONS ON FEEDSTOCK COST AND QUALITY FOR BIOENERGY APPLICATIONS

*Jaya Shankar Tumuluru**, *Erin Searcy*, *Kevin L. Kenney*,
William A. Smith, *Garold L. Gresham* and *Neal A Yancey*
Idaho National Laboratory, ID, US

ABSTRACT

The economical and sustainable production of bioenergy depends on efficient feedstock supply systems. The development of feedstock supply systems requires balancing cost of delivered feedstock, feedstock quality, and the quantity of biomass available for feedstock production to meet the demand. Relevant quality characteristics of feedstocks depend on the conversion process, but usually include moisture, carbohydrates, particle size and distribution, and ash content and composition. These properties are highly variable even within a species and are dependent on a variety of factors, including the methods used to harvest, preprocessing operations, type of biomass, and climatic condition at the time of harvest. This chapter addresses various unit operations within the feedstock supply system, including harvest and collection, preprocessing, and storage, that impact the quality of feedstock delivered to the biorefinery. This chapter also addresses the impact of feedstock logistics on the feedstock quality attributes and mitigation methods that can help to manage biomass moisture content, improve the biomass quality specifications in terms of ash, carbohydrate, and particle size, and density for biofuels production.

Keywords: biomass, quality, harvesting, storage, preprocessing, logistics.

* Biofuels and Renewable Energy Technology, Idaho National Laboratory, P.O. Box 1625, MS 3570, Idaho Falls, ID 83415, USA. Email: JayaShankar.Tumuluru@inl.gov.

INTRODUCTION

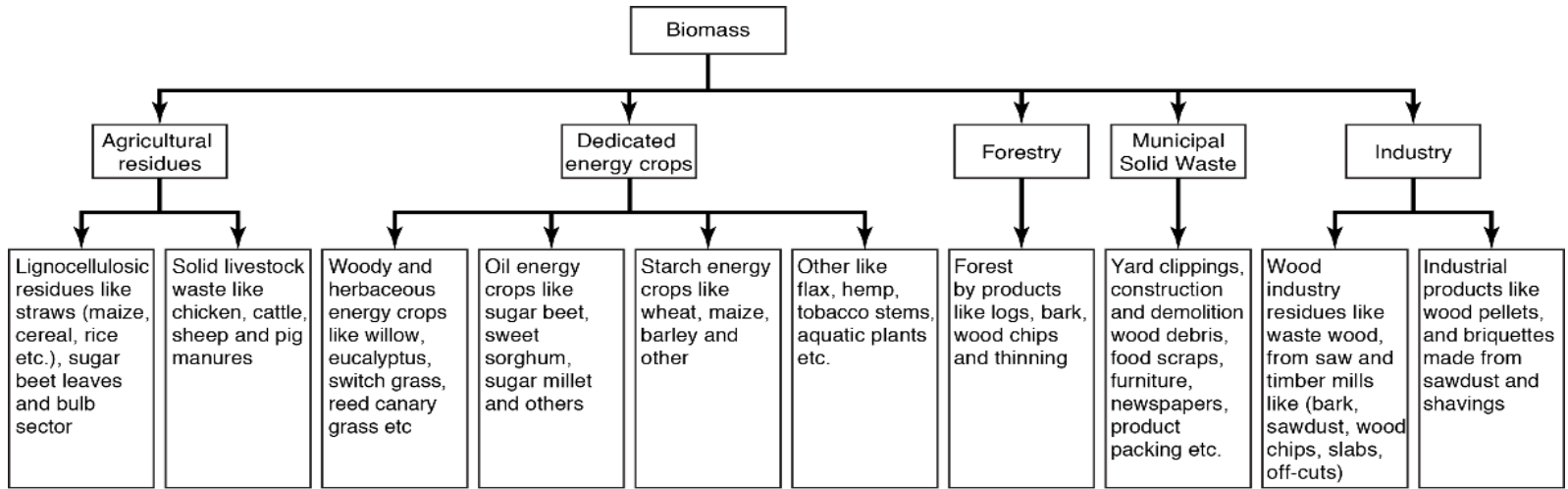
Biomass is a renewable resource that can be made into a variety of end products including, chemicals, electricity, feed, biobased materials, and fuels. Energy production from cellulosic biomass, such as herbaceous energy crops, annual agricultural crop residues, and woody biomass, is considered a potential solution for addressing climate change, energy security, and rural economic development (Greene et al., 2004; McLaughlin et al., 2002). Biomass conversion technologies used to make these products can generally be categorized as biological or thermochemical, although other approaches are also being utilized. Biological conversion includes fermentation of carbohydrate components to produce energy carriers like ethanol, butanol, hydrogen, and biogas, or extraction of oils for biodiesel production. Thermochemical conversion includes direct combustion for heat and electricity, as well as indirect processes like pyrolysis and gasification (Humbird et al., 2011). Feedstock in-feed specifications vary between conversion processes; for example, the desired ash content is <1% for many thermochemical conversions but is <5% for biochemical conversion processes (Kenney, Smith, Gresham, & Westover, 2013a).

Achieving the feedstock quality attributes or performance-driven targets in terms of intrinsic composition and physical characteristics, while meeting cost targets and supplying desired feedstock quantities, is challenging. The performance-driven targets or quality attributes are determined based on the requirements of the biorefinery to meet conversion performance and limitations of the system infrastructure (e.g., system requirements for flowability and minimization of catalyst contamination). Specifications are based on the inherent characteristics of the feedstock material itself and may include moisture, total ash, hemicellulose, cellulose, lignin, and elemental ash content (Lee, Owens, Boe, & Jeranyama, 2007), as well as physical characteristics (e.g., grind size, particle size distribution, fines content, flowability, and durability).

FEEDSTOCK SUPPLY SYSTEM: COMPOSITION AND QUALITY CHALLENGES

According to the *U.S. Billion-Ton Update* report released by the U.S. Department of Energy (DOE, 2011), the potential exists for more than a billion tons of biomass to be available annually by the year 2030 to support biofuels production. Although the broad-scale use of agricultural crops and woody biomass for the production of bioenergy are emerging, feedstock supply systems inherit the experience of mature agriculture and logging industries and are therefore based on these conventional systems. Other lignocellulosic biomass sources include residues, energy crops, municipal solid waste (yard clippings, construction and demolition wood debris), and energy crops (Figure 1).

Research has been ongoing for decades to improve conventional agricultural and forestry feedstock supply systems, designed to support traditional industries such as pulpwood and animal feed. However, supplying biomass for energy requires at least adaptations to the conventional systems and potentially new systems altogether.



10-GA50774-43a

Figure 1. Biomass feedstocks for bioenergy (Tumuluru, Hess, Boardman, Wright, & Westover, 2012).

Certain operations are common across all feedstock supply systems. For example, whether the biomass is woody or herbaceous, the biomass must be harvested and gathered within a given harvest window; for woody biomass, this window may be year-round in some locations. Biomass logistics are complicated by the wide geographical distribution of resources, time- and weather-sensitive crop maturity, a short window for biomass collection, and competition from concurrent harvest operations. The major physiological and geographical challenges associated with using biomass as a feedstock for energy production are high-moisture content, irregular shapes and sizes, low-bulk density, and spatially scattered biomass, making the feedstock difficult to handle, transport, store, and utilize in its original form (Igathinathane et al., 2014; Tumuluru, Hess, Wright, & Kenney, 2011a). To minimize costs while meeting the required conversion in-feed specifications, biomass must be processed and handled efficiently. Herbaceous crops are often baled to make the material easier to handle, while woody material is often chipped prior to transport to the biorefinery. This chapter examines the impact of the unit operations involved in the supply system on cost and quality attributes like biomass moisture content ash, carbohydrate, particle size, and density.

FEEDSTOCK SUPPLY SYSTEM AND COST

Feedstock supply chain logistics includes biomass production, harvesting, collection, preprocessing (size reduction & densification), transportation, and storage. The main function of a feedstock supply system is to access biomass in a cost-effective manner while maintaining quality. The development of efficient, sustainable biomass feedstock supply systems supports a diverse energy portfolio and increased competitiveness in the global quest for clean energy technologies. The Department of Energy Bioenergy Technologies Office has shaped the vision of a national, commodity-scale feedstock supply systems. Much progress has been made in developing and reaching this vision through optimizing biomass logistics and defining commodity attributes compatible with existing commodity-scale, solids-handling infrastructure.

Advanced feedstock commodity system was designed to support expansion of the bioenergy industry in the United States by providing strategies and mechanisms for reliably and sustainably supplying biorefineries with on-spec, affordable feedstock at the volumes required for sustainable operation (Searcy, Lamers, Hansen, Jacobson & Webb, 2015). This supply system helps to transform different raw biomass resources from a highly variable, aerobically unstable, low-density form into a fairly uniform, aerobically stable, high-density, tradable, aggregatable commodity.

Unit Operations in Biomass Feedstock Supply Systems

Feedstock supply systems involve different unit operations to move the lignocellulosic biomass from the production place to the reactor throat of the biorefinery (Hess, Thompson, Hoskinson, Shaw, & Grant, 2003). All these unit operations have an impact on the quality of the feedstock delivered to the biorefinery.

- Biomass production involves producing biomass feedstocks at the point of harvest. Various factors which influence the biomass production are: (a) selection of feedstock type, (b) land-use issues, (c) policy issues, (d) agronomic practices that drive biomass yield rates, and (e) directly affected by harvest and collection operations.
- Harvest and collection operations include getting the biomass from its production source to the storage or queuing location. The various unit operations in the harvest and collection are cutting (e.g., combining, swathing, or felling), hauling, and baling, bundling, or chipping for easy movement.
- Storage and queuing are essential operations used to accommodate seasonal harvest times, limited operational windows, variable yields, and delivery schedules. Low cost storage methods are employed to hold the biomass in a stable format until they are required by the biorefinery.
- Preprocessing changes the biomass to a format that is required by the biorefinery. Preprocessing can be as simple as grinding and densification increasing the bulk density or improving conversion efficiency, or it can be as complex as improving feedstock quality through fractionation, tissue separation, drying, and blending.
- Transportation and handling consists of moving the biomass from one point to another point in the supply system. The most commonly used transportation methods are truck, rail, barge, or pipeline. Transportation and handling methods are dependent on the biomass format and bulk density. Biomass format has a great impact on the transportation distance (Tumuluru, Igathinathane, Archer, & McCulloch, 2015a). In general, for a given location transportation options are mostly fixed.

Feedstock Delivered Cost

Delivered feedstock cost depends on many factors, such as feedstock type, conversion process, the quality of feedstock, location of biomass resource, available technology, supply chain design, etc. For example, grower payment in highly productive resource areas may be less than in low-resource areas. Many case studies have performed supply chain analysis to quantify delivered feedstock cost based on feedstock supply chain design (Muth et al., 2014; Ren et al., 2015; Roni, Eksioglu, Cafferty, & Jacobson, 2016; Roni, Eksioglu, Searcy, & Jha, 2014; Searcy & Hess, 2010). Table 1 presents an example of feedstock supply system costs supplying material for biochemical conversion targeted for the year 2017, incorporating design improvements to reduce feedstock supply system costs, while maintaining (or even enhancing) feedstock quality, and increasing access to feedstock resources (DOE, 2015). The goal of the 2017 Design Case is to enable expansion of biofuels production beyond highly productive resource areas by breaking the reliance of cost-competitive biofuel production on a single, abundant, low-cost feedstock. For the 2017 Design Case scenario located in western Kansas, it worked out that both the cost and quality criteria could be achieved through blending. Additional information on the design case assumptions and harvesting, storage, and preprocessing process improvement has been discussed in detail by Kenney et al. (2013).

Table 1. Modeled cost for blended herbaceous feedstock supply systems supplying material for biochemical conversion in the year 2017, presented in 2011\$. Costs are presented on a per dry ton basis (DOE, 2015)

	Cost(\$dry ton)
Feedstock	Blend of Herbaceous Feedstocks
Total delivered cost*	\$80
Grower payment	\$27.12
Harvest and collection	\$13.90
Storage and queuing	\$6.00
Preprocessing and In-Plant receiving	\$21.90
Transportation and handling	\$10.50

Note: *Total delivered cost is the sum of grower payment and feedstock logistics cost, from the point of harvest through to in-feed of the conversion reactor.

The various unit operations impact the quality of the feedstock delivered to the biorefinery. Research has touched on many aspects of the feedstock supply chain including, improving the collection scenarios (Igathinathane et al., 2014) and improving the harvesting and preprocessing machinery performance and efficiencies (Kenney et al., 2013a), with most of the research focused on a) improving the harvesting and storage operational windows, b) reducing the material and quality loss in the supply chain, and c) improving the cost-to-value relationship (Kenney et al., 2013a; Shinnars, Boettcher, Muck, Weimer, & Casler, 2010). Currently, size reduction and densification unit operations are gaining importance as they offer several advantages like: a) improved handling and conveyance efficiencies throughout the supply system and biorefinery infeed, b) controlled particle size distribution for improved feedstock uniformity and density, c) fractionated structural components for improved compositional quality, and d) conformance to pre-determined conversion technology and supply system specifications (Tumuluru et al., 2011a). Recent research has proven that size reduction and densification helps to improve the performance of biomass in both thermochemical and biochemical conversion pathways (Ray, Hoover, Nagle, Chen, & Gresham, 2013; Sarkar, Kumar, Tumuluru, Patil, & Bellmer, 2014; Yang, Sarkar, Kumar, Tumuluru, & Huhnke, 2014).

Feedstock quality impacts conversion performance and therefore the overall economics of bioenergy production. The quality of field-run biomass is impacted by a variety of factors including: a) inherent species variability, b) production conditions, c) differing harvest methods and time, d) collection, e) storage practices, and f) weather fluctuations. Even the process of cutting biomass and laying it on the ground before collecting it introduces ash and other contaminants that can affect the overall chemical composition (Kenney et al., 2013a). Commercialization of the biorefineries has led to understanding the importance of the quality (moisture, ash, and sugar content) and physical properties (particle size and shape). Although in-feed specifications vary between conversion processes, feedstock supply systems invariably impact biorefinery performance.

BIOMASS COMPOSITION

Moisture Content

Feedstock moisture content is a critical quality attribute, impacting both cost and quality of the feedstock. In addition to quality impacts, high moisture increases transportation costs, because more moisture and less biomass is being transported. High moisture makes biomass handling and feeding difficult, largely due to plugging of the feeders and hoppers due to its cohesive nature (Dai, Cui, & Grace, 2012). High moisture can also reduce throughput and quality of the product during grinding operations. Grinding energy increases with increased moisture content (Tumuluru, Tabil, Song, Iroba, & Meda, 2014a; Yancey, Tumuluru, & Wright, 2013). Moisture content also impacts conversion performance, particularly for thermochemical conversion. High moisture biomass needs to be dried to make it aerobically stable. According to (Lamers et al., 2015) drying of biomass from 30% to 10% is the most significant cost in the preprocessing of biomass. Figure 2 indicates the typical moisture content of non-irrigated corn stover harvested over a period of time. It is very clear from the figure that the moisture content fluctuations are higher in these crops from year to year and is dependent on the precipitation received. The bars in the Figure 2 indicate the combined moisture frequency and lines indicate the moisture frequency by year.

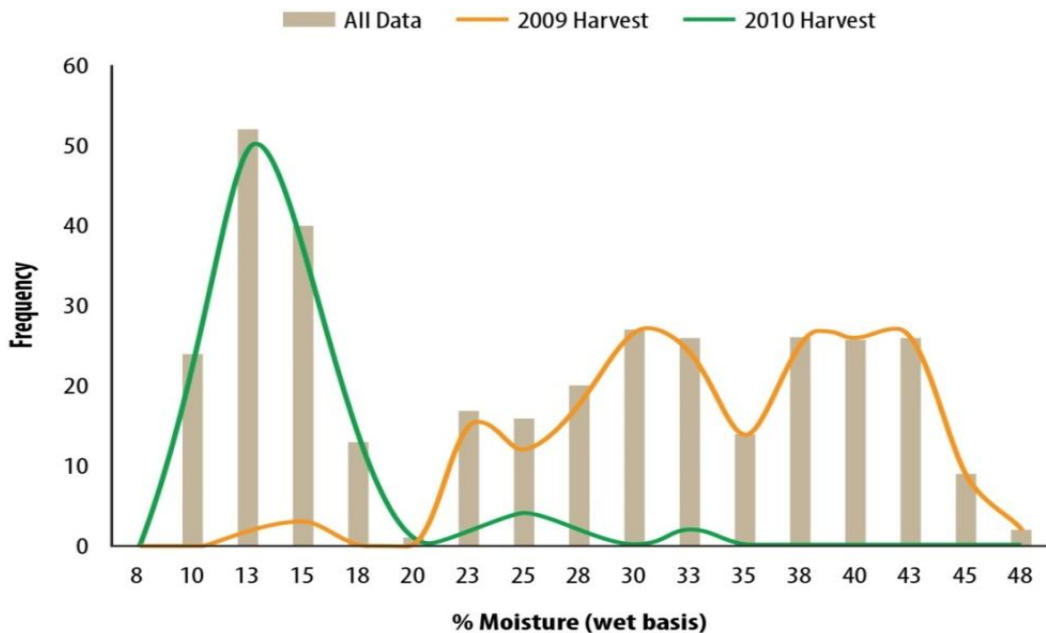


Figure 2. Year-to-year variability of corn stover moisture content over the 2009 and 2010 Midwest harvest seasons (N = 339) adapted from (Kenney et al., 2013a).

Ash Content

Ash is an inert component of biomass, and has a larger impact on thermochemical conversion compared to biochemical conversion (Humbird et al., 2011). According to Kenney et al. (2013a), there are three types of ash in the biomass: a) introduced ash (primarily soil), b) biological and/or c) structural ash. The introduced ash is largely due to harvesting and handling methods used in the field (harvest, collection, handling, and storage). Harvesting methods have the greatest influence on soil contamination in baled herbaceous feedstock materials whereas, the biological and structural ash is a part of the vascular tissues and plant cell walls and is more dependent on intrinsic biomass properties such as plant type, maturity, growing conditions, irrigation practices, anatomical fractions and growth conditions.

In the case of biochemical conversion, ash in the biomass can decrease the convertibility by displacing convertible carbohydrates and reducing the efficiency of dilute acid pretreatment (Weiss, Farmer, & Schell, 2010). In thermochemical conversion applications, higher ash content can lead to slagging, fouling, and corrosion of the equipment (Das, Ganesh, & Wangikar, 2004; Tumuluru et al., 2012). Studies conducted by Carpenter et al. (2010) indicated that herbaceous biomass like corn stover, switchgrass, and others result in varying gas composition during gasification. The results from this are a higher tar concentration and reduced gasifier efficiency. Woody biomass species are generally lower in ash content compared to herbaceous biomass, and are therefore, preferred for thermochemical conversion. In general, the ash content range is higher for herbaceous biomass compared to woody biomass (Table 2). In Figure 3, total ash (% , dry basis) presented reflects anatomical ash. The authors' purpose (Tao, Lestander, Geladi, & Xiong, 2012) was to link biomass properties to fuels characteristics based on physiological properties rather than logistics operations of harvesting and handling. As a result, the ash contents are more representative of the biological properties contributing to structural and vascular ash, rather than ash introduced from harvesting or storage operations. Currently, examples of ash specifications for biochemical conversion and thermochemical conversion are <5 and 1%, respectively (Aden & Foust, 2009; Das et al., 2004; Kenney et al., 2013a). As shown in Table 2 and Figure 3 most of the samples have ash contents in the range of 7–9%, which is well above the specifications (Kenney et al., 2013a).

Table 2. Mean values and ranges for selected lignocellulosic biomass feedstocks (both the soil and anatomical ash) (Tao et al., 2012)

Feedstock	Mean Ash, %*	Reported Range, %
<i>Herbaceous</i>		
Corn cob	2.9 (13)	1.0 – 8.8
Corn stover	6.6 (28)	2.9 – 11.4
Miscanthus straw	3.3 (13)	1.1 – 9.3
Reed Canary grass	6.7 (11)	3.0 – 9.2
Rice straw	17.5 (22)	7.6 – 25.5
Sorghum straw	6.6 (5)	4.7 – 8.7
Sugarcane bagasse	5.6 (27)	1.0 – 15.2
Switchgrass straw	5.8 (21)	2.7 – 10.6
Wheat straw	8.0 (50)	3.5 – 22.8

Feedstock	Mean Ash, %*	Reported Range, %
<i>Woody</i>		
Oak residue	2.5 (5)	1.5 – 4.1
Oak wood	0.6 (11)	0.2 – 1.3
Pine residue	2.6 (4)	0.3 – 6.0
Pine wood	1.0 (40)	0.1 – 6.0
Poplar wood	2.1 (14)	0.5 – 4.3
Spruce residue	4.3 (2)	2.2 – 6.4
Spruce wood	0.8 (5)	0.3 – 1.5
Willow residue	2.0 (1)	2.0 – 2.0
Willow wood	1.5 (18)	1.0 – 2.3

* Mean value presented with number of reported samples in parenthesis.

A recent study by Mullen, Boateng, Dadson, & Hashem, (2014) found a positive correlation between ash content and carbon conversion to aromatic hydrocarbons. Their study indicated that iron present in the biomass has a positive influence, whereas potassium has a negative impact. Correlations between elemental species in the ash, the chemical intermediates from the incipient pyrolysis process, and the final CFP products suggest that the main influence of potassium is on the initial pyrolysis reactions. However, iron may affect the catalytic reactions over HZSM-5. In contrast, Wu (2015) suggested that ash has a negative effect on the gasification reaction rate. He observed that high ash fuels react more slowly compared to low ash fuels.

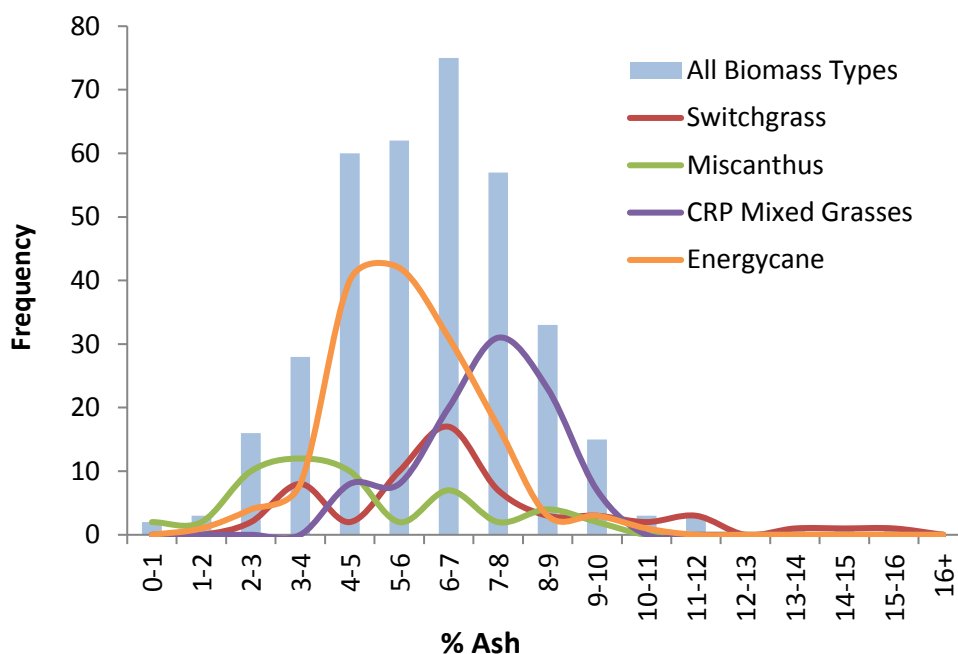


Figure 3. Histogram of percent ash (anatomical) from four biomass types. Each datapoint is an average of all of the replicates from a field trial. (Frequency is the number of samples that fit each percentage (%) bin; Number of samples (n): Switch grass = 60; Miscanthus = 53; CRP Mixed grasses = 97; Energy cane = 150; All other biomass types = 360) (Idaho National Laboratory (INL), 2016). (Source: Bioenergy Feedstock Library).

Carbohydrates

Raw biomass generally consists of about 26–47% cellulose, 19–33% hemicelluloses, 14–23% lignin, and 1–5% ash for many of the lignocellulosic biomasses (Idaho National Laboratory (INL), 2016; Lee et al., 2007; Phyllis2, 2015). Carbohydrate is a main constituent of lignocellulosic biomass and is an important parameter for biochemical conversion, as structural sugars and the ratio of C₅ and C₆ sugars impact the pretreatment process and fermentation process. Figure 4 illustrates how combined glucan plus xylan content of different bioenergy feedstocks can vary both within a single feedstock type and among feedstock types.

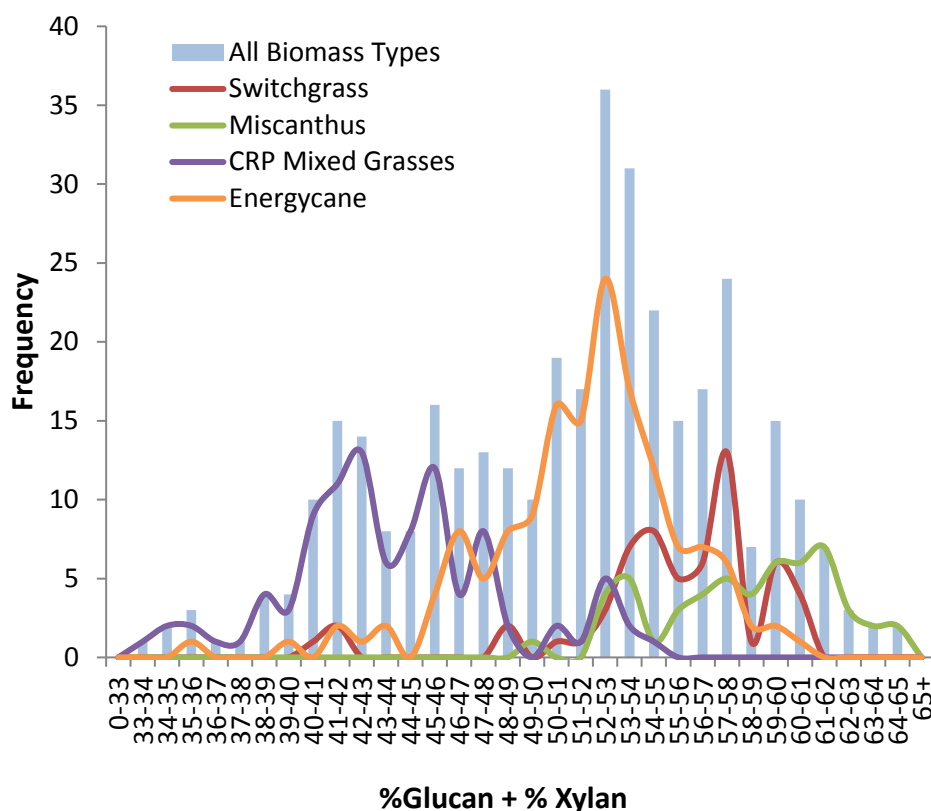


Figure 4. Histogram of percent glucan + xylan summed from four biomass types. Each data point is an average of all of the replicates from a treatment combination from a field trial. Frequency is the number of samples that fit each percentage (%) bin. (Number of samples: Switch grass = 60; Miscanthus = 53; CRP = 98; Energy cane = 150; All biomass types = 361). (Idaho National Laboratory (INL), 2016). (Source: Bioenergy Feedstock Library).

Particle Size and Bulk Density

Particle size and density are important specifications for both biochemical and thermochemical conversion pathways. Also, both these parameters influence the feeding,

handling, storage and transportation (Tumuluru et al., 2011a). Preprocessing operations like size reduction, drying, and densification will help to meet the desired specifications in terms of moisture content, particle size and bulk density. In general, hammer mills are suitable for low moisture biomass whereas shear mills are used for high moisture biomass feedstocks. The desired particle size is dependent on both the conversion pathway and the reactor design. The particle size desirable for most of the thermochemical applications like gasification and pyrolysis is 2 mm (Bridgwater, 1999; Jones et al., 2009), whereas the particle size can vary from 6 to 75 mm in the case of biochemical conversion. In general, ground biomass has lower bulk density of 50-80 kg/m³ (Tumuluru et al., 2014a) which is a major limitation for transporting it longer distance. Densification helps to overcome low bulk density limitations and improves the transportation efficiencies (Tumuluru et al., 2011a). In general, densifying biomass using a pellet mill increases the bulk density of the ground biomass by about 10 times. Yancey et al. (2013) indicated that while the energy input to preprocess and densify the feedstock is significant, the energy value of the pellet far outweighs the cost of creating it. There are different densification systems which can be used for making biomass into a commodity like product (Tumuluru et al., 2011a). Table 3 indicates some of the commonly used densification systems, operating and product characteristics and their suitability for conversion applications (Tumuluru et al., 2011a). These products have better handling, storage and transportation characteristics.

Table 3. Densification systems, operating conditions, product properties and their suitability for conversion pathway

	Pellet mill	Piston press	Cuber	Screw press
<i>Operating characteristics</i>				
Optimum moisture content of the raw material (%)	10–15	10–15	15-25	4-8
Particle size requirements (mm)	< 3	6-12	12-16	2-6
Addition of binder	Not required	Not required	Required	Not required
Wear of contact parts	High	Low	Low	High
Output from machine	Continuous	In strokes	Continuous	Continuous
Specific energy consumption (kWh/ton)	16.4–74.5	37.4–77	28-75	36.8–150
Through puts (ton/hr)	5	2.5	5	0.5-1
Maintenance	High	Low	Low	Low
<i>Physical properties</i>				
Unit density (g/cm ³)	1.1-1.2	<0.1	0.8	1–1.4
Bulk density (g/cm ³)	0.65-0.75	0.4-0.5	0.45-0.55	0.5-0.6
Homogeneity of densified biomass	Homogeneous	Not homogenous	Not homogeneous	Homogenous
<i>Suitability for conversion pathway</i>				
Combustion performance	Very good	Moderate	No information	Very good
Carbonization of charcoal	Not possible	Not possible	Not possible	Makes good charcoal
Suitability in gasifiers	Suitable	Suitable	Suitable	Suitable
Suitability for cofiring	Suitable	Suitable	Suitable	Suitable
Suitability for biochemical conversion	Suitable	Suitable	Suitable	Not suitable

SUPPLY SYSTEM UNIT OPERATIONS IMPACT ON MOISTURE AND QUALITY

Harvesting and Storage

Moisture

Factors impacting feedstock moisture include: harvest timing, age (particularly in the case of trees), type of biomass, the region where it is grown, water availability, and irrigation practices (Kenney et al., 2013a). According to Gamble et al. (2014) harvest date affect the biomass yield, moisture content and mineral concentration of switchgrass and mixed grasses. According to these authors, biomass moisture content was lowest in late spring averaging 156 g kg⁻¹ across all locations and years when harvested after April 1st. The same authors indicated that biomass N concentration did not change across harvest dates; however, P and K concentrations declined dramatically from late summer to late spring. Many herbaceous crops are harvested at times when field drying becomes impractical (Shinners, Binversie, Muck, & Weimer, 2007). Additionally, high moisture content (i.e., over 20% w.b.) poses challenges to aerobic storage, whereas low moisture biomass feedstocks the dry matter losses are often less than 7% per year (Coble & Egg, 1987; Emery & Mosier, 2012; Jirjis, 1995; Sanderson, Egg, & Wiseloge, 1997). Degradation during storage also results in significant loss of sugars in the biomass.

One way to reduce the impact of the variability in the moisture content of harvested biomass is by employing best management practices, such as identifying proper harvest and storage methods (Kenney et al., 2013a). Shinners et al. (2010) suggested that proper storage of high-moisture biomass can reduce the dry matter losses to acceptable levels. An alternative method is to store the material anaerobically, while this method is used for high-value animal feed (e.g., silage where biomass is stored in poly bags under wet conditions) this storage method is expensive and labor intensive. Moisture in the biomass can also be managed by drying. Typically, biomass is dried in the field using passive drying methods. Passive drying is done by leaving the harvested biomass or logs in the field to dry by evaporation or evapotranspiration. The rate of passive drying is impacted by a variety of factors including: the material to be dried (e.g., shape and size of pieces, wood density, and presence of leaves and bark,) and the storage conditions (e.g., method of storage and stacking, air flow, temperature, humidity, and precipitation). The effectiveness of passive drying of woodchips, for example can be enhanced by covering the material (i.e., protecting it from being re-hydrated) (Afzal, Bedane, Sokhansanj, & Mahmood, 2010), or by orienting baled herbaceous materials to improve airflow through the stack (Smith, Bonner, Kenney, & Wendt, 2013). In general, if the desired moisture in the biomass is below 10%, then active drying is necessary. The major limitations of passive drying are: a) long drying times to reach the desired moisture level, b) the larger foot print to dry larger volumes of materials, c) higher dry matter losses and emission of CO₂ and CH₄, d) limitation of the final moisture content that exceeds most of the preprocessing (grinding and densification) requirements, and e) soil contamination which increases the total ash content (Klavina, Zandekis, Rochas, & Zagorskis, 2014).

Ash

The studies conducted by various researchers indicated that ash content decreases in forages with maturity. For example, when the harvest is delayed from fall to late winter, as a result of environmental factors like soil type, soil chemistry, water quality, fertilization chemistry, and the elemental composition of the soil (Adler, Sanderson, Boateng, Weimer, & Jung, 2006; Burvall, 1997; Davidsson, Pettersson, & Nilsson, 2002; Duguid et al., 2009; Jarchow, Liebman, Rawat, & Anex, 2012; Jorgensen, 1997; Lewandowski & Kicherer, 1997; Lewandowski et al., 2003; Madakadze, Stewart, Peterson, Coulman, & Smith, 1999; Sanderson & Wolf, 1995). Another important variable that impacts the ash content is the anatomical fraction (Duguid et al., 2007). For instance, the leaves may be high in silica and inorganic nutrients such as nitrate and phosphate (Lindsey, Johnson, Kim, Jackson, & Labbe, 2013).

Feedstock selection is one approach to ash management. For example, woody biomass can be a suitable feedstock for the thermochemical conversion process where the conversion is sensitive to the amount of ash content in the biomass. Mechanical separation of the leaves and other anatomical fractions that carry most of the ash from the herbaceous biomass can make it suitable for the thermochemical conversion pathway. For instance, the ash content of the corn stover is about 2.3 times that of cobs (see Table 2). Harvesting selected parts of the crop can be cost-intensive, but can help to produce feedstock lower in ash.

Modifying harvest and collection operations can significantly reduce ash intake. For example, when comparing ground-driven wheel-rake windrowing to mechanical bar-rake windrowing, the weighted mean ash content is extremely elevated at 28.2%, which is 10% greater than the bar-rake (Bonner et al., 2014). The harvesting results using different equipment indicated that the practice of windrowing with a wheel rake has a heavy negative impact on soil entrainment in corn stover bales as a result of its intense ground contact and incorporation of soil-laden root crowns. The use of a wheel rake is not recommended unless changes in equipment operation can reduce soil disturbance (Bonner et al., 2014). The shred-flail treatment showed the most dramatic impact on bale ash content compared to the bar-rake. More than 66% of the samples collected were below 11.5% ash, and 95% were below 21.5% ash. This impressive shift in sample distribution resulted in a weighted mean ash content of 11.5%. This study indicated that the removal of a raking step by shredding reduces ground contact and soil entrainment in the windrowed material. Of the conditions tested, the shred-flail combination provided the most desirable results and is recommended in similar soil conditions, where soil contamination is a primary concern.

Bonner et al. (2014) also indicated the ash content varies considerably across and within locations/fields, equipment used, and harvest yield. The bar rake with a baler resulted in the lowest ash content of 7.2%, but yielded an average ash content of 11.3% across the ten fields harvested, with a maximum ash of 15.6%. The other conditions that influence the variability in the ash composition are field conditions (soil type, moisture content and previous crop) or collection settings (degree of soil disturbance). Similar observations were seen in other fields where the equipment combination (rotary rake and self-propelled baler) influenced the ash content. The ash content ranged from 9.5% to 22.3%. This study indicated that selection of

the right equipment has an impact on the ash content of the harvested biomass. Studies conducted by Bonner (2016) on three windrowing systems (bar rake, wheel rake, and flail shredder) indicated that the ash content also escalates with increasing the collection rate, which is influenced by the speed of the tractor and amount of material collected (Table 4). Results from multi-pass corn stover bales from Palo Alto County, Iowa (2014) that were harvested from 10 different fields using either 2-pass (material other than grain or “MOG) or bar rakes to form windrows showed that the average ash content ranged from 3.9% to 8.2%; values for individual bales ranged from 2.8% to 18.5%. These results highlight the range of variation within an individual field for a particular collection method (Figure 5)

Single-pass harvesting results in less soil contact by the stover and the harvesting equipment, and therefore, lower total ash content (Table 5). Table 5 compares the two - and single-pass harvesting conducted using commercially-available harvesting equipment. The results indicate there is nearly 10% more ash in two-pass bales than in single-pass bales of the same year, highlighting the negative impacts of ground contact in the process of stover collection. Nonetheless, compared to traditional multi-pass bales, two-pass bales have less ash content. Even though the ash content of the bales is less in single-pass bales, the bales harvested by this method are higher in moisture content. Single-pass harvesting relies on baling directly behind the combine during grain harvest, when stover moisture contents may exceed 45% (Shinners, Huenink, Muck, & Albrecht, 2009; Shinners, Wepner, Muck, & Weimer, 2011). The material harvested by this method needs to be stored properly in order to reduce the dry matter losses resulting from microbial and fungal growth. However, multi-pass or two-pass harvest provides the opportunity for in-field drying, which reduces potential for biological degradation.

In addition to introduced ash, the other category of ash is anatomical. According to Jorgensen (1997), Madakadze et al. (1999), and Sanderson & Wolf (1995), anatomical ash content in herbaceous biomass decreases with maturity. This delay in the harvest can help reduce the ash content. Some of the environmental factors that can impact the ash composition are: soil type, soil water chemistry, and fertilization rate (Davidsson et al., 2002; Duguid et al., 2007; Jarchow et al., 2012; Lewandowski et al., 2003). Johnson & Gresham (2013) in their studies indicated that harvesting time has an impact on the elemental composition of biomass. Their studies indicated that N, P, K and S declined from July/August to October/ November for switchgrass.

Table 4. Multi-pass corn stover collected from Nebraska in 2010, focusing on residue removal rates (Smith, 2015)

Windrower	Removal	% Ash
Bar rake	Low	12.9
Bar rake	High	14.5
Wheel rake	Low	8.8
Wheel rake	High	11.5
Flail shredder	Low	8.1
Flail shredder	High	9.3
Flail shredder	High	10.9

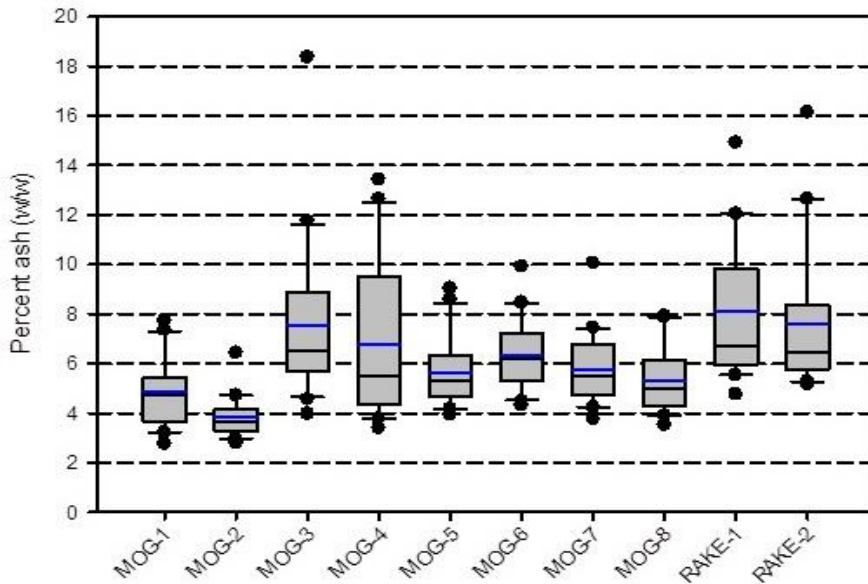


Figure 5. Impact of within-field conditions and harvesting method on the ash content of the harvested biomass (Smith, 2015).

Table 5. Mean ash content of single- and two-pass corn stover (Standard deviation in parenthesis) (Smith, 2015)

Location	Year	Collection Method	% Ash
Palo Alto County, IA	2009	Single-Pass	2.5 (0.1)
Palo Alto County, IA	2010	Single-Pass	3.5 (0.4)
Palo Alto County, IA	2010	Single-Pass	3.5 (0.4)
Stevens County, KS	2011	Single-Pass	3.8 (0.5)
Texas County, OK	2011	Single-Pass	4.0 (0.3)
Palo Alto County, IA	2010	Two-Pass	13.3 (4.5)

Carbohydrates

One of the factors that greatly impact the carbohydrate content of the biomass is the harvesting period. According to Kenney et al. (2013a), seasonal time of harvest, as well as the specific machinery used to harvest biomass, has a great impact on the carbohydrate content of the biomass. Adler et al. (2006) also indicated that the carbohydrate content of the switchgrass between fall and spring influences the structural carbohydrates. The switchgrass harvested in spring has higher structural carbohydrates due to leaching of soluble components like simple sugars, inorganic nutrients, proteins, and organic acids during the winter season. The other seasonal factor that can influence carbohydrate content is the loss of some of the plant's anatomical fractions, resulting in less capability to withstand weather changes. The loss of leaves, husks, and upper stalks in corn stover (Shinners et al., 2007) and the loss of seed in switchgrass (Adler et al., 2006) during delayed harvesting resulted in quick drying of the biomass, making it brittle and susceptible to physical damage (bent or broken stems). The delay in harvest from spring to fall resulted in a reduction in the starch content of both the biomasses.

Prewitt et al. (2007) indicated that harvesting machinery has an impact on the carbohydrate content of the biomass. For example, a wheel rake, which operates as a result of ground contact, collects more cobs than a bar rake or a flail shredder, which do not normally contact the ground. A mower, such as a flail shredder, collects lower stalk material where rakes usually do not. Dropping a windrow behind a combine or single-pass harvest both collect more corn cobs over systems that utilize a rake or flail shredder. Pordesimo, Hames, Sokhansanj, & Edens (2005) and Duguid et al. (2007) observed that different proportions of glucan and xylan among stalk, leaf, and husk fractions have different carbohydrate content. Prewitt et al. (2007); Hoskinson, Karlen, Birrell, Radtke, & Wilhelm, (2007); Karlen, Birell, & Hess, (2011) indicated that harvester cut height has an impact on the total carbohydrate content available in the biomass. The studies conducted by Hoskinson et al. (2007) and Karlen et al. (2011) indicated that single-pass harvesting differentiated by cut height resulted in different concentrations of glucan and xylan content. The glucan content increased with a higher amount of lower stalk, and xylan increased with higher amounts of cob and husk fractions.

Templeton, Sluiter, Hayward, Hames, & Thomas (2009) indicated that normalizing year-to-year agronomic practices and harvesting strategies can help to maintain consistent composition in biomass. Kenney et al. (2013a) suggested that best management practices along with the right selection of harvest time and storage systems can help to preserve the biomass quality and can result in consistent carbohydrate content. Moisture content of plants during harvest and during storage has a great impact on the carbohydrate content of the biomass. Management of moisture is critical for preserving the carbohydrate content (Darr & Shah, 2012). Many studies have indicated that proper moisture can extend the biomass shelf life, maintaining carbohydrate content, and reduce formation of soluble sugars and organic acids. In their review on biomass variability, Kenney et al. (2013a) indicated that baled feedstock stored outdoors is most susceptible to dry matter loss. This does not happen uniformly. It is more likely to occur within regions of the bale that retain water over time such as, directly under tarps or in contact with the soil. This results in reduced carbohydrates and relative increase in lignin content in the biomass. Shah, Darr, Webster, & Hoffman (2001) and Shinnars et al. (2010) showed increased lignin and cellulose fractions and decreased hemicellulose fraction in corn stover and switchgrass. The results of dry matter loss in baled corn stover can be contributed to the decrease in xylan content in the remaining biomass.

Recent studies by Wendt (2015) on switchgrass harvested at low moisture (13%, wet basis) and stored uncovered and exposed to local weather conditions for 18 months had a 0.6% decrease in reactivity (fraction of glucan and xylan released in conversion) per every 1% dry matter loss suffered in storage, up to a 26.5% reduction in reactivity at 44% dry matter loss (Figure 6). These results indicate that moisture management (i.e., tarping) during outdoor switchgrass storage is critical to preserve dry matter and convertibility. The study results further indicated that the relationship between reactivity and dry matter loss in corn stover is different than switchgrass, and wet-harvested corn stover requires lower pretreatment severity for sugar conversion, which could favor single-pass harvesting.

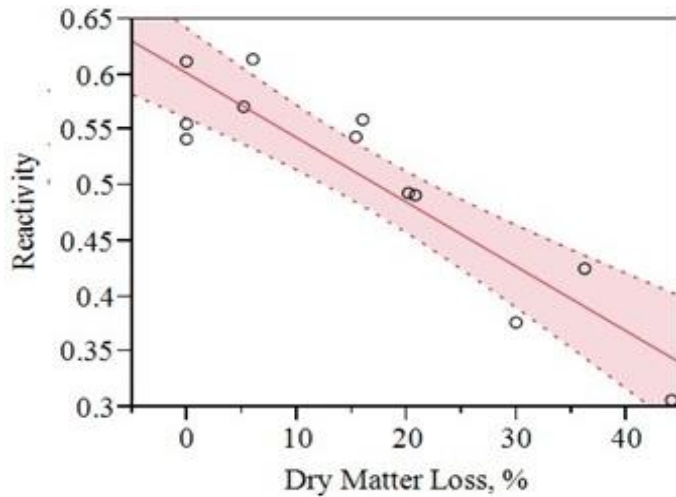


Figure 6. Conversion reactivity loss (fraction of glucan and xylan originally present in biomass feedstock released as glucose or xylose) due to dry matter losses during storage (Wendt, 2015).

Biomass Preprocessing

Biomass preprocessing includes size reduction, drying and densification. Size reduction and densification are the mechanical preprocessing operations used to make biomass meet the specifications needed for conversion applications. Drying is thermal pretreatment technique which is typically used to make biomass aerobically stable.

Size Reduction

Size reduction is required to meet the particle size specifications for the conversion process. In the case of high-moisture biomass, drying may also be needed (e.g., using a rotary drier prior to milling). Drying not only stabilizes the biomass for storage, but increases the efficiency of the grinders. Particle size, distribution, and shape play major roles in feeding biomass into reactors. In general, herbaceous biomass is transported in bales to biorefineries or satellite storage points. The biomass received is stored in storage yards, and is further processed to create a flowable format for feeding the biorefineries. The biomass is size reduced to a particle size of less than <1 inch typically using hammer mills. This reduced size allows the biomass to be fed to the bioreactors or biochemical conversion processes in a more flowable format and at a particle most effective for the conversion process. In the case of thermochemical conversion like pyrolysis and gasification, the particle size of the finely ground biomass plays a major role, because it controls the reaction kinetics (Dibble, Shatova, Jorgenson, & Stickel, 2011; van Walsum et al., 1996). Grinding or milling the biomass from its harvested condition to the size required by the conversion process is typically the most costly part of the conversion process. Several factors, such as moisture, screen size, crop type,

and harvest method, influence the energy required to grind the biomass from its field condition to the format suitable for the conversion process. Table 6 indicate how hammer mill screen size in the range of 19.05-31.75 mm impact the grinding energy in a laboratory scale hammer mill (Tumuluru et al., 2014a). Both the screen size and type of the feedstock has an influence on the grinding energy. Bigger screen sizes resulted in lower specific energy consumption. In the case of canola straws, it consumed the least energy whereas oat straws consumed the maximum.

Table 6. Specific energy consumption for chopping and grinding of agricultural straws (n = 3) (Tumuluru et al., 2014a) Grinding energy (kWh^t⁻¹)

Agricultural straw	Hammer mill/ 31.75 mm screen		Hammer mill/ 25.40 mm screen		Hammer mill/ 19.05 mm screen	
	Mean	SD	Mean	SD	Mean	SD
Barley	1.70 ^a	0.23	2.99 ^a	0.56	3.23 ^a	0.42
Wheat	2.05 ^a	0.25	3.10 ^a	0.34	3.52 ^a	0.13
Canola	1.46 ^a	0.56	1.47 ^b	0.39	2.91 ^a	0.44
Oat	5.68 ^b	0.19	7.51 ^c	0.33	8.05 ^b	0.37

Different scripts in the table indicate that the means are statistically significant based on the Holms-Sidak method and a significance level of 0.05 and 'n' indicates the number of samples.

In general, the ground material has a variety of size fractions including, fine, medium and coarse particles. The fines generated in the grinding process have a higher amount of ash and soil, which erodes conveying and handling systems and has negative effects on most conversion processes. Material handling also creates fines (Bell, 2005). The general consensus of many industrial partners is that fines in the ground material limit the success of downstream processes. In addition, ash content is a concern in most processes, decreasing the value of the preprocessed feedstock. The ash content of the ground biomass is typically highest in the fines. Therefore, removal of the fines would create a more beneficial product from a particle size standpoint, and would result in a reduction in the ash content. Studies on the concentration of ash based on the particle size of ground corn stover in two stage in grinding test conducted, indicated that concentration of ash in the fines, less than 600 microns can be as much as 70%, while the concentration of ash in the fraction greater than 3 mm was only 2.5%. In addition, the larger particles can be problematic as they are less flowable and may cause plugging issues in the conveyance, handling and processing system.

Bale moisture content and screen size of the grinder has a great impact on the particle size distribution of ground biomass. Biomass bale moisture not only impacts particle size distribution, but also the grinding energy and throughput of the grinder. Experiments were conducted using the prototype horizontal hammermill bale grinder (BG480E, Vermeer Cooperation, USA) associated with the Biomass Feedstock National User Facility at Idaho National Laboratory to determine effect of bale moisture content, harvest method and screen size on the energy consumption, and particle size distribution. The BG-480E grinder uses two 200 HP electric motors to drive two grinding drums with 96 swinging hammers on each drum. The corn stover tested was harvested in the fall of 2014, and delivered to the INL for

testing in January of 2015. The material was harvested using single and multi-pass (stover cut, windrowed in the field, and baled) harvest methods from Palo Alto County Iowa. The bale moisture was in the range of 8-15% (w.b.). Testing was conducted using the User Facility stage 1 bale grinder fitted with 1 inch- screen. The results indicated that single pass bales required an average grinding energy of 18-24 kWhr/dry ton, whereas multi-pass required about 22-38 kWhr/dry ton.

Grinding tests were further conducted using the multi-pass harvested corn stover bales to understand the effect of screen size and bale moisture on the grinding energy, and mean particle size of the ground biomass. Biomass bale moisture not only impacts particle size distribution, but also the grinding energy and throughput of the grinder. To determine the effect of moisture on grinding energy, the moisture was plotted against grinding energy (kWh/dry ton), as shown in Figure 7. The figure shows that increasing moisture contents resulted in an increase in energy consumption, whereas increasing the screen size reduced the grinding energy. Feedstock moisture content and screen size have impact on the average mean particle size of the grind (Figure 8). The results indicate that there is an interactive effect between biomass bale moisture content, screen size on the grinding energy, and mean particle size. The other variable which can have an impact on the particle size and grinding energy is the feed rate of the grinder. Yancey et al. (2013) indicated that particle size is also dependent on the feed rate.

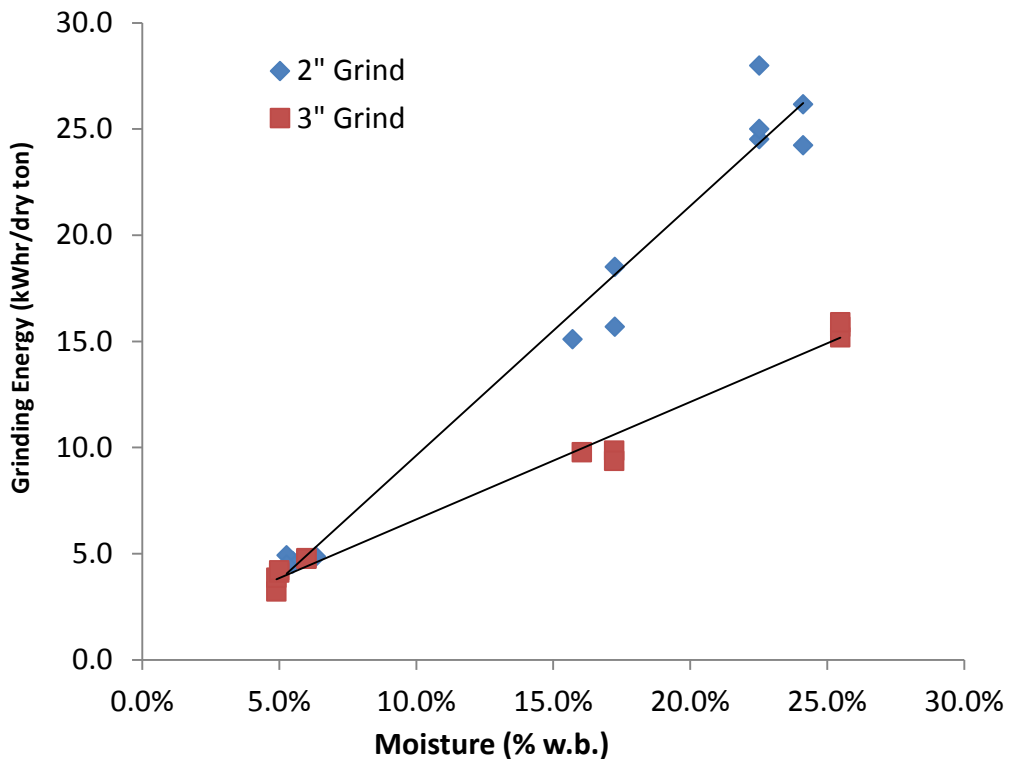


Figure 7. Effect of screen size and moisture content on the grinding energy (Idaho National Laboratory (INL), 2016a) (Source: Biomass National User Facility, Idaho National Laboratory, Idaho Falls, ID).

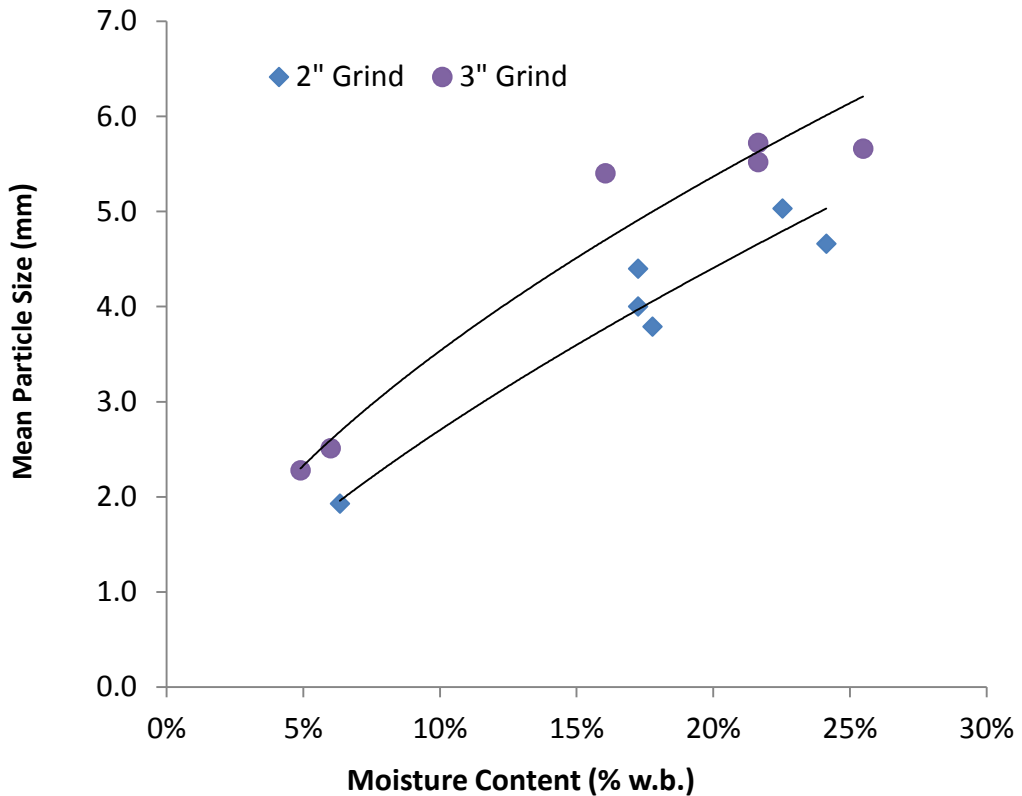


Figure 8. Effect of screen size and moisture content on the particle size (Idaho National Laboratory (INL), 2016a) (Source: Biomass National User Facility, Idaho National Laboratory, Idaho Falls, ID).

Drying

To make biomass aerobically stable and to dry large quantities of biomass, active drying methods are employed. Active drying is needed to remove the moisture that is more tightly bound to biomass (moisture which may be caught in capillaries, fibers or held onto via chemical reactions). Active drying involves using some kind of dryer and consumes energy such as, natural gas or electricity. Active drying is carried out using industrial dryers for higher volume drying. A rotary dryer is typically used for drying large quantities of biomass (Figure 9). Drying tests conducted at the INL Biomass Feedstock National User Facility utilized the Balke Rullman SD 75-22 Rotary Direr. According to Yancey et al. (2013) herbaceous biomass takes less energy compared to woody biomass. Typical consumption of drying energy for woody biomass are in the range 340-400 kWhr/ton, whereas herbaceous biomasses are in the range of 200-300 kWhr/ton. Lamers et al. (2015) indicated that drying of biomass using rotary dryer takes about \$15/dry ton, whereas pelleting takes about \$7.82/dry ton. Among the preprocessing unit operations, drying is the most energy intensive operation.



Figure 9. Rotary dryer used in biomass industry (Idaho National Laboratory (INL), 2016a) (Source: Biomass National User Facility, Idaho National Laboratory, Idaho Falls, ID).

When compared to active drying, passive drying is generally less expensive, requires less equipment, and requires less external energy input. However, it is slower and is dependent on climatological conditions which change annually and cannot be predicted ahead of time. Much of the free water in the biomass can be removed by passive drying, which can be used to achieve a moisture content of 25–30% (w.b.) depending on the equilibrium moisture content of the material in the ambient storage conditions. This final moisture content may be suitable for combustion application, but for other thermochemical applications like pyrolysis and gasification, a lower moisture content of 5–15% (w.b.) (Jahirul, Rasul, Chowdhury, & Ashwath, 2012) is desirable and is generally achieved by active drying. In active drying, external heat is provided to the biomass to speed the drying process. Typically, the temperatures that are used in active drying are about 160–180°C and rotary dryers are commonly used for this operation. However, the challenge in using commercial dryers is the cost. Energy analysis of grinding, drying, and pelleting indicated that drying takes about 65–70% of the total energy (Tumuluru, Cafferty, & Kenney, 2014b). Another major disadvantage of high temperature drying is emission of volatile organic compounds (VOCs) which can lead to environmental issues (Tumuluru, 2014; Tumuluru, 2015). Currently, low temperature drying methods are gaining importance in Europe to avoid high drying costs and environmental issues. One example, is forced air convective method where lower drying temperatures in the range of 60–80°C and low air flow rates are used for drying of biomass materials. Some of the examples of forced air convective dryers are cabinet dryers, grain and belt dryers. The major advantages of these dryers are they operate at lower temperature and are not capital intensive (Lamers et al., 2015). The other major advantage of low temperature methods are: a) greater efficiency, b) reduced fire hazard, c) does not need high quality heat,

d) reduced volatile organic compound (VOC) emissions, e) reduced particulate emissions, and f) does not agglomerate high clay or sticky biomass (Tumuluru, Conner, & Hoover, 2016; Tumuluru, 2016).

Densification

A major limitation of ground agricultural biomass is its low bulk density resulting in lower bin density and transportation efficiencies. Some of the densification systems like baling, pelleting, and briquetting help to increase the bulk density and make biomass easier to handle and transport. Densifying the biomass after grinding can help to reduce handling, storage, and transportation problems and improves the flow characteristics. Densification of biomass by pellet mill increases the bulk density by about 5-10 times compared to ground biomass (Tumuluru et al., 2011a). Typically, the ground herbaceous biomass has a density of about 80–150 kg/m³ (Table 7) (Tumuluru et al., 2014a; Yancey et al., 2013). The bulk, tapped and particle density of the ground biomass changes with screen size selected (Tumuluru et al., 2014a). Table 8 indicated how the flow indices like Carr index and Hausner ratio are influenced by the hammer mill screen size. In case of wood pellets the Hausner ratio and Carr Index calculated based on the tapped and bulk density values provided by Tumuluru et al., 2010 is 1.09 and 8.40. Recommend Hausner ratio for free flowing is <1.25 and Carr index should be between 5-15 and 1-16 for excellent and good flow properties. Carr index values of >23 indicates poor flow properties (Tumuluru et al., 2014a). It is very clear from the data that pellets have higher flow characteristics compared to ground biomass.

Table 7. Bulk, tapped and particle density of chopped and ground agricultural straws (n = 3) (Tumuluru et al., 2014a)

Agricultural straw	Hammer mill/31.75 mm screen		Hammer mill/25.40 mm screen		Hammer mill/19.05 mm screen	
	Bulk density (kg/m ³)					
	Mean	SD	Mean	SD	Mean	SD
Barley	48.54 ^a	3.45	64.9 ^a	3.56	67.2 ^b	2.34
Wheat	49.68 ^a	2.11	58.8 ^{a, b}	2.90	58.2 ^a	3.12
Canola	67.15 ^b	1.88	73.6 ^c	2.29	80.4 ^c	3.09
Oat	54.35 ^a	2.01	53.5 ^b	2.39	58.3 ^a	2.87
	Tapped density (kg/m ³)					
Barley	65.05 ^a	3.23	99.4 ^b	3.89	101 ^b	3.45
Wheat	59.39 ^b	2.01	80.7 ^a	2.87	88.2 ^a	3.05
Canola	79.66 ^c	1.97	113 ^c	2.39	119 ^c	3.89
Oat	68.94 ^a	2.36	85.1 ^a	2.77	90.6 ^a	3.07
Barley	817.5 ^a	16.4	869.5 ^b	19.2	873.6 ^a	20.1
Wheat	663.2 ^b	10.2	709.0 ^a	12.78	781.4 ^b	15.6
Canola	818.2 ^a	9.9	969.4 ^c	12.2	1219.7 ^c	17.3
Oat	620.9 ^c	8.9	714.2 ^a	12.1	839.3 ^d	18.9

Different superscripts indicate the means are statistically significant based on the Holms-Sidak method and a significance level of 0.05 and 'n' indicates the number of samples.

Table 8. Hausner ratio and Carr index of chopped and ground agricultural straws (Tumuluru et al., 2014a)

Straw	Hausner ratio		
	Hammer mill/31.75 mm screen	Hammer mill/25.4 mm screen	Hammer mill/19.05 mm screen
Oat	1.27	1.59	1.55
Barley	1.34	1.53	1.50
Canola	1.19	1.53	1.48
Wheat	1.19	1.37	1.52
Straw	Carr Index		
	Hammer mill/31.75 mm screen	Hammer mill/25.4 mm screen	Hammer mill/19.05 mm screen
Oat	21.16	37.13	35.65
Barley	25.38	34.71	33.46
Canola	15.70	34.87	32.44
Wheat	16.35	27.14	34.01

Note: 6 mm diameter wood pellets have Hausner ratio and Carr index of 1.09 and 8.40 (calculated based on bulk and tapped density data provided by Tumuluru et al., 2010).

Densifying the biomass using the densification systems indicated in Table 3 increases the bulk density. Pellets produced using pellet mill are commonly used for bioenergy applications. Typically, the bulk density of pellets is in the range of 700-750 kg/m³ (Tumuluru et al., 2010; Yancey et al., 2013). Also, once the material is densified, it can be handled easily with the conveying and handling systems that are typically used in grain-processing industries. Figure 10 indicates the density comparison of bales, grounds and pellets. Figure 11 indicates the durability values of the woody, herbaceous and formulated pellets. Durability of the pellets is defined as the ability of the pellets to withstand the frictional and impact resistances (Tumuluru et al., 2011a). The higher the durability values the greater is the integrity of the pellets during handling, storage and transport. Another interesting outcome of this research was that the hardwood pellets, which have lower durability values and higher drying energy, when blended with corn stover, switchgrass, and lodgepole pine resulted in higher durability values of >97.5 and reduced grinding and drying energies (Yancey et al., 2013). Briquetting of biomass is another option to increase the bulk density of the ground biomass (Table 6). The major advantage of briquette is that it requires larger particle sizes which results in lower energy consumption during the grinding process (Tumuluru, Tabil, Song, Iroba, & Meda, 2015). The typical bulk density and durability of the briquettes produced using woody and herbaceous biomass for material ground using hammer mill fitted with different screens is given in Figures 12 and 13.

Additionally, pellets and briquettes when crumbled resulted in higher particle density and uniform particle size with fewer fines making biomass more suitable for thermochemical conversion pathway. Laboratory studies conducted on performance of pellets for both biochemical and thermochemical conversion pathways indicated that pellets perform better compared to ground biomass (Ray et al., 2013; Rijal, Igathinathane, Karki, Yu, & Pryor,

2012; Yang et al., 2014). Currently most of the wood pellets produced at commercial scale are used for biopower generation (Tumuluru et al., 2010).

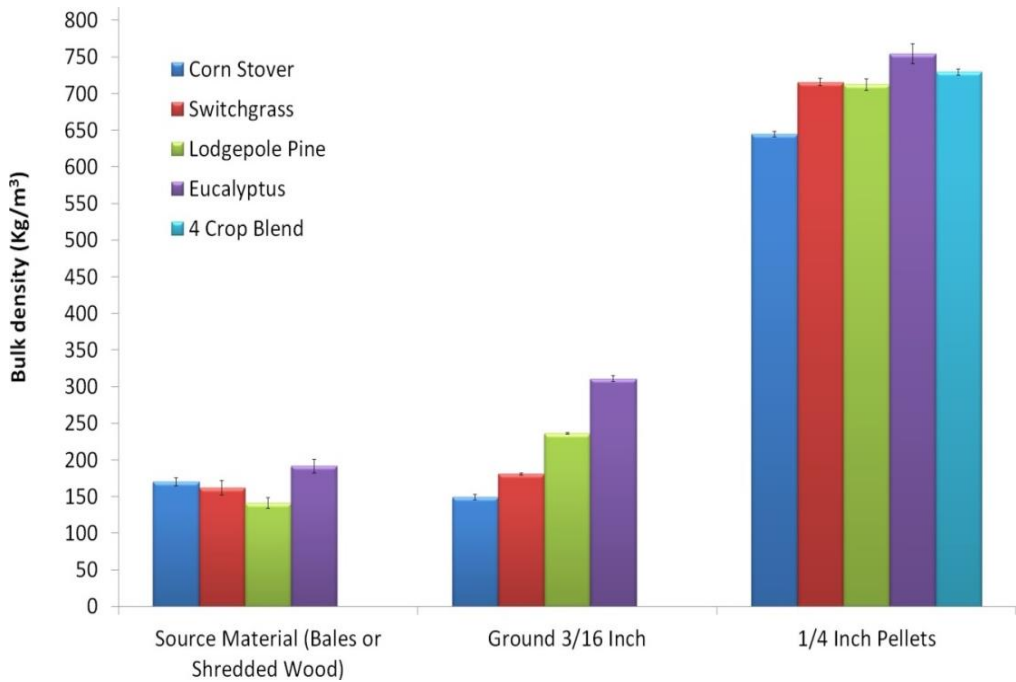


Figure 10. Bulk density of raw, ground and pelleted woody and herbaceous (Yancey et al., 2013).

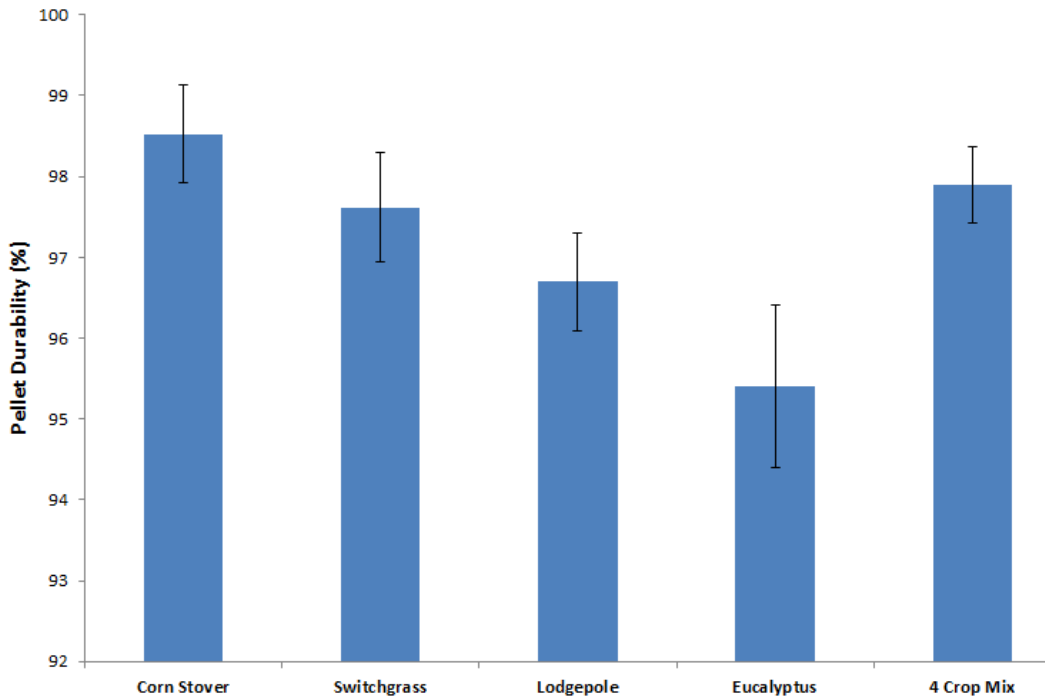


Figure 11. Durability of herbaceous, woody and formulated biomass pellets (Yancey et al., 2013).

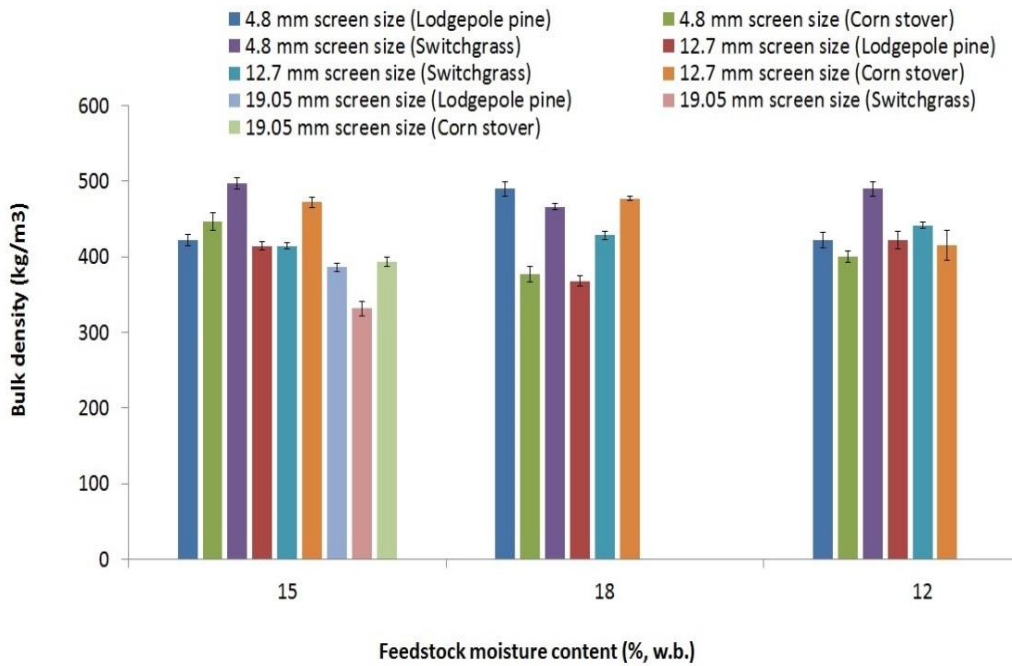


Figure 12. Bulk density of woody and herbaceous biomass briquettes (Tumuluru, Dansie, Johnson, & Conner, 2015b).

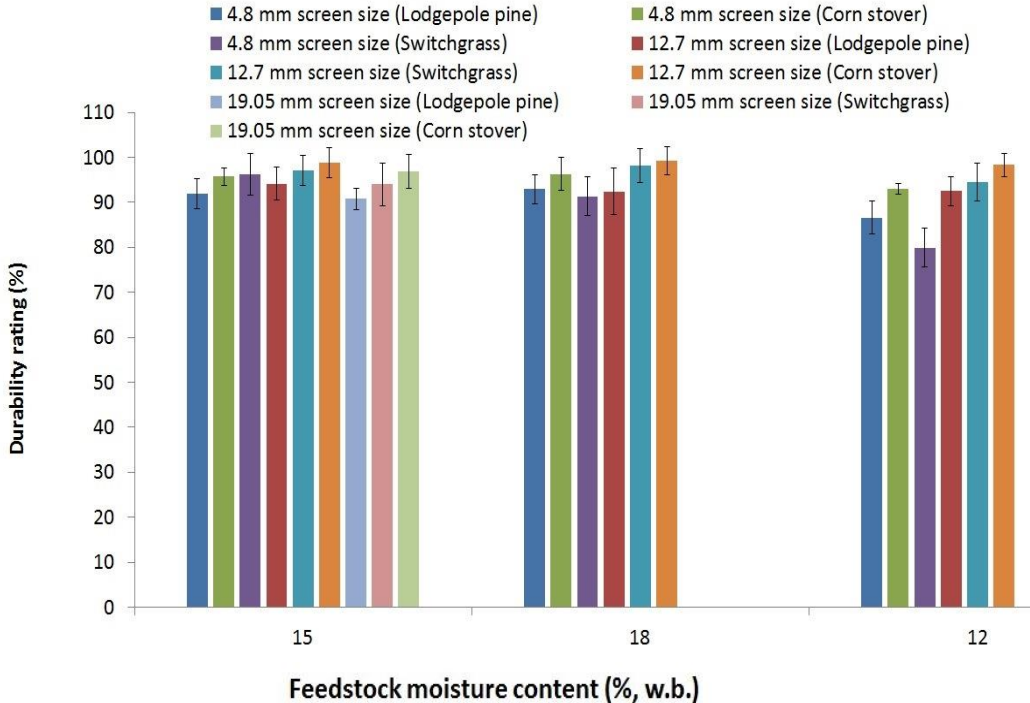


Figure 13. Durability rating of different woody and herbaceous biomass briquettes (Tumuluru et al., 2015b).

ADVANCED PREPROCESSING TECHNIQUES TO IMPROVE BIOMASS QUALITY

In general, the raw biomass physical properties (lower mass density, high-moisture content, irregular size and shape, and hydrophilic in nature), chemical properties (low carbon and high hydrogen, oxygen, and volatiles), and energy properties (high hydrogen/carbon and oxygen/carbon ratios, and lower heating values) do not make them suitable for thermochemical applications like gasification, pyrolysis, and cofiring (Tumuluru et al., 2015b). Tumuluru et al. (2012) in their review it was indicated that raw biomass physical properties and chemical composition do not make them suitable for co-firing higher percentages with coal. The authors stated that boiler inefficiency due to higher moisture and volatiles and lower energy content of the biomass fuels, as compared to coal is a major limitation to cofiring higher percentages of biomass with coal. The shortcoming of lignocellulosic biomass in terms of physical and chemical properties can be overcome by thermal pretreatments. Currently, thermal (dry torrefaction, hydrothermal carbonization, steam explosion, and ionic treatment) and chemical (acid, alkali, and ammonia fiber expansion (AFEX)) treatment techniques are being investigated to improve the biomass quality for both thermochemical and biochemical conversion applications (Karki et al., 2015; Lynam, Reza, Vasquez, & Coronella, 2012; Reza, Lynam, Uddin, & Coronella, 2013; Singh et al., 2015; Tumuluru et al., 2012; Tumuluru, Sokhansanj, Hess, Wright, & Boardman, 2011b; Tumuluru et al., 2011a). Sarkar et al. (2014) and Yang et al. (2014) have successfully used torrefied and torrefied-densified switchgrass for gasification and pyrolysis application. Their results indicated that syngas quality and bio-oil quality were better compared to products produced with raw biomass. In case of biochemical conversion, chemical pretreatments (acid, alkali and ammonia fiber explosion) and further densification helps to increase the conversion performance (Hoover, Tumuluru, Teymouri, Moore, & Gresham, 2014).

The unit operations like grinding, drying, thermal and chemical treatments and densification are energy intensive. However, the advantages of performing these unit operations need to be quantified in terms of reducing the transportation, storage, and handling costs, and increasing the conversion performance. Kenney et al. (2013a) suggested that there are two approaches to solving handling problems. One is to engineer the equipment to suit the biomass material properties. The second approach is to perform preprocessing operations on the biomass to make it suitable for the existing commercial conveying, storage, and handling equipment. In the present day, the first approach is more common compared to the second, but it is advantageous to use both approaches to reduce the many storage, handling, and conveying problems and to improve the conversion performance and to produce high quality bioenergy products.

DISCUSSION

Biomass feedstock quality attributes profoundly impact biofuels production. The main quality attributes that affect biofuels production are moisture, ash, carbohydrates, particle size, and density. In the case of the thermochemical conversion pathway, ash is targeted to be less than 1%, whereas in the case of the biochemical conversion pathway, maximum

carbohydrates are desirable to ensure economical product yields. Particle size influences the reaction kinetics of biomass during conversion, whereas the density influences the transportation and handling logistics. Based on the current analysis, it can be concluded that the harvesting methods used impact ash composition and carbohydrate content in the biomass. Single-pass harvest results in lower ash content, but higher moisture content in the harvested biomass. Storage is another important variable that can influence dry matter loss in biomass. Storing higher-moisture biomass for longer periods results in dry matter loss and, in turn, decreases the carbohydrate and energy content in the biomass.

Ash in the biomass is influenced by the harvesting and preprocessing methods. Recent study by researchers has indicated that separating the biomass of certain component in the biomass can reduce the total ash content in the biomass. Separating the leaves from the biomass using air classification methods can reduce the ash composition of the recovered biomass. Lacey, Aston, Westover, Cherry, & Thompson (2015) in their studies on removal of introduced inorganic ash content from chipped forest biomass using air classification, found that the ash concentrations are highest in the lightest fractions (5.8-8.5 wt%) and in a heavy fraction of the fines (8.9-15.1 wt%). They found that high inorganic content fractions were about 7 wt % of the total biomass, but they had greater than 40% of the ash content by mass. Alternatively the fines can be separated during the grinding process to selectively remove the fines which contain a higher percentage of ash. Ash content in biomass is also dependent on the harvesting methods, harvesting time, sampling rate, sampling location, environmental variables, and storage conditions.

Other methods of reducing the ash content of the harvested biomass include washing, leaching, and acid or alkali pretreatment. Washing and leaching help to remove most of the soil contamination, whereas acid or alkali pretreatment will help to remove the anatomical ash content. Das et al. (2004) reported on the effectiveness of a dilute hydrofluoric acid pretreatment for reducing ash concentrations in sugarcane bagasse from 2% (dry mass) to less than 0.05%. The method was shown to be very effective for removing ash and provided the baseline for Das et al.'s study of other ash removal methods. The major limitation of using the additional preprocessing steps can be the associated equipment and chemical costs. The additional cost with this preprocessing can be offset by reducing the operational cost of the biorefineries, because these pretreatments can result in less maintenance (reduce wear and tear of the handling systems due to erosion) of the machinery in the biorefineries. One way to reduce the impact of ash on the thermochemical conversion process is by mechanical separation of various biomass components like leaves, stalk etc. In general, leaves have higher ash content compared to other biomass components. The data presented will help the farmers to identify the harvesting periods and suitable environmental conditions that can result in lower ash content in the biomass which will result by providing the biorefineries suitable material for maximizing the conversion efficiencies.

Carbohydrates content in the biomass is influenced by the harvesting and storage methods introduced. Another alternative to improve the biomasses having fewer carbohydrates is blending or formulating the different feedstocks. Blending is widely used in the livestock feed industry to make up the protein, carbohydrates, or fats in the feed constituents. In the thermal power industry, different coals are mixed to maintain the specification desired for the boilers. Tumuluru et al. (2012) suggested that biomass can be formulated with coal to improve the specifications to co-fire in coal-fired power plants. Formulation can be a good alternative to make up the lost biomass consistent during

harvesting and storage. According to Betancur & Pereira (2010), low-carbohydrate biomasses can be mixed with biomasses that are high in carbohydrates to meet the desired specifications. According to Kenney et al. (2013a), formulation can be implemented at a preprocessing facility or at the throat of the reactor to meet the specification needed by the biorefineries in terms of carbohydrates.

Preprocessing of the biomass helps to improve the particle size and density specification needed for both biochemical and thermochemical conversion pathway. Grinding and further pelleting of the biomass helps to reduce the storage issues (e.g., dry matter losses, storage foot print, and feedstock recovery) and improve the transportation logistics. Improving the size-reducing systems to handle high-moisture feedstocks is critical to reducing the preprocessing costs. Also, the design of bulk flowable systems to handle high-moisture biomass feedstock will be critical for efficient management of high-moisture biomass feedstock. Novel thermal (torrefaction, hydrothermal carbonization) and chemical preprocessing (ammonia fiber explosion, acid and alkali and ionic) techniques are being developed to modify biomass to meet the quality specification needed for biochemical and thermochemical conversions.

CONCLUSION

The cost of biomass supplied to the biorefineries is dependent on the unit operations like harvesting, storage and preprocessing. These unit operations also influence the biomass quality attributes such as moisture, ash, carbohydrates, particle size, and density. Feedstock moisture content is a critical quality attribute, impacting both cost and quality of the feedstock and also influencing transportation costs. Factors impacting feedstock moisture include: a) harvest timing, b) age (particularly in the case of trees), c) the type of biomass, d) the region where it is grown, e) water availability, and f) irrigation practices. Typically, moisture in biomass is managed in the field using passive drying methods. Ash is an inert component of biomass, and has a larger impact on thermochemical conversion compared to biochemical conversion. Ash content decreases in forages with maturity when the harvest is delayed from fall to late winter. Additionally, agronomic factors play a part such as, soil type, soil chemistry, water quality, fertilization chemistry, and the elemental composition of the soil. Selecting the right feedstock, harvesting equipment, and preprocessing equipment also influence the ash content in the biomass. Carbohydrate content in the lignocellulosic biomass is important for biochemical conversion and is influenced by the harvesting equipment and storage methods. Particle size and density of the biomass has an influence on the storage, transportation and handling, and can be improved by size reduction and densification methods. A major limitation of ground biomass is low bulk density and this limitation can be overcome by mechanical densification using a pellet mill or briquette press. Finally, to manage high volumes of high moisture biomass feedstocks, active drying methods may need to be employed to make biomass aerobically stable.

ACKNOWLEDGMENTS

This work was supported by the Department of Energy, Office of Energy Efficiency and Renewable Energy under the Department of Energy Idaho Operations Office Contract DE-AC07-05ID14517.

DISCLAIMER

This information was prepared as an account of work sponsored by an agency of the U.S. government. Neither the U.S. government nor any agency thereof, nor any of their employees, makes any warranty, express or implied, or assumes any legal liability or responsibility for the accuracy, completeness, or usefulness of any information, apparatus, product, or process disclosed, or represents that its use would not infringe privately owned rights. References herein to any specific commercial product, process, or service by trade name, trademark, manufacturer, or otherwise, do not necessarily constitute or imply its endorsement, recommendation, or favoring by the U.S. government or any agency thereof. The views and opinions of the authors expressed herein do not necessarily state or reflect those of the U.S. government or any agency thereof.

Conflict of Interest Statement

The authors declare that the research was conducted in the absence of any commercial or financial relationships that could be construed as a potential conflict of interest.

REFERENCES

- Aden, A. & Foust, T. (2009). Technoeconomic analysis of the dilute sulfuric acid and enzymatic hydrolysis process for the conversion of corn stover to ethanol. *Cellulose*, 16(4), 535-545.
- Adler, P. R., Sanderson, M. A., Boateng, A. A., Weimer, P. I., & Jung, H. J. G. (2006). Biomass yield and biofuel quality of switchgrass harvested in fall or spring. *Agronomy Journal*, 98(6), 1518-1525.
- Afzal, M. T., Bedane, A. H., Sokhansanj, S., & Mahmood, W. (2010). Storage of comminuted and uncomminuted forest biomass and its effect on fuel quality. *BioResources*, 5(1), 55-69.
- Bell, T. A. (2005). Challenges in the scale-up of particulate processes - An industrial perspective. *Powder Technology*, 150(2), 60-71.
- Betancur, G. J.V., & Pereira Jr, N. (2010). Sugar cane bagasse as feedstock for second generation ethanol production. Part I: Diluted acid pretreatment optimization. *Electronic Journal of Biotechnology*, 13(5).
- Bonner, I. J. (2016). [Principle scientist biomass storage project, Idaho National Laboratory].

- Bonner, I. J., Cafferty, K. G., Muth, D. J., Jr., Tomer, M. D., James, D. E., Porter, S. A., & Karlen, D. L. (2014). Opportunities for Energy Crop Production Based on Subfield Scale Distribution of Profitability. *Energies*, 7(10), 6509-6526
- Bridgwater, A. V. (1999). Principles and practice of biomass fast pyrolysis processes for liquids. *Journal of Analytical and Applied Pyrolysis*, 51(1-2), 3-22.
- Burvall, J. (1997). Influence of harvest time and soil type on fuel quality in reed canary grass (*Phalaris arundinacea* L.). *Biomass & Bioenergy*, 12(3), 149-154.
- Carpenter, D. L., Bain, R. L., Davis, R. E., Dutta, A., Feik, C. J., Gaston, K. R., . . . Nimlos, M. R. (2010). Pilot-Scale Gasification of Corn Stover, Switchgrass, Wheat Straw, and Wood: 1. Parametric Study and Comparison with Literature. *Industrial & Engineering Chemistry Research*, 49(4), 1859-1871.
- Coble, C. G., & Egg, R. (1987). Dry matter losses during hay production and storage of sweet sorghum used for methane production. *Biomass*, 14(3), 209-217.
- Dai, J. J., Cui, H. P., & Grace, J. R. (2012). Biomass feeding for thermochemical reactors. *Progress in Energy and Combustion Science*, 38(5), 716-736.
- Darr, M. J., & Shah, A. (2012). Biomass storage: and update on industrial solutions for baled biomass feedstocks. *Biofuels*, 3(3), 321-332.
- Das, P., Ganesh, A., & Wangikar, P. (2004). Influence of pretreatment for deashing of sugarcane bagasse on pyrolysis products. *Biomass & Bioenergy*, 27(5), 445-457.
- Davidsson, K. O., Pettersson, J. B. C., & Nilsson, R. (2002). Fertiliser influence on alkali release during straw pyrolysis. *Fuel*, 81(3), 259-262.
- Dibble, C. J., Shatova, T. A., Jorgenson, J. L., & Stickel, J. J. (2011). Particle morphology characterization and manipulation in biomass slurries and the effect on rheological properties and enzymatic conversion. *Biotechnology Progress*, 27(6), 1751-1759.
- DOE. (2011). U.S. Billion-Ton Update: Biomass Supply for a Bioenergy and Bioproducts Industry. In R. D. Perlack & B. J. Stokes (Eds.), (pp. 227). Oak Ridge National Laboratory, Oak Ridge, TN: U.S. Department of Energy.
- DOE (2015). Multi-Year Program Plan, U.S. Department of Energy, from www.energy.gov/sites/prod/files/2015/04/f22/mypp_beto_march2015.pdf, March 2015.
- Duguid, K.B., Montross, M.D., Radtke, C.W., Crofcheck, C.L., Wendt, L.M., Shearer, S.A. (2009). Effect of anatomical fractionation on the enzymatic hydrolysis of acid and alkaline pretreated corn stover. *Bioresource Technology*, 100(21), 5189-5195.
- Emery, I. R., & Mosier, N. S. (2012). The impact of dry matter loss during herbaceous biomass storage on net greenhouse gas emissions from biofuels production. *Biomass & Bioenergy*, 39, 237-246.
- Gamble, J. D., Jungers, J. M., Wyse, D. L., Johnson, G. A., Lamb, J. A. and Sheaffer, C. C. Harvest date effects on biomass yield, moisture content, mineral concentration and mineral export in switchgrass and native polycultures managed for bioenergy. *Bioenergy Research*, 8, 740-749.
- Greene, N., Celik, F. E., Dale, B., Jackson, M., Jayawardhana, K., Jin, H., Larson, E. D., Laser, M., Lynd, L., MacKenzie, D., Mark, J., McBride, J., McLaughlin, S., & Saccardi, D. (2004). Growing energy: How biofuels can help end America's oil dependence [Press release].
- Hess, J., Thompson, D., Hoskinson, R., Shaw, P., & Grant, D. R. (2003). Physical separation of straw stem components to reduce silica. *Applied Biochemistry and Biotechnology*, 105, 43-51.

- Hoover, A. N., Tumuluru, J. S., Teymouri, F., Moore, J., & Gresham, G. (2014). Effect of pelleting process variables on physical properties and sugar yields of ammonia fiber expansion pretreated corn stover. *Bioresource Technology*, 164(0), 128-135.
- Hoskinson, R. L., Karlen, D. L., Birrell, S. J., Radtke, C. W., & Wilhelm, W. W. (2007). Engineering, nutrient removal, and feedstock conversion evaluations of four corn stover harvest scenarios. *Biomass & Bioenergy*, 31(2-3), 126-136.
- Humbird, D., Davis, R., Tao, L., Kinchin, C., Hsu, D., Aden, A., Schoen, P., Lukas, J., Olthof, B., Worley, M., Sexton, D., & Dudgeon, D. (2011). Process design and economics for biochemical conversion of lignocellulosic biomass to ethanol. National Renewable Energy Laboratory. (Vol. NRL/TP-5100-47764). from www.nrel.gov/docs/fy11osti/47764.pdf.
- Idaho National Laboratory (INL). (2016). Biomass Feedstocks Library, Biofuels and Renewable Energy Technology. from bioenergylibrary.inl.gov.
- Idaho National Laboratory (INL). (2016a). Biomass National User Facility. from www.inl.gov/bfnuf/.
- Igathinathane, C., Archer, D., Gustafson, C., Schmer, M., Hendrickson, J., Kronberg, S., Keshwani, D. R., Backer, L., Hellevang, K., & Faller, T. (2014). Biomass round bales infield aggregation logistics scenarios. *Biomass & Bioenergy*, 66, 12-26.
- Jahirul, M. I., Rasul, M. G., Chowdhury, A. A., & Ashwath, N. (2012). Biofuels Production through Biomass Pyrolysis-A Technological Review. *Energies*, 5(12), 4952-5001.
- Jarchow, M. E., Liebman, M., Rawat, V., & Anex, R. P. (2012). Functional group and fertilization affect the composition and bioenergy yields of prairie plants. *Global Change Biology Bioenergy*, 4(6), 671-679.
- Jirjis, R. (1995). Storage and drying of wood fuel. *Biomass & Bioenergy*, 9(1-5), 181-190.
- Johnson, J. M. F & Gresham, G. L. 2014. Do Yield and Quality of Big Bluestem and Switchgrass Feedstock Decline over Winter?, *Bioenergy Research*, 7, 68-77
- Jones, S. B., Valkenburg, C., Walton, C. W., Elliott, D. C., Holliday, J. E., Stevens, D. J., Kinchin, C., & Czernik, S. (2009). Production of gasoline and diesel from biomass via fast pyrolysis, hydrotreating and hydrocracking: a design case (Vol. PNNL-18284): Pacific Northwest National Laboratory.
- Jorgensen, U. (1997). Genotypic variation in dry matter accumulation and content of N, K and Cl in *Miscanthus* in Denmark. *Biomass & Bioenergy*, 12(3), 155-169.
- Karlen, D. L., Birell, S. J., & Hess, J. R. (2011). A five-year assessment of corn stover harvest in central Iowa, USA. *Soil & Tillage Research*, 115, 47-55.
- Karki, B., Muthukumarappan, K., Wang, Y., Dale, B. E., Balan, V., Gibbons, W. R., & Karunanithy, C. (2015). Physical characteristics of AFEX-pretreated and densified switchgrass, prairie cord grass, and corn stover. *Biomass & Bioenergy*, 78, 164-174.
- Kenney, K. L., Cafferty, K. G., Jacobson, J. J., Bonner, I. J., Gresham, G. L., Hess, J. R., Ovard, L. P., Smith, W. A., Thompson, D. N., Thompson, V. S., Tumuluru, J. S., & Yancey, N. (2013). Feedstock Supply System Design and Economics for Conversion of Lignocellulosic Biomass to Hydrocarbon Fuels. Conversion Pathway: Biological Conversion of Sugars to Hydrocarbons: The 2017 Design Case. (Vol. INL/EXT-13-30342).
- Kenney, K. L., Smith, W. A., Gresham, G. L., & Westover, T. L. (2013a). Understanding biomass feedstock variability. *Biofuels*, 4, 111-127.

- Klavina, K., Zandeckis, A., Rochas, C., & Zagorskis. (2014). *Low temperature drying as a solution for sustainable use of biomass*. In: *Environmental Protection Engineering*. Paper presented at the Proceedings of the 17th Conference for Junior Researchers "Science - Future of Lithuania", Lithuania, Vilnius.
- Lacey, A.L., Aston, J.E., Westover, T.L., Cherry, R.S., & Thompson, D.N. (2015). Removal of introduced inorganic content from the chipped forest residues via air classification. *Fuel*, 160, 265-273.
- Lamers, P., Roni, M. S., Tumuluru, J. S., Jacobson, J. J., Cafferty, K. G., Hansen, J. K., Kenney, K., Teymouri, F., & Bals, B. (2015). Techno-economic analysis of decentralized biomass processing depots. *Bioresource Technology*, 194, 205-213.
- Lee, D., Owens, V. N., Boe, A., & Jeranyama, P. (2007). Compostion of Herbaceous Biomass Feedstocks In S. D. S. U. North Central Sun Grant Center (Ed.). Brookings, South Dakota.
- Lewandowski, I., and Kicherer, A. (1997). Combustion quality of biomass: Practical relevance and experiments to modify the biomass quality of *Miscanthus x giganteus*. *European Journal of Agronomy*, 6(3-4), 163-177.
- Lewandowski, I., Clifton-Brown, J. C., Andersson, B., Basch, G., Christian, D. G., Jorgensen, U., Jones, M. B., Riche, A. B., Schwarz, K. U., Tayebi, K., & Teixeira, F. (2003). Environment and harvest time affects the combustion qualities of *Miscanthus* genotypes. *Agronomy Journal*, 95(5), 1274-1280.
- Lindsey, K., Johnson, A., Kim, P., Jackson, S., & Labbe, N. (2013). Monitoring switchgrass composition to optimize harvesting periods for bioenergy and value-added products. *Biomass & Bioenergy*, 56, 29-37.
- Lynam, J. G., Reza, M. T., Vasquez, V. R., & Coronella, C. J. (2012). Pretreatment of rice hulls by ionic liquid dissolution. *Bioresource Technology*, 114, 629-636.
- Madakadze, I. C., Stewart, K., Peterson, P. R., Coulman, B. E., & Smith, D. L. (1999). Switchgrass biomass and chemical composition for biofuel in eastern Canada. *Agronomy Journal*, 91(4), 696-701.
- McLaughlin, S. B., De La Torre Ugarte, D. G., Garten Jr., C. T., Lynd, L. R., Sanderson, M. A., Tolbert, V. R., & Wolf, D. D. (2002). High-value renewable energy from prairie grasses. *Environmental Science & Technology*, 36, 2122-2129.
- Mullen, C., Boateng, A. A., Dadson, R. B., & Hashem, F. M. (2014). Biological mineral range effects on biomass conversion to aromatic hydrocarbons via catalytic fast pyrolysis over HZSM-5. *Energy & Fuels* 28, 7014-7024.
- Muth, D. J., Langholtz, M. H., Tan, E. C. D., Jacobson, J. J., Schwab, A., Wu, M. M., Searcy, E. M. (2014). Investigation of thermochemical biorefinery sizing and environmental sustainability impacts for conventional supply system and distributed pre-processing supply system designs. *Biofuels Bioproducts & Biorefining-Biofpr*, 8(4), 545-567.
- Phyllis2, E. (2015). Databased for biomass and waste from <https://www.ecn.nl/phyllis2/>
- Pordesimo, L. O., Hames, B. R., Sokhansanj, S., & Edens, W. C. (2005). Variation in corn stover composition and energy content with crop maturity. *Biomass & Bioenergy*, 28(4), 366-374.
- Prewitt, R. M., Montross, M. D., Shearer, S. A., Stombaugh, T. S., Higgins, S. F., McNeill, S. G., & Sokhansanj, S. (2007). Corn stover availability and collection efficiency using typical hay equipment. *Transactions of the ASABE*, 50(3), 705-711.

- Ray, A. E., Hoover, A. N., Nagle, N., Chen, X., & Gresham, G. L. (2013). Effect of pelleting on the recalcitrance and bioconversion of dilute-acid pretreated corn stover under low- and high-solids conditions. *Biofuels*, 4(3), 271-284.
- Ren, L., Cafferty, K., Roni, M., Jacobson, J., Xie, G., Ovard, L., & Wright, C. (2015). Analyzing and Comparing Biomass Feedstock Supply Systems in China: Corn Stover and Sweet Sorghum Case Studies. *Energies* 5577-5597, 8(6), 5577-5597.
- Reza, M. T., Lynam, J. G., Uddin, M. H., & Coronella, C. J. (2013). Hydrothermal carbonization: Fate of inorganics. *Biomass & Bioenergy*, 49, 86-94.
- Rijal, B., Igathinathane, C., Karki, B., Yu, M., & Pryor, S. W. (2012). Combined effect of pelleting and pretreatment on enzymatic hydrolysis of switchgrass. *Bioresource Technology*, 116, 36-41.
- Roni, M. S., Eksioğlu, S. D., Cafferty, K. G., & Jacobson, J. J. (2016). A multi-objective, hub-and-spoke model to design and manage biofuel supply chains. *Annals of Operations Research*, 1-30.
- Roni, M. S., Eksioğlu, S. D., Searcy, E., & Jha, K. (2014). A supply chain network design model for biomass co-firing in coal-fired power plants. *Transportation Research Part E-Logistics and Transportation Review*, 61, 115-134.
- Sanderson, M. A., Egg, R. P., & Wiseloge, A. E. (1997). Biomass losses during harvest and storage of switchgrass. *Biomass & Bioenergy*, 12(2), 107-114.
- Sanderson, M. A., & Wolf, D. D. (1995). Switchgrass biomass composition during morphological development in diverse environments. *Crop Science*, 35(5), 1432-1438.
- Sarkar, M., Kumar, A., Tumuluru, J. S., Patil, K. N., & Bellmer, D. D. (2014). Gasification performance of switchgrass pretreated with torrefaction and densification. *Applied Energy*, 127, 194-201.
- Searcy, E., & Hess, J. (2010). Uniform-format feedstock supply system: A commodity-scale design to produce an infrastructure-compatible biocrude from lignocellulosic biomass. (Vol. INL/EXT09-15423). Idaho National Laboratory.
- Searcy, E., Lamers, P., Hansen, J., Jacobson, J., & Webb, E. (2015) Advanced feedstock supply system validation workshop. Golden, Colorado. (Vol. INL/EXT-10-18930).
- Shah, A., Darr, M. J., Webster, K., & Hoffman, C. (2001). Outdoor storage characteristics of single-pass large square corn stover bales in Iowa. *Energies*, 4(10), 1687-1695.
- Shinners, K. J., Binversie, B. N., Muck, R. E., & Weimer, P. (2007). Comparison of wet and dry corn stover harvest and storage. *Biomass & Bioenergy*, 31(4), 211-221
- Shinners, K. J., Boettcher, G. C., Muck, R. E., Weimer, P. J., & Casler, M. D. (2010). Harvest and storage of two perennial grasses as biomass feedstocks. *Transactions of the ASABE*, 53(2), 359-370.
- Shinners, K. J., Huenink, B. M., Muck, R. E., & Albrecht, K. A. (2009). Storage characteristics of large round and square alfalfa bales: low-moisture wrapped bales. *Transactions of the ASABE*, 52(2), 401-407.
- Shinners, K. J., Wepner, A. D., Muck, R. E., & Weimer, P. J. (2011). Aerobic and anaerobic storage of single-pass, chopped corn stover. *Bioenergy Research*, 4(1), 61-75.
- Singh, S., Cheng, G., Sathitsuksanoh, N., Wu, D., Varanasi, P., George, A., ... Simmons, B. A. (2015). Comparison of different biomass pretreatment techniques and their impact on chemistry and structure. *Frontiers in Energy Research*, 2(62), 1-12.
- Smith, W. A. (2015). [Biomass storage & harvesting project lead at Idaho National Laboratory].

- Smith, W. A., Bonner, I., Kenney, K. L., & Wendt, L. M. (2013). Practical considerations of moisture in baled biomass feedstocks. *Biofuels*, 4, 95-110.
- Tao, G. C., Lestander, T. A., Geladi, P., & Xiong, S. J. (2012). Biomass properties in association with plant species and assortments I: A synthesis based on literature data of energy properties. *Renewable & Sustainable Energy Reviews*, 16(5), 3481-3506.
- Templeton, D. W., Sluiter, A. D., Hayward, T. K., Hames, B. R., & Thomas, S. R. (2009). Assessing corn stover composition and sources of variability via NIRS. *Cellulose*, 16(4), 621-639.
- Tumuluru, J. S. (2014). Effect of process variables on the density and durability of the pellets made from high moisture corn stover. *Biosystems Engineering*, 119, 44-57.
- Tumuluru, J.S. (2015). High moisture corn stover pelleting in a flat die pellet mill fitted with a 6 mm die: physical properties and specific energy consumption. *Energy Science & Engineering*, 3 (4), 327-341.
- Tumuluru, J. S. (2016). Specific energy consumption and quality of wood pellets produced using high-moisture lodgepole pine grind in a flat die pellet mill. *Chemical Engineering Research and Design*, 110, 82-97.
- Tumuluru, J.S., Cafferty, K.G., & Kenney, K.L. (2014b). Techno-economic analysis of conventional, high moisture pelletization and briquetting process. American Society of Agricultural and Biological Engineer Annual Meeting, Paper No. 141911360, Montreal, Quebec Canada July 13 –16, doi: 10.13031/aim.20141911360, (2014).
- Tumuluru, J. S., Conner, C. C., & Hoover, A. N. (2016). Method to produce high durable pellets at lower energy consumption using high moisture corn stover and a corn starch binder in a flat die pellet mill. *Journal of Visualized Experiments (JoVE)*, In Press.
- Tumuluru, J. S., Dansie, T., Johnson, I., & Conner, C. C. (2015b). Specific energy consumption and quality of briquettes produced using woody and herbaceous biomass. Paper presented at the American Society of Agricultural and Biological Engineers Annual International Meeting, New Orleans Marriott, New Orleans, LA, USA.
- Tumuluru, J. S., Hess, J. R., Boardman, R. D., Wright, C. T., & Westover, T. L. (2012). Formulation, pretreatment, and densification options to improve biomass specifications for co-firing high percentages with coal. *Industrial Biotechnology*, 8(3), 113-132.
- Tumuluru, J. S., Igathinathane, C., Archer, D. W., & McCulloch, R. (2015a). Energy analysis and break-even distance for transportation for biofuels in comparison to fossil fuels. Paper presented at the American Society of Agricultural and Biological Engineers Annual International Meeting, New Orleans Marriott, New Orleans, LA, USA.
- Tumuluru, J. S., Sokhansanj, S., Hess, J. R., Wright, C. T., & Boardman, R. D. (2011b). A review on biomass torrefaction process and product properties for energy applications. *Industrial Biotechnology*, 7(5), 384-401.
- Tumuluru, J. S., Sokhansanj, S., Lim, C. J., Bi, T., Lau, A., Melin, S., ... & Oveisi, E. (2010). Quality of wood pellets produced in british columbia for export. *Applied Engineering in Agriculture*, 26(6), 1013-1020.
- Tumuluru, J. S., Tabil, L. G., Song, Y., Iroba, K. L., & Meda, V. (2014a). Grinding energy and physical properties of chopped and hammer-milled barley, wheat, oat, and canola straws. *Biomass & Bioenergy*, 60, 58-67.
- Tumuluru, J. S., Tabil, L. G., Song, Y., Iroba, K. L., & Meda, V. (2015c). Impact of process conditions on the density and durability of wheat, oat, canola, and barley straw briquettes. *Bioenergy Research*, 8(1), 388-401.

- Tumuluru, J. S., Wright, C. T., Hess, J. R., & Kenney, K. L. (2011a). A review of biomass densification systems to develop uniform feedstock commodities for bioenergy application. *Biofuels Bioproducts & Biorefining-Biofpr*, 5(6), 683-707.
- van Walsum, G. P., Allen, S. G., Spencer, M. J., Laser, M. S., Antal, M. J., & Lynd, L. R. (1996). Conversion of lignocellulosics pretreated with liquid hot water to ethanol. *Applied Biochemistry and Biotechnology*, 57-8, 157-170.
- Weiss, N. D., Farmer, J. D., & Schell, D. J. (2010). Impact of corn stover composition on hemicellulose conversion during dilute acid pretreatment and enzymatic cellulose digestibility of the pretreated solids. *Bioresource Technology*, 101(2), 674-678.
- Wendt, L. (2015). [Principle scientist biomass storage project, Idaho National Laboratory].
- Wu, R. 2015. Development of kinetic models of biomass gasification. American Institute of Chemical Engineers 2015 Annual Meeting from www3.aiche.org/proceedings/Abstract.aspx?PaperID=432007.
- Yancey, N., Tumuluru, J. S., & Wright, C. (2013). Grinding and Densification Studies on Raw and Formulated Woody and Herbaceous Biomass Feedstocks. *Journal of Biobased Materials and Bioenergy*, 7(5), 549-558.
- Yang, Z., Sarkar, M., Kumar, A., Tumuluru, J. S., & Huhnke, R. L. (2014). Effects of torrefaction and densification on switchgrass pyrolysis products. *Bioresource Technology*, 174, 266-273.

Chapter 2

ANALYTICAL METHODS FOR BIOMASS CHARACTERIZATION DURING PRETREATMENT AND BIOCONVERSION*

*Yunqiao Pu^{1,2}, Xianzhi Meng³, Chang Geun Yoo^{1,2},
Mi Li^{1,2} and Arthur J. Ragauskas^{1,2,3,†}*

¹Biosciences Division, BioEnergy Science Center,
Oak Ridge National Laboratory, Oak Ridge, TN, US

²UT-ORNL Joint Institute for Biological Science,
Oak Ridge National Laboratory, Oak Ridge, TN, US

³Department of Chemical and Biomolecular Engineering
and Department of Forestry, Wildlife, and Fisheries,
University of Tennessee, Knoxville, TN, US

ABSTRACT

Lignocellulosic biomass has been introduced as a promising resource for alternative fuels and chemicals because of its abundance and complement for petroleum resources. Biomass is a complex biopolymer and its compositional and structural characteristics largely vary depending on its species as well as growth environments. Because of complexity and variety of biomass, understanding its physicochemical characteristics is a key for effective biomass utilization. Characterization of biomass does not only provide critical information of biomass during pretreatment and bioconversion, but also give valuable insights on how to utilize the biomass. For better understanding of biomass characteristics, good grasp and proper selection of analytical methods are necessary. This chapter introduces existing analytical approaches that are widely employed for biomass

* This manuscript has been authored by UT-Battelle, LLC, under Contract No. DE-AC05-00OR22725 with the U.S. Department of Energy. The United States Government retains and the publisher, by accepting the article for publication, acknowledges that the United States Government retains a non-exclusive, paid-up, irrevocable, world-wide license to publish or reproduce the published form of this manuscript, or allow others to do so, for United States Government purposes.

† Corresponding author address: Department of Chemical and Biomolecular Engineering & Department of Forestry, Wildlife, and Fisheries, University of Tennessee, Knoxville, TN, US. Email: aragausk@utk.edu.

characterization during biomass pretreatment and conversion process. Diverse analytical methods using Fourier transform infrared (FTIR) spectroscopy, gel permeation chromatography (GPC), and nuclear magnetic resonance (NMR) spectroscopy for biomass characterization are reviewed. In addition, biomass accessibility methods by analyzing surface properties of biomass are also highlighted in this chapter.

Keywords: biomass characterization, pretreatment, structures, accessibility, NMR

1. INTRODUCTION

The production of biofuels and biobased chemicals/materials from lignocellulosic biomass is a global research theme and has garnered extensive interest worldwide. The biological route to produce biofuels from lignocellulosic materials usually involves three steps: biomass pretreatment, enzymatic hydrolysis of pretreated biomass, and fermentation of simple sugars to biofuels (Ragauskas et al., 2006; Yang & Wyman, 2008). The purpose of pretreatment is to alter biomass structures thus reducing its recalcitrance which is an inherent property of biomass due to the structural complexity of plant cell walls (Pu, Hu, Huang, Davison, & Ragauskas, 2013; Pu, Hu, Huang, & Ragauskas, 2015). Extensive research on biomass characterization has been focused on the structural characteristics of biomass that influence recalcitrance. Equally important is to understand the effects of pretreatment on biomass properties changes as well as how such changes affect biomass-biocatalyst interactions during deconstruction by enzymes and microorganisms. Such knowledge will provide fundamental information that is required to develop efficient and cost-competitive pretreatment technologies, to improve effectiveness of biomass deconstruction using microorganism or enzyme complexes, and to engineer feedstocks with low recalcitrance and high productivity through genetic modification of cell wall biosynthesis pathways (Pu, Chen, Ziebell, Davison, & Ragauskas, 2009). These demand an array of efficient and informative analytical methods for biomass characterization. This chapter reviews analytical methods that are frequently employed for biomass characterization during biomass pretreatment and conversion process in a combination to yield a comprehensive picture of physical/chemical properties of biomass, such as compositional contents, accessibility, cellulose crystallinity/ultrastructure, cellulose and hemicellulose degree of polymerization, and lignin molecular weights and structures. The characterization of bulk biomass and isolated major structural components (i.e., cellulose, hemicellulose, and lignin) are highlighted. Specifically, application of Fourier transform infrared (FTIR) spectroscopy, gel permeation chromatography (GPC), and various solution/solid state nuclear magnetic resonance (NMR) spectroscopy techniques on characterization of structural and physicochemical properties of cellulose, hemicellulose and lignin are discussed.

2. CHARACTERIZATION OF BULK BIOMASS

2.1. Compositions

Lignocellulosic biomass mainly consists of cellulose, hemicellulose, lignin, pectin, ash and extractives. Depending on plant species and/or various treatments such as pretreatment,

enzymatic hydrolysis, and fermentation, the composition of these compounds varies. In particular, lignin content and major sugars (i.e., glucose, xylose, arabinose, galactose, and mannose) from carbohydrate fractions are mainly analyzed for elucidating the characteristics of raw biomass and residual solids after treatments. The compositional profiles of raw material and their changes during pretreatment and conversion process are basic and important characteristics of biomass, providing key information on mechanism of biomass recalcitrance, pretreatment efficiency, and enzymatic hydrolysis performance.

2.1.1. Sample Preparation

For keeping consistency of compositional analysis results, moisture content and particle size of biomass should be prepared in suitable ranges. The moisture content of biomass samples needs to be below 10% prior to any milling (Hames et al., 2008). Air-drying, drying in a convection oven (at 45°C), or freeze-drying is a suitable method for biomass drying. After drying, the particle size of dried biomass is controlled by various milling methods followed by sieving. Generally, the milled biomass between 20-mesh and 80-mesh is collected for compositional analysis. This is because the deviation to a smaller or larger particle size results in a bias in carbohydrate and lignin contents by excessive carbohydrate degradation or incomplete hydrolysis of polysaccharides (Hames et al., 2008). In addition, extractives, the non-structural components in the biomass, are usually removed prior to compositional analysis through solvent extraction. Depending on the plant species, a variety of solvents such as water, ethanol, dichloromethane, acetone or toluene-ethanol (2:1) mixture are used (Table 1) (Sluiter, Ruiz, Scarlata, Sluiter, & Templeton, 2005; Tappi, 2007a and 2007b). The residual solids after extraction step are dried again for carrying out compositional analysis.

Table 1. Solvent extraction methods for biomass (Sluiter et al., 2005; Tappi, 2007b)

Biomass	Solvent	Soluble extractives
Pine, oak, aspen, pulp	Ethanol-benzene, dichloromethane, acetone	Waxes, fats, resins, sterols, non-volatile hydrocarbons, low-molecular weight carbohydrates, salts, polyphenols, fatty acids and their ester, unsaponifiable substances
Corn stover, wheat straw, hybrid poplar, pine	Water-ethanol	Inorganic material, non-structural sugars, nitrogenous material, chlorophyll, waxes

2.1.2. Compositional Analysis

The extractive-free biomass sample is fractionated by a two-step acid hydrolysis for analyzing structural carbohydrates and lignin (Sluiter et al., 2008b). In the first step, biomass sample is hydrolyzed using 72% sulfuric acid at room temperature-30°C for ~1-2 h. For the second-step, the mixture is diluted to 4% concentration of sulfuric acid, and then hydrolyzed at 121°C using autoclave for 1 h. While carrying the second hydrolysis step, sugar standards including glucose, xylose, galactose, arabinose, and mannose are also prepared in 4% sulfuric acid and loaded in autoclave for correcting sugar degradation during the hydrolysis.

The hydrolysate and residual solids after two-step acid hydrolysis are separated by filtration. Sugar compositional analysis is carried out by using high performance liquid

chromatography (HPLC) or high performance anion exchange chromatography equipped with pulsed amperometric detection (HPAEC-PAD). HPAEC-PAD measurement enables well separation of sugar peaks for accurate quantification. Figure 1 shows a representative ion chromatogram for detection of arabinose, galactose, glucose, xylose, and mannose in biomass using HPAEC-PAD. A diluted NaOH (2.0 mM) solution was used as the mobile phase and fucose as an internal standard.

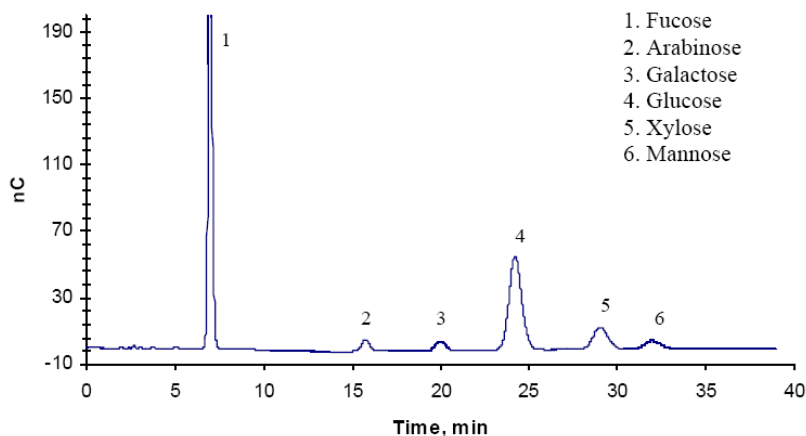


Figure 1. A representative ion chromatogram of sugar composition analysis using Dionex DX-500 ion chromatography. Flow rate: 1.0 ml/min; Column: CarboPac PA20 (Dionex Inc., USA).

The liquid fraction is also used for determining acid soluble lignin (ASL) content by using UV-Vis spectroscopy as well as acetyl content by using HPLC if necessary (Sluiter et al., 2008b). Different types of biomass need different wavelength and absorptivity constants for ASL measurement. Table 2 shows the absorptivity constants of ASL for selected biomass. The calculation of ASL with these constants is as below:

$$\% \text{ ASL} = \frac{UV_{\text{abs}} \times Vol_{\text{filtrate}} \times Dilution}{\varepsilon \times ODW_{\text{sample}} \times Pathlength} \times 100$$

where UV_{abs} is average UV-Vis absorbance for the sample at appropriate wavelength, Vol_{filtrate} is volume of filtrate (mL), ε is absorptivity of biomass at specific wavelength, and ODW_{sample} is oven dry weight of sample (mg). The path length of UV-Vis cell is usually 1 cm.

Table 2. Absorptivity and recommended wavelength for acid soluble lignin analysis (Sluiter et al., 2008b)

Biomass	Wavelength (nm)	Absorptivity (L/g cm)
Pine	240	12
Bagasse	240	25
Corn Stover	320	30
Poplar	240	25

The solid acid insoluble residue (AIR) fraction from the filtration is rinsed with deionized water, and then dried at 105°C until a constant weight. The dried residue is weighed and placed in a muffle furnace at 575°C for 24 h to obtain the insoluble ash. The Klason lignin content can be calculated as follows:

$$\% \text{ Klason} = \% \text{ AIR} - \% \text{ Ash}$$

Therefore, total lignin in the biomass is:

$$\% \text{ Lignin} = \% \text{ ASL} + \% \text{ Klason lignin}$$

Biomass usually contains certain amounts of moisture after subjecting to pretreatments. For an accurate analysis of biomass composition, it is important to know the exact biomass moisture content. Generally, the moisture content of Wiley-milled biomass samples (between 20-mesh and 80-mesh) can be measured by drying in a convection oven at 105°C or using a moisture analyzer (Hames et al., 2008; Sluiter et al., 2008a). The oven dry weight, which is the mathematically corrected biomass sample weight for moisture content, is used for calculation of biomass compositional analysis. Table 3 shows compositions of several hardwood, softwood, and grass biomass.

Table 3. Compositions (wt.%; dry basis) of various biomass (Li et al., 2010; Pan, Xie, Yu, Lam, & Saddler, 2007; Sannigrahi, Ragauskas, & Tuskan, 2010; Xu & Tschirner, 2011; Yoo et al., 2015)

Biomass	Glucan	Xylan	Galactan	Arabinan	Mannan	Lignin	Ash
Poplar	45.1	17.8	1.5	0.5	1.7	21.4	-
Corn stover	35.3	23.9	1.9	4.0	ND	19.9	-
Switchgrass	39.5	20.3	2.6	2.1	ND	2.18	4.1
Pine	45.4	6.3	2.0	1.3	11.8	25.1	0.3
Aspen	44.5	17.7	1.3	0.5	1.7	21.1	0.5

Note: ND: not detected; -: not reported.

2.2. FTIR Spectroscopic Analysis

Fourier transform infrared (FTIR) spectroscopy has been widely employed to perform qualitative and quantitative study of lignocellulosic biomass (Kačuráková & Wilson, 2001; Xu, Yu, Tesso, Dowell, & Wang, 2013). As a result of molecular vibration, a unique spectrum representing the adsorption and transmission is produced when IR radiation is passed through a sample. The main advantages of FTIR technology are non-destructive, simple sample preparation, fast analysis, and comprehensive analysis for multi-constituents. The infrared wavelength range is usually divided into three regions: near-infrared (12800-4000 cm⁻¹), mid-infrared (4000-400 cm⁻¹), and far-infrared (400-10 cm⁻¹). FTIR in the mid-infrared region is a preferred technique for functional group analysis and has the advantage of high throughput. There are two commonly used sampling tools: conventional transmission and attenuated total reflectance (ATR). In the transmission IR spectroscopy, the IR beam

passes through a sample and the effective path length is determined by the thickness of the sample and its orientation to the directional plane of the IR beam. In the ATR sampling, the IR beam hits onto a crystal of relatively higher refractive index and reflects. The reflective beam creates an evanescent wave which projects orthogonally into the sample in intimate contact with the ATR crystal.

FTIR can provide compositional and structural information of biomass through absorbance bands of functional groups. The characteristic functional groups detected in lignocellulosics are most likely consisted of hydroxyl (O–H), alkene (C=C), ester (–COO–), aromatics (Ar), ketone (C=O), and ether (C–O–C) etc. An exemplary FTIR spectrum of poplar is shown in Figure 2. The typical absorbance bands and assignments of functional groups in biomass are summarized in Table 4.

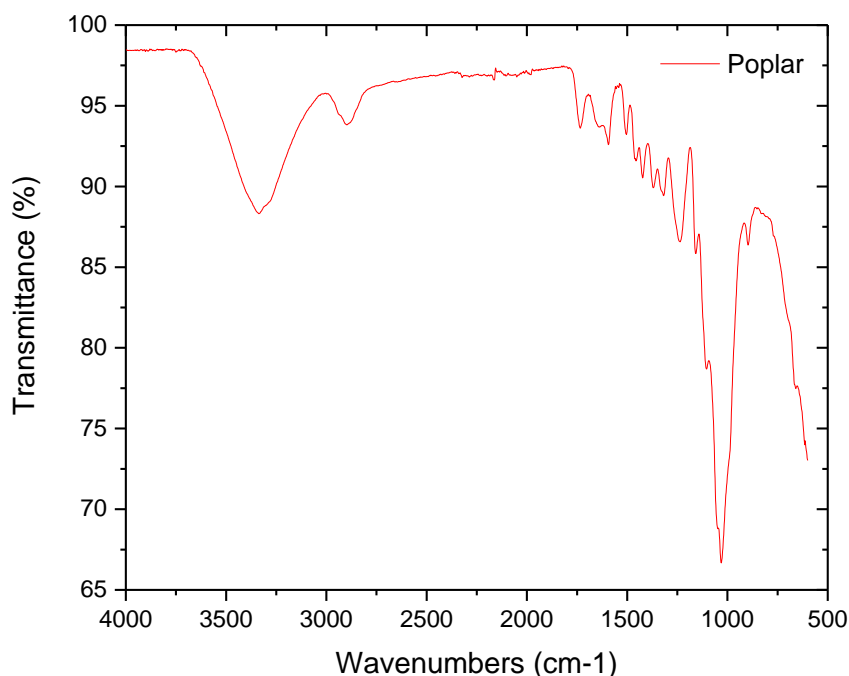


Figure 2. An exemplary FTIR spectrum of poplar.

FTIR spectroscopy has been used successfully for compositional analysis as well as structural analysis on a variety of biomass, including wood, wheat straw, sugar cane, barley, canola, oat, isolated hemicellulose, lignin, and cellulose (Ali, Emsley, Herman, & Heywood, 2001; Bilba & Ouensanga, 1996; Donohoe, Decker, Tucker, Himmel, & Vinzant, 2008; Pandey, 1999; Sun, Sun, Fowler, & Baird, 2005; Sun, Xu, Sun, Fowler, & Baird, 2005; Szymanska-Chargot, Chylinska, Kruk, & Zdunek, 2015; Tjeerdsma & Militz, 2005; Yang, Yan, Chen, Lee, & Zheng, 2007). Coupled with chemometric tools, FTIR spectroscopic techniques have been calibrated to predict chemical components of biomass such as lignin content in wood and straw, carbohydrates and extractives content in straw, protein and lipids in microbiological biomass, and pectin content in onion and rice (Pistorius, DeGrip, & Egorova-Zachernyuk, 2009; Raikila et al., 2007; Sene, McCann, Wilson, & Grinter, 1994;

Tamaki & Mazza, 2011). For example, Pandey investigated the structural difference of Klason lignin isolated from hardwood and softwood by comparing signal intensities of guaiacyl and syringyl units in FTIR (Pandey, 1999). FTIR has also been used for identification of cellulose type and determination of crystallinity index of cellulose (Oh et al., 2005). In addition, FTIR was employed to determine hemicellulose and lignin removal in steam explosion and alkaline peroxide pretreatment and compositional changes in wood decay (Pandey & Pitman, 2003; Sun et al., 2005). Gierlinger et al. developed an *in situ* FTIR technique coupled with microscopy to enhance the structural quantification of poplar wood on enzymatic treatment (Gierlinger et al., 2008).

Table 4. Absorbance bands and assignment in FTIR spectrum of lignocellulosic biomass. (Kubo & Kadla, 2005; Le Trodec et al., 2008; Pandey, 1999; Schwanninger, Rodrigues, Pereira, & Hinterstoisser, 2004; Sills & Gossett, 2012; Yang et al., 2007)

Wavenumber (cm ⁻¹)	Assignment	Compounds	Polymer
3600-3000	O–H stretching (hydrogen bonded)	Acid, alcohol	Lignin, cellulose, hemicellulose
2970-2860	C–H stretching	Alkyl, aliphatic, aromatic	Lignin, cellulose, hemicellulose
2850	CH ₂ symmetrical stretching	Alkyl	Wax
1750	–COO–	Free ester	Hemicellulose
1730-1700	C=O stretch (unconjugated)	Ketone, carbonyl	Lignin, hemicellulose
1650-1640	–OH	Water	Water
1632	C=C	Benzene ring	Lignin
1613-1600	C=C vibration with C=O stretching	Aromatic skeleton	Lignin
1560-1510	C=O stretching	Ketone, carbonyl	Hemicellulose
1505	C=C aromatic symmetrical stretching	Aromatic skeleton	Lignin
1470-1430	O–CH ₃	Methoxyl	Lignin
1425	C–H bending	Ar-H	Lignin
1380	C–H bending	C–H	Cellulose, hemicellulose, lignin
1232	C–O–C stretching	Aryl-alkyl ether	Lignin
1310-1218	C–O stretching	phenol	Lignin
1170-1160	C–O–C asymmetrical stretching	Pyranose ring	Cellulose, hemicellulose
1108	OH association	C-OH	Cellulose, hemicellulose
1060	C–O stretching and C–O deformation	alcohol	Cellulose, hemicellulose
1035	C–O, C=C, and C–C–O stretching	Ar, C–O	Cellulose, hemicellulose, lignin
996-985	C–O valence vibration	C–O	Cellulose
930, 875	C–O–C	Glycosidic linkage	Cellulose, hemicellulose
900-700	C–H out of plane vibration	Ar-H	Lignin
700-400	C–C stretching	C–C	Cellulose, hemicellulose

2.3. Whole Cell Wall NMR

Nuclear magnetic resonance (NMR) is one of robust analysis methods for plant cell walls. Diverse NMR analysis methods have been studied for biomass characterization usually with isolated components from cell walls (Mansfield, Kim, Lu, & Ralph, 2012). Kim and Ralph introduced a solution-state 2D NMR analysis with cell wall gels (Kim & Ralph, 2010). This method directly swells and gels cell wall materials in DMSO- d_6 in a NMR tube. The other solvent mixtures such as DMSO- d_6 /*N*-methylimidazole- d_6 (Yelle, Ralph, Lu, & Hammel, 2008) and DMSO- d_6 /[Hpyr]Cl- d_6 (Jiang, Pu, Samuel, & Ragauskas, 2009) are also applicable for cell wall dissolution. Whole cell wall dissolution does not include chemical derivatization like an acetylation; therefore, observation of “native” cell walls is available. In addition, information on acetylation in native cell walls can be detected by this method.

Sample preparation is an important step for whole cell wall NMR analysis. Non-structural components need to be removed from cell walls, because signals from these components hinder detection of signals from major cell wall components. In particular, biomass with high extractives and protein content should be treated for extractives and protein removal. In addition, a milling step is essential for dissolving biomass cell walls. Milling time varies depending on biomass species, particle size, biomass loading, and mill spinning speed. Biomass cell walls need to be sufficiently milled for successful cell wall dissolution, but excessive milling can cause degradation to some degree of cell wall components (Holtman, Chang, Jameel, & Kadla, 2006; Kim & Ralph, 2010). Table 5 shows examples of ball-milling time for different biomass samples.

Table 5. Ball-milling time for various biomass and their sample loading (Kim & Ralph, 2010)

Sample loading	Pine	Aspen	Corn & kenaf
100 mg	1 h 20 min	40 min	25 min
200 mg	2 h 20 min	1 h 10 min	45 min
300 mg	3 h 20 min	1 h 40 min	1 h 5 min
400 mg	4 h 20 min	2 h 10 min	1 h 25 min
500 mg	5 h 20 min	2 h 40 min	1 h 45 min
1 g	10 h 20 min	5 h 10 min	3 h 25 min
2 g	20 h 20 min	10 h 10 min	6 h 45 min

Note: Ball-milling was performed at 600 rpm with zirconium dioxide vessels (50 mL) containing ZrO₂ ball bearings (10 mm × 10).

Ball-milled cell wall materials are directly loaded into a NMR tube, and then distributed well in the horizontally positioned NMR tubes. DMSO- d_6 solvent mixture is then loaded into NMR tubes using a syringe and the NMR tubes are sonicated for ~1-5 h until formation of homogeneous gels in the tubes. Two-dimensional heteronuclear single quantum correlation (HSQC) NMR experiments are mostly used for characterizing structures of whole cell wall biomass. Figure 3 presents representative HSQC NMR spectra of whole cell wall aspen, poplar, and switchgrass.

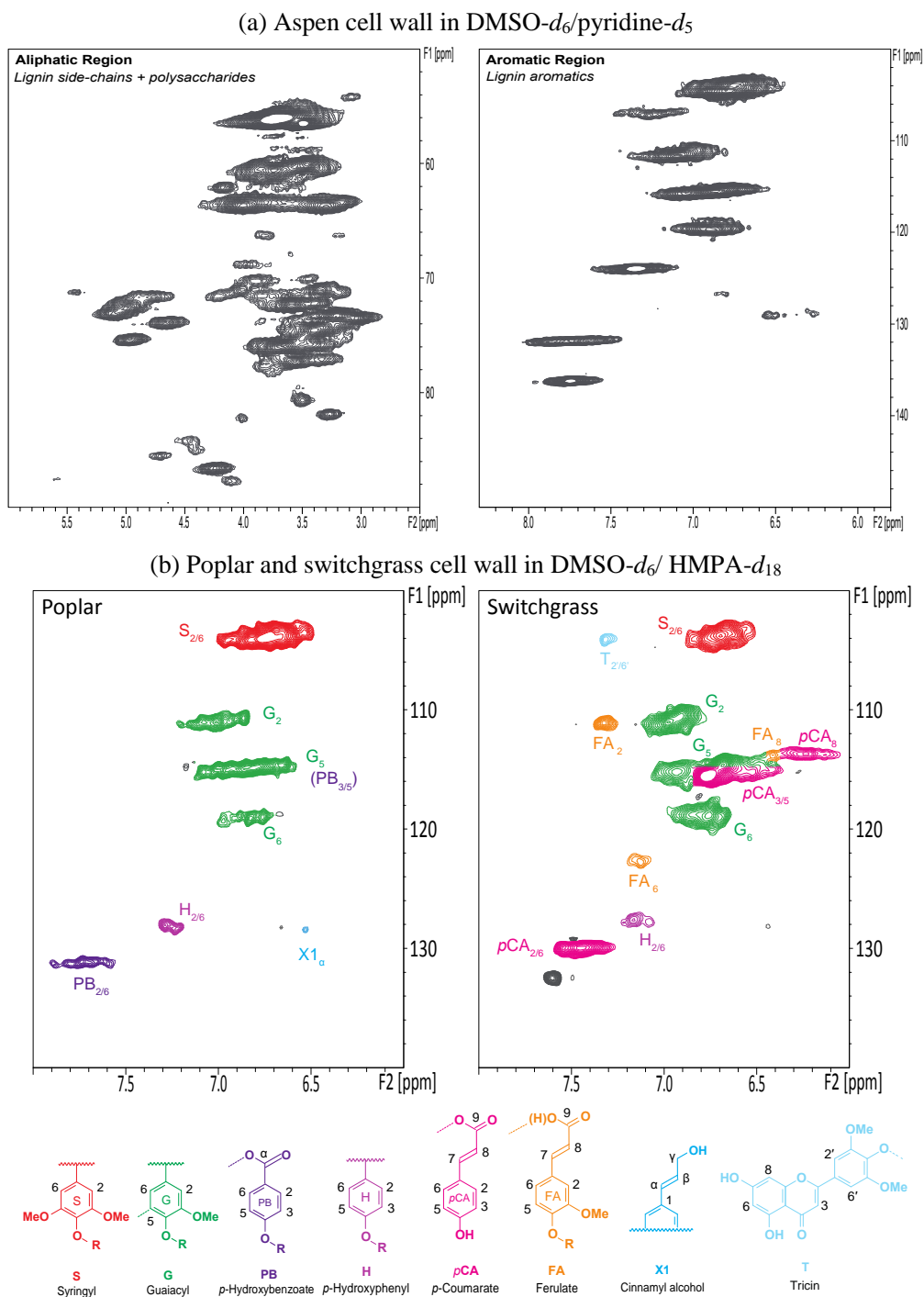


Figure 3. HSQC NMR spectra of (a) aspen cell wall in DMSO- d_6 /pyridine- d_5 (4:1); (b) poplar and switchgrass cell wall in DMSO- d_6 /HMPA- d_{18} (4:1).

Whole cell wall NMR analysis method can cover from raw biomass to process residues without chemical modification of materials and has been used to investigate the structural changes including linkage cleavages and compositional changes during bioconversion

processes. Various biomass samples have been analyzed by using the whole cell wall NMR methods. Kim and Ralph proposed the whole cell wall NMR method using DMSO- d_6 and DMSO- d_6 /pyridine- d_5 mixture with pine, aspen, kenaf, and corn stover (Kim & Ralph, 2010; Kim, Ralph, & Akiyama, 2008). Mansfield and his co-workers characterized whole plant cell wall of poplar, pine, corn stover, and Arabidopsis and compared this method with traditional cell wall composition analysis (Mansfield, Kim, Lu, & Ralph, 2012). Jiang and his co-workers conducted whole cell wall analysis with poplar and switchgrass by mixture of ionic liquid and DMSO- d_6 (Jiang et al., 2009). Cheng et al. characterized *Miscanthus* with DMSO- d_6 containing [Emim]OAc (Cheng, Sorek, Zimmermann, Wemmer, & Pauly, 2013). Recently, Yoo et al. proposed a new bi-solvent system composed of DMSO- d_6 and hexamethylphosphoramide (HMPA- d_{18}) for enhancing mobility of biomass samples and signals of NMR spectra with poplar, switchgrass, and Douglas fir (Yoo et al., 2016). In addition, the application of whole cell wall NMR methods has been expanded to the pretreated materials and/or residues after diverse conversion processes such as technical lignin and residual lignin (Samuel et al., 2011; Wen, Sun, Xue, & Sun, 2013; Yoo et al., 2015).

2.4. Biomass Accessibility Methods

Surface properties such as surface area and porosity are two important physical properties that could impact the quality and utility of biomass material during the process of converting biomass to biofuels (Hinkle, Ciesielski, Gruchalla, Munch, & Donohoe, 2015). To convert biomass to biofuels, depolymerization of cellulose is an essential step to produce simple sugars by applying biomass degrading enzymes on pretreated biomass. The intimate contact between cellulose and cellulase, such as *Trichoderma reesei* cellobiohydrolases (CBH I & CBH II) and endoglucanases (EGs), is the prerequisite step for efficient enzymatic hydrolysis, thus the surface area of cellulose plays a critical role in enzymatic hydrolysis yield and rate (Arantes & Saddler, 2010). Biomass surface area can be divided into exterior surface area which is governed by individual particle size, and interior surface area which is largely determined by size and number of fiber pores (Arantes & Saddler, 2011). Biomass material is anisotropic in spatial structure which induces difference in mechanical properties with various contents of cellulose, hemicellulose, and lignin (Guo, Chen, & Liu, 2012). Image analysis could be used to determine biomass particle size and shape and it has been found that the decrease of particle size normally leads to an increase of aspect ratio and exterior specific surface area. The interior surface area is essentially reflected by biomass porosity. Wang et al. reported that approximately over 90% of the substrate enzymatic digestibility is affected by the accessible pore surfaces (Wang et al., 2012).

There exist several scales of porosity in biomass including cell lumen, pits, and nanopores formed between coated micro fibrils (Davison, Parks, Davis, & Donohoe, 2013). The cell lumen represents the largest scale of biomass porosity with its size in the range of tens of micrometers. Pits are the regions where the secondary cell wall is absent and an open pore is maintained between adjacent cell lumen in plant cell walls. Neither of these types of pore represents a fundamental barrier to cellulolytic enzymes that typically have a nominal diameter of ~ 5.1 nm, and the fundamental barrier to effective enzymatic hydrolysis is obviously the accessibility of a reactive cellulose surface. Study on transport phenomena

suggests that pore size should be at least in the range of 50-100 nm to allow sufficient penetration of enzymes into cell walls (Davison et al., 2013). Unlike the exterior surface area, many researches have indicated a positive relationship between interior surface area/porosity and enzymatic hydrolysis rate (Luo & Zhu, 2011; Meng, Wells, Sun, Huang, & Ragauskas, 2015). Nevertheless, the accurate measurement of cellulose accessibility is the prerequisite step for understanding the role of cellulose accessibility in biomass recalcitrance. Considerable amounts of work have been done to develop promising analytical techniques that can be directly applied on biomass materials to measure its cellulose accessibility, and each technique has its own advantages and disadvantages (Meng & Ragauskas, 2014).

2.4.1. Nitrogen Adsorption Method

One of the classic techniques to measure the specific surface area is the Brunauer-Emmett-Teller (BET) method using gas adsorption. Inert gas, mostly nitrogen, could be adsorbed on the outer surface of solid material and also on the surface of pores in case of porous material such as biomass. Adsorption of nitrogen at a temperature of 77 K can lead to the so-called adsorption isotherm which also refers to the BET isotherm. The typical nitrogen adsorption instrument consists of an adsorption cell to hold the material, a gas burette, a manometer, and a pumping system (Loebenstein & Deitz, 1951). Accordingly, samples are dried, degassed, and then cooled in the presence of nitrogen gas allowing nitrogen gas to condense on the surfaces and within the pores. The quantity of gas adsorbed can be then determined from the pressure decrease after the sample was exposed to gas, and the specific surface area is calculated using BET model that relates the gas pressure to the volume of gas adsorbed. Table 6 shows the BET specific surface area of lignocellulosic materials before and after pretreatment as determined by nitrogen adsorption. The results demonstrated that all different pretreatments increased the BET surface area and as the pretreatment severity factor increased, so did the specific surface area. On the one hand, nitrogen can pass readily through plant cell walls and its uptake provides a quick and robust method for determination of the surface area accessible to nitrogen. On the other hand, this measurement requires a prior drying of the substrate which makes it typically less effective due to the partial irreversible collapse of pores (Meng & Ragauskas, 2014). In addition, the small size of nitrogen molecules compared to cellulase enzymes could cause over-estimation in terms of cellulose accessibility to cellulase (CAC) measurement.

Table 6. Summary of BET surface area of untreated and pretreated lignocellulosic materials

Samples	BET surface area (m ² /g)	Refs
Untreated spruce	0.4	(Wiman et al., 2012)
2% SO ₂ pretreated spruce at 194°C, 7 min	1.3	
2% SO ₂ pretreated spruce at 220°C, 7 min	8.2	
Untreated corn stover	8.5	(Li, Zhao, Qu, & Lu, 2014)
Hot water pretreated corn stover at 190°C, 20 min	17.1	
Untreated switchgrass	0.5	(Dougherty et al., 2014)
Dilute acid pretreated switchgrass at 160°C, 20 min	0.8	
Ionic liquid pretreated switchgrass at 120°C, 240 min	3.2	

2.4.2. Solute Exclusion Method

The solute exclusion technique is based on the accessibility of probe molecules to the substrate pores of different sizes (Rolleri, Burgos, Bravo-Linares, Vasquez, & Droppelmann, 2014). A known concentration of a solution containing the probe solute molecule is added to the swollen substrate, causing possible dilution of the solution by the water contained in the initial substrate. If all the pores in the substrate are accessible to the solute molecules after thorough mixing, then all the water from the initial substrate can contribute to the dilution process, while the water presented in the pores that is not accessible to the probe molecules will not contribute to the dilution. As a result, the substrate pore size and volume distribution can be determined using the concentration of the probe molecule in the final substrate mixture. The typical solute molecules used in solute exclusion include polyethylene glycol and dextran which are not adsorbed on nor chemically react with lignocellulosic substrate. The concentration of these probe molecules can be measured by HPLC with a refractive index detector or thermoporometry methods using differential scanning calorimetry (DSC) and ^1H NMR (Stone & Scallan, 1965; Grethlein, 1985; Ishizawa, Davis, Schell, & Johnson, 2007). To assess the cellulose accessibility to cellulase, 5.1 nm is normally selected as the cutoff for the pore size for which cellulase can transverse to access the interior surface (Huang, Su, Qi, & He, 2010). The accuracy of the solute exclusion technique for pore size or volume measurements is based on several assumptions: (1) the concentration of the probe molecules in the accessible pores is equal to that in the solution surrounding the porous materials and (2) complete penetration of probe molecules into the pores should occur when the diameter of the probe molecule is less than the diameter of the pores into which it will diffuse (Lin, Ladisch, Voloch, Patterson, & Noller, 1985). Table 7 presents exemplary data on the accessible surface area to the 5.1 nm molecular probes of biomass after various pretreatment, indicating that pretreatments result in a higher accessible interior surface area. Compared to nitrogen adsorption technique, one of the advantages for this technique is that the measurement can be directly performed quantitatively in wet state of biomass. There are some limitations to this method as well. It is laborious, unspecific to cellulose, and cannot account for the external surface area. Ink-bottle effect and osmotic pressure were also reported to affect the determination of pore size distribution when using the solute exclusion method (Beecher, Hunt, & Zhu, 2009).

Table 7. Accessible interior surface area of untreated and pretreated lignocellulosic materials

Samples	Accessible surface area available to solute of 5.1 nm (m^2/g)	Refs
Untreated mixed hardwood	14.8	(Grethlein, 1985)
Hydrogen peroxide pretreated mixed hardwood	24.5	
Ethylenediamine pretreated mixed hardwood	30.7	
Untreated corn cob	51.2	(Huang et al., 2010)
Sulfuric acid pretreated corn cob	55.2	
Lime pretreated corn cob	93.4	
Sodium hydroxide pretreated corn cob	104.0	

2.4.3. Simons' Stain Method

An alternative approach to examine pore size is to employ direct dyes such as Simons' stain (SS) to estimate the total available surface area of lignocellulosic substrates as a semi-quantitative method (Chandra, Ewanick, Hsieh, & Saddler, 2008). It evaluates the large-to-small pore ratio of a substrate by applying two different dyes: Direct Blue 1 and Direct Orange 15. Dyes are well known as sensitive probes for characterization of cellulose structure, and direct dyes are particularly appropriate because of their linear structures and outstanding substantivity toward cellulose (Inglesby & Zeronian, 2002). Direct Blue 1 has a well-defined chemical formula $C_{34}H_{24}N_6Na_4O_{16}S_4$ with a molecular diameter of ~ 1 nm. Direct Orange 15 is a condensation product of 5-nitro-o-toluenesulfonic acid in aqueous alkali solution with a diameter in the range of ~ 5 -36 nm, and it also has much higher binding affinity for hydroxyl groups on a cellulosic surface compared to Direct Blue dye (Meng et al., 2013). When lignocellulosic biomass is treated with a mixed solution of the direct orange and blue dyes, the blue dye enters all the pores with a diameter larger than ~ 1 nm, while the orange dye only populates the larger pores. After a pore size increase either by physical or chemical action, the orange dye will gain further access to the enlarged pores because of the higher affinity of orange dye for the hydroxyl groups on a cellulosic surface. Therefore, the ratio of adsorption capacity between the Direct Orange 15 and Direct Blue 1 dyes can be calculated as a measure of large-to-small pore ratio of a substrate.

It has been reported that the use of Orange/Blue (O/B) ratio as a molecular probe is a good indicator of the total surface area of cellulose available to enzymes (Chandra et al., 2008). Others reported that the higher the O/B ratio, the lower the protein loading required for the efficient hydrolysis (Arantes & Saddler, 2010). Table 8 presents the cellulose accessibility of untreated and pretreated lignocellulosic substrates as determined by the O/B ratio in Simons' stain. Although the O/B ratio has been related to the cellulose accessibility and cellulase activity, large amounts of the smaller Direct Blue dye adsorbed by a substrate can cause a decrease of the overall O/B ratio. In this case, even when there may be a significant amount of large pore and cellulose accessibility, the analysis based solely on the low O/B ratio may skew data interpretation. In addition, the method is not considered fully quantitative and the measurement is also significantly affected by pore shapes and tortuosity. Despite the shortcomings of Simons' stain technique, it provides a relatively fast, simple and sensitive method for the measurement of exterior and interior accessible surface area and relative porosity of lignocellulosic substrate in its wet state.

Table 8. Cellulose accessibility of untreated and pretreated lignocellulosic biomass as determined by Simons' stain

Samples	Orange/Blue (O/B) ratio	Refs
Untreated poplar	0.19	(Meng et al., 2013)
Steam explosion pretreated poplar	0.25	
Dilute acid pretreated poplar	0.39	
Untreated switchgrass	0.08	(Keshwani & Cheng, 2010)
Lime pretreated switchgrass	0.26	
Sodium hydroxide pretreated switchgrass	0.39	

2.4.4. NMR Cryoporometry Method

NMR cryoporometry has also been used for pore size distribution measurements through observation of melting point of a confined liquid in biomass non-destructively. The method is based on the principle that small crystals formed from liquid within pores melt at a lower temperature than bulk liquid. The melting point depression of liquid that confined within a pore can be related to the pore size through the Gibbs-Thompson equation (Strange, Rahman, & Smith, 1993):

$$\Delta T = T_m - T_m(x) = k/x$$

where T_m is the normal melting point, $T_m(x)$ is the melting point of a crystal in pores of diameter x , and k is a characteristic constant of the liquid. The pore volume v is a function of pore diameter x , so the melting temperature of the liquid $T_m(x)$ can be related to the pore size distribution by the formula below:

$$\frac{dv}{dx} = \frac{dv}{dT_m(x)} \frac{dT_m(x)}{dx}$$

From Gibbs-Thompson equation, $dT_m(x)/dx = k/x^2$, so the pore size distribution can be written as:

$$\frac{dv}{dx} = \frac{dv}{dT_m(x)} \frac{k}{x^2}$$

Accordingly, liquid probe such as water is imbibed into a porous lignocellulosic substrate, and the sample is cooled until all the liquid is frozen and then slowly warmed up. A CPMG NMR sequence is used to measure the quantity of the liquid that has melted due to the fact that the coherent transverse nuclear spin magnetization decays much more rapidly in a solid than that in a mobile liquid. As a result, the NMR cryoporometry data collected contains liquid proton signal intensity proportional to the integral pore volume v which varies as a function of temperature T . At each temperature, v is the volume of liquid in cell wall pores with a dimension less than or equal to x . So the measurement of $dv/dT_m(x)$ which can be obtained from the slope of the curve of v against T will allow the pore size distribution curve to be determined (Meng et al., 2013). The pore size distribution gives information about the incremental volume of the pores at a particular pore diameter. Pore size distributions obtained with NMR cryoporometry have been shown to compare favorably with other methods such as gas adsorption (Mitchell, Webber, & Strange, 2008).

Using NMR cryoporometry, Ostlund et al. revealed the decrease in porosity within the fiber cell wall of bleached softwood Kraft pulp that was exposed to a series of drying procedures, suggesting drying the pulp at 105°C decreases the pore volume to 55% of the never-dried pulp (Ostlund, Kohnke, Nordasierna, & Nyden, 2010). Meng et al. estimated the representative pore diameter roughly from the peak maximums in the pore size distribution curve for untreated and dilute acid pretreated poplar (Meng et al., 2013). The positions of the main peaks attributed to meso-scale pores for untreated, 10 min steam explosion pretreated,

10 min dilute acid pretreated, and 60 min dilute acid pretreated poplar were at 1.5 nm, 3 nm, 6 nm, and 9 nm, respectively. NMR cryoporometry was also successfully applied on water swollen flax and cotton fibers, suggesting that swelling substantially increases the pore volume by a factor of 20-30 of fibers in the mesoporous region with 1 to 10 nm (Mikhalovsky et al., 2012). DSC thermoporosimetry follows the same principal as the NMR cryoporometry, except that the actual melting point instead of the amount of water that melts at a certain temperature is recorded (Ponni, Vuorinen, & Kontturi, 2012). Park et al. characterized the surface and pore structure of cellulose fibers during enzymatic hydrolysis via DSC thermoporosimetry (Park et al., 2006). Their results showed that the concentration of large pores decreased more than that of small pores through the cellulase treatment.

2.4.5. NMR Relaxometry

Like NMR cryoporometry, there are other NMR based techniques which can be used to track changes in cellulose accessibility of biomass, such as proton NMR relaxometry. Fluid molecules such as water confined into pores are usually subjected to interactions that can change NMR relaxation times of the fluid materials. Therefore, information about the pore size distribution of the material can be obtained through determining the relaxation time distribution. In terms of lignocellulosic biomass, adsorbed water has been found spatially localized on and within cellulosic micro fibrils, existing as capillary water in a lumen, or between fibers and within the lignin-hemicellulose matrix (Menon et al., 1987). The nature and strength of the association between water and cell walls is directly related to the ultrastructural and chemical state of the biomass, making it possible to study the changes in biomass pore surface area to volume ratio by monitoring the amount and the relative nature of nuclear relaxation of the adsorbed water.

Spin-spin relaxation, also known as T_2 relaxation, is the mechanism by which the transverse component of the magnetization vector exponentially decays towards its equilibrium value in NMR. Biomass with a more hydrophilic pore surface or reduced pore size distribution will contain a higher proportion of bound to unbound water. In a T_2 relaxation curve, the signal intensity decays as a function of local inhomogeneity in the magnetic field mainly due to perturbation by nuclei through space or dipolar interactions (Araujo, Mackay, Whittall, & Hailey, 1993). Basically, as the T_2 relaxation time of adsorbed water increase, the degrees of freedom or average local mobility of the water in pores also increases. Similarly, an increase in T_2 relaxation time of adsorbed water can be correlated with a decrease in the proportion of bound to unbound water or amount of water located at the pore surface versus pore interior. Therefore, in systems of increasing average pore size, the pore surface area to volume ratio will decrease and is therefore detected by an increase in the T_2 relaxation time.

NMR relaxometry has been used to characterize pore size or surface area of various lignocellulosic materials including native biomass, pretreated biomass, and enzymatic hydrolyzed cellulose (Felby, Thygesen, Kristensen, Jorgensen, & Elder, 2008; Menon et al., 1987). Foston and Ragauskas studied the changes in the structure of cellulose fiber walls during dilute acid pretreatment in *Populus* by generating the Inverse Laplace distributions on T_2 decays, and the results demonstrated not only a shift in T_2 times to longer relaxation or a more mobile state but also indicated that the population of water with longer relaxation times increased after pretreatment (Foston & Ragauskas, 2010). This suggests that the dilute acid pretreatment breaks down and loosens the cellulosic ultrastructure within biomass. Karuna et

al. studied the impact of alkali pretreatment on the surface properties of rice straw affecting cellulose accessibility to cellulases by NMR relaxometry. The spin-spin relaxation times of the samples indicated increased porosity in alkali pretreated rice straw (Karuna et al., 2014). Felby et al. studied the cellulose-water interactions during enzymatic hydrolysis of filter paper by determining the T_2 distributions via time domain NMR, suggesting the action of enzyme system is a breakdown and loosening of the cellulose therefore introducing more water into the structure and providing better access for the enzymes during the initial enzymatic hydrolysis of cellulose (Felby et al., 2008). However, the NMR relaxometry technique is usually expensive, and requires complicated setup and long experiment time.

2.4.6. Mercury Porosimetry Method

This technique provides a wide range of information including pore size distribution, total porosity, apparent density, and specific surface area (Giesche, 2006). The non-wetting property of mercury combined with its high surface tension uniquely qualifies mercury for use in probing pore space. Unlike water, mercury cannot penetrate pores by capillary action spontaneously, therefore an external pressure needs to be applied to force it into the pores. The external pressure can be related to the pore size according Washburn equation:

$$D = -4\gamma\cos\theta/P$$

where D is the pore diameter, γ is the surface tension of mercury, θ is the contact angle, and P is the external pressure. The inverse relationship between the pore diameter and pressure indicate that only slight pressure is required to intrude mercury into large macro pores, whereas much larger pressures are required to force mercury into small pores. Therefore, the volume of pores in the corresponding size can be determined by measuring the volume of mercury which intrudes into the porous material with each pressure change. Because mercury porosimetry requires a prior drying of samples, organic solvent exchange drying is normally applied on samples to avoid unnecessary pore collapse (Foston & Ragauskas, 2010). In this manner, water can be removed from biomass step by step, preserving the maximally swollen pore structure of the biomass samples in an absolutely dry state.

Using mercury porosimetry, Meng et al. reported the total area, average pore diameter, and pore tortuosity of untreated, hot water, dilute acid, and alkaline pretreated poplar (Meng et al., 2015). The results showed that dilute acid pretreatment had the largest pore area among these three pretreatments. In addition, both hot water and alkaline pretreatments were found to slightly increase the average pore diameter, while the severe dilute acid pretreatment significantly decreased the average diameter. The average pore diameter was observed to decrease by 90% after 60 min of 160°C dilute acid pretreatment as compared to untreated poplar.

3. CHARACTERIZATION OF ISOLATED MAJOR COMPONENTS

3.1. Cellulose Analysis

Cellulose, consisting of approximately 40-50% of the total feedstock dry matter, is a linear glucose polymer linked by β -1,4 glycosidic bonds with cellobiose as its repeating unit.

Cellulose chain has a strong tendency to form inter and intra-molecular hydrogen bonds by hydroxyl groups on these linear cellulose chains, which stiffen the chains and promote aggregation into a crystalline structure (Sannigrahi et al., 2010). Degree of polymerization (DP) and crystallinity are two important structural properties of cellulose that may affect its digestibility. It is generally believed that amorphous cellulose should be hydrolyzed at a much faster rate than crystalline cellulose, indicating the initial degree of crystallinity of cellulose might play a major role as a rate determinant in hydrolysis reaction (Zhang & Lynd, 2004). It is also reported that cellulose crystallinity could affect the ability of cellulase enzyme modules to adsorb or function on cellulose, and the maximum adsorption constant has been shown to be greatly enhanced at low crystallinity index (Lee, Shin, Ryu, & Mandels, 1982). Cellulose chain length could also affect the solubility of cellulose in a given solvent, the mechanical properties of composite materials, and the efficiency of enzymatic hydrolysis of biomass (Yang, Dai, Ding, & Wyman, 2011). Hence, it is important to measure the cellulose DP and crystallinity during biomass conversion process.

3.1.1. Degree of Polymerization

Cellulose DP can be measured by various analytical techniques including viscometer and gel permeation chromatography (GPC). Determination of cellulose DP via viscometer after nitration was developed in early 1940s, in which lignocellulosic biomass was treated with nitric acid, phosphoric acid, and phosphorous pentoxide in a ratio of 64:26:10 at 17°C for 40 h, resulting in the formation of cellulose nitrates that can be subsequently solubilized in ethyl acetate or acetone (Timell, 1955). Although this technique has the advantage of eliminating pre-isolation of cellulose through holocellulose pulping and base catalyzed hydrolysis of hemicellulose, it is rarely used nowadays due to the uncertainty arising from possible change of cellulose chain during derivatization as well as the instability of the derivative (Hallac & Ragauskas, 2011).

GPC is another technique that can be used to measure cellulose DP and it also involves cellulose derivatization known as cellulose tricarbanilate. The derivatization of cellulose starts with the isolation of cellulose, including two steps: delignification of extractive-free material to generate holocellulose by oxidative degradation of lignin, followed by an alkaline extraction to remove hemicellulose. One of the conventional delignification methods to selectively remove lignin from biomass with only limited amount of glucan and xylan being solubilized is treating samples with glacial acetic acid and sodium chlorite (Hubbell & Ragauskas, 2010). However, the addition of acetic acid might increase the likelihood of chain degradation. Kumar et al. reported nearly 75% in the average DP of filter paper remained after delignification using acid-chlorite (Kumar, Mago, Balan, & Wyman, 2009). Hubbell and Ragauskas reported that the introduction of even a small portion of lignin to the system instead of completely removing lignin greatly reduced the negative DP effect (Hubbell & Ragauskas, 2010). To address this issue, several delignification methods were compared for their selectivity and impacts on physiochemical characteristics of cellulosic biomass in a recent study. The results showed that delignification using peracetic acid at room temperature is much more selective than the traditional chlorite-acetic acid method, and more importantly, has less severe impacts on cellulose DP (Kumar, Hu, Hubbell, Ragauskas, & Wyman, 2013). Once cellulose is isolated from lignin-hemicellulose matrix, derivatization of cellulose is usually performed by reaction of cellulose with phenyl isocyanate in pyridine. Typically, ~4.00 mL of anhydrous pyridine and 0.5 mL of phenyl isocyanate is added to ~15 mg of dried

cellulose samples, and the reaction mixture is kept at $\sim 66^\circ\text{C}$ with stirring until the cellulose is completely dissolved. It should be noted that the temperature needs to be kept lower than 70°C thus avoiding cellulose degradation. Afterwards, methanol is added to the reaction to eliminate the unreacted phenyl isocyanate, and the mixture is then poured into a water-methanol mixture to precipitate the cellulose tricarbanilate which can then be analyzed by GPC for its molecular weight.

3.1.2. Crystallinity and Ultrastructure

Cellulose crystallinity index (CrI) can be used to describe the relative amount of crystalline portion in cellulose, and can be typically measured using several analytical techniques including X-ray diffraction (XRD), Infrared (IR) spectroscopy, and solid-state ^{13}C NMR. XRD can provide strong signals from the crystalline fraction of cellulose, and the CrI is usually defined as (Segal, Creely, Martin, & Conard, 1959)

$$\text{CrI} = [(I_{002} - I_{\text{amorphous}})/I_{002}] \times 100$$

where I_{002} is the diffraction intensity at 002 peak position at $2\theta = 22.5^\circ$ and $I_{\text{amorphous}}$ is the scattering intensity of amorphous region at $2\theta = 18.7^\circ$. The non-crystalline part of cellulose is represented by broader and less clearly refined features in the XRD pattern, leading to challenges in evaluation of signals for a quantitative crystallinity measurement. In addition, information about cellulose crystallinity can be also obtained by FTIR spectroscopy, which gives only relative values of crystallinity. The ratio of amorphous to crystalline cellulose usually associates with the ratio of intensities of the bands at 900 cm^{-1} and 1098 cm^{-1} in FTIR spectra (Stewart, Wilson, Hendra, & Morrison, 1995).

Another promising method to analyze ultrastructural features of cellulose is the ^{13}C cross polarization magic angle spinning (CP/MAS) NMR spectroscopy. In CP/MAS ^{13}C NMR, CrI is defined as (Newman, 2004):

$$\text{CrI} = [A_{86-92\text{ppm}}/(A_{79-86\text{ppm}} + A_{86-92\text{ppm}})] \times 100$$

where $A_{86-92\text{ppm}}$ represents the area of crystalline C_4 signal, $A_{79-86\text{ppm}}$ is the area of amorphous C_4 signal. Similar to other biological materials, the NMR spectra of cellulose contains multiple broad and overlapping peaks. To address this problem, a least-squared model and spectra fitting method was proposed to quantitatively estimate the relative fraction of ultrastructural components, including crystalline cellulose (i.e., cellulose I_α and I_β), paracrystalline cellulose, and amorphous domain of accessible or inaccessible fibril surfaces (Foston, Hubbell, & Ragauskas, 2011). Figure 4 shows a non-linear least-squared line fitting of the C_4 region for a ^{13}C CP/MAS spectrum of isolated cellulose, with the peak assignments of signals presented in Table 9. Lorentzian line shapes were applied to the carbon signals attributed to the domain of cellulose I_α , I_β , $\text{I}_{\alpha+\beta}$, while Gaussian lines were used to describe the signals from inaccessible and accessible fibril surfaces comprising the amorphous domains (Foston & Ragauskas, 2010).

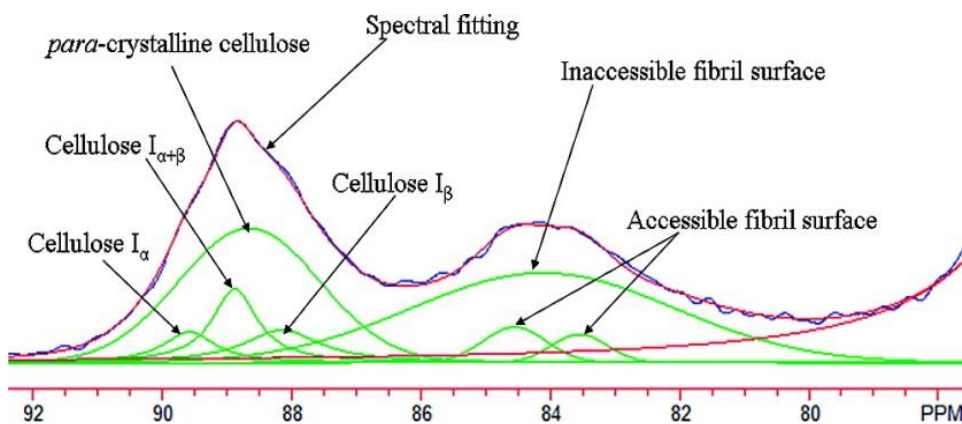


Figure 4. Spectra fitting for the C₄ region of the CP/MAS ¹³C NMR spectrum of cellulose (Hallac et al., 2009).

Table 10 lists the relative contents of amorphous, para-crystalline, and crystalline portion of cellulose isolated from *Populus*, *Buddleja Davidii*, and switchgrass. Para-crystalline cellulose is the largest fraction observed for *Populus*, while inaccessible fibril surface of cellulose is the largest fraction observed for *Buddleja Davidii* and switchgrass. *Populus* is composed of relatively higher crystallinity (~63%) and accessible fibril surface (~10.2%) as compared to switchgrass and *Buddleja Davidii*.

Table 9. Assignments of signals in the C-4 region of the CP/MAS ¹³C NMR spectrum (Foston, Hubbell, Davis, & Ragauskas, 2009)

Assignment	Chemical shift (ppm)	Intensity (%)	Line type
Cellulose I _α	89.6	4.2	Lorentz
Cellulose I _{α+β}	88.9	8.7	Lorentz
Para-crystalline cellulose	88.7	32.9	Gauss
Cellulose I _β	88.2	6.5	Lorentz
Accessible fibril surface	84.6	3.9	Gauss
Inaccessible fibril surface	84.1	41.1	Gauss
Accessible fibril surface	83.6	2.7	Gauss

Table 10. Crystallinity index and line fitting results of cellulose by CP/MAS ¹³C NMR

Biomass feedstock	CrI	I _α	I _{α+β}	I _β	Para-crystalline	Accessible fibril surface	Inaccessible fibril surface	Refs
<i>Populus</i>	63	5.0	14.2	19.8	31.1	10.2	18.3	(Foston et al., 2009)
<i>Buddleja Davidii</i>	55	4.2	8.7	6.5	32.9	6.6	41.1	(Foston et al., 2009)
Switchgrass	44	2.3	8.0	4.8	27.3	6.2	51.3	(Samuel, Pu, Foston, & Ragauskas, 2010)

Besides FTIR and NMR spectroscopy, Raman spectroscopy could be also used for the assessment of structural differences in celluloses of various origins (Szymanska-Chargot, Cybulska, & Zdunek, 2011). Cellulose I crystallinity can be calculated based on the Raman band intensity ratio of 378 and 1096 cm^{-1} using an FT-Raman spectroscopy (Agarwal, Reiner, & Ralph, 2007). In addition, cellulose polymorphic modifications I and II as well as amorphous structure can be also identified. Schenzel and Fischer investigated cellulose I and II using FT-Raman experiments, confirming the difference in the conformational arrangements. The authors reported that simultaneous presence of two stereo chemically non-equivalent CH_2OH groups was observed in cellulose I resulting from the rotation of side chains about C(5)-C(6) atoms, while there was only one type of CH_2OH groups present in cellulose II (Schenzel & Fischer, 2004).

3.2. Hemicellulose Analysis

Hemicelluloses are heterogeneous polysaccharides, representing generally 15-35% of plant biomass. Hemicellulose in biomass may contain pentoses (xylose, arabinose, rhamnose), hexoses (mannose, glucose, galactose, fucose), uronic acids (glucuronic and galacturonic acids), and acetyl substitutes (Gírio et al., 2010; Sun, Fang, Tomkinson, Geng, & Liu, 2001). Prior to hemicellulose extraction, the Wiley milled and dried biomass is extracted with solvents to remove wax and lipids, and the dewaxed biomass is further delignified by sodium chloride or peracetic acid to obtain holopulp. Hemicellulose is usually extracted from biomass holopulp with high alkali (e.g., 2-17.5% sodium hydroxide or potassium hydroxide) at room temperature (Cao, Pu, Studer, Wyman, & Ragauskas, 2012; Kumar et al., 2013). The hemicellulose is obtained by precipitation of the alkali extracts in ethanol (75%, v/v) followed by washing with additional ethanol (75%, v/v). The characteristics of hemicellulose that are general required to assess are listed in Table 11.

Table 11. Hemicellulose characteristics and the characterization techniques

Samples	Techniques
Chemical compositions	HPLC
Molecular weights distribution	GPC
Functional groups	FTIR
Structures and linkages	NMR

3.2.1. Chemical Compositions

The chemical compositions such as xylose, mannose, glucose, arabinose, galactose, uronic acids, and acetyl groups of hemicelluloses can be analyzed following a modified two-step acid hydrolysis (Sluiter et al., 2008b). The isolated hemicellulose is soaked first in 72% sulfuric acid at 45°C for 7 min and is followed by hydrolysis in ~ 3% sulfuric acid at 121°C for another 30 min. The concentrations of monomeric sugars in the soluble fraction can be determined by HPLC or an ion chromatography. Uronic acids can be quantified either by the sulfuric acid-carbazole procedure or gas chromatography after derivatization (Filisetti-Cozzi & Carpita, 1991; Li, Kisara, Danielsson, Lindström, & Gellerstedt, 2007). The chemical compositions of hemicellulose usually vary depending on various fractions and extraction

solvents employed (Jin et al., 2009; Xue, Wen, Xu, & Sun, 2012). The monosaccharides and uronic acids contents of hemicellulose from several lignocelluloses are given in Table 12.

Table 12. The contents of monosaccharides and uronic acids in hemicellulose. (Brienzo, Siqueira, & Milagres, 2009; Jin et al., 2009; Patwardhan, Brown, & Shanks, 2011; Peng et al., 2012; Sun et al., 2001; Xue et al., 2012)

Biomass	Xylose	Mannose	Glucose	Arabinose	Galactose	Rhamnose	Uronic acids
Barley straw ^a	28-77%	0.3-2.5%	8-30%	12-19%	0.3-10%	2-11%	5-8%
Maize stem ^a	26-61%	0.1-6%	7-25%	23-30%	0.2-12%	1-8%	3-7%
Pine wood ^a	20-59%	20-48%	6-12%	7-10%	6-14%	-	-
Poplar wood ^a	79-89%	2-9%	4-7%	0.9-1.3%	1.9-2.8%	1.6-2.2%	8-12%
Sugarcane bagasse ^b	73-83%	-	4-7%	4-7%	-	-	4-7%
Sweet sorghum leaves ^b	9-89%	<3%	8-50%	1-43%	2-20%	1-9%	1-3%
Switchgrass ^a	66.2%	-	3.3%	14.2%	3.8%	-	-

^a: based on total sugar weight; ^b: based on hemicellulose weight; -: not reported.

3.2.2. GPC Analysis

The average molecular weights of hemicelluloses can be determined by GPC based on calibration with pullulan standards of molecular weights ranging from ~780 up to 1600,000 Da. Sodium acetate buffer or sodium phosphate buffer in pH 7-12 is used as the mobile phase. The polydispersity index (PDI) is calculated by dividing weight-average molecular weight (M_w) over number-average molecular weight (M_n) of hemicellulose. The hemicellulose molecular weights and its distributions also vary widely upon the hemicellulose fraction extracted with different solvents. Molecular weights of hemicellulose isolated from several biomass are listed in Table 13.

3.2.3. FTIR Spectroscopic Analysis

FTIR spectra can be used to determine the structure of isolated hemicellulose. The characteristic absorbance bands of functional groups in hemicellulose include hydroxyl (OH), glycosidic linkage (C–O–C), ester group (–COO–), and carbonyl group (C=O). The hemicellulose containing lignin residual shows aromatic skeletal absorbance at 1500-1560 cm^{-1} (Sun, Jing, Fowler, Wu, & Rajaratnam, 2011; Xue et al., 2012). The identified functional groups and assignments in FTIR spectra of hemicellulose are summarized in Table 14.

Table 13. Weight-average (M_w) and number-average (M_n) molecular weights (g/mol) and polydispersity index (M_w/M_n) of hemicellulose from various biomass. (Ayoub, Venditti, Pawlak, Sadeghifar, & Salam, 2013; Jin et al., 2009; Peng et al., 2012; Sun et al., 2001; Xue et al., 2012)

	M_w	M_n	PDI
Barley straw	14,600-28,840	5,030-10,080	2.6-3.0
Maize stem	13,370-23,590	4,840-8,780	2.7-2.8
Pine wood	16,500-79,840	12,760-40,020	1.3-2.0
Poplar wood	38,360-42,230	4,910-7,580	5.1-8.0
Sweet sorghum leaves	17,300-128,000	1,400-20,100	2.5-12.4
Switchgrass	3,500-85,700	460-20,900	4.1-7.6

Table 14. The main functional groups assignment of hemicellulose in FTIR spectra (Jin et al., 2009; Sun et al., 2001; Sun et al., 2005)

Wave numbers (cm ⁻¹)	Functional group	Compounds
3343	O–H stretching	Hemicellulose
2950-2850	C–H stretching	hemicellulose
1745	C=O	Acetyl, uronic, and ferulic ester
1584	C–H deformation	Hemicellulose
1456	C–H vibration of polysaccharides	Hemicellulose
1420	–COO– symmetric stretching	Uronic acids
1374	C–H vibration of polysaccharides	Cellulose
1258	–COOH vibration	Glucuronic acid
1249	–C–O–	Acetyl, uronic, and ferulic ester
1149	C–OH vibration and C–O–C stretching	Glycosidic bond
1028	O–H	Glucose unit
897, 903	C–O–C	Glycosidic linkage
873	Pyranose ring stretching	Hexose units

Table 15. Chemical shifts and signals assignments of hemicellulose in HSQC spectra (Sun et al., 2011; Sun et al., 2005)

Chemical shift, ppm (δ_C/δ_H)	Assignment
110.00/5.21	α -arabinose unit
109.56/4.88	α -arabinose unit
100.08/4.64	C-1/H-1 of mannose residue
106.50/4.46	C-1/H-1 of galactose residue
102.52/4.32	C-1/H-1 of glucose and xylose residue
97.6/5.19	C-4/H-4 of 4- <i>O</i> -methyl-D-glucuronic acid
86.70/4.15	C-4/H-4 of α -arabinose unit
83.20/3.15	4- <i>O</i> -methyl-D-glucuronic acid
78.96/3.54	C-4/H-4 of 4-linked β -glucose
78.60/3.71	C-5/H-5 of 4-linked β -glucose
76.90/3.68	C-4/H-4 of 4-linked β -mannose
76.00/3.59	C-4/H-4 of β -xylose
75.88/3.45	C-5/H-5 of 4-linked β -mannose
75.10/3.28	C-3/H-3 of β -xylose
74.12/3.47	C-3/H-3 of 4-linked β -glucose
73.80/3.19	C-2/H-2 of 4-linked β -glucose
73.20/3.07	C-2/H-2 of β -xylose
72.12/3.67	C-3/H-3 of 4-linked β -mannose
71.21/3.98	C-3/H-3 of 4-linked β -mannose
63.91/3.85, 3.17	C-5/H-5 of β -xylose
60-63.50/3.40-4.00	C-6/H-6 of 4-linked β -mannose and β -glucose
60.82/3.47	<i>O</i> -methyl group
23.20/1.83	Acetyl group

3.2.4. NMR Spectroscopic Analysis

The structure of isolated hemicellulose has also been analyzed by ¹H, ¹³C, and heteronuclear single quantum coherence (HSQC) NMR. The solvent used for NMR analysis are generally D₂O. In a ¹H-NMR spectrum, signal around δ 2.1 ppm indicates the presence of acetyl group in polysaccharides of hemicellulose (Lundqvist et al., 2002). The signals in the region between 4.8 and 4.5 ppm were attributed to the anomeric protons of substituted β -D-

xylose (Jin et al., 2009). The anomeric proton chemical shifts of 4.77 and 4.52 ppm correspond to the presence of (1-4)-linked β -mannopyranosyl and β -glucopyranosyl residues, respectively (Sun et al., 2005). In a ^{13}C -NMR spectrum, five signals at 102.6 (C-1), 78.3 (C-4), 77.7 (C-3), 76.2 (C-2), and 66.0 (C-5) ppm, were assigned to the (1,4) linked β -D-Xyl residues (Jin et al., 2009). HSQC NMR spectra are very useful in elucidating the structure of hemicellulose. The cross peaks in HSQC spectra of hemicellulose and their assignments are summarized in Table 15.

3.3. Lignin Analysis

Lignin is a natural aromatic polymer mainly composed of coniferyl, sinapyl and *p*-coumaryl alcohols by aryl ether linkages (e.g., β -O-4, 4-O-5) and carbon-carbon bonds (e.g., β - β , β -1, β -5, 5-5). It is a major cell wall component and provides structural strength and rigidity of plant tissues, and is also an important component for water transportation in plants (Whetten & Sederoff, 1995). In addition, lignin is also connected with carbohydrates forming lignin-carbohydrate complex (LCC) in cell walls. While whole cell wall NMR can provide useful information on lignin structures such as monolignol types and interunit linkages, isolation of lignin from plant cell walls is a required step for characterization of certain key structural properties of lignin such as molecular weights and hydroxyl groups. Efforts in isolation process should focus on minimizing structural modification of lignin that might occur during isolation (Guerra, Filpponen, Lucia, Saquing, et al., 2006). Three types of isolated lignins have been widely used for lignin characterization: milled wood lignin (MWL), cellulolytic enzyme lignin (CEL), and enzymatic mild acidolysis lignin (EMAL). In addition, Wen et al. recently proposed a new method for lignin isolation from Eucalyptus wood based on mild alkaline preswelling and enzymatic hydrolysis (Wen, Sun, Yuan, & Sun, 2015). The isolated lignin was termed as swollen residual enzyme lignin (SREL) and a high yield of SREL up to 95% was reported. Figure 5 presents an overall isolation procedure for MWL, CEL, and EMAL. The structural features of lignin such as molecular weights, functional groups contents, monolignol types/ratios, and interunit linkages are generally investigated by using GPC and a variety of NMR techniques.

Milled wood lignin, also called as Björkman lignin, is separated from plant cell walls without enzymatic or chemical hydrolysis (Björkman, 1957). Biomass samples need to be prepared as described in the previous section before milling. The dry extractives-free biomass is milled using a ball mill. Milling time and other milling conditions such as milling speed and amount of loading biomass need to be optimized based on biomass species, particle size, and even types of ball mills. Ball-milled biomass is extracted in dioxane/water mixture (96:4, v/v) at room temperature for 24 h, and then centrifuged for recovering the extracts. The residues are extracted again with a fresh dioxane-water mixture for another 24 h. The extracts from the dioxane extraction are combined and dried by either freeze-drying or vacuum drying. Although this crude MWL is useful for many experiments, it still has ~5-10% residual carbohydrate contaminants (Obst & Kirk, 1988). For the further purification of the crude MWL, the lignin is dissolved in 90% acetic acid, and then precipitated in water. The precipitated lignin is freeze-dried and dissolved in ethylene chloride and ethanol (2:1, v/v) and remove the solid fraction by centrifugation. The lignin in solution is precipitated in anhydrous ethyl ether and recovered by centrifugation and freeze-drying.

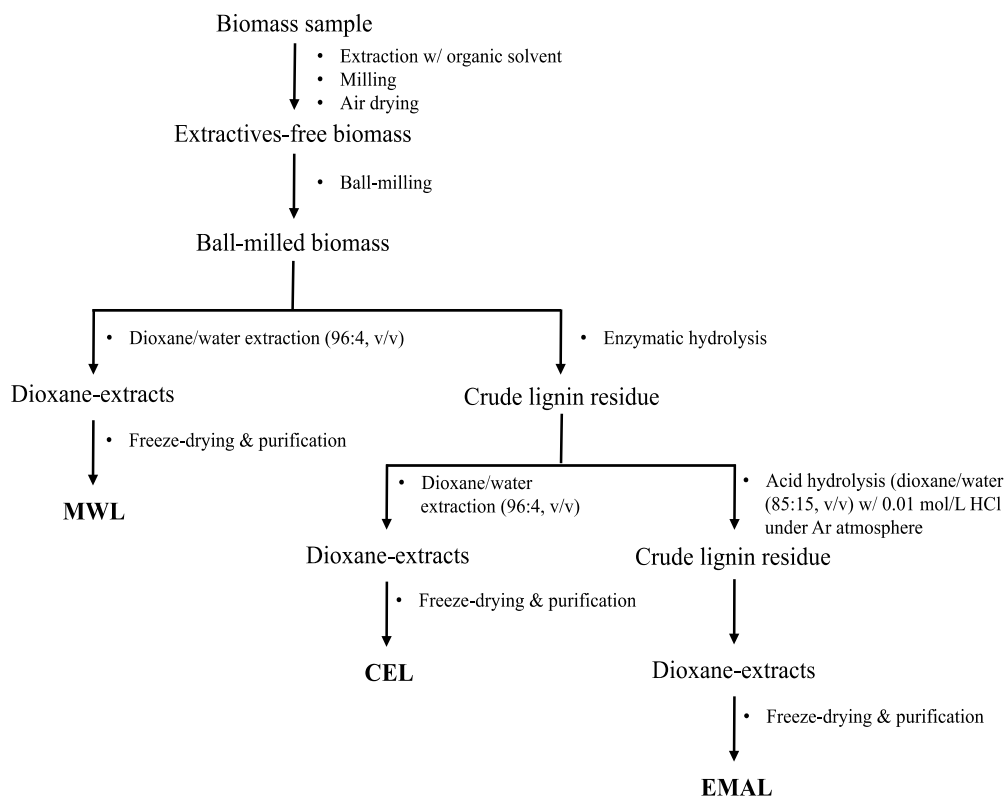


Figure 5. An overall isolation procedure for MWL, CEL, and EMAL lignin from biomass.

Another lignin isolation method was introduced by using enzymatic hydrolysis for enhancing the lignin isolation (Chang, Cowling, & Brown, 1975; Holtman, Chang, & Kadla, 2004). Typically, it has a higher lignin yield compared to MWL, while it potentially contains some protein impurities from the enzyme residues and carbohydrates from LCC complexes. The biomass preparation and ball-milling steps are the same as MWL isolation, except that the ball-milled biomass is hydrolyzed by enzyme cocktails including cellulase, hemicellulase, and β -glucosidase before conducting dioxane extraction. Enzymatic hydrolysis conditions (pH of solution, enzyme loading, and temperature) vary depending on the types of enzymes employed. Enzymatic hydrolysis is usually conducted for 24-72 h in a buffer with repeatedly adding fresh enzymes. The solid residues from enzymatic hydrolysis are recovered by centrifugation, and then washed with DI-water before freeze-drying. The residues are extracted by 96% dioxane/water (v/v) as similar to MWL isolation.

Enzymatic mild acidolysis lignin is isolated by combination of enzymatic hydrolysis and a mild acid hydrolysis, reportedly yielding a lignin with high yield and improved purity (Guerra, Filpponen, Lucia, Saquing, et al., 2006; Wu & Argyropoulos, 2003). Significant amount of carbohydrates can be removed from ball-milled biomass during the enzymatic hydrolysis. The solid residues are washed with acidified DI water (pH 2), and then freeze-dried for the following mild acid hydrolysis step. The acid hydrolysis is conducted by fluxing an azeotrope of dioxane/water (85:15, v/v) with 0.01 mol/L HCl under an inert (i.e., argon) atmosphere to cleave linkages between lignin and carbohydrates. The resultants are

centrifuged and the supernatants are neutralized with sodium bicarbonate, and then added dropwise into acidified DI water (~pH 2.0). The precipitated lignin is then kept in solution overnight, centrifuged and washed with DI water before freeze-drying. Table 16 shows typical lignin yields from different biomass by MWL, CEL, and EMAL isolation procedures.

Table 16. Lignin yields from different biomass by different isolation methods for MWL, CEL, and EMAL (Guerra, Filpponen, Lucia, & Argyropoulos, 2006; Guerra, Filpponen, Lucia, Saquing, et al., 2006; Tolbert, Akinosho, Khunsupat, Naskar, & Ragauskas, 2014)

Biomass species	Isolated lignin yield ^a [%]		
	MWL	CEL	EMAL
Norway Spruce	11.4	23.4	44.5
Douglas Fir	1.4	7.1	24.8
Redwood	15.7	13.2	56.7
White Fir	11.3	11.5	42.9
Eucalyptus globulus	34.0	32.5	63.7
Southern Pine	11.9	12.4	56.3

^aCalculation is based on Klason lignin contents in biomass.

3.3.1. Molecular Weights Analysis

Molecular weight is one of key physicochemical properties of lignin. It has been analyzed by different methods including vapor pressure osmometry (VPO), ultrafiltration, light scattering, mass spectrometry, and gel permeation chromatography (GPC) (Baumberger et al., 2007; Gidh, Decker, Vinzant, Himmel, & Williford, 2006; Gosselink et al., 2004; Jönsson, Nordin, & Wallberg, 2008). Among these methods, GPC is widely used for lignin molecular weight analysis because of its advantages: (1) broad range of molecular weights, (2) tolerance of synthetic and natural polymers, (3) small quantity analysis (milligram size), and (4) relatively short processing time (Robards, Robards, Haddad, & Jackson, 1994; Seidel, 2008; Tolbert et al., 2014). Weight-average molecular weight (M_w) and number-average molecular weight (M_n) of lignin can be calculated through a calibration curve established with polystyrene standards. Lignin polydispersity index, which represents the heterogeneity of lignin particle sizes, can also be calculated.

For GPC analysis, derivatization of isolated lignin is usually performed to achieve good solubility of lignin samples in organic solvents. Derivatization can be conducted by methylation, acetylation, or silylation (Tolbert et al., 2014). Acetylation using acetic anhydride-pyridine mixture (1:1, v/v) is the most employed derivatization method for lignin GPC analysis (Gellerstedt, 1992). The isolated lignin is dissolved in acetic anhydride-pyridine mixture and stirred at room temperature for 24 h. After reaction, ethanol is loaded in the mixture, and then evaporated using rotary evaporator to remove solvents. This ethanol addition and evaporation is repeated until unreacted acetic anhydride and pyridine are completely removed. The acetylated lignin is dissolved in THF and filtered using a hydrophobic PTFE membrane filter before GPC analysis. Polystyrene standards are used for the calibration curves of molecular weights. Details for GPC system and calculation of M_n , M_w , and PDI are similar to cellulose molecular weight analysis (Section 3.1.1). Using GPC analysis, Hallac et al. reported that degree of polymerization of lignin in *Buddleja davidii* significantly decreased (i.e., by ~85%) with an increase in polydispersity index after ethanol

organosolv pretreatment, thus facilitating lignin solubilization in ethanol (Hallac et al., 2010). Table 17 shows molecular weights and PDI of lignin isolated from various biomass.

Table 17. Molecular weights and polydispersity index of lignin from various biomass (Cao et al., 2012; Hu, Cateto, Pu, Samuel, & Ragauskas, 2011; Rahikainen et al., 2013; Tolbert et al., 2014; Wen et al., 2013)

Biomass	Isolation	M_n [g/mol]	M_w [g/mol]	PDI (M_w/M_n)
Spruce	EMAL	3,100	13,700	4.4
Wheat Straw	EMAL	2,000	3,600	1.8
Birch	CEL	7,810	18,300	2.3
Poplar	MWL	4,176	13,250	3.2
Switchgrass	MWL	2,070	5,100	2.5

3.3.2. ^1H NMR

^1H NMR spectroscopy has long been used as a valuable technique for structural characterization of lignin. This technique provides a high signal to noise (S/N) ratio in a short experimental time (typically within several minutes). However, it usually suffers from severe signal overlapping due to its short chemical shift ranges (i.e., $\sim \delta$ 12–0 ppm) and complexity of lignin structures. ^1H NMR can quantitatively examine lignin samples either as acetate derivatives or underivatized forms, providing information of some key lignin functionalities, such as carboxylic acids, aromatic hydrogens, methoxyl group, and monolignol types in lignin. Acetylated lignin can provide improved spectral resolution; however, some unwanted chemical modifications probably occur to the sample to some extent due to the acetylation procedure. Table 18 shows chemical shifts and signals assignments of acetylated spruce milled wood lignin in a ^1H NMR spectrum.

Table 18. Typical signals assignment and chemical shifts in ^1H NMR spectrum of acetylated spruce lignin (solvent: deuterated chloroform) (Lundquist, 1992)

δ (ppm)	Assignment
1.26	Hydrocarbon contaminant
2.01	Aliphatic acetate
2.28	Aromatic acetate
2.62	Benzylic protons in β - β structures
3.81	Protons in methoxyl groups
4.27	H_γ in several structures
4.39	H_γ in, primarily, β -O-4 structures and β -5 structures
4.65	H_β in β -O-4 structures
4.80	Inflection possibly due to H_α in pinoresinol units and H_β in noncyclic benzyl aryl ethers
5.49	H_α in β -5 structures
6.06	H_α in β -O-4 structures (H_α in β -1 structures)
6.93	Aromatic protons (certain vinyl protons)
7.41	Aromatic protons in benzaldehyde units and vinyl protons on the carbon atoms adjacent to aromatic rings in cinnamaldehyde units
7.53	Aromatic protons in benzaldehyde units
9.64	Formyl protons in cinnamaldehyde units
9.84	Formyl protons in benzaldehyde units

3.3.3. ^{13}C NMR

Compared to ^1H NMR, ^{13}C NMR spectroscopy benefits from a broader spectral window (i.e., $\sim \delta$ 240–0 ppm), better resolution, and less signals overlapping, while needing longer experimental time due to the low natural isotopic abundance of ^{13}C nucleus. ^{13}C NMR can provide comprehensive information about lignin structure and functional groups including methoxyl, condensed and noncondensed carbons, interunit linkages, and monolignol ratio. Both qualitative and quantitative ^{13}C NMR spectra are applicable for lignin characterization. A qualitative ^{13}C NMR spectrum for lignin analysis usually requires ~ 2 -5 h depending on sample concentration and experimental conditions. In order to perform quantitative analysis of lignin, a ^{13}C NMR spectrum needs to obtain under quantitative requirement conditions using an inversed-gated decoupling pulse sequence and long relaxation delay of at least 5 times the longest ^{13}C longitudinal relaxation time. A quantitative ^{13}C NMR spectrum with a satisfactory signal-to-noise ratio can be obtained using a 90° pulse, a pulse delay of ~ 12 s, and thousands of scan numbers. The quantitative ^{13}C NMR spectra are usually time consuming with the total experiment time being up to 24–36 h. Recently, Holtman et al. reported a shortened time of quantitative ^{13}C NMR spectra for lignin analysis by adding relaxation agent chromium (III) acetylacetonate (0.01 M) into lignin solution samples which provided complete relaxation of all nuclei in lignin (Holtman et al., 2006). The experimental condition was reported not affecting the quality of the spectra while allowing a 4-fold decrease in the experimental time with a shorter pulse delay (i.e., 1.7 s). Table 19 summarizes signal assignments and chemical shifts of structural features of a spruce milled wood lignin in a ^{13}C NMR spectrum measured using DMSO- d_6 as solvent. Figure 6 shows a quantitative ^{13}C NMR spectrum for a milled wood lignin isolated from a hardwood poplar (Cao et al., 2012).

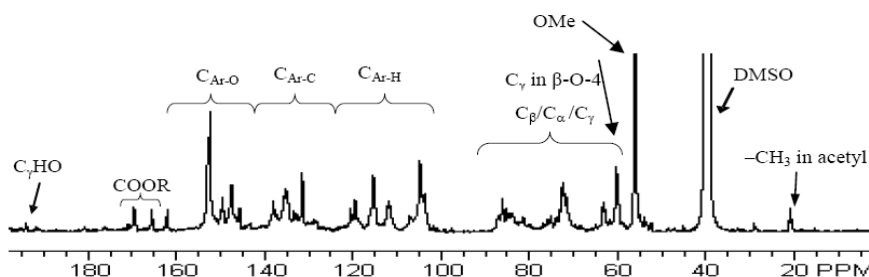


Figure 6. A quantitative ^{13}C NMR spectrum of a milled wood lignin isolated from a hardwood poplar (Cao et al., 2012). Ar: aromatic; OMe: methoxyl; DMSO: dimethyl sulfoxide.

^{13}C NMR spectroscopy has been widely used for lignin characterization in biomass feedstock and pretreatment. For example, Pu et al. employed quantitative ^{13}C NMR to study structure of lignin in genetically engineered alfalfa and reported that *p*-coumarate 3-hydroxylase (C3H) and hydroxycinnamoyl CoA:shikimate/quinic acid hydroxycinnamoyl transferase (HCT) C3H gene down-regulation reduced the methoxyl content by up to $\sim 58\%$ and 73% in lignin, respectively (Pu et al., 2009). Hallac et al. investigated structural transformations of *Buddleja davidii* lignin during ethanol organosolv pretreatment using ^{13}C NMR (Hallac, Pu, & Ragauskas, 2010). The results demonstrated a decrease of β -O-4 linkages up to $\sim 57\%$ and S/G ratio remained relatively unchanged after the pretreatments. Similarly, Sannigrahi et al. investigated lignin isolated from loblolly pine before and after

ethanol organosolv pretreatment and observed a ~50% decrease in β -O-4 linkages from quantitative ^{13}C NMR analysis, which suggested that acid-catalyzed cleavage of β -O-4 linkages was a major mechanism for lignin degradation during organosolv pretreatment (Sannigrahi, Ragauskas, & Miller, 2008; Sannigrahi, Ragauskas, & Miller, 2010).

3.3.4. ^{31}P NMR

Lignin hydroxyl groups, especially free phenoxy groups, as well as their contents in lignin, are key structural characteristics that impact physical and chemical properties of lignin. These functional groups have a prominent role in defining reactivity of lignin to promote cleavage of inter-unit linkages and/or oxidative degradation during pretreatment processes. ^{31}P NMR can provide quantitative information for various types of major hydroxyl groups including aliphatic, carboxylic, phenolic hydroxyls, and *p*-hydroxyphenyls in a relatively short experimental time and with small sample size requirements. The ^{31}P NMR technique usually involves treating lignin samples with the phosphorylation reagent 2-chloro-4,4,5,5 tetramethyl-1,3,2-dioxaphospholane (TMDP) to phosphorylate the labile hydroxyl protons in lignin and then determine their concentration by ^{31}P NMR (Pu, Cao, & Ragauskas, 2011). An internal standard such as cyclohexanol or N-hydroxy-5-norbornene-2,3-dicarboximide is used in ^{31}P NMR analysis. A mixture of anhydrous pyridine and deuterated chloroform (~1.6:1.0, v/v) containing a relaxation agent (i.e., chromium (III) acetylacetonate) and an internal standard is employed as a solvent. Typically, an accurately weighed dried lignin sample (10~25 mg) is dissolved in a NMR solvent mixture (0.50 ml) and TMDP reagent (~ 0.05 – 0.10 ml) is added and stirred for a short period of time at room temperature. ^{31}P NMR spectrum with a satisfactory signal to noise (S/N) ratio is usually acquired with a 90° pulse width, a 25-s pulse delay, and 64 - 256 acquisitions (~ 0.5– 2 h) at room temperature. Figure 7 shows a ^{31}P NMR spectrum of a hardwood lignin derivatized with 2-chloro-4,4,5,5 tetramethyl-1,3,2-dioxaphospholane. Table 20 summarizes chemical shifts/integration ranges of hydroxyl groups in lignin using TMDP/ ^{31}P NMR analysis.

^{31}P NMR has been shown to be very effective for determining the presence and contents of various hydroxyl groups in starting and pretreated biomass. Using ^{31}P NMR methodology, Cao et al. documented that the syringyl and guaiacyl phenolic OH contents in poplar lignin increased after dilute acid pretreatment (Cao et al., 2012). Similarly, Hallac et al. applied ^{31}P NMR to determine hydroxyl contents in lignin of *Buddleja davidii* during ethanol organosolv pretreatments and reported the amount of phenolic OH increased significantly in ethanol organosolv lignin EOLs as compared to milled wood lignin from native *B. davidii* (Hallac et al., 2010). ^{31}P NMR analysis by Samuel et al. demonstrated that dilute acid pretreatment led to a 27% decrease in aliphatic hydroxyl content and a 25% increase in phenolic hydroxyl content in switchgrass lignin (Samuel, Pu, Raman, & Ragauskas, 2010). Akim et al. investigated structural features of lignins in wild type and COMT down-regulated transgenic poplar and documented that COMT down-regulation (90% deficient) yielded a poplar lignin with a lower content of syringyl and aliphatic OH group as well as an increased guaiacyl phenolic OH amount when compared to the wild type control (Akim et al., 2001).

3.3.5. HSQC NMR Analysis

Two-dimensional heteronuclear single quantum coherence (HSQC) ^1H - ^{13}C correlation NMR is one of the most commonly applied techniques in structural characterization of lignin. HSQC has an increased sensitivity of ^{13}C nuclei by polarization transfer from abundant ^1H

nuclei and also can avoid signal overlapping that usually occurs in one-dimensional (1D) spectra. The application of HSQC NMR in lignin enables reliable assignments of proton and carbon nuclei signals in lignin molecules. It is a very efficient tool for lignin structural analysis which not only is useful for structural identification but also can provide estimation of relative abundance of interunit linkages and monolignol composition in lignin from native and genetically altered plants as well as pretreated biomass (Ralph & Landucci, 2010; Balakshin, Capanema, & Chang, 2007; Ralph et al., 2006; Moinuddin et al., 2010; Rencoret et al., 2008). HSQC analysis of lignin can be performed with solution of lignin in deuterated dimethyl sulfoxide (DMSO- d_6) by applying a 90° pulse width, a 1.0-2.0 s pulse delay, a $^1J_{C-H}$ of 145 Hz (i.e., CNST2), and 32 or more scans depending on the concentration of lignin samples. The concentration of ~5-15% is usually used which requires at least ~25 mg of lignin in 0.50 mL of DMSO- d_6 solvent. The lignin amount can be decreased dramatically to ~5 mg in ~0.15 mL of DMSO- d_6 if a Shigemi NMR microtube is used, which still provides a satisfactory S/N ratio in NMR spectra. Signals assignments and respective chemical shifts in HSQC spectra for typical interunit linkages and/or subunits in lignin are shown in Table 21.

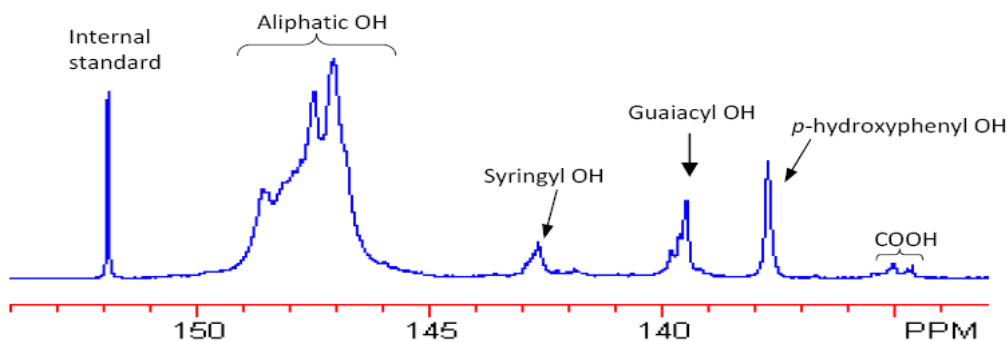


Figure 7. A quantitative ^{31}P NMR spectrum of a hardwood lignin derivatized with TMDP using N-hydroxy-5-norbornene-2,3-dicarboximide as internal standard.

Table 19. Typical chemical shifts and signal assignments in a ^{13}C NMR spectrum of lignin.(Robert, 1992; Drumond, Aoyama, Chen, & Robert, 1989; Pan, Lachenal, Neirinck, & Robert, 1994)

δ (ppm)	Assignment
193.4	C=O in Ar-CH=CH-CHO; C=O in Ar-CO-CH(-OAr)-C-
191.6	C=O in Ar-CHO
169.4	Ester C=O in R'-O-CO-CH ₃
166.2	C=O in Ar-COOH Ester C=O in Ar-CO-OR
156.4	C-4 in H-units
152.9	C-3/C-3' in etherified 5-5 units; C- α in Ar-CH=CH-CHO units
152.1	C-3/C-5 in etherified S units and B ring of 4-O-5 units
151.3	C-4 in etherified G units with α -C=O
149.4	C-3 in etherified G units
149.1	C-3 in etherified G type β -O-4 units
146.8	C-4 in etherified G units
146.6	C-3 in non-etherified G units (β -O-4 type)
145.8	C-4 in non-etherified G units
145.0	C-4/C-4' of etherified 5-5 units
143.3	C-4 in ring B of β -5 units; C-4/C-4' of non-etherified 5-5 units

Table 19. (Continued)

δ (ppm)	Assignment
134.6	C-1 in etherified G units
132.4	C-5/C-5' in etherified 5-5 units
131.1	C-1 in non-etherified 5-5 units
129.3	C- β in Ar-CH=CH-CHO
128.0	C- α and C- β in Ar-CH=CH-CH ₂ OH
125.9	C-5/C-5' in non-etherified 5-5 units
122.6	C-1 and C-6 in Ar-CO-C-C units
119.9	C-6 in G units
118.4	C-6 in G units
115.1	C-5 in G units
114.7	C-5 in G units
111.1	C-2 in G units
110.4	C-2 in G units
86.6	C- α in G type β -5 units
84.6	C- β in G type β -O-4 units (threo)
83.8	C- β in G type β -O-4 units (erythro)
71.8	C- α in G type β -O-4 units (erythro)
71.2	C- α in G type β -O-4 units (threo); C- γ in G type β - β
63.2	C- γ in G type β -O-4 units with α -C=O
62.8	C- γ in G type β -5, β -1 units
60.2	C- γ in G type β -O-4 units
55.6	C in Ar-OCH ₃
53.9	C- β in β - β units
53.4	C- β in β -5 units
40-15	CH ₃ and CH ₂ in saturated aliphatic chain

Ar: aromatic.

Table 20. Chemical shifts and signals assignments in ³¹P NMR spectra of lignin (Zawadzki, 1999; Pu et al., 2011)

Chemical shift (ppm)	Assignment
145.4 – 150.0	Aliphatic OH
137.6 – 144.0	Phenols
140.2 – 144.5	C ₅ substituted phenols
~143.5	beta-5
~142.7	Syringyl
~142.3	4-O-5
~141.2	5-5
139.0 – 140.2	Guaiacyl
~138.9	Catechol
~137.8	<i>p</i> -hydroxyphenyl
133.6 – 136.0	Carboxylic OH

While HSQC is typically not considered quantitative, it has been widely employed as a semi-quantitative method to provide relative comparisons of structural features in lignin. For interunit linkages comparison, side chain α -carbon contours in various linkages are usually used for volume integration, and the relative abundance of each respective interunit linkage is then calculated as the percentage of integrals of total linkages. For monolignol profiling analysis, aromatic contours from S units (C_{2,6}), G units (C₂), and H units (C_{2,6}) are employed

for volume integration. Figure 8 illustrates exemplary ^1H - ^{13}C correlation signals in aromatic regions and aliphatic side chain ranges of lignin in a wild type switchgrass. Using HSQC analysis, Samuel et al. investigated lignin structures of wild type and caffeic acid 3-O-methyltransferase (COMT) down-regulated transgenic switchgrass (Samuel et al., 2014). Compared to the wild type plant, COMT down-regulation resulted in a significant increase in G units and formation of benzodioxane, as well as a concomitant decrease in S units and β -O-4 ether linkage. Cao et al. characterized the structures of poplar lignin during dilute acid pretreatment and observed a decrease in β -O-4 content and diminished cinnamaldehyde unit after pretreatment (Cao et al., 2012).

Table 21. Chemical shifts and assignment of signals in HSQC spectra of lignin (DMSO as solvent) (del Río et al., 2008; Stewart, Akiyama, Chapple, Ralph, & Mansfield, 2009; Ralph et al., 1999; Samuel et al., 2014)

δ_c/δ_H (ppm)	Assignment ^a
53.1/3.44	C β /H β in phenylcoumaran substructure (B)
53.6/3.03	C β /H β in resinol substructure (C)
55.7/3.70	C/H in methoxyl group
59.8/3.28,3.62	C γ /H γ in β -O-4 ether linkage (A)
61.7/4.09	C γ /H γ in cinnamyl alcohol (F)
62.3/4.08,3.95	C γ /H γ in dibenzodioxocin
62.8/3.76	C γ /H γ in phenylcoumaran substructure (B)
71.1/3.77, 4.13	C γ /H γ in resinol substructure (C)
71.4/4.76	C α /H α in β -O-4 linked to a G unit (A)
72.1/4.86	C α /H α in β -O-4 linked to a S unit (A)
76.0/4.81	C α /H α in benzodioxane
78.2/4.00	C β /H β in benzodioxane
81.4/5.1	C β /H β in spirodienone substructure
83.7/4.31	C β /H β in β -O-4 linked to a G unit (A)
84.2/4.69	C α /H α in dibenzodioxocin
84.7/4.7	C α /H α in spirodienone substructure
85.2/4.63	C α /H α in resinol substructure (C)
86.3/4.13	C β /H β in β -O-4 linked to a S unit (A)
86.6/4.08	C β /H β in dibenzodioxocin
87.0/5.52	C α /H α in phenylcoumaran substructure (B)
103.8/6.70	C $_{2,6}$ /H $_{2,6}$ in syringyl units (S)
105.5/7.3	C $_{2,6}$ /H $_{2,6}$ in oxidized syringyl (S') units with C α = O
111.0/6.98	C $_2$ /H $_2$ in guaiacyl units (G)
114.8/6.73	C $_{3,5}$ /H $_{3,5}$ in <i>p</i> -hydroxyphenyl units (H)
115.1/6.72, 6.98	C $_5$ /H $_5$ in guaiacyl units
119.1/6.80	C $_6$ /H $_6$ in guaiacyl units
128.0/7.17	C $_{2,6}$ /H $_{2,6}$ in <i>p</i> -hydroxyphenyl units
128.2/6.75	C β /H β in cinnamaldehyde unit (E)
128.3/6.45	C α /H α in cinnamyl alcohol (F)
128.3/6.25	C β /H β in cinnamyl alcohol (F)
130.6/7.65, 7.87	C $_{2,6}$ /H $_{2,6}$ in <i>p</i> -hydroxybenzoate units (D)
153.6/7.62	C α /H α in cinnamaldehyde unit (E)

^a G: guaiacyl; S: syringyl; S' = oxidized syringyl with C α =O; H: *p*-hydroxyphenyl; A: β -O-4 ether linkage; B: β -5/ α -O-4 phenylcoumaran; C: resinol (β - β); D: *p*-hydroxybenzoate; E: cinnamaldehyde; F: cinnamyl alcohol.

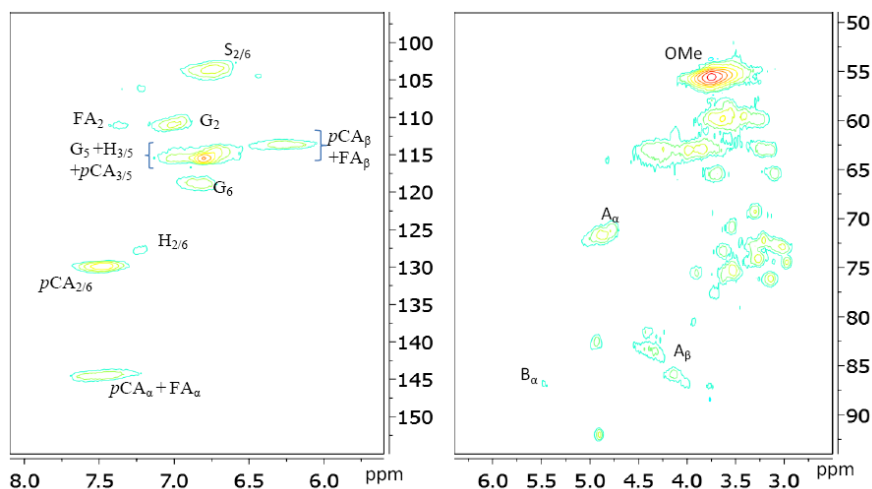


Figure 8. HSQC spectra of enzyme lignins isolated from switchgrass (Left: aromatic region; right: aliphatic region) (Samuel et al., 2014). G: guaiacyl; S: syringyl; H: p-hydroxyphenyl; pCA: p-coumarate; FA: ferulate; A: β -O-4 ether; B: phenylcoumaran; OMe: methoxyl.

CONCLUSION

Biomass characterization is a key and essential part in the area of biomass pretreatment and conversion to biofuels, chemicals, and biomaterials. Many analytical methods have been developed and applied in biomass characterization. There is not a single perfect method for biomass characterization providing a complete picture of its structures and properties. Each analytical approach has specific advantages and limitations. A combination of analytical methods reviewed in this chapter yields a comprehensive picture of physical and chemical properties of biomass, such as compositions, biomass accessibility, cellulose crystallinity and ultrastructure, cellulose and hemicellulose molecular weights, and lignin molecular weights and structures. The results from these analyses can help investigate and understand the fundamental structures of plant biomass and chemistry in biomass pretreatment and conversion process. It should be noted that besides the analytical methods reviewed in this chapter, there are a number of methods which currently are also widely applied in biomass characterization for surface properties and morphological properties, such as Raman spectroscopy, atomic force microscopy, time-of-flight secondary ion mass spectrometry (TOF-SIMS), and X-ray spectroscopy. The choice of optimal analytical strategy to give best results depends on research objectives, biomass species, samples quantities as well as the available instruments and other variables. New analytical methods which can generate new structural information (such as LCC linkages) and/or allow comprehensive analysis with a small amount of samples in a short experimental time are still needed and will have broad applicability for biomass characterization during pretreatment and conversion.

ACKNOWLEDGMENT

This work was supported and performed as part of the BioEnergy Science Center (BESC). The BioEnergy Science Center is a U.S. Department of Energy Bioenergy Research Center supported by the Office of Biological and Environmental Research in the DOE Office of Science.

REFERENCES

- Agarwal, U. P., Reiner, R. S., & Ralph, S. A. (2007, 3/25-29). Dependable cellulose I crystallinity determination using near-IR FT-Raman. Cell Division, Abstract 95, 233rd *ACS National Meeting*; Chicago.
- Akim, L.G., Argyropoulos, D.S., Jouanin L., Lepage J.-C., Pilate G., Pollet B., & Lapierre C. (2001). Quantitative P-31 NMR spectroscopy of lignins from transgenic poplars. *Holzforschung*, 55, 386-390.
- Ali, M., Emsley, A., Herman, H., & Heywood, R. (2001). Spectroscopic studies of the ageing of cellulosic paper. *Polymer*, 42(7), 2893-2900.
- Arantes, V., & Saddler, J. N. (2010). Access to cellulose limits the efficiency of enzymatic hydrolysis: the role of amorphogenesis. *Biotechnology for Biofuels*, 3(4), 1-11.
- Arantes, V., & Saddler, J. N. (2011). Cellulose accessibility limits the effectiveness of minimum cellulase loading on the efficient hydrolysis of pretreated lignocellulosic substrates. *Biotechnology for Biofuels*, 4(3), 1-16.
- Araujo, C. D., MacKay, A. L., Whittall, K. P., & Hailey, J. R. T. (1993). A diffusion model for spin-spin relaxation of compartmentalized water in wood. *Journal of Magnetic Resonance, Series B*, 101(3), 248-261.
- Ayoub, A., Venditti, R. A., Pawlak, J. J., Sadeghifar, H., & Salam, A. (2013). Development of an acetylation reaction of switchgrass hemicellulose in ionic liquid without catalyst. *Industrial Crops and Products*, 44, 306-314.
- Balakshin, M.Y., Capanema, E.A., & Chang, H.M. (2007). MWL fraction with a high concentration of lignin-carbohydrate linkages: isolation and 2D NMR spectroscopic analysis. *Holzforschung*, 61, 1-7.
- Baumberger, S., Abaecherli, A., Fasching, M., Gellerstedt, G., Gosselink, R., Hortling, B., de Jong, E. (2007). Molar mass determination of lignins by size-exclusion chromatography: towards standardisation of the method. *Holzforschung*, 61(4), 459-468.
- Beecher, J.F., Hunt, C.G., & Zhu, J.Y. (2009). Tools for the characterization of biomass at the nanometer scale. In: *The Nanoscience and Technology of Renewable Biomaterials*, John Wiley & Sons, Ltd, 61-90.
- Bilba, K., & Ouensanga, A. (1996). Fourier transform infrared spectroscopic study of thermal degradation of sugar cane bagasse. *Journal of Analytical and Applied Pyrolysis*, 38(1), 61-73.
- Björkman, A. (1957). Lignin and lignin-carbohydrate complexes. *Industrial & Engineering Chemistry*, 49(9), 1395-1398.

- Brienzo, M., Siqueira, A., & Milagres, A. M. F. (2009). Search for optimum conditions of sugarcane bagasse hemicellulose extraction. *Biochemical Engineering Journal*, 46(2), 199-204.
- Cao, S., Pu, Y., Studer, M., Wyman, C., & Ragauskas, A. J. (2012). Chemical transformations of *Populus trichocarpa* during dilute acid pretreatment. *RSC Advances*, 2(29), 10925-10936.
- Chandra, R., Ewanick, S., Hsieh, C., & Saddler, J.N. (2008). The characterization of pretreated lignocellulosic substrates prior to enzymatic hydrolysis. Part 1: a modified Simons' staining technique. *Biotechnology Progress*, 24(5), 1178 – 1185.
- Chang, H.-m., Cowling, E. B., & Brown, W. (1975). Comparative studies on cellulolytic enzyme lignin and milled wood lignin of sweetgum and spruce. *Holzforschung*, 29(5), 153-159.
- Cheng, K., Sorek, H., Zimmermann, H., Wemmer, D. E., & Pauly, M. (2013). Solution-state 2D NMR spectroscopy of plant cell walls enabled by a dimethylsulfoxide-*d*₆/1-ethyl-3-methylimidazolium acetate solvent. *Analytical Chemistry*, 85(6), 3213-3221.
- Davison, B. H., Parks, J., Davis, M. F., & Donohoe, B. S. (2013). Plant Cell Walls, Basics of Structure, Chemistry, Accessibility and the Influence on Conversion. In: Aqueous Pretreatment of Plant Biomass for Biological and Chemical Conversion to Fuels and Chemicals, *John Wiley & Sons*, Ltd, 23-38.
- del Río, J.C., Rencoret, J., Marques, G., Gutiérrez, A., Ibarra, D., Santos, J.I., ... Martínez, Á.T. (2008). Highly acylated (acetylated and/or *p*-coumaroylated) native lignins from diverse herbaceous plants. *Journal of Agricultural and Food Chemistry*, 56(20), 9525-9534.
- Donohoe, B. S., Decker, S. R., Tucker, M. P., Himmel, M. E., & Vinzant, T. B. (2008). Visualizing lignin coalescence and migration through maize cell walls following thermochemical pretreatment. *Biotechnology and Bioengineering*, 101(5), 913-925.
- Dougherty, M. J., Tran, H. M., Stavila, V., Knierim, B., George, A., Auer, M., Adams, P. D., & Hadi, M. Z. (2014). Cellulosic biomass pretreatment and sugar yields as a function of biomass particle size. *PLoS ONE*, 9(6), e100836.
- Drumond, M., Aoyama, M., Chen, C.-L., & Robert, D. (1989). Substituent effects on C-13 chemical shifts of aromatic carbons in biphenyl type lignin model compounds. *Journal of Wood Chemistry and Technology*, 9, 421-411.
- Felby, C., Thygesen, L. G., Kristensen, J. B., Jorgensen, H., & Elder, T. (2008). Cellulose-water interactions during enzymatic hydrolysis as studied by time domain NMR. *Cellulose*, 15(5), 703-710.
- Filisetti-Cozzi, T. M., & Carpita, N. C. (1991). Measurement of uronic acids without interference from neutral sugars. *Analytical Biochemistry*, 197(1), 157-162.
- Foston, M., & Ragauskas, A. J. (2010). Changes in lignocellulosic supramolecular and ultrastructure during dilute acid pretreatment of *Populus* and switchgrass. *Biomass and Bioenergy*, 34(12), 1885-1895.
- Foston, M., & Ragauskas, A. J. (2010). Changes in the structure of the cellulose fiber wall during dilute acid pretreatment in *Populus* studied by ¹H and ²H NMR. *Energy & Fuels*, 24(10), 5677-5685.
- Foston, M., Hubbell, C. A., & Ragauskas, A. J. (2011). Cellulose isolation methodology for NMR analysis of cellulose ultrastructure. *Materials*, 4, 1985-2002.

- Foston, M., Hubbell, C.A., Davis, M., & Ragauskas, A. J. (2009). Variations in cellulosic ultrastructure of poplar. *Bioenergy Research*, 2, 193-197.
- Gellerstedt, G. (1992). Gel permeation chromatograph. In: Methods in lignin chemistry. Lin SY and Dence CW, editors. Springer-Verlag: New York, NY, pp. 487-497.
- Gidh, A. V., Decker, S. R., See, C. H., Himmel, M. E., & Williford, C. W. (2006). Characterization of lignin using multi-angle laser light scattering and atomic force microscopy. *Analytica Chimica Acta*, 555(2), 250-258.
- Gidh, A. V., Decker, S. R., Vinzant, T. B., Himmel, M. E., & Williford, C. (2006). Determination of lignin by size exclusion chromatography using multi angle laser light scattering. *Journal of Chromatography A*, 1114(1), 102-110.
- Gierlinger, N., Goswami, L., Schmidt, M., Burgert, I., Coutand, C., Rogge, T., & Schwanninger, M. (2008). In situ FT-IR microscopic study on enzymatic treatment of poplar wood cross-sections. *Biomacromolecules*, 9(8), 2194-2201.
- Giesche, H. (2006). Mercury porosimetry: A general (practical) overview. *Particle & Particle Systems Characterization*, 23(1), 9-19.
- Gírio, F., Fonseca, C., Carvalheiro, F., Duarte, L., Marques, S., & Bogel-Lukasik, R. (2010). Hemicelluloses for fuel ethanol: a review. *Bioresource Technology*, 101(13), 4775-4800.
- Gosselink, R., Abächerli, A., Semke, H., Malherbe, R., Käuper, P., Nadif, A., & Van Dam, J. (2004). Analytical protocols for characterisation of sulphur-free lignin. *Industrial Crops and Products*, 19(3), 271-281.
- Grethlein, H.E. (1985). The effect of pore size distribution on the rate of enzymatic hydrolysis of cellulosic substrates. *Nature Biotechnology*, 3(2), 155-160.
- Guerra, A., Filpponen, I., Lucia, L. A., & Argyropoulos, D. S. (2006). Comparative evaluation of three lignin isolation protocols for various wood species. *Journal of Agricultural and Food Chemistry*, 54(26), 9696-9705.
- Guerra, A., Filpponen, I., Lucia, L. A., Saquing, C., Baumberger, S., & Argyropoulos, D. S. (2006). Toward a better understanding of the lignin isolation process from wood. *Journal of Agricultural and Food Chemistry*, 54(16), 5939-5947.
- Guo, Q., Chen, X., & Liu, H. (2012). Experimental research on shape and size distribution of biomass particle. *Fuel*, 94, 551-555.
- Hallac, B. B., & Ragauskas, A. J. (2011). Analyzing cellulose degree of polymerization and its relevancy to cellulosic ethanol. *Biofuels, Bioproducts and Biorefining*, 5(2), 215-225.
- Hallac, B. B., Sannigraha, P., Pu, Y., Ray, M., Murphy, R. J., & Ragauskas, A. J. (2010). Effect of ethanol organosolv pretreatment on enzymatic hydrolysis of *Buddleja davidii* stem biomass. *Industrial & Engineering Chemistry Research*, 49(4), 1467-1472.
- Hallac, B. B., Sannigrahi, P., Pu, Y., Ray, M., Murphy, R. J., & Ragauskas, A. J. (2009). Biomass characterization of *Buddleja davidii*: A potential feedstock for biofuel production. *Journal of Agricultural and Food Chemistry*, 57, 1275-1281.
- Hallac, B.B., Pu, Y., Ragauskas, A.J. (2010). Chemical transformations of *Buddleja davidii* lignin during ethanol organosolv pretreatment. *Energy & Fuels*, 24, 2723-2732.
- Hames, B., Ruiz, R., Scarlata, C., Sluiter, A., Sluiter, J., & Templeton, D. (2008). *Preparation of samples for compositional analysis*. (NREL/TP-510-42620) Retrieved from <http://www.nrel.gov/docs/gen/fy08/42620.pdf>.
- Hinkle, J. D., Ciesielski, P. N., Gruchalla, K., Munch, K. R., & Donohoe, B. S. (2015). Biomass accessibility analysis using electron tomography. *Biotechnology for Biofuels*, 8, 212.

- Holtman, K.M., Chang, H.-M., & Kadla, J. F. (2004). Solution-state nuclear magnetic resonance study of the similarities between milled wood lignin and cellulolytic enzyme lignin. *Journal of Agricultural and Food Chemistry*, 52(4), 720-726.
- Holtman, K.M., Chang, H.-M., Jameel, H., & Kadla, J. F. (2006). Quantitative ^{13}C NMR characterization of milled wood lignins isolated by different milling techniques. *Journal of Wood Chemistry and Technology*, 26, 21-34.
- Hu, G., Cateto, C., Pu, Y., Samuel, R., & Ragauskas, A. J. (2011). Structural characterization of switchgrass lignin after ethanol organosolv pretreatment. *Energy & Fuels*, 26(1), 740-745.
- Huang, R., Su, R., Qi, W., & He, Z. (2010). Understanding the key factors for enzymatic conversion of pretreated lignocellulose by partial least square analysis. *Biotechnology Progress*, 26(2), 384-392.
- Hubbell, C.A., & Ragauskas, A. J. (2010). Effect of acid-chlorite delignification on cellulose degree of polymerization. *Bioresource Technology*, 101(19), 7410-7415.
- Inglesby, M. K., & Zeronian, S. H. (2002). Direct dyes as molecular sensors to characterize cellulose substrates. *Cellulose*, 9(1), 19-29.
- Ishizawa, C.I., Davis, M.F., Schell, D.F., & Johnson, D.K. (2007). Porosity and its effect on the digestibility of dilute sulfuric acid pretreated corn stover. *Journal of Agricultural and Food Chemistry*, 55(7), 2575-2581.
- Jiang, N., Pu, Y., Samuel, R., & Ragauskas, A. J. (2009). Perdeuterated pyridinium molten salt (ionic liquid) for direct dissolution and NMR analysis of plant cell walls. *Green Chemistry*, 11(11), 1762.
- Jin, A., Ren, J., Peng, F., Xu, F., Zhou, G., Sun, R., & Kennedy, J. (2009). Comparative characterization of degraded and non-degradative hemicelluloses from barley straw and maize stems: Composition, structure, and thermal properties. *Carbohydrate Polymers*, 78(3), 609-619.
- Jönsson, A.-S., Nordin, A.-K., & Wallberg, O. (2008). Concentration and purification of lignin in hardwood kraft pulping liquor by ultrafiltration and nanofiltration. *Chemical Engineering Research and Design*, 86(11), 1271-1280.
- Kačuráková, M., & Wilson, R. (2001). Developments in mid-infrared FT-IR spectroscopy of selected carbohydrates. *Carbohydrate Polymers*, 44(4), 291-303.
- Karuna, N., Zhang, L., Walton, J. H., Couturier, M., Oztop, M. H., Master, E. R., McCarthy, M. J., & Jeoh, T. (2014). The impact of alkali pretreatment and post-pretreatment conditioning on the surface properties of rice straw affecting cellulose accessibility to cellulases. *Bioresource Technology*, 167, 232-240.
- Keshwani, D.R., & Cheng, J.J. (2010). Microwave-based alkali pretreatment of switchgrass and coastal bermudagrass for bioethanol production. *Biotechnology Progress*, 26(3), 644-652.
- Kim, H., & Ralph, J. (2010). Solution-state 2D NMR of ball-milled plant cell wall gels in $\text{DMSO-}d_6/\text{pyridine-}d_5$. *Organic & Biomolecular Chemistry*, 8(3), 576-591.
- Kim, H., Ralph, J., & Akiyama, T. (2008). Solution-state 2D NMR of ball-milled plant cell wall gels in $\text{DMSO-}d_6$. *BioEnergy Research*, 1(1), 56-66.
- Kubo, S., & Kadla, J. F. (2005). Hydrogen bonding in lignin: a Fourier transform infrared model compound study. *Biomacromolecules*, 6(5), 2815-2821.

- Kumar, R., Hu, F., Hubbell, C. A., Ragauskas, A. J., & Wyman, C. E. (2013). Comparison of laboratory delignification methods, their selectivity, and impacts on physiochemical characteristics of cellulosic biomass. *Bioresource Technology*, *130*, 372-381.
- Kumar, R., Mago, G., Balan, V., & Wyman, C. E. (2009). Physical and chemical characterizations of corn stover and poplar solids resulting from leading pretreatment technologies. *Bioresource Technology*, *100*(17), 3948-3962.
- Le Troedec, M., Sedan, D., Peyratout, C., Bonnet, J. P., Smith, A., Guinebretiere, R., Gloaguen, V., & Krausz, P. (2008). Influence of various chemical treatments on the composition and structure of hemp fibres. *Composites Part A: Applied Science and Manufacturing*, *39*(3), 514-522.
- Lee, S.B., Shin, H. S., Ryu, D. D. Y., & Mandels, M. (1982). Adsorption of cellulase on cellulose, Effect of physicochemical properties of cellulose on adsorption and rate of hydrolysis. *Biotechnology and Bioengineering*, *24*(10), 2137-2153.
- Li, C., Knierim, B., Manisseri, C., Arora, R., Scheller, H. V., Auer, M., Vogel, K. P., & Singh, S. (2010). Comparison of dilute acid and ionic liquid pretreatment of switchgrass: biomass recalcitrance, delignification and enzymatic saccharification. *Bioresource Technology*, *101*(13), 4900-4906.
- Li, J., Kisara, K., Danielsson, S., Lindström, M. E., & Gellerstedt, G. (2007). An improved methodology for the quantification of uronic acid units in xylans and other polysaccharides. *Carbohydrate Research*, *342*(11), 1442-1449.
- Li, X., Zhao, J., Qu, Y., & Lu, J. (2014). Characteristics of corn stover pretreated with liquid hot water and fed-batch semi-simultaneous saccharification and fermentation for bioethanol production. *PLoS ONE*, *9*(4), e95455.
- Lin, K.W., Ladisch, M.R., Voloch, M., Patterson, J.A., & Noller, C.H. (1985). Effect of pretreatments and fermentation on pore size in cellulosic materials. *Biotechnology and Bioengineering*, *27*(10), 1427-1433.
- Loebenstein, W.V., & Deitz, V.R. (1951). Surface-area determination by adsorption of nitrogen from nitrogen-helium mixtures. *Journal of Research of the National Bureau of Standards*, *46*(1), 51-55.
- Lundquist, K. (1992). Proton (¹H) NMR spectroscopy. In: Methods in Lignin Chemistry. Lin SY and Dence CW, editors. Springer-Verlag: New York, NY, pp. 242-249.
- Lundqvist, J., Teleman, A., Junel, L., Zacchi, G., Dahlman, O., Tjerneld, F., & Stålbrand, H. (2002). Isolation and characterization of galactoglucomannan from spruce (*Picea abies*). *Carbohydrate Polymers*, *48*(1), 29-39.
- Luo, X. L., & Zhu, J.Y. (2011). Effects of drying-induced fiber hornification on enzymatic saccharification of lignocelluloses. *Enzyme and Microbial Technology*, *48*(1), 92-99.
- Mansfield, S. D., Kim, H., Lu, F., & Ralph, J. (2012). Whole plant cell wall characterization using solution-state 2D NMR. *Nature Protocols*, *7*(9), 1579-1589.
- Meng, X., & Ragauskas, A.J. (2014). Recent advances in understanding the role of cellulose accessibility in enzymatic hydrolysis of lignocellulosic substrates. *Current Opinion in Biotechnology*, *27*, 150-158.
- Meng, X., Foston, M., Leisen, J., DeMartini, J., Wyman, C.E., & Ragauskas, A.J. (2013). Determination of porosity of lignocellulosic biomass before and after pretreatment by using Simons' stain and NMR techniques. *Bioresource Technology*, *144*, 467-476.

- Meng, X., Wells, T., Sun, Q., Huang, F., & Ragauskas, A. J. (2015). Insights into the effect of dilute acid, hot water or alkaline pretreatment on the cellulose accessible surface area and the overall porosity of *Populus*. *Green Chemistry*, 17(8), 4239-4246.
- Menon, R. S., MacKay, A. L., Hailey, J. R. T., Bloom, M., Burgess, A. E., & Swanson, J. S. (1987). An NMR determination of the physiological water distribution in wood during drying. *Journal of Applied Polymer Science*, 33(4), 1141-55.
- Mikhailovsky, S.V., Gun'ko, V.M., Bershtein, V.A., Turov, V.V., Egorova, L. M., Morvan, C., & Mikhailovska, L. I. (2012). A comparative study of air-dry and water swollen flax and cotton fibres. *RSC Advances*, 2(7), 2868-2874.
- Mitchell, J., & Webber, J. B. W. (2008). Strange JH, Nuclear magnetic resonance cryoporometry. *Physics Report*, 461(1), 1-36.
- Moinuddin, S.G.A., Jourdes, M., Laskar, D.D., Ki, C., Cardenas, C.L., Kim, K.W., Lewis, N.G. (2010). Insights into lignin primary structure and deconstruction from *Arabidopsis thaliana* COMT (caffeic acid O-methyl transferase) mutant *Atomt1*. *Organic & Biomolecular Chemistry*, 8, 3928-3946.
- Newman, R. H. (2005). Homogeneity in cellulose crystallinity between samples of Pinus radiata wood. *Holzforschung*, 58(1), 91-96.
- Obst, J. R., & Kirk, T. K. (1988). Isolation of lignin. In W. A. Wood & S. T. Kellogg (Eds.), *Methods in enzymology-Biomass, Part B: Lignin, Pectin, and Chitin* (Vol. 161, pp. 3-12). San Diego: *Academic Press, Inc.*
- Oh, S. Y., Yoo, D. I., Shin, Y., Kim, H. C., Kim, H. Y., Chung, Y. S., ... Youk, J. H. (2005). Crystalline structure analysis of cellulose treated with sodium hydroxide and carbon dioxide by means of X-ray diffraction and FTIR spectroscopy. *Carbohydrate Research*, 340(15), 2376-2391.
- Ostlund, A., Kohnke, T., Nordstierna, L., & Nyden, M. (2010). NMR cryoporometry to study the fiber wall structure and the effect of drying. *Cellulose*, 17(2), 321-328.
- Pan, X., Lachenal, D., Neirinck, V., & Robert, D. (1994). Structure and reactivity of spruce mechanical pulp lignins IV: ¹³C-NMR spectral studies of isolated lignins. *Journal of Wood Chemistry and Technology*, 14, 483-506.
- Pan, X., Xie, D., Yu, R. W., Lam, D., & Saddler, J. N. (2007). Pretreatment of lodgepole pine killed by mountain pine beetle using the ethanol organosolv process: fractionation and process optimization. *Industrial & Engineering Chemistry Research*, 46(8), 2609-2617.
- Pandey, K. (1999). A study of chemical structure of soft and hardwood and wood polymers by FTIR spectroscopy. *Journal of Applied Polymer Science*, 71(12), 1969-1975.
- Pandey, K., & Pitman, A. (2003). FTIR studies of the changes in wood chemistry following decay by brown-rot and white-rot fungi. *International Biodeterioration & Biodegradation*, 52(3), 151-160.
- Park, S., Venditti, R. A., Abrecht, D. G., Jameel, H., Pawlak, J. J., & Lee, J. M. (2006). Surface and pore structure modification of cellulose fibers through cellulase treatment. *Journal of Applied Polymer Science*, 103(6), 3833-3839.
- Patwardhan, P. R., Brown, R. C., & Shanks, B. H. (2011). Product distribution from the fast pyrolysis of hemicellulose. *ChemSusChem*, 4(5), 636-643.
- Peng, F., Bian, J., Peng, P., Guan, Y., Xu, F., & Sun, R.-C. (2012). Fractional separation and structural features of hemicelluloses from sweet sorghum leaves. *BioResources*, 7(4), 4744-4759.

- Pistorius, A. M., DeGrip, W. J., & Egorova-Zachernyuk, T. A. (2009). Monitoring of biomass composition from microbiological sources by means of FT-IR spectroscopy. *Biotechnology and Bioengineering*, *103*(1), 123-129.
- Ponni, R., Vuorinen, T., & Kontturi, E. (2012). Proposed nano-scale coalescence of cellulose in chemical pulp fibers during technical treatments. *BioResources*, *7*(4), 6077-6108.
- Pu, Y., Cao, S., & Ragauskas, A.J. (2011). Application of quantitative ^{31}P NMR in biomass lignin and biofuel precursors characterization. *Energy & Environmental Science*, *4*(9), 3154-316.
- Pu, Y., Chen, F., Ziebell, A., Davison, B.H., & Ragauskas, A.J. (2009). NMR characterization of C3H and HCT down-regulated alfalfa lignin. *BioEnergy Research*, *2*, 198-208.
- Rahikainen, J. L., Martin-Sampedro, R., Heikkinen, H., Rovio, S., Marjamaa, K., Tamminen, T., Rojas, O. J., & Kruus, K. (2013). Inhibitory effect of lignin during cellulose bioconversion: the effect of lignin chemistry on non-productive enzyme adsorption. *Bioresource Technology*, *133*, 270-278.
- Raiskila, S., Pulkkinen, M., Laakso, T., Fagerstedt, K., Loija, M., Mahlberg, R., Paajanen, L., Ritschkoff, A., & Saranpaa, P. (2007). FTIR spectroscopic prediction of Klason and acid soluble lignin variation in Norway spruce cutting clones. *Silva Fennica*, *41*(2), 351.
- Ralph, J., & Landucci, L.L. (2010). NMR of lignins. In: Lignin and Lignans. Heitner C, Dimmel DR, and Schmidt JA, editors. CRC Press, Boca Raton, Fla, pp. 137-244.
- Ralph, J., Akiyama, T., Kim, H., Lu, F., Schatz, P.F., Marita, J.M., Dixon, R.A. (2006). Effects of coumarate 3-hydroxylase down-regulation on lignin structure. *Journal of Biological Chemistry*, *281*, 8843-8853.
- Ralph, J., Marita, J.M., Ralph, S.A., Hatfield, R.D., Lu, F., Ede, R.M., Peng, J., & Landucci, L.L. (1999). Solution state NMR of lignins. In: Advances in lignocellulosics characterization. Tappi Press, Atlanta, GA.
- Rencoret, J., Marques, G., Gutierrez, A., Ibarra, D., Li, J., Gellerstedt, G., & del Río, J.C. (2008). Structural characterization of milled wood lignins from different eucalypt species. *Holzforschung*, *62*, 514-526.
- Robards, K., Robards, K., Haddad, P. R., & Jackson, P. E. (1994). Principles and practice of modern chromatographic methods: *Academic Press*, Inc.
- Robert, D. (1992). Carbon-13 nuclear magnetic resonance spectroscopy. In: Methods in lignin chemistry. Lin SY and Dence CW, editors. Springer-Verlag: New York, NY, pp. 250-273.
- Rolleri, A., Burgos, F., Bravo-Linares, C., Vasquez, E., & Droppelmann, F. (2014). Determining pore size distribution in wet earlywood cell wall by solute exclusion using total organic carbon technique (TOC). *Wood Science and Technology*, *48*(4), 787-795.
- Samuel, R., Foston, M., Jaing, N., Cao, S., Allison, L., Studer, M., Wyman, C., & Ragauskas, A. J. (2011). HSQC (heteronuclear single quantum coherence) ^{13}C - ^1H correlation spectra of whole biomass in perdeuterated pyridinium chloride-DMSO system: an effective tool for evaluating pretreatment. *Fuel*, *90*(9), 2836-2842.
- Samuel, R., Pu, Y., Foston, M., Ragauskas, A. J. (2010). Solid-state NMR characterization of switchgrass cellulose after dilute acid pretreatment. *Biofuels*, *1*, 85-90.
- Samuel, R., Pu, Y., Jiang, N., Fu, C., Wang, Z.Y., & Ragauskas, A.J. (2014). Structural characterization of lignin in wild-type versus COMT down-regulated switchgrass. *Frontiers in Bioenergy and Biofuels*, *1*, 1-9.

- Samuel, R., Pu, Y., Raman, B., & Ragauskas, A.J. (2010). Structural characterization and comparison of switchgrass lignin before and after dilute acid pretreatment. *Applied Biochemistry and Biotechnology*, 162, 62-74.
- Sannigrahi, P., Ragauskas, A. J., & Tuskan, G. A. (2010). Poplar as a feedstock for biofuels: A review of compositional characteristics. *Biofuels, Bioproducts and Biorefining*, 4, 209-226.
- Sannigrahi, P., Ragauskas, A.J., & Miller, S.J. (2008). Effects of two-stage dilute acid pretreatment on the structure and composition of lignin and cellulose in loblolly pine. *BioEnergy Research*, 1, 205-214.
- Sannigrahi, P., Ragauskas, A.J., & Miller, S.J. (2010). Lignin structural modifications resulting from ethanol organosolv treatment of loblolly pine. *Energy & Fuels*, 24, 683-689.
- Schenzel, K., & Fischer, S. (2004). Applications of FT Raman spectroscopy for the characterization of cellulose. *Lenzinger Berichte*, 83, 64-70.
- Schwanninger, M., Rodrigues, J., Pereira, H., & Hinterstoisser, B. (2004). Effects of short-time vibratory ball milling on the shape of FT-IR spectra of wood and cellulose. *Vibrational Spectroscopy*, 36(1), 23-40.
- Segal, L., Creely, J. J., Martin, A. E. Jr., & Conrad, C. M. (1959). An empirical method for estimating the degree of crystallinity of native cellulose using the x-ray diffractometer. *Textile Research Journal*, 29(10), 786-794.
- Seidel, A. (2008). Characterization and analysis of polymers: *John Wiley & Sons*.
- Sene, C. F., McCann, M. C., Wilson, R. H., & Grinter, R. (1994). Fourier-transform Raman and Fourier-transform infrared spectroscopy (an investigation of five higher plant cell walls and their components). *Plant Physiology*, 106(4), 1623-1631.
- Sills, D. L., & Gossett, J. M. (2012). Using FTIR to predict saccharification from enzymatic hydrolysis of alkali-pretreated biomasses. *Biotechnology and Bioengineering*, 109(2), 353-362.
- Sluiter, A., Hames, B., Hyman, D., Payne, C., Ruiz, R., Scarlata, C., Sluiter, J., Templeton, D., & Wolfe, J. (2008a). *Determination of total solids in biomass and total dissolved solids in liquid process samples*. (NREL/TP-510-42621) Retrieved from <http://www.nrel.gov/biomass/pdfs/42621.pdf>.
- Sluiter, A., Hames, B., Ruiz, R., Scarlata, C., Sluiter, J., Templeton, D., & Crocker, D. (2008b). *Determination of structural carbohydrates and lignin in biomass*. (NREL/TP-510-42618) Retrieved from <http://www.nrel.gov/biomass/pdfs/42618.pdf>.
- Sluiter, A., Ruiz, R., Scarlata, C., Sluiter, J., & Templeton, D. (2005). *Determination of extractives in biomass*. (NREL/TP-510-42619) Retrieved from <http://www.nrel.gov/biomass/pdfs/42619.pdf>.
- Stewart, D., Wilson, H. M., Hendra, P. J., & Morrison, I. M. (1995). Fourier-Transform infrared and Raman spectroscopic study of biochemical and chemical treatments of oak wood (*Quercus rubra*) and barley (*Hordeum vulgare*) straw. *Journal of Agricultural and Food Chemistry*, 43(8), 2219-2225.
- Stewart, J.J., Akiyama, T., Chapple, C., Ralph, J., & Mansfield, S.D. (2009). The effects on lignin structure of overexpression of ferulate 5-hydroxylase in hybrid poplar. *Plant Physiology*, 150, 621-635.

- Stone, J.E., & Scallan, A.M. (1965). Effect of component removal upon the porous structure of the cellwalls of wood. *Journal of Polymer Science Part C: Polymer Letters*, 11(1), 13-25.
- Strange, J.H., Rahman, M., & Smith, E.G. (1993). Characterization of porous solids by NMR. *Physical Review Letter*, 71(21), 3589-3591.
- Sun, R., Fang, J., Tomkinson, J., Geng, Z., & Liu, J. (2001). Fractional isolation, physico-chemical characterization and homogeneous esterification of hemicelluloses from fast-growing poplar wood. *Carbohydrate Polymers*, 44(1), 29-39.
- Sun, X. F., Jing, Z., Fowler, P., Wu, Y., & Rajaratnam, M. (2011). Structural characterization and isolation of lignin and hemicelluloses from barley straw. *Industrial Crops and Products*, 33(3), 588-598.
- Sun, X., Xu, F., Sun, R., Fowler, P., & Baird, M. (2005). Characteristics of degraded cellulose obtained from steam-exploded wheat straw. *Carbohydrate Research*, 340(1), 97-106.
- Sun, X.-F., Sun, R., Fowler, P., & Baird, M. S. (2005). Extraction and characterization of original lignin and hemicelluloses from wheat straw. *Journal of Agricultural and Food Chemistry*, 53(4), 860-870.
- Szymanska-Chargot, M., Chylinska, M., Kruk, B., & Zdunek, A. (2015). Combining FT-IR spectroscopy and multivariate analysis for qualitative and quantitative analysis of the cell wall composition changes during apples development. *Carbohydrate Polymers*, 115, 93-103.
- Szymanska-Chargot, M., Cybulska, J., & Zdunek, A. (2011). Sensing the structural differences in cellulose from apple and bacterial cell wall materials by Raman and FT-IR spectroscopy. *Sensors*, 11(6), 5543-5560.
- Tamaki, Y., & Mazza, G. (2011). Rapid determination of carbohydrates, ash, and extractives contents of straw using attenuated total reflectance Fourier transform mid-infrared spectroscopy. *Journal of Agricultural and Food Chemistry*, 59(12), 6346-6352.
- TAPPI. (2007a). *Solvent extractives of wood and pulp*. (T204cm-97) Retrieved from <http://www.tappi.org/content/sarg/t204.pdf>.
- TAPPI. (2007b). *Standard test method for ethanol-toluene solubility of wood*. (T204os-76).
- Timell, T. E. (1955). Chain length and chain-length distribution of native white spruce cellulose. *Pulp and Paper Magazine of Canada*, 56(7), 104-114.
- Tjeerdsmas, B., & Militz, H. (2005). Chemical changes in hydrothermal treated wood: FTIR analysis of combined hydrothermal and dry heat-treated wood. *Holz als Roh-und Werkstoff*, 63(2), 102-111.
- Tolbert, A., Akinosho, H., Khunsupat, R., Naskar, A. K., & Ragauskas, A. J. (2014). Characterization and analysis of the molecular weight of lignin for biorefining studies. *Biofuels, Bioproducts and Biorefining*, 8(6), 836-856.
- Wang, Q. Q., He, Z., Zhu, Z., Zhang, Y. H. P., Ni, Y., Luo, X. L., & Zhu, J. Y. (2012). Evaluations of cellulose accessibilities of lignocelluloses by solute exclusion and protein adsorption techniques. *Biotechnology and Bioengineering*, 109(2), 381-389.
- Wen, J.-L., Sun, S.-L., Xue, B.-L., & Sun, R.-C. (2013). Quantitative structures and thermal properties of birch lignins after ionic liquid pretreatment. *Journal of Agricultural and Food Chemistry*, 61(3), 635-645.

- Wen, J.-L., Sun, S.-L., Yuan, T.-Q., & Sun, R.-C. (2015). Structural elucidation of whole lignin from Eucalyptus based on preswelling and enzymatic hydrolysis. *Green Chemistry*, 17, 1589-1596.
- Whetten, R., & Sederoff, R. (1995) Lignin biosynthesis. *The Plant Cell*, 7, 1001-1013.
- Wiman, M., Dienes, D., Hansen, M. A. T., van der Meulen, T., Zacchi, G., & Lidén, G. (2012). Cellulose accessibility determines the rate of enzymatic hydrolysis of steam-pretreated spruce. *Bioresource Technology*, 126, 208-215.
- Wu, S., & Argyropoulos, D. (2003). An improved method for isolating lignin in high yield and purity. *Journal of Pulp and Paper Science*, 29(7), 235-240.
- Xu, F., Yu, J., Tesso, T., Dowell, F., & Wang, D. (2013). Qualitative and quantitative analysis of lignocellulosic biomass using infrared techniques: a mini-review. *Applied Energy*, 104, 801-809.
- Xu, L., & Tschirner, U. W. (2012). Peracetic acid pretreatment of alfalfa stem and aspen biomass. *BioResources*, 7(1), 203-216.
- Xue, B. L., Wen, J. L., Xu, F., & Sun, R. C. (2012). Structural characterization of hemicelluloses fractionated by graded ethanol precipitation from *Pinus yunnanensis*. *Carbohydrate Research*, 352, 159-165.
- Yang, B., Dai, Z., Ding, S. Y., & Wyman, C. E. (2011). Enzymatic hydrolysis of cellulosic biomass. *Biofuels*, 2(4), 421-450.
- Yang, H., Yan, R., Chen, H., Lee, D. H., & Zheng, C. (2007). Characteristics of hemicellulose, cellulose and lignin pyrolysis. *Fuel*, 86(12), 1781-1788.
- Yelle, D. J., Ralph, J., Lu, F., & Hammel, K. E. (2008). Evidence for cleavage of lignin by a brown rot basidiomycete. *Environmental Microbiology*, 10(7), 1844-1849.
- Yoo, C.G., Kim, H., Lu, F., Azarpira, A., Pan, X., Oh, K. K., Kim, J. S., Ralph, J., & Kim, T. H. (2015). Understanding the physicochemical characteristics and the improved enzymatic saccharification of corn stover pretreated with aqueous and gaseous ammonia. *BioEnergy Research*, 1-10.
- Yoo, C.G., Pu, Y., Li, M., & Ragauskas, A.J. (2016). Elucidating structural characteristics of biomass using solution-state 2D NMR with a mixture of deuterated dimethylsulfoxide and hexamethylphosphoramide. *ChemSusChem*, 9(10), 1090-1095.
- Zawadzki, M. (1999). Ph.D. Dissertation. Quantitative determination of quinone chromophore changes during ECF bleaching of kraft pulp. Institute of Paper Science and Technology, Atlanta, GA.
- Zhang, Y-H. P., & Lynd, L. R. (2004). Toward an aggregated understanding of enzymatic hydrolysis of cellulose: Noncomplexed cellulase systems. *Biotechnology and Bioengineering*, 88(7), 797-824.

Chapter 3

BIOCHEMICAL CONVERSION OF BIOMASS TO BIOFUELS

Ximing Zhang¹, Arun Athmanathan² and Nathan S. Mosier^{1,}*

¹Laboratory of Renewable Resources Engineering,
Department of Agricultural and Biological Engineering,
Purdue University, West Lafayette, IN, US

²National Corn to Ethanol Research Center, Edwardsville, IL, US

ABSTRACT

Lignocellulosic biomass is a potentially rich resource for carbohydrates for biochemical conversion to biofuels. In this chapter, we outline the critical processing steps for lignocellulosic biofuel production: pretreatment, enzymatic hydrolysis, and mixed C5 and C6 ethanol fermentation. Pretreatment is necessary to convert the recalcitrant cellulose in biomass into a more reactive form. Both acid and alkali chemistries can be used to remove hemicellulose, remove and/or rearrange the lignin, and improve the accessibility of the β -1-4 glycosidic bonds that form the cellulose polymer to enzymatic attack. Enzymatic hydrolysis of cellulose requires multiple enzyme activities that work in concert to completely depolymerize cellulose to fermentable glucose. While glucose is the predominant sugar in lignocellulosic biomass, xylose from hemicellulose represents up to 40% of the total sugars. Fermentation to biofuels requires complete conversion of this five carbon sugar along with glucose in order for the process to be economically viable.

Keywords: pretreatment, cellulose, cellulase, fermentation, saccharomyces, distillation

1. INTRODUCTION

For the past few decades, significant efforts have been focused on developing technologies for the biochemical conversion of lignocellulose to liquid transportation fuels

* Corresponding author: mosiern@purdue.edu.

and chemicals (Jin et al., 2016; Jönsson, Alriksson, & Nilvebrant, 2013; Mosier et al., 2005; Ximenes, Kim, & Ladisch, 2013). The most prevalent utilization is conversion of lignocellulose to bioethanol production. Bioethanol is of great importance to complement gasoline use in the US (Lichts, 2011). Brazil and the United States lead the industrial production of ethanol fuel, accounting together for 83.4 percent of the world's production in 2014 (Renewable Fuels Association, 2015). However, corn starch and sugar cane sucrose are the primary sources of fermentable sugars while lignocellulose provides a small fraction of that total. Yue et al. gives a summary of current main commercial-scale cellulosic ethanol projects in the world in Table 1 (Yue, Wu, & Lin, 2014).

**Table 1. Commercial-scale cellulosic ethanol projects worldwide
(based upon Tables 1 and 2 from Yue et al., 2014)**

<i>Company & Country</i>	<i>Capacity (k ton/year)</i>	<i>Feedstock & Product</i>	<i>Process Technology</i>	<i>Operation Year</i>
Longlive, China	50	Corn cob residue; Ethanol + xylitol	Xylose isolated after dilute acid pretreatment for xylitol production, residue via enzymatic hydrolysis to hexose, fermentation to ethanol.	2012
Shengquan, China	20	Corn cob residue; Ethanol+furfural	Xylose isolated after dilute acid pretreatment for furfural production, enzymatic hydrolysis to hexose, fermentation to ethanol	2013
Beta-Renewable, Italy	60	Arundo; Ethanol & power	Steam explosion, enzymatic hydrolysis, C5/C6 co-fermentation	Oct. 2013
Ineos bio, US.	24	Plants and wood waste; Ethanol & 6MW power	Gasification & bacterial fermentation to ethanol	Aug. 2013
POET-DSM, US.	75	Corn stover/cob; Ethanol & biogas	Dilute acid pretreatment enzymatic hydrolysis C5/C6 co-fermentation	2014
Abengoa, US.	75	Corn stover, wheat straw; Ethanol & 18MW power	Dilute acid pretreatment enzymatic hydrolysis C5/C6 co-fermentation	2014
Tianguan, China	40	Corn stover, wheat straw; Ethanol + biogas	Batch steam explosion, enzymatic hydrolysis, hexose fermentation to ethanol, pentose to biogas	2014
DuPont, US.	83	Corn stover/cob; Ethanol	Ammonia pretreatment, enzymatic hydrolysis, C5/C6 co-fermentation	2015
Beta-Renewables, US.	60	Miscanthus, Switchgrass; Ethanol	Steam explosion, enzymatic hydrolysis C5/C6 fermentation	2015

Lignocellulose refers to plant cell wall tissues of woody crops, agricultural residuals, energy crops, and municipal solid wastes. Cellulose, hemicellulose, and lignin are the three main components of lignocellulosic materials (Rowell, 2012). Cellulose accounts for approximately 40-50% of dry weight of biomass (Mosier et al., 2005; Rowell, 2012). Cellulose is composed of linear polymers of D-glucose subunit linked by β -1,4 glycosidic bonds that form linear microfibrils of approximately 30-40 hydrogen bonded chains. These microfibrils have highly crystalline structures with native polymerization of approximately 10,000-15,000, which the plant assembles into larger structures in the cell wall (Yang, Dai, Ding, & Wyman, 2011).

Hemicellulose accounts for 23-35% of the dry weight in lignocellulosic biomass. Unlike cellulose, hemicellulose is a branched polymer with a linear backbone consisting typically of xylose. The branching side chains of hemicellulose can contain subunits such as D-xylose, D-mannose, D-galactose, D-glucose, L-arabinose, D-galacturonic, D-glucuronic, and 4-O-methyl-glucuronic acids as well as non-glycosides such as ferulates and *p*-coumarates (Carvalho, Duarte, & Gírio, 2008). Hemicellulose structure and composition varies significantly across major plant types (Zhao, Zhang, & Liu, 2012).

Lignin makes up approximately 15-28% of lignocellulosic biomass and is physically and/or chemically linked to both cellulose and hemicellulose to form a physical seal in the plant cell wall which improves plant strength and stiffness (Ritter, 2008). The phenyl propanoid subunits of lignin are covalently linked to form an amorphous heteropolymer that is not water soluble (Pérez, Munoz-Dorado, de la Rubia, & Martinez, 2002). Lignin has a complex structure with multiple types of bonds; the lignin molecule is random polymerized from three main subunits: *p*-coumaryl alcohol (hydroxyphenyl units, H), coniferyl alcohol (guaiacyl units, G), and sinapyl alcohol (sinapyl units, S). The random cross-linked subunits build up the amorphous three-dimensional lignin molecule biologically by enzyme-catalyzed oxidation (Boerjan, Ralph, & Baucher, 2003; Freudenberg & Neish, 1968; Hu et al., 1999; Humphreys & Chapple, 2002).

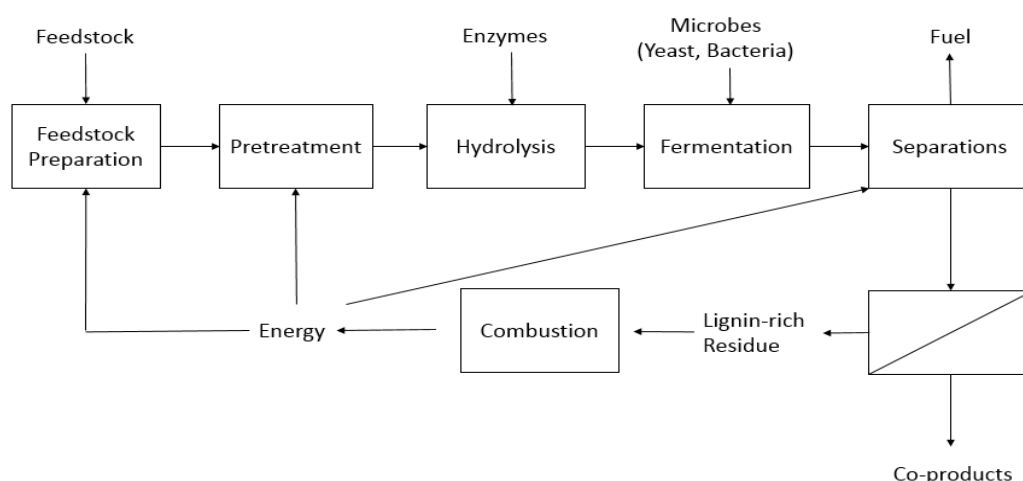


Figure 1. Block flow diagram of major unit operations in producing cellulosic ethanol.

Nearly all of the cellulosic bioethanol currently produced is made through a biological conversion pathway that consists of three unique processing steps: 1) pretreatment to disrupt the lignin and plant cell wall structure of lignocellulose, 2) enzymatic hydrolysis to release fermentable sugars from the cellulose and hemicellulose, and 3) bacterial or yeast fermentation to convert a mixture of 5 and 6 carbon sugars to ethanol (Figure 1).

This chapter will provide a review of current technologies and the current understanding of how these three processing steps make the production of cellulosic ethanol technologically and economically feasible. To make the process technically feasible, pretreatment is a key step which increases the enzyme-accessible surface area and reactivity of cellulose in order to enhance the subsequent enzymatic hydrolysis yields and rates of release of fermentable sugars (Sousa, Chundawat, Balan, & Dale, 2009; Mosier et al., 2005; Severian, 2008). The pretreated lignocellulosics are hydrolyzed by a complex mixture of enzymes that act synergistically to fully hydrolyze cellulose to fermentable glucose. Improvements to the production of these enzymes and the tailoring of the exact ratio of enzymatic activities to maximize yields and rates also have been crucial accomplishments to enable commercial production of cellulosic ethanol (Bras et al., 2011; Wyman, 2013). The polysaccharides in lignocellulose, cellulose and hemicellulose, contain both C6 and C5 sugars (primarily glucose and xylose), both of which must be fermented to ethanol at yields, rates, and final titers that allow recovery of fuel-grade ethanol, economically. Since no known microorganism in nature possess the appropriate characteristics, significant efforts were made to develop novel ethanologens (yeast and bacteria) capable of effectively producing ethanol from the mixture of sugars found in lignocellulose. Utilization of the separation stream products such as lignin-rich residue or byproducts derived from pretreatment such as furfural and 5-hydroxymethylfurfural is a research hotspot as these unutilized products would make bioethanol process more cost-effective (Ragauskas et al., 2014).

2. BIOMASS PRETREATMENT PROCESS

2.1. Necessity of Biomass Pretreatment and Source of Cellulose Recalcitrance

Plants naturally synthesize cell walls that are resistant to microbial and fungal degradation, as a result of which the complex polymer matrix of the plant cell wall resists the action of fungal or bacterial enzymes that hydrolyze cellulose and hemicellulose into monosaccharides. Due to this resistance-termed 'recalcitrance' - typical yields of glucose by enzymatic hydrolysis of native cellulose in minimally processed plant matter average below 10% (Mosier et al., 2005; Wyman et al., 2011). Pretreatments have been correspondingly developed to 1) enhance the rate of hydrolysis, 2) enhance the yield of monosaccharides from cellulose and hemicellulose, 3) lower the amount of enzymes needed to accomplish 1, 2, and 4) improve the material handling of the lignocellulose through the downstream processing steps (Kumar, Mago, Balan, & Wyman, 2009; Mosier et al., 2005; Zhu & Pan, 2010). Yang & Wyman pointed out the cellulose after pretreatment should achieve higher than 90% yields of sugar after 72 h enzymatic hydrolysis with enzyme loading less than 10 FPU/g cellulose (Yang & Wyman, 2008). Pretreatment processes reduce recalcitrance through a combination of carbohydrate (cellulose and/or hemicellulose) solubilization and depolymerization and the

removal or relocation of lignin, the mechanism varying between processes. The removal of hemicellulose from the microfibrils is thought to expose the crystalline cellulose core, which can be further hydrolyzed by cellulase enzymes. In addition, as the macroscopic rigidity of biomass is interrupted, the physical barriers to mass transport are decreased significantly (Himmel et al., 2007).

Lignin binds cellulosic fibers together in a composite structure with excellent mechanical and water resistive properties, but also reduces the accessibility of cellulose to enzymes (Wyman et al., 2005). Various studies reported cellulose hydrolysis was improved with increasing lignin removal, although differences were reported in the degree of lignin removal needed (Chum et al., 1988; Converse, 1993; Grethlein, 1984; Yang, Boussaid, Mansfield, Gregg, & Saddler, 2002). Douglas-fir was pretreated by 1% H₂O₂ to remove 90% of lignin and 45% hydrolysis improvement was achieved (Yang et al., 2002). With the same feedstock, by using pressurized oxygen and 15% NaOH, 84% lignin was removed and gave a 55% hydrolysis improvement (Pan, Zhang, Gregg, & Saddler, 2004). Another significant limitation of the effect of lignin is on swelling of the cell wall matrix through hydration, which then limits the accessibility of the cellulose to the enzymes (Mansfield, Mooney, & Saddler, 1999; Mooney, Mansfield, Touhy, & Saddler, 1998). Lignin has been shown to partially depolymerize and then redeposit on the surface of the cellular matrix during pretreatment, although no doubt in a different morphology that changes the impact of the lignin on cellulose digestion (Donohoe, Decker, Tucker, Himmel, & Vinzant, 2008; Ramos, Nazhad, & Saddler, 1993; Shevchenko, Beatson, & Saddler, 1999). Researchers also find the relocation of lignin through pretreatment also make significant improvement of hydrolysis even the lignin is removed by a small portion. For example, when douglas-fir was treated by cold 1% NaOH, only 7% of lignin was removed but yields a 30% improvement for hydrolysis (Pan, Xie, Gilkes, Gregg, & Saddler, 2005). The removal of lignin not only increased cellulose accessibility but also allowed more cellulase action (Chum et al., 1988). Kawamoto et al. found that lignin and its derivatives favored in precipitation and bonding with protein, and lignin in the condensed phase can adsorb protein from aqueous solutions (Kawamoto, Nakatsubo, & Murakami, 1992). Multiple phenomenon observed through studies show lignin can irreversibly adsorb cellulase physically and chemically, which make the hydrolysis step inefficient (Lu, Yang, Gregg, Saddler, & Mansfield, 2002). To overcome this problem, removal of lignin is a reasonable choice to facilitate enzyme hydrolyze cellulose and avoid enzyme nonspecific adsorption of lignin (Chum et al., 1988).

The chemical makeup and structure of lignin also affects the digestibility of the cellulose in plant tissue. Lignin that has altered monomer ratios through changes in the genes that synthesize these monomers (H, G, and S lignin units) has been shown to either decrease or increase recalcitrance to saccharification. Specifically, the ratio of syringyl to guaiacyl subunits (S/G ratio) in the lignin has been shown to be significant. Hybrid poplar with S/G ratio of 1.8 showed higher xylose release resulting from dilute acid hydrolysis compared to native poplar with S/G ratio of 2.3, even though the total lignin content was approximately the same (Davison, Drescher, Tuskan, Davis, & Nghiem, 2006).

In addition to lignin, the structure and presence of hemicellulose affects the ability of cellulolytic enzymes to release fermentable sugars from cellulose. Separation of hemicellulose from cellulose also enhances pore size as well as reduces the cellulose crystallinity. Both aspects make the cellulose hydrolysis step more efficient (Galbe & Zacchi, 2007). Besides, removing hemicellulosic sugars separated from the cellulosic sugar (glucose)

results in two different processing streams that contain fermentable sugars. This can add to overall processing costs. Hemicellulose is naturally acetylated in many varieties of biomass and the degree of acetylation has been shown to correlate negatively with cellulose digestibility (Kumar & Wyman, 2009a). Hemicellulose deacetylation can significantly increase the cellulose digestibility; however, the degree of hemicellulose deacetylation to make significant cellulose digestibility is controversial (Teixeira, Linden, & Schroeder, 2000; Kim & Lee, 2005). Yang et al. in his review summarized some conflicting conclusions from multiple groups on the degree of removal of hemicellulose in effectively changing the cellulose digestibility (Yang et al., 2011). Grohmann et al. pointed out that after removal of 75% of acetyl groups, the effectiveness is regressive; while Kong et al. reported there are improvements up to full removal of hemicellulose (Grohmann, Mitchell, Himmel, & Dale, 1989; Kong, Engler, & Soltes, 1992). This is hypothesized to be because lignin can physically and chemically interact with the acetyl groups which may hinder hydration of the matrix and removal of the lignin (Chang & Holtzapfel, 2000).

Pretreatment processes are also optimized to minimize degradation of the sugars into non-fermentable compounds. For example, when harsh conditions are used, degradation of C5 and C6 sugars will generate furan derivatives. Sufficient amounts of any by-products generated through the pretreatment step can severely inhibit the downstream processing steps like enzymatic hydrolysis and microbial fermentation. The inhibitors can be classified as mainly four categories: phenolic compounds, weak acids, furan derivatives, and inorganic compounds (Casey, Sedlak, Ho, & Mosier, 2010).

Pretreatment processes should be able to treat biomass from a wide variety of plant sources and enable biorefineries to utilize a variety of feedstocks as growing seasons, availability, and costs change over time. For example, acid-catalyzed pretreatments are more effective across variations in lignocellulose sources and characteristics, but it is relatively expensive (Mosier et al., 2005). Alkali-catalyzed pretreatment is effective in reducing the lignin content for agricultural residues but less effective on softwoods (Chandra et al., 2007).

2.2. Mechanisms of Pretreatment

The major obstacle in effective lignocellulose utilization is its unreactivity, specifically towards depolymerizing enzymes. Pretreatments increase the digestibility of substrates by different mechanisms; however, it is clear that the increase of cellulose accessibility is resulted by modification of chemical compositions in couple with alteration of physical structures. Increasing accessible surface area of cellulose to cellulases is the primary objective of pretreatment. Accessibility of the substrate to the cellulolytic enzymes is one of the major factors influencing hydrolysis process. Thus, one of the main objectives of the pretreatment is to increase the available surface area for the enzymatic attack. Previous studies have concluded that the pore size of the substrate in relation to the size of the enzymes is the main limiting factor in the enzymatic hydrolysis of lignocellulosic biomass (Chandra et al., 2007). Pretreatment processes can significantly increase porosity in the biomass which improves the hydrolysis rates and yields. Several review papers pointed out the role of glucan accessibility and its change with conversion, with a few studies showing that glucan accessibility becomes limiting with conversion (Kim, Jia, & Wang, 2006) and others showing no significant decrease of accessibility with conversion or even no change at all (Kumar & Wyman, 2009b).

Table 2. Methods for lignocellulosic pretreatment
(Compiled from Verardi et al., 2012, Kumar et al., 2009, and Mosier et al., 2005)

<i>Pretreatment</i>	<i>Method</i>	<i>Operating conditions</i>	<i>Advantages</i>	<i>Disadvantages</i>
Physical	Chipping Grinding Milling	Room temperature Energy input < 30Kw per ton biomass	Reduces cellulose crystallinity	Power consumption higher than inherent biomass energy
Chemical	Steam pretreatment	160-260°C (0.69- 4.83MPa) for 5-15 min	Causes hemicellulose auto hydrolysis and lignin transformation; cost-effective for hardwoods and agricultural residues	Destruction of a portion of the xylan fraction; incomplete disruption of the lignin-carbohydrate matrix; generation of inhibitory compounds; less effective for softwoods
	CO ₂ explosion	4 kg CO ₂ /kg fiber at 5.62 Mpa 160 bar for 90 min at 50°C under supercritical Carbon dioxide	Increases accessible surface area, does not cause formation of inhibitory compounds	It is not suitable for biomass with high lignin content (such as woods and nut shells). Does not modify lignin neither hydrolyze hemicelluloses
	Liquid hot water	200-230°C up to 15 min	Reduces lignin content; removes most of the hemicellulose; no need to neutralize the waste; no chemical cost.	Generate acetic acid and other organic acids.
	Ozonolysis	Room temperature	Reduces lignin content; does not produce toxic residues	Expensive for the ozone required
	Wet oxidation	148-200°C for 30 min	Efficient removal of lignin; low formation of inhibitors; low energy demand	High cost of oxygen and alkaline catalyst
	AFEX (Ammonia fiber Expansion)	90-140°C for 30 min. 1-2 kg ammonia /kg dry biomass	Increases accessible surface area	Does not modify lignin neither hydrolyzes hemicellulose;
	ARP (Ammonia Recycled Percolation method)	150-170°C for 14 min. Fluid velocity 1 ml/min	Increases accessible surface area, removes lignin and hemicellulose	Does not modify lignin neither hydrolyzes hemicellulose;

Table 2. (Continued)

<i>Pretreatment</i>	<i>Method</i>	<i>Operating conditions</i>	<i>Advantages</i>	<i>Disadvantages</i>
	Acid hydrolysis: dilute-acid pretreatment	Type I: T>160°C, continuous-flow process for low solid loading 5-10%,- Type II: T < 160°C, batch process for high solid loadings (10-40%)	Hydrolyzes hemicellulose to xylose and other sugar; alters lignin structure	Equipment corrosion; formation of toxic substances
	Alkaline hydrolysis	Room temperature; Long time high. Concentration of the base; For soybean straw: ammonia liquor (10%) for 24 h at room temperature	Removes hemicelluloses and lignin; increases accessible surface area	Residual salts in biomass
	Organosolv	150-200°C with or thout addition of catalysts (oxalic,	Hydrolyzes lignin and hemicelluloses	High costs due to the solvents recovery
		salicylic, acetylsalicylic acid)		
Biological		Several fungi (brown-, white- and soft-rot fungi)	Degrades lignin and hemicelluloses; low energy requirements	Slow hydrolysis rates

A wide spectrum of pretreatment protocols has been investigated for hydrolysis and only a few of these have been developed sufficiently to be called technologies. A variety of pretreatment procedures have been evaluated for their effectiveness towards cellulose biodegradation and possibly the suitability of pretreatment procedures may vary depending on the raw material selected. Kumar et al. has summarized some major pretreatment technologies (Table 2). The selection of a pretreatment method has an impact on the subsequent enzymatic hydrolysis and must be based on various considerations. To commercialize pretreatment technology, the economic and technical aspect will account great potential. For example, biological pretreatment, which is known for delignification by using enzymes such as lignin peroxidase, manganese peroxidase, and laccase which can be derived from fungi, has a significant disadvantage that large amount of space and substantial longer residence time (10-14 days) are required which make it less attractive and difficult to commercialize (Himmel et al., 2007).

No matter which pretreatment technology is used, a pre-pretreatment step, called physical pretreatment, is widely adopted. Physical pretreatment refers to the process of mechanical

comminution by a combination of chipping, grinding, and milling (Mosier et al., 2005). The size of the feedstock is usually 10-30 mm after chipping and 0.2-2 mm after milling or grinding (McMillan, 1997). Size reduction is associated with increase of specific surface area (SSA) (Zhu, 2011). Yeh et al. studied that after media milling, particle size of microcrystalline cellulose was decreased from 25.52 μm to 0.78 μm and the SSA increased from 0.24 m^2/g to 25.50 m^2/g (Yeh, Huang, & Chen, 2010).

Mosier et al. summarized the features of promising technologies for pretreatment of lignocellulosic biomass (Mosier et al., 2005), in which several pretreatment technologies were described in detail. In this chapter, in regard to large scale application for practical applications in biorefineries, the pretreatment technologies mainly fall into three categories: acidic pretreatment, alkaline pretreatment, and solvent assisted pretreatment.

2.3. Acid-Catalyzed Pretreatment

Acid-catalyzed pretreatment of biomass has long been recognized as a critical technology to produce materials with acceptable enzymatic digestibilities (digestibilities >80% are routinely obtained) (Schell, Farmer, Newman, & McMillan, 2003). Acid-catalyzed pretreatments are usually further classified by whether or not Brønsted acid catalysts, such as sulfuric or hydrochloric acid, are added or whether the acidic environment of water at high temperatures or the acids released from the biomass (e.g., acetic acid from acetylated hemicellulose) are the catalytic agents (Mosier et al., 2005).

The uncatalyzed steam explosion is conducted by using high-pressure saturated steam and the pressure is swiftly reduced, making the materials undergo an explosive decompression (Sun & Cheng, 2002). Steam explosion has been described as a thermo-mechano-chemical process, because the massive disruption of lignocellulosic structure is aided by heat of steam (thermo), shear forces due to the expansion of moisture (mechano), and hydrolysis of glycosidic bonds (chemical) (Chornet & Overend, 1991), which leads to cleavages of some accessible glycosidic links, β -ether linkages of lignin and lignin-carbohydrate complex bonds, and minor chemical modifications of lignin and carbohydrate (Glasser & Wright, 1998). More specifically, during auto-catalyzed steam explosion, a significant portion of the hemicellulose is hydrolyzed and releases organic acids such as acetic acid and uronic acid (Jeoh, 1998). Under acidic conditions, lignin is partially degraded through the hydrolytic cleavage of β -O-4 ether and other acid-labile linkages (Ramos, 2003). The cellulose surface becomes exposed after hemicelluloses are removed from the microfibrils (Kabel, Bos, Zeevalking, Voragen, & Schols, 2007). During steam pretreatment, lignin is not removed from the solid matrix but it is redistributed on the fiber surfaces because of melting and depolymerization and repolymerization reactions (Li, Henriksson, & Gellerstedt, 2007). However, sugar degradation also inevitably happens during steam explosion to form furfural and 5-hydroxymethylfurfural, both of which show strong inhibitions to microorganisms in subsequent fermentations.

Similar to steam explosion pretreatment, liquid hot water pretreatment uses water as media to pretreat biomass under pressures to maintain the water in the liquid state at elevated temperatures (Kumar, Barrett, Delwiche, & Stroeve, 2009; Mosier, Hendrickson, Ho, Sedlak, & Ladisch, 2005; Weil et al., 1997). This pretreatment is also sometimes called hydrothermolysis. It removes approximately 40-60% of the total biomass with 4-22% of the

cellulose and nearly all of the hemicellulose to form liquid soluble oligosaccharides (Athmanathan, Emery, Kuczek, & Mosier, 2015). The decrease in cellulose crystallinity, lower association of cellulose with lignin, and depolymerization of cellulose by liquid hot water pretreatment also contribute to the enhancement of cellulose accessibility (Kumar et al., 2009). Organic acids are formed by cleavage of O-acetyl and uronic acid substitutions from hemicellulose, which further help to catalyze hemicellulose solubilization (Mosier et al., 2005). Most of the acetyl groups can be cleaved at high temperature, whereas only partial deacetylation is found to occur at moderate treatment temperature (Tjeerdsma & Militz, 2005). Lignin is partially depolymerized and solubilized but complete delignification is not possible using hot water alone, since water cannot dissolve lignin well (Donohoe, Decker, Tucker, Himmel, & Vinzant, 2008).

Dilute aqueous acid pretreatment has received considerable attention over the past several decades. It is the main technology used in the commercial scale cellulosic bioethanol production facility. In dilute acid pretreatment, a mineral acid such as sulfuric acid, is dissolved in water to a concentration in between 0.5% to 5% (w/w). As is true for all acid-catalyzed pretreatments, hemicellulose is hydrolyzed to monosaccharides and the sugars can be further degraded to form other products such as furfural and 5-hydroxymethylfurfural. It has been thought that the increase of cellulose accessibility by dilute acid pretreatment is mainly attributed to the removal of hemicellulose; however, dilute acid pretreatment under mild conditions (<120°C) can remove most of hemicellulose, but the cellulose digestibility is only somewhat increased (Xu, Zhang, Sharma-Shivappa, & Eubanks, 2012; Zhao et al., 2012; Xiao, Zhang, Wang, Niu, & Han, 2015). Higher temperature should be employed to further disrupt the biomass structure, especially lignin. Therefore, effective dilute acid pretreatment is usually conducted at temperatures between 160 and 220°C for periods ranging from minutes to seconds to significantly disrupt and redistribute lignin in cell wall (Yang & Wyman, 2004). However, under acid conditions, lignin can quickly condense and precipitate onto solid surface and this condensation reaction become more pronounced with higher acid concentrations or at higher reaction temperatures (Shevchenko, Beatson, & Saddler, 1999). The monomeric sugars under acidic condition also tend to have condensation reaction which makes side reaction products called humins (Zhang, Hewetson, & Mosier, 2015; Hu, Jung, & Ragauskas, 2012; Kumar et al., 2013; Sannigrahi, Kim, Jung, & Ragauskas, 2011).

2.4. Alkaline Pretreatment

Alkaline pretreatment involves the processes with various alkalis or bases such as NaOH, KOH, aqueous ammonia, and lime to pretreat biomass. It is believed that during alkaline pretreatment the intermolecular ester bonds cross-linking xylan hemicellulose and lignin are saponified, thus resulting in delignification of biomass (Sun & Cheng, 2002). Removal of lignin increases access to the remaining polysaccharides and eliminates nonproductive adsorption of cellulases (Zhang, Xu, & Cheng, 2011). Alkaline pretreatment also causes the depolymerization of lignin molecules by cleavage of inner-molecular α - and β -aryl ether linkages, which essentially contributes to lignin degradation (Xu, Zhang, & Cheng, 2012). Especially, the cleavage of β -O-4 linkages leads to the formation of new phenolic hydroxyl groups, causing substantial decrease in the molecular mass of residual lignin and imparting it a more hydrophilic character (Naik, Goud, Rout, & Dalai, 2010). Moreover, during alkaline

treatment, cellulose undergoes some hydration, depending on the reaction temperature and alkali concentration. Alkalis are good agents to swell cellulose and alter cellulose crystalline polymorphs (Agbor, Cicek, Sparling, Berlin, & Levin, 2011).

Alkali pretreatment may be carried out at room temperature, but pretreatment times at these low temperatures are measured in terms of hours or days rather than minutes or seconds (Mosier et al., 2005; Kumar et al., 2009; Zhang, Xu, & Cheng, 2011). This is because during alkaline pretreatment, some of the alkali is irreversibly converted to salts or incorporated as salts into biomass (Chou, Lu, & Lee, 2005).

Pretreatment processes based on alkaline rapid decompression have been proposed with considerable success. The alkaline process, known as ammonia fiber expansion (AFEX), partially displaces hemicellulose and lignin to the surface of the biomass, generating walls that are considerably more amendable to enzyme hydrolysis (Alizadeh, Teymouri, Gilbert, & Dale, 2005; Chundawat et al., 2011). During the pretreatment, lignocellulosic materials is permeated with liquid ammonia followed by increasing temperature to about 90°C or above (Mosier et al., 2005; Kumar et al., 2009). The formed gas ammonia interacts with biomass under pressure and the pressure is then rapidly released, which results in cellulose decrystallization, hemicellulose prehydrolysis, and alternation of lignin structure (Chundawat et al., 2011).

2.5. Solvent-Assisted Pretreatment

Solvent-assisted pretreatments mainly fall in two categories: organosolv and cellulose-solvent-based pretreatments. Organosolv pretreatment refers to the process to pretreat lignocellulosic feedstocks in organic solvents or their aqueous solution systems with or without added catalysts in temperature range of 100-250°C (Zhao et al., 2009). Organosolv pretreatment uses solvents such as methanol, ethanol, acetone, ethylene glycol, triethylene glycol, and phenols (Galbe & Zacchi, 2007). In a typical experiment, the solvent (such as ethanol) mixed with water (~40-60: 50 w/w), added sulfuric acid as catalyst, with a liquid to solid ratio of 7-10:1 with desired temperature (Pan et al., 2005). Organosolv pretreatment extensively removes lignin and hemicellulose, with resulting increase of accessible surface area and pore volume. The biomass structure becomes loosened after organosolv pretreatment due to lignin and hemicellulose dissolution thus increasing the adsorption of cellulase enzymes onto solid substrates (Koo et al., 2011). The lignin degradation and dissolution during organosolv pretreatment are mainly attributed to the hydrolysis of the internal bonds in lignin as well as lignin-hemicellulose bonds (ether and 4-O-methylglucuronic acid ester bonds to the α -carbons of the lignin units) (Zhao et al., 2009). More specifically, cleavage of ether linkages is the major factor in lignin breakdown.

In recent years, pretreatment of lignocellulosic biomass based on cellulose solvents has attracted attention due to the substantial increase of cellulose hydrolysis rate and degree after pretreatment. The solvents that have received the most attention in pretreatment of lignocellulose are concentrated phosphoric acid (CPA) and ionic liquids (IL). A biomass fractionation process based on CPA has been successfully applied to pretreat pure cellulose substrate, corn stover, switchgrass, hybrid poplar, douglas fir, reed, and bamboo (Zhang et al., 2007). For corn stover, before CPA treatment, the plant cell wall structures and elementary cellulose fibers can be clearly identified, but after pretreatment, no fibers structures can be

observed, which indicates that CPA not only disrupts all linkages among cellulose, hemicellulose, and lignin, but also breaks up the orderly hydrogen bonds among glucan chains (Zhang et al., 2007). After precipitated from CPA, cellulose becomes completely amorphous and contains little lignin and hemicellulose. This amorphous cellulose thus shows a very high hydrolysis rate even with an enzyme loading as low as 5 FPU/g glucan, because of the breakup of highly ordered hydrogen-bonding networks and resulting significant increase of accessible surface area (Sathitsuksanoh, Zhu, Wi, & Zhang., 2011).

IL is another solvent for cellulose dissolution, since ILs can dissolve large amount of cellulose under considerably mild conditions (Dadi, Schall, & Varanasi, 2007; Dadi, Varanasi, & Schall, 2006; Zheng, Pan, & Zhang, 2009). Some hydrophilic ionic liquids, for example, 1-butyl-3-methylimidazolium chloride (BMIMCl) and 1-allyl-3-methylimidazolium chloride (AMIMCl) were proven to be effective ILs for biomass pretreatment (Zhu et al., 2006; Zhu, 2008). After regeneration from solution, the regenerated cellulose has the same or lower DP compared with the initial cellulose, but significantly different macro and micro structure, especially for the degree of crystallinity (Dadi et al., 2007; Dadi et al., 2006). Being similar to CPA, ILs increase cellulose accessibility by breakup both inter- and intra-molecular hydrogen bonds networks, resulting in the increase of accessible binding sites of cellulose for cellulase enzymes. While cellulose solvents are highly effective at producing very reactive cellulose, the costs of the solvents and/or the costs for recycling the solvents have hindered the adoption of these approaches beyond the laboratory scale.

Shi et al. demonstrated a one-pot, wash-free process with combined the IL pretreatment and saccharification into a single vessel (Shi et al., 2013). 1-ethyl-3-methylimidazolium acetate ([C2mim][OAc]) was used to treat switchgrass, and then subsequently water diluted to a IL slurry with concentration of 10%. The thermostable IL tolerant enzyme cocktail (enzyme loading of 5.75 mg g⁻¹ of biomass) was added to directly hydrolyze the slurry. The glucose and xylose were liberated at yield of 81.2% and 87.4% after 72 h at 70°C and separated by liquid-liquid extraction with over 90% efficiency. The one-pot, wash-free approach reduces the cost of the IL solvents and recycling steps and makes IL pretreatment promising for further development.

Pretreatment typically solubilizes a fraction of the available carbohydrates and renders a larger fraction vulnerable to enzymatic action. It is followed by the conversion of the polysaccharides into more soluble monosaccharides, typically termed hydrolysis.

3. ENZYMATIC HYDROLYSIS USING BIOMASS DEGRADING ENZYMES

Enzymatic hydrolysis refers to the process of depolymerizing carbohydrates to monomeric sugars by means of a protein catalyst with high selectivity operating under mild temperatures and pH. Enzymatic hydrolysis using amylases is typically carried out to convert grain starches into monosaccharides. In case of lignocellulose, it involves the conversion of cellulose and hemicellulose into their component monosaccharides using a family of enzymes collectively termed '(hemi) cellulases'. Compared to enzymatic hydrolysis, chemical hydrolysis, mainly referring to acid hydrolysis, requires harsh reaction conditions, resulting in low selectivity due to side reactions with monosaccharides and equipment corrosion (Rinaldi & Schüth, 2009; Bhosale, Rao, & Deshpande, 1996; Yang et al., 1996). However,

commercialization of enzymatic hydrolysis in industry faces several issues, chiefly the low stability of the enzyme under extreme reactions conditions and difficulties in its recovery and purification for re-use (Verardi, Ricca, De Bari, & Calabrò, 2012).

3.1. Cellulase Mechanistic Action during Enzyme Hydrolysis

Cellulase is a combination of enzymes mainly includes endoglucanases, exoglucanases or cellobiohydrolase, and β -glucosidase. During the hydrolytic process, insoluble cellulose is first depolymerized by endoglucanases and cellobiohydrolases to release shorter oligosaccharide molecules synergistically. The released short chains (short cello-oligosaccharides and cellobiose) are further cleaved by β -glucosidase to generate soluble glucose. The accessory enzymes such as hemicellulases and pectinases also synergistically facilitate the cellulose decomposition.

3.2. Fungal vs. Bacterial Based Cellulase

In order to significantly improve the efficiency of enzymatic hydrolysis of cellulosic biomass and lower costs, approaches have been taken to find more robust enzymes and advance the understanding of enzyme interactions with cellulosic biomass. In nature, various cellulolytic microorganisms produce enzymes that function synergistically and associate with the microorganism (such as cellulosomes) or act independently (such as most fungal and many bacterial cellulases).

Based on different composition of lignocellulose, corresponding enzymes are discovered responsible to degrade the lignocellulosic components to monomers. Table 3 lists various enzymes effective in degrading the corresponding biopolymers in biomass. However, researchers found it is not limited to the enzymes listed in Table 3 that are responsible for degradation of the corresponding biopolymer, some proteins may also contribute the degradation with unclear mechanism. For example, a protein named *Zea h* secreted from *Z. mays* itself doesn't have cellulase activity but has synergistic effect with cellulases on cellulose hydrolysis (Han, & Chen, 2007).

Table 3. Major enzyme for degrading lignocellulose
(Table 2 from Van Dyk & Pletschke, 2012)

Lignin	Laccase, Manganese peroxidase, Lignin Peroxidase
Pectin	Pectin methyl esterase, pectate lyase, polygalacturonase, rhamnogalacturonan lyase
Hemicellulose	Endo-xylanase, acetyl xylan esterase, β -xylosidase, endo-mannanase, β -mannosidase, α -L-arabinofuranosidase, α -glucuronidase, ferulic acid esterase, α -galactosidase, p-coumaric acid esterase
Cellulose	Cellobiohydrolases, endoglucanases, β -glucosidase

As cellulose and hemicellulose together in lignocellulose account for 60-70% of the carbohydrate mass, which can be hydrolyzed into fermentable sugars, understanding cellulases and hemicellulases functions is of great importance (Gellerstedt, Li, Kleinert, &

Barth, 2008). Hydrolysis of hemicellulose is more complicated than hydrolysis of cellulose. Hemicellulose consists not only of carbohydrates such as xylose, mannose, galactose, arabinose, and glucose, but also substituent moieties such as acetyl groups, ferulates, etc. These components are interconnected and thus the enzyme cocktail showed in Table 3 is needed to hydrolyze the hemicellulose into sugar monomers synergistically (Meyer, Rosgaard, & Sorensen, 2009).

The cellulases and hemicellulases are mainly secreted from bacteria or fungi. However, different strategies for degrading cellulose are used by various microorganisms. They mainly fall two categories: complexed and non-complexed cellulase system (Lynd, Weimer, van Zyl, & Pretorius, 2002; Verardi et al., 2012; Sun & Cheng, 2002). Aerobic bacteria and fungi, such as *Trichoderma reesei* and *Aspergillus niger*, secrete soluble extracellular enzymes known as non-complexed cellulase system (Zhang & Lynd, 2004); anaerobic cellulolytic microorganisms, such as *clostridia*, *Butyrivibrio fibrisolvens*, *Acetovibrio cellulolyticus*, *Bacteroides cellulosolvens*, *Ruminococcus albus*, and *Ruminococcus flavefaciens*, produce complexed cellulase systems, called cellulosomes (Bayer, Chanzy, Lamed, & Shoham, 1998; Van Dyk & Pletschke, 2012; Verardi et al., 2012). The cellulosomes consist of multiple hemicellulases, cellulases, and lichenases.

3.3. *Trichoderma reesei* and Its Cellulase Systems

Generally, *T. reesei* secretes at least two cellobiohydrolases (CBHI and CBHII), five to six endoglucanases (EGI, EGII, EGIII, EGIV, EGV, and EGVI), two β -glucosidases (BGL I and II), two xylanases, and various accessory hemicellulases (Vinzant et al., 2001). The effectiveness of cellulase components acting on insoluble substrates, and especially crystalline cellulose, is affected by the proportion of these components, with some ratios being particularly effective due to their synergistic action (Henrissat, Driguez, Viet, & Schulein, 1985; Kanda, Wakabayashi, & Nisizawa, 1980). There are three kinds of enzymes that act together to hydrolyze cellulose into glucose: endo-1,4- β -glucanases, exo-1,4- β -glucanases (cellobiohydrolases), and β -glucosidases (cellobiases) (Ximenes et al., 2013).

Crystalline cellulose is hydrolyzed by the synergistic action of endo-acting (with respect to the cellulose chain) enzymes known as endoglucanases, and exo-acting enzymes, known as exo-glucanases. The endoglucanases locate surface sites at locations, probably found randomly, along the cello-dextrin and insert a water molecule in the β -(1, 4) bond, creating a new reducing and non-reducing chain end pair. β -D-glucosidases (cellobiases) act to hydrolyze cellobiose, the product of cellulase action, and thus relieve the system from end-product inhibition. Exoglucanases or cellobiohydrolase attack cellulose chain ends and hydrolyze the 1, 4-glycosidyl linkages to form cellobiose. Endo-1, 4- β -glucanases attacks low crystallinity regions in the cellulose fibers by endoaction, decreasing the degree of polymerization and creating free chain-ends. β -glucosidase converts cello-oligosaccharides and disaccharide cellobiose into glucose residues in a processive manner (Verardi et al., 2012).

3.4. Enzymatic Hydrolysis Process

During hydrolysis of a substrate, enzymes adsorb onto the substrate, desorb and re-adsorb again, dynamically equilibrating between the solid and the liquid fractions of the reaction medium. It has been indicated that the extent of adsorption affects the rate and extent of hydrolysis and that adsorption is a prerequisite in enzymatic hydrolysis of cellulose (Ximenes et al., 2013). Various factors are said to affect adsorption, including substrate characteristics such as the presence of lignin, the method of pretreatment, as well as surface area and pore volume in the substrate. From reports in the literature, it appears that the characteristics of the enzymes also play a role in adsorption behavior (Lynd et al., 2002).

Enzymes represent a significant cost in bioconversion and therefore the total amount of protein used in saccharification is important (Van Dyk & Pletschke, 2012). The efficiency of the process can be measured as the amount of sugars produced per mg protein applied per g of cellulose. In addition to enzyme loadings, substrate loadings are a factor in making bioconversion economical and have to be high enough to achieve sufficient sugar concentrations for fermentation and to yield a high ethanol concentration. Thus the optimal enzyme and substrate loadings have to be identified for optimal efficiency and economy (mg of protein/g of substrate).

Enzyme loading may differ depending on the specific substrate and its composition, as well as the type of pretreatment. Substrates with a high lignin composition may require higher enzyme loadings due to non-productive adsorption of enzymes to the lignin portions (Ximenes, Kim, Mosier, Dien, & Ladisch, 2011). Enzyme loading may also depend on whether the enzyme combination is optimal for the substrate.

Pretreatments used on substrates may also have an impact on the enzyme loadings (Kumar et al., 2009e). For example, Wyman et al. (2011) found that higher protein loadings were required for alkaline pretreated switchgrass, whereas dilute acid, SO₂, and liquid hot water pretreated solids required lower enzyme loadings for the same levels of hydrolysis. This was related to the hemicellulose content remaining after pretreatment which required additional enzymes such as xylanases (Wyman et al., 2011).

Several factors can reduce enzyme loading. Washing of the substrate to remove any inhibitory compounds prior to enzyme hydrolysis can lead to reduced enzyme loading, as well as the addition of compounds such as Tween 20, BSA, and PEG 6000 which reduce non-productive adsorption of enzymes to residual lignin (Yang & Wyman, 2006; Kumar & Wyman, 2009d; Ximenes et al., 2011, 2013). Cellulase loadings can be reduced if xylanases are added which improves overall cellulose digestion; in the same manner, supplementation with β -glucosidase can reduce cellulase loadings by removing cellobiose which would inhibit cellulases (Wyman et al., 2011). Inhibition of enzymes such as β -glucosidase can also be overcome by the type of process used in bioconversion, such as SSF, where glucose is immediately converted into ethanol. Such processes can therefore also assist in reducing enzyme loadings. Enzyme loadings can also be reduced by using enzymes with higher specific activity. Enzyme recycling over several batches can also reduce enzyme loading (Tu et al., 2006).

3.5. Enzymatic Hydrolysis Process Challenge

During the pretreatment, especially under acidic environment, by-products generated through the pretreatment step can severely inhibit on the following enzymatic hydrolysis and fermentation processes. The inhibitors can be classified as mainly four categories: phenolic compounds, aliphatic acids, furan derivatives, and inorganic compounds (Casey et al., 2010). For the group of inhibitors aliphatic acids, referring to acetic acid, formic acid, and levulinic acid. All of these three aliphatic acids relate to sugar degradation during the pretreatment. Formic acid is a product of hydrolysis of HMF (5-hydroxymethylfurfural) and furfural. Levulinic acid is a degradation product from HMF. The yeast *S. cerevisiae* commonly used for fermentation can be deactivated by binding with all these acids. Acetic acid is a weak acid generated by hydrolysis of acetyl groups of hemicellulose (Palmqvist, & Hahn-Hägerdal, 2000a, 2000b). Acetic acid has negative impact on fermentative performance of microorganisms by inhibition of biomass growth, substrate consumption and ethanol volumetric productivity (Casey et al., 2010). The furan derivatives mainly refer to HMF (degraded from glucose) and furfural (degraded from xylose). The inhibition caused by these compounds and phenolic compounds are similar to acetic acid, including reduced growth rate of yeast and decreased ethanol yield and productivity (Larsson, Reimann, Nilvebrant, & Jönsson, 1999; Lee, Chung, & Willis, 1985; Liu et al., 2004).

Enzyme activity may be affected by the products of their own actions as well as the products formed by other enzymes (Ximenes et al., 2011). Jing, Zhang, and Bao (2009) reported the inhibition strength by the lignocellulose degradation products to cellulase is lignin derivatives > furan derivatives > organic acids > ethanol. Ximenes et al., (2011) reported that water-soluble phenol derivatives from lignin deactivate up to 80% of cellulase activity within 24 hours. The degree of deactivation varied between the species of fungus from which the enzyme was produce and specific enzyme, with b-glucosidase being the most sensitive (Ximenes et al., 2011). Szengyel and Zacchi (2000) studied the effect of acetic acid and furfural on cellulase production from *T. reesei* RUT C30 by using steam-pretreated willow as the carbon source, results showed that furfural could cause a significant decrease in both cellulase and β -glucosidase production (Szengyel, & Zacchi, 2000). As the inhibitors can decrease the enzyme activity during the enzymatic hydrolysis, washing the solid fraction with excess water prior to enzymatic hydrolysis proved to be an effective method; alternatively, fermenting the prehydrolysate prior to enzymatic hydrolysis also can increase the cellulose conversion yield (Tengborg, Galbe, & Zacchi, 2001). Separation technologies were tested to detoxify a dilute acid pretreated biomass slurry by sequential using polyelectrolyte polymer adsorption and resin-wafer electrodeionization. Results showed acetic acid, HMF and furfural could be removed by 77%, 60% and 74% respectively, and a 94% cellulose conversion yield can be achieved (Gurram, Datta, Lin, Snyder, & Menkhaus, 2011). During SSF or CBP processes, the ethanol formed may also have an inhibitory impact on enzymes as well as on the organisms involved in the following fermentation (Hahn-Hägerdal, Galbe, Gorwa-Grauslund, Lidén, & Zacchi, 2006).

For the aspect of substrate, the moisture content of the substrate can affect the ability of enzymes to hydrolyze it and drying of a substrate can result in decreased hydrolysis, this is related to a collapse in the pore structure, which probably causes a reduction in total surface area (Chandra et al., 2007). According to Ding et al. (2008), dehydration has a significant effect on the structure and arrangement of cell wall micro fibrils (Ding et al., 2008). It is

indicated that there is a relationship between drying of the substrate and adsorption capacity. The standard NREL protocol for enzymatic degradation of biomass indicates that no drying must take place after aqueous pretreatments, as it will cause “irreversible pore collapse in the microstructure” which will decrease hydrolysis (Selig et al., 2008). Drying can cause an irreversible loss of water binding ability which results in a loss of pores. The pores are indicated to be more important for accessibility of the enzymes than the external surface area (Luo & Zhu, 2011). Zhang & Lynd (2004) indicated that pore sizes should be large enough to accommodate a typical enzyme with a 51 Å diameter. Although rehydration may increase the surface area, pores are not restored (Zhang & Lynd, 2004).

Through enzymatic hydrolysis step, product inhibition and nonproductive binding to lignin need ten to hundred times of theoretical enzyme loading to gain high sugar yield to compensate the inhibition effect (Wyman et al., 2013). In order to have high sugar yield, the cellulase dose costs around \$1.00/gal ethanol (\$1.50/gal equivalent gasoline) (Klein-Marcuschamer, Oleskowicz-Popiel, Simmons, & Blanch, 2012), which further weakens the profitability of cellulosic ethanol especially when the gasoline price is low. To deal with this issue, many scientists are focusing on mitigating pretreatment side effects on enzymes and develop methods to reuse the enzymes. On the other hand, adaptation of enzyme to make it more resistant to inhibitors and reduce their production cost are research hot topics (Ximenes et al., 2011). Understanding the inhibition behavior of enzymes is a key factor in achieving optimal hydrolysis as steps may be taken to prevent or remove the inhibitory compounds.

3.5.1. Product Inhibition

During enzymatic hydrolysis, oligosaccharides, disaccharides and monomers are formed and may cause inhibition of the enzymes involved when they reach high concentrations, impacting enzymatic hydrolysis efficiency. According to García-Aparicio et al. (2006), inhibition by sugars have a greater impact than pretreatment inhibitors (García-Aparicio et al., 2006). This is the advantage of processes such as SSF where inhibition is prevented by the direct fermentation of sugars as they are produced.

It has been well documented that enzymes are inhibited by the products of their action. Cellulases are inhibited by cellobiose (Gruno, Våljamäe, Pettersson, & Johansson, 2004), while β -glucosidases is inhibited by glucose (Andrić et al., 2010). For this reason, excess β -glucosidase is generally added to cellulase in bioconversion processes to prevent inhibition of cellulase. Endo-xylanases have been reported to be inhibited by xylose and xylobiose (Khanna, 1993). However, β -xylosidase has been found to be inhibited by xylose and xylobiose (de Vargas Andrade, de Moraes, Terenzi, & Jorge, 2004). Feruloyl esterases have also been found to be inhibited by ferulic acid (Xiros, Moukouli, Topakas, & Christakopoulos, 2009). Some researchers have further investigated the impact oligosaccharides and sugars other than cellobiose and glucose on cellulases and found that hemicellulose-derived sugars (xylose, arabinose, mannose, and galactose) inhibited cellulose conversion (García-Aparicio et al., 2006). Some reports even indicate that xylooligomers are stronger inhibitors of cellulase than glucose and cellobiose (Kumar, & Wyman, 2009; Qing, Yang, & Wyman, 2010; Kont, Kurašin, Teugjas, & Våljamäe, 2013).

3.5.2. Nonproductive Binding to Lignin

When working with complex substrates such as lignocellulose, it was observed that adsorption did not correlate with hydrolysis efficiency. It was demonstrated that high levels of

non-productive adsorption took place during hydrolysis of lignocellulosic substrates, specifically onto lignin, which decreased the hydrolysis efficiency and required high enzyme loadings to overcome this phenomenon (Ximenes et al., 2010, 2011). Non-productive adsorption of cellulases to lignin has been demonstrated to be as a result of the CBM that cellulases contain. It has been shown that, unless hydrolysis of the substrate is complete, enzymes remain adsorbed to the recalcitrant, unhydrolysed part of the substrate and this could affect the reuse of enzymes in subsequent batches (Van Dyk, & Pletschke, 2012).

Many studies have investigated ways in which non-productive adsorption can be overcome by alkali extraction of lignin or by the addition of compounds such as surfactants (Tween), protein (BSA) or other additives (e.g., poly ethylene glycol) (Hatti-Kaul, Törnvall, Gustafsson, & Börjesson, 2007). The increased cost for adding additives may be compensated by improved enzymatic hydrolysis step. This also has particular relevance in terms of recycling of enzymes for reuse. If the enzymes could be released from the substrate at the end of a batch hydrolysis, they could be recycled, reducing enzyme cost.

3.5.3. Cellulase Deactivation

The phenolic compounds and related aromatics released from lignin have the inhibition and deactivation effects on cellulolytic enzymes, which require increased enzyme doses to achieve high conversion yields. The LORRE research group from Purdue University conducted in-depth studies on the deactivation of enzyme caused by phenols. Results showed that phenols are major inhibitors and deactivators of cellulolytic enzymes (Ximenes et al., 2011). Two approaches were proposed: use of lignin-free cellulose or prevention of cellulase adsorption on lignin. These approaches help to minimize the phenolic compounds' deactivation and inhibition effect in order to have higher glucose yield meanwhile with lower enzyme loading (Kim, Ximenes, Mosier, & Ladisch, 2011).

In summary, the inhibitors released by the pretreatment step can significantly reduce the yield of alcohol and make the enzymatic hydrolysis step more expensive. Coupled with the high capital costs associated with pretreatment and handling the low bulk-density lignocellulose, the increased costs associated with higher enzyme use and lower fermentation productivity continue to be the most significant economic hurdles to expanding cellulosic ethanol production (Wyman, 2007).

Effective pretreatment and saccharification are essential for the release of monosaccharides into liquid media. Sugar release must be followed by effective bioconversion into ethanol or similar fermentation fuels, the unit operation termed 'fermentation'.

4. FERMENTATION

The term 'fermentation' generically refers to a biological process where microbial cellular activity transforms a feedstock molecular into a specific product of interest (Mosier & Ladisch, 2009). In the case of ethanol fermentation, it refers to the generation of ethanol following the breakdown of glucose molecules into pyruvic acid/pyruvate. The process, termed glycolysis, varies between eukaryote (Figure 2) and prokaryote cells (Figure 3), but generates the same end product – pyruvate – that is then converted into ethanol, typically in

the absence or limited presence of oxygen. Ethanol being a direct product of cellular energy metabolism, its fermentation is sometimes classified as a type I fermentation (Mosier & Ladisch, 2009), meaning that cellular growth, consumption of a carbon source (sugar) and generation of the product (ethanol) are closely coupled. Ethanol fermentation is currently the largest-scale microbial process in industrial practice (Gray, Zhao, & Emptage, 2006; Rudolf, Karhumaa, & Hähn-Hägerdal, 2009).

4.1. Ethanol Process Overview

An industrial fermentation process begins with the extraction of the constituent sugars from the feedstock into a liquid medium. In order for the manufacturing process to be commercially viable, the ethanologen must meet the following critical requirements (Picataggio & Zhang, 1996):

1. High fermentative ethanol yield and titer are foremost, as well as tolerance for the high concentrations of ethanol generated.
2. A broad substrate (sugar) range is necessary, as the carbohydrate composition of fuel ethanol feedstocks can be expected to be heterogeneous.
3. Tolerance for the fermentation media – corn mash, cane or sorghum juice, cellulosic hydrolysate, etc. – composition is critical, given the costs of additional treatments on a commercial scale.
4. The ethanologen must not consume oxygen during fermentation, as oxygen typically leads to complete carbohydrate/pyruvate breakdown.
5. The fermentation must also take place at low pH, to reduce microbial contamination.

In addition to the essential traits listed above, the following properties are desirable in the ethanologen:

1. High specific growth and sugar consumption rates.
2. The capacity to grow in minimal media, as nutrient supplementation is costly at the commercial scale.
3. High temperature and shear tolerance.
4. Being Generally Regarded as Safe (GRAS).

While several microbial species are capable of ethanol fermentation, commercial significance is restricted to *Saccharomyces cerevisiae* (Rudolf et al., 2009; Russell, 2003), commonly known as baker's yeast, and *Zymomonas mobilis*, a bacterium (Geddes, Nieves, & Ingram, 2011; Rogers, Jeon, Lee, & Lawford, 2007). These species alone are capable of tolerating the high concentrations of ethanol that must be generated for commercial-scale viability. A brief overview of their properties is presented below.

4.1.2. *Saccharomyces cerevisiae*

Yeasts belonging to the *Saccharomyces* genus are the oldest known ethanologens, having been used since antiquity in the brewing of alcoholic beverages such as wine and ale. While other *Saccharomyces* species such as *S. pastorianus* are capable of generating ethanol on a

large scale (D'Amore, Panchal, & Russell, 1989; Kodama, Kielland-Brandt, & Hansen, 2006), *S. cerevisiae* is currently the most commonly used ethanologen across the world, for beverage and fuel ethanol fermentation.

Yeasts are naturally capable of fermenting hexose sugars. *S. cerevisiae* is capable of fermenting monosaccharides such as glucose, fructose, mannose, and galactose. It can ferment the disaccharides maltose and sucrose, and the trisaccharides maltotriose and raffinose (Russell, 2003). Yeast cells are incapable of metabolizing longer chain polysaccharides such as starch or cellulose. Commercial fermentations involving the same are carried out following their chemical or enzymatic depolymerization into fermentable mono-, di- or trisaccharides.

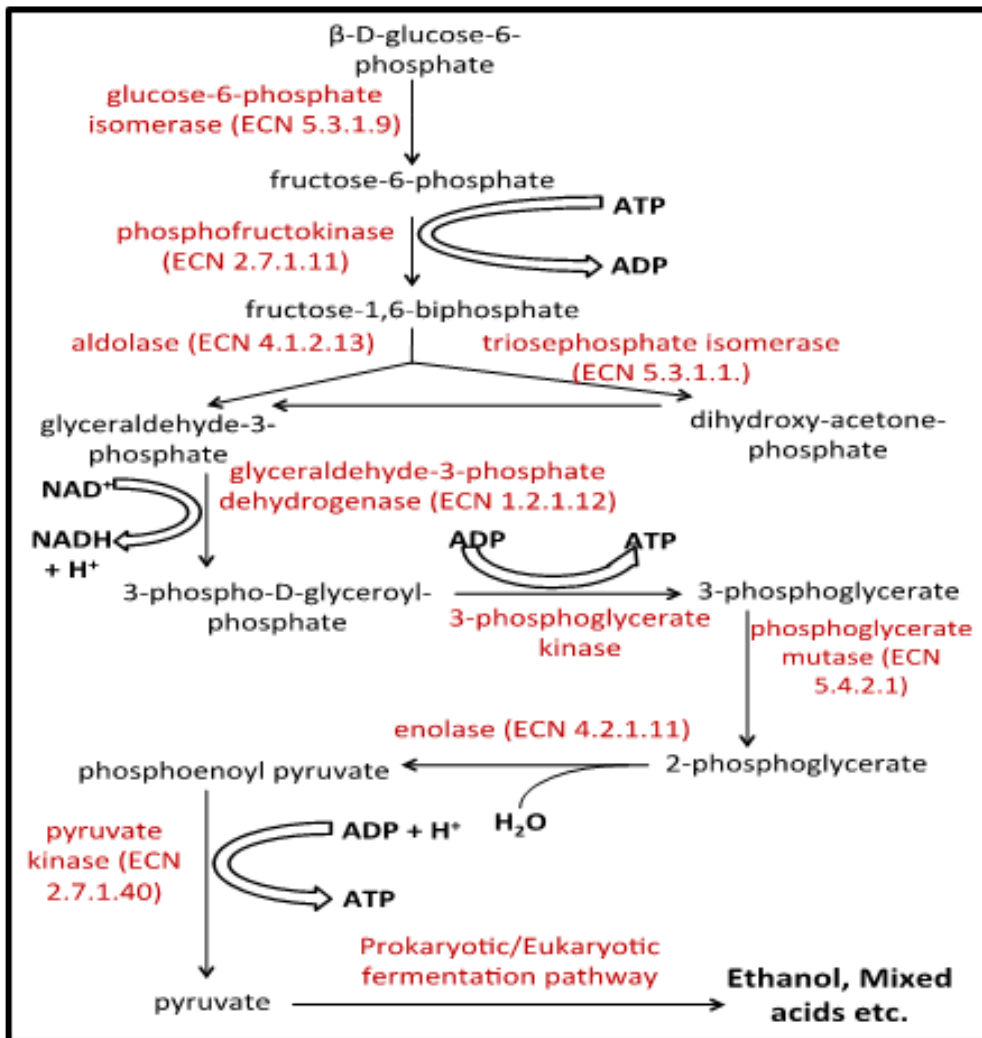


Figure 2. Glucose breakdown through the Embden-Meyerhof-Parnas pathway. (Reproduced from MetaCyc).

Following hexose entry into the yeast cell, it is phosphorylated, isomerized into glucose- or fructose-6-phosphate, and broken down through the Embden-Meyerhoff-Parnas pathway

into pyruvic acid (Figure 2). The latter molecule is then de-carboxylated into acetaldehyde, which is then reduced to ethanol (Russell, 2003). Significantly, in the presence of sufficiently high (>10% w/v) hexose concentrations, *Saccharomyces* is capable of ethanol fermentation irrespective of aeration or oxygen concentration, a characteristic known as the Crabtree effect (Pronk, Steensma, & Van Dijken, 1996; Russell, 2003). Metabolomic and genomic analyses indicate this mechanism to be an evolutionary adaptation, giving the yeast the advantage in sugar rich environments (Hagman & Piskur, 2015). As a result of the Crabtree effect, yeast ethanol fermentation can be maintained by adjusting glucose concentrations in the reactor, which is more economical on a large-scale than maintaining anaerobic or limited-aerobic conditions. Depending upon the strain and culturing conditions – temperature, pH, nutrient concentration – *S. cerevisiae* is capable of generating and tolerating ethanol concentrations as high as 30% w/v, although most industrial applications limit the concentration to 15% w/v (Benitez, Del Castillo, & Aguilera, 1983; D'Amore et al., 1989).

4.1.3. *Zymomonas mobilis*

Z. mobilis is a gram-negative bacteria capable of ethanol fermentation. It was first identified as a cause of cider and beer spoilage in Europe, and subsequently as the fermenting agent responsible for the formation of pulque in Mexico and palm wines in tropical regions across the world (Swings & De Ley, 1977). The only species of its genus, *Zymomonas mobilis* was projected as a potential biocatalyst as a result of its high ethanol yields (97% of theoretical) and productivity rates (Bai, Anderson, & Moo-Young, 2008; Lee, Pagan, & Rogers, 1983; Park & Baratti, 1991; Rogers, Lee, & Tribe, 1979; Skotnicki, Lee, Tribe, & Rogers, 1981).

Zymomonas is capable of natively fermenting glucose and fructose, with select strains also being capable of fermenting sucrose (Panesar, Marwaha, & Kennedy, 2006; Swings & De Ley, 1977). The fermentation of the latter is however less efficient due to the formation of levan, fructans, and sorbitol upon sucrose hydrolysis (Doelle, Kirk, Crittenden, Toh, & Doelle, 1993; Park & Baratti, 1991). Following the sugar entry into the cell, it is converted into glucose, phosphorylated and absorbed through the Enter-Doudoroff pathway, eventually being converted into pyruvic acid, and then into ethanol. While the end products are the same as in yeast, the pathways in *Zymomonas* differ in enzymes, byproducts, and resulting redox balance in the cell, which has ramifications for cell ethanol tolerance. At present, *Z. mobilis* is capable of fermenting and tolerating ethanol concentrations of up to 12% w/v (Dien, Cotta, & Jeffries, 2003; Sprenger, 1996).

4.2. Cellulosic Ethanol and Xylose Fermentation

While cellulose, a polymer of glucose, is the primary constituent of lignocellulose, hemicellulose is a substantial source of potentially fermentable sugars. Hemicellulose has a structure significantly different from cellulose, showing more variation in composition and structure across plant classes and species. While cellulose is a homogeneous polymer of glucose, hemicellulose consists of several different monomeric units. Hemicellulose contains hexoses (glucose, galactose and mannose), pentoses (xylose and arabinose) and sugar acids such as glucuronic acid. The monomers are linked to form various classes of hemicellulosic polysaccharides, such as xylo-glucans, arabino-xylans, mannans, etc. Hemicelluloses

comprise 25+% by dry weight of grass-based feedstocks such as corn stover (25-28%), switchgrass (20-26%), and wheat straw (30-50%). They are also important components of woody biomass, comprising 14-18% by dry weight of willow and poplar (Byrt, Grof, & Furbank, 2011; Saha, 2003). As such, the utilization of hemicellulose and its constituent sugars is critical to effective lignocellulose conversion. Xylose is the predominant component of hemicellulose, typically making up 20-35% by dry weight on average of grass-based lignocellulose and 10-20% on average by dry weight of hard wood lignocelluloses (Saha, 2003; Wiselogel, Tyson, & Johnson, 1996).

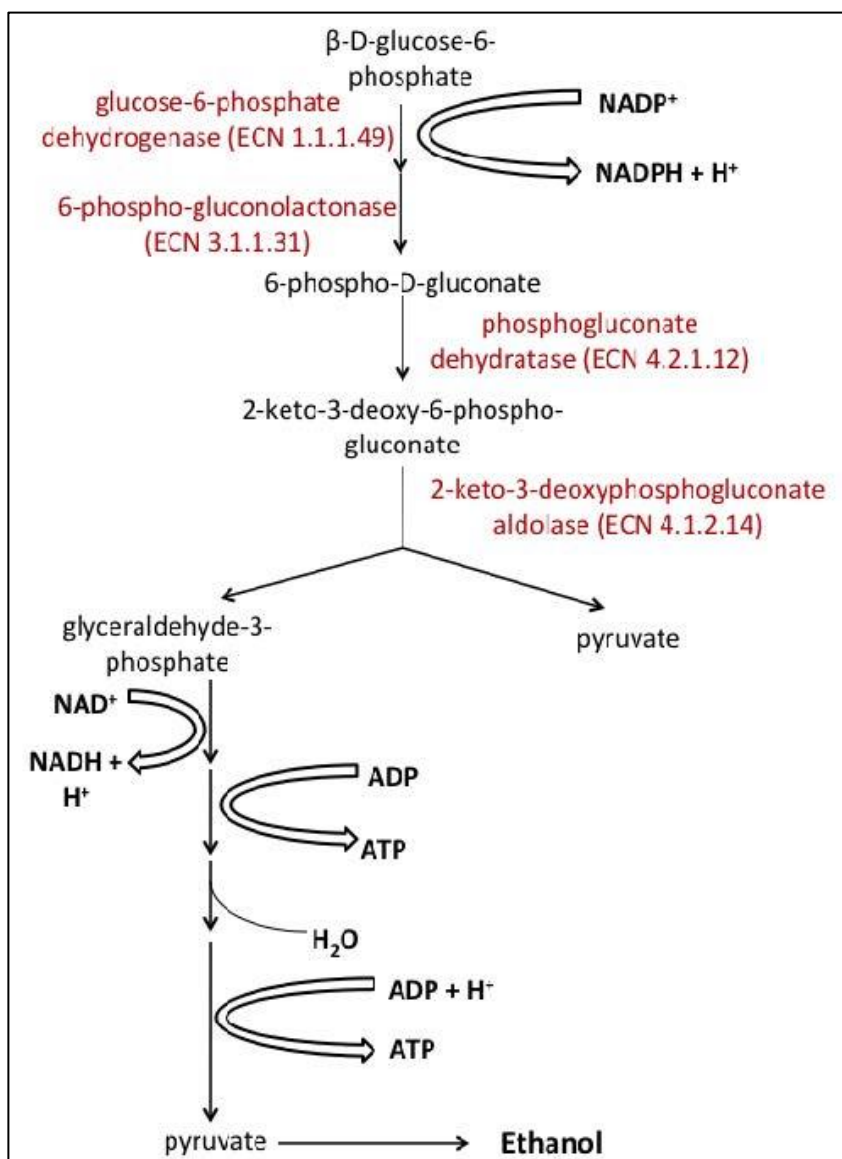


Figure 3. Glucose breakdown through the Entner-Doudoroff pathway (Reproduced from MetaCyc).

As a result of its abundance, xylose must be fermented to effectively make use of hemicellulose and lignocellulose as a whole. As neither *S. cerevisiae* nor *Z. mobilis* natively ferment xylose, genetic engineering is required to give them the capacity to do so. A summary of these efforts is presented in Section 4.3 below.

4.3. Genetic Engineering Strategies for Xylose Utilization

Xylose utilization in the cell requires its conversion into xylulose, a ketose isomer with the same molecular formula. Xylulose upon phosphorylation can be absorbed into the pentose phosphate pathway, a sequence of cellular reactions universal to all cells. While the pathway is required to generate ribose and erythrose for biosynthetic purposes, and NADPH for cellular redox reactions, it also generates glycolytic end products, which can then be fermented (Figure 4). Depending upon glucose availability, xylose fermentation in this pathway theoretically generates 1.5-1.66 moles of ethanol per mole xylose.

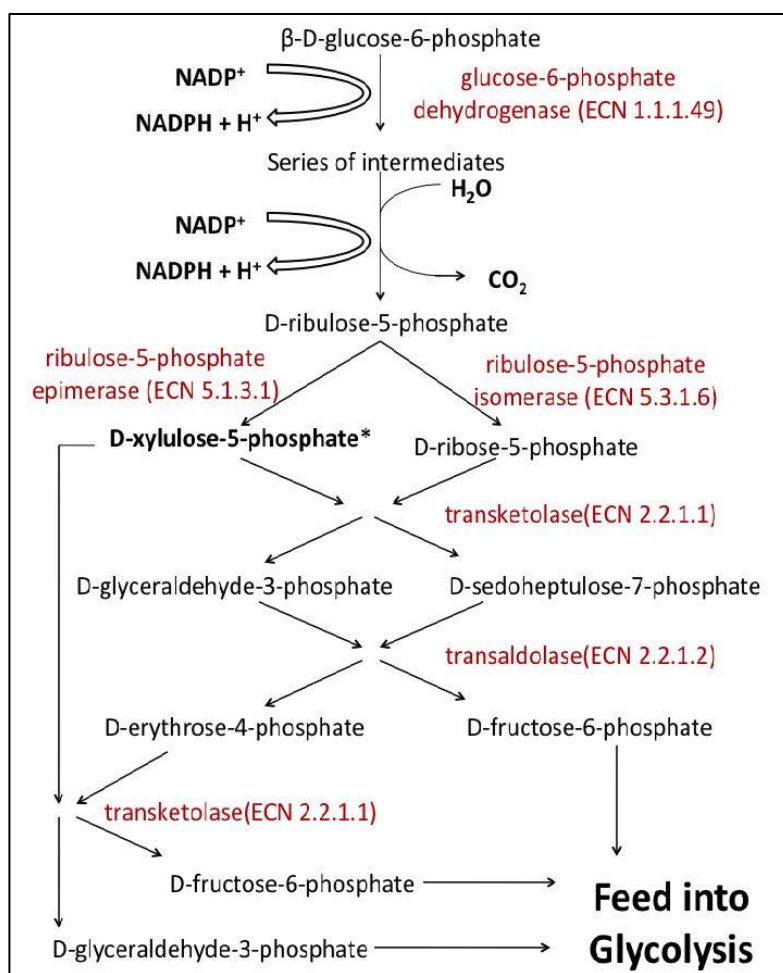


Figure 4. Pentose Phosphate Pathway. Asterisk marks the point of entry of xylose, following conversion into xylulose and phosphorylation.

The conversion of xylose to xylulose can occur through two currently known metabolic pathways:

1. *Xylose Isomerase (XI) pathway*: Xylose isomerase (ECN 5.3.1.5) is an enzyme capable of converting xylose into xylulose in a single, non-redox step. The sugars being aldose-ketose isomers, the isomerization reaction is redox neutral.
2. *Xylose Reductase/Xylitol Dehydrogenase (XR/XDH) pathway*: In this pathway, xylose is converted to xylulose through a two-step reduction-oxidation process. Xylose is first reduced to xylitol, the reaction catalyzed by xylose reductase (EC 1.1.1.21). Xylitol is subsequently oxidized into xylulose, the reaction catalyzed by xylitol dehydrogenase (EC 1.1.1.9). The reactions consume one molecule of NADPH and generate a molecule of NADH.

Following its generation, xylulose is phosphorylated by (EC 2.7.1.17), to form D-xylulose-5-phosphate, which is absorbed into the pentose phosphate pathway.

Several efforts have been made recently to develop industrial-scale ethanologens capable of xylose fermentation. Attempts have been made both to confer xylose-fermenting capacity on known ethanologens as well as to enhance the ethanol fermenting capacity of microbial species capable of native xylose fermentation. Three species have been the focus of the most effort, namely *Saccharomyces cerevisiae*, *Zymomonas mobilis*, and *Escherichia coli*.

Wild-type *S. cerevisiae* is capable of xylose uptake through facilitated diffusion (Jeffries, 1983; Leao & Van Uden, 1984a). Xylose entry into *S. cerevisiae* cells is carried out by hexose transporters encoded by the HXT family of genes (Hamacher, Becker, Gárdonyi, Hähn-Hägerdal, & Boles, 2002; Kruckeberg, 1996; Sedlak & Ho, 2004), specifically HXT2, HXT6, and HXT7, which have a high affinity for glucose and are repressed by high concentrations of the same. These high affinity transporters are strongly expressed during glucose depletion, and transport xylose into the cell at this point. Additionally, Gal2, a galactose permease, was found capable of transporting xylose as well (Hamacher et al., 2002). Attempts have been made to engineer xylose-fermenting ability in *S. cerevisiae* through both the xylose isomerase (XI) and xylose reductase/xylitol dehydrogenase (XR/XDH) pathways.

The XI pathway is attractive as it circumvents redox conditions, is independent of co-factors, and does not generate intermediates. Attempts to express bacterial xylose isomerases in *S. cerevisiae* (Amore, Wilhelm, & Hollenberg, 1989; Ho, Stevis, & Rosenfeld, 1983; Moes, Pretorius, & Van Zyl, 1996; Sarthy et al., 1987; Walfridsson et al., 1996) met with failure as the gene products had severely reduced or no activity, attributed to differences in protein expression, post-translational modification and optimal temperatures between bacteria and yeasts (Chu & Lee, 2007; Walfridsson et al., 1996). Additionally, xylitol formation was observed, which inhibited further isomerase activity. Subsequent efforts focused on increasing expression of the isomerase and xylulokinase genes and reducing expression of specific cellular transaldolase (Lönn, Gárdonyi, Van Zyl, Hahn-Hägerdal, & Otero, 2002; Träff, Cordero, Van Zyl, & Hahn-Hägerdal, 2001), which catalyzed the formation of xylitol. Further improvement was achieved through the overexpression of pentose phosphate pathway genes (Karhumaa, Hahn-Hägerdal, & Gorwa-Grauslund, 2005), and identification of a fungal xylose isomerase gene (Harhangi et al., 2003). Following the incorporation of the fungal gene (Kuyper et al., 2003), work has continued on improving the fermentative performance of the

engineered *S. cerevisiae* through various genetic and metabolic engineering (Aeling et al., 2012; Kuyper, Hartog, et al., 2005a; Kuyper, Toirkens, et al., 2005b; Kuyper, Winkler, Van Dijken, & Pronk, 2004; Ma, Liu, & Moon, 2012; Zhou, Cheng, Wang, Fink, & Stephanopoulos, 2012). A persistent bottleneck has been lower ethanol titer and productivity, even at high fermentative yields, in comparison with yeasts engineered with the XR/XDH pathway (Bettiga, Hahn-Hagerdal, & Gorwa-Grauslund, 2008; Karhumaa, Sanchez, Hähn-Hägerdal, & Gorwa-Grauslund, 2007).

Expression of xylose reductase (XR) and xylitol dehydrogenase (XDH) genes in *S. cerevisiae* was reported first by Kotter et al. (Kotter & Ciriacy, 1993; Kotter, Amore, Hollenberg, & Ciriacy, 1990), who transferred genes from *P. stipitis*, a yeast capable of native xylose fermentation. While the transformed yeast could grow on xylose, fermentative yields were low, xylitol being the predominant product. Similar results were reported elsewhere (Tantirungkij, Nakashima, Seki, & Yoshida, 1993). Optimization of the cellular redox mechanism – the NADH/NAD⁺ ratio – was predicted to improve xylose metabolism (Bruinenberg, 1986). Efforts were made to improve xylose metabolism by engineering increased expression of pentose phosphate pathway enzymes and more suitable cellular redox conditions during xylose fermentation (Walfridsson, Anderlund, Bao, & Hahn-Hagerdal, 1997; Walfridsson, Hallborn, Penttila, Keranen, & Hahn-Hagerdal, 1995). While the resulting strains showed improved aerobic growth on xylose as well as reduced xylitol production, ethanol yield and titer did not improve.

The first successful glucose-xylose co-fermentation in *S. cerevisiae* was reported by Ho et al. (1998). *S. cerevisiae* strain 1400 was transformed to express *P. stipitis* XR, XDH and Xylulokinase (XK) genes. The resulting strain 1400(pLNH32) was reported capable of fermenting a glucose-xylose mixture of 5% w/v each to produce an ethanol concentration of approximately 4.8% in 36 hours, achieving 78% of the theoretical ethanol yield from pure xylose (Krishnan, Ho, & Tsao, 1999). Eliasson et al. subsequently reported chemostat-based xylose fermentation using *S. cerevisiae*, similarly engineered to express XR, XDH and XK, observing initially low consumption (Eliasson, Christensson, Wahlbom, & Hahn-Hagerdal, 2000) and improvements upon modifying the expression ratios of the enzymes (Eliasson, Hofmeyr, Pedler, & Hähn-Hägerdal, 2001). Following the demonstration of xylose fermentation, efforts are ongoing to optimize the process through metabolic engineering (Hahn-Hagerdal, Karhumaa, Jeppsson, & Gorwa-Grauslund, 2007; Jeffries, 2006). Points of focus include improving cellular redox conditions (Jeffries, 2006; Jeppsson et al., 2006; Khattab & Kodaki, 2014; Khattab, Saimura, & Kodaki, 2013; Lee, Kodaki, Park, & Seo, 2012; Petschacher & Nidetzky, 2008; Verho, Londesborough, Penttila, & Richard, 2003), increasing the expression profiles and activity of enzymes to shift specific reaction equilibria forward (Karhumaa, Fromanger, Hähn-Hägerdal, & Gorwa-Grauslund, 2006; Matsushika et al., 2012; Träff-Bjerre, Jeppsson, Hahn-Hagerdal, & Gorwa-Grauslund, 2004) and increasing xylose entry and uptake (Bertilsson, Andersson, & Lidén, 2007; Fonseca et al., 2011; Hector, Qureshi, Hughes, & Cotta, 2008; Saloheimo et al., 2006). Using an *S. cerevisiae* strain patented by Ho et al. (Ho & Tsao, 1998), the complete consumption of 9% w/v pure xylose and co-fermentation of 9% w/v xylose and 17% w/v glucose in batch fermentations was reported by Athmanathan et al. (Athmanathan, Sedlak, Ho, & Mosier, 2011), which is currently the highest concentration reported co-fermented (Table 4).

Table 4. Reported xylose fermentations to ethanol for various microbial species

Reported By		Fermenting Strain	Feed Concentrations (% w/v)	Ethanol Production		
				Titer (% w/v)	Yield (% _{theoretical})	Time (hours)
(Mohagheghi et al.)	2002	<i>Z. mobilis</i> AX 101	Glucose: 4% w/v Xylose: 4% w/v Arabinose: 4% w/v	4.2	84	48
	2004	<i>Z. mobilis</i> 8b	Glucose: 7.5% w/v Xylose: 5% w/v	5.4	91	48
(Yomano et al., 2008)		<i>E. coli</i> LY160	Xylose: 9% w/v	4.5	83% (Mineral media) 81% (LB media)	24
(Kuyper et al., 2004; Kuyper, Hartog, et al., 2005a)		<i>S. cerevisiae</i> RWB 202-AFX	Glucose: 2% w/v Xylose: 2% w/v	1.7	83	40
(Sedlak et al., 2004)		<i>S. cerevisiae</i> 424A (LNH-ST)	Glucose: 7% w/v Xylose: 4% w/v (YEP)	4.7	80	30
			Glucose: 4% w/v Xylose: 4% w/v (Hydrolysate)	3.0	36	48
(Athmanathan et al., 2011)		<i>S. cerevisiae</i> 424A (LNH-ST)	Xylose: 9%	4.6	84	48
			Glucose: 17% Xylose: 9%	11	77	125

Zymomonas mobilis was found to have a native facilitated diffusion system capable of xylose uptake (DiMarco & Romano, 1985). Liu et al. reported the transfer of xylose-catabolizing genes from *Xanthomonas* (Liu, Goodman, & Dunn, 1988). *Zymomonas* has so far been engineered with the isomerase (XI) pathway, due to a greater degree of compatibility with bacterial isomerase genes. Xylose fermentation was demonstrated by *Z. mobilis* CP4 (pZB5), a strain transformed with *E. coli* xylose isomerase and xylulokinase genes (pZB5 plasmid) (Zhang, Eddy, Deanda, Finkelstein, & Picataggio, 1995). A range of batch and fed-batch fermentations were subsequently reported with CP4 (pZB5) and strains derived from it, 6.5% w/v being the maximum concentration of xylose reported completely consumed during co-fermentation with glucose (Joachimsthal & Rogers, 2000; Joachimsthal, Hagggett, & Rogers, 1999; Krishnan, Blanco, Shattuck, Nghiem, & Davison, 2000; Mohagheghi, Evans, Finkelstein, & Zhang, 1998). A new strain, AX101, derived from CP4 (pZB5), was developed to co-ferment arabinose with glucose and xylose (Mohagheghi, Evans, Chou, & Zhang, 2002). Most recently, 10% w/v xylose was reported fermented by Agrawal et al., using a *Z. mobilis* strain developed through directed adaptation (Agrawal, Mao, & Chen, 2010).

While initial strain engineering focused on improving the substrate range, *Zymomonas* tolerance towards fermentation inhibitors is an additional concern. Low xylose consumption and ethanol titers were reported when carrying out fermentations on wood pretreatment liquor using *Z. mobilis* strains transformed with the pZB5 plasmid (Lawford, Rousseau, Mohagheghi, & McMillan, 1998, 1999). The bacteria is particularly susceptible to acetic acid/acetate ion inhibition (Joachimsthal, Hagggett, Jang, & Rogers, 1998; Sáez-Miranda, Saliceti-Piazza, & McMillan, 2006). A series of strains have been developed with acetate

tolerance, through mutagenesis (Jeon, Svenson, Joachimsthal, & Rogers, 2002; Joachimsthal et al., 1998), gene integration (Mohagheghi et al., 2004) and directed adaptation (Agrawal, Wang, & Chen, 2012). Efforts are ongoing to analyze and engineer resistance to other fermentation inhibitors commonly found in cellulosic hydrolysates (Franden, Pienkos, & Zhang, 2009; Franden, Pilath, Mohagheghi, Pienkos, & Zhang, 2013a; Yang et al., 2014).

Escherichia coli have been projected as potential ethanologens predominantly because of their native ability to metabolize hexose and pentose sugars. *E. coli* are capable of actively absorbing xylose (Lam, Daruwalla, Henderson, & Jones-Mortimer, 1980; Song & Park, 1997) and isomerizing it into xylulose. Correspondingly, they present a significant advantage by way of substrate range and uptake rates. A substantial body of knowledge moreover exists on *E. coli* genetics and metabolism, making engineering them easier than other species.

The principal drawback with *E. coli* is their fermentation pathway. Following the generation of pyruvate, it is broken down through the pyruvate formate lyase pathway, generating formic acid as a byproduct. The pathway is unbalanced by the way of redox agents (NADH/NAD⁺), which the cell must compensate for through the formation of acetic and succinic acids. Ethanol yields thus typically average 50% of theoretical in native *E. coli* (Dien et al., 2003), compared to 90+% in *S. cerevisiae* or *Z. mobilis*.

To reduce the NADH use per molecule of ethanol, pyruvate decarboxylase/alcohol dehydrogenase genes from *Zymomonas* were expressed in *E. coli*. Ingram et al. first reported successful expression of the genes in *E. coli* (Ingram, Conway, Clark, Sewell, & Preston, 1987). Chromosomal integration of the expressed construct into *E. coli* resulted in the development of strain KO11 (Ohta, Beall, Mejia, Shanmugam, & Ingram, 1991), with which ethanol fermentations were reported using corn residues and rice hulls (Beall et al., 1992; Moniruzzaman & Ingram, 1998; Moniruzzaman et al., 1996). A series of strains were since developed from KO11 through metabolic engineering and directed evolution (Jarboe, Grabar, Yomano, Shanmugam, & Ingram, 2007; Yomano, York, & Ingram, 1998), with which ethanol fermentation from cellulosic hydrolysates has been demonstrated (Brandon et al., 2008; 2011; Lau, Dale, & Balan, 2007). While the fermentative percentage yields are high (90+%), 6% w/v is the maximum ethanol titer achieved with *E. coli* KO11 or its derivatives. Complete fermentation of 9% w/v xylose was reported by Yomano et al. (Yomano, York, Zhou, Shanmugam, & Ingram, 2008), which is the highest pure xylose concentration fermented (Table 4). In parallel, recombinant strains of *E. coli* were developed at the Fermentation Biochemistry Research Unit at Peoria, Illinois through transformation with the construct developed by Ingram et al. (Hespell, Wyckoff, Dien, & Bothast, 1996). The strains – termed FBR – have been used to demonstrate co-fermentation of glucose, xylose, and arabinose both with reagent sugars and cellulosic hydrolysates (Dien, Hespell, Wyckoff, & Bothast, 1998; Dien, Nichols, O'Bryan, & Bothast, 2000). In particular, *E. coli* FBR5 has been tested with a variety of pretreated cellulosic feedstocks, under a variety of batch and continuous fermentation configurations (Martin, Knepper, Zhou, & Pamment, 2006; Qureshi, Dien, Nichols, Saha, & Cotta, 2006; Saha & Cotta, 2006; 2007b; 2007a; 2008; 2010; 2011; Saha, Iten, Cotta, & Wu, 2005; 2008; Saha, Nichols, & Cotta, 2011a; Saha, Nichols, Qureshi, & Cotta, 2011b; Saha, Qureshi, Kennedy, & Cotta, 2015; Saha, Yoshida, Cotta, & Sonomoto, 2013). While the fermentative yields could be raised to 98% of theoretical by altering fermentation parameters, final ethanol titers ranged 2-4% w/v throughout, from a total sugar concentration of 5-9% w/v (corresponding to 2-3% w/v xylose), which is significantly lower

than what can be achieved from *Saccharomyces* or *Zymomonas*. The FBR strains moreover require nutrient-rich fermentation media, which would prove costly at the commercial scale.

In addition to fermentative capacity, *E. coli* engineering is also focused on its tolerance of inhibitors commonly found in cellulosic hydrolysates. Work is ongoing to develop strains tolerant of ethanol and furfural (Wang, Miller, Yomano, Shanmugam, & Ingram, 2012; Wang et al., 2013).

4.4. Fermentation Inhibitors

The fermentation media, while sugar rich, is a typically heterogeneous mixture containing components that might be toxic to the fermenting organism, and which cannot be feasibly removed. Lignocellulosic hydrolysates in particular contain compounds generated by the harsh conditions under which the biomass is pretreated (Mosier et al., 2005; Yang & Wyman, 2008), which reduce fermentation yield, rate, and final ethanol output. Their effect on the fermenting organism must therefore be understood. Fermentation inhibitors can be categorized into two major groups:

1. Pretreatment-generated inhibitors are compounds generated through lignocellulose pretreatment. They are generated from the breakdown of hemicellulose and lignin into toxic monomers or oligomers. The most common pretreatment-generated inhibitors are furan aldehydes generated from hemicellulose and cellulose sugars, acetic acid from hemicellulose residues and solubilized phenolics from lignin.
2. Fermentation-generated inhibitors are compounds generated during the fermentation process that are inhibitory to the yeast. As such, their mechanism is typically product inhibition. The two most common inhibitors are acetic acid and ethanol, both generated from sugar fermentation.

A description of their generation and impact is presented below.

4.4.1. Pretreatment-Generated Inhibitors

Pretreatment is an essential step in the bio-based conversion of lignocellulose into biofuels, required for the separation of lignin from structural hydrocarbons and render them susceptible to enzyme depolymerization. While methods such as mechanical extrusion (Karunanithy & Muthukumarappan, 2009; 2012) occur under milder conditions, the process typically employs extremes in temperature and pH (Mosier, 2013; Mosier et al., 2005; Ramirez, Holtzapple, & Piamonte, 2013; Trajano & Wyman, 2013) to chemically degrade and remove the lignin. The extremity of the pretreatment is termed as severity factor which is calculated by a pseudo-first order equation relating pH, temperature, pressure, and residence time of the pretreatment. Due to the severity factor applied in the pretreatment, the reactions also degrade the hemicellulose and cellulose, optimal pretreatment conditions maximizing lignin removal while minimizing sugar degradation (Galbe & Zacchi, 2012). The degradation of lignin and the structural carbohydrates produces different inhibitory components, all of which reduce ethanol yields and titers upon fermentation of lignocellulosic hydrolysates (Larsson et al., 1999; Mills, Sandoval, & Gill, 2009; Palmqvist & Hähn-Hägerdal, 2000a; 2000b). Described below are the inhibitors generated from the degradation of each polymer.

Lignin, being a phenolic polymer, generates a mixture of phenyl-substituted molecules (Klinke, Thomsen, & Ahring, 2004; Liu, 2011; Ximenes et al., 2013), the exact mixture varying with feedstock and pretreatment conditions. The species generated include phenol derivatives such as hydroxybenzaldehyde, hydroxybenzoic and hydroxycinnamic acid, cresol and catechol, guaiacol derivatives such as coniferol, vanillin and ferulic acid, syringol derivatives such as syringaldehyde, sinapyl alcohol and sinapic acid and polyphenolic molecules such as tannic acid. Several of these molecular species have been found to have inhibitory effects on cellulolytic enzymes (Kim et al., 2011; Ximenes, Kim, Mosier, Dien, & Ladisch, 2010), tannic acid being reported as reducing cellulase and β -glucosidase activities by up to 60% (Ximenes et al., 2011).

Hydrolysate phenolics were found to inhibit fermentative activity in *Saccharomyces* (Ando, Arai, Kiyoto, & Hanai, 1986; Jönsson et al., 2013; Larsson et al., 1999; Liu & Blaschek, 2010; Martín & Jönsson, 2003; Palmqvist & Hähn-Hägerdal, 2000b; Xiros & Olsson, 2014), *E. coli* (Chandel, da Silva, & Singh, 2013; Klinke et al., 2004; Palmqvist & Hähn-Hägerdal, 2000b) and *Zymomonas* (Frandsen, Pilath, Mohagheghi, Pienkos, & Zhang, 2013b; Klinke et al., 2004; Liu & Blaschek, 2010; van der Pol, Bakker, Baets, & Eggink, 2014). Their inhibitory effect has been primarily attributed to their solvent properties. Due to the hydrophobic nature of the phenyl structure, phenolic compounds enter the cell membrane, where their interactions with the constituent lipids and embedded proteins affects membrane fluidity and integrity, disrupting cellular metabolic functions and putting severe stress on the organism (Fitzgerald et al., 2004; Keweloh, Weyrauch, & Rehm, 1990; Piotrowski et al., 2014; van der Pol et al., 2014; Zeng, Zhao, Yang, & Ding, 2014). While tolerance depends upon strain, species and hydrolysate conditions, it has been found to increase with phenolic molecular size, smaller phenolic molecules reported as more toxic (Chandel et al., 2013; Larsson, Quintana-Sáinz, Reimann, Nilvebrant, & Jönsson, 2000; Palmqvist & Hähn-Hägerdal, 2000b). The substitution is also a factor in toxicity, with phenyl aldehydes being reported more toxic than the corresponding carboxylic acids which are in turn more toxic than the corresponding alcohols (Jönsson et al., 2013; van der Pol et al., 2014).

The pretreatment reactions expose and subsequently break down hemicellulose and cellulose, following lignin removal. Fractions of cellulose and hemicellulose are thus solubilized into oligosaccharides, monosaccharides and eventually sugar degradation products (Klinke et al., 2004; Palmqvist & Hähn-Hägerdal, 2000b; Ximenes et al., 2013). Cellulose solubilization generates glucose alone, while hemicellulose solubilization generates a mixture of hexoses – glucose, mannose, and galactose – and pentoses – xylose and arabinose. Upon further degradation, pentose sugars are dehydrated into furfural (IUPAC name: furan-2-carbaldehyde), and pentose sugars into 5-hydroxymethylfurfural (IUPAC name: 5-(hydroxymethyl)-2-furaldehyde). Both compounds are severely inhibitory to fermenting organisms.

Furfural and 5-hydroxymethyl furfural have both been observed to reduce growth and ethanol productivity rates across fermenting organisms. The effect has been attributed to oxidative stress, brought about by interactions between cellular molecular species and the formyl or carbonyl group of the aldehyde (Almeida, Bertilsson, Gorwa-Grauslund, Gorsich, & Lidén, 2009; Taylor, Mulako, Tuffin, & Cowan, 2012). As with phenolic compounds, the furan aldehyde is more toxic than the corresponding alcohol or carboxylic acid. Correspondingly, a common stress response of the cell is to convert furfural into furfuryl alcohol (IUPAC name: 2-furanmethanol) or furoic acid (IUPAC name: furan-2-carboxylic

acid) (Palmqvist & Hähn-Hägerdal, 2000b; Wierckx, Koopman, Ruijsenaars, & de Winde, 2011; Ximenes et al., 2013). The exact mechanisms of the stress are still unclear, as glucose and xylose fermentation have been reported affected in different ways (Ask, Bettiga, Duraiswamy, & Olsson, 2013; Klinke et al., 2004).

Neutral and low-pH pretreatments typically generate carboxylic acids, either directly from the hemicellulose or from the degradation of its component monosaccharides. Hemicellulose branches typically contain acetate substitutions, which upon pretreatment are hydrolyzed into acetic acid (Davison, Parks, Davis, & Donohoe, 2013). In addition, a fraction of the furan aldehydes generated, furfural and 5-hydroxymethylfurfural, typically break down further into formic and levulinic (IUPAC name: 2-oxopentanoic acid) acids, respectively. In addition to the acids generated, the low pH of the fermentation environment is itself an inhibitor, reducing cell viability and fermentative rates.

The impact of the acids depends upon the pH of the hydrolysate medium (Casey et al., 2010; Ximenes et al., 2013). Being weak acids (pKa ranging 3.6-4.8), all three stay protonated at low pH. Entering the microbial cell in their protonated form, they dissociate in the higher pH of the cytosol and acidify it. To combat the acidification, cells have to divert energy in the form of ATP toward the proton pump machinery that maintains pH homeostasis (Casey et al., 2010; Taylor et al., 2012). The resulting metabolic stress reduces fermentation yields and titers and causes cell death when the outward proton flux is slower than the acidification rate. Even in the absence of the carboxylic acids generated, microbial cells must constantly counter passive proton influx at low pH, making an acidic lignocellulosic hydrolysate highly stressful for growth and fermentation.

Lignocellulosic hydrolysates typically contain multiple pretreatment-generated inhibitors, which results in a synergistic inhibitory effect. Due to this synergy, the overall impact on hydrolysate fermentation is difficult to predict from analysis of the chemical composition alone. Work is ongoing in analyzing and countering their toxicity (Piotrowski et al., 2014; Zeng et al., 2014). Various solutions have been proposed to address their presence, including enzyme supplementation to convert them, chemical treatment of the hydrolysate, genetic engineering of more tolerant biocatalysts and physical separation of the compounds from the pretreated hydrolysate (Chandel et al., 2013; Dhamole, Wang, & Feng, 2013; Grzenia et al., 2012; Jönsson et al., 2013; Liu, 2011; Luo, Zeuner, Morthensen, Meyer, & Pinelo, 2015; Palmqvist & Hähn-Hägerdal, 2000a; van Walsum, 2013). Suitable solutions must balance the inhibitor removal against the added costs. In addition to the above, the fermenting biocatalyst must also combat the stress from fermentation-generated inhibitors, described in further detail below.

4.4.2. Fermentation- Generated Inhibitors

The products generated by type I fermentation are typically cytotoxic upon accumulation. Under sufficiently high concentrations they cause loss of cell viability and eventual cell death. The main fermentation generated inhibitors are ethanol itself, and fermentation generated carboxylic acids – chiefly lactic and acetic acid. Due to their predominant usage, the impacts of these inhibitors on yeast cells have been best documented. This section will correspondingly focus on their impact on yeasts, specifically *Saccharomyces cerevisiae*.

4.4.2.1. Ethanol

Ethanol is cytotoxic, particularly at the concentrations reached during commercial-scale fermentation (> 10% w/v). Yeasts in general produce and can tolerate greater amounts of ethanol in comparison to other microbes (Taylor, Tuffin, Burton, Eley, & Cowan, 2008), a trait viewed as a possible evolutionary defense mechanism (Culberson & Culberson, 1981; Hagman & Piskur, 2015). As ethanol concentration increases, three major symptoms have been observed, in the increasing order of severity (D'Amore et al., 1989):

1. Loss of cell viability: The initial effects of ethanol are to reduce cell growth (Thomas & Rose, 1979) replication ceasing at concentrations of 10 – 14% w/v ethanol (Benítez, del Castillo, Aguilera, Conde, & Cerdáolmedo, 1983).
2. Cessation of fermentation: Upon further ethanol buildup, cells cease fermentation. Depending on strain and culturing conditions, cessation has been reported to occur at concentrations of 14 – 30% w/v ethanol in *Saccharomyces* (Benítez et al., 1983; D'Amore et al., 1989).
3. Cell death: At high enough concentrations, ethanol brings about cell death.

Based on factors such as strain, culturing conditions, etc. the severity of the symptoms has varied. All three being highly undesirable from a production standpoint, it is important to develop biocatalysts resistant to ethanol toxicity, as well as the cause for the same.

Early analyses of ethanol toxicity found it interfering with yeast membrane transport (Thomas & Rose, 1979; Thomas, Hossack, & Rose, 1978), including glucose, ammonium and amino acids (Leao & Van Uden, 1982; 1983; 1984b), increasing passive proton influx into the cell (Leao & Van Uden, 1984a; Pascual, Alonso, Garcia, Romay, & Kotyk, 1988) and altering membrane permeability (Walker-Caprioglio, Rodriguez, & Parks, 1985). Ethanol inhibition was correlated to its lipid/water partition coefficient, indicating the membrane to be the site of attack, and similar results were observed with propanol and butanol. The inhibitory effects of the alcohols were observed to increase with alcohol carbon number, indicating lipid solubility to be a key factor in alcohol stress. Based on these observations, the primary site of alcohol damage was deduced to be the cell membrane (Ingram, 1986). Ethanol diffuses into the hydrophobic regions of the lipid bilayer, where its buildup increases hydration and polarity in the hitherto-hydrophobic region, disrupts hydrogen bonding and increases the rate of lipid desorption (Slater, Ho, Taddeo, Kelly, & Stubbs, 1993). While a high concentration is required for complete fluidization of the membrane and cell death, ethanol poses metabolic stress to the cell at sub-lethal concentrations, necessitating expenditure of energy to combat the membrane destabilization.

Concordant to its impact on membrane stability, ethanol stress is exacerbated by high temperatures (Gray, 1941; Nagodawithana & Steinkraus, 1976) to which it has similar stress response (D'Amore et al., 1989; Gibson, Lawrence, Leclair, Powell, & Smart, 2007; Henderson, Zeno, Lerno, Longo, & Block, 2013b; Plesset, Palm, & McLaughlin, 1982), low pH (Cardoso & Le O, 1992; Pampulha & Loureiro-Dias, 1989) and high enough solute concentrations to cause osmotic stress (D'Amore et al., 1989; D'Amore, Panchal, Russeil, & Stewart, 1988; Koppram, Tomás-Pejó, Xiros, & Olsson, 2014). Yeasts respond to ethanol stress by altering membrane compositions to be more unsaturated and correspondingly hydrophobic (Aguilera, Peinado, Millan, Ortega, & Mauricio, 2006; Ciesarová, Šajbidor, Šmogrovičová, & Bafrcová, 1996; Gibson et al., 2007; Henderson & Block, 2014;

Henderson, Lozada-Contreras, Jiranek, Longo, & Block, 2013a; Koukkou, Tsoukatos, & Drainas, 1993; Mannazzu et al., 2008), generating heat-shock proteins (D'Amore et al., 1989; Gibson et al., 2007) and trehalose (Gibson et al., 2007) and up-regulating the activity of active transport proteins, chiefly H⁺-ATPase (Aguilera et al., 2006; Gibson et al., 2007; Monteiro & Sá-Correia, 1997). All the responses being strongly dependent upon glucose metabolism, ethanol stress response during pentose fermentation is likely to be different (Athmanathan et al., 2011). Concordant with its impact on the cell machinery, nutrient supplementation in the fermentation media can mitigate ethanol stress, specifically nitrogen (Casey, Magnus, & Ingledew, 1984; Gibson et al., 2007), fatty acids (Casey et al., 1984; Casey, Magnus, & Ingledew, 1983; D'Amore & Stewart, 1987; Ohta & Hayashida, 1983) and magnesium (Birch & Walker, 2000; Walker, 1994).

Product inhibition from ethanol is a critical bottleneck during very high gravity (VHG) fermentation, which is a standard industrial practice. As nutrient supplementation is likely cost-ineffective for the manufacture of fuel ethanol, feeding and product removal strategies must be employed to reduce ethanol stress and keep the fermentation continuous.

4.4.2.2. Lactic and Acetic acid

Carboxylic acids, chiefly acetic and lactic acid, are generated as fermentation by-products as well as during pretreatment (Maiorella, Blanch, & Wilke, 1983). As described earlier, the impact of the acids especially at low pH is to enter the cell and acidify the cytosol, putting metabolic stress on the fermenting organism. Both acids can be generated during fermentation from the sugars present in the media. Acetic acid is generated in small amounts from glucose by *Saccharomyces* (Thomas, Hynes, & Ingledew, 2001; 2002) during ethanol fermentation. It is generated in much larger quantities however, by bacterial contaminants present in the fermentation media (Beckner, Ivey, & Phister, 2011; Bischoff, Liu, Leathers, Worthington, & Rich, 2009; Narendranath, Thomas, & Ingledew, 2001; Skinner & Leathers, 2004), predominantly members of the *Lactobacillus* genus (Bayrock & Ingledew, 2004; Beckner et al., 2011; Narendranath, Hynes, Thomas, & Ingledew, 1997; Schell et al., 2007). While less common in pretreated hydrolysates, bacterial contamination is a significant issue in the fermentation of first generation feeds (Gombert & van Maris, 2015; Khullar et al., 2012) such as corn starch (Beckner et al., 2011; Narendranath et al., 1997; Schell et al., 2007; Skinner & Leathers, 2004) and cane juice (Basso et al., 2013; Lucena et al., 2010), wherein the contaminants both generate inhibitory acids and compete for necessary nutrients (Bayrock & Ingledew, 2004). In case of cellulosic fermentations moreover, the bacteria can natively ferment pentoses into lactic and acetic acid (Schell et al., 2007), making carboxylic acid inhibition a significant issue at the commercial scale. Early, large infusions of yeast cells reduce the likelihood of contamination by generating sufficient alcohol to inhibit growth, but the possibility remains.

While bacterial contamination can be prevented through the use of antibiotics, their continued usage can lead to the evolution of resistant strains (Bischoff et al., 2009; Muthaiyan, Limayem, & Ricke, 2011; Rasmussen, Koziel, Jane, & Pometto, 2015). Efforts are ongoing to develop cost-effective alternative strategies such as chemically sterilizing the fermentation mash (Muthaiyan et al., 2011; Rasmussen et al., 2015), using phages to limit contaminants (Worley-Morse, Deshusses, & Gunsch, 2015), engineering yeasts to counter contaminant bacteria (Khatibi, Roach, Donovan, Hughes, & Bischoff, 2014) and engineering

growth and culturing conditions so as to prevent contamination (Katakura, Moukamnerd, Harashima, & Kino-oka, 2011).

4.5. Process Considerations: Ethanol Fermentation Requirements

The fermentation process must fulfill specific requirements in order for the overall manufacturing process to be commercially and environmentally viable. The primary constraint on ethanol fermentation is posed by the subsequent distillation step, wherein ethanol is separated from the fermentation beer. Distillation can account for 60-74% of the energy consumed during ethanol manufacture (Galbe, Wallberg, & Zacchi, 2013), and has long been identified as a driver of the overall manufacturing costs (Maiorella, Blanch, & Wilke, 1984). While efforts are ongoing to optimize distillation configurations so as to lower its energy requirements (Vane, 2008), the predominant factor affecting it is the final ethanol concentration after fermentation (Galbe et al., 2007; 2013; Madson, 2003; Maiorella et al., 1984). High final concentrations of ethanol are thus extremely important to reduce distillation costs. Post-fermentation liquids, beers, generated from starch-based ethanol fermentation typically comprise >8% w/w ethanol (10-12% v/v) (Klein-Marcuschamer, Holmes, Simmons, & Blanch, 2011). In comparison, some lignocellulosic fermentations are currently projected to generate 4-5% w/w ethanol, which is the minimum required to offset the energy requirements of distillation (Figure 5) (Galbe & Zacchi 2007). High ethanol concentrations are also required upon lignocellulosic fermentation to offset the added costs of biomass collection, packaging and transportation, chemical pretreatment to separate the cellulose and the use of enzymes to convert structural carbohydrates into monosaccharides (Klein-Marcuschamer et al., 2011; Klein-Marcuschamer & Blanch, 2015; Stephen, Mabee, & Saddler, 2011). Thus pretreatment processes, enzymes, and microorganisms able to generate high sugar concentrations and ferment all of these sugars to ethanol are critical to reducing product recovery costs.

As a corollary to high final titers, the fermentative process must have a high yield. The theoretical yields of ethanol are 0.51 g/g from hexoses and 0.51 g/g from pentoses. The yields are lower in practice as the sugars are diverted towards other metabolic routes. In particular, sugars are converted into sugar alcohols – predominantly glycerol, but also including xylitol, mannitol and sorbitol – as a response to osmotic stress (Gibson et al., 2007; Krallish, Jeppsson, Rapoport, & Hahn-Hagerdal, 1997; Shen, Hohmann, Jensen, & Bohnert, 1999; Singh, Johnston, Rausch, & Tumbleson, 2010a), which is common during high-gravity (high sugar concentration) fermentations. Care must be taken to ensure that sugars are diverted towards ethanol fermentation. This is critical in case of lignocellulosic fermentations, as lignocellulose bioprocessing is difficult at high dry matter concentrations (Modenbach & Nokes, 2012; 2013), limiting final ethanol concentrations.

The final requirement is a high productivity rate. Current commercial-scale corn or sugarcane ethanol fermentations are complete within 48-72 hours, accounting for liquefaction and saccharification. A comparable or faster turnover is required for fuel ethanol to be commercially viable, especially from cellulosic sources. To improve the turnover rate and reduce the high capital cost and high enzyme cost for the current technologies used by biorefineries, attempts are continuing developed to overcome the bottlenecks mentioned. Jin et al. (2016) reported that using AFEX processing technologies combined with cycles of

recycling enzyme for hydrolysis would shorten the overall process time and avoid subjecting all the biomass to the slower hydrolysis rate period (Jin et al., 2016). They called the new system “RaBIT”, shorten for Rapid Bioconversion with Integrated recycle Technology. The system combined with AFEX process reduced the enzyme loading to 11.9 mg protein per g glucan, which is attractive for biorefinery application.

4.5.1. Commercial Considerations: Ethanol Usage

Ethanol is the leading biofuel currently in usage. The world production in 2014 was 24.5 billion gallons (<http://ethanolrfa.org/pages/World-Fuel-Ethanol-Production>). The United States of America leads the production of fuel ethanol at 14.3 billion gallons. Corn is the predominant feedstock (98%), with sorghum accounting for the rest. Brazil is the second-largest producer of ethanol at 6.19 billion gallons, produced from sugarcane juice or molasses. Fuel ethanol production was begun in 1975, under the National Alcohol Fuel Program (PROALCOOL), a series of government mandates and subsidies that were phased out in the early 2000s. While its production is significantly lower than that of the US, Brazil is significant in using ethanol blends ranging from 25% to 100%, compared to 15% in the United States. In particular, automobile engines in Brazil have been developed capable of running on hydrous (95% w/w) ethanol (Kramer & Belanger, 2011).

Fuel ethanol usage in the United States is driven by the Renewable Fuel Standard (RFS), a Federal program administered by the Environmental Protection Agency (EPA) (<http://www.epa.gov/otaq/fuels/renewablefuels/index.htm>). The program mandates the sale of specific volumes of ethanol by petroleum refiners, blenders and importers, decided by the EPA and increased annually. The RFS is aimed at establishing the utilization of 35-36 billion gallons of renewable fuels, including cellulosic ethanol, biodiesel and other advanced fuels. Despite improvements in production, ethanol utilization is limited by the availability and turnover rate for automobiles capable of utilizing it, termed the ‘blend wall’ (Tyner, Taheripour, & Perkis, 2010).

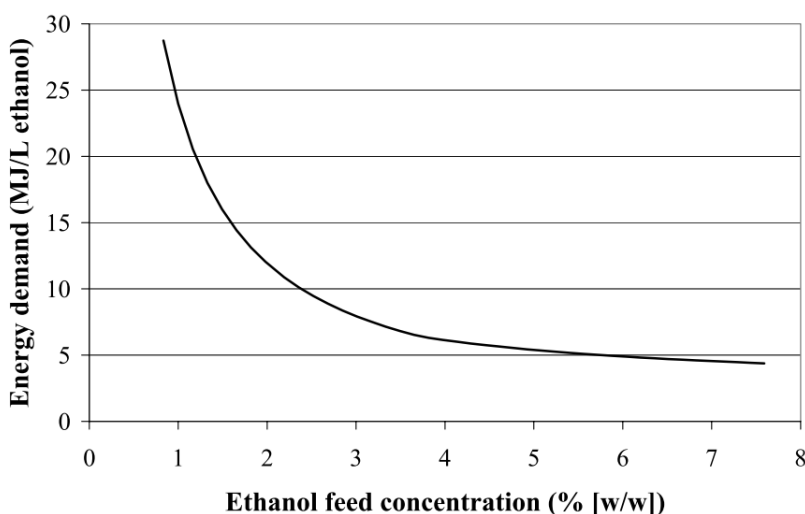


Figure 5. Distillation energy demand as a function of ethanol concentration in the beer (Figure 6 from Galbe & Zacchi 2007).

While the unit operations involved in cellulosic ethanol manufacture have been researched extensively, including multiple analyses on the requirements and features of a viable process (Davis et al., 2015; Dutta et al., 2011; Humbird et al., 2011), cellulosic ethanol is not as yet a commercially manufactured product. Several plants are being established for the same across the world (Klein-Marcuschamer & Blanch, 2015; Mutturi, Palmqvist, & Lidén, 2014). Within in the United States, the leading projects are by Abengoa Bioenergy (Hugoton, KS), Poet-DSM (Emmetsburg, IA), and DuPont Energy (Nevada, IA), all based on the breakdown of corn stover. The plants are designed to manufacture 20-30 million gallons of cellulosic ethanol annually, and are projected to begin full function in 2015-16. Other plants in the Americas include Iogen-Raizen (São Paulo, Brazil) and GranBio Bioflex 1 (Alagoas, Brazil), based on sugarcane bagasse. Near commercial-scale demonstration units have been built by Inbicon (Denmark), SEKAB (Sweden) and Weyland (Norway), all aiming to manufacture cellulosic ethanol from wheat straw, wood chips and bagasse. Efforts are ongoing to address the various bottlenecks that have prevented commercialization to this point.

4.6. Alternative Fermentation Fuels: Bio-Butanol

While ethanol is the most common alkanol/alcohol generated through fermentation, microbes are capable of generating longer chain alcohols, including propanol, butanol, isobutanol, and butanediol (Atsumi & Liao, 2008; Choi, Lee, Jang, & Lee, 2014; Jang et al., 2012; Mainguet & Liao, 2010; Yu, Cao, Zou, & Xian, 2010). Due to their longer chain length, their calorific value and solvent polarity are closer to those of gasoline, making them fuels that can be utilized in current-generation engines (termed ‘drop-in’ fuels). The higher chain length also makes them more cytotoxic than ethanol, as a result of which they are typically generated in much smaller concentrations. Efforts are ongoing to engineer biocatalysts for their commercially feasible manufacture.

Butanol is considered a suitable ‘drop in’ biofuel (Qureshi & Ezeji, 2008), as well as a feedstock for bio-based plastics and polymers. It is produced from sugars by bacteria of the *Clostridium* genus, *C. acetobutylicum* and *C. beijerinckii* being the predominant species used to make it. Bio-based butanol had been manufactured from starch and molasses on a commercial scale from 1912 until between 1960, when it became cost-ineffective compared to butanol synthesized from petroleum (Green, 2011; Qureshi & Blaschek, 2010). The concept was revived in recent times, following the increased focus on bio-based fuels and chemicals. An added attraction is the native ability *Clostridium* species have to ferment pentose sugars (Tracy, Jones, Fast, Indurthi, & Papoutsakis, 2012), making lignocellulose a suitable feedstock. The metabolic pathway generates acetone and ethanol as by-products and is termed ABE fermentation.

The ABE pathway follows the glycolytic breakdown of hexoses and pentoses into pyruvate. Following its generation, pyruvate can be directed towards several possible coenzyme moieties, predominantly acetyl, acetoacetyl, and butyryl. Depending upon the cell metabolic conditions, these are converted into the corresponding carboxylic acids or into ethanol, acetone and butanol, respectively. Pyruvate can also be directed towards acrylyl coenzyme, propionyl coenzyme, or α -acetolactic acid, eventually generating propionic acid, acrylic acid, and 2, 3-butanediol, respectively. These are generated in much smaller

concentrations, depending upon the *Clostridium* strain (Tracy et al., 2012). While the yields are currently very low, the ABE pathway could be theoretically engineered to generate isobutanol and 1, 4-butanediol.

The principal bottleneck in the commercialization of ABE fermentation is the high cytotoxicity of butanol. Butanol inhibits cell metabolism at concentrations as low as 0.5-1% w/v, compared to 8-10% w/v for ethanol fermentation in yeasts (Qureshi & Ezeji, 2008). As a result of the cytotoxicity, ABE batch fermentations result in fermentation yields averaging 30% of theoretical, with correspondingly low titers. While higher yields can be achieved through flow-through reactor configurations, the resulting product stream is dilute, making distillation unfeasible. In case of lignocellulosic fermentations, the toxicity is further exacerbated by the fermentation inhibitors released upon pretreatment (Baral & Shah, 2014). A recent innovation is the development of perstraction, to remove the fermented butanol and acetone as soon as they are generated. This is achieved by having an organic extractant in the reaction vessel, separated from the fermentation broth by a membrane. Due to its lower polarity, butanol spontaneously migrates into the extraction media, reducing the load on the fermenting cells (Maddox, Qureshi, & Roberts-Thomson, 1995; Qureshi & Maddox, 2005). Perstraction enabled the fermentation of 20-23% w/v lactose to 10% w/v total product. Further updates to the process were reported recently (Qureshi, Friedl, & Maddox, 2014). Efforts are also ongoing to improve the butanol tolerance of the fermenting *Clostridium* species through genetic engineering, as well as transfer the relevant genes into better fermenting biocatalysts such as *E. coli* or *Saccharomyces* (Branduardi, de Ferra, Longo, & Porro, 2013). At present, *Clostridium* species remain the best producers of butanol, with final product concentrations ranging 1-5% w/v under batch fermentation conditions, and 0.5-15% under fed-batch conditions (Köhler, Rühl, Blank, & Schmid, 2015). Various methods have also been proposed to better separate the butanol from the product stream (Abdehagh, Tezel, & Thibault, 2014; Qureshi & Ezeji, 2008). Despite its better fuel properties, butanol fermentation is currently unfeasible at the commercial scale due to low product concentration, yield and productivity, compared to ethanol fermentation in yeast.

CONCLUSION

Commercialization of biological processes for cellulose conversion to biofuels has required the integration of fundamental and applied biology with process engineering to develop robust, economical systems of technology to efficiently convert a mixture of sugars locked in plant cell wall polysaccharides. As described above, these efforts required the metabolic engineering of ethanologens to efficiently convert all plant biomass sugars to ethanol at high yields and a high final titers so that the resulting ethanol could be distilled efficiently. The development of a carefully balanced suite of enzymes was needed to hydrolyze cellulose to glucose for fermentation. While significant process has been made, the cost of enzymes required are a significant hurdle to cost-effective cellulosic ethanol. Third, pretreatment processes to enhance the reactivity of cellulose toward enzymatic hydrolysis that is robust and low cost is critical. Finally, these processing steps must be integrated in a way that takes into account the fact that plant cell wall components and derivatives thereof formed during processing can have significant harmful effects on downstream processes. A

technology and the underlying fundamental research that enables them continue to develop, future biological conversion of cellulose to biofuels may involve integrated biorefining approaches that result in processing facilities that make and sell a variety of products, including fuels. The market for renewable and sustainable carbon-based fuels, chemicals, and materials is likely to continue to be a significant one into the future. Processes that can realize value in these markets using plant biomass as a raw material have the potential to have significant economic, environmental, and societal impacts.

REFERENCES

- Abdehagh, N., Tezel, F. H. & Thibault, J. (2014). Separation techniques in butanol production: Challenges and developments. *Biomass and Bioenergy*, 60(C), 222–246.
- Aeling, K. A., Salmon, K. A., Laplaza, J. M., Li, L., Headman, J. R., Hutagalung, A. H. & Picataggio, S. (2012). Co-fermentation of xylose and cellobiose by an engineered *Saccharomyces cerevisiae*. *Journal of Industrial Microbiology & Biotechnology*, 39(11), 1597–1604.
- Agrawal, M., Mao, Z. & Chen, R. R. (2010). Adaptation yields a highly efficient xylose-fermenting *Zymomonas mobilis* strain. *Biotechnology and Bioengineering*, 108(4), 777–785.
- Agrawal, M., Wang, Y. & Chen, R. R. (2012). Engineering efficient xylose metabolism into an acetic acid-tolerant *Zymomonas mobilis* strain by introducing adaptation-induced mutations. *Biotechnology Letters*, 34(10), 1825–1832.
- Aguilera, F., Peinado, R., Millan, C., Ortega, J. & Mauricio, J. (2006). Relationship between ethanol tolerance, ATPase Activity and the Lipid Composition of the Plasma Membrane in Different Wine Yeast Strains. *International Journal of Food Microbiology*, 110(1), 34–42.
- Agbor, V. B., Cicek, N., Sparling, R., Berlin, A. & Levin, D. B. (2011). Biomass pretreatment: fundamentals toward application. *Biotechnology Advances*, 29(6), 675–685.
- Almeida, J. R. M., Bertilsson, M., Gorwa-Grauslund, M. F., Gorsich, S. & Lidén, G. (2009). Metabolic effects of furaldehydes and impacts on biotechnological processes. *Applied Microbiology and Biotechnology*, 82(4), 625–638.
- Alizadeh, H., Teymouri, F., Gilbert, T. I. & Dale, B. E. (2005). Pretreatment of switchgrass by ammonia fiber explosion (AFEX). *Applied Biochemistry and Biotechnology*, 124(1-3), 1133–1141.
- Amore, R., Wilhelm, M. & Hollenberg, C. P. (1989). The fermentation of xylose - An analysis of the expression of *Bacillus* and *Actinoplanes* xylose isomerase genes in yeast. *Applied Microbiology and Biotechnology*, 30(4), 351–357.
- Ando, S., Arai, I., Kiyoto, K. & Hanai, S. (1986). Identification of aromatic monomers in steam-exploded poplar and their influences on ethanol fermentation by *Saccharomyces cerevisiae*. *Journal of Fermentation Technology*, 64(6), 567–570.
- Andrić, Pavle, Meyer., Anne S., Jensen., Peter, A. & Dam-Johansen, Kim. (2010). Reactor design for minimizing product inhibition during enzymatic lignocellulose hydrolysis: I. Significance and mechanism of cellobiose and glucose inhibition on cellulolytic enzymes. *Biotechnology Advances*, 28(3), 308–324.

- Ask, M., Bettiga, M., Duraiswamy, V. R. & Olsson, L. (2013). Pulsed addition of HMF and furfural to batch-grown xylose-utilizing *Saccharomyces cerevisiae* results in different physiological responses in glucose and xylose consumption phase. *Biotechnology for Biofuels*, 6, 181–181.
- Athmanathan, A., Sedlak, M., Ho, N. W. Y. & Mosier, N. S. (2011). Effect of Product Inhibition on Xylose Fermentation to Ethanol by *Saccharomyces cerevisiae* 424A (LNH-ST). *Biological Engineering Transactions*, 3(2), 111–124.
- Athmanathan, A., Emery, I. R., Kuczek, T. & Mosier, N. S. (2015). Impact of Temperature, Moisture, and Storage Duration on the Chemical Composition of Switchgrass, Corn Stover, and Sweet Sorghum Bagasse. *BioEnergy Research*, 8(2), 843–856.
- Atsumi, S., & Liao, J. C. (2008). Metabolic engineering for advanced biofuels production from *Escherichia coli*. *Current Opinion in Biotechnology*, 19(5), 414–419.
- Bai, F. W., Anderson, W. A. & Moo-Young, M. (2008). Ethanol fermentation technologies from sugar and starch feedstocks. *Biotechnology Advances*, 26(1), 89–105.
- Baral, N. R. & Shah, A. (2014). Microbial inhibitors: formation and effects on acetone-butanol-ethanol fermentation of lignocellulosic biomass. *Applied Microbiology and Biotechnology*, 98(22), 9151–9172.
- Basso, T. O., Gomes, F. S., Lopes, M. L., de Amorim, H. V., Eggleston, G. & Basso, L. C. (2013). Homo- and heterofermentative lactobacilli differently affect sugarcane-based fuel ethanol fermentation. *Antonie Van Leeuwenhoek*, 105(1), 169–177.
- Bayrock, D. P. & Ingledew, W. M. (2004). Inhibition of yeast by lactic acid bacteria in continuous culture: nutrient depletion and/or acid toxicity? *Journal of Industrial Microbiology & Biotechnology*, 31(8), 362–368.
- Bayer, E. A., Chanzy, H., Lamed, R. & Shoham, Y. (1998). Cellulose, cellulases and cellulosomes. *Current Opinion in Structural Biology*, 8(5), 548–557.
- Beall, D. S., Ingram, L. O., Ben-Bassat, A., Doran, J. B., Fowler, D. E., Hall, R. G. & Wood, B. E. (1992). Conversion of hydrolysates of corn cobs and hulls into ethanol by recombinant *Escherichia coli* B containing integrated genes for ethanol production. *Biotechnology Letters*, 14(9), 857–862.
- Beckner, M., Ivey, M. L. & Phister, T. G. (2011). Microbial contamination of fuel ethanol fermentations. *Letters in Applied Microbiology*, 53(4), 387–394.
- Benítez, T., del Castillo, L., Aguilera, A., Conde, J. & Cerdáolmedo, E. (1983). Selection of Wine Yeasts for Growth and Fermentation in the Presence of Ethanol and Sucrose. *Applied and Environmental Microbiology*, 45(5), 1429–1436.
- Berlin, A., Balakshin, M., Gilkes, N., Kadla, J., Maximenko, V., Kubo, S. & Saddler, J. (2006). Inhibition of cellulase, xylanase and β -glucosidase activities by softwood lignin preparations. *Journal of Biotechnology*, 125(2), 198–209.
- Bertilsson, M., Andersson, J. & Lidén, G. (2007). Modeling simultaneous glucose and xylose uptake in *Saccharomyces cerevisiae* from kinetics and gene expression of sugar transporters. *Bioprocess and Biosystems Engineering*, 31(4), 369–377.
- Bettiga, M., Hahn-Hagerdal, B. & Gorwa-Grauslund, M. F. (2008). Comparing the xylose reductase/xylytol dehydrogenase and xylose isomerase pathways in arabinose and xylose fermenting *Saccharomyces cerevisiae* strains. *Biotechnology for Biofuels*, 1(1), 16.
- Bhosale, S. H., Rao, M. B. & Deshpande, V. V. (1996). Molecular and industrial aspects of glucose isomerase. *Microbiological Reviews*, 60(2), 280–300.

- Birch, R. M. & Walker, G. M. (2000). Influence of magnesium ions on heat shock and ethanol stress responses of *Saccharomyces cerevisiae*. *Enzyme and Microbial Technology*, 26(9-10), 678–687.
- Bischoff, K. M., Liu, S., Leathers, T. D., Worthington, R. E. & Rich, J. O. (2009). Modeling bacterial contamination of fuel ethanol fermentation. *Biotechnology and Bioengineering*, 103(1), 117–122.
- Boerjan, W., Ralph, J. & Baucher, M. (2003). Lignin biosynthesis. *Annual Review of Plant Biology*, 54(1), 519–546.
- Bras, J. L., Cartmell, A., Carvalho, A. L. M., Verze, G., Bayer, E. A., Vazana, Y. & Romao, M. J. (2011). Structural insights into a unique cellulase fold and mechanism of cellulose hydrolysis. *Proceedings of the National Academy of Sciences of the United States of America*, 108(13), 5237–5242.
- Brandon, S. K., Eiteman, M. A., Patel, K., Richbourg, M. M., Miller, D. J., Anderson, W. F. & Doran Peterson, J. (2008). Hydrolysis of Tifton 85 bermudagrass in a pressurized batch hot water reactor. *Journal of Chemical Technology & Biotechnology*, 83(4), 505–512.
- Brandon, S. K., Sharma, L. N., Hawkins, G. M., Anderson, W. F., Chambliss, C. K. & Doran Peterson, J. (2011). Ethanol and co-product generation from pressurized batch hot water pretreated T85 bermudagrass and Merkeron napiergrass using recombinant *Escherichia coli* as biocatalyst. *Biomass and Bioenergy*, 35(8), 3667–3673.
- Branduardi, P., de Ferra, F., Longo, V. & Porro, D. (2013). Microbial n-butanol production from Clostridia to non-Clostridial hosts. *Engineering in Life Sciences*, 14(1), 16–26.
- Bruinenberg, P. M. (1986). The NADP (H) redox couple in yeast metabolism. *Antonie Van Leeuwenhoek*, 52(5), 411–429.
- Byrt, C. S., Grof, C. P. L. & Furbank, R. T. (2011). C4 Plants as Biofuel Feedstocks: Optimising Biomass Production and Feedstock Quality from a Lignocellulosic Perspective Free Access. *Journal of Integrative Plant Biology*, 53(2), 120–135.
- Cardoso, H. & Leo, C. (1992). Mechanisms underlying the low and high enthalphy death induced by short-chain monocarboxylic acids and ethanol in *Saccharomyces cerevisiae*. *Applied Microbiology and Biotechnology*, 38(3), 388–392–392.
- Casey, E., Sedlak, M., Ho, N. W. Y. & Mosier, N. S. (2010). Effect of acetic acid and pH on the cofermentation of glucose and xylose to ethanol by a genetically engineered strain of *Saccharomyces cerevisiae*. *FEMS Yeast Research*, 10(4), 385–393.
- Carvalho, Florbela., Duarte, Luís, C. & Gírio, Francisco, M. (2008). Hemicellulose biorefineries: a review on biomass pretreatments. *Journal of Scientific & Industrial Research*, 67(11), 849–864.
- Casey, G. P., Magnus, C. A. & Ingledew, W. M. (1983). High gravity brewing: Nutrient enhanced production of high concentrations of ethanol by brewing yeast. *Biotechnology Letters*, 5(6), 429–434.
- Casey, G. P., Magnus, C. A. & Ingledew, W. M. (1984). High-Gravity Brewing: Effects of Nutrition on Yeast Composition, Fermentative Ability, and Alcohol Production. *Applied and Environmental Microbiology*, 48(3), 639–646.
- Chandel, A. K., da Silva, S. S. & Singh, O. V. (2013). Detoxification of Lignocellulose Hydrolysates: Biochemical and Metabolic Engineering Toward White Biotechnology. *BioEnergy Research*, 6(1), 388–401.

- Chandra, R. P., Bura, R., Mabee, W. E., Berlin, A., Pan, X. & Saddler, J. N. (2007). Substrate Pretreatment: The Key to Effective Enzymatic Hydrolysis of Lignocellulosics? *Adv Biochem Eng Biotechnol*, 108, 67-93.
- Chang, V. S. & Holtzapple, M. T. (2000). Fundamental factors affecting biomass enzymatic reactivity. *Applied Biochemistry and Biotechnology*, 84-86, 5-37.
- Choi, Y. J., Lee, J., Jang, Y. S. & Lee, S. Y. (2014). Metabolic Engineering of Microorganisms for the Production of Higher Alcohols. *mBio*, 5(5), e01524-14.
- Chornet, E. & Overend, R. P. (1991). Phenomenological kinetics and reaction engineering aspects of steam/aqueous treatments. *Steam Explosion Techniques: Fundamentals and Industrial Applications*, 21-58.
- Chou, K. S., Lu, Y. C. & Lee, H. H. (2005). Effect of alkaline ion on the mechanism and kinetics of chemical reduction of silver. *Materials Chemistry and Physics*, 94(2), 429-433.
- Chu, B. C. H. & Lee, H. (2007). Genetic improvement of *Saccharomyces cerevisiae* for xylose fermentation. *Biotechnology Advances*, 25(5), 425-441.
- Chum, H. L., Johnson, D. K., Black, S., Baker, J., Grohmann, K., Sarkanen, K. V. & Schroeder, H. A. (1988). Organosolv Pretreatment for Enzymatic-Hydrolysis of Poplars .1. Enzyme Hydrolysis of Cellulosic Residues. *Biotechnology and Bioengineering*, 31(7), 643-649.
- Chundawat, S. P., Donohoe, B. S., da Costa Sousa, L., Elder, T., Agarwal, U. P., Lu, F. & Dale, B. E. (2011). Multi-scale visualization and characterization of lignocellulosic plant cell wall deconstruction during thermochemical pretreatment. *Energy & Environmental Science*, 4(3), 973-984.
- Converse, A. O. (1993). Substrate factors limiting enzymatic hydrolysis. In J. N. Saddler (Ed.), *Bioconversion of Forest and Agricultural Plant Residues* (pp. 93-106). Wallingford, UK: CAB International.
- Ciesarova, Z., Sajbidor, J., Smogroviciova, D. & Bafrcnova, P. (1996). Effect of ethanol on fermentation and lipid composition in *Saccharomyces cerevisiae*. *Food Biotechnology*, 10(1), 1-12.
- Culberson, W. L. & Culberson, C. F. (1981). Yeast, ethanol and chemical competition. *American Naturalist*, 117(4), 567.
- Dadi, A. P., Schall, C. A. & Varanasi, S. (2007). Mitigation of cellulose recalcitrance to enzymatic hydrolysis by ionic liquid pretreatment. *Applied Biochemistry and Biotechnology*, 137, 407-421.
- Dadi, A. P., Varanasi, S. & Schall, C. A. (2006). Enhancement of cellulose saccharification kinetics using an ionic liquid pretreatment step. *Biotechnology and Bioengineering*, 95(5), 904-910.
- Davison, B. H., Drescher, S. R., Tuskan, G. A., Davis, M. F. & Nghiem, N. P. (2006). Variation of S/G ratio and lignin content in a *Populus* family influences the release of xylose by dilute acid hydrolysis. In *Twenty-Seventh Symposium on Biotechnology for Fuels and Chemicals* (pp. 427-435).
- D'Amore, T. & Stewart, G. G. (1987). Ethanol tolerance of yeast. *Enzyme and Microbial Technology*, 9(6), 322-330.
- D'Amore, T., Panchal, C. J. & Russell, I. (1989). A study of ethanol tolerance in yeast. *Critical Reviews in Biotechnology*, 9(4), 287-304.

- D'Amore, T., Panchal, C. J., Russeil, I. & Stewart, G. G. (1988). Osmotic pressure effects and intracellular accumulation of ethanol in yeast during fermentation. *Journal of Industrial Microbiology*, 2(6), 365–372.
- Davis, R., Tao, L., Scarlata, C., Tan, E. C. D., Ross, J., Lukas, J. & Sexton, D. (2015). Process Design and Economics for the Conversion of Lignocellulosic Biomass to Hydrocarbons: Dilute-Acid and Enzymatic Deconstruction of Biomass to Sugars and Catalytic Conversion of Sugars to Hydrocarbons (No. NREL/TP-5100-62498). National Renewable Energy Laboratory.
- Davison, B. H., Parks, J., Davis, M. F. & Donohoe, B. S. (2013). Plant Cell Walls: Basics of Structure, Chemistry, Accessibility and the Influence on Conversion. In C. E. Wyman, Aqueous Pretreatment of Plant Biomass for Biological and Chemical Conversion to Fuels and Chemicals (pp. 23–38). Chichester, UK: John Wiley & Sons, Ltd.
- de Vargas Andrade, S., de Moraes, M. D. L. T., Terenzi, H. F. & Jorge, J. A. (2004). Effect of carbon source on the biochemical properties of β -xylosidases produced by *Aspergillus versicolor*. *Process Biochemistry*, 39(12), 1931–1938.
- de Vargas Andrade, S., de Moraes, Maria., de Lourdes, Teixeira., Terenzi, Héctor Francisco. & Jorge, João Atilio. (2004). Effect of carbon source on the biochemical properties of β -xylosidases produced by *Aspergillus versicolor*. *Process Biochemistry*, 39(12), 1931–1938.
- Dhamole, P. B., Wang, B. & Feng, H. (2013). Detoxification of corn stover hydrolysate using surfactant-based aqueous two phase system. *Journal of Chemical Technology & Biotechnology*, 88(9), 1744–1749.
- Dien, B. S., Cotta, M. A. & Jeffries, T. W. (2003). Bacteria engineered for fuel ethanol production: current status. *Applied Microbiology and Biotechnology*, 63(3), 258–266.
- Dien, B. S., Hespell, R. B., Wyckoff, H. A. & Bothast, R. J. (1998). Fermentation of hexose and pentose sugars using a novel ethanologenic *Escherichia coli* strain. *Enzyme and Microbial Technology*, 23(6), 366–371.
- Dien, B. S., Nichols, N. N., O'Bryan, P. J. & Bothast, R. J. (2000). Development of new ethanologenic *Escherichia coli* strains for fermentation of lignocellulosic biomass. *Applied Biochemistry and Biotechnology*, 84-86(1-9), 181–196.
- DiMarco, A. A. & Romano, A. H. (1985). D-Glucose transport system of *Zymomonas mobilis*. *Applied and Environmental Microbiology*, 49(1), 151–157.
- Ding, S., Xu, Q., Crowley, M., Zeng, Y., Nimlos, M., Lamed, R. & Himmel, M. E. (2008). A biophysical perspective on the cellulosome: new opportunities for biomass conversion. *Current Opinion in Biotechnology*, 19(3), 218–227.
- Doelle, H. W., Kirk, L., Crittenden, R., Toh, H. & Doelle, M. B. (1993). *Zymomonas Mobilis*—Science and Industrial Application. *Critical Reviews in Biotechnology*, 13(1), 57–98.
- Donohoe, B. S., Decker, S. R., Tucker, M. P., Himmel, M. E. & Vinzant, T. B. (2008). Visualizing lignin coalescence and migration through maize cell walls following thermochemical pretreatment. *Biotechnology and Bioengineering*, 101(5), 913–925.
- Dutta, A., Talmadge, M., Hensley, J., Worley, M., Dudgeon, D., Barton, D., et al. (2011). Process Design and Economics for Conversion of Lignocellulosic Biomass to Ethanol: Thermochemical Pathway by Indirect Gasification and Mixed Alcohol Synthesis (No. NREL/TP-5100-51400) (pp. 1–187). National Renewable Energy Laboratory.

- Eliasson, A., Christensson, C., Wahlbom, C. F. & Hahn-Hägerdal, B. (2000). Anaerobic xylose fermentation by recombinant *Saccharomyces cerevisiae* carrying XYL1, XYL2, and XKS1 in mineral medium chemostat cultures. *Applied and Environmental Microbiology*, 66(8), 3381–3386.
- Eliasson, A., Hofmeyr, J. H. S., Pedler, S. & Hahn-Hägerdal, B. (2001). The xylose reductase/xylytol dehydrogenase/xylylulokinase ratio affects product formation in recombinant xylose-utilising *Saccharomyces cerevisiae*. *Enzyme and Microbial Technology*, 29(4–5), 288–297.
- Esteghlalian, A. R., Bilodeau, M., Mansfield, S. D. & Saddler, J. N. (2001). Do enzymatic hydrolyzability and Simons' stain reflect the changes in the accessibility of lignocellulosic substrates to cellulase enzymes? *Biotechnology Progress*, 17(6), 1049–1054.
- Fitzgerald, D. J., Stratford, M., Gasson, M. J., Ueckert, J., Bos, A. & Narbad, A. (2004). Mode of antimicrobial action of vanillin against *Escherichia coli*, *Lactobacillus plantarum* and *Listeria innocua*. *Journal of Applied Microbiology*, 97(1), 104–113.
- Fonseca, C. S., Olofsson, K., Ferreira, C., Runquist, D., Fonseca, L. L., Hahn-Hägerdal, B. & Lidén, G. (2011). The glucose/xylose facilitator Gxf1 from *Candida intermedia* expressed in a xylose-fermenting industrial strain of *Saccharomyces cerevisiae* increases xylose uptake in SSCF of wheat straw. *Enzyme and Microbial Technology*, 48(6-7), 518–525.
- Franden, M. A., Pienkos, P. T. & Zhang, M. (2009). Development of a high-throughput method to evaluate the impact of inhibitory compounds from lignocellulosic hydrolysates on the growth of *Zymomonas mobilis*. *Journal of Biotechnology*, 144(4), 259–267.
- Franden, M. A., Pilath, H. M., Mohagheghi, A., Pienkos, P. T. & Zhang, M. (2013). Inhibition of growth of *Zymomonas mobilis* by model compounds found in lignocellulosic hydrolysates. *Biotechnology for Biofuels*, 6, 99–99.
- Freudenberg, Karl. & Neish, Arthur Charles. (1968). Constitution and biosynthesis of lignin. *Constitution and Biosynthesis of Lignin*.
- Galbe, M. & Zacchi, G. (2007). Pretreatment of lignocellulosic materials for efficient bioethanol production Biofuels (pp. 41-65): Springer.
- Galbe, M. & Zacchi, G. (2012). Pretreatment: The key to efficient utilization of lignocellulosic materials. *Biomass and Bioenergy*, 46(C), 70–78.
- Galbe, M., Sassner, P., Wingren, A. & Zacchi, G. (2007). Process Engineering Economics of Bioethanol Production. In L. Olsson, *Biofuels*, (Vol. 108, pp. 303–327). Springer Berlin Heidelberg.
- Galbe, M., Wallberg, O. & Zacchi, G. (2013). Cellulosic Bioethanol Production. In S. Ramaswamy, H.-J. Huang, & B. V. Ramarao, *Separation and Purification Technologies in Biorefineries* (pp. 487–501). Chichester, UK: John Wiley & Sons, Ltd.
- García-Aparicio, MA Prado., Ballesteros, Ignacio., González, Alberto., Oliva, José Miguel., Ballesteros, Mercedes. & Negro, MA José. (2006). Effect of inhibitors released during steam-explosion pretreatment of barley straw on enzymatic hydrolysis. At the Twenty-Seventh Symposium on Biotechnology for Fuels and Chemicals.
- García-Aparicio, M. P., Ballesteros, M., Manzanares, P., Ballesteros, I., González, A. & Negro, M. J. (2007). Xylanase contribution to the efficiency of cellulose enzymatic hydrolysis of barley straw. *Applied Biochemistry and Biotechnology*, 137(1-12), 353–365.
- Geddes, C. C., Nieves, I. U. & Ingram, L. O. (2011). Advances in ethanol production. *Current Opinion in Biotechnology*, 22(3), 312–319.

- Gellerstedt, G., Li, J., Eide, I., Kleinert, M. & Barth, T. (2008). Chemical structures present in biofuel obtained from lignin. *Energy & Fuels*, 22(6), 4240-4244.
- Gibson, B. R., Lawrence, S. J., Leclaire, J. P. R., Powell, C. D. & Smart, K. A. (2007). Yeast responses to stresses associated with industrial brewery handling. *FEMS Microbiology Reviews*, 31(5), 535-569.
- Glasser, W. G. & Wright, R. S. (1998). Steam-assisted biomass fractionation. II. Fractionation behavior of various biomass resources. *Biomass and Bioenergy*, 14(3), 219-235.
- Goldemberg, J., Coelho, S. T. & Guardabassi, P. (2008). The sustainability of ethanol production from sugarcane. *Energy Policy*, 36(6), 2086-2097.
- Gombert, A. K. & van Maris, A. (2015). Improving conversion yield of fermentable sugars into fuel ethanol in 1st generation yeast-based production processes. *Current Opinion in Biotechnology*, 33, 81-86.
- Gray, K. A., Zhao, L. & Emptage, M. (2006). Bioethanol. *Current Opinion in Chemical Biology*, 10(2), 141-146.
- Gray, W. D. (1941). Studies on the Alcohol Tolerance of Yeasts. *Journal of Bacteriology*, 42(5), 561-574.
- Green, E. M. (2011). Fermentative production of butanol-the industrial perspective. *Current Opinion in Biotechnology*, 22(3), 337-343.
- Grethlein, Hans E. (1984). Pretreatment for enhanced hydrolysis of cellulosic biomass. *Biotechnology Advances*, 2(1), 43-62.
- Grohmann, K., Mitchell, D. J., Himmel, M. E., Dale, B. E. & Schroeder, H. A. (1989). The role of ester groups in resistance of plant cell wall polysaccharides to enzymatic hydrolysis. *Applied Biochemistry and Biotechnology*, 20(1), 45-61.
- Gruno, M., Våljamäe, P., Pettersson, G. & Johansson, G. (2004). Inhibition of the *Trichoderma reesei* cellulases by cellobiose is strongly dependent on the nature of the substrate. *Biotechnology and Bioengineering*, 86(5), 503-511.
- Grzenia, D. L., Dong, R. W., Jasuja, H., Kipper, M. J., Qian, X. & Wickramasinghe, S. R. (2012). Conditioning biomass hydrolysates by membrane extraction. *Journal of Membrane Science*, 415-416(C), 75-84.
- Gurram, R. N., Datta, S., Lin, Y. J., Snyder, S. W. & Menkhous, T. J. (2011). Removal of enzymatic and fermentation inhibitory compounds from biomass slurries for enhanced biorefinery process efficiencies. *Bioresource Technology*, 102(17), 7850-7859.
- Hagman, A. & Piskur, J. (2015). A Study on the Fundamental Mechanism and the Evolutionary Driving Forces behind Aerobic Fermentation in Yeast. *PLoS ONE*, 10(1), e0116942.
- Hahn-Hägerdal, B., Karhumaa, K., Jeppsson, M. & Gorwa-Grauslund, M. F. (2007). Metabolic engineering for pentose utilization in *saccharomyces cerevisiae*. In *L. Olssen, Biofuels*, (Vol. 108, pp. 147-177).
- Hahn-Hägerdal, B., Galbe, M., Gorwa-Grauslund, M. F., Lidén, G. & Zacchi, G. (2006). Bio-ethanol—the fuel of tomorrow from the residues of today. *Trends in Biotechnology*, 24(12), 549-556.
- Hamacher, T., Becker, J., Gárdonyi, M., Hahn-Hägerdal, B. & Boles, E. (2002). Characterization of the xylose-transporting properties of yeast hexose transporters and their influence on xylose utilization. *Microbiology*, 148(9), 2783-2788.

- Han, Y. & Chen, H. Z. (2007). Synergism between corn stover protein and cellulase. *Enzyme and Microbial Technology*, 41(5), 638-645.
- Harhangi, H. R., Akhmanova, A. S., Emmens, R., van der Drift, C., de Laat, W. T. A. M., van Dijken, J. P., et al. (2003). Xylose metabolism in the anaerobic fungus *Piromyces* sp. strain E2 follows the bacterial pathway. *Archives of Microbiology*, 180(2), 134-141.
- Hatti-Kaul, R., Törnqvall, U., Gustafsson, L. & Börjesson, P. (2007). Industrial biotechnology for the production of bio-based chemicals—a cradle-to-grave perspective. *Trends in Biotechnology*, 25(3), 119-124.
- Hayes, D. J. & Hayes, M. H. B. (2009). The role that lignocellulosic feedstocks and various biorefining technologies can play in meeting Ireland's biofuel targets. *Biofuels, Bioproducts and Biorefining*, 3(5), 500-520.
- Hector, R. E., Qureshi, N., Hughes, S. R. & Cotta, M. A. (2008). Expression of a heterologous xylose transporter in a *Saccharomyces cerevisiae* strain engineered to utilize xylose improves aerobic xylose consumption. *Applied Microbiology and Biotechnology*, 80(4), 675-684.
- Henderson, C. M. & Block, D. E. (2014). Examining the role of membrane lipid composition in determining the ethanol tolerance of *Saccharomyces cerevisiae*. *Applied and Environmental Microbiology*, 80(10), 2966-2972.
- Henderson, C. M., Lozada-Contreras, M., Jiranek, V., Longo, M. L. & Block, D. E. (2013a). Ethanol production and maximum cell growth are highly correlated with membrane lipid composition during fermentation as determined by lipidomic analysis of 22 *Saccharomyces cerevisiae* strains. *Applied and Environmental Microbiology*, 79(1), 91-104.
- Henderson, C. M., Zeno, W. F., Lerno, L. A., Longo, M. L. & Block, D. E. (2013b). Fermentation temperature modulates phosphatidylethanolamine and phosphatidylinositol levels in the cell membrane of *Saccharomyces cerevisiae*. *Applied and Environmental Microbiology*, 79(17), 5345-5356.
- Hendriks, A. T. W. M. & Zeeman, G. (2009). Pretreatments to enhance the digestibility of lignocellulosic biomass. *Bioresource Technology*, 100(1), 10-18.
- Henrissat, B., Driguez, H., Viet, C. & Schülein, M. (1985). Synergism of cellulases from *Trichoderma reesei* in the degradation of cellulose. *Nature Biotechnology*, 3(8), 722-726.
- Hespell, R. B., Wyckoff, H., Dien, B. S. & Bothast, R. J. (1996). Stabilization of pet operon plasmids and ethanol production in *Escherichia coli* strains lacking lactate dehydrogenase and pyruvate formate- lyase activities. *Applied and Environmental Microbiology*, 62(12), 4594-4597.
- Himmel, M. E., Ding, S. Y., Johnson, D. K., Adney, W. S., Nimlos, M. R., Brady, J. W. & Foust, T. D. (2007). Biomass recalcitrance: Engineering plants and enzymes for biofuels production. *Science*, 315(5813), 804-807.
- Ho, N. W. Y. & Tsao, G. T. (1998). Recombinant yeasts for effective fermentation of glucose and xylose. (Purdue Research Foundation). Google Patents.
- Ho, N. W. Y., Chen, Z. & Brainard, A. P. (1998). Genetically engineered *Saccharomyces* yeast capable of effective cofermentation of glucose and xylose. *Applied and Environmental Microbiology*, 64(5), 1852-1859.
- Ho, N. W. Y., Stevis, P. & Rosenfeld, S. (1983). Expression of the *E. coli* xylose isomerase gene by a yeast promoter. *Biotechnology Bioengineering Symposium*, VOL. 13(13), 245-250.

- Humbird, D., Davis, R., Tao, L., Kinchin, C., Hsu, D., Aden, A., et al. (2011). Process Design and Economics for Biochemical Conversion of Lignocellulosic Biomass to Ethanol: Dilute-Acid Pretreatment and Enzymatic Hydrolysis of Corn Stover, (No. NREL/TP-5100-47764) (pp. 1–147). Golden, CO: National Renewable Energy Laboratory.
- Hu, F., Jung, S. & Ragauskas, A. (2012). Pseudo-lignin formation and its impact on enzymatic hydrolysis. *Bioresource Technology*, *117*, 7-12.
- Hu, W., Harding, S. A., Lung, J., Popko, J. L., Ralph, J., Stokke, D. D. & Chiang, V. L. (1999). Repression of lignin biosynthesis promotes cellulose accumulation and growth in transgenic trees. *Nature Biotechnology*, *17*(8), 808-812.
- Humphreys, John M. & Chapple, Clint. (2002). Rewriting the lignin roadmap. *Current Opinion in Plant Biology*, *5*(3), 224-229.
- Ingram, L. O. (1986). Microbial tolerance to alcohols: role of the cell membrane. *Trends in Biotechnology*, *4*(2), 40–44.
- Ingram, L. O., Conway, T., Clark, D. P., Sewell, G. W. & Preston, J. F. (1987). Genetic engineering of ethanol production in *Escherichia coli*. *Applied and Environmental Microbiology*, *53*(10), 2420–2425.
- Ilmen, Marja., Saloheimo, Anu., Onnela, Maija-Leena. & Penttilä, MERJA E. (1997). Regulation of cellulase gene expression in the filamentous fungus *Trichoderma reesei*. *Applied and Environmental Microbiology*, *63*(4), 1298-1306.
- Jang, Y. S., Kim, B., Shin, J. H., Choi, Y. J., Choi, S., Song, C. W., et al. (2012). Bio-based production of C2–C6 platform chemicals. *Biotechnology and Bioengineering*, *109*(10), 2437–2459.
- Jarboe, L. R., Grabar, T. B., Yomano, L. P., Shanmugan, K. T. & Ingram, L. O. (2007). Development of ethanologenic bacteria. *Biofuels*, (Vol. 108, pp. 237–261).
- Jeffries, T. W. (1983). Utilization of xylose by bacteria, yeasts, and fungi. *Advances in Biochemical Engineering/Biotechnology*, *27*, 1–32.
- Jeffries, T. W. (2006). Engineering yeasts for xylose metabolism. *Current Opinion in Biotechnology*, *17*(3), 320–326.
- Jeoh, Tina. (1998). Steam explosion pretreatment of cotton gin waste for fuel ethanol production. Virginia Polytechnic Institute and State University.
- Jeon, Y. J., Svenson, C. J., Joachimsthal, E. L. & Rogers, P. L. (2002). Kinetic analysis of ethanol production by an acetate-resistant strain of recombinant *Zymomonas mobilis*. *Biotechnology Letters*, *24*(10), 819–824.
- Jeppsson, M., Bengtsson, O., Franke, K., Lee, H., Hähn-Hägerdal, B. & Gorwa-Grauslund, M. F. (2006). The expression of a *Pichia stipitis* xylose reductase mutant with higher KM for NADPH increases ethanol production from xylose in recombinant *Saccharomyces cerevisiae*. *Biotechnology and Bioengineering*, *93*(4), 665–673.
- Jin, M., da Costa Sousa, L., Schwartz, C., He, Y., Sarks, C., Gunawan, C. & Dale, B. E. (2016). Toward lower cost cellulosic biofuel production using ammonia based pretreatment technologies. *Green Chemistry*, *18*(4), 957-966.
- Jing, X., Zhang, X. & Bao, J. (2009). Inhibition performance of lignocellulose degradation products on industrial cellulase enzymes during cellulose hydrolysis. *Applied Biochemistry and Biotechnology*, *159*(3), 696-707.
- Joachimsthal, E. L. & Rogers, P. L. (2000). Characterization of a high-productivity recombinant strain of *Zymomonas mobilis* for ethanol production from glucose/xylose mixtures. *Applied Biochemistry and Biotechnology*, *84-86*(1-9), 343–356.

- Joachimsthal, E., Haggett, K. & Rogers, P. L. (1999). Evaluation of recombinant strains of *Zymomonas mobilis* for ethanol production from glucose/xylose media. *Applied Biochemistry and Biotechnology*, 77(1-3), 147–157.
- Joachimsthal, E., Haggett, K., Jang, J. H. & Rogers, P. L. (1998). A mutant of *Zymomonas mobilis* ZM4 capable of ethanol production from glucose in the presence of high acetate concentrations. *Biotechnology Letters*, 20(2), 137–142.
- Jönsson, L. J., Alriksson, B. & Nilvebrant, N. O. (2013). Bioconversion of lignocellulose: inhibitors and detoxification. *Biotechnology for Biofuels*, 6, 16–16.
- Kabel, M. A., Bos, G., Zeevalking, J., Voragen, A. G. J. & Schols, H. A. (2007). Effect of pretreatment severity on xylan solubility and enzymatic breakdown of the remaining cellulose from wheat straw. *Bioresource Technology*, 98(10), 2034–2042.
- Kanda, T., Wakabayashi, K. & Nisizawa, K. (1980). Modes of Action of Exo-Cellulases and Endo-Cellulases in the Degradation of Cellulose-I and Cellulose-II. *Journal of Biochemistry*, 87(6), 1635–1639.
- Karhumaa, K., Fromanger, R., Hähn-Hägerdal, B. & Gorwa-Grauslund, M. F. (2006). High activity of xylose reductase and xylitol dehydrogenase improves xylose fermentation by recombinant *Saccharomyces cerevisiae*. *Applied Microbiology and Biotechnology*, 73(5), 1039–1046.
- Karhumaa, K., Hahn-Hagerdal, B. & Gorwa-Grauslund, M. F. (2005). Investigation of limiting metabolic steps in the utilization of xylose by recombinant *Saccharomyces cerevisiae* using metabolic engineering. *Yeast*, 22(5), 359–368.
- Karhumaa, K., Sanchez, R. G., Hähn-Hägerdal, B. & Gorwa-Grauslund, M. F. (2007). Comparison of the xylose reductase-xylitol dehydrogenase and the xylose isomerase pathways for xylose fermentation by recombinant *Saccharomyces cerevisiae*. *Microbial Cell Factories*, 6, 5–5.
- Karunanithy, C. & Muthukumarappan, K. (2009). Influence of Extruder Temperature and Screw Speed on Pretreatment of Corn Stover while Varying Enzymes and Their Ratios. *Applied Biochemistry and Biotechnology*, 162(1), 264–279.
- Karunanithy, C. & Muthukumarappan, K. (2012). A comparative study on torque requirement during extrusion pretreatment of different feedstocks. *BioEnergy Research*, 5(2), 263–276.
- Katakura, Y., Moukamnerd, C., Harashima, S. & Kino-oka, M. (2011). Strategy for preventing bacterial contamination by adding exogenous ethanol in solid-state semi-continuous bioethanol production. *Journal of Bioscience and Bioengineering*, 111(3), 343–345.
- Katzen, R., Madson, P. W. & Moon Jr, G. D. (1999). Ethanol distillation: the fundamentals. *The Alcohol Textbook*, 269–299.
- Kawamoto, H., Nakatsubo, F. & Murakami, K. (1992). Protein-adsorbing capacities of lignin samples. *Journal of the Japan Wood Research Society*, 38(1), 81–84.
- Keweloh, H., Weyrauch, G. & Rehm, H.-J. R. (1990). Phenol-induced membrane changes in free and immobilized *Escherichia coli*. *Applied Microbiology and Biotechnology*, 33(1), 66–71.
- Khanna, Sunil. (1993). Regulation, purification, and properties of xylanase from *Cellulomonas fimi*. *Enzyme and Microbial Technology*, 15(11), 990–995.

- Khatibi, P. A., Roach, D. R., Donovan, D. M., Hughes, S. R. & Bischoff, K. M. (2014). *Saccharomyces cerevisiae* expressing bacteriophage endolysins reduce *Lactobacillus* contamination during fermentation. *Biotechnology for Biofuels*, 7(1), 104.
- Khattab, S. M. R. & Kodaki, T. (2014). Efficient bioethanol production by overexpression of endogenous *Saccharomyces cerevisiae* xylulokinase and NADPH-dependent aldose reductase with mutated strictly NADP⁺-dependent *Pichia stipitis* xylitol dehydrogenase. *Process Biochemistry*, 49(11), 1838–1842.
- Khattab, S. M. R., Saimura, M. & Kodaki, T. (2013). Boost in bioethanol production using recombinant *Saccharomyces cerevisiae* with mutated strictly NADPH-dependent xylose reductase and NADP⁺-dependent xylitol dehydrogenase. *Journal of Biotechnology*, 165(3-4), 153–156.
- Khullar, E., Kent, A. D., Leathers, T. D., Bischoff, K. M., Rausch, K. D., Tumbleson, M. E. & Singh, V. (2012). Contamination issues in a continuous ethanol production corn wet milling facility. *World Journal of Microbiology and Biotechnology*, 29(5), 891–898.
- Kim, J., Jia, H. & Wang, P. (2006). Challenges in biocatalysis for enzyme-based biofuel cells. *Biotechnology advances*, 24(3), 296–308.
- Kim, T. H. & Yoon Y. Lee. (2005). Pretreatment and fractionation of corn stover by ammonia recycle percolation process. *Bioresource Technology*, 96(18), 2007–2013.
- Kim, Y., Ximenes, E., Mosier, N. S. & Ladisch, M. R. (2011). Soluble inhibitors/deactivators of cellulase enzymes from lignocellulosic biomass. *Enzyme and Microbial Technology*, 48(4-5), 408–415.
- Klein-Marcuschamer, D., Oleskowicz-Popiel, P., Simmons, B. A. & Blanch, H. W. (2012). The challenge of enzyme cost in the production of lignocellulosic biofuels. *Biotechnology and Bioengineering*, 109(4), 1083–1087.
- Klein-Marcuschamer, D. & Blanch, H. W. (2015). Renewable fuels from biomass: Technical hurdles and economic assessment of biological routes. *AIChE Journal*, 61(9), 2689–2701.
- Klein-Marcuschamer, D., Holmes, B., Simmons, B. A. & Blanch, H. W. (2011). *Biofuel Economics. Plant Biomass Conversion*, (pp. 329–354). Hoboken, NJ, USA: John Wiley & Sons, Inc.
- Klinke, H. B., Thomsen, A. B. & Ahring, B. K. (2004). Inhibition of ethanol-producing yeast and bacteria by degradation products produced during pre-treatment of biomass. *Applied Microbiology and Biotechnology*, 66(1), 10–26.
- Kodama, Y., Kielland-Brandt, M. C. & Hansen, J. (2006). Lager brewing yeast. In P. Sunnerhagen & J. Piskur, *Comparative Genomics* (Vol. 15, pp. 145–164). Berlin, Heidelberg: Springer Berlin Heidelberg.
- Kong, F., Engler, C. R. & Soltes, E. J. (1992). Effects of cell-wall acetate, xylan backbone, and lignin on enzymatic hydrolysis of aspen wood. *Applied Biochemistry and Biotechnology*, 34(1), 23–35.
- Kont, R., Kurašin, M., Teugjas, H. & Väljamäe, P. (2013). Strong cellulase inhibitors from the hydrothermal pretreatment of wheat straw. *Biotechnology for Biofuels*, 6(1), 135.
- Koo, Bon-Wook., Kim, Ho-Yong., Park, Nahyun., Lee, Soo-Min., Yeo, Hwanmyeong. & Choi, In-Gyu. (2011). Organosolv pretreatment of *Liriodendron tulipifera* and simultaneous saccharification and fermentation for bioethanol production. *Biomass and Bioenergy*, 35(5), 1833–1840.

- Koppram, R., Tomás-Pejó, E., Xiros, C. & Olsson, L. (2014). Lignocellulosic ethanol production at high-gravity: challenges and perspectives. *Trends in Biotechnology*, 32(1), 46–53.
- Kotiranta, P., Karlsson, J., Siika-Aho, M., Medve, J., Viikari, L., Tjerneld, F. & Tenkanen, M. (1999). Adsorption and activity of *Trichoderma reesei* cellobiohydrolase I, endoglucanase II, and the corresponding core proteins on steam pretreated willow. *Applied Biochemistry and Biotechnology*, 81(2), 81–90.
- Kotter, P. & Ciriacy, M. (1993). Xylose fermentation by *Saccharomyces cerevisiae*. *Applied Microbiology and Biotechnology*, 38(6), 776–783.
- Kotter, P., Amore, R., Hollenberg, C. P. & Ciriacy, M. (1990). Isolation and characterization of the *Pichia stipitis* xylitol dehydrogenase gene, XYL2, and construction of a xylose-utilizing *Saccharomyces cerevisiae* transformant. *Current Genetics*, 18(6), 493–500.
- Koukkou, A. I., Tsoukatos, D. & Drainas, C. (1993). Effect of ethanol on the sterols of the fission yeast *Schizosaccharomyces pombe*. *FEMS Microbiology Letters*, 111(2-3), 171–175.
- Köhler, K. A. K., Rühl, J., Blank, L. M. & Schmid, A. (2015). Integration of biocatalyst and process engineering for sustainable and efficient n-butanol production. *Engineering in Life Sciences*, 15(1), 4–19.
- Krallish, I., Jeppsson, H., Rapoport, A. & Hahn-Hagerdal, B. (1997). Effect of xylitol and trehalose on dry resistance of yeasts. *Applied Microbiology and Biotechnology*, 47(4), 447–451.
- Kramer, R. & Belanger, H. (2011). Fermentation-Based Biofuels. In E. E. Hood, P. Nelson, & R. Powell, *Plant Biomass Conversion*, (pp. 255–274). Hoboken, NJ, USA: John Wiley & Sons, Inc.
- Krishnan, M. S., Blanco, M., Shattuck, C. K., Nghiem, N. P. & Davison, B. H. (2000). Ethanol production from glucose and xylose by immobilized *Zymomonas mobilis* CP4 (pZB5). *Applied Biochemistry and Biotechnology*, 84-86(1-9), 525–541.
- Krishnan, M. S., Ho, N. W. Y. & Tsao, G. T. (1999). Fermentation kinetics of ethanol production from glucose and xylose by recombinant *Saccharomyces* 1400(pLNH33). *Applied Biochemistry and Biotechnology - Part a Enzyme Engineering and Biotechnology*, 77-79, 373–388.
- Kristensen, J. B., Felby, C. & Jørgensen, H. (2009). Yield-determining factors in high-solids enzymatic hydrolysis of lignocellulose. *Biotechnology for Biofuels*, 2(1), 11.
- Kruckeberg, A. L. (1996). The hexose transporter family of *Saccharomyces cerevisiae*. *Archives of Microbiology*, 166(5), 283–292.
- Kumar, P., Barrett, D. M., Delwiche, M. J. & Stroeve, P. (2009). Methods for pretreatment of lignocellulosic biomass for efficient hydrolysis and biofuel production. *Industrial & Engineering Chemistry Research*, 48(8), 3713–3729.
- Kumar, R., Mago, G., Balan, V. & Wyman, C. E. (2009). Physical and chemical characterizations of corn stover and poplar solids resulting from leading pretreatment technologies. *Bioresource Technology*, 100(17), 3948–3962.
- Kumar, R. & Wyman, C. E. (2009a). Cellulase Adsorption and Relationship to Features of Corn Stover Solids Produced by Leading Pretreatments. *Biotechnology and Bioengineering*, 103(2), 252–267.

- Kumar, R. & Wyman, C. E. (2009b). Does change in accessibility with conversion depend on both the substrate and pretreatment technology? *Bioresource Technology*, 100(18), 4193-4202.
- Kumar, R. & Wyman, C. E. (2009c). Effects of cellulase and xylanase enzymes on the deconstruction of solids from pretreatment of poplar by leading technologies. *Biotechnology Progress*, 25(2), 302-314.
- Kumar, R. & Wyman, C. E. (2009d). Effect of additives on the digestibility of corn stover solids following pretreatment by leading technologies. *Biotechnology and Bioengineering*, 102(6), 1544-1557.
- Kumar, R. & Wyman, C. E. (2009e). Effect of enzyme supplementation at moderate cellulase loadings on initial glucose and xylose release from corn stover solids pretreated by leading technologies. *Biotechnology and Bioengineering*, 102(2), 457-467.
- Kumar, R., Hu, F., Sannigrahi, P., Jung, S., Ragauskas, A. J. & Wyman, C. E. (2013). Carbohydrate derived-pseudo-lignin can retard cellulose biological conversion. *Biotechnology and Bioengineering*, 110(3), 737-753.
- Kuyper, M., Harhangi, H., Stave, A., Winkler, A., Jetten, M., Delaat, W., et al. (2003). High-level functional expression of a fungal xylose isomerase: the key to efficient ethanolic fermentation of xylose by *FEMS Yeast Research*, 4(1), 69-78.
- Kuyper, M., Hartog, M., Toirkens, M., Almering, M., Winkler, A., vanDijken, J. & Pronk, J. (2005a). Metabolic engineering of a xylose-isomerase-expressing strain for rapid anaerobic xylose fermentation. *FEMS Yeast Research*, 5(4-5), 399-409.
- Kuyper, M., Toirkens, M. J., Diderich, J. A., Winkler, A. A., Van Dijken, J. P. & Pronk, J. T. (2005b). Evolutionary engineering of mixed-sugar utilization by a xylose-fermenting *Saccharomyces cerevisiae* strain. *FEMS Yeast Research*, 5(10), 925-934.
- Kuyper, M., Winkler, A. A., Van Dijken, J. P. & Pronk, J. T. (2004). Minimal metabolic engineering of *Saccharomyces cerevisiae* for efficient anaerobic xylose fermentation: A proof of principle. *FEMS Yeast Research*, 4(6), 655-664.
- Lam, V. M. S., Daruwalla, K. R., Henderson, P. J. F. & Jones-Mortimer, M. C. (1980). Proton-linked D-xylose transport in *Escherichia coli*. *Journal of Bacteriology*, 143(1), 396-402.
- Larsson, S., Quintana-Sáinz, A., Reimann, A., Nilvebrant, N. O. & Jönsson, L. J. (2000). Influence of Lignocellulose-Derived Aromatic Compounds on Oxygen-Limited Growth and Ethanolic Fermentation by *Saccharomyces cerevisiae*. *Applied Biochemistry and Biotechnology*, 84-86(1-9), 617-632.
- Larsson, S., Reimann, A., Nilvebrant, N. O. & Jönsson, L. J. (1999). Comparison of different methods for the detoxification of lignocellulose hydrolyzates of spruce. *Applied Biochemistry and Biotechnology*, 77(1-3), 91-103.
- Lau, M. W., Dale, B. E. & Balan, V. (2007). Ethanolic fermentation of hydrolysates from ammonia fiber expansion (AFEX) treated corn stover and distillers grain without detoxification and external nutrient supplementation. *Biotechnology and Bioengineering*, 99(3), 529-539.
- Laureano-Perez, Lizbeth., Teymouri, Farzaneh., Alizadeh, Hasan. & Dale, Bruce E. (2005). Understanding factors that limit enzymatic hydrolysis of biomass. *Applied Biochemistry and Biotechnology*, 124(1-3), 1081-1099.

- Lawford, H. G., Rousseau, J. D., Mohagheghi, A. & McMillan, J. D. (1998). Continuous culture studies of xylose-fermenting *Zymomonas mobilis*. *Applied Biochemistry and Biotechnology*, 70-72(1), 353–367.
- Lawford, H. G., Rousseau, J. D., Mohagheghi, A. & McMillan, J. D. (1999). Fermentation performance characteristics of a prehydrolyzate-adapted xylose-fermenting recombinant *Zymomonas* in batch and continuous fermentations. *Applied Biochemistry and Biotechnology*, 77(1-3), 191–204.
- Leao, C. & Van Uden, N. (1982). Effects of ethanol and other alkanols on the glucose transport system of *Saccharomyces cerevisiae*. *Biotechnology and Bioengineering*, 24(11), 2601–2604.
- Leao, C. & Van Uden, N. (1983). Effects of ethanol and other alkanols on the ammonium transport system of *Saccharomyces cerevisiae*. *Biotechnology and Bioengineering*, 25(8), 2085–2089.
- Leao, C. & Van Uden, N. (1984a). Effects of ethanol and other alkanols on passive proton influx in the yeast *Saccharomyces cerevisiae*. *Biochimica Et Biophysica Acta - Biomembranes*, 774(1), 43–48.
- Leao, C. & Van Uden, N. (1984b). Effects of ethanol and other alkanols on the general amino acid permease of *Saccharomyces cerevisiae*. *Biotechnology and Bioengineering*, 26(4), 403–405.
- Lee, K. H., Chung, J. M. & Willis Jr, W. D. (1985). Inhibition of primate spinothalamic tract cells by TENS. *Journal of Neurosurgery*, 62(2), 276-287.
- Lee, J. H., Pagan, R. J. & Rogers, P. L. (1983). Continuous simultaneous saccharification and fermentation of starch using *Zymomonas mobilis*. *Biotechnology and Bioengineering*, 25(3), 659–669.
- Lee, S. H., Kodaki, T., Park, Y. C. & Seo, J. H. (2012). Effects of NADH-preferring xylose reductase expression on ethanol production from xylose in xylose-metabolizing recombinant *Saccharomyces cerevisiae*. *Journal of Biotechnology*, 158(4), 184–191.
- Li, J., Henriksson, G. & Gellerstedt, G. (2007). Lignin depolymerization/ repolymerization and its critical role for delignification of aspen wood by steam explosion. *Bioresource Technology*, 98(16), 3061-3068.
- Lights, F. O. (2011). Industry statistics: 2010 world fuel ethanol production. Renewable Fuels Association, accessed in “<http://www.ethanolrfa.org/pages/statistics>.”
- Liu, C. Q., Goodman, A. E. & Dunn, N. W. (1988). Expression of cloned *Xanthomonas* d-xylose catabolic genes in *Zymomonas mobilis*. *Journal of Biotechnology*, 7(1), 61–70.
- Liu, Z. L. (2011). Molecular mechanisms of yeast tolerance and *in situ* detoxification of lignocellulose hydrolysates. *Applied Microbiology and Biotechnology*, 90(3), 809–825.
- Liu, Z. L. & Blaschek, H. P. (2010). Biomass Conversion Inhibitors and *In Situ* Detoxification. In A. A. Verts, N. Qureshi, H. P. Blaschek, & H. Yukawa, *Biomass to Biofuels*, (pp. 233–259). Blackwell Publishing Ltd.
- Liu, Z. L., Slininger, P. J., Dien, B. S., Berhow, M. A., Kurtzman, C. P. & Gorsich, S. W. (2004). Adaptive response of yeasts to furfural and 5-hydroxymethylfurfural and new chemical evidence for HMF conversion to 2, 5-bis-hydroxymethylfuran. *Journal of Industrial Microbiology and Biotechnology*, 31(8), 345-352.
- Lönn, A., Gárdonyi, M., Van Zyl, W., Hahn-Hagerdal, B. & Otero, R. C. (2002). Cold adaptation of xylose isomerase from *Thermus thermophilus* through random

- PCR mutagenesis: Gene cloning and protein characterization. *European Journal of Biochemistry*, 269(1), 157–163.
- Lu, Y., Yang, B., Gregg, D., Saddler, J. N. & Mansfield, S. D. (2002). Cellulase adsorption and an evaluation of enzyme recycle during hydrolysis of steam-exploded softwood residues. *Applied Biochemistry and Biotechnology*, 98(1-9), 641–654.
- Lucena, B. T., Santos, dos, B. M., Moreira, J. L., Moreira, A. P. B., Nunes, A. C., Azevedo, V., et al. (2010). Diversity of lactic acid bacteria of the bioethanol process. *BMC Microbiology*, 10, 298–298.
- Luo, J., Zeuner, B., Morthensen, S. T., Meyer, A. S. & Pinelo, M. (2015). Separation of phenolic acids from monosaccharides by low-pressure nanofiltration integrated with laccase pre-treatments. *Journal of Membrane Science*, 482(C), 83–91.
- Luo, X. L. & Zhu, J. Y. (2011). Effects of drying-induced fiber hornification on enzymatic saccharification of lignocelluloses. *Enzyme and Microbial Technology*, 48(1), 92–99.
- Lynd, L. R., Wyman, C. E. & Gerngross, T. U. (1999). Biocommodity Engineering. *Biotechnology Progress*, 15(5), 777–793.
- Lynd, L. R., Weimer, P. J., van Zyl, W. H. & Pretorius, I. S. (2002). Microbial cellulose utilization: fundamentals and biotechnology. *Microbiology and Molecular Biology Review*, 66(3), 506–577.
- Ma, M., Liu, Z. L. & Moon, J. (2012). Genetic Engineering of Inhibitor-Tolerant *Saccharomyces cerevisiae* for Improved Xylose Utilization in Ethanol Production. *BioEnergy Research*, 5(2), 459–469.
- Maddox, I. S., Qureshi, N. & Roberts-Thomson, K. (1995). Production of acetone-butanol-ethanol from concentrated substrate using *Clostridium acetobutylicum* in an integrated fermentation-product removal process. *Process Biochemistry*, 30(3), 209–215.
- Mansfield, S. D., Mooney, C. & Saddler, J. N. (1999). Substrate and enzyme characteristics that limit cellulose hydrolysis. *Biotechnology Progress*, 15(5), 804–816.
- Mainguet, S. E. & Liao, J. C. (2010). Bioengineering of microorganisms for C3 to C5 alcohols production. *Biotechnology Journal*, 5(12), 1297–1308.
- Maiorella, B. L., Blanch, H. W. & Wilke, C. R. (1984). Economic evaluation of alternative ethanol fermentation processes. *Biotechnology and Bioengineering*, 26(9), 1003–1025.
- Maiorella, B., Blanch, H. W. & Wilke, C. R. (1983). By-product inhibition effects on ethanolic fermentation by *Saccharomyces cerevisiae*. *Biotechnology and Bioengineering*, 25(1), 103–121.
- Mannazzu, I., Angelozzi, D., Belviso, S., Budroni, M., Farris, G. A., Goffrini, P., et al. (2008). Behaviour of *Saccharomyces cerevisiae* wine strains during adaptation to unfavourable conditions of fermentation on synthetic medium: Cell lipid composition, membrane integrity, viability and fermentative activity. *International Journal of Food Microbiology*, 121(1), 84–91.
- Martin, G. J. O., Knepper, A., Zhou, B. & Pamment, N. B. (2006). Performance and stability of ethanologenic *Escherichia coli* strain FBR5 during continuous culture on xylose and glucose. *Journal of Industrial Microbiology & Biotechnology*, 33(10), 834–844.
- Martin, C. & Jönsson, L. J. (2003). Comparison of the Resistance of Industrial and Laboratory Strains of *Saccharomyces* And *Zygosaccharomyces* To Lignocellulose-Derived Fermentation Inhibitors. *Enzyme and Microbial Technology*, 32(3–4), 386–395.
- Matsushika, A., Goshima, T., Fujii, T., Inoue, H., Sawayama, S. & Yano, S. (2012). Characterization of non-oxidative transaldolase and transketolase enzymes in the pentose

- phosphate pathway with regard to xylose utilization by recombinant *Saccharomyces cerevisiae*. *Enzyme and Microbial Technology*, 51(1), 16–25.
- McMichael, P. (2009). Banking on agriculture: a review of the World Development Report 2008. *Journal of Agrarian Change*, 9(2), 235–246.
- McMillan, J. D. (1997). Bioethanol production: status and prospects. *Renewable energy*, 10(2), 295–302.
- Meyer, A. S., Rosgaard, L. & Sørensen, H. R. (2009). The minimal enzyme cocktail concept for biomass processing. *Journal of Cereal Science*, 50(3), 337–344.
- Mills, T. Y., Sandoval, N. R. & Gill, R. T. (2009). Cellulosic hydrolysate toxicity and tolerance mechanisms in *Escherichia coli*. *Biotechnology for Biofuels*, 2(1), 26.
- Modenbach, A. A. & Nokes, S. E. (2012). The use of high-solids loadings in biomass pretreatment—a review. *Biotechnology and Bioengineering*, 109(6), 1430–1442.
- Modenbach, A. A. & Nokes, S. E. (2013). Enzymatic hydrolysis of biomass at high-solids loadings. *Biomass and Bioenergy*, 56(C), 526–544.
- Moes, C. J., Pretorius, I. S. & Van Zyl, W. H. (1996). Cloning and expression of the clostridium thermosulfurogenes d-xylose isomerase gene (xylA) in *saccharomyces cerevisiae*. *Biotechnology Letters*, 18(3), 269–274.
- Mohagheghi, A., Dowe, N., Schell, D., Chou, Y. C., Eddy, C. & Zhang, M. (2004). Performance of a newly developed integrant of *Zymomonas mobilis* for ethanol production on corn stover hydrolysate. *Biotechnology Letters*, 26(4), 321–325.
- Mohagheghi, A., Evans, K., Chou, Y. C. & Zhang, M. (2002). Cofermentation of glucose, xylose, and arabinose by genomic DNA-integrated xylose/arabinose fermenting strain of *Zymomonas mobilis* AX101. *Applied Biochemistry and Biotechnology*, 98–100(1–9), 885–898.
- Mohagheghi, A., Evans, K., Finkelstein, M. & Zhang, M. (1998). Cofermentation of glucose, xylose, and arabinose by mixed cultures of two genetically engineered *Zymomonas mobilis* strains. *Applied Biochemistry and Biotechnology*, 70–72(1), 285–299.
- Moniruzzaman, M. & Ingram, L. (1998). Ethanol production from dilute acid hydrolysate of rice hulls using genetically engineered *Escherichia coli*. *Biotechnology Letters*, 20(10), 943–947.
- Moniruzzaman, M., Dien, B. S., Ferrer, B., Hespell, R. B., Dale, B. E., Ingram, L. O. & Bothast, R. J. (1996). Ethanol production from AFEX pretreated corn fiber by recombinant bacteria. *Biotechnology Letters*, 18(8), 985–990.
- Monteiro, G. A. & Sá-Correia, I. (1997). *In vivo* activation of yeast plasma membrane H⁺-ATPase by ethanol: effect on the kinetic parameters and involvement of the carboxyl-terminus regulatory domain. *Biochimica Et Biophysica Acta - Biomembranes*, 1370(2), 310–316.
- Mooney, C. A., Mansfield, S. D., Touhy, M. G. & Saddler, J. N. (1998). The effect of initial pore volume and lignin content on the enzymatic hydrolysis of softwoods. *Bioresource Technology*, 64(2), 113–119.
- Mosier, N., Hendrickson, R., Ho, N., Sedlak, M. & Ladisch, M. R. (2005). Optimization of pH controlled liquid hot water pretreatment of corn stover. *Bioresource Technology*, 96(18), 1986–1993.
- Mosier, N., Wyman, C., Dale, B., Elander, R., Lee, Y. Y., Holtzapfle, M. & Ladisch, M. (2005). Features of promising technologies for pretreatment of lignocellulosic biomass. *Bioresource Technology*, 96(6), 673–686.

- Mosier, N. S. (2013). Fundamentals of Aqueous Pretreatment of Biomass. In C. E. Wyman, Aqueous Pretreatment of Plant Biomass for Biological and Chemical Conversion to Fuels and Chemicals. Chichester, UK: John Wiley & Sons, Ltd.
- Mosier, N. S. & Ladisch, M. R. (2009). Microbial Fermentations. *Modern Biotechnology*, (pp. 73–109). Hoboken, NJ, USA: John Wiley & Sons, Inc.
- Murzin, Dmitry Yu. & Salmi, Tapio. (2012). Catalysis for Lignocellulosic Biomass Processing: Methodological Aspects. *Catalysis Letters*, 142(7), 817–829.
- Muthaiyan, A., Limayem, A. & Ricke, S. C. (2011). Antimicrobial strategies for limiting bacterial contaminants in fuel bioethanol fermentations. *Progress in Energy and Combustion Science*, 37(3), 351–370.
- Mutturi, S., Palmqvist, B. & Lidén, G. (2014). Developments in bioethanol fuel-focused biorefineries. *Advances in Biorefineries*, (pp. 259–302). Woodhead Publishing Limited.
- Nagodawithana, T. W. & Steinkraus, K. H. (1976). Influence of the rate of ethanol production and accumulation on the viability of *Saccharomyces cerevisiae* in “rapid fermentation.” *Applied and Environmental Microbiology*, 31(32), 158–162.
- Naik, SN, Goud., Vaibhav V, Rout., Prasant, K. & Dalai, Ajay K. (2010). Production of first and second generation biofuels: a comprehensive review. *Renewable and Sustainable Energy Reviews*, 14(2), 578–597.
- Narendranath, N. V., Hynes, S. H., Thomas, K. C. & Ingledew, W. M. (1997). Effects of lactobacilli on yeast-catalyzed ethanol fermentations. *Applied and Environmental Microbiology*, 63(11), 4158–4163.
- Narendranath, N. V., Thomas, K. C. & Ingledew, W. M. (2001). Effects of acetic acid and lactic acid on the growth of *Saccharomyces cerevisiae* in a minimal medium. *Journal of Industrial Microbiology & Biotechnology*, 26(3), 171–177.
- Ohta, K. & Hayashida, S. (1983). Role of Tween 80 and Monoolein in a Lipid-Sterol-Protein Complex Which Enhances Ethanol Tolerance of Sake Yeasts. *Applied and Environmental Microbiology*, 46(4), 821–825.
- Ohta, K., Beall, D. S., Mejia, J. P., Shanmugam, K. T. & Ingram, L. O. (1991). Genetic Improvement of *Escherichia Coli* for Ethanol Production: Chromosomal Integration of *Zymomonas Mobilis* Genes Encoding Pyruvate Decarboxylase and Alcohol Dehydrogenase II. *Applied and Environmental Microbiology*, 57(4), 893–900.
- Olofsson, K., Bertilsson, M. & Lidén, G. (2008). A short review on SSF – an interesting process option for ethanol production from lignocellulosic feedstocks. *Biotechnology for Biofuels*, 1, 7–7.
- Palmqvist, E. & Hähn-Hägerdal, B. (2000a). Fermentation of lignocellulosic hydrolysates. I: inhibition and detoxification. *Bioresource Technology*, 74(1), 17–24.
- Palmqvist, E. & Hähn-Hägerdal, B. (2000b). Fermentation of Lignocellulosic Hydrolysates. II: Inhibitors and Mechanisms of Inhibition. *Bioresource Technology*, 74(1), 25–33.
- Pampulha, M. E. & Loureiro-Dias, M. C. (1989). Combined effect of acetic acid, pH and ethanol on intracellular pH of fermenting yeast. *Applied Microbiology and Biotechnology*, 31-31(5-6), 547–550.
- Pan, X. J., Arato, C., Gilkes, N., Gregg, D., Mabee, W., Pye, K. & Saddler, J. (2005). Biorefining of softwoods using ethanol organosolv pulping: Preliminary evaluation of process streams for manufacture of fuel-grade ethanol and co-products. *Biotechnology and Bioengineering*, 90(4), 473–481.

- Pan, X. J., Xie, D., Gilkes, N., Gregg, D. J. & Saddler, J. N. (2005). Strategies to enhance the enzymatic hydrolysis of pretreated softwood with high residual lignin content. At the Twenty-Sixth Symposium on Biotechnology for Fuels and Chemicals.
- Panesar, P. S., Marwaha, S. S. & Kennedy, J. F. (2006). *Zymomonas mobilis*: an alternative ethanol producer. *Journal of Chemical Technology & Biotechnology*, 81(4), 623–635.
- Park, S. C. & Baratti, J. (1991). Comparison of ethanol production by *Zymomonas mobilis* from sugar beet substrates. *Applied Microbiology and Biotechnology*, 35(3), 283–291.
- Pascual, C., Alonso, A., Garcia, I., Romay, C. & Kotyk, A. T. (1988). Effect of ethanol on glucose transport, key glycolytic enzymes, and proton extrusion in *Saccharomyces cerevisiae*. *Biotechnology and Bioengineering*, 32(3), 374–378.
- Pérez, J., Munoz-Dorado, J., de la Rubia, T. D. L. R. & Martinez, J. (2002). Biodegradation and biological treatments of cellulose, hemicellulose and lignin: an overview. *International Microbiology*, 5(2), 53–63.
- Perlack, R. D. & Stokes, B. J. (2011). U.S. Billion-Ton Update: *Biomass Supply for a Bioenergy and Bioproducts Industry*, (No. ORNL/TM-2011/224) (pp. 1–235). Oak Ridge, TN: US Dept. of Energy.
- Perlack, R. D., Wright, L. L., Turhollow, A. F., Graham, R. L., Stokes, B. J. & Erbach, D. C. (2005). Biomass as Feedstock for a Bioenergy and Bioproducts Industry: The Technical Feasibility of a Billion-Ton Annual Supply, (pp. 1–78). Oak Ridge National Laboratory.
- Petschacher, B. & Nidetzky, B. (2008). Altering the coenzyme preference of xylose reductase to favor utilization of NADH enhances ethanol yield from xylose in a metabolically engineered strain of *Saccharomyces cerevisiae*. *Microbial Cell Factories*, 7, 9–9.
- Picataggio, S. & Zhang, M. (1996). Biocatalyst Development for Bioethanol Production from Hydrolysates. In C. E. Wyman, *Handbook on Bioethanol: Production and Utilization*, (pp. 163–178).
- Piotrowski, J. S., Zhang, Y., Bates, D. M., Keating, D. H., Sato, T. K., Ong, I. M. & Landick, R. (2014). Death by a thousand cuts: the challenges and diverse landscape of lignocellulosic hydrolysate inhibitors. *Frontiers in Microbiology*, 5, 90.
- Plesset, J., Palm, C. & McLaughlin, C. S. (1982). Induction of heat shock proteins and thermotolerance by ethanol in *Saccharomyces cerevisiae*. *Biochemical and Biophysical Research Communications*, 108(3), 1340–1345.
- Power, R. F. (2003). Enzymatic conversion of starch to fermentable sugars. In K. A. Jacques, T. P. Lyons, & D. R. Kelsall, *The Alcohol Textbook*, (4 ed., pp. 23–32). Nottingham University Press.
- Pronk, J. T., Steensma, H. Y. & Van Dijken, J. P. (1996). Pyruvate metabolism in *Saccharomyces cerevisiae*. *Yeast*, 12(16), 1607–1633.
- Puri, V. P. (1984). Effect of crystallinity and degree of polymerization of cellulose on enzymatic saccharification. *Biotechnology and Bioengineering*, 26(10), 1219–1222.
- Qi, B., Chen, X., Su, Y. & Wan, Y. (2011). Enzyme adsorption and recycling during hydrolysis of wheat straw lignocellulose. *Bioresource Technology*, 102(3), 2881–2889.
- Qing, Q., Yang, B. & Wyman, C. E. (2010). Xylooligomers are strong inhibitors of cellulose hydrolysis by enzymes. *Bioresource Technology*, 101(24), 9624–9630.
- Qureshi, N. & Blaschek, H. P. (2010). Clostridia and Process Engineering for Energy Generation. In A. A. Verts, N. Qureshi, H. P. Blaschek, & H. Yukawa, *Biomass to Biofuels*, (pp. 347–358). Oxford, UK: Blackwell Publishing Ltd.

- Qureshi, N. & Ezeji, T. C. (2008). Butanol, “a superior biofuel” production from agricultural residues (renewable biomass): recent progress in technology. *Biofuels, Bioproducts and Biorefining*, 2(4), 319–330.
- Qureshi, N. & Maddox, I. S. (2005). Reduction in Butanol Inhibition by Perstraction: Utilization of Concentrated Lactose/Whey Permeate by *Clostridium acetobutylicum* to Enhance Butanol Fermentation Economics. *Food and Bioproducts Processing*, 83(1), 43–52.
- Qureshi, N., Dien, B. S., Nichols, N. N., Saha, B. C. & Cotta, M. A. (2006). Genetically engineered *Escherichia coli* for ethanol production from xylose. *Food and Bioproducts Processing*, 84(2), 114–122.
- Qureshi, N., Friedl, A. & Maddox, I. S. (2014). Butanol production from concentrated lactose/whey permeate: Use of pervaporation membrane to recover and concentrate product. *Applied Microbiology and Biotechnology*, 98(23), 9859–9867.
- Ragauskas, A. J., Beckham, G. T., Biddy, M. J., Chandra, R., Chen, F., Davis, M. F. & Wyman, C. E. (2014). Lignin valorization: improving lignin processing in the biorefinery. *Science*, 344(6185), 1246843.
- Ramirez, R. S., Holtzapple, M. & Piamonte, N. (2013). Fundamentals of Biomass Pretreatment at High pH. In C. E. Wyman, *Aqueous Pretreatment of Plant Biomass for Biological and Chemical Conversion to Fuels and Chemicals*, (pp. 145–167). Chichester, UK: John Wiley & Sons, Ltd.
- Ramos, L. P., Nazhad, M. M. & Saddler, J. N. (1993). Effect of enzymatic hydrolysis on the morphology and fine structure of pretreated cellulosic residues. *Enzyme and Microbial Technology*, 15(10), 821–831.
- Ramos, L. P. (2003). The chemistry involved in the steam treatment of lignocellulosic materials. *Química Nova*, 26(6), 863–871.
- Rasmussen, M. L., Koziel, J. A., Jane, J. L. & Pometto, A. L., III. (2015). Reducing Bacterial Contamination in Fuel Ethanol Fermentations by Ozone Treatment of Uncooked Corn Mash. *Journal of Agricultural and Food Chemistry*, 63(21), 5239–5248.
- Renewable Fuels Association (RFA), (2015). Going global-2015 ethanol industry outlook. RFA.
- Rinaldi, R. & Schüth, F. (2009). Design of solid catalysts for the conversion of biomass. *Energy & Environmental Science*, 2(6), 610–626.
- Ritter, S. K. (2008). Lignocellulose: A complex biomaterial. *Plant Biochemistry*, 86(49), 15.
- Rowell, R. M. (2012). *Handbook of wood chemistry and wood composites*: CRC press.
- Rogers, P. L., Jeon, Y. J., Lee, K. J. & Lawford, H. G. (2007). *Zymomonas mobilis* for Fuel Ethanol and Higher Value Products. In L. Olsson, *Biofuels*, (Vol. 108, pp. 263–288). Springer Berlin Heidelberg.
- Rogers, P. L., Lee, K. & Tribe, D. E. (1979). Kinetics of alcohol production by *Zymomonas mobilis* at high sugar concentrations. *Biotechnology Letters*, 1(4), 165–170.
- Rudolf, A., Karhumaa, K. & Hähn-Hägerdal, B. (2009). Ethanol Production from Traditional and Emerging Raw Materials. In T. Satyanarayana & G. Kunze, *Yeast Biotechnology: Diversity and Applications*, (pp. 489–513). Dordrecht: Springer Netherlands.
- Russell, I. (2003). Understanding yeast fundamentals. In K. A. Jacques, T. P. Lyons, & D. R. Kelsall, *The Alcohol Textbook*, (4 ed., pp. 85–120). Nottingham University Press.
- Saha, B. C. (2003). Hemicellulose bioconversion. *Journal of Industrial Microbiology & Biotechnology*, 30(5), 279–291.

- Saha, B. C. & Cotta, M. A. (2006). Ethanol production from alkaline peroxide pretreated enzymatically saccharified wheat straw. *Biotechnology Progress*, 22(2), 449–453.
- Saha, B. C. & Cotta, M. A. (2007a). Enzymatic hydrolysis and fermentation of lime pretreated wheat straw to ethanol. *Journal of Chemical Technology & Biotechnology*, 82(10), 913–919.
- Saha, B. C. & Cotta, M. A. (2007b). Enzymatic saccharification and fermentation of alkaline peroxide pretreated rice hulls to ethanol. *Enzyme and Microbial Technology*, 41(4), 528–532.
- Saha, B. C. & Cotta, M. A. (2008). Lime pretreatment, enzymatic saccharification and fermentation of rice hulls to ethanol. *Biomass and Bioenergy*, 32(10), 971–977.
- Saha, B. C. & Cotta, M. A. (2010). Comparison of pretreatment strategies for enzymatic saccharification and fermentation of barley straw to ethanol. *New Biotechnology*, 27(1), 10–16.
- Saha, B. C. & Cotta, M. A. (2011). Continuous ethanol production from wheat straw hydrolysate by recombinant ethanologenic *Escherichia coli* strain FBR5. *Applied Microbiology and Biotechnology*, 90(2), 477–487.
- Saha, B. C., Iten, L. B., Cotta, M. A. & Wu, Y. V. (2005). Dilute acid pretreatment, enzymatic saccharification and fermentation of wheat straw to ethanol. *Process Biochemistry*, 40(12), 3693–3700.
- Saha, B. C., Iten, L. B., Cotta, M. A. & Wu, Y. V. (2008). Dilute Acid Pretreatment, Enzymatic Saccharification, and Fermentation of Rice Hulls to Ethanol. *Biotechnology Progress*, 21(3), 816–822.
- Saha, B. C., Nichols, N. N. & Cotta, M. A. (2011a). Ethanol production from wheat straw by recombinant *Escherichia coli* strain FBR5 at high solid loading. *Bioresource Technology*, 102(23), 10892–10897.
- Saha, B. C., Nichols, N. N., Qureshi, N. & Cotta, M. A. (2011b). Comparison of separate hydrolysis and fermentation and simultaneous saccharification and fermentation processes for ethanol production from wheat straw by recombinant *Escherichia coli* strain FBR5. *Applied Microbiology and Biotechnology*, 92(4), 865–874.
- Saha, B. C., Qureshi, N., Kennedy, G. J. & Cotta, M. A. (2015). Enhancement of xylose utilization from corn stover by a recombinant *Escherichia coli* strain for ethanol production. *Bioresource Technology*, 190(C), 182–188.
- Saha, B. C., Yoshida, T., Cotta, M. A. & Sonomoto, K. (2013). Hydrothermal pretreatment and enzymatic saccharification of corn stover for efficient ethanol production. *Industrial Crops and Products*, 44, 367–372.
- Saloheimo, A., Rauta, J., Stasyk, O. V., Sibirny, A. A., Penttilä, M. & Ruohonen, L. (2006). Xylose transport studies with xylose-utilizing *Saccharomyces cerevisiae* strains expressing heterologous and homologous permeases. *Applied Microbiology and Biotechnology*, 74(5), 1041–1052.
- Sarthy, A. V., McConaughy, B. L., Lobo, Z., Sundstrom, J. A., Furlong, C. E. & Hall, B. D. (1987). Expression of the *Escherichia coli* xylose isomerase gene in *Saccharomyces cerevisiae*. *Applied and Environmental Microbiology*, 53(9), 1996–2000.
- Sáez-Miranda, J. C., Saliceti-Piazza, L. & McMillan, J. D. (2006). Measurement and analysis of intracellular ATP levels in metabolically engineered *Zymomonas mobilis* fermenting glucose and xylose mixtures. *Biotechnology Progress*, 22(2), 359–368.

- Sathitsuksanoh, N., Zhu, Z. G., Wi, S. & Zhang, Y. H. P. (2011). Cellulose Solvent-Based Biomass Pretreatment Breaks Highly Ordered Hydrogen Bonds in Cellulose Fibers of Switchgrass. *Biotechnology and Bioengineering*, 108(3), 521-529.
- Sannigrahi, P., Kim, D. H., Jung, S. & Ragauskas, A. (2011). Pseudo-lignin and pretreatment chemistry. *Energy & Environmental Science*, 4(4), 1306-1310.
- Schell, D. J., Dowe, N., Ibsen, K. N., Riley, C. J., Ruth, M. F. & Lumpkin, R. E. (2007). Contaminant occurrence, identification and control in a pilot-scale corn fiber to ethanol conversion process. *Bioresource Technology*, 98(15), 2942-2948.
- Searchinger, T. & Heimlich, R. (2009). Likely impacts of biofuel expansion on midwest land and water resources. *International Journal of Biotechnology*, 11(1-2), 127-149.
- Searchinger, T., Heimlich, R., Houghton, R. A., Dong, F., Elobeid, A., Fabiosa, J., et al. (2008). Use of U.S. Croplands for Biofuels Increases Greenhouse Gases Through Emissions from Land-Use Change. *Science*, 319(5867), 1238-1240.
- Sedlak, M. & Ho, N. W. Y. (2004). Characterization of the effectiveness of hexose transporters for transporting xylose during glucose and xylose co-fermentation by a recombinant *Saccharomyces* yeast. *Yeast*, 21(8), 671-684.
- Selig Michael, J., Knoshaug Eric, P., Adney William, S., Himmel Michael, E. & Decker, Stephen R. (2008). Synergistic enhancement of cellobiohydrolase performance on pretreated corn stover by addition of xylanase and esterase activities. *Bioresource Technology*, 99(11), 4997-5005.
- Severian, D. (2008). Polysaccharides: structural diversity and functional versatility. Marcel Dekker, New York.
- Shahir, S. A., Masjuki, H. H., Kalam, M. A., Imran, A., Fattah, IM Rizwanul. & Sanjid, A. (2014). Feasibility of diesel-biodiesel-ethanol/bioethanol blend as existing CI engine fuel: An assessment of properties, material compatibility, safety and combustion. *Renewable and Sustainable Energy Reviews*, 32, 379-395.
- Shen, B., Hohmann, S., Jensen, R. G. & Bohnert, A. H. J. (1999). Roles of Sugar Alcohols in Osmotic Stress Adaptation. Replacement of Glycerol by Mannitol and Sorbitol in Yeast. *Plant Physiology*, 121(1), 45-52.
- Shevchenko Sergey, M., Beatson Rodger, P. & Saddler John, N. (1999). The nature of lignin from steam explosion/enzymatic hydrolysis of softwood. *Applied Biochemistry and Biotechnology*, 79(1-3), 867-876.
- Shi, J., Gladden, J. M., Sathitsuksanoh, N., Kambam, P., Sandoval, L., Mitra, D. & Singh, S. (2013). One-pot ionic liquid pretreatment and saccharification of switchgrass. *Green Chemistry*, 15(9), 2579-2589.
- Singh, V., Johnston, D. B., Rausch, K. D. & Tumbleson, M. E. (2010a). Improvements in Corn to Ethanol Production Technology Using *Saccharomyces cerevisiae*. In A. A. Verts, N. Qureshi, H. P. Blaschek, & H. Yukawa, *Biomass to Biofuels*, (pp. 185-198). Oxford, UK: Blackwell Publishing Ltd.
- Skinner, K. A. & Leathers, T. D. (2004). Bacterial contaminants of fuel ethanol production. *Journal of Industrial Microbiology & Biotechnology*, 31(9), 401-408.
- Skotnicki, M. L., Lee, K. J., Tribe, D. E. & Rogers, P. L. (1981). Comparison of ethanol production by different *Zygomonas* strains. *Applied and Environmental Microbiology*, 41(4), 889-893.
- Slater, S. J., Ho, C., Taddeo, F. J., Kelly, M. B. & Stubbs, C. D. (1993). Contribution of hydrogen bonding to lipid-lipid interactions in membranes and the role of lipid order:

- Effects of cholesterol, increased phospholipid unsaturation, and ethanol. *Biochemistry*, 32(14), 3714–3721.
- Smith, K. A. & Searchinger, T. D. (2012). Crop-based biofuels and associated environmental concerns. *GCB Bioenergy*, 4(5), 479–484.
- Song, S. & Park, C. (1997). Organization and regulation of the D-xylose operons in *Escherichia coli* K-12: XylR acts as a transcriptional activator. *Journal of Bacteriology*, 179(22), 7025–7032.
- Sousa, L. D., Chundawat, S. P. S., Balan, V. & Dale, B. E. (2009). ‘Cradle-to-grave’ assessment of existing lignocellulose pretreatment technologies. *Current Opinion in Biotechnology*, 20(3), 339–347.
- Sprenger, G. A. (1996). Carbohydrate metabolism in *Zymomonas mobilis*: A catabolic highway with some scenic routes. *FEMS Microbiology Letters*, 145(3), 301–307.
- Sreejit, P., Kumar, Suresh. & Verma Rama, S. (2008). An improved protocol for primary culture of cardiomyocyte from neonatal mice. *In Vitro Cellular & Developmental Biology-Animal*, 44(3-4), 45-50.
- Stephen, J. D., Mabee, W. E. & Saddler, J. N. (2011). Will second-generation ethanol be able to compete with first-generation ethanol? Opportunities for cost reduction. *Biofuels, Bioproducts and Biorefining*, 6(2), 159–176.
- Stone, K. C., Hunt, P. G., Cantrell, K. B. & Ro, K. S. (2010). The potential impacts of biomass feedstock production on water resource availability. *Bioresource Technology*, 101(6), 2014–2025.
- Sun, Ye. & Cheng, Jiayang. (2002). Hydrolysis of lignocellulosic materials for ethanol production: a review. *Bioresource Technology*, 83(1), 1-11.
- Swatloski, R. P., Spear, S. K., Holbrey, J. D. & Rogers Robin, D. (2002). Dissolution of cellulose with ionic liquids. *Journal of the American Chemical Society*, 124(18), 4974-4975.
- Swings, J. & De Ley, J. (1977). The biology of *Zymomonas*. *Bacteriological Reviews*, 41(1), 1–46.
- Szengyel, Z. & Zacchi, G. (2000). Effect of acetic acid and furfural on cellulase production of *Trichoderma reesei* RUT C30. *Applied Biochemistry and Biotechnology*, 89(1), 31-42.
- Tantirungkij, M., Nakashima, N., Seki, T. & Yoshida, T. (1993). Construction of xylose-assimilating *Saccharomyces cerevisiae*. *Journal of Fermentation and Bioengineering*, 75(2), 83–88.
- Taylor, M. P., Mulako, I., Tuffin, M. & Cowan, D. (2012). Understanding Physiological Responses to Pretreatment Inhibitors in Ethanologenic Fermentations. *Biotechnology Journal*, 7(9), 1169–1181.
- Taylor, M., Tuffin, M., Burton, S., Eley, K. & Cowan, D. (2008). Microbial responses to solvent and alcohol stress. *Biotechnology Journal*, 3(11), 1388–1397.
- Teixeira, L. C., Linden, J. C. & Schroeder, H. A. (2000). Simultaneous saccharification and cofermentation of peracetic acid-pretreated biomass. *Applied Biochemistry and Biotechnology*, 84-6, 111-127.
- Tengborg, C., Galbe, M. & Zacchi, G. (2001). Reduced inhibition of enzymatic hydrolysis of steam-pretreated softwood. *Enzyme and Microbial Technology*, 28(9), 835-844.
- Thomas, D. S. & Rose, A. H. (1979). Inhibitory effect of ethanol on growth and solute accumulation by *Saccharomyces cerevisiae* as affected by plasma-membrane lipid composition. *Archives of Microbiology*, 122(1), 49–55.

- Thomas, D. S., Hossack, J. A. & Rose, A. H. (1978). Plasma-Membrane lipid composition and ethanol tolerance in *Saccharomyces cerevisiae*. *Archives of Microbiology*, 117(3), 239–245.
- Thomas, K. C., Hynes, S. H. & Ingledew, W. M. (2001). Effect of lactobacilli on yeast growth, viability and batch and semi-continuous alcoholic fermentation of corn mash. *Journal of Applied Microbiology*, 90(5), 819–828.
- Thomas, K. C., Hynes, S. H. & Ingledew, W. M. (2002). Influence of medium buffering capacity on inhibition of *Saccharomyces cerevisiae* growth by acetic and lactic acids. *Applied and Environmental Microbiology*, 68(4), 1616–1623.
- Tjeerdsmas, B. F. & Militz, H. (2005). Chemical changes in hydrothermal treated wood: FTIR analysis of combined hydrothermal and dry heat-treated wood. *Holz als Roh-und Werkstoff*, 63(2), 102–111.
- Tracy, B. P., Jones, S. W., Fast, A. G., Indurthi, D. C. & Papoutsakis, E. T. (2012). Clostridia: the importance of their exceptional substrate and metabolite diversity for biofuel and biorefinery applications. *Current Opinion in Biotechnology*, 23(3), 364–381.
- Trajano, H. L. & Wyman, C. E. (2013). Fundamentals of Biomass Pretreatment at Low pH. In C. E. Wyman, *Aqueous Pretreatment of Plant Biomass for Biological and Chemical Conversion to Fuels and Chemicals*. Chichester, UK: John Wiley & Sons, Ltd.
- Träff, K. L., Cordero, R. R. O., Van Zyl, W. H. & Hahn-Hagerdal, B. (2001). Deletion of the GRE3 Aldose Reductase Gene and Its Influence on Xylose Metabolism in Recombinant Strains of *Saccharomyces cerevisiae* Expressing the xylA and XKS1 Genes. *Applied and Environmental Microbiology*, 67(12), 5668–5674.
- Träff-Bjerre, K. L., Jeppsson, M., Hahn-Hagerdal, B. & Gorwa-Grauslund, M. F. (2004). Endogenous NADPH-dependent aldose reductase activity influences product formation during xylose consumption in recombinant *Saccharomyces cerevisiae*. *Yeast*, 21(2), 141–150.
- Tu, M., Zhang, X., Kurabi, A., Gilkes, N., Mabee, W. & Saddler, J. (2006). Immobilization of β -glucosidase on Eupergit C for lignocellulose hydrolysis. *Biotechnology Letters*, 28(3), 151–156.
- Tyner, W. E., Taheripour, F. & Perkis, D. (2010). Comparison of fixed versus variable biofuels incentives. *Energy Policy*, 38(10), 5530–5540.
- van der Pol, E. C., Bakker, R. R., Baets, P. & Eggink, G. (2014). By-products resulting from lignocellulose pretreatment and their inhibitory effect on fermentations for (bio)chemicals and fuels. *Applied Microbiology and Biotechnology*, 98(23), 9579–9593.
- Van Dyk, J. S. & Pletschke, B. I. (2012). A review of lignocellulose bioconversion using enzymatic hydrolysis and synergistic cooperation between enzymes—factors affecting enzymes, conversion and synergy. *Biotechnology Advances*, 30(6), 1458–1480.
- van Walsum, G. P. (2013). Separation and Purification of Lignocellulose Hydrolyzates. In S. Ramaswamy, H.-J. Huang, & B. V. Ramarao, *Separation and Purification Technologies in Biorefineries*, (pp. 513–532). Chichester, UK: John Wiley & Sons, Ltd.
- Vane, L. M. (2008). Separation technologies for the recovery and dehydration of alcohols from fermentation broths. *Biofuels, Bioproducts and Biorefining*, 2(6), 553–588.
- Verardi, A., Ricca, E., De Bari, I. & Calabrò, V. (2012). Hydrolysis of lignocellulosic biomass: current status of processes and technologies and future perspectives. INTECH Open Access Publisher.

- Verho, R., Londesborough, J., Penttila, M. & Richard, P. (2003). Engineering Redox Cofactor Regeneration for Improved Pentose Fermentation in *Saccharomyces cerevisiae*. *Applied and Environmental Microbiology*, 69(10), 5892–5897.
- Vinzant, T. B., Adney, W. S., Decker, S. R., Baker, J. O., Kinter, M. T., Sherman, N. E. & Himmel, M. E. (2001). Fingerprinting *Trichoderma reesei* hydrolases in a commercial cellulase preparation. *Applied Biochemistry and Biotechnology*, 91(1-9), 99-107.
- Vorotnikova, Ekaterina. & Seale Jr, James L. (2014). US Ethanol Mandate Is a Hidden Subsidy to Corn Producers.
- Walfridsson, M., Anderlund, M., Bao, X. & Hahn-Hagerdal, B. (1997). Expression of different levels of enzymes from the *Pichia stipitis* XYL1 and XYL2 genes in *Saccharomyces cerevisiae* and its effects on product formation during xylose utilisation. *Applied Microbiology and Biotechnology*, 48(2), 218–224.
- Walfridsson, M., Bao, X., Anderlund, M., Lilius, G., Bülow, L. & Hahn-Hagerdal, B. (1996). Ethanol fermentation of xylose with *Saccharomyces cerevisiae* harboring the *Thermus thermophilus* xylA gene, which expresses an active xylose (glucose) isomerase. *Applied and Environmental Microbiology*, 62(12), 4648–4651.
- Walfridsson, M., Hallborn, J., Penttila, M., Keranen, S. & Hahn-Hagerdal, B. (1995). Xylose-metabolizing *Saccharomyces cerevisiae* strains overexpressing the TKL1 and TAL1 genes encoding the pentose phosphate pathway enzymes transketolase and transaldolase. *Applied and Environmental Microbiology*, 61(12), 4184–4190.
- Walker, G. M. (1994). The roles of magnesium in biotechnology. *Critical Reviews in Biotechnology*, 14(4), 311–354.
- Walker-Caprioglio, H. M., Rodriguez, R. J. & Parks, L. W. (1985). Recovery of *Saccharomyces cerevisiae* from ethanol-induced growth inhibition. *Applied and Environmental Microbiology*, 50(3), 685–689.
- Walter, A. (2009). Bio-Ethanol Development(s) in Brazil. In *Biofuels*, (pp. 55–75). John Wiley & Sons, Ltd.
- Wang, X., Miller, E. N., Yomano, L. P., Shanmugam, K. T. & Ingram, L. O. (2012). Increased Furan Tolerance in *Escherichia coli* Due to a Cryptic *ucpA* Gene. *Applied and Environmental Microbiology*, 78(7), 2452–2455.
- Wang, X., Yomano, L. P., Lee, J. Y., York, S. W., Zheng, H., Mullinnix, M. T., et al. (2013). Engineering furfural tolerance in *Escherichia coli* improves the fermentation of lignocellulosic sugars into renewable chemicals. *Proceedings of the National Academy of Sciences of the United States of America*, 110(10), 4021–4026.
- Weil, Joe., Sarikaya, Ayda., Rau, Shiang-Lan., Goetz, Joan., Ladisch., Christine, M., Brewer, Mark. & Ladisch Michael, R. (1997). Pretreatment of yellow poplar sawdust by pressure cooking in water. *Applied Biochemistry and Biotechnology*, 68(1-2), 21-40.
- Wierckx, N., Koopman, F., Ruijssenaars, H. J. & de Winde, J. H. (2011). Microbial degradation of furanic compounds: biochemistry, genetics, and impact. *Applied Microbiology and Biotechnology*, 92(6), 1095–1105.
- Wiseloge, A. E., Tyson, S. & Johnson, D. (1996). Biomass Feedstock Resources and Composition. In C. E. Wyman, *Handbook on Bioethanol Production and Utilization*, (pp. 105–118).
- Worley-Morse, T. O., Deshusses, M. A. & Gunsch, C. K. (2015). Reduction of invasive bacteria in ethanol fermentations using bacteriophages. *Biotechnology and Bioengineering*, 112(8), 1544–1553.

- Wyman, C. E. (2013). Introduction. Aqueous Pretreatment of Plant Biomass for Biological and Chemical Conversion to Fuels and Chemicals, 1–15.
- Wyman, C. E. (2007). What is (and is not) vital to advancing cellulosic ethanol. *TRENDS in Biotechnology*, 25(4), 153-157.
- Wyman, C. E., Balan, V., Dale, B. E., Elander, R. T., Falls, M., Hames, B. & Warner, R. E. (2011). Comparative data on effects of leading pretreatments and enzyme loadings and formulations on sugar yields from different switchgrass sources. *Bioresource Technology*, 102(24), 11052-11062.
- Wyman, C. E., Dale, B. E., Elander, R. T., Holtzapple, M., Ladisch, M. R. & Lee, Y. Y. (2005). Coordinated development of leading biomass pretreatment technologies. *Bioresource Technology*, 96(18), 1959-1966.
- Wyman, C. E., Dale, B. E., Elander, R. T., Holtzapple, M., Ladisch, M. R., Lee, Y. Y. & Saddler, J. N. (2009). Comparative Sugar Recovery and Fermentation Data Following Pretreatment of Poplar Wood by Leading Technologies. *Biotechnology Progress*, 25(2), 333-339.
- Xu, J. L., Zhang, X. & Cheng, J. J. (2012). Pretreatment of corn stover for sugar production with switchgrass-derived black liquor. *Bioresource Technology*, 111, 255-260.
- Xu, J. L., Zhang, X., Sharma-Shivappa, R. R. & Eubanks, M. W. (2012). Gamagrass varieties as potential feedstock for fermentable sugar production. *Bioresource technology*, 116, 540-544.
- Xiao, W. H., Zhang, X. M., Wang, X., Niu, W. & Han, L. (2015). Rapid Liquefaction of Corn Stover with Microwave Heating. *BioResources*, 10(3), 4038-4047.
- Ximenes, E., Kim, Y. & Ladisch, M. R. (2013). Biological Conversion of Plants to Fuels and Chemicals and the Effects of Inhibitors. In C. E. Wyman, Aqueous Pretreatment of Plant Biomass for Biological and Chemical Conversion to Fuels and Chemicals, (pp. 39–60). Chichester, UK: John Wiley & Sons, Ltd.
- Ximenes, E., Kim, Y., Mosier, N. S., Dien, B. & Ladisch, M. R. (2010). Inhibition of cellulases by phenols. *Enzyme and Microbial Technology*, 46(3-4), 170–176.
- Ximenes, E., Kim, Y., Mosier, N. S., Dien, B. & Ladisch, M. R. (2011). Deactivation of cellulases by phenols. *Enzyme and Microbial Technology*, 48(1), 54–60.
- Xiros, C. & Olsson, L. (2014). Comparison of strategies to overcome the inhibitory effects in high-gravity fermentation of lignocellulosic hydrolysates. *Biomass and Bioenergy*, 65(C), 79–90.
- Xiros, C., Moukouli, M., Topakas, E. & Christakopoulos, P. (2009). Factors affecting ferulic acid release from Brewer's spent grain by *Fusarium oxysporum* enzymatic system. *Bioresource Technology*, 100(23), 5917-5921.
- Yang, B. & Wyman, C. E. (2008). Pretreatment: the key to unlocking low-cost cellulosic ethanol. *Biofuels, Bioproducts and Biorefining*, 2(1), 26–40.
- Yang, S., Franden, M. A., Brown, S. D., Chou, Y. C., Pienkos, P. T. & Zhang, M. (2014). Insights into acetate toxicity in *Zymomonas mobilis* 8b using different substrates. *Biotechnology for Biofuels*, 7, 140.
- Yang, S. W., Burgin, A. B., Huizenga, B. N., Robertson, C. A., Yao, K. C. & Nash, H. A. (1996). A eukaryotic enzyme that can disjoin dead-end covalent complexes between DNA and type I topoisomerases. *Proceedings of the National Academy of Sciences*, 93(21), 11534-11539.

- Yang, B., Boussaid, A., Mansfield, S. D., Gregg, D. J. & Saddler, J. N. (2002). Fast and efficient alkaline peroxide treatment to enhance the enzymatic digestibility of steam-exploded softwood substrates. *Biotechnology and Bioengineering*, 77(6), 678-684.
- Yang, B., Dai, Z., Ding, S. Y., & Wyman, C. E. (2011). Enzymatic hydrolysis of cellulosic biomass. *Biofuels*, 2(4), 421-449.
- Yang, B., & Wyman, C. E. (2008). Pretreatment: the key to unlocking low-cost cellulosic ethanol. *Biofuels, Bioproducts and Biorefining*, 2(1), 26-40.
- Yang, B. & Wyman, C. E. (2004). Effect of xylan and lignin removal by batch and flowthrough pretreatment on the enzymatic digestibility of corn stover cellulose. *Biotechnology and Bioengineering*, 86(1), 88-98.
- Yang, B. & Wyman, C. E. (2006). BSA treatment to enhance enzymatic hydrolysis of cellulose in lignin containing substrates. *Biotechnology and Bioengineering*, 94(4), 611-617.
- Yeh, An-I., Huang, Yi-Ching. & Chen, Shih Hsin. (2010). Effect of particle size on the rate of enzymatic hydrolysis of cellulose. *Carbohydrate Polymers*, 79(1), 192-199.
- Yomano, L. P., York, S. W. & Ingram, L. O. (1998). Isolation and characterization of ethanol-tolerant mutants of *Escherichia coli* KO11 for fuel ethanol production. *Journal of Industrial Microbiology & Biotechnology*, 20(2), 132-138.
- Yomano, L. P., York, S. W., Zhou, S., Shanmugam, K. T. & Ingram, L. O. (2008). Re-engineering *Escherichia coli* for ethanol production. *Biotechnology Letters*, 30(12), 2097-2103.
- Yu, C., Cao, Y., Zou, H. & Xian, M. (2010). Metabolic engineering of *Escherichia coli* for biotechnological production of high-value organic acids and alcohols. *Applied Microbiology and Biotechnology*, 89(3), 573-583.
- Yue, G., Wu, G. & Lin, X. (2014). [Insights into engineering of cellulosic ethanol]. *Sheng wu gong cheng xue bao= Chinese Journal of Biotechnology*, 30(6), 816-827.
- Zeng, Y., Zhao, S., Yang, S. & Ding, S.-Y. (2014). Lignin plays a negative role in the biochemical process for producing lignocellulosic biofuels. *Current Opinion in Biotechnology*, 27(0), 38-45.
- Zhang, M., Eddy, C., Deanda, K., Finkelstein, M. & Picataggio, S. (1995). Metabolic Engineering of a Pentose Metabolism Pathway in *Ethanologenic Zymomonas mobilis*. *Science*, 267(5195), 240-243.
- Zhang, X., Hewetson, B. B. & Mosier, N. S. (2015). Kinetics of Maleic Acid and Aluminum Chloride Catalyzed Dehydration and Degradation of Glucose. *Energy & Fuels*, 29(4), 2387-2393.
- Zhang, X., Xu, J. & Cheng, J. J. (2011). Pretreatment of corn stover for sugar production with combined alkaline reagents. *Energy & Fuels*, 25(10), 4796-4802.
- Zhang, Y. H. P., Ding, S. Y., Mielenz, J. R., Cui, J. B., Elander, R. T., Laser, M. & Lynd, L. R. (2007). Fractionating recalcitrant lignocellulose at modest reaction conditions. *Biotechnology and Bioengineering*, 97(2), 214-223.
- Zhang, Y. H. P. & Lynd, L. R. (2004). Toward an aggregated understanding of enzymatic hydrolysis of cellulose: Noncomplexed cellulase systems. *Biotechnology and Bioengineering*, 88(7), 797-824.
- Zhang, Y. H. P. (2008). Reviving the carbohydrate economy via multi-product lignocellulose biorefineries. *Journal of Industrial Microbiology & Biotechnology*, 35(5), 367-375.

- Zhao, X., Zhang, L. & Liu, D. (2012). Biomass recalcitrance. Part I: the chemical compositions and physical structures affecting the enzymatic hydrolysis of lignocellulose. *Biofuels, Bioproducts and Biorefining*, 6(4), 465-482.
- Zhao, X., Cheng, K. & Liu, D. (2009). Organosolv pretreatment of lignocellulosic biomass for enzymatic hydrolysis. *Applied Microbiology and Biotechnology*, 82(5), 815-827.
- Zhao, X., Peng, F., Cheng, K. & Liu, D. (2009). Enhancement of the enzymatic digestibility of sugarcane bagasse by alkali-peracetic acid pretreatment. *Enzyme and Microbial Technology*, 44(1), 17-23.
- Zheng, Y., Pan, Z. & Zhang, R. (2009). Overview of biomass pretreatment for cellulosic ethanol production. *International Journal of Agricultural and Biological Engineering*, 2(3), 51-68.
- Zhou, H., Cheng, J. S., Wang, B. L., Fink, G. R. & Stephanopoulos, G. (2012). Xylose isomerase overexpression along with engineering of the pentose phosphate pathway and evolutionary engineering enable rapid xylose utilization and ethanol production by *Saccharomyces cerevisiae*. *Metabolic Engineering*, 14(6), 611-622.
- Zhu, J. Y. & Pan, X. J. (2010). Woody biomass pretreatment for cellulosic ethanol production: Technology and energy consumption evaluation. *Bioresource Technology*, 101(13), 4992-5002.
- Zhu, J. Y. (2011). Physical pretreatment—woody biomass size reduction—for forest biorefinery. Sustainable production of fuels, chemicals, and fibers from forest biomass. American Chemical Society, Washington, DC, 89-107.
- Zhu, S. (2008). Use of ionic liquids for the efficient utilization of lignocellulosic materials. *Journal of Chemical Technology and Biotechnology*, 83(6), 777-779.
- Zhu, S., Wu, Y., Chen, Q., Yu, Z., Wang, C., Jin, S. & Wu, G. (2006). Dissolution of cellulose with ionic liquids and its application: a mini-review. *Green Chemistry*, 8(4), 325-327.

Chapter 4

OPTIMIZATION OF BIOGAS PRODUCTION BY ANAEROBIC CO-DIGESTION

Raphael M. Jingura and Reckson Kamusoko*

Chinhoyi University of Technology,
School of Agricultural Sciences and Technology,
Chinhoyi, Zimbabwe

ABSTRACT

The use of biomass as an energy source has escalated in recent times as a result of global initiatives in pursuit of alternative and renewable fuels. Biofuels comprise liquid, solid and gaseous fuels. Biogas is one of the common gaseous biofuels. It is a high methane fuel. The technology of producing biogas is relatively not sophisticated. Biogas has gained traction as an energy carrier with potential to contribute significantly to the global energy mix. Biogas is produced from degradable organic matter by anaerobic digestion. Anaerobic digestion is a technology that breaks down organic matter in the absence of oxygen, and the process produces biogas. Biogas typically consists of methane (50-75%), carbon-dioxide (25-50%), and trace quantities of contaminant gases. There is need to optimise anaerobic digestion in order to maximise biogas yields. Co-digestion is one option of optimising anaerobic digestion. Co-digestion refers to the synchronized digestion of a homogenous mixture of multiple substrates in a single digester. Co-digestion enhances the efficiency of anaerobic digestion and increases biogas yields for substrates that have low methane potential. Co-digestion increases methane yields from low-yielding or difficult to digest materials. Examples of co-substrates for co-digestion include food wastes, press-cakes, crop residues and animal manures. For the co-digestion process, selected feedstocks must be compatible to enhance methane yields. The co-substrates must complement each other in terms of carbon to nitrogen ratio, nutrients and other physical and chemical factors. This chapter presents an overview of the co-digestion process, focusing on the principles, selecting co-feedstocks, biomethane potential of feedstocks, merits and limits of co-digestion.

Keywords: anaerobic digestion, biogas, co-digestion, feedstock, organic matter

*Corresponding Author: e-mail: rjingura@gmail.com, Tel: +263 774 663 587.

INTRODUCTION

The depleting supply of fossil fuels which have negative environmental impacts has increased interest in search for alternative and cleaner energy sources such as biogas (Sidik, Razali, Alwi, & Maigari, 2013). Biomass can make a substantial contribution to supplying future energy demand in a sustainable way (World Energy Council (WEC), 2013). By 2013, biomass supplied some 50 EJ globally, which represented 10% of global annual primary energy consumption (WEC, 2013). Biofuels include liquid fuels such as bioethanol and biodiesel; solid fuels such as fuelwood and charcoal; and gaseous fuels such as biogas.

Biogas is made up of methane (CH₄), carbon dioxide (CO₂), and traces of gases generated from biomass or organic materials under anaerobic conditions (Solomon & Lora, 2009). Biogas is a high methane fuel. Methane is a fuel that is comparatively clean. In addition, the technology of producing biogas is relatively not sophisticated (Taleghani & Kia, 2005). Biogas can be used as an alternative to fossil fuels in power and heat production processes and can be used as a gaseous vehicle fuel (Weiland, 2010). After removal of contaminants, the methane-rich biogas (biomethane) can replace natural gas as a feedstock for producing chemicals and materials (Weiland, 2010).

Biogas is produced by anaerobic digestion (AD) of biodegradable organic matter. Typical feedstocks for biogas production are manure and sewage, crop residues, the organic fraction of the waste from households and industry, as well as energy crops including maize and grass silage (World Bioenergy Association, 2013). The production of biogas through AD offers significant advantages over other forms of bioenergy production (Weiland, 2010). It is one of the most energy-efficient and environmentally beneficial technologies for bioenergy production (Al-Masri, 2001). Traditionally, AD of organic matter (OM) has mainly been based on a single substrate. However, some feedstocks used for AD have low biodegradability which leads to low biogas yields. In some cases, although biodegradable OM can be used as a sole feedstock in AD, the digestion process tends to fail without the addition of external nutrients and buffering agents (Demirel and Scherer, 2008). This is the basis of co-digestion as shall be described in this chapter.

One of the approaches of enhancing the economics of AD of OM is to improve the biogas yield rate by co-digesting more than one substrate as long as such substrates can augment the missing nutrients in the digesters (Mata-Alvarez, Mace, & Llabres, 2000). Co-digestion generally refers to the AD of multiple biodegradable substrates. It refers to the digestion of a combination of selected substrates with a base substrate that an AD system was designed to handle. Its primary objective is to maximise biogas yields in an AD system by adding substrates that produce much more biogas per unit mass than the base substrate.

PRINCIPLES OF ANAEROBIC DIGESTION

Anaerobic Digestion as a Conversion Technology

Methane can be produced from biomass by either thermal gasification or biological gasification. Biological gasification is commonly referred to as AD. The AD process is one of the most efficiently used methods for conversion of biomass to methane. It is a complex microbial process occurring naturally in oxygen-free environments (Switzenbaum, 1995;

Ward, Hobbs, Holliman, & Jones, 2008). The process is carried out by several different anaerobic bacteria. In the absence of oxygen, anaerobic bacteria ferment biodegradable matter into methane and carbon dioxide. The gas mixture is called biogas.

Biogas contains 60 – 70% methane (CH₄) and 30 – 40% carbon dioxide depending on the feedstock type (Taleghani & Kia, 2005). Trace amounts of hydrogen sulphide, ammonia, hydrogen, nitrogen, carbon monoxide, oxygen and siloxanes are occasionally present in the biogas (Monnet, 2003). Usually, the mixed gas is saturated with water vapour (Abdelgadir et al., 2014). A general framework of AD as an energy conversion technology is shown in Figure 1.

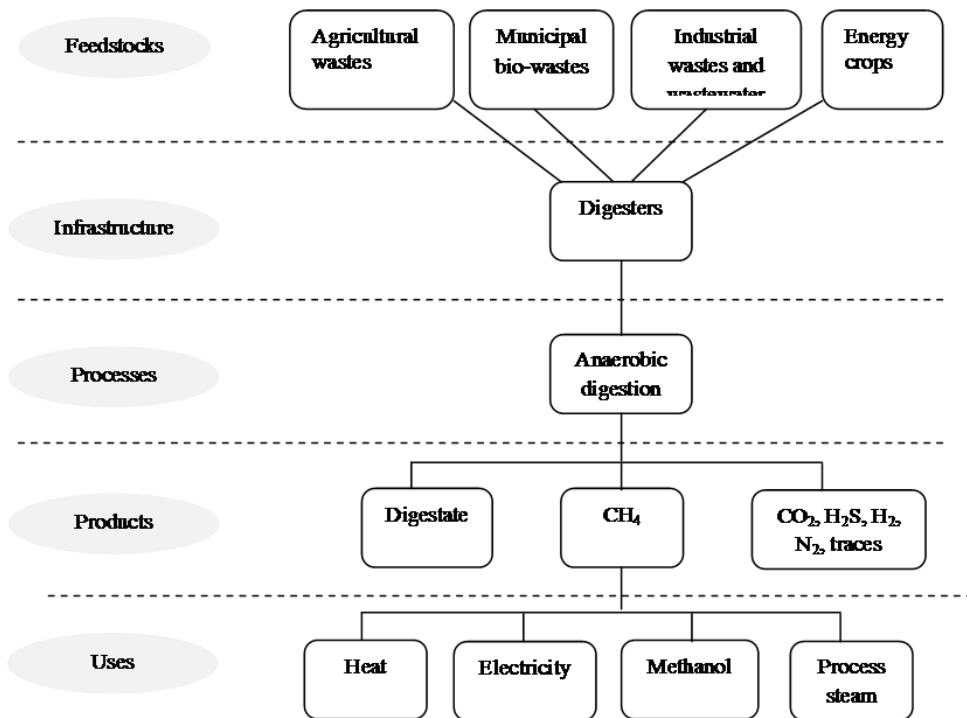


Figure 1. Biomass conversion to bioenergy by anaerobic digestion.

Figure 1 shows five key parameters of AD in the conversion of biomass to biogas. The AD infrastructure, which is principally the digesters, is outside the scope of this chapter. However, there are many different types of digesters that can be used for AD. The digesters can be broadly grouped based on their ability to process liquid (wet) and solid (dry) OM (PEW Centre, 2011).

Digestion Process

Fermentation of OM is a complex process. The process can be divided into four phases. These are hydrolysis, acidogenesis, acetogenesis/dehydrogenation, and methanogenesis (Raju, 2012). Hydrolysis is an extracellular process, while the other three steps are intracellular processes (Demirel and Scherer, 2008). The individual degradation steps are

carried out by different microorganisms, which partly stand in syntrophic interrelation and place different requirements on the environment (Angelidaki et al., 1993). The microbes responsible for the first and second steps, as well as microbes for the third and fourth steps are linked closely with each other (Schink, 1997). Therefore, the process can be accomplished in two stages. Figure 2 is a generalised flow chart of methane production from organic precursors.

The first microbial groups to intervene are hydrolytic or facultative anaerobes, or anaerobes which hydrolyse complex organic molecules such as lipids, polysaccharides, proteins and nucleic acids into simpler products (Giard, 2011). The products are soluble and transportable through cellular membranes for further degradation (Giard, 2011). The anaerobes secrete extracellular enzymes that solubilise solids via three mechanisms (Raju, 2012). Firstly, enzymes secreted into the bulk of the liquid adsorb onto a substrate. Secondly, the microbes attach themselves onto a substrate and release enzymes. Lastly, the anaerobes attach themselves to the substrate whilst the enzymes are also attached to the anaerobes (Raju, 2012). Besides their hydrolytic roles, the enzymes also act as receptors to transport the products to the interior of the cells.

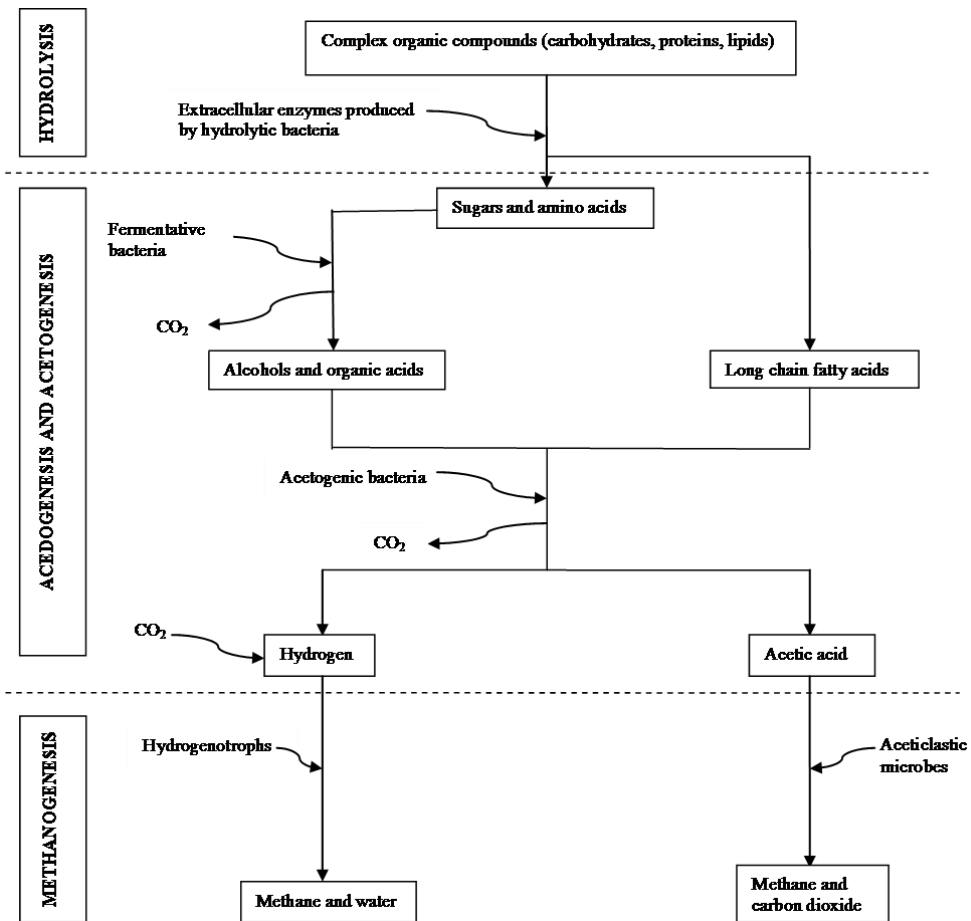


Figure 2. Generalised framework of methane production from organic substrates (Modified from Raju, 2012).

Hydrolysis is often considered as rate-limiting (Appels, Baeyens, Degreve, & Dewil, 2008). This is due to lignocelluloses which act as a barrier to the hydrolysis of insoluble organic material (Appels et al., 2008). Hydrolysis produces soluble compounds, such as amino acids, simple sugars and long chain fatty acids. These are readily degraded by the next anaerobic microbial group called the acidogenesis bacteria. The products are alcohols and volatile fatty acids (VFA) such as acetic, propionic and butyric acids, along with NH_3 , H_2S , CO_2 and other by-products (Appels et al., 2008).

The next stage is acetogenesis. In this stage, acetogens use the products from acidogenesis (such as VFAs and alcohols) and the residues of hydrolysis to produce acetic acid, CO_2 and H_2 (Giard, 2011). The final stage is methanogenesis. Methanogens use the products of acidogenesis and acetogenesis, such as H_2 , CO_2 , and acetate to produce biogas, which is around 55-70 percent CH_4 and 30-45 percent CO_2 (Monnet, 2003). This is either by breaking down the acids to CH_4 and CO_2 , or by reducing CO_2 with hydrogen (Monnet, 2003). In addition, carbon monoxide (CO), formate (HCOOH), methanol (CH_3OH), and methylamine (CH_3NH_2) can also be utilised to produce methane (Raju, 2012). There are three main groups of methanogens that vary according to utilisation of substrates (Gerardi, 2003). These are:

- Acetoclastic methanogens use acetate as substrate to produce CH_4 and CO_2 .
 $\text{CH}_3\text{COOH} \rightarrow \text{CO}_2 + \text{CH}_4$
- Hydrogenotrophic methanogens utilise hydrogen to convert CO_2 to CH_4 .
 $\text{CO}_2 + 4\text{H}_2 \rightarrow \text{CH}_4 + 2\text{H}_2\text{O}$
- Methylotrophic methanogens use methyl groups such as methanol and methylamines.
 $3\text{CH}_3\text{OH} + 6\text{H} \rightarrow 3\text{CH}_4 + 3\text{H}_2\text{O}$

Feedstock Parameters

Many factors affect the performance of AD processes. The factors are related to feedstock characteristics, reactor design, and operational conditions (Babae and Shayegan, 2011). Important feedstock parameters include volatile solids (VS), chemical oxygen demand (COD), biological (biochemical) oxygen demand (BOD), carbon to nitrogen ratio (C/N), and presence of inhibitory substances (Babae and Shayegan, 2011; Kwietniewska and Tys, 2014). In AD, the difference between the OM contained before and after treatment is a significant parameter that it is necessary to control the process. This is measured in term of total solids (TS), VS, total organic carbon (TOC), COD or BOD (Boe et al., 2005).

The TS content of solid waste influences AD performance, especially biogas production efficiency (Pavan, Battistoni, Mata-Alvarez, & Cecchi, 2000). Systems used to digest solid waste are classified according to the percentage of TS in the feedstock (Yi, Dong, Jin, & Dai, 2014). These are: conventional wet ($\leq 10\%$ TS), semi-dry (10–20% TS) and modern dry ($\geq 20\%$ TS) (Yi et al., 2014). Abbassi-Guendouz et al., (2012) showed that total methane yield decreased with TS contents increasing from 10% to 25% in batch AD of cardboard under mesophilic conditions. Similarly, Forster-Carneiro et al., (2008) showed that biogas and methane production decreased when the TS contents increased from 20% to 30% in dry batch AD of food waste.

TS contain both organic and inorganic matter. Usually, OM is measured by the amount of carbon in a feedstock (Hamilton, 2012). TOC is the total organic carbon in feedstocks. VS are the OM component of TS and these are degraded during AD. Methane production is directly related to VS degradation (Moody et al., 2009). The COD is used to quantify the amount of OM in feedstocks and predict the potential for biogas production (des Mes et al., 2003). The COD measures the OM concentration by measuring the oxidant consumption for the oxidation of the OM in aerobic conditions (Van Haandel and van der Lubbe, 2007). Theoretical methane yield can be calculated from the COD of a substrate (Kwietniewska and Tys, 2014).

Biogas production in relation to COD is about 0.5 l g^{-1} COD removed, corresponding to a methane production of approximately 0.35 l g^{-1} of COD removed (Angelidaki and Sanders, 2004). The COD has a stoichiometric correlation with methane production, therefore and is frequently used to express the loading rate of anaerobic digesters (Banks and Zhang, 2010). COD is also a good indicator of the progress of the AD process, as any undigested material will require oxygen (in an aerobic environment) to complete the degradation (Ward et al., 2008). However, a considerable fraction of the input COD may not be anaerobically biodegradable (Batstone et al., 2002).

Another widely used parameter is the BOD. This involves the measurement of dissolved oxygen used by aerobic microorganisms in biochemical oxidation of OM (de Mes et al., 2003). It is a measure of the oxygen used by microorganisms to decompose OM. BOD is similar to COD in that both measure the amount of OM. Examples of typical BOD values include pig slurry 20,000 – 30,000, cattle slurry 10,000 – 20,000 and wastewater 1000 – 5000 mg/l (Korres et al., 2013).

Another important factor is the C/N ratio. The ratio represents the relationship between the amount of nitrogen and carbon in a feedstock. The optimum C/N ratio for AD is 20-35:1. (Kwietniewska and Tys, 2014). If the ratio is low it means that the material is protein rich. AD of such material results in increased content of free ammonia that causes high pH leading to methanogenic inhibition (Salminen & Rintala, 2002; Khalid, Arshad, Anjum, Mahmood, & Dawson, 2011). A high ratio causes rapid depletion of nitrogen causing lower gas production. A feedstock C/N ratio of 25:1 produces optimal gas production (Gerardi, 2003). Wang et al., (2014) reported an interactive effect between temperature and C/N on AD performance. When temperature was increased, Wang et al., (2014) observed that an increase was required in the feed C/N ratio in order to reduce the risk of ammonia inhibition. Typical C/N ratios for some feedstocks are: cattle manure 13:1, chicken manure 15:1, grass silage 25:1 and rice husks 47:1 (Dioha et al., 2013).

A wide variety of inhibitory substances cause anaerobic digester upset or failure when they are present in substantial concentrations in wastes (Chen, Cheng, & Creamer, 2008). A material may be judged inhibitory when it causes an adverse shift in the microbial population or inhibition of bacterial growth (Chen et al., 2008). The inhibitors are commonly NH_3 , H_2S and heavy metals (Gerardi, 2003). Free NH_3 is the main cause of inhibition since it is freely membrane-permeable (de Baere, Devocht, Van Assche, & Verstraete, 1984). Methanogens have the least tolerance to NH_3 inhibition amongst all the microbes in anaerobic digesters (Chen et al., 2008). Normally, H_2S produced from degradation of compounds and sulphate reduction is a growth requirement for bacteria (Gerardi, 2003). However, large quantities are toxic to methanogenic bacteria since they restrain their metabolic activity (Chen et al., 2008). It is necessary to prevent sulphide toxicity by diluting the input of the digester (Gerardi,

2003). Alternatively, free H₂S can be removed from digesters by production of CO₂, H₂ and CH₄, or by incorporating physico-chemical processes such as stripping, coagulation, oxidation, precipitation, and biological conversions (Chen et al., 2008). Nonetheless, sulphides reduce heavy metal toxicity to microbial cells by precipitating heavy metals into insoluble metal sulphides (Khanal, 2008). In order to manage the concentrations of toxic substances in anaerobic slurries, maximum permissible limits were set as shown in Table 1.

In addition to the substances shown in Table 1, heavy metals such as lead, zinc, cobalt and cadmium are of particular concern in AD (Chen et al., 2008). Heavy metals, unlike many other toxic substances, are not biodegradable and can accumulate to potentially toxic concentrations (Chen et al., 2008).

Table 1. Maximum permissible limits for concentrations of toxic substances in anaerobic slurries

Substance	Unit	Maximum permissible limit
Cyanide (CN ⁻)	mg/L	< 25
Copper (Cu)	mg/L	100
Chromium (Cr)	mg/L	200
Nickel (Ni)	mg/L	200 - 500
Sulphate (SO ₄ ²⁻)	ppm	5 000
Sodium chloride (NaCl)	ppm	40 000
Magnesium (Mg)	mg/L	1 000 – 1 500
Ammonia (NH ₃)	mg/L	1 500 – 3 000
Calcium (Ca)	mg/L	2 500 – 4 500
Potassium (K)	mg/L	2 500 – 4 500
Sodium (Na)	mg/L	3 500 – 5 500

Source: OLGPB, 1976 cited by Sattler, 2011.

Process Parameters of Anaerobic Digestion

The complex microbial community that is responsible for AD survives in specific environmental conditions. The main process parameters are oxidation reduction potential (ORP), pH, temperature and nutrient concentrations (Cantrell, Ducey, Ro, & Hunt, 2008; Raju, 2012). Optimisation of biogas production requires good control of these parameters.

Firstly, AD takes place in the absence of oxygen. To keep a system under anaerobic conditions, the ORP must remain well below -200 mV (Appels et al., 2008). Hydrolysis, the first stage in digestion, requires ORP around -300 mV, while methanogenesis takes place at ORP reaching -500 mV (Colmenarejo, Sánchez, Bustos, García, & Borja, 2004). Oxygen increases the relative CO₂ production during the degradation of acetate, at the expense of CH₄ (Giard, 2011). The introduction of oxygen may also inhibit and/or decrease the population of methanogens by favouring facultative anaerobes competing for reducing equivalents (Hedrick, Guckert, & White, 1991). Thus, digester design and operation must minimise the presence of oxygen during the digestion process.

Anaerobic digesters can be designed for psychrophilic, mesophilic or thermophilic operations. The effect of temperature on AD is well known (Kwietniewska and Tys, 2014).

Temperature affects the rate of biological processes. Temperatures must be carefully regulated during AD. Table 2 provides general information on psychrophilic, mesophilic and thermophilic digestion.

Table 2. Anaerobic digestion at three temperature ranges

Descriptors	References
<i>Psychrophilic (0 – 20 °C)</i>	
<ul style="list-style-type: none"> - Microbial communities acclimated to psychrophilic conditions are available for AD - For temperate regions, psychrophilic conditions reduce digesters substrate heating costs and produce less sensitive digesters - Psychrophilic conditions result in less extensive hydrolysis of organic compounds 	Kashyap, Dadhich, & Sharma, 2003; Halalsheh, Kassab, Yazajeen, Qumsieh, & Field, 2010; Giard, 2011
<i>Mesophilic (25 – 45 °C)</i>	
<ul style="list-style-type: none"> - Most favourable for AD - Optimises biogas production rate of livestock manure as livestock manure originates from a mesophilic environment (38-40°C) 	Kim, Ahn, & Speece, 2002; Cantrell et al., 2008
<i>Thermophilic (45 – 65 °C)</i>	
<ul style="list-style-type: none"> - Faster and more extensive hydrolysis for a higher biogas production rate - A smaller consortium of anaerobic organisms is adapted to thermophilic conditions - Thermophilic methanogens exhibit a growth rate 2-3 times faster than mesophilic methanogens thus, a lower sludge retention time can be used - Hyper-thermophilic temperatures (70°C-75°C) have been used to further improve the rate of the process - Populations of microorganisms found under such extreme temperatures are very limited 	Cantrell et al., 2008; Lee, Hidaka, & Tsuno, 2008

Generally, an increased temperature has a positive effect on the metabolic rate of microorganisms and the AD process runs faster (Kwietniewska and Tys, 2014). For example, at 55°C more rapid degradation of fatty acids was found than at 38°C (Ward et al., 2008). In addition, retention time was shorter as 95% of the methane yield was obtained after 11 days under thermophilic conditions compared to 27 days under mesophilic conditions (Ward et al., 2008).

It is not just absolute temperature that matters in AD. Fluctuations in temperature influence the stability and efficiency of AD (Giard, 2011). This is by affecting the relative rate of microbial growth and metabolism of the various groups and thus CH₄ production (Cantrell et al., 2008). Chae et al., (2008) reported that biogas production rate was reduced due to even small changes in temperature. Appels et al., (2008) reported that the AD process can fail at temperature fluctuations of even 1°C per day. Methanogenic bacteria are more sensitive to changes in temperature than other organisms present in digesters (Marchaim, 1992). Of the methanogenic group of bacteria, acetoclastic methanogens are the most

temperature-sensitive group (Appels et al., 2008). Rapid temperature drops also tend to lead to higher VFA concentrations (Colmenarejo et al., 2004) because of very low metabolic activity of the bacteria degrading the VFAs (Collins, Woods, McHugh, Carton, & O'Flaherty, 2003).

AD is influenced by pH. A fundamental issue in AD is that equilibrium has to be maintained between acid and methanogenic fermentation (Marchaim, 1992). Acetate and fatty acids produced during digestion tend to lower the pH of digester liquor. Most microorganisms grow best under neutral pH conditions. Other pH values may adversely affect metabolism by altering the chemical equilibrium of enzymatic reactions, or by actually destroying the enzymes. Methanogenic bacteria are extremely sensitive to pH fluctuations and prefer pH around 7.0 as their growth is greatly reduced at pH below 6.6 (Ward et al., 2008; Ogejo et al., 2009). Low pH can cause the chain of biological reactions in digestion to cease. Each different phase of AD has its own optimum pH range. A pH range of 7-8 is normally recommended for methanogens and acetogens. However, pH of less than 6 and greater than 8.5 is considered to have some inhibitory effects on methanogenesis (Raju, 2012).

Macro- and micronutrients supply the basic requirements for bacterial growth. Nitrogen and phosphorous are the principal macronutrients for all biological reactions occurring in digesters (Strik, Domnanovich, & Holubar, 2006). For methanogens, they are available in the form of ammonical-nitrogen ($\text{NH}_4^+\text{-N}$) and orthophosphate-phosphorous ($\text{HPO}_4\text{-P}$). Methane-forming bacteria utilise $\text{NH}_4^+\text{-N}$ (Gerardi, 2003). A minimum concentration of 40-70 mg nitrogen/L is necessary to prevent a drop in microbial activity and lower biogas production (Strik et al., 2006). Ammonium concentrations exceeding 3 000 mg/L can affect methane production. For AD, the preferred N range stands between 150 mg/L (Dolfing and Bloeman, 1985; Strik et al., 2006) and 200 mg/L (Chen et al., 2008). In addition to macronutrients, micronutrients (Co, Fe, Ni) are required for methanogen enzymes to transform acetate into methane (Gerardi, 2003).

Biogas Composition

Biogas is primarily composed of 50 – 60 % CH_4 , 38 - 48 % CO_2 (Bothi, 2007). Other gases present include N_2 , H_2 , H_2S and NH_3 (Kwietniewska and Tys, 2014). The gas also contains water vapour (Kwietniewska and Tys, 2014). A comparison of the typical composition of biogas, natural gas and landfill gas is given in Table 3.

Merits and Demerits of Anaerobic Digestion

There is no doubt in literature that AD presents a cost-effective way to deal with biodegradable wastes. The process produces valuable products such as biogas and digestate from wastes. Stabilisation of wastes is an important practice (Tambone, Genevini, D'Imporzano, & Adani, 2009). As an example, a study on pig slurry by Tambone et al. (2015) produced results that indicated that AD by itself promoted a high biological stability of biomass with a Potential Dynamic Respiration Index (PDRI) close to 1000 mg $\text{O}_2 \text{ kg VS}^{-1} \text{ h}^{-1}$. In an earlier study, Tambone et al., (2009), working on transformation of organic matter during AD of mixtures of energetic crops, cow slurry, agro-industrial waste

and organic fraction of municipal solid waste (OFMSW) concluded that AD caused a higher degree of biological stability of the digestate with respect to the starting mixture. The merits and demerits of AD are shown in Table 4.

Table 3. The typical composition of biogas, natural gas, and landfill gas

Components	Biogas	Landfill gas	Natural gas
<i>Bulk components</i>			
Carbon dioxide (Vol %)	25-45	12-45	0.61
Methane (Vol %)	50-75	45-88	91
<i>Trace components</i>			
Carbon monoxide (ppm)	0	Trace	0
Hydrogen (Vol %)	0	0	Trace to <1%
Volatile organic compounds (Vol %)	0	0	0.25-0.50
Nitrogen (Vol %)	0-2	0-3	0.32
Water vapour (Vol %)	2-7	-	-
Ammonia (ppm)	~100	0	0
Hydrogen sulphide (ppm)	~500	10-200	~1

‘-’ means value not stated.

Sources: (Monnet, 2003; Graaf & Fendler, 2010 as cited by Ziemiński and Frąç, 2012).

Table 4. Merits and demerits of anaerobic digestion

Merits	Demerits
<ul style="list-style-type: none"> - Reduces greenhouse gases and provides an energy source with no net increase in atmospheric carbon which contributes to global climate change - Feedstock for AD is a renewable resource - Digestate can be used as bio-fertiliser - Provides an integrated management system for soil and water pollution in relation to disposal of untreated manure/slurries - Reduction of up to 80 % of the odour and destroys weed seeds, thus reducing the use of herbicides and other weed control methods - Transforms wastes into useful products (biogas, soil conditioner and liquid fertiliser) 	<ul style="list-style-type: none"> - Has the potential to generate some risks and negative environmental effects - Has significant capital and operational costs - Traffic movements are created by all waste management systems and can be problematic in centralised anaerobic digestion (CAD) plants since transport greatly influences costs and emissions - Risks to human health associated with pathogenic load of the feedstock - Larger CAD plants may pose some visual impact although to a certain extent may be reduced by partially sinking the digester into the ground

Source: (Monnet, 2003).

FEEDSTOCKS

All types of biomass can be used as feedstocks for biogas production as long as they contain carbohydrates, proteins, fats, cellulose, and hemicelluloses as main components (Weiland, 2010). The choice of substrate determines the organic loading rate (OLR), amount of biogas and the methane content of the biogas produced (Raju, 2012). The mass balance of products of AD depends on three fundamental factors; viz, the feedstock type, the digestion

system, and the retention time (Braun, 2007). Biomass resources differ significantly in their chemical composition. This affects their potential for biogas production by AD.

The gamut of biomass resources amenable to AD includes animal manure, MSW, sewage sludge, food waste, crops and crop residues. Use of the term ‘waste’ when referring to feedstocks for bioenergy is resisted by some scholars on the basis that it precludes their value as sources of energy. However, the term will be used in this chapter cognisant of this observation. AD has been regarded as the waste-to-energy technology and is widely used in the treatment of various organic wastes.

There are significant populations of livestock in many countries. Livestock produce large amounts of manure which are suitable substrates for AD. Animal manure is one of the common feedstocks for AD. Estimates of quantities of manure obtainable from various livestock species and the associated energy potential are shown in Table 5.

Various organic wastes from households and municipal authorities provide MSW. Worldwide there are many AD plants in operation using MSW or organic industrial waste as their principal feedstock. An example of economic sustainability of three different biogas full-scale plants, fed with different organic matrices: energy crops, manure, agro-industrial and OFMSW is provided by Riva et al., (2014). They showed that unit costs of biogas and electric energy were differently distributed, depending on the type of feed and plant. In their study, the plant using OFMSW showed high management/maintenance cost for OFMSW treatment. The plant using energy crops had high cost for crop supply (Riva et al., 2014). The plant using agro-industrial waste showed higher impact on the total costs because of the depreciation charge (Riva et al., 2014).

Table 5. Livestock manure output and their energy potential

Species	Dry dung output* (kg head ⁻¹ day ⁻¹)	Energy value* (GJ t ⁻¹)
Cattle	1.80	18.5
Pigs	0.80	11.0
Sheep	0.40	14.0
Goats	0.40	14.0
Poultry	0.06	11.0

*Source: Hemstock and Hall, 1995.

Table 6. Classification of municipal solid waste

Type of waste	Waste description
Household waste	Organic kitchen wastes, sweepings, rags, paper, cardboard, plastic, bone, metals
Commercial refuse	Sources include markets, shops, offices, restaurants, warehouses, hotels
Institutional refuse	Sources include schools, government offices, hospitals, religious buildings
Street sweepings	These consist of sand, stones, litter

Source: Ministry of Local Government, Rural and Urban Development, Zimbabwe, 1995.

MSW is a heterogeneous mixture of multiple wastes produced in urban areas. Typical composition of MSW is shown in Table 6. Municipal solid waste consists of several different fractions, both of organic and inorganic nature. MSW is normally sorted into six categories, namely, food residue, wood waste, paper textiles, plastics, and rubber (Zhou, Meng, Long, Li, & Zhang, 2014).

Separation of MSW into the putrescible organic fraction has been known to provide the best quality feedstock for AD (Jingura and Matengaifa, 2009). This fraction of MSW is called the OFMSW. In some urban centres there is source-sorting of MSW such that the OFMSW is readily available (Jingura and Matengaifa, 2009). The composition of the OFMSW strongly depends on the place and time of collection for a specific municipality or area (Alibardi and Cossu, 2015). The OFMSW is characterised by high moisture and high biodegradability due to a large content of food waste, kitchen waste and leftovers from residences, restaurants, cafeterias, factory lunch-rooms and markets (Zhang et al., 2007; Lebersorger and Schneider, 2011).

Crop residues have high potential for AD (Jingura and Matengaifa, 2009). Several crop residues have been shown to be suitable for AD and these include cotton, maize and rice residues (Isci and Demir, 2007). However, high lignin content in some straws and other residues can lead to poor biodegradability and low biogas production.

A number of crops demonstrate good biogas potentials. In fact, all C₄ plants have very good growth yields and produce large amounts of biomass. The most important parameter for choosing energy crops is their net energy yield per hectare (Weiland, 2010). Many conventional forage crops produce large amounts of easily degradable biomass which is necessary for high biogas yields (Braun et al., 2009). Different cereal crops and perennial grasses have potential as energy crops. Gross crop yield and energy potential are shown in Table 7.

Table 7. Gross crop yield and biogas potential of different crops

Crop	Crop yield (t FM/ha)	Biogas yield (Nm ³ /(t VS))	Methane content (%)
Fodder beet	80-120	750-800	53
Sorghum	40-80	520-580	55
Sugar beet	40-70	730-770	53
Maize	40-60	560-650	52
Wheat	30-50	650-700	54
Sunflower	31-42	420-540	55
Triticale	28-33	590-620	54
Grass	22-31	530-600	54
Red clover	17-25	530-620	56
Corn cob mix	10-15	660-680	53
Wheat grain	6-10	700-750	53
Rye grain	4-7	560-780	53

Source: Weiland, 2010.

Non-food crops can be used for biogas production. An example shown in Table 7 is grass which has high biogas yields. Other examples of non-food crops that can be used in AD are *Jatropha curcas* L. press-cake (Jingura, Musademba, & Matengaifa, 2010) and *Arundo donax* L. (Corno, Pilu, & Adani, 2014). *A. donax* can be used for biogas production in substitution or partial integration with the traditional energy crops in co-digestion with animal slurries and/or other biomasses (Corno et al., 2014). Production of biogas by AD of *J. curcas* press-cake has been demonstrated (Singh, Vyas, Srivastava, & Narra, 2008). Radhakrishma (2007) obtained 0.5 m³ biogas kg⁻¹ of solvent extracted *J. Curcas* press-cake and 0.6 m³ biogas kg⁻¹ of mechanically de-oiled cake. Singh et al., (2008) observed that biogas production from *J. Curcas* press-cake was about 60% higher than that from cattle dung and the gas contained 66% methane.

Sewage sludge abounds in urban areas the world over. It is a vast resource that is amenable to AD. Wastewater treatment facilities employ anaerobic digesters to break down sewage sludge and eliminate pathogens in wastewater (Scaglia, D'Imporzano, Garuti, Negri, & Adani, 2014). A standard practice is to use a small amount of ammonia in full-scale plants to partially sanitize sewage sludge, thereby allowing successive biological processes to enable the high biological stability of the OM (Scaglia et al., 2014). However, Scaglia et al., (2014) have demonstrated that sludge sanitation can be achieved without the addition of ammonia. Worldwide, the anaerobic stabilization of sewage sludge is probably the most important AD process (Braun and Wellinger, 2009). In Europe, typically between 30% and 70% of sewage sludge is treated by AD (IEA, 2009). In developing countries, AD is in most cases the only treatment of wastewater.

CO-DIGESTION

Principle of Co-Digestion

Co-digestion is the simultaneous digestion of a mixture of two or more different substrates (Wu, 2000; Barz, 2014). The most common situation is when a major amount of a main substrate (e.g., manure or sewage sludge) is mixed and digested together with minor amounts of a single, or a variety of additional substrates (Braun and Wellinger, 2009; Kangle, Kore, Kore, & Kulkarni, 2012). The expression co-digestion is applied independently to the ratio of the respective substrates used simultaneously (Braun and Wellinger, 2009). The use of co-substrates usually improves the biogas yields from anaerobic digesters due to positive synergisms established in the digestion medium and the supply of missing nutrients by the co-substrates (Alvarez and Liden, 2008).

Historically, AD was a single substrate, single purpose technology (Kangle et al., 2012). For example, each type of livestock manure would be digested as a sole substrate in digesters to produce biogas. Examples can be used to illustrate the principle of co-digestion. For example, C/N ratio and buffer capacity are important aspects of digester performance (Murto, Bjornsson, & Mattiasson, 2004). Blood and pig manure have high N content and can be co-digested with waste that has low N content (Alverz and Liden, 2008). The N and P content in fruit and vegetable wastes is often low and for this reason it has been used in co-digestion with wastes with higher N and P content (Callaghan, Wase, Thayanithy, & Forster, 2002).

The concept of co-digestion is premised on the fact that the biogas yield of individual substrates varies. The biogas yield of the individual substrates varies considerably dependent on their origin, content of organic substance, and substrate composition (Weiland, 2010). Thus, the principle of co-digestion is to increase methane production from low-yielding or difficult to digest feedstocks and enhance synergistic effects between feedstocks (Alverz and Liden, 2008; Kangle et al., 2012).

Selecting Feedstocks for Co-Digestion

The fundament of co-digestion is to select compatible feedstocks that enhance methane production and to avoid materials that may inhibit methane generation (Kangle et al., 2012). In addition, anaerobic digester systems must be able to handle the significant increase in methane output that is common with co-digestion (USEPA, 2014).

There are multiple choices for co-digestion feedstocks, including restaurant or cafeteria food wastes, food processing wastes or byproducts, fats, oil and grease from restaurant grease traps, energy crops, crop residues, and others (USEPA, 2014). Methods for testing potential co-digestion feedstocks include biochemical methane potential (BMP) and anaerobic toxicity assays (ATAs) (Moody et al., 2009). While BMPs provide information regarding the methane production of a substrate, they are typically highly diluted and may mask potential substrate toxicity (Moody et al., 2009).

ATAs determine how a particular substrate inhibits methane production by examining methane production from a mixture of a known degradable substrate and the test substrate (Sell et al., 2010). An ATA evaluates a substrate's ability to inhibit methane production and thus determine its potential toxicity (Sell et al., 2010; Moody, Burns, Sell, & Bishop, 2011). ATAs provide additional information that could be utilized with BMP results to assist with co-substrate selection (Moody et al., 2011). The ATA procedure is documented in significant detail in the ISO (2003) standard.

Examples of substrates that could be toxic have been given in literature. Campos et al., (2008), working with liquid livestock waste treated with polyacrylamide (PAM), observed some indirect inhibitory phenomena of PAM, such as a limited hydrolysis rate due to particle aggregation, and inhibition of methanogenesis by high ammonia concentration. This could affect use of such material as a co-substrate. Moody et al., (2011) demonstrated toxicity of 'enzyme process by-product' material in AD. Therefore, ATAs are required to thoroughly evaluate co-digestion co-substrates (Moody et al., 2011).

Although critical to early stage design, BMP, and ATA results may be misleading when applied directly to full-scale operation due to their lack of information addressing hydraulic retention time (HRT), substrate interaction, and continuous organic loading (Sell et al., 2010). However, there are other factors that determine suitability of co-substrates. USEPA (2012) provided a practical checklist of things to consider when selecting substrates for co-digestion. The factors stated in their Co-digestion Fact Sheet can be disaggregated and placed into the categories as adumbrated in Figure 3.

Economic and Legal Factors

Both the availability and cost of co-digestion feedstocks are important factors to consider (USEPA, 2012). It makes sense to use co-substrates that are readily available within the location of a plant. Cost of the substrate, in addition to cost of transportation, affects the

economic merits of co-digestion (USEPA, 2012). In some jurisdictions, co-digesting multiple feedstocks may require an anaerobic digester system to obtain additional air, water, or solid waste permits (USEPA, 2012).

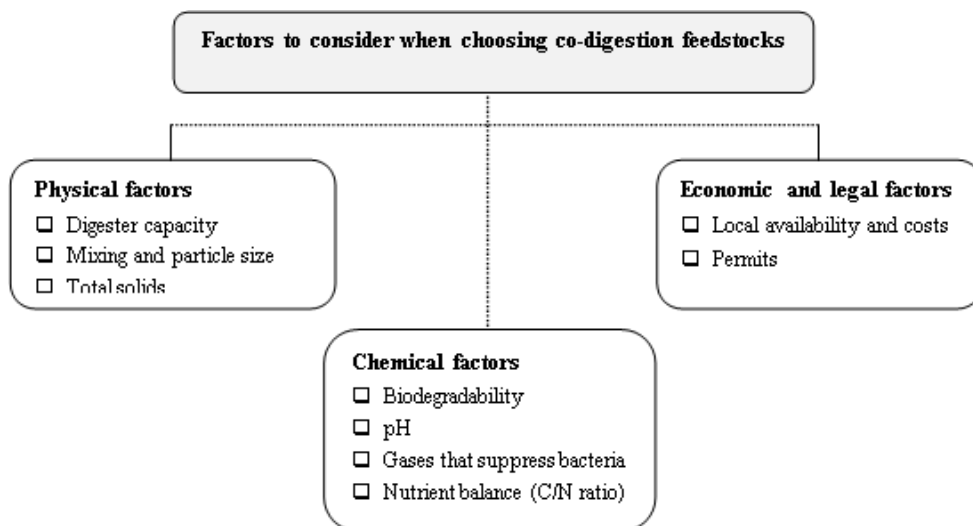


Figure 3. Factors to consider when selecting substrates for co-digestion.

Physical Factors

Capacity considerations for digesters are at several fronts (USEPA, 2012). First, the digester must have enough capacity to handle the additional substrate. The second factor is organic loading rate (OLR). The OLR is the amount of VS fed into the digester each day in a continuous process (Kwietniewska and Tys, 2014). As the OLR rate increases, the biogas yield increases to some extent, but above the optimal OLR the VS degradation and biogas yield decreases due to overloading (Babae and Shayegan, 2011).

Typical values of OLR ranges between 0.5 and 3 kg VS/m³/d (Poliafico, 2007). Ehimen et al., (2011) reported that the most effective ORL was 5 g VS l⁻¹ AD substrate.

The third factor is retention time. There are two significant types of retention time. The hydraulic retention time (HRT) is the time that the fluid element of the feedstock remains in the digester (Kwietniewska and Tys, 2014). The solid retention time (SRT) is the residence time of the bacteria in the digester (Kwietniewska and Tys, 2014). The retention time for wastes treated in mesophilic digesters ranges from 10 to 40 days (Kangle et al., 2012). Lower retention times, for example 14 days, are required for digesters operated in the thermophilic range (Kangle et al., 2012). Given the relatively long generation time of methanogens, SRT should be over 12 days in order to avoid microbial washout (Gerardi, 2003).

The purpose of mixing in a digester is to create a homogenous feed in the digester and to ensure blending of fresh material with digestate containing microbes. Co-substrates may vary widely in particle size. Small particle size has been shown to increase biogas yield because methane-producing bacteria have better contact with the volatile solids (USEPA, 2012). Mixing prevents scum formation and avoids temperature gradients within the digester (Kangle et al., 2012). Thus, co-substrates must complement each other on these variables.

A general guide is that a low solid AD contains less than 10% TS, medium solids about 15-20%, and high solids 22-40% (Kangle et al., 2012). An increase in TS results in a decrease in digester volume. For example, mixing liquid manures with drier feedstocks may increase the TS of feedstock in the digester. The implication is that enough moisture must be maintained to support AD.

Chemical Factors

The issue of biodegradability of feedstocks varies quite markedly. Generally, animal manures are digested lower than other organic substrates. This subject will be covered in the section on BMP of feedstocks. Addition of substrates for co-digestion must increase VS in the mixture and enhance biogas yield (Kangle et al., 2012).

pH as a process parameter has been discussed in an earlier section. The pH requirements of microbes involved in AD varies between the acidogenic and methanogenic bacteria. The dynamic of pH effects is that each different phase of AD has its own optimum range. The effects of inhibitory substances and C/N ratios have been covered in an earlier section.

Methane Potential of Feedstocks

The biogas yield of the individual substrates varies considerably dependent on their origin, content of organic substance, and substrate composition (Weiland, 2010). The main constituents of organic feedstocks are carbohydrates, proteins, and fats. Feedstocks differ markedly in their chemical composition. Baserga (1998), cited by Weiland (2010), provided information on gas yields and methane potential of various feedstock constituents. The data are shown in Table 8.

Table 8. Maximal gas yields and theoretical methane contents

Substrate	Biogas (Nm ³ /t TS)	CH ₄ (%)	CO ₂ (%)
Raw fat	1 200-1 250	67-68	32-33
Carbohydrates ^a	790-800	50	50
Raw protein	700	70-71	29-30
Lignin	0	0	0

^aOnly polymers from hexoses, not inulins and single hexoses.

Sources: (Baserga, 1998 cited by Weiland, 2010).

It is quite evident from Table 8 that fats and oils have high potential for methane production. Anaerobic biogasification potential (ABP) assay, also known as BMP, can be used in evaluating biogas potential of both organic matrices composing an ingestate mixture and residual biogas in digestates (Schievano, Pognani, D'Imporzano, & Adani, 2008). It is prudent at this juncture to define BMP before we situate it in the context of co-digestion. The BMP provides an indication of the biodegradability of a substrate and its potential to produce methane via AD (Sell et al., 2010). Such information allows a direct assessment of biogas yields achieved by the AD process (Schievano et al., 2008). The BMP is a good method of establishing baseline performance data for AD (Speece, 1996). However, as stated earlier, ATAs also need to be considered in co-substrate selection (Moody et al., 2011).

Table 9. Multiple stepwise linear regression for predicting ABP

Model	Equation	Variables involved
1	$ABP = 20.497 * VS * 1241.534$	VS
2	$ABP = 13.782 * VS + 26.161 * OD20^{1/2} - 997.890$	VS, $OD20^{1/2}$
3	$ABP = 10.480 * VS + 23.178 * OD20^{1/2} + 10.979 * TOC - 1038.667$	VS, $OD20^{1/2}$, TOC
4	$ABP = 8.445 * VS + 19.173 * OD20^{1/2} + 10.942 * TOC + 2.913 * CS - 1067.198$	VS, $OD20^{1/2}$, TOC, CS

OD20 – Oxygen demand in a 20-h respirometric test. CS – Cell soluble. Source: (Schievano et al., 2008).

Table 10. Chemical composition and cumulative and ultimate methane yields of substrates

Substrate	n	pH	TS	VS	Cumulative methane yield		Ultimate methane yield
			g kg ⁻¹	g kgTS ⁻¹	L kgTS ⁻¹	L kgVS ⁻¹	L kgVS ⁻¹
Grass silage	4	4.5	314	928	296	319	320
Maize silage	3	4.2	174	952	292	307	339
Hay	4	-	913	937	268	286	292
Pig slurry	1	7	69.9	794	252	317	321
Cattle slurry	9	7.7	78	782	186	238	247
Raw milk	1	-	128	993	508	512	517
Distillery slop	1	3.2	55.4	912	306	335	385

Source: (Luna-delRisco et al., 2011).

BMP assays are a useful tool for determining the best substrate and co-digestion configurations (Nielfa, Cano, & Fdz-Polanco, 2015). However, there are some methodologies designed to save costs and time from this process by using the theoretical final methane potential of a substrate from its organic composition (Nielfa et al., 2015). Several methods could help to determine theoretical methane potential based on COD characterisation, elemental composition or organic fraction composition (Nielfa et al., 2015). An example is given by Schievano et al., (2008). Considering both quantitative (VS and TOC) and qualitative aspects of OM, four models were proposed to predict ABP (Schievano et al., 2008). The models are shown in Table 9.

BMP assays have been widely used to determine the methane yield of organic substrates in specific conditions (Gunaseelan, 2004). A study by Luna-delRisco et al., (2011) provides some data that can be used as an exemplar of BMP of some feedstocks. The data are shown in Table 10.

A study by Gunaseelan (2004) showed that the ultimate methane yields of fruit wastes ranged from 0.18 to 0.732 l g⁻¹ VS, and that of vegetable wastes ranged from 0.19 to 0.41 l g⁻¹ VS. Labatut et al., (2011) reported the BMP of used vegetable oil as 648 mL g⁻¹ VS. In fact, crop materials (energy crops, maize, etc) and non-agricultural wastes (biowaste, food waste) have higher BMP than animal manures. Zhang et al., (2009) reported that the average methane content of biogas from AD of food waste was 73%. This explains why co-digestion of animal manure or feedstocks with low carbon content with food waste can improve process stability and methane production (Zhang et al., 2008). Literature abounds with a plethora of studies on co-digestion of animal manure with food and vegetable wastes. Examples of such studies are shown in Table 11.

Table 11. Examples of studies that have demonstrated the advantages of co-digestion

Study co-substrates	Findings	References
Different mixing ratios of cattle waste and cassava peels (1:1; 2:1, 3:1, 4:1)	Biogas yield increased to 21.3, 19.5, 15.8, and 11.2 L/kg TS, respectively	Adelekan and Bamgboye, 2009
Cow dung and pig manure in a ratio of 1:1	Maximum increase of seven and three fold of biogas compared to mono cow and pig manure substrates, respectively	Muyiyya and Kasisira, 2009
Dairy manure and food waste in ratios 100/0, 68/32 and 52/48	Biogas yield was 241, 282 and 311 L/kg VS	El-Mashad and Zhang, 2010
Mixtures of dairy manure with various different food wastes	Methane yields increased by 2 to 4.6 times over the control (dairy manure only)	Zhu, Wan, & Li, 2011
Cattle manure with organic kitchen waste	Substantially increased the biogas yields by 24 to 47% over the control (organic kitchen waste and dairy manure only)	Aragaw, Andargie, & Gessesse, 2013

Numerous energy crops have been tested for their methane formation potential. Examples of energy crops used in AD plants include maize, sunflower, miscanthus, and various grasses. In principle, many varieties of grasses, clover, cereals and maize including whole plants, as well as rape or sunflower have proved feasible for methane production (Braun et al., 2009). Depending on numerous conditions, a fairly wide range of methane yields, between 120–658 m³ t⁻¹VS, was reported in literature from AD of different crops (Braun et al., 2009). For example, methane yields for miscanthus, Sudan grass, and ryegrass were 179-215, 213-303, and 390-410 m³ t⁻¹VS, respectively (Braun et al., 2009).

Selected Examples of Co-Digestion Plants

The numbers of co-digestion plants are continuously increasing, particularly in many European countries and this has become a standard practice (Braun and Wellinger, 2009). Germany is a notable leader in biogas production. The typology of plant types is as follows:

- Sewage sludge
- Biowaste
- Agriculture
- Industrial waste
- Landfill (valorisation)

A good number of new sewage treatment plants or plant extensions are increasingly using co-substrates. The co-substrates include source-separated biowaste, kitchen waste, fat waste, flotation sludges, and various other materials. In agriculture, co-digestion has become a

standard technology. In Austria, 293 plants were implementing co-digestion, 11 in Finland, and 29 in Switzerland (International Energy Agency, 2014).

Developments in AD technology continue to rise as more possibilities are explored. For example, biorefineries for production of several products and by-products such as biofuels, heat, and/or electricity have been in focus in the recent years (Chen et al., 2005; Zhang, 2008). Production of multiple types of biofuels and energy products from a commercial biorefinery is a compelling alternative to maximise the energy value of available biomass resources (Papa et al., 2015). In a biorefinery, biomass can be converted to useful biomaterials and/or energy carriers in an integrated manner (Thomsen, 2005). The advantage of this practice is that it can maximize the economic value of the biomass used while reducing the waste streams produced (Thomsen, 2005).

Papa et al., (2015) demonstrated the benefits of ionic liquid pretreatment of biomass as strategy to optimise total energy production by combining bioethanol and biogas production. Kaparaju et al., (2009) investigated the production of bioethanol, biohydrogen, and biogas from wheat straw within a biorefinery framework. Their work (Kaparaju et al., 2009) showed that either use of wheat straw for biogas production or multi-fuel production were the energetically most efficient processes compared to production of mono-fuels such as bioethanol when fermenting C₆ sugars alone. This is ongoing work that is important for integrated biorefinery technology.

Merits and Limits of Co-Digestion

Several studies have demonstrated that using co-substrates in AD system improves the biogas yields (Wu, 2000; Braun and Wellinger, 2009; Kangle et al., 2012). This is due to the positive synergisms established in the digestion medium and the supply of missing nutrients by the co-substrates (Wu, 2000; Kangle et al., 2012). Studies, as those shown in Table 11, have demonstrated that co-digestion of a variety of substrates, especially the utilization of animal manure together with solid agricultural residues and/or energy crops, improves the nutrient balance and the AD process is more stable (Barz, 2014). A further advantage of co-digestion is optimisation of use of digester volume which will result in increased plant capacities and the equalization of solid matter distribution in the digester (Barz, 2014). The utilization of agricultural residues as feedstocks in AD contributes to economic, environmental and social sustainability (Barz, 2014).

Kangle et al., (2012) have summarised the merits and limits of co-digestion as given below. These are:

Advantages:

- Improved nutrient balance and digestion
- Additional biogas collection
- Possible gate fees for waste treatment
- Additional fertilizer i.e., soil conditioner
- Renewable biomass disposable for digestion in agriculture
- Optimisation of use of digester space

Disadvantages:

- Increased digester effluent COD
- Additional pre-treatment requirements
- Increased mixing requirements
- Wastewater treatment requirement
- Hygienisation requirements
- Restrictions of land use for digestate
- Economically dependent on crops

It is important to note that the main benefits of co-digestion, as given above, relate to enhanced biogas yields, economic merits, and benefits to agriculture. However, agricultural wastes have other uses within farming systems which are not necessarily for energy production. The disadvantages do not apply in all cases. For example, land use for digestate might not be a concern in crop situations that rely on bio-fertilisers.

CONCLUSION

Biogas is a growing fuel in the 21st century and this is not a disputable fact. Co-digestion is a technology that can be used to optimise production of biogas. Evidence abounds in literature that co-digestion can be used to enhance biogas yields of the AD process. The principle of co-digestion is to enhance the synergistic effect between feedstocks. Where feedstocks complement each other, the co-substrates improve biogas yields. There are also economic benefits brought about by this technology due to shared equipment and increased gas yields.

REFERENCES

- Abbassi-Guendouz, A., Brockmann, D., Trably, E., Dumas, C., Delgene`s, J.P., et al., (2012). Total solids content drives high solid anaerobic digestion via mass transfer limitation. *Bioresource Technology*, 111, 55–61.
- Abdelgadir, A., Chen, X. G., Liu, J. S., Xie, X. H., Zhang, J., Zhang, K., Liu, N. (2014). Characteristics, Process Parameters, and Inner Components of Anaerobic Bioreactors. *Biomed Research International*.
- Adelekan, F. & Bamgboye, A. (2009). Comparison of biogas productivity of cassava peels mixed in selected ratios with major livestock waste types. *African Journal of Agricultural Research*, 4(7), 571-577.
- Alibardi, I. & Cossu, R. (2015). Composition variability of the organic fraction of municipal solid waste and effects on hydrogen and methane production potentials. *Waste Management*, 36, 147–155.
- Al-Masri, M. R. (2001). Changes in biogas production due to different ratios of some animal and agricultural wastes. *Bioresource Technology*, 77(1), 97-100.

- Angelidaki, I., Ellegaard, L., & Ahring, B. K. (1993). A mathematical model for dynamic simulation of anaerobic digestion of complex substrates: focusing on ammonia inhibition. *Biotechnology and Bioengineering*, 42(2), 159–166.
- Angelidaki, I., & Sanders, W. (2004). Assessment of the anaerobic biodegradability of macropollutants. *Reviews in Environmental Science and Bio/Technology*, 3(2), 117–129.
- Appels, L., Baeyens, J., Degrève, J., & Dewil, R. (2008). Principles and potential of the anaerobic digestion of waste-activated sludge. *Progress in Energy and Combustion Science*, 34(6), 755–781.
- Aragaw, T., Andargie, M., & Gessesse, A. (2013). Co-digestion of cattle manure with organic kitchen waste to increase biogas production using rumen fluid as inoculums. *International Journal of Physical Sciences*, 8(11), 443–450.
- Alvarez, R., & Liden, G. (2008). Semi-continuous co-digestion of solid slaughterhouse waste, manure, and fruit and vegetable waste. *Renewable Energy*, 33(4), 726–734.
- Babae, A., & Shayegan, J. (2011). Effect of organic loading rates (OLR) on production of methane from anaerobic digestion of vegetables waste. World renewable energy congress. Sweden: Linköping; (8–13 May).
- Banks, C.J. & Zhang, Y. (2010). Optimising inputs and outputs from anaerobic digestion process. School of Engineering and the Environment, University of Southampton. Technical Report Defra WR 0212.
- Barz, M. (2014). Ecological, technological, and economic advantages of co-digestion for biogas production. 5th International Conference on Sustainable Energy and Environment, Bangkok, Thailand, 19–21 November.
- Batstone, D. J., Keller, J., Angelidaki, I., Kalyuzhnyi, S. V., Pavlostathis, S. G., Rozzi, A., et al., (2002). The IWA anaerobic digestion model no1 (ADM1). *Water Science and Technology*, 45(10), 65–73.
- Braun, R. (2007). Anaerobic digestion: a multi-faceted process for energy, environmental management and rural development. In: Ranalli, P (Ed) Improvement of crop plants for industrial end uses. Springer, Dordrecht pp. 335–415.
- Braun, R., Weiland, P., & Wellinger, A. (2009). Biogas from energy crop digestion. IEA Task 37 Brochure, International Energy Agency, Paris, France.
- Braun, R., & Wellinger, A. (2009). Potential of Co-digestion, International Energy Agency (IEA) Bioenergy, 2009.
- Boe, K., Batstone, D. J. & Angelidaki, I. (2005). Optimisation of serial CSTR biogas reactors using modeling by ADM1, In: The First International Workshop on the IWA Anaerobic Digestion Model No.1 (ADM1), 2–4 September, Lyngby, Denmark. Proceedings, pp. 219–221. International Water Association, London, UK.
- Bothi, K. L. (2007). Characterisation of biogas from anaerobically digested dairy waste for energy use. MSc Thesis, Cornell University, Ithaca, New York.
- Callaghan, F. J., Wase, D. A. J., Thayanithy, K., & Forster, C. F. (2002). Continuous co-digestion of cattle slurry with fruit and vegetable wastes and chicken manure. *Biomass and Bioenergy*, 22(1), 71–77.
- Cantrell, K. B., Ducey, T., Ro, K. S., & Hunt, P. G. (2008). Livestock waste-to-bioenergy generation opportunities. *Bioresource Technology*, 99(17), 7941–7953.
- Chae, K. J., Jang, A., Yim, S. K., & Kim, I. S. (2008). The effects of digestion temperature and temperature shock on the biogas yields from the mesophilic anaerobic digestion of swine manure. *Bioresource Technology*, 99, 1–6.

- Chen, Y., Cheng, J. J. & Creame, K. S. (2008). Inhibition of anaerobic digestion process: A review, *Bioresource Technology*, 99, 4044 – 4064.
- Chen, S., Wen, Z., Liao, W., Liu, C., Kincaid, R., Harrison, J., Elliott, D., Brown, M. & Stevens, D. (2005). Studies into using manure in a biorefinery concept. *Applied Biochemistry and Biotechnology*, 124 (1), 999–1015.
- Collins, G., Woods, A., McHugh, S., Carton, M. W., & O'Flaherty, V. (2003). Microbial community structure and methanogenic activity during start-up of psychrophilic anaerobic digesters treating synthetic industrial wastewaters. *FEMS Microbiology Ecology*, 46(2), 159-170.
- Colmenarejo, M. F., Sánchez, E., Bustos, A., García, G., & Borja, R. (2004). A pilot-scale study of total volatile fatty acids production by anaerobic fermentation of sewage in fixed-bed and suspended biomass reactors. *Process Biochemistry*, 39(10), 1257-1267.
- Corno, L., Pilu, R., & Adani, F. (2014). Arundo donax L.: A non-food crop for bioenergy and bio-compound production. *Biotechnology Advances*, 32(8), 1535-1549.
- Campos, E., Almirall, M., Mtnez-Almela, J., Palatsi, J., & Flotats, X. (2008). Feasibility study of the anaerobic digestion of dewatered pig slurry by means of polyacrylamide. *Bioresource Technology*, 99(2), 387-395.
- de Baere, L. A., Devocht, M., van Assche, P., & Verstraete, W. (1984). Influence of high NaCl and NH₄Cl salt levels on methanogenic associations. *Water Research*, 18(5), 543–548.
- de Mes, T. Z. D., Stams, A. J. M., Reith, J. H. & Zeeman, G. (2003). Methane production by anaerobic digestion of wastewater and solid wastes. In: Reith, J. H., Wijffels, R. H. & Barten, H. (eds) Bio-methane & biohydrogen: status and perspectives of biological methane and hydrogen production. Dutch Biological Hydrogen Foundation, Petten, The Netherlands, pp. 58–102.
- Demirel, B. & Scherer, P. (2008). Production of methane from sugar beet silage without manure addition by a single-stage anaerobic digestion process. *Biomass and Bioenergy*, 32, 203–209.
- Dioha, J., Ikeme, C. H., Nafi'u, T., Soba, N. I. & Yusuf M. B. S. (2013). Effect of carbon to nitrogen ratio on biogas production. *International Research Journal of Natural Sciences*, 1(3), 1 -10.
- Dolfing, J., & Bloeman, W. G. B. M. (1985). Activity measurements as a tool to characterize the microbial composition of methanogenic environments. *Journal of Microbiological Methods*, 4(1), 1-12.
- El-Mashad. H. & Zhang, R. (2010). Biogas production from co-digestion of dairy manure and food waste. *Bioresource Technology*, 101(11), 4021-4028.
- Ehimen, E. A., Sun, Z. F., Carrington, C. G., Bircj, E. J. & Eaton-Rye, J. J. (2011). Anaerobic digestion of microalgae residues resulting from the biodiesel production process. *Applied Energy*, 88(10), 3454-3463.
- Forster-Carneiro, T., Pe´rez, M. & Romero, L. (2008). Influence of total solid and inoculum contents on performance of anaerobic reactors treating food waste. *Bioresource Technology*. 99: 6994–7002.
- Gerardi, M. (2003). The microbiology of anaerobic digesters. John Wiley & Sons, Inc. Hoboken, 33, 726-734.
- Giard, D. (2011). Biogas Production Regime for In-Storage-Psychrophilic-Anaerobic-Digestion. MSc Thesis, McGill University, Ste-Anne-de-Bellevue, Québec, Canada.

- Gunaseelan, V.N. (2004). Biochemical methane potential of fruits and vegetable solid waste feedstocks. *Biomass and Bioenergy*, 26, 389–399.
- Halalsheh, M., Kassab, G., Yazajeen, H., Qumsieh, S., & Field, J. (2010). Effect of increasing the surface area of primary sludge on anaerobic digestion at low temperature. *Bioresource Technology*, 102(2), 748-752.
- Hamilton, D. W. (2012). Organic Matter Content of Wastewater and Manure, BAE 1760. Stillwater, OK: Oklahoma Cooperative Extension Service.
- Hedrick, D. B., Guckert, J. B., & White, D. C. (1991). The effects of oxygen and chloroform on microbial activities in a high-solids, high-productivity anaerobic biomass reactor. *Biomass and Bioenergy*, 14, 207-212.
- Hemstock, S. L. & Hall, D. O. (1995). Biomass energy flows in Zimbabwe. *Biomass and Bioenergy*, 8(3), 151–173.
- International Energy Agency. (2009). Biogas production and utilization. IEA Task 37 Brochure, International Energy Agency, Paris, France.
- International Energy Agency. (2014). IEA Bioenergy Task 37 - Country Reports Summary 2014. IEA Task 37 Brochure, International Energy Agency, Paris, France.
- Isci, A. & Demir, G.N. (2007). Biogas production potential from cotton wastes. *Renewable Energy*, 32,750–757.
- ISO. (2003). Water quality – determination of inhibition of gasproduction of anaerobic bacteria – Part 1: General test. International Standards Organization 13641-1. Geneva,Switzerland: ISO.
- Jingura, R. M. & Matengaifa, R. (2009). Optimization of biogas production by anaerobic digestion for sustainable energy development in Zimbabwe. *Renewable and Sustainable Energy Reviews*, 135, 1116-1120.
- Jingura, R. M., Musademba, D. & Matengaifa, R. (2010). An evaluation of utility of *Jatropha curcas* L. as a source of multiple energy carriers. *International Journal of Engineering, Science and Technology*, 2(7), 115-122.
- Kangle, K. M., Kore, S. V., Kore, V. S. & Kulkarni, G. S. (2012). Recent trends in anaerobic codigestion: A review. *Universal Journal of Environmental Research and Technology*, 2(4), 201-219.
- Kaparaju, P., Serrano, M., Thomsen, A. B., Kongjan, P. & Angelidaki, I. (2009). Bioethanol, biohydrogen and biogas production from wheat straw in a biorefinery concept. *Bioresource Technology*, 100, 2562–2568.
- Kashyap, D. R., Dadhich, K. S., & Sharma, S. K. (2003). Biomethanation under psychrophilic conditions: a review. *Bioresource Technology*, 87(2), 147-153.
- Khalid, A., Arshad, M., Anjum, M., Mahmood, T., & Dawson, L. (2011). The anaerobic digestion of solid organic waste. *Waste Management*, 31(8), 1737-44.
- Khanal, S.K. (2008). Microbiology and biochemistry of anaerobic biotechnology. In Khanal, S. K. (Ed.), *Anaerobic biotechnology for bioenergy production - principles and applications*. Wiley-Blackwell, Singapore.
- Kim, M., Ahn, Y. H., & Speece, R. E. (2002). Comparative process stability and efficiency of anaerobic digestion; mesophilic vs. thermophilic. *Water Research*, 36(17), 4369-4385.
- Korres, N., O'Kiely, P., John A. H., Benzie, J. A. H. & West, J. S. (2013). *Bioenergy Production by Anaerobic Digestion: Using Agricultural Biomass and Organic Wastes*. Routledge, London.

- Kwietniewska, E., & Tys, J. (2014). Process characteristics, inhibition factors and methane yields of anaerobic digestion process, with particular focus on microalgal biomass fermentation. *Renewable and Sustainable Energy Reviews*, 34, 491-500.
- Labatut, R. A., Largus T. Angenent, L. T. & Scott, N. R. (2011). Biochemical methane potential and biodegradability of complex organic substrates. *Bioresource Technology*, 102, 2255–2264.
- Lee, M., Hidaka, T., & Tsuno, H. (2008). Effect of temperature on performance and microbial diversity in hyperthermophilic digester system fed with kitchen garbage. *Bioresource Technology*, 99(15), 6852-6860.
- Lebersorger, S. & Schneider, F. (2011). Discussion on the methodology for determining food waste in household waste composition studies. *Waste Management*, 31, 1924–1933.
- Luna-delRisco, M., Normak, A. & Orupõld, K. (2011). Biochemical methane potential of different organic wastes and energy crops from Estonia. *Agronomy Research*, 9(1-2), 331-342.
- Marchaim, U. (1992). Biogas processes for sustainable development. Food and Agriculture Organization of the United Nations, Viale delle Terme di Caracalla, Rome, Italy.
- Mata-Alvarez, J., Mace, S., & Llabres, P. (2000). Anaerobic digestion of organic solid wastes. An overview of research achievements and perspectives. *Bioresource Technology*, 74(1), 3-16.
- Ministry of Local Government, Rural and Urban Development. (1995). Zimbabwe urban solid waste management study. Harare: Tevera–Mubvumi and Associates.
- Monnet, F. (2003). An Introduction to the Anaerobic Digestion of Organic Waste. Available from: www.biogasmx.co.uk/.../introanaerobicdigestion__073323000_1011_2.pdf (accessed 4 May 2015).
- Moody, L. R., Burns, R.T., Wu-Haan, W. & Spajić, R. (2009). Use of biochemical methane potential (BMP) assays for predicting and enhancing anaerobic digester performance. In proceedings of the 4th International and 44th Croatian Symposium of Agriculture. Optija, Croatia.
- Moody, L. B., Burns, R. T., Sell, S. T., & Bishop, G. (2011). Using anaerobic toxicity assays to aid in co-substrate selection for co-digestion. *Applied Engineering in Agriculture*, 27(3), 441-447.
- Muyiyya, N. & Kasisira, L. (2009). Assessment of the Effect of Mixing Pig and Cow Dung on Biogas Yield. *Agricultural Engineering International: the CIGR E. J. Manuscript PM 1329*, Vol. XI.
- Murto, M., Björnsson, L. & Mattiasson, B. (2004). Impact of food industrial waste on anaerobic co-digestion of sewage sludge and pig manure. *Journal of Environment Management*, 70(2), 101–107.
- Nielfa, A., Cano, R., & Fdz-Polanco, M. (2015). Theoretical methane production generated by the co-digestion of organic fraction municipal solid waste and biological sludge. *Biotechnology Reports*, 5, 14-21.
- Ogejo, J. A., Wen, Z., Ignosh, J., Bendfeldt, E. & Collins, E. R. (2009). Biomethane technology. Virginia Cooperative Extension. Publication, 442–881.
- Papa, G., Rodriguez, S., George, A., Schievano, A., Orzi, V., Sale., K. L., Singh, S., Adani, F. & Simmons, B. A. (2015). Comparison of different pretreatments for the production of bioethanol and biomethane from corn stover and switchgrass. *Bioresource Technology*, 183, 101-110.

- Pavan, P., Battistoni, P., Mata-Alvarez, J., & Cecchi, F. (2000). Performance of thermophilic semi-dry anaerobic digestion process changing the feed biodegradability. *Water Science and Technology*, 41(3), 75-81.
- Poliafico, M. (2007). Anaerobic digestion: decision support software. Master's thesis, Department of Civil, Structural and Environmental Engineering. Cork institute of technology, Cork, Ireland.
- PEW Centre. (2011). Anaerobic digesters. Available from: <http://www.c2es.org/docUploads/AnaerobicDigesters.pdf> (accessed 12 May 2015).
- Radhakrishma, P. (2007). Contribution of de-oiled cakes in carbon sequestration and as a source of energy, in Indian agriculture-need for a policy initiative. In: Proceedings of the fourth international biofuels conference, New Delhi, India, February 1-2, New Delhi: Winrock International India, pp. 65-70.
- Raju, C. S. (2012). Optimization of the anaerobic digestion process by substrate pre-treatment and the application of NIRS. Department of Engineering, Aarhus University. Denmark. Technical report BCE -TR-1, pp. 96
- Riva, C., Schievano, A., D'Imporzano, G. & Adani, F. (2014). Production costs and operative margins in electric energy generation from biogas. Full-scale case studies in Italy. *Waste Management*, 34(8), 1429-1435.
- Salminen, E., & Rintala, J. (2002). Semi-continuous anaerobic digestion of solid poultry slaughter house waste: effect of hydraulic retention time and loading. *Water Research*, 36(13), 3175-3182.
- Sattler, M. (2011). Anaerobic processes for waste treatment and energy generation. In: Kumar, S. (Ed.), Integrated waste management – Volume II. ISBN: 978-953-307-447-4, InTech, Available from: <http://www.intechopen.com/books/integrated-waste-management-volume-ii/anaerobic-processes-for-waste-treatment-and-energy-generation>
- Scaglia, B., D'Imporzano, G., Garuti, G., Negri, C. & Adani, F. (2014). Sanitation ability of anaerobic digestion performed at different temperature on sewage. *Science of the Environment*, 466-467, 888-897.
- Schievano, A., Pognani, M., D'Imporzano, G., & Adani, F. (2008). Predicting anaerobic biogasification potential of ingestates and digestates of full-scale biogas plant using chemical and biological parameters. *Bioresource Technology*, 99(17), 8112-8117.
- Schink, B. (1997). Energetics of syntrophic cooperation in methanogenic degradation. *Microbiology and Molecular Biology Review*, 61, 262-280.
- Sell, S. T., Burns, R. T., Raman, D. R. & Moody, L. B. (2010). Approaches for Selecting Anaerobic Digestion Co-Substrates for a Full-Scale Beef Manure Digester Using Biochemical Methane Potentials and Anaerobic Toxicity Assays. *Proceedings of the International Symposium on Air Quality and Manure Management for Agriculture, Agricultural and Biosystems Engineering Conference*, Dallas Texas, USA.
- Sidik, U. H., Razali, F. B., Alwi, S. R., & Maigari, F. (2013). Wan Biogas production through co-digestion of palm oil mill effluent with cow manure. *Nigerian Journal of Basic and Applied Science*, 21(1), 79-84.
- Singh, R. N., Vyas, D. K., Srivastava, N. S. L., & Narra, M. (2008). SPRERI experience on holistic approach to utilize all parts of *Jatropha curcas* fruit for energy. *Renewable Energy*, 33(8), 1868-1873.
- Solomon, K. R. & Lora, E. E. S. (2009). Estimate of the electric energy generating potential for different sources of biogas in Brazil. *Biomass and Bioenergy*, 33(9), 1101-1107.

- Speece, R. (1996). *Anaerobic biotechnology for industrial wastewaters*. Archae Press. Nashville, Tennessee, U.S.A.
- Strik, D. P. B. T. B., Domnanovich, A. M. & Holubar, P. (2006). A pH-based control of ammonia in biogas during anaerobic digestion of artificial pig manure and maize silage. *Process Biochemistry*, 41(6), 1235-1238.
- Switzenbaum, M. S. (1995). Obstacles in the implementation of anaerobic treatment technology. *Bioresource Technology*, 53(3), 255-262.
- Taleghani, G. & Kia, A. S. (2005). Technical–economical analysis of the Saveh biogas power plant. *Renewable Energy*, 30(3), 441-446.
- Tambone, F., Genevini, P., D’Imporzano, G., & Adani, F. (2009). Assessing amendment properties of digestate by studying the organic matter composition and the degree of biological stability during the anaerobic digestion of the organic fraction of MSW. *Bioresource Technology*, 100(12), 3140-3142.
- Tambone, F., Terruzzi, L., Scaglia, B. & Adani, F. (2015). Composting of the solid fraction of digestate derived from pig slurry: Biological processes and compost properties. *Waste Management*, 35, 55-61.
- Thomsen, M. (2005). Complex media from processing of agricultural crops for microbial fermentation. *Applied Microbiology and Biotechnology*, 68 (5), 598–606.
- United States Environmental Protection Agency (USEPA). (2012). Increasing Anaerobic Digester Performance with Co-digestion. Available from: <http://www.epa.gov/agstar/documents/codigestion.pdf> (accessed 4 June 2015)
- United States Environmental Protection Agency (USEPA). (2014). Co-digestion. Available from: <http://www.epa.gov/agstar/anaerobic/codigestion.html> (accessed 4 June 2015).
- Van Haandel, A.C. & van der Lubbe, J. G. M. (2007). *Handbook of biological wastewater treatment—design of activated sludge systems*. Leidschendam, The Netherlands: QuistPublishing.
- Wang, X., Lu, X., Li, F. & Yang, G. (2014). Effects of Temperature and Carbon-Nitrogen (C/N) Ratio on the Performance of Anaerobic Co-Digestion of Dairy Manure, Chicken Manure and Rice Straw: Focusing on Ammonia Inhibition. *PLoS ONE* 9(5): e97265. doi:10.1371/journal.pone.0097265.
- Ward, A. J., Hobbs, P. J., Holliman, P. J., & Jones, D. L. (2008). Optimisation of the anaerobic digestion of agricultural resources. *Bioresource Technology*, 99(17), 7928-7940.
- Wu, W. (2000). *Anaerobic Co-digestion of Biomass for Methane Production: Recent Research Achievements*.
- Weiland, P. (2010). Biogas production: current state and perspectives. *Applied Microbiology and Biotechnology*, 85(4), 849-860.
- World Bioenergy Association. (2013). *Biogas – An important renewable energy source*. WBA Fact Sheet, First Edition.
- World Energy Council. (2013). *World Energy Resources – 2013 Survey*. World Energy Council, London.
- Yi, J., Dong, B., Jin, J. & Dai, X. (2014). Effect of Increasing Total Solids Contents on Anaerobic Digestion of Food Waste under Mesophilic Conditions: Performance and Microbial Characteristics Analysis. *PLoS ONE* 9(7):e102548. doi:10.1371/journal.pone.0102548.

- Zhang, Y. (2008). Reviving the carbohydrate economy via multi-product lignocellulose biorefineries. *Journal of Industrial Microbiology and Biotechnology*, 35(5), 367–375.
- Zhang, R., El-Mashad, H. M., Hartman, K., Wang, F., Liu, G., Choate, C. & Gamble, P. (2007). Characterization of food waste as feedstock for anaerobic digestion. *Bioresource Technology*, 98, 929–935.
- Zhang, L. X., Yang, Z. F., Chen, B. & Chen, G. Q. (2009). Rural energy in China: pattern and policy. *Renewable Energy*, 34, 2813-2823.
- Zhou, H., Meng, A., Long, Y., Li, Q. & Zhang, Y. (2014). Classification and comparison of municipal solid waste based on thermochemical characteristics. *Journal of Air and Waste Management Association*, 64(5), 597-616.
- Zhu, D., Wan, C. & Li, Y. (2011). Anaerobic Co-digestion of Food Wastes and Dairy Manure for Enhanced Methane Production. *Biological Engineering*, 4(4), 195-206.
- Ziemiński, K & Frąc, M. (2012). Methane fermentation process as anaerobic digestion of biomass: Transformations, stages and microorganisms. *African Journal of Biotechnology*, 11(18), 4127-4139.

Chapter 5

CURRENT DEVELOPMENTS IN THERMOCHEMICAL CONVERSION OF BIOMASS TO FUELS AND CHEMICALS

Chan Seung Park and Arun S. K. Raju†*

College of Engineering - Center for Environmental Research and Technology,
University of California, Riverside, CA, US

ABSTRACT

Biomass is the largest concentrated carbon source available for producing renewable energy. Thermochemical conversion of biomass has been used for centuries in various settings. Biomass typically has a higher oxygen and volatile matter content than other solid carbon feedstocks, resulting in increased reactivity during conversion by thermochemical pathways. Moisture content of the biomass feedstock exerts significant influence on the conversion process and is an important criteria used to classify various thermochemical conversion technologies. This chapter discusses the current status and future outlook of thermochemical biomass conversion processes.

Keywords: biomass, gasification, pyrolysis, hydrothermal treatment, steam hydrogasification, combustion

INTRODUCTION

Biomass can be defined as plant materials and animal waste, although broader definitions that include other forms of carbonaceous waste are used in the renewable energy context. Earth's primary source of biomass is the plant matter that grows through photosynthesis. The carbon stored in biomass is from the carbon dioxide consumed during photosynthesis and is ultimately converted back to carbon dioxide during any energy generation application. As is

* Corresponding author: cspark@cert.ucr.edu.

† Corresponding author: arun@enr.ucr.edu.

well known, biomass based processes are often carbon neutral, i.e., do not add additional carbon dioxide to the atmosphere, or have a very low carbon footprint. For these reasons, biomass is the largest and most widespread carbon source for producing renewable energy and is relatively free of the fluctuation problems inherent to wind and solar energy. A comprehensive inventory of biomass resources in the United States potentially available for energy production is available in the ‘billion-ton study’ by the U.S. Department of Energy (Perlack et al., 2005).

The oldest energy conversion process used by humans is biomass combustion in open air to produce heat. Biomass burning is still a dominant process in many parts of the world and thermochemical conversion of biomass to energy has a long scientific history. Since then, various thermochemical processes for biomass conversion have been developed to overcome the primary limitation of combustion: it only produces thermal energy along with the flue gases. Thermochemical biomass conversion to gaseous and liquid fuels has been studied and practiced for centuries. Production of chemicals and other non-fuel, high value products from biomass is another important application of thermochemical processes. The first such example is charcoal production from wood, practiced as early as around 4,000 B.C.

Compared to coal, which is the most widely used conventional solid fuel for energy production, the oxygen and volatile matter content of biomass is typically higher whereas the ash content is lower (Drift, 2015). This high oxygen content makes biomass a good fuel although oxygen itself does not contribute towards the energy value of the fuel. The higher oxygen content results in reduced air (oxygen) requirement during the combustion reaction. Table 1 summarizes the Lower Heating Value (LHV) of different fuels. Coal has a higher LHV than biomass per unit mass of the fuel. However, once the volume of air required for complete combustion is taken into account (LHV per mass per air mix), biomass’ value is higher than that of coal, and is even comparable to methane.

Nearly 80% of the carbon in the biomass is typically considered ‘organic’, i.e., bounded to hydrogen or oxygen. Organic carbon is highly reactive compared to elementary carbon, resulting in improved conversion and thus makes biomass an attractive feedstock for thermochemical production of fuels and chemicals, especially from the conversion perspective. Table 2 summarizes the typical oxygen and volatile content of coal and biomass. Conversion of the volatile portion of the biomass feedstock into gaseous species starts around 225 to 300°C and is mostly complete around 500 to 600°C (Gaur & Reed, 1998). While elemental, non-volatile carbon decomposes at temperatures above 800°C, much higher temperatures (>1200°C) are desirable to avoid potential problems associated with ash softening (Higman & Burgt, 2011). Thus, thermochemical conversion of biomass can be performed at much lower temperatures than is needed for coal, with a higher conversion efficiency.

Table 1. Comparison of LHV values of methane, coal, biomass and hydrogen

LHV	Methane	Bituminous Coal	Biomass	Hydrogen
MJ/kg fuel (GREET, 2010)	47	27	18	120
MJ/kg fuel/air mix	2.62	2.44	2.60	3.36

Table 2. Oxygen and volatiles content of coal and biomass

Components	Bituminous Coal	Biomass
Oxygen (wt. %, daf*)	14	43
Volatiles (wt. %, daf)	42	82

*daf: dry ash free.

From the thermodynamic point of view, at the typical biomass conversion temperature of 800°C, the product gas typically has higher concentrations of more valuable C₂₊ species. Table 3 shows product gas composition of a biomass gasifier operated by the Milena project (Milena indirect gasifier, <http://www.milenatechnology.com>), a well-known biomass gasification demonstration project in Europe. The typical coal gasifier is operated at higher temperatures (1400°C) and the product gas composition is closer to thermodynamic equilibrium values.

Table 3. Comparison of product gas composition under equilibrium conditions with those from a biomass gasifier

Mole Fraction, %	H ₂	CO	CO ₂	CH ₄	C ₂₊
Equilibrium value	51	45	3	1	0
Measured (Milena FB gasifier)	25	33	18	15	6

The composition also shows that the product gas has a lower syngas ratio (syngas or synthesis gas is a mixture of hydrogen and carbon monoxide and syngas ratio is the molar ratio of H₂ to CO), which typically provides more flexibility during use in downstream processes that require specific syngas ratios. Syngas ratio can be increased using the well-known, commercially mature, water-gas shift process. Syngas ratio reduction is achieved through techniques such as membrane separation, and presents a number of technical challenges (Peer, Mahdeyarfar, & Mohammadi, 2009). Higher CH₄ content is also beneficial since the product gas is often used as a fuel in combustion engines or boilers. C₂₊, i.e., gaseous carbon species with a higher carbon number, can potentially be used as a feedstock in chemical production. Such high value co-products can provide an additional revenue stream, improving the overall economics of the conversion plant.

In conclusion, biomass is the only concentrated renewable carbon source that can be converted into fuels and chemicals with a zero or very low carbon footprint. Unlike biological processes that only convert part of the biomass, thermochemical processes can generally convert all the carbon in the feedstock. Biomass is a reactive, desirable feedstock for thermochemical processes due to the higher oxygen content compared to coal. Thermochemical conversion of biomass offers significant versatility since the product gas can be converted into fungible liquid fuels, thereby offering a pathway to reduce the carbon intensity of all major energy use sectors, including transportation. The product gas from most thermochemical processes can also be converted into high value chemicals such as ethylene, BTX (Benzene, Toluene, and Xylene).

Some thermochemical processes such as fast pyrolysis and hydrothermal liquefaction directly produce a liquid product. Thermochemical processes can also handle intermediate products and waste biomass from biological conversion processes (Öhrman et al., 2013).

High value chemicals production from biomass in a 'bio-refinery' setting with energy as a major co-product may be the path to economic viability in the near future.

This chapter presents an overview of the different thermochemical processes that convert biomass into a high energy content gaseous or liquid product and/or additional thermal energy. A discussion of the unique aspects of different technologies from different end use perspectives is also provided.

CLASSIFICATION OF THERMOCHEMICAL BIOMASS CONVERSION PROCESSES

Biomass consists of organic and inorganic matter and often significant amounts of moisture. Organic matter in biomass contributes to its calorific value. Organic matter can be further classified into cellulose, hemicellulose, and lignin. The inorganic matter is conventionally referred to as ash. Compared to conventional fuels, the oxygen content of biomass is typically very high, approximately ranging from 20~50% by weight. The moisture content plays a very important role in selecting the appropriate thermochemical conversion process. Heating value of biomass is heavily dependent on the moisture content. The LHV value is negative for biomass with a high moisture content (80%), since the heat released during the combustion process is not sufficient to evaporate all the water (Swaaij & Kersten, 2015). Therefore, biomass is usually dried under sunlight or through other methods, e.g., using recycled thermal energy as part of feed preparation. Solar and air drying in the production field is the preferred method of drying, primarily due to the lower cost. However, there are several conversion routes that use wet biomass feedstocks without the need for drying. Whether a conversion process uses wet or dry biomass as the feedstock is an important criterion for the classification of biomass conversion processes. A technology is categorized as a wet biomass process based on whether the moisture in the feedstock plays an important role in the process, either as a major reactant, or as physical media to maintain the reaction environment. In other words, wet biomass processes do not benefit from drying the feedstock, and often require the feedstock to have a certain quantity of moisture. Table 4 lists the wet and dry biomass feedstock processes, and these processes are discussed in detail in the rest of the chapter.

Recently, the bio-refinery concept has emerged as an important option. A bio-refinery integrates several conversion and resource recovery processes with the aim of maximizing process efficiency, minimizing waste and improving profits (Patel, Zhang, & Kumar, 2016). An integrated bio-refinery may use additional feedstocks besides biomass and will produce multiple products including fuels, chemicals and thermal or electrical energy. The bio-refinery concept is still evolving, and has the potential to be an important biomass utilization option in the future that incorporates a wide range of options including biological and thermochemical processes to overcome the limitations of specific technologies.

Table 4. Classification of biomass conversion processes

Feedstock	Technology	Features
Wet biomass	Biological*	Anaerobic digestion, or alcohol production from sugars by biomass hydrolysis and fermentation
	Hydrothermal conversion	High pressure conversion to a hydrophobic oil. Often involves further catalytic conversion to methane, liquid fuels or chemicals
	Supercritical gasification	Conversion occurs under supercritical conditions
	Steam hydrogasification	Uses hydrogen and steam as the gasifying agents
Dry biomass	Oil extraction from seeds*	Trans-esterification or hydrogenation of vegetable oil from oil seeds to produce bio-diesel
	Direct combustion	Generate heat or power through the direct combustion of biomass
	Slow pyrolysis	Heating up the biomass in the absence of air (or oxygen) with slow heating rates to produce biochar and gaseous products
	Fast pyrolysis	Extremely fast pyrolysis of biomass with very high heating rates resulting in crude oil like bio-oil and gaseous products
	Gasification	Biomass is converted into syngas using air or oxygen or hydrogen as the gasifying agent

*These processes are outside the scope of this chapter and are not covered.

BIOMASS CONVERSION PROCESSES

Wet Thermochemical Processes

Hydrothermal Conversion Process

Hydrothermal conversion has been studied for more than a hundred years. Friedrich Bergius, who would later receive the 1931 Nobel Prize in Chemistry along with Carl Bosch, developed the Bergius process that produces liquid fuel through hydrogenation of crude oil derived from hydrothermal treatment of coal. The technology was also applied to peat and plant material (Bergius, 1912). Hydrothermal conversion converts biomass into 'bio-crude' through thermal depolymerization under high pressures and moderate temperatures and has since then been studied by several research groups. A comprehensive review of the hydrothermal conversion process of the biomass is provided by (Peterson et al., 2008).

Hydrothermal processes can convert all types of biomass, including wet organic biomass, and typically involves the use of a catalyst to improve conversion efficiency. The product bio-crude can be further processed into high quality diesel or kerosene. The fast pyrolysis process, discussed later, is a dry conversion process that produces a bio-crude (or bio-oil) from dry biomass feedstock. Hydrothermal conversion process has lower efficiencies caused by the significant energy requirement of water evaporation.

Hydrothermal conversion processes can be further divided into supercritical and subcritical hydrothermal conversion processes. A supercritical hydrothermal conversion process developed by Aalborg University and commercialized by Steeper Energy under the name of “Hydrofaction” converts organic wastes into a raw bio-crude under supercritical conditions in the presence of K_2CO_3 catalyst (Hoffmann, 2013). Another process, referred to as the “Catliq” process uses Zirconia catalyst under supercritical conditions to produce a bio-crude with less than 6% oxygen content (Toor et al., 2012).

Shell research group has demonstrated a subcritical process named Hydro Thermal Upgrading (HTU) that converts the biomass into bio-crude with and without a catalyst (Berends, Zeevalkink, & Naber, 2004). Research has shown that in the presence of a catalyst with adequate activity, conversion could be accomplished at conditions that are less severe than supercritical. A number of catalysts including ones based on Ru, Carbon, and Ni have been proposed with the ultimate goal of developing an optimal hydrothermal conversion process under subcritical conditions (Elliott, 2011).

Supercritical Gasification

The supercritical condition for water is the combination of $T > 374^\circ\text{C}$ and $P > 218$ atm. Under these conditions, distinct liquid and vapor phases do not exist and the water exists as a single phase fluid (Peterson et al., 2008). The general reason to use supercritical conditions for wet feedstocks is to minimize the energy loss associated with water evaporation. Transition of liquid water to the gas phase (steam) requires a large amount of heat, so called “the heat of vaporization”, which can be recovered in theory, but needs very efficient heat exchanger design. By operating the conversion process under supercritical conditions, uniform temperature profile along the reactor can be expected without the formation of multiple phases of water (liquid water, steam and/or superheated steam), which in turn results in efficient heat transfer between the product gas and feed inlet of the gasifier.

Supercritical biomass gasifiers typically operate around 500 to 750°C without a catalyst or at temperatures below 500°C in the presence of a catalyst. The presence of supercritical water leads to rapid hydrolysis of biomass and high solubility of intermediate reaction products including gaseous species. These features make supercritical gasification as excellent tool for the conversion of very wet feedstocks such as aquatic biomass and sewage sludge (a.k.a. biosolids) that normally require considerable drying before they can be gasified economically. Supercritical gasification also produces a high pressure product gas, thereby eliminating the need for the product gas compression required by most down-stream processes. A detailed discussion of process efficiency and other aspects of supercritical gasification is available in the article by (Dinjus & Kruse, 2004). For example, the gasification efficiency of a biomass feedstock with 80% water content using conventional steam reforming reaction is only 10%, while that of supercritical gasification can be as high as 70%.

However, there are several technological issues that must be overcome in order for supercritical processes to be commercially viable:

- Supercritical gasification processes need large heat input. Design of highly effective heat transfer methods is critical to achieve desired energy conversion efficiency.

- The feeding of wet biomass is another barrier, although slurry pumps have been used to feed into high pressure vessels. However, achieving reliable feeding into a supercritical gasifier operating under very high pressures is still a significant challenge.
- Other issues such as fouling, plugging of the feedstock, and corrosion are well reviewed by (Marrone & Hong, 2008).
- Higher capital costs due the high operating pressure also has a negative impact on economic performance.

For these reasons, supercritical gasification processes are still in the development stage (Antal, Allen, Schulman, Xu, & Divilio, 2000). University of Twente operates a pilot plant and is involved in active research and development (Knezevic, 2009). The VERENA group operates a somewhat larger pilot plant with 100 kg per hour throughput in Karlsruhe, Germany (Fritz, 2009).

Steam Hydrogasification

Steam hydrogasification uses steam and hydrogen as the gasifying agents and is especially suited for the conversion of wet feedstocks since it utilizes the water from the feedstock as a major reactant (Hydrogasification, 2010). Hydrogasification, using only hydrogen as the gasifying agent, is a well-known conversion technology but is not considered commercially viable due to several issues, including low conversion efficiencies and requirement of an external hydrogen source (Mozafarriani & Zwart, 2000). Research has shown that hydrogasification in the presence of steam significantly enhances the rate of methane formation under specific process conditions, thereby improving the overall process efficiency (Jeon et al., 2007; Raju et al. 2009). This process, referred to as “steam hydrogasification”, produces a product gas with a high methane content. The product gas also contains considerable amount of unreacted steam along with CO, CO₂, H₂, and some higher molecule hydrocarbons. The product gas can then be converted into various fuels or chemical products.

An example block flow diagram for Renewable Natural Gas (RNG) production is shown in Figure 1. The feedstock is turned into a slurry through a hydrothermal pretreatment process (HTP) and is transported into the steam hydrogasification reactor (SHR) using a slurry pump. A portion of the necessary steam enters the reactor as water that is part of the slurry along with additional superheated steam and recycled hydrogen.

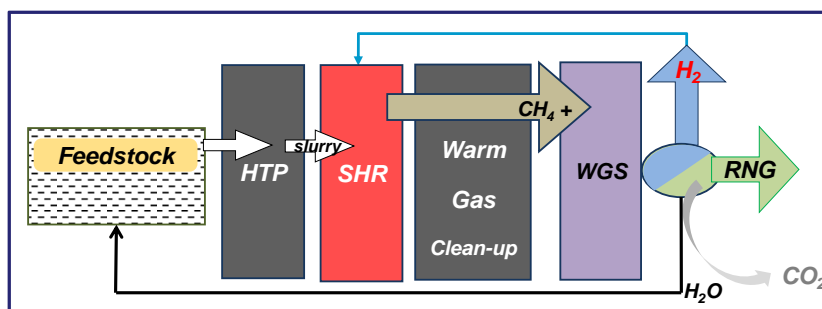


Figure 1. Block flow diagram of RNG production by steam hydrogasification process.

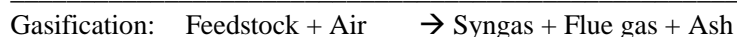
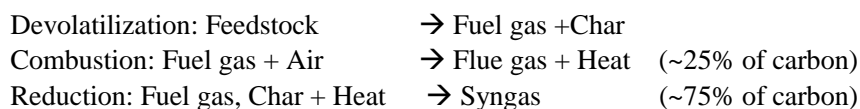
The methane-rich gasifier product gas is then subjected to warm gas cleanup in order to remove contaminants such as sulfur and other species. Following this, the excess steam and CO is converted into hydrogen in a water gas shift reactor (WGS). This is an important aspect of the process: Even though the steam hydrogasification process needs hydrogen, it does not require an external source of hydrogen. The hydrogen is separated and fed back into the gasifier, making the process self-sustained in terms of the hydrogen supply. The process is currently undergoing demonstration (Park & Norbeck, 2011).

Dry Thermochemical Processes

Gasification

Gasification, which implies incomplete combustion (also commonly referred to as partial oxidation) of the carbonaceous feedstock, is one of the most attractive options to convert biomass into high value products including liquid and gaseous fuels, chemicals and electricity. Gasification is the most popular among the thermochemical conversion processes with the exception of direct combustion. Gasification processes have several advantages and disadvantages over other conversion technologies. The main advantages are that the gasification feedstock can be any type of biomass including agricultural residues, forestry residues, byproducts from chemical processes, and even organic municipal wastes. Moreover, gasification typically converts all the carbon in the feedstock, making it more attractive than enzymatic ethanol production or anaerobic digestion where only portions of the biomass material are converted to fuel. The second advantage is that the product gas can be converted into a variety of fuels (H_2 , RNG, synthetic diesel and gasoline, etc.) and chemicals (methanol, acetic acid). Thus gasification is most suitable to produce chemicals that can be alternatives to petroleum based products.

Gasification processes are primarily designed to produce synthesis gas (syngas, a mixture of hydrogen and carbon monoxide) by converting the feedstock under reducing (oxygen deficient) conditions in the presence of a limited amount of gasifying agent such as air or oxygen (Higman & Burgt, 2011). Gasification consists of 3 major steps. The first step is devolatilization of the dried feedstock to produce the fuel gas for the second step, which is combustion. The combustion step produces the necessary heat and reducing environment required for the final step. The final step (so-called reduction step, char gasification step or syngas production step), is the slowest reaction phase in gasification, and often governs the overall gasification reaction rate. These 3 steps can be shown as:



Approximately 25% of carbon in the feedstock is consumed in the combustion step to provide the heat and reducing environment for the reduction step. A detailed discussion of

gasification, including minor steps and considerations is available elsewhere (Higman & Burgt, 2011).

The dual fluidized bed reactor configuration is a well-known option for the gasification of biomass feedstock. This configuration uses two separate reactors, one for the combustion and the other for the reduction reaction.

Benefits of the dual bed configuration for biomass gasification are (Basu, 2010):

- Provides improved process efficiencies and avoids the challenges related to ash melting by operating at lower gasification temperatures (normally greater than 800°C but below the ash softening point).
- Other fuel sources can be used for the combustion step to overcome the low heating value of the biomass feedstock. These fuels include char bi-product from the reduction reactor or other designated fuels such as methane.
- Air is only used in the combustion reactor and does not enter the reduction reactor, thereby preventing nitrogen dilution of syngas, a major problem in air blown gasifiers (Pröll, Rauch, Aichernig, & Hofbauer, 2005).

The heat required for the reduction reaction is supplied through the bed material (typically sand) from the combustion reactor. The bed material is continuously circulated between the two reactors while the ash is removed from the bed material using cyclones and the gases from the two reactors are not allowed to mix. The Milena project gasifier uses the two reactor configuration (Van der Meijden, Veringa, Van der Drift, & Vreugdenhil, 2008).

A major challenge of biomass gasification is to overcome the higher specific capital and operating costs. This is due to the much smaller plant sizes (normally less than five hundred tons per day of feedstock throughput) compared to coal gasification plants (tens of thousands of tons per day). The plant size is determined by biomass availability and related logistic issues and transportation costs inherent to any distributed resource. Other challenges include the presence of undesirable species such as alkali compounds in biomass ash. Alkali materials such as sodium and potassium cause slagging and fouling problems (Huber, Iborra, & Corma, 2006). Most biomass gasifiers operate below the ash softening temperature to avoid ash melting. The lower temperatures also lead to lower capital cost requirement, resulting in favorable process economics. However, lower temperatures often result in the formation of undesired tar, which leads to severe operational problems. A number of catalysts and process configurations have been developed to address this issue, but tar problems still persist (Knoef, 2012). Addition of a catalytic tar cracker to the outlet of the gasifier to decompose the tars into smaller molecules has been considered (Bridgwater & Boocock, 1997). Washing out the tars while the product gas is cooling down has also been proposed, but this approach requires rigorous treatment of the washing water. Tar formation is still a major challenge and is regarded as the “Achilles heel” of biomass gasification processes. These issues are not to be underestimated and careful attention is required in the design and operation of biomass gasifiers.

Slow/Fast Pyrolysis

Pyrolysis is the thermal decomposition of the feedstock in the absence of oxygen. The products of biomass pyrolysis are char, bio-oil (also referred to as bio-crude) and gases

including methane, hydrogen, carbon monoxide, and carbon dioxide. Pyrolysis can be further classified into slow and fast pyrolysis based on the residence time of the solid biomass in the reactor. Fast pyrolysis, also known as flash pyrolysis, is normally conducted under medium to high temperatures (usually 450°C to 550°C) at very high heating rates and a short residence time (e.g., milliseconds to a few seconds).

The objective of the process is to maximize the liquid yield and minimize the production of char and gases. This requires fast heating of the biomass and produces bio-oil (~60% by weight) and other products including gas and char (Scott & Piskorz, 1982). On the other hand, slow pyrolysis takes several hours to complete with bio-char being the main product. Fast pyrolysis has attracted considerable attention in recent years. Fast pyrolysis efficiency, in addition to the residence time and operating temperature, is strongly dependent on the particle size of the feedstock as rapid and efficient heat transfer through the particle is critical. Most fast pyrolysis processes use a maximum particle size of 2 mm. Pyrolysis processes can be built in relatively small scales and are well suited for lignocellulosic feedstocks. Efficient thermal energy input to the reactor is critical since the pyrolysis process is endothermic and heat transfer rates play a major role in the conversion process. High moisture content biomass must be dried prior to the conversion process. Besides oil and gas, bio-char is an important pyrolysis product. Bio-char is well-known as a soil amendment as it is highly absorbent and increases the soil's ability to retain water and nutrients.

Fast pyrolysis is an emerging technology and there are several key issues that need to be addressed. The most critical problems are associated with the quality of the 'bio-oil', dictated by the physical and the chemical properties. Some of these problems are discussed below. Ideally, bio-oil should be interchangeable with petroleum crude oil so that the transportation and refining infrastructure can be used in existing form or with minor modifications. Based on this reasoning, the properties of bio-oil are often compared to that of petroleum crude oil. However, bio-oil has serious physical and chemical property issues and it is difficult to use it in existing petroleum refineries (Toor et al., 2012; Berends et al., 2004; Elliott, 2011; Peterson et al., 2008; Dinjus & Kruse, 2004; Marrone & Hong, 2008; Antal et al., 2000).

Bio-oil is known to be extremely corrosive and this causes serious problems related to handling and transportation. The Total Acid Number (TAN) required for crude oil refineries is normally less than 2. Typical bio-oil TAN values range from 50 to as high as 200 (Knezevic, 2009). Bio-oil typically contains 15-30% water. Besides water, components present in high concentrations are hydroxyacetaldehyde and acetic and formic acids. These oxygenated compounds along with various other species such as phenolic compounds contribute towards the acidity of the bio-oil. Typical pH of the bio-oil is in the range of 2.0 to 3.0 (Berends et al., 2004). The viscosity of bio-oils increases during storage and the physical properties undergo considerable changes (Dinjus & Kruse, 2004). The changes in the physical properties are attributed to the self-reaction of various compounds in the bio-oil including polymerization reactions (Marrone & Hong, 2008; Fritz, 2009). These reactions, occurring during storage, increase the average molecular weight of the bio-oil and also lead to other storage related issues such as phase separation.

The resulting corrosive nature presents serious obstacles to any efforts aimed at the transportation and centralized refining or upgrading of the bio-oils. Also, the unstable nature of bio-oils often necessitates minimizing storage times and local upgrading, instead of transportation to a centralized facility. Such local upgrading is done by means of hydrodeoxygenation using hydrogen, often in the presence of catalysts. This normally adds capital

and operating cost to the bio-oil production process. Gasification and co-gasification of bio-crude to syngas have been tried, with reasonable success (Higman & Burt, 2011).

Most of the fast pyrolysis projects are still in laboratory scale with the exception of a few, including KIOR project (KiOR, Inc. - Home, n.d.) and BTG-BV in the Netherlands, which was originally developed by University of Twente (Wagenaar, Prins, & van Swaaij, 1994). These processes are regarded as pre-commercial, or demonstration stage technologies.

Direct Combustion

Direct combustion of biomass is the oldest energy production process in human history. It is still by far the most widely practiced biomass conversion process. A wide range of technology options ranging from the simple fire stove to the advanced boiler with fluidized bed furnace using pulverized fuel are available. Precise control of mixing between the biomass fuel and oxygen source (generally, air) is a critical aspect of advanced combustion systems in order to achieve improved thermal efficiency and minimized criteria pollutant emissions including particulate matter (PM), nitrogen oxides (NO_x), carbon monoxide (CO) and hydrocarbons.

For industrial and centralized domestic heat and power generation, several designs including stoker burners, grate boilers and dense fluid-bed combustor are used ranging from a few kilowatts to 10 MW of output. Combustion efficiency has improved remarkably in recent decades and has reached over 90% from around 55% in 1980 (FBC). Recently, development of combustion systems with pressurized fluidized beds have enabled direct electricity production without requiring steam generation, since the process utilizes the fluidized bed as combustion chamber of the gas turbine (Huang et al., 2006).

For very large scale direct combustion (larger than 300 MW), co-firing biomass with pulverized coal has been recommended. Pulverized coal combustion technology is well established and co-firing is an attractive option that can reduce the net greenhouse gas (GHG) emissions from coal. However, challenges associated with co-firing with biomass such as changes in ash properties, fouling of heat exchanger, etc. still need to be addressed (Loo & Koppejan, 2015). Biomass torrefaction is promising process that improves the usefulness of biomass as a fuel by heating the biomass in the absence of air under mild temperatures (230°C to 300°C), similar to slow pyrolysis. The resulting biomass fuel is a desirable feedstock for entrained-flow reactors or in pulverized coal fired boilers employing biomass co-firing (Bach & Skreiberg, 2016).

Oxy-combustion is an emerging technology that uses pure oxygen in the combustor. The advantage is that after the cooling of flue gas, nearly pure carbon dioxide is produced without any nitrogen or nitrogen oxides. However, the use of pure oxygen (or oxygen enriched air) results in higher capital and operating costs. This needs to be balanced against the cost/energy savings related to carbon dioxide capture. This technology is still in the research and demonstration stage. As more cost effective processes for oxygen production, including membrane separation, are developed, oxy-combustion will presumably become a more attractive option for both biomass and fossil feedstocks.

CONCLUSION

Renewable carbon based energy sources are critical to address future energy needs, especially in the transportation sector. Biomass is the largest and most widespread carbon source for producing renewable energy, fuels and chemicals and can be a constant, reliable resource compare to other renewable sources such as solar or wind energy. A wide range of biomass conversion processes are available and are under development. Among these, thermochemical processes offer several advantages, including product versatility, and high conversion rates and efficiencies, although challenges to commercialization still remain.

Wet thermochemical processes including hydrothermal conversion, supercritical gasification and steam hydrogasification are still under development, but have many attractive aspects for use in decentralized, low cost applications, especially for high moisture content biomass. Dry thermochemical conversion processes including direct combustion, gasification and pyrolysis have several specific technology options that are mature. However, economic viability issues and technical challenges related to tar formation and alkaline ash presence still need to be addressed.

Emerging approaches such as the bio-refinery concept that integrate different conversion technologies and generate multiple products are expected to play a key role in addressing the technical and economic barriers of thermochemical and other conversion processes.

REFERENCES

- Antal, M. J., Allen, S. G., Schulman, D., Xu, X., & Divilio, R. J. (2000). Biomass Gasification in Supercritical Water. *Industrial & Engineering Chemistry Research*, 39(11), 4040-4053.
- Bach, Q.V., & Skreiberg, Ø. (2016). Upgrading biomass fuels via wet torrefaction: A review and comparison with dry torrefaction. *Renewable and Sustainable Energy Reviews*, 54, 665–677.
- Basu, P. (2010). Biomass Gasification and Pyrolysis: Practical Design and Theory, Elsevier Science. ISBN 978-0-12-374988-8, page 167.
- Berends R. H., Zeevalkink J. A., Naber J. E. (2004), Results of the first long duration run of the HTU pilot plant at TNO-MEP, Proceedings of the 2nd World Biomass Conference: Biomass for Energy, Industry and Climate Protection, Rome 535.
- Bergius, F. K. R. (1912). Die Anwendung hoher Drucke bei chemischen Vorgängen und eine Nachbildung des Entstehungsprozesses der Steinkohle, Verlag Wilhelm Knapp, Halle, Germany. (n.d.). Retrieved December 4, 2015, from http://www.nobelprize.org/nobel_prizes/chemistry/laureates/1931/bergius-lecture.pdf.
- Bridgwater, A. V., & Boocock, D. G. B. (Eds.). (1997). Cleaning of hot producer gas in a catalytic adiabatic packed bed reactor with periodic flow reversal, Development in Thermochemical Biomass Conversion, Dordrecht: Springer Netherlands 907-920.
- Dinjus, E., & Kruse, A. (2004). Hot compressed water—a suitable and sustainable solvent and reaction medium? *Journal of Physics: Condensed Matter*, 16(14), S1161–S1169.
- Drift, A. (2015). Role of Gasification in a Bio-Based Future, presented at 24th European Biomass Conference and Exhibition, Vienna, Austria, June 1-4, ECN-L--15-063 EN.

- Elliott, D. C. (2011). Hydrothermal processing in Thermochemical processing of Biomass: Conversion into Fuels, Chemicals and Power, 200-231, Ed. Brown, R. C., John Wiley and Sons, Chichester, UK.
- FBC, Fluidised Bed Combustion. (n.d.). Retrieved July 16, 2015, from <http://www.photomemorabilia.co.uk/FBC.html>.
- Fritz, R. (2009). KIT - IKFT - VERENA Pilot Plant. Roland Fritz. Retrieved July 16, 2015, from <http://www.ikft.kit.edu/english/138.php>.
- Gaur, S., Reed, T. B. (1998). Thermal Data for Natural and Synthetic Fuels, Chapter 6, Marcel Dekker, ISBN 0-8247-0070-8, page 102-108.
- GREET, The Greenhouse gases, Regulated Emissions, and Energy use in Transportation Model, GREET 1.8d.1, developed by Argonne National Laboratory, Argonne, IL, released August 26, 2010.
- Higman, C., van der Burgt, M. (2011). Gasification, Elsevier Science. ISBN 978-0-7560-8528-3, page 163-173.
- Higman, C., van der Burgt, M. (2011). Gasification, Elsevier Science. ISBN 978-0-7560-8528-3, page 33.
- Hoffmann, J. (2013). Upgrading of bio-crude from hydrothermal Liquefaction, presented at TCBIomass 2013. Or see <http://www.steeperenergy.com>.
- Huang, Y., McIlveen-Wright, D., Rezvani, S., Wang, Y. D., Hewitt, N., & Williams, B. C. (2006). Biomass co-firing in a pressurized fluidized bed combustion (PFBC) combined cycle power plant: A techno-environmental assessment based on computational simulations. *Fuel Processing Technology*, 87(10), 927–934.
- Huber, G. W., Iborra, S., & Corma, A. (2006). Synthesis of transportation fuels from biomass: chemistry, catalysts, and engineering. *Chemical Reviews*, 106(9), 4044–98.
- Hydrogasification/FT production with electricity & electricity only cases CERT-1 thru CERT-6 conceptual study. 2010, DOE-NETL. Or <http://www.netl.doe.gov/research/coal/energy-systems/gasification/gasifipedia/hydro>.
- Jeon, S. K., Park, C. S., Hackett, C. E., & Norbeck, J. M. (2007). Characteristics of steam hydrogasification of wood using a micro-batch reactor. *Fuel*, 86(17-18), 2817–2823.
- KiOR, Inc. - Home. (n.d.). Retrieved July 16, 2015, from <http://www.kior.com/>
- Knezevic, D. (2009). Hydrothermal conversion of Biomass. (n.d.). University of Twente, Retrieved December 5, 2015, from http://doc.utwente.nl/67359/1/thesis_D_Knezevic.pdf.
- Knoef, H. A. M., Ed. (2012). Handbook of Biomass Gasification, 2nd Edition, BTG Biomass Technology Group BV, the Netherlands.
- Loo, S., Koppejan, J. (2015). Biomass Power for the World, Ed. Pan Stanford Publishing, ISBN 978-981-4669-24-5, page 248-264.
- Marrone, P. A., & Hong, G. T. (2008). Corrosion Control Methods In Supercritical Water Oxidation And Gasification Processes. CORROSION 2008. NACE International, New Orleans. Retrieved from <https://www.onepetro.org/conference-paper/NACE-08422>.
- Van der Meijden, C. M., Veringa, H. J., Van der Drift, A., & Vreugdenhil, B. J. (2008). The 800 kWth allothermal biomass gasifier MILENA, presented at 16th European Biomass Conference and Exhibition, Valencia, Spain Retrieved from <ftp://130.112.2.101/pub/www/library/report/2008/m08054.pdf>.
- Milena indirect gasifier: www.milenatechnology.com.

- Mozafarriani, M. Zwart, R. (2000). Production of Substitute Natural Gas by Biomass Hydrogasification, ECN-RX-00-38, Netherlands Energy Research Foundation, (ECN), Petten.
- Öhrman, O. G. W., Weiland, F., Pettersson, E., Johansson, A.-C., Hedman, H., & Pedersen, M. (2013). Pressurized oxygen blown entrained flow gasification of a biorefinery lignin residue. *Fuel Processing Technology*, *115*, 130–138.
- Park, C., Norbeck, J. M. (2011). Development of Steam Hydrogasification Process Demonstration Unit-5 Lb/Hr PDU Design Report. (n.d.). CEC-500-2013-092, California Energy Commission, Sacramento, CA. Retrieved December 5, 2015, from <http://www.energy.ca.gov/2013publications/CEC-500-2013-092/CEC-500-2013-092.pdf>.
- Patel, M., Zhang, X., & Kumar, A. (2016). Techno-economic and life cycle assessment on lignocellulosic biomass thermochemical conversion technologies: A review. *Renewable and Sustainable Energy Reviews*, *53*, 1486–1499.
- Peer, M., Mahdeyarfar, M., & Mohammadi, T. (2009). Investigation of syngas ratio adjustment using a polyimide membrane. *Chemical Engineering and Processing: Process Intensification*, *48*(3), 755–761.
- Perlack, R. D., Wright, L. L., Turhollow, A. F., Graham, R. L., Stokes, B. J., & Erbach, D. C. (2005). Biomass as Feedstock for a Bioenergy and Bioproducts Industry: The Technical Feasibility of a Billion-Ton Annual Supply. Oak Ridge National Laboratory, Oak Ridge, Tennessee, DOE/GO-102995-2135.
- Peterson, A. A., Vogel, F., Lachance, R. P., Fröling, M., Antal, Jr., M. J., & Tester, J. W. (2008). Thermochemical biofuel production in hydrothermal media: A review of sub- and supercritical water technologies. *Energy & Environmental Science*, *1*(1), 32–65.
- Pröll, T., Rauch, R., Aichernig, C., & Hofbauer, H. (2005). Fluidized Bed Steam Gasification of Solid Biomass: Analysis and Optimization of Plant Operation Using Process Simulation. In 18th International Conference on Fluidized Bed Combustion (Vol. 2005, pp. 763–770). ASME. <http://doi.org/10.1115/FBC2005-78129>.
- Raju, A. S. K., Park, C. S., & Norbeck, J. M. (2009). Synthesis gas production using steam hydrogasification and steam reforming. *Fuel Processing Technology*, *90*(2), 330–336.
- Scott, D., & Piskorz, J. (1982). The flash pyrolysis of Aspen-poplar wood. *The Canadian Journal of Chemical Engineering*, *60*(5), 666–674.
- Swaij, W., Kersten S. (2015). Biomass Power for the World, Ed. Pan Stanford Publishing, ISBN 978-981-4669-24-5, page 33
- Toor, S. S., Rosendahl, L., Nielsen, M. P., Glasius, M., Rudolf, A., & Iversen, S. B. (2012). Continuous production of bio-oil by catalytic liquefaction from wet distiller's grain with solubles (WDGS) from bio-ethanol production. *Biomass and Bioenergy*, *36*, 327–332.
- Wagenaar, B. M., Prins, W., & van Swaij, W. P. M. (1994). Pyrolysis of biomass in the rotating cone reactor: modelling and experimental justification. *Chemical Engineering Science*, *49*(24), 5109–5126.

Chapter 6

HYDROTHERMAL LIQUEFACTION OF BIOMASS FOR BIOFUEL

*Florin G. Barla and Sandeep Kumar**

Department of Civil and Environmental Engineering,
Old Dominion University, Norfolk, VA, US

ABSTRACT

In recent years, significant research interests have been placed on the conversion of non-food biomass resources such as lignocellulosic biomass (terrestrial) and algae (aquatic) to biofuels. However, high moisture content of fresh biomass or algae is one of the major challenges in developing logistics and downstream processing for an economical design of bio-refineries. Hydrothermal liquefaction (HTL) of biomass has a number of advantages including high throughputs, high energy and separation efficiencies, and feedstock flexibility. The production of liquid fuels from biomass can be achieved by HTL to an intermediate product (bio-oil or biocrude) followed by catalytic upgradation of the bio-oil/biocrude. Generally, HTL is conducted in seconds or minutes of residence time in the temperature range of 250-350°C under subcritical water conditions in a batch/flow-through/ continuous flow reactor. In this chapter, we review the recent developments of HTL of lignocellulosic biomass and microalgae along with the techno-economic analysis (TEA) and life cycle assessments (LCA).

Keywords: lignocellulose, microalgae, biocrude, life cycle assessment, techno-economic analysis

1. INTRODUCTION

Over the last two decades, mostly corn and soy, as well as other food crops have been used for production of first generation biofuels. Since 2006, the US Government has encouraged the development of alternative lignocellulosic biomass crops because of the

* Corresponding author: skumar@odu.edu.

adverse impact first generation biofuels can have on food markets. The biofuels industry has focused on using lignocellulosic biomass mainly from agricultural/forestry waste such as corn stover, straw, wood and other byproducts, as well as dedicated crops like switchgrass, miscanthus, hybrid poplar, and energy tobacco to produce second-generation or advanced biofuels (Adrianov et al., 2010). In addition to these terrestrial crops, aquatic biomass such as microalgae has attracted much attention because it has shown great productivity compared to terrestrial plants. Nevertheless, the main challenge with microalgae is the high water content, with usually only 1 g of dry algal biomass recovered per liter of water (Kumar, 2012).

From a policy perspective, alternative and sustainable energy sources, especially to those that reduce carbon dioxide emissions, are highly recommended for numerous environmental and energy security reasons. Biofuels produced from non-edible feedstock such as lignocellulosic biomass offer some benefits like: being renewable and sustainable, indirectly helping carbon dioxide fixation in the atmosphere, diversification of energy output based on geography, boosting and stimulating the local economy, bringing energy security for countries dependent on imported oil, creating high technology jobs for engineers, fermentation specialists, process engineers, and scientists. At a most basic level, plants and trees are the raw material for biofuels, and because they need carbon dioxide to grow, their conversion into biofuels does not add CO₂ to the atmosphere, but rather just recycles what was already there. It is well known that the critical factors in the selection of a biofuel feedstock for commercial use are productivity, storage logistics, scalability and a continuous supply of biomass (Neveux et al., 2014). After a plant is harvested, it can be converted into biocrude utilizing a thermochemical process such as hydrothermal liquefaction (HTL) process. Biocrude also called bio-oil is a product that is obtained when the biomass (forestry residues, crop residues, waste paper and organic waste) is treated with water at high temperature and pressure. There are several other competing pathways such as fast pyrolysis or gasification for converting the biomass to liquid fuel, chemicals, and/or hydrogen. Among these, the HTL or subcritical water liquefaction process has attracted much attention due its versatility to utilize mixed biomass feedstock sometimes without, or with a slight pretreatment such as mild alkaline pretreatment, at a comparatively low temperature (Jazrawi et al., 2015; Kumar & Gupta, 2009; Li et al., 2015). Biocrude can be upgraded into liquid hydrocarbons (green gasoline or jet fuel) through catalytic upgradation using hydrogen.

With all feedstock, across the three generations of biofuels, a primary economic and environmental challenge is conversion from natural state into sugar, oil and other biocrude products. Each crop must be evaluated for its productivity from an agricultural perspective, taking into account all of the inputs relative to outputs, and for its efficiency from a conversion perspective, taking into account the economic and environmental consequences of conversion to biocrude. The goal is economic efficiency and minimal net carbon impact. Carbon impact is measured in a Life Cycle Analysis (LCA), which calculates the full contribution of carbon to the atmosphere from all inputs (fertilizers, transportation, energy, etc.) and outputs (burned biofuels), as well as the full capture of carbon from plant growth to generate a net carbon impact determination. The LCA is an important step required by the U.S. Environmental Protection Agency (EPA) in recognizing the advance fuel status (EPA-420-F-10-006, 2010).

Over the last few years, with a focus on “green” and economical conversion of biomass to biocrude, some venture companies have invested in efforts to develop new technological flows based on HTL using biomass from dedicated fuel crops such as switchgrass, corn

stover, tobacco, pinewood, and microalgae. For example, Tyton Biosciences, a renewable energy company located in Virginia, USA, has made significant progress in making tobacco into a biofuel crop, and it utilizes HTL to hydrolyze carbohydrates from tobacco because of the low energy consumption and environmentally-benign process. A fresh-cut tobacco biomass can contain 85-90% of water on dry basis and this excess moisture reduces the need of extra water during hydrothermal hydrolysis for sugars recovery. Hydrothermal processes may significantly reduce carbon impact and lower processing costs when paired with appropriately productive feedstock.

Historically, biomass has been used to generate electricity or produce heat through direct combustion (Tumuluru, Boardman, Wright, & Hess, 2012). However, these renewable resources can potentially be used in a more efficient way for producing liquid transportation fuels to partly replace petroleum derived fuels. In this paper, we have divided non-food based biomass into two categories including (i) lignocellulosic biomass (agricultural residues, forest residues/woody biomass, and energy crops and (ii) aquatic biomass (microalgae) and reviewed the HTL process for these feedstocks.

2. HYDROTHERMAL LIQUEFACTION (HTL)

For biomass with high moisture content (in some cases 90%), the use of subcritical water will minimize or eliminate in some cases the need of adding water as a reactant to the reaction medium. Hydrothermal or sub/super-critical water (critical point: 374°C, 22.1 MPa) technology can utilize wet biomass by using the bi-polar versatile solvent properties of water at high temperature for converting biomass to biofuels. In this case the moisture removal it is not required, much energy being saved, this becoming a major advantage of this hydrothermal technology. This method provides an environmental-friendly and relatively inexpensive medium for chemical reactions. In sub- and supercritical water processes, water is kept in liquid phase by applying pressure greater than the vapor pressure of water. Therefore, the incremental heat increase required for phase change of water from liquid to vapor phase (2.26 MJ/kg of water) is not needed. Normally 2.869 MJ/kg of energy is needed to convert water from 25°C to 250°C at 0.1 MPa (steam phase) while about 1 MJ/kg of energy is required to heat water from 25°C to subcritical-water condition at 250°C and 5 MPa, the amount of energy is equivalent to 8-10% of energy content of dry biomass (Kumar, 2012).

The ionization constant of water increases with temperature in the subcritical region and is about three times higher than that of ambient water the dielectric constant of water drops from 80 to 20 (Kumar, Popov, Majeranowski, & Kostenyuk, 2014). Organic compounds present in the biomass are dissolved in water at a low dielectric constant value while a high ionization constant provides acidic conditions for the hydrolysis during subcritical water extraction; these ionic reactions are dominant due to liquid-like properties of the subcritical water. In the supercritical ($\geq 374^\circ\text{C}$) region, density of water drops down to lower value this means that ionic product of water is much lower and ionic reactions are inhibited because of the low dielectric constant of water. The lower density favors free-radical reactions, which may be favorable for gasification. Hence, subcritical water at temperatures between 200-350°C and variable residence time is mainly used for the liquefaction of biomass for biocrude or for the production of green coal/hydrochar.

Liquefaction of biomass in hydrothermal medium proceeds through a series of complex structural and chemical transformations involving (i) solvolysis of biomass resulting in micellar like structure, (ii) depolymerization of cellulose, hemicelluloses, proteins, and lignin, and (iii) chemical and thermal decomposition and re-condensation of intermediate products (Kumar & Gupta, 2009). The products from HTL mainly consist of biocrude, aqueous phase (dissolved organics), light gases, and insoluble residual solids. Biocrude is a complex mixture of ketones, aldehydes, phenols, alkenes, fatty acids, esters, aromatics, and nitrogen containing heterocyclic compounds. Acetic acid among other organic acids is one of the main components of the aqueous-phase.

Biocrude derived from the HTL of biomass can be converted to liquid fuel, hydrogen gas, or chemicals. In HTL studies, typically 15-25 wt% biomass slurry in water is treated at temperatures of 300-350°C, catalysts, and 12-18 MPa pressures for 5-30 min to yield a mixture of liquid, gas (mainly CO₂), and water. The liquid is a mixture with a wide molecular weight distribution and consists of various kinds of molecules. A large proportion of the oxygen is removed as carbon dioxide and the resulting biocrude contains only 10-13% oxygen, as compared to 40% in the dried biomass (Gourdiaan & Peferoen, 1990). In a conceptual process scheme, it was shown that each ton (dry basis) of biomass could produce 300 kg (or 95 gallons) of liquid fuel (Gourdiaan & Peferoen, 1990). The overall schematics of lignocellulosic biomass to liquid fuels via HTL are shown in Figure 1.

The U.S. Department of Energy (DOE) has considered subcritical water/hydrothermal process as a viable technology, which can process wet biomass for biofuels. In fact, Elliott et al., at Pacific Northwest National Laboratory (PNNL), National Advanced Biofuels Consortium (NABC), and National Alliance for Advanced Biofuels and Bioproducts (NAABB) team has been leading the HTL scale up efforts (Elliott et al., 2013; Elliott et al., 2014; Zhu, Biddy, Jones, Elliott, & Schmidt, 2014). Recently, the group published the pilot-scale studies on hydrothermal processing of microalgae and woody biomass in continuous-flow reactors, which successfully demonstrated the technical feasibility, and scalability of the HTL-based processes (Elliott et al., 2013; Elliott et al., 2014; Zhu et al., 2014).

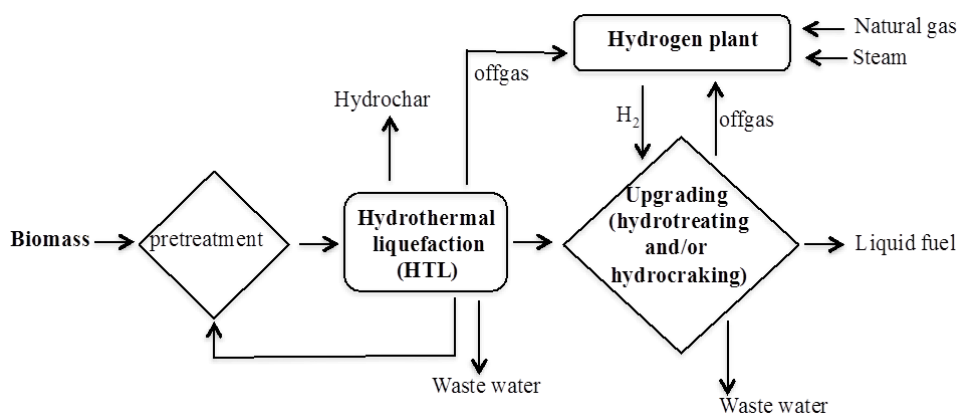


Figure 1. The simplified diagram of biomass to liquid hydrocarbons via HTL.

Use of homogeneous catalyst: The addition of alkali metal salts (e.g., KHCO₃, KOH, Na₂CO₃, K₂CO₃) during HTL reduces coke formation and catalyzes the water-gas shift

reaction (Hao, Gio, , Mao, Zhang, & Chen, 2003). For example, the addition of KHCO_3 leads to an increase in gas formation and a decrease in the amount of carbon monoxide (Sinag, Kruse & Schwarzkopf, 2003). The use of K_2CO_3 in the reaction mixture during depolymerization of cellulose in subcritical water substantially enhanced gas formation (Kumar & Gupta, 2008). Ramsurn and Gupta proposed a novel two-step process in which acidic subcritical water (200°C) followed by alkaline supercritical water (380°C) media used to optimize biocrude yield and minimize hydrochar (solid residue) production for switchgrass (Ramsurn & Gupta, 2012). The yield of biocrude was 40 wt% on mass basis and 67% on energy basis of the feedstock biomass. In another similar study by the same group, calcium formate ($\text{Ca}(\text{HCOO})_2$) was used as an *in-situ* source of hydrogen to enhance deoxygenation and the quality of the biocrude. The study concluded that by simply using an inexpensive hydrogen donor such as calcium formate, a good quality biocrude could be produced due to the hydrodeoxygenation of the depolymerized biomass components (Ramsurn & Gupta, 2013).

Use of heterogeneous catalyst: In bio-renewables industry, development of heterogeneous catalysts that could tolerate hydrothermal degradation is very important (Liu et al., 2013). Carbon materials are recalcitrant to hydrothermal conditions but for solid acid sulfonated carbon materials, the current reports did not fully clarify the stability of the sulfonic-acid groups on the aromatic rings, in this respect model compounds containing sulfonic acid groups linked to aromatic, alkene or cycloalkane carbon atoms were exposed to hydrothermal conditions. There are several reports that underline the advantages of a heterogeneous catalyst when various supports were used such as: alumina (Morejkar & Fernandes, 2010), silica (Murkute, Jackson & Miller, 2011), zeolites (Hyun, Song, & Kwak, 1999; Roh, Won, Woo, & Venkataraman, 2004; Zheng et al., 2009), resins (Kapura & Gates, 1973; Turbak, 1963), carbon based polymer (Shaabani, Rahmati, & Badri, 2008), and carbon amorphous or highly structured (Tan et al., 2011; Zhao, Wang, Zhao, & Shen, 2010). Unfortunately, the silica, alumina, zeolites and resins collapse under subcritical conditions (Budarin et al., 2007; Petrus, Stamhuis & Joosten, 1981). Therefore only the stable carbon remains as a support for a potential catalyst in subcritical water process, satisfying two green chemistry directives: using safer solvents (water vs. organic solvents) and utilizing renewable feedstock. As a particular case, Duan and Savage used six different heterogeneous catalysts (Pd/C, Pt/C, Ru/C, Ni/SiO₂-Al₂O₃, CoMo/y-Al₂O₃ (sulfide and zeolite) under inert He and high-pressure reducing (hydrogen) conditions. The results indicate that in the absence of added H₂ all the tested catalysts produced higher yields of bio-oil from the liquefaction of *Nannochloropsis sp.* (Duan & Savage, 2010).

3. PRODUCT SEPARATION AFTER HTL

For the efficient liquefaction process, most of the carbon and hydrogen in the present biomass should appear in biocrude/bio-oil for the maximizing carbon efficiency (Kumar, 2010; Kumar, 2012; Kumar, 2013). Therefore, product separation is one of the most important aspects of HTL. In standard laboratory practices, an organic solvent such as dichloromethane, chloroform, hexane, and cyclohexane is used to separate biocrude/bio-oil from the product mixture by liquid-liquid extraction step. Subsequently, organic solvent is

evaporated to recover biocrude. Figure 2 shows the general schematics of product separation methods used after HTL in a laboratory scale study. The solid and liquid products were rinsed with DI water separated by vacuum filtration. The solid products are dried and quantified, and the liquid products are immediately analyzed for total organic carbon (TOC). The sum of light bio-oil (LBO) and heavy bio-oil (HBO) is labeled as total bio-oil/biocrude. The remaining solids are oven-dried, quantified, and labeled as hydrochar.

A typical gas phase composition from HTL is CO₂ (66.2%), CH₄ (1.9%), and H₂ (29.7%) along with nitrogen and traces of C₂ and C₃ gases (Brown, Duan & Savage, 2010). Generally CO₂ consists of more than 85% of gas phase when reaction is conducted at lower temperature ($\leq 300^{\circ}\text{C}$) which goes down with temperature and hydrogen becomes a significant component of the gas phase at higher temperature ($\geq 350^{\circ}\text{C}$).

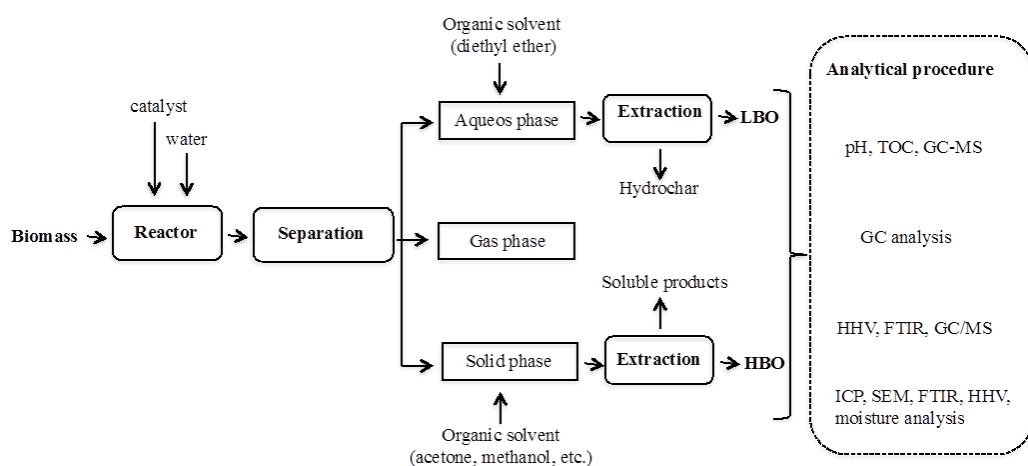


Figure 2. A representative product separation scheme after HTL (Popov, Kumar, & Balan, 2012).

4. HTL OF TERRESTRIAL BIOMASS

Lignocellulosic biomass is mainly composed of carbohydrates including cellulose (35-50 wt%) and hemicelluloses (20-35 wt%) and non-carbohydrate/aromatic portion lignin (15-20 wt%). The carbohydrates fraction contains different sugar monomers (C₅ and C₆ carbon sugars) that are tightly bound to lignin. It is well known that these three major chemical components of lignocellulosic biomass behave differently under hydrothermal conditions (Peterson et al., 2008).

Hydrothermal upgrading of lignocellulosic biomass was first developed by Shell, where biomass was subjected to subcritical water at 330°C to produce biocrude (Gourdiaan & Peferoen, 1990). Biocrude was further upgraded to liquid fuels via hydrodeoxygenation process. In one of the prior studies, switchgrass was effectively liquefied to produce biocrude in subcritical water in a flow through reactor. Biocrude composed of aqueous phase (water-soluble compound) and solid precipitates (Kumar & Gupta, 2009). The aqueous phase contained oligomers and monomers of five and six carbon sugars, degradation products (5-HMF and furfural), organic acids (lactic, formic and acetic acid), 2-furancarboxaldehyde and other phenolic products containing 5 to 9 carbon atoms. More than 50 wt% of carbon present

in switchgrass could be converted to biocrude in the presence of K_2CO_3 . Most of the studies related to HTL of lignocellulosic biomass employed alkali catalysts to increase biocrude yields and suppress hydrochar formation (Minowa, Fang, Ogi, & Varhegyi, 1998; Karagoz, Bhaskar, Muto, Sakata, & Uddin, 2004). It has been reported that all the biopolymeric components (carbohydrates, lipids, and proteins) contribute the biocrude production during HTL process (Elliott et al., 2013; Liu et al., 2013).

In general, woody and herbaceous biomass has similar thermochemical properties but extractives (e.g., chlorophyll, waxes, terpenes, and aliphatic acids) are higher in herbaceous biomass. The supply chain of herbaceous biomass also faces several other challenges including lower energy density, seasonal variations, and more susceptibility to biodegradation in comparison to woody biomass. This may affect the properties and composition of biocrude and also the hydrogen efficiency during upgradation stage (Kenney et al., 2013). In some areas, switching between woody and herbaceous feedstocks, or blending of the two or with others, may be necessary to keep large-scale operation near constant year round.

Karagoz et al., investigated the distribution of HTL (280°C for 15 min) products when wood (sawdust) and non-wood biomass (rice husk), and model components (lignin, cellulose) were used as the feedstock (Karagoz, Bhaskar, Muto, & Sakata, 2005). Sawdust and rice husk had almost similar conversions. Liquid products were recovered with various solvents (ether, acetone, and ethyl acetate) and analyzed by GC-MS. The composition of oils (ether extract) from sawdust and rice husk contained both phenolic compounds and furans, however phenolic compounds were dominant. Rice husk derived oil consists of more benzenediols than sawdust derived oil. The volatility distribution of oxygenated hydrocarbons showed that the majority of oxygenated hydrocarbons from sawdust, rice husk and lignin were distributed at n-C₁₁, whereas they were distributed at n-C₈ and n-C₁₀ in cellulose-derived oil (Karagoz et al., 2005; Karagoz, Bhaskar, Muto, & Sakata, 2006).

5. HTL OF AQUATIC BIOMASS

Microalgae primarily comprise of varying proportion of proteins (30-70 wt%), carbohydrates (15-50 wt%), lipids (15-60 wt%) and ash (up to 15 wt%) and the percentage fluctuate depending upon species (Becker, 2007; Kumar, 2012), in some cases could reach 26% (Elliott, Biller, Ross, Schmidt, & Jones, 2015). Microalgae consume the atmospheric CO₂ and also remove nitrogen and phosphorus from water. The microalgae production system can be integrated into an industrial ecology framework where the culture of microalgae in wastewater provides bioremediation, mineral processing and aquaculture (Neveux et al., 2014). A general scheme of liquid fuels production from microalgae using HTL is shown in Figure 3.

Wet algae slurry was successfully converted into an upgradeable biocrude with high levels of carbon conversion to gravity separable biocrude product at 350°C and 20 MPa in a continuous-flow reactor under subcritical water environment. The group reported high conversions even with high slurry concentrations of up to 35 wt% of dry solids (Elliott et al., 2013; Elliott et al., 2014). Though the hydrothermal technology is being rapidly adopted for industrial scale applications, the expanded process development is still needed to take it to a scale for wide-scale industrial applications. In some studies, heterogeneous catalysts (noble

and bimetallic catalysts on different supports) were used for direct liquefaction of algal biomass in hydrothermal media (Duan & Savage, 2010). However, they seem to be more efficient for upgradation/hydrodeoxygenation of resulting bio-oils (Furimsky, 2000).

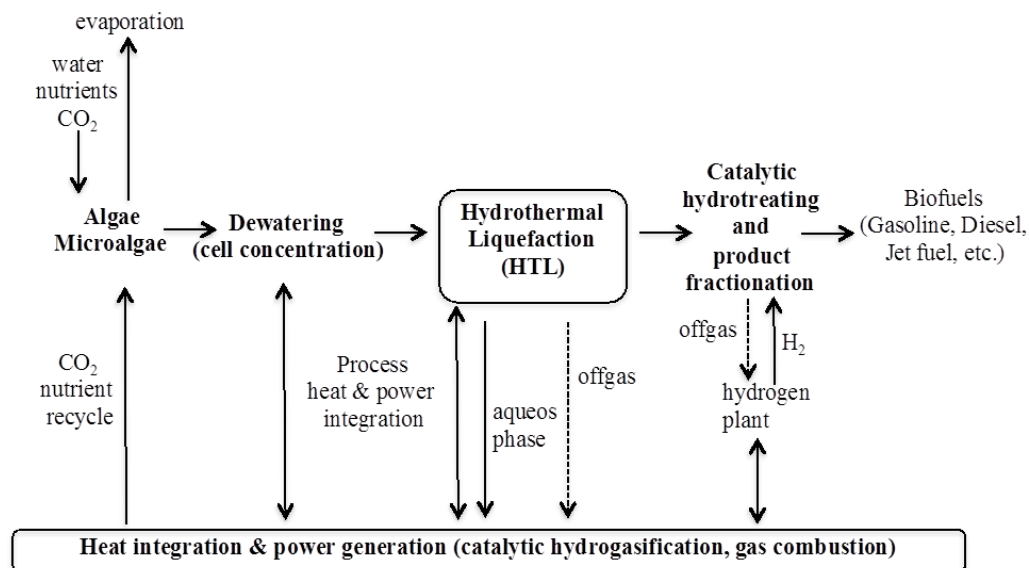


Figure 3. A general diagram of HTL of microalgae for biofuels production.

Biller and Ross compared the biocrude production from three different microalgae strains and a cyanobacteria conducting hydrothermal liquefaction at 350°C and 20 MPa (Biller & Ross, 2011). The yields of biocrude were 5-25 wt% higher than the lipid content of the algae depending upon biochemical composition. The yields of biocrude followed the trend lipids > proteins > carbohydrates. The study showed that each biochemical component (lipid, carbohydrate, and protein) of feedstock contributes to the bio-oil production which is a distinct advantage of HTL process. The HTL for algal biomass offers numerous advantages over pyrolysis through the use of wet biomass thus avoiding energy losses associated with drying, and also through enhanced reaction rates and an efficient separation of products (Peterson et al., 2008). Faeth et al., showed that high yields of energy-dense biocrudes can be obtained by rapidly heating algae slurries in minutes, using HTL process (Faeth, Valdez, & Savage, 2013).

6. TECHNO-ECONOMICAL ANALYSIS (TEA) AND LCA OF HTL

Transportation fuels based on algae or terrestrial biomass are being developed as an important step in achieving energy independence, reduction of fossil fuel use and greenhouse gas (GHG) emissions reduction. In order to accomplish these, the final product (biofuel) must be produced at a satisfactory price with no high engineering risk and on the other hand with consume of land, water and nutrients reliable with existing resources (Davis et al., 2014). The HTL shows a particular commercial interest because effortlessly integrates with the existing petroleum-refining infrastructure, once the biomass is liquefied, the bio-crude can be

separated and subsequently blended with petroleum crude to produce drop-in fuels in conventional refineries (Liu et al., 2013). Liu et al. showed that at the pilot-scale cultivation of algae would produce lower GHG emission than petroleum and bioethanol standard processes (Liu et al., 2013).

The TEA is an engineering costing analysis method that could determinate the process feasibility, evaluate and quantify the economic implications and the selling price of product, on the other hand LCA is used widely to estimate the environmental implications, basically evaluates the process energy consumption and GHG emissions (Figure 4), in other words, LCA methods consider all energy and emissions accumulated during production and use of a biofuel. Costs can be obtained through TEA and GHG emissions through LCA, a methodology that sums direct process emissions with those from upstream supporting technological operations.

Substantial amount of work has been done recently, concerning the environmental implications of a large-scale algae growing design for producing biofuels, using LCA approach (Davis et al., 2014). Liu et al. described a structured modeling based on three scenarios: lab-scale, pilot-scale, and full-scale, designed to highlighting the evolution of algae-to-energy industry (Liu et al., 2013). The major parameters, energy and materials input corresponding to the mentioned scenarios are detailed in the Tables 1 and 2.

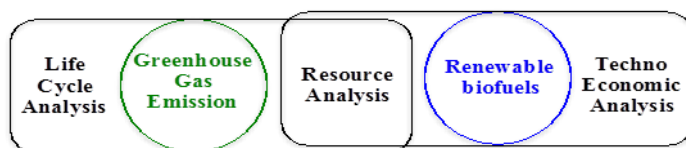


Figure 4. The biofuel pathways combine resource assessment, techno-economic analysis, and environmental analysis integrated.

Table 1. Summary of major input parameters for algae cultivation at three scenarios – adapted from (Liu et al., 2013)

Major input parameters of the model	Lab value (range)	Pilot value (range)	Full-scale value (range)
Growth rate (g/m ² /d) ^{a,b}	25 (15-35)	12 (12-24)	16 (12-25)
Carbon in algae biomass (%)	51 (48-53)	47 (41-50)	52
Nitrogen in algae biomass (%)	7 (5-9)	8 (7-9)	9
Phosphorus in algae biomass (%)	1 (0.9-1.3)	1.0 (0.9-1.3)	1.3
Biocrude yield (%)	60 (26-65)	20 (5-20)	50 (40-65)
Carbon in biocrude (%)	73 (68.1-75.4)	75 (65-77)	78.3 (65-79)
Nitrogen in biocrude (%)	5.7 (4-8.1)	4 (3-10)	4.2 (3-10)
CO ₂ recycle from CH ₄ combustion	No	No	Yes
Nutrients recycle efficiency (%)	90 (0-95)	12.5	75 (70-90)
Solvent	Toluene	Hexane	Toluene
Biogas production (%)	8 (2-35)	3	3 (1-6)

^a ash-free dry weight

^b a growth rate range 15-35 g/m²/d was used

Table 2. Major energy and material inputs at lab, pilot, and full-scale design in producing algae biofuels via HTL – adapted from (Liu et al., 2013)

Major energy and material inputs	process phase	Lab	Pilot	Full-scale
Electricity use for cultivation (MJ/bbl)	cultivation	116.4	529.1	171.6
CO ₂ supply (kg/bbl)	CO ₂	450.7	464.5	472.5
Nitrogen fertilizer input (kgN/bbl)	N	8.8	48.7	10.8
Phosphorus fertilizer input (kgP ₂ O ₅ /bbl)	P	0.1	0.4	0.21
Electricity use for harvest & dewatering (MJ/bbl)	(daf)	146.5	459.5	123.7
Natural gas use for HTL (MJ/bbl)	HTL	102.9	359.4	147.6
Electricity use for biocrude extraction (MJ/bbl)	extraction	18.8	18.8	18.8
Heat use for solvent recovery (MJ/bbl)	extraction	0.3	0.3	0.3

(daf)-dissolved air floatation

Recently, Davis et al., investigated the possibility of producing 5 billion gallons yr⁻¹ (BGY) of renewable diesel from *Chlorella* by HTL (Davis et al., 2014). The process was scaled-up based on previous results and on the data from a continuous one-liter reactor as well as on geographically and climatically distributed sites required to produce 5 BGY. The production of 5 BGY of renewable diesel required 1671 sites of 485 ha each. The TEA showed that a plant could produce 4-million gallons per year (annualized scenario) of naphtha and 27 million gallons per year of diesel, however, the productivity seems to vary 10-fold between seasons at some sites (Davis et al., 2014). The LCA model studied GHG emissions in detail for every representative site (geographical) and season for 30 years using a computer simulation program was recently described by Davis et al. The results showed that during winter three of the five sites exceeded the emissions for petroleum diesel (95 g CO₂e MJ⁻¹) in addition none of the sites reached a 2-fold emission reduction. According with these results the LCA imply 3-season operation following the shutdown operation during winter to reduce the GHG emissions but this is contrary to TEA that indicates 90% stream factor for each operating season including winter. However, the algae-to-energy modeling is at an early stage, there is lack of process data and on the other hand the pathway is a complex industrial pathway regarding the algae production, processing, regional upgrading facilities, refineries, and fuel blending (Davis et al., 2014).

Typically liquefaction processes of woody biomass could be done by fast pyrolysis and by HTL. One of the major difference between these two processes is that the oxygen content in the HTL bio-oil is 10-20 wt% considerably lower than that measured in the pyrolysis bio-oil which is about 40 wt%, in addition, the heating value of HTL bio-oil is about 35 MJ/kg which is twice higher than that of pyrolysis bio-oil 16-19 MJ/kg (Zhu et al., 2014). Zhu et al., implemented TEA to make an evaluation regarding the feasibility of developing a large-scale (2000 dry metric ton/day) woody biomass HTL and upgrading plant to produce liquid fuel (Zhu et al., 2014). Two cases were evaluated: a State-of-Technology case with HTL experimental testing and the Goal case, where the assumption of reducing the organic matter loss in the water phase, may lead to a significant reduction of the production cost. It is assumed that the Goal case displays (Zhu et al., 2014), (as in Table 3), an nth-of-a-kind (NOAK) plant design and the major improvements include: lower pressure in HTL process, less organics loss in the water phase, hydrocracking for heavy oils treatment and using a single reactor hydrotreating process. As it is shown in the Table 3, the operating pressure for

the HTL in the Goal case is lower than that of the State-of-Technology case with the same biomass conversion efficiency, actually this assumption is based on the recently HTL operating pressure range reported in the literature, that suggests a cost reduction due to lower pressure requirement for the equipment including pumps, heat exchangers and for the HTL reactor. The bio-oil yield in the Goal case it is higher than in the State-of-Technology case, this assumption is based on the improvements that could be achieved in the oil/water phase separation for an NOAK plant. Additionally, lower organic loss in the water phase improves the off gas generated by the HTL wastewater treatment.

Table 3. The major process inputs and assumptions in the State-of-Technology and Goal cases –adapted from (Zhu et al., 2014)

Cases	State of Technology	Goal
Biomass rate, metric ton/day, dry basis	2000	2000
Dry biomass wt% in biomass-water slurry	15	15
HTL		
Temperature (°C)	355	336
Pressure (Mpa)	20.3	16.6
Biomass conversion (%)	99.9	99.9
Liquid hourly space velocity (h ⁻¹)	4	4
Yields, (kg/100kg dry wood)		
Bio-oil	29.4	40.5
Gas	17.8	17.8
Water (with dissolved organics)	49.7	38.6
Solid wastes	3	3
Gas composition (wt%)		
CO ₂	88.3	88.3
H ₂	0.9	0.9
CH ₄	1.8	1.8
other hydrocarbons	9	9
Water composition (wt%)		
H ₂ O	67.2	72.9
Dissolved organics	32.8	27.1
Hydrotreating		
	Two-stage fixed bed	Single-stage fixed bed
Temperature (°C) inlet	165	165
Pressure (Mpa) inlet	13.5	13.5
Liquid hourly space velocity (h ⁻¹)	0.54 (stage 1) 0.18 (stage 2)	0.18
H ₂ consumption (gH ₂ /g dry bio-oil)	0.033	0.033
Product distribution (wt%)		
Deoxygenated oil	81.7	79
Water	15.7	18.5
Gas	2.5	2.5
Deoxygenated oil distillation streams (wt%)		
Light hydrocarbons (C ₄)	0.8	0.8
Gasoline (C ₅ -C ₁₀)	41.3	41.3
Diesel (C ₁₀ - 400°C boiling point)	39.6	39.6
Heavy oil (boiling point >400°C)	18.4	18.4
Hydrocracking		
Temperature (°C) inlet	n/a	376
Pressure (Mpa) inlet	n/a	10.5
Liquid hourly space velocity (h ⁻¹)	n/a	1

Table 4. The results and performance for the biomass HTL and upgrading system – adapted from (Zhu et al., 2014)

Case	State of Technology	Goal
Raw materials		
Biomass feedstock flowrate ton/day, dry	2000	2000
Natural gas flowrate (kg/h)	165	1420
Overall process yields		
Hydrocarbon (final product)production (L/h)	18.560	30.24
Hydrocarbon production rate (million GGE/yr)	42.9	69.9
Hydrocarbon yields, dry feedstock (L/kg)	0.22	0.36
Heavy oil (by-product) production rate (L/h)	3358	0
Heavy oil yield, dry feedstock (L/kg)	0.04	0
Hydrogen consumption		
Hydrogen feed to hydrotreater (kg/kg bio-oil)	0.041	0.038
Hydrogen feed to hydrotreater (kg/kg bio-oil)	0	0.006
Water usage		
Cooling water makeup (L/L product)	9.44	3.96
Boiler feed water makeup (L/L product)	0.96	0.66
Total water usage (L/L product)	10.4	4.62
Electricity usage		
Electricity consumption (MWe)	29.4	26.8
Electricity generation (MWe)	16.2	11
Net electricity requirement (kWh/L product)	0.71	0.52
Carbon efficiency		
Overall carbon efficiency (%) ^a	43.7	56.4
Hydrocarbon % C based on biomass only	35.1	57.8
Hydrocarbon % C based on biomass + natural gas	35	56.4
Energy efficiency		
Energy input		
Biomass feedstock (GJ/h) HHV basis	1627	1627
Natural gas (GJ/h) HHV basis	9.2	79.4
Energy output		
Hydrocarbon (GJ/h) HHV basis	714	1163
Heavy oil (GJ/h) HHV basis	162.3	0
Energy efficiency for hydrocarbon only ^b % HHV basis	42.4	65.9
Overall energy efficiency ^c % HHV basis	52	65.9

^a the overall carbon efficiency is calculated as the total carbon moles in final liquid fuel and by-product heavy oil divided by the total carbon input in the biomass feedstock and natural gas

^b energy efficiency is calculated as the total energy output divided by total energy inputs. The total energy inputs include energy in biomass, natural gas and required electricity

^c Overall energy efficiency is for all fuel products including both final liquid fuel product and by-product heavy oil.

Table 4 shows the major performance results in the State-of-Technology and Goal cases for the biomass HTL processed and upgrading system. In the both cases, the same amount of biomass, as a feed flow rate, is assumed, the natural gas consumption in the Goal case is higher because is assumed to produce more bio-oil and has a hydrocracker that require more hydrogen consumption.

Zhu et al., concluded that in the Goal case the hydrocarbon production could be with 63% higher than in the State-of-technology case because fewer organics are expected to be lost in the water phase this significantly increase the bio-oil production (Zhu et al., 2014). The heavy oil is treated as a by-product in the case of State-of-Technology case while in the case of Goal case hydrocracking process turns the heavy oil into additional biofuel products. Finally the efficiency is 14% higher in the case of Goal case, which is mainly due to the substantial improvement of organic matter loss management that translates into higher product yield.

7. ENGINEERING CHALLENGES OF HTL

Though excellent results have been achieved during laboratory experiments; there are certain engineering issues with the scale of the technology, which need to be addressed. These challenges include feeding of biomass slurry, corrosive medium, and possibility of deactivation of heterogeneous catalysts. There are several existing examples of lab- to pilot/demo-scale unit or product demonstration units (PDU) based on HTL technology. One of the challenges in scaling up HTL technology is use of a high pressure biomass slurry pump. The NABC led by PNNL has published a report (prepared for the) in 2012 on review and assessment of commercial vendors/options for feeding and pumping biomass slurries for subcritical water reactions in continuous reactor (Berglin, Enderlin, & Schmidt, 2012). PNNL and NABC team has been leading the efforts of scale up of hydrothermal/subcritical water based processing of biomass for biofuels. The recent pilot-scale studies on algae (NAABB) or woody biomass (NABC) feedstock in continuous-flow reactors and the related TEA and LCA successfully demonstrated the scale up feasibility of HTL process.

CONCLUSION

Hydrothermal liquefaction of biomass for biofuels production has been in the forefront among the other competing technologies. HTL has been successfully applied for producing biocrude from terrestrial biomass as well as aquatic biomass at laboratory, demonstrations, and in some cases at commercial scales. In the case of aquatic biomass, pumping biomass at a high pressure to achieve the HTL process conditions seem less challenging when compared to terrestrial/fibrous biomass. Homogeneous and heterogeneous catalysts are used to increase the degree of biomass liquefaction.

The results of LCA and TEA studies focusing on HTL as intermediate process in the overall conversion of biomass to biofuels, has shown some encouraging results. In one of the examples, the TEA showed that a plant could produce 4-million gallons per year of naphtha and 27 million gallons per year of renewable diesel from *Chlorella*. The DOE has led the HTL-based technology development for processing biomass for more than two decades. The continuous-flow reactors for HTL have been operated at pilot-scales and it has immensely helped in demonstrating the scale up feasibility of HTL process.

REFERENCES

- Andrianov, V., Borisjuk, N., Pogrebnyak, N., Brinker, A., Dixon, J., Spitsin, S., Koprowski, H. (2010). Tobacco as a production platform for biofuel: overexpression of Arabidopsis DGAT and LEC2 genes increases accumulation and shifts the composition of lipids in green biomass. *Plant Biotechnology Journal*, 8(3), 277-287.
- Berglin, E. J., Enderlin, C. W., & Schmidt, A. J. (2012). Review and Assessment of commercial Vendors/Option for Feeding and Pumping Biomass Slurries for Hydrothermal Liquefaction. DE-AC05-76RL01830, PNN-21981.

- Biller, P., & Ross, A. B. (2011). Potential yields and properties of oil from the hydrothermal liquefaction of microalgae with different biochemical content. *Bioresource Technology*, 102(1), 215-225.
- Brown, T. M., Duan, P., & Savage, P. E. (2010). Hydrothermal Liquefaction and Gasification of *Nannochloropsis* sp. *Energy & Fuels*, 24(6), 3639-3646.
- Becker, E. W. (2007). Micro-algae as a source of protein. *Biotechnology Advances*, 25, 207-210.
- Budarin, V. L., Clark, J. H., Luque, R., Macquarrie, D. J., Koutinas, A., & Webb, C. (2007). Tunable mesoporous materials optimized for aqueous phase esterifications. *Green Chemistry*, 9(9), 992-995.
- Davis, R. E., Fishman, D. B., Frank, E. D., Johnson, M. C., Jones, S. B., Kinchin, C. M., . . . Wigmosta, M. S. (2014). Integrated Evaluation of Cost, Emissions, and Resource Potential for Algal Biofuels at the National Scale. *Environmental Science & Technology*, 48(10), 6035-6042.
- Duan, P., & Savage, P. E. (2010). Hydrothermal Liquefaction of a Microalga with Heterogeneous Catalysts. *Industrial & Engineering Chemistry Research*, 50(1), 52-61.
- Elliott, D. C., Biller, P., Ross, A. B., Schmidt, A. J., & Jones, S. B. (2015). Hydrothermal liquefaction of biomass: Development from batch to continuous process. *Bioresource Technology*, 178, 147-156.
- Elliott, D. C., Hart, T. R., Schmidt, A. J., Neuenschwander, G. G., Rotness, L. J., Olarte, M. V., Zacher, A. H., Albrecht, K. O., Hallen, R. T., & Holladay, J. E. (2013). Process development for hydrothermal liquefaction of algae feedstocks in a continuous-flow reactor. *Algal Research*, 2(4), 445-454.
- Elliott, D. C., Hart, T. R., Neuenschwander, G. G., Rotness, L. J., Roesijadi, G., Zacher, A. H., & Magnuson, J. K. (2014). Hydrothermal Processing of Macroalgal Feedstocks in Continuous-Flow Reactors. *ACS Sustainable Chemistry & Engineering*, 2(2), 207-215.
- EPA Lifecycle Analysis of Greenhouse Gas Emissions from Renewable Fuels, EPA-420-F-10-006, Feb. (2010). <http://www3.epa.gov/otaq/renewablefuels/420f10006.pdf>.
- Faeth, J. L., Valdez, P. J., & Savage, P. E. (2013). Fast Hydrothermal Liquefaction of *Nannochloropsis* sp. To Produce Biocrude. *Energy & Fuels*, 27(3), 1391-1398.
- Furimsky, E. (2000). Catalytic hydrodeoxygenation. *Applied Catalysis A: General*, 199(2), 147-190.
- Gourdiaan, F., & Peferoen, D. (1990). Liquid fuels from biomass via a hydrothermal process. *Chemical Engineering Science*, 45, 2729-2734.
- Hao, X. H., Gio, L. J., Mao, X., Zhang, X. M., & Chen, X. J. (2003). Hydrogen production from glucose used as a model compound of biomass gasified in supercritical water. *International Journal of Hydrogen Energy*, 28(1), 55-64.
- Hyun, S. H., Song, J. K., & Kwak, B. I. (1999). Synthesis of ZSM-5 zeolite composite membranes for CO₂ separation. *Journal of Materials Science*, 34(13), 3095-3103.
- Jazrawi, C., Biller, P., He, Y., Montoya, A., Ross, A., Maschmeyer, T., & Haynes, B. (2015). Two-stage hydrothermal liquefaction of high-protein microalga. *Algal Research*, 8, 15-22.
- Kapura, J. M., & Gates, B. C. (1973). Sulfonated polymers as alkylation catalysts. *Industrial & Engineering Chemistry Product Research and Development*, 12(1), 62-7.

- Karagoz, S., Bhaskar, T., Muto, A., & Sakata, Y. (2005). Comparative studies of oil compositions produced from sawdust, rice husk, lignin and cellulose by hydrothermal treatment. *Fuel*, 84(7-8), 875-884.
- Karagoz, S., Bhaskar, T., Muto, A., & Sakata, Y. (2006). Hydrothermal upgrading of biomass: Effect of K_2CO_3 concentration and biomass/water ratio on product distribution. *Bioresource Technology*, 97, 90-98.
- Karagoz, S., Bhaskar, T., Muto, A., Sakata, Y., & Uddin, A. (2004). Low temperature hydrothermal treatment of biomass: Effect of reaction parameters on products and boiling point distributions. *Energy & Fuels*, 18, 234-241.
- Kenney, K. L., Smith, W. A., Gresham, G. L., & Westover, T. L. (2013). Understanding biomass feedstock variability. *Biofuels*, 4(1), 117-127.
- Kumar, S. (2010). Hydrothermal Treatment for Biofuels: Lignocellulosic Biomass to Bioethanol, Biocrude, and Biochar. *Chemical Engineering*, Auburn University: Auburn, 258.
- Kumar, S. (2012). *Sub-and Supercritical Water-Based Processes for Microalgae to Biofuels, in The Science of Algal Fuels*. R. Gordon and J. Seckbach, Editors, Springer Netherlands, pp. 467-493.
- Kumar, S. (2013). Sub-and Supercritical Water Technology for Biofuels. *Advanced Biofuels and Bioproducts*, JW Lee ed., 147-183.
- Kumar, S., & Gupta, R. B. (2008). Hydrolysis of Microcrystalline Cellulose in Subcritical and Supercritical Water in a Continuous Flow Reactor. *Industrial and Engineering Chemistry Research*, 47(23), 9321-9329.
- Kumar, S., & Gupta, R. B. (2009). Biocrude Production from Switchgrass using Subcritical Water. *Energy & Fuels*, 23(10), 5151-5159.
- Kumar, S., Popov, S., Majeranowski, P., & Kostenyuk, I. (2014). Subcritical water assisted oil extraction and green coal production from oilseed. US20150267141, May.
- Li, Z., Hong, Y., Cao, J., Huang, Z., Huang, K., Gong, H., Huang, L., Shi, S., Kawashita, M. & Li, Y. (2015). Effects of Mild Alkali Pretreatment and Hydrogen-Donating Solvent on Hydrothermal Liquefaction of Eucalyptus Woodchips. *Energy & Fuels*, 29(11), 7335-7342.
- Liu, X., Saydah, B., Eranki, P., Colosi, L.M., Mitchell, B.G., Rhodes, J., & Clarens, A. F. (2013). Pilot-scale data provide enhanced estimates of the life cycle energy and emissions profile of algae biofuels produced via hydrothermal liquefaction. *Bioresource Technology*, 148(0), 163-171.
- Minowa, T., Fang, Z., Ogi, T., & Varhegyi, G. (1998). Decomposition of cellulose and glucose in hot-compressed water under catalyst-free conditions. *Journal of Chemical Engineering of Japan*, 31(1), 131-134.
- Morajkar, P. ., & Fernandes, J.B. (2010). A new facile method to synthesize mesoporous gamma -Al₂O₃ of high surface area and catalytic activity. *Catalysis Communications*, 11(5), 414-418.
- Murkute, A. D., Jackson, J. E., & Miller, D. J. (2011). Supported mesoporous solid base catalysts for condensation of carboxylic acids. *Journal of Catalysis*, 278(2), 189-199.
- Neveux, N., Yuen, A. K., Jazrawi, C., Mannusson, M., Haynes, B., Masters, A., Montoya, A., Paul, N., Maschmeyer, T., & de Nys, R. (2014). Biocrude yield and productivity from the hydrothermal liquefaction of marine and freshwater green macroalgae. *Bioresource Technology*, 155(0), 334-341.

- Peterson, A. A., Vogel, F., Lachance, R. P., Froling, M., Antal, M. J., & Tester, J. W. (2008). Thermochemical biofuel production in hydrothermal media: A review of sub- and supercritical water technologies. *Energy and Environmental Science*, *1*, 32-65.
- Petrus, L., Stamhuis, E. J., & Joosten, G. E. H. (1981). Thermal deactivation of strong-acid ion-exchange resins in water. *Industrial & Engineering Chemistry Product Research and Development*, *20*(2), 366-371.
- Popov, S., Kumar, S., Balan, V., Uppugunda, N., Sousa, L., & Dale, B. E. (2012). Hydrothermal Processing of Un-Hydrolyzed Biomass for Biocrude and Biochar Production. *American Institute of Chemical Engineers (AIChE) annual conference*, Pittsburgh, PA: AIChE.
- Ramsurn, H., & Gupta, R. B. (2012). Production of Biocrude from Biomass by Acidic Subcritical Water Followed by Alkaline Supercritical Water Two-Step Liquefaction. *Energy & Fuels*, *26*(4), 2365-2375.
- Ramsurn, H., & Gupta, R. B. (2013). Deoxy-liquefaction of switchgrass in supercritical water with calcium formate as an in-situ hydrogen donor. *Bioresource Technology*, *143*, 575-583.
- Roh, H. S., Won, J. K., Woo, K. J., & Venkataraman, V. (2004). Superior dehydration of CH₃OH over double layer bed of solid acid catalysts-A novel approach for dimethyl ether (DME) synthesis. *Chemistry Letters*, *33*(5), 598-599.
- Sinag, A., Kruse, A., & Schwarzkopf, V. (2003). Key compounds of the hydrolysis of glucose in supercritical water in the presence of K₂CO₃. *Industrial and Engineering Chemistry Research*, *42*, 3516-3521.
- Shaabani, A., Rahmati, A., & Badri, Z. (2008). Sulfonated cellulose and starch: New biodegradable and renewable solid acid catalysts for efficient synthesis of quinolones. *Catalysis Communications*, *9*(1), 13-16.
- Tan, X. J., Liu, H. J., Wen, Y. W., Lv, H. Y., Pan, L., Shi, J., & Tang, X. F. (2011). Thermoelectric Properties of Ultrasmall Single-Wall Carbon Nanotubes. *Journal of Physical Chemistry C*, *115* (44), 21996- 22001.
- Tumuluru, J., Boardman, R., Wright, C., & Hess, J. (2012). Some Chemical Compositional Changes in Miscanthus and White Oak Sawdust Samples during Torrefaction. *Energies*, *5*(10), 3928-3947.
- Turbak, A. F. (1963). Sulfonation with organic phosphorus compound-sulfur trioxide adducts. US3072618 A, Jan, Esso Research and Engineering Co., 6.
- Zhao, Y., Wang, H., Zhao, Y., & Shen, J. (2010). Preparation of a novel sulfonated carbon catalyst for the etherification of isopentene with methanol to produce tert-amyl methyl ether. *Catalysis Communications*, *11*(9), 824-828.
- Zheng, J. J., Ma, J., Wang, Y., Bai, Y., Zhang, X., & Li, R. (2009). Synthesis and Catalytic Property of a Zeolite Composite for Preparation of Dimethyl Ether from Methanol Dehydration. *Catalysis Letters*, *130*(3-4), 672-678.
- Zhu, Y., Bidy, M. J., Jones, S. B., Elliott, D. C., & Schmidt, A. J. (2014). Techno-economic analysis of liquid fuel production from woody biomass via hydrothermal liquefaction (HTL) and upgrading. *Applied Energy*, *129*(0), 384-394.

Chapter 7

APPLICATION OF HETEROGENEOUS CATALYSTS FOR THE PRODUCTION OF FUEL AND FUEL ADDITIVES FROM LIGNOCELLULOSIC BIOMASS

*Małgorzata Wąchala, Agnieszka M. Ruppert,
Olga Sneka-Platek and Jacek Grams**

Institute of General and Ecological Chemistry,
Faculty of Chemistry, Lodz University of Technology, Lodz, Poland

ABSTRACT

Lignocellulosic biomass is considered to be one of the most abundant alternative energy sources. Its great potential results from low price, wide availability, and no impact on the increase in the carbon dioxide emission. Moreover, lignocellulosic biomass, consisting mainly of cellulose, hemicellulose, and lignin, does not compete with the production of food. However, its use is dependent on the development of highly efficient conversion methods allowing to obtain high valuable products which can replace traditional resources. Therefore, this work is focused on their role in biomass conversion processes. The application of heterogeneous catalysts as a sustainable solution applied for biomass conversion is highlighted. The examples of the influence of the catalysts on the yield of the products of low and high temperature reactions are described. The relation between catalysts activity and their surface properties in the mentioned processes are demonstrated. In this chapter, we concentrate on fuel and fuel additives approach. Therefore, on the example of chosen chemicals, which have an application as fuel additives (GVL and HMF), the recent development in the field of heterogeneous catalysis is described. The second focus is put on the thermochemical way of biofuel synthesis as competitive approach.

Keywords: lignocellulosic biomass, biomass conversion, heterogeneous catalysts, platform molecules, levulinic acid, hydroxymethylfurfural, γ -valerolactone, bio-oil upgrading

* Corresponding author: jacek.grams@p.lodz.pl.

1. INTRODUCTION

The growing consumption of fossil fuels associated with intensive development of civilization has been observed over the past years (Chheda, Huber, & Dumesic, 2007). Different social sectors, which became an indicator of the level of public development, such as transport, industry, residential, and commercial, require permanent supply of energy from fossil fuels resources. Some of the most serious problems nowadays are global warming and climate changes caused by increasing emission of carbon dioxide into the atmosphere. The formation of CO₂ is related to intensive utilization of carbon-rich fossil fuels for obtaining energy in combustion processes (Serrano-Ruiz, & Dumesic, 2011). The concentration of CO₂ in the atmosphere has increased from 280 ppm since before the industrial revolution to 390 ppm in 2010 and is further predicted to be 570 ppm by the end of the 21st century. Therefore, many countries were required to reduce their CO₂ release into the atmosphere and develop a CO₂ capture system (Wang, Wang, Ma, & Gong, 2011).

The second challenge associated with the industrialization of society is depletion of fossil fuels reserves. Unfortunately, the formation of that feedstock took millions of years, while the utilization process is incredibly fast, making oil, natural gas, and coal non-renewable energy sources. Researchers are therefore constantly looking for new solutions which could be helpful in finding their replacement. Biomass which can be converted to biofuels and chemicals seems to be the most promising (Wang et al., 2011).

Biofuels can be divided into different generations, according to the origin. First generation of biofuels is produced from edible feedstock: sugars, starches, and vegetable oil. The most common fuels in this category are biodiesel and bioethanol. As a result, a lot of controversy arise over the food vs fuel competition and the cultivation of specific crops to be transformed into biofuels (Luque et al., 2008). Therefore, research on the use of non-edible feedstock for biofuels production has begun, and their second generation produced by the conversion of lignocellulosic biomass seems to be a promising alternative, since it does not compete with food, because it is based on waste plant feedstock (Wang et al., 2011; Shuttleworth et al., 2014). Lignocellulosic materials are the most abundantly available renewable source of energy, and most importantly, CO₂ released into the atmosphere in their combustion is later consumed in the regrowth process, i.e., photosynthesis (Chheda et al., 2007; Serrano-Ruiz, & Dumesic, 2011).

Lignocellulosic biomass can be converted into valuable platform chemicals referred to as “platform molecules” which were selected by the US Department of Energy according to their industrial potential to be transformed into fuels and chemicals. These biomass derivatives include 12 compounds, such as organic acids: succinic, itaconic, fumaric, lactic and levulinic, as well as glycerol, sorbitol, and xylitol. These industrially important compounds can be transformed into “secondary chemicals,” i.e., substrates for the synthesis of many useful products like surfactants, polymers, fabrics, resins, solvents, plastic or textiles (Figure 1). Platform molecules can also be transformed into liquid hydrocarbon biofuels or fuel additives (Chatterjee, Pong, & Sen, 2015; Serrano-Ruiz, Luque, & Sepulveda-Escribano, 2011). Blending of those additives with conventional fuels decreases the greenhouse gas emission, and also protects the engine against damage and nozzle choking. The corrosive nature of the fuel additives is highly undesirable. Therefore, liquid fuels obtained from lignocellulosic

materials should be compatible with combustion engines and their chemical properties should be identical to those of currently used petroleum (Climent, Corma, & Iborra, 2014).

Hydrocarbon fuels obtained from lignocellulosic biomass supply an energy on the same level as the conventional fuels. In contrast to ethanol, the most common fuel additive (Serrano-Ruiz, & Dumesic, 2011) lignocellulosic biomass-derived fuels are hydrophobic which eliminates the risk of engine damage and low miscibility problems which can appear in the latter case. Moreover, liquid hydrocarbon fuels have the ability to self-separate from water, allowing to avoid the distillation steps needed for the purification of ethanol. Forecasting, ethanol can be replaced by liquid hydrocarbon fuels (LHFs) obtained from non-edible lignocellulosic biomass, as LHFs are chemically similar to the fuels currently used in internal combustion engines (Serrano-Ruiz, & Dumesic, 2011).

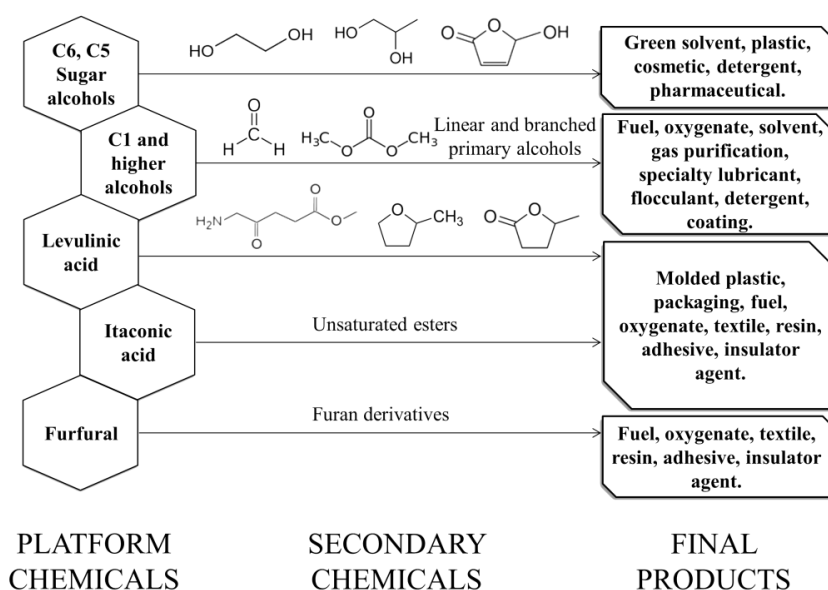


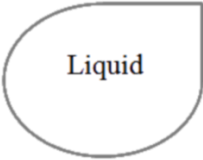
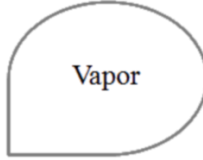
Figure 1. Platform molecules and possible paths for further upgrading together with example of industrial applications.

The lignocellulosic biomass can be converted into platform molecules and fuel/fuel additives in three possible pathways:

- Biochemical, based on enzymatic or biological (using microorganisms) decomposition of biomass into simple compounds, such as acids or sugars, which can be transformed into larger molecules and then into fuels or building block chemicals.
- Liquid phase catalytic process. The conversion of biomass into lower oxygenates is conducted in the presence of homo- and/or heterogeneous catalysts at low temperature. This kind of method requires biomass pretreatment.
- Thermochemical methods including pyrolytic processes, conversion of lignocellulosic biomass into gas, char and bio-oil, further transformed into biofuels at high temperature (Mushrif, Vasudevan, Krishnamurthy, & Venkatesh, 2015).

Below we listed examples of thermochemical processes and required reaction conditions for the formation of platform molecules (Table 1).

Table 1. Examples of thermochemical processes leading to the formation of platform molecules

PHASE	CATALYTIC PROCESS	PRESSURE [bar]	TEMPERATURE [°C]
	<i>Hydrogenation</i> <i>Hydrogenolysis</i>	0 – 182	30 – 200
	<i>Aqueous - Phase Reforming</i>	10 – 76	100 – 200
	<i>Dehydration Hydrolysis</i>	10 – 35	30 – 120
	<i>Isomerization</i> <i>Aldol Condensation</i> <i>Oxidation</i>	0 – 20	0 – 100
	<i>Liquefaction</i>	41 – 193	300 – 500
	<i>Vapor - Phase Reforming</i>	0 – 35	200 – 1000
	<i>Pyrolysis</i>	0 – 20	400 – 700
	<i>Gasification</i>	0 – 25	700 – 1000
	<i>Petrochemical Processes</i>	0 – 182	200 – 900
	<i>Super Critical Water Gasification</i>	203 – 250	400 – 700

2. STRUCTURE OF LIGNOCELLULOSIC BIOMASS

Lignocellulosic biomass is a composite material, which consists of three polymers irregularly distributed within the cell walls: cellulose, hemicellulose, and lignin (Figure 2). Owing to the composite and rigid structure, conversion of biomass into chemicals or fuels requires fractionation by using different pretreatment methods (chemical and physical). Unfortunately, depolymerization of biomass is a complicated process and its performance entails high cost (Alonso, Bond, & Dumesic, 2010; Isikgor & Becer, 2015).

Depending on the species, tissue growth conditions, maturity of the plant, structure and amount of cellulose, hemicellulose and lignin in plant cell wall the lignocellulosic materials can be different. It is assumed that lignocellulosic biomass consists of 35-50% cellulose, 10-25% lignin, and 20-35% hemicellulose (Figure 3). Nevertheless, plant cells contain not only these three fractions but also pectin, proteins, ash, waxes, chlorophyll, and nitrogenous material (Isikgor & Becer, 2015; Kumar, Barrett, Delwiche, & Stroeve, 2009).

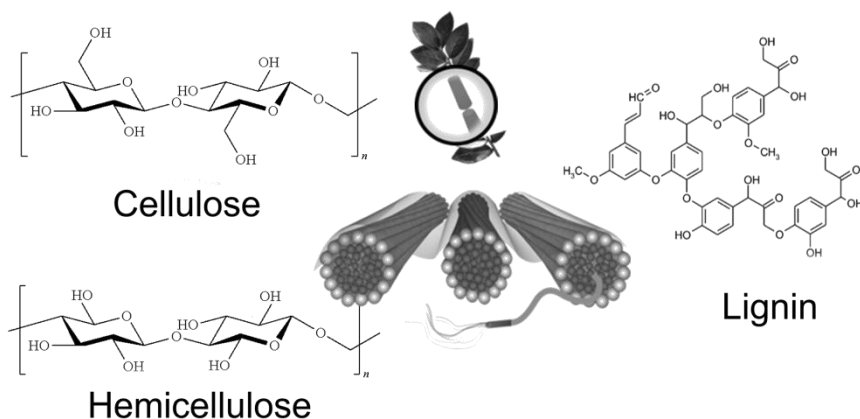


Figure 2. The composition of lignocellulosic biomass.

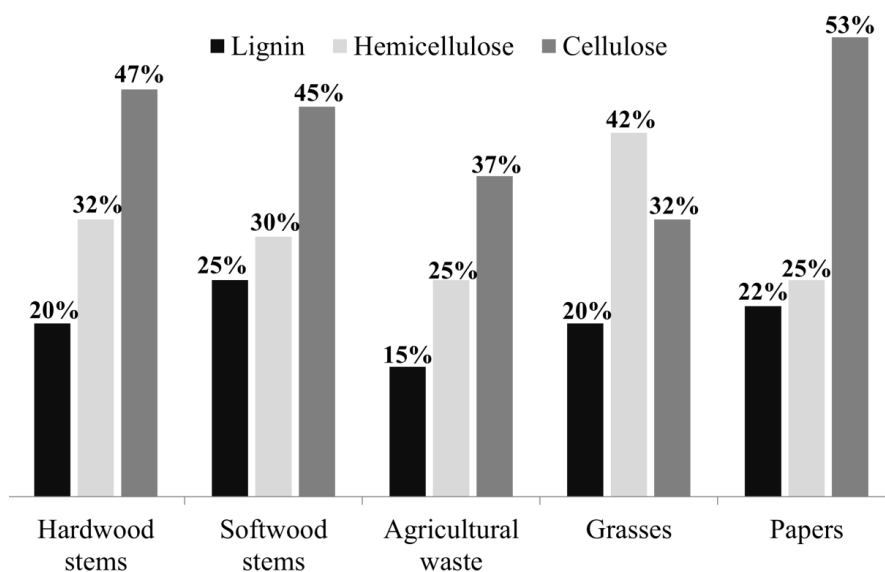


Figure 3. Composition of different lignocellulosic biomass feedstocks (Isikgor & Becer, 2015; Kumar et al., 2009).

a) Cellulose

Cellulose is a linear polymer consisting of glucose units joined by β -1,4-glycosidic bonds, forming long chains. Van der Waals interactions and hydrogen bonds aggregate these chains into microfibrils enveloped by hemicellulose and lignin. Cellulose has different polymorphic forms, crystalline ($I\alpha$, $I\beta$, II, III, and IV) and amorphous. Interestingly, the amorphous form of cellulose, without a highly organized structure, is more available to reactants and water than the crystalline one (Brandt, Gräsvik, Hallett, & Welton, 2013; Chatterjee et al., 2015; Zhao et al., 2006).

Only I α and I β forms are present in natural cellulose. The others are formed as a result of changes initiated by the (alkaline or ammonia) pretreatment of cellulose (Chatterjee et al., 2015).

b) Hemicellulose

Hemicellulose is a fraction of lignocellulosic biomass consisting of branched amorphous polymer with short lateral chains, made of pentoses (xylose, rhamnose, and arabinose), hexoses (glucose, mannose, and galactose), and uronic acids (4-methylglucuronic, D-glucuronic, and D-galacturonic acids). The main skeleton of hemicellulose is usually composed of hetero- or homopolymers with short branches linked by β -(1,4)-glycosidic bonds and occasionally β -(1,3)-glycosidic bonds (Kumar et al., 2009). In contrast to cellulose, hemicellulose has lower molecular weight, branches with short side chains and containing different sugars (Hendriks & Zeeman, 2009). Moreover, the amorphous character of hemicellulose makes it more prone to depolymerization than cellulose (Chatterjee et al., 2015). In plants, hemicellulose acts as a connection between the lignin and cellulose fibers, making the lignocellulose more rigid (Hendriks & Zeeman, 2009).

c) Lignin

Lignin is a biomass component with amorphous character. This polymer is made of three monomers: coniferyl alcohol, cumaryl alcohol and sinaphyl alcohol, combined with different bonds: acryl-acryl, alkyl-alkyl or alkyl-acryl. The structure of this fraction, which provide rigidity and hydrophobic character, makes it chemically and biologically resistant (Alonso et al., 2010; Hendriks, & Zeeman, 2009; Kumar et al., 2009).

3. PRETREATMENT OF LIGNOCELLULOSIC BIOMASS

While lignocellulosic biomass is an abundant and inexpensive renewable source of fuels, its depolymerization is a difficult task due to its complex structure, hydrophobicity and structure rigidity caused mainly by the presence of lignin. Thus, lignocellulosic materials need to be separated into cellulose, hemicellulose and lignin before their conversion into fuels. A wide range of pretreatment methods can be used for this purpose (Alonso et al., 2010). The main goals of biomass pretreatment are breaking down the lignin and exposing cellulose and hemicellulose, destroying crystalline structure of cellulose in order to make it more available for chemical and enzymatic conversion and reducing the size of biomass particles (Figure 4). Then, the hydrolysis of such pretreated carbohydrates into sugars is conducted easily (Kumar et al., 2009).

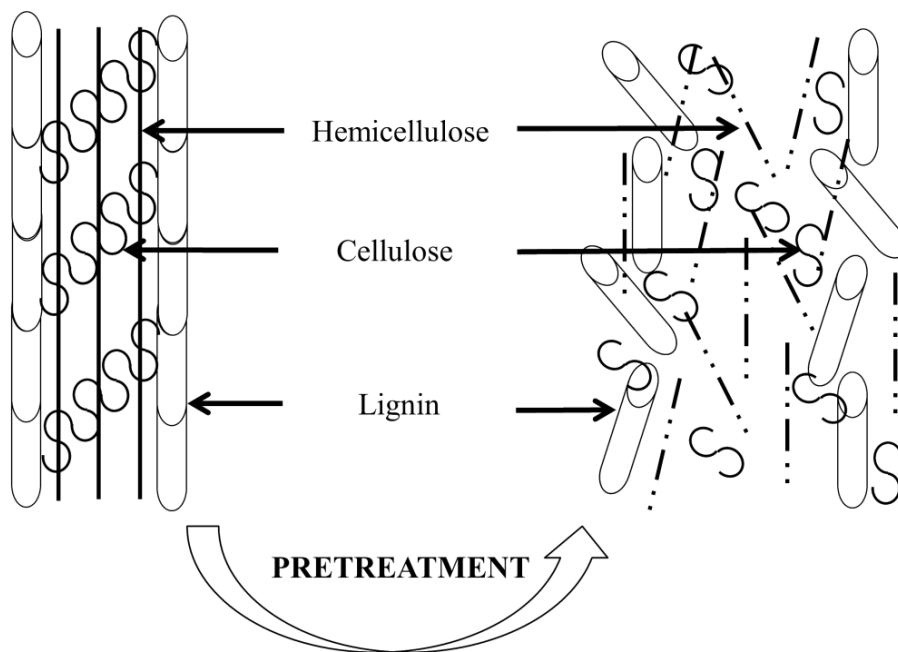


Figure 4. Schematic representation of the biomass pretreatment.

The main biomass pretreatment methods can be divided into physical (milling, grinding, chipping), chemical (acid, alkali, organic solvent, ionic liquid), and physicochemical (hydrothermolysis, steam pretreatment, wet oxidation).

The literature data (Guo, Fang, Xu, & Smith, 2012) shows that chemical pretreatment of lignocellulosic biomass is the most efficient and cost effective among all biomass pretreatment methods. Although physical treatment (e.g., chipping, grinding, milling, and thermal methods) is usually less efficient and requires more energy, those methods are often used in order to improve the yield of conversion of lignocellulosic material into biofuels.

3.1. Physical Pretreatment of Lignocellulose Biomass

The main goal of physical pretreatment of lignocellulosic biomass is to reduce its size and the crystallinity of cellulose. After milling the size of the treated biomass could be minimized to about 0.2-2 mm in comparison to 10-30 mm after chipping (Sun, & Cheng, 2002). Moreover, mechanical ball milling significantly decreases the amount of crystalline fraction of cellulose by breaking hydrogen bonds, reducing the degree of polymerization, opening the structure, and making β -1,4 bonds more available to acids (liquid or solid) which facilitates the sugar production (glucose), followed by conversion into hydroxymethylfurfural or levulinic acid (Guo et al., 2012; Hendriks & Zeeman, 2009; Zhao et al., 2006).

3.2. Chemical Methods of Lignocellulosic Biomass Pretreatment

Acid Pretreatment

The aim of acid pretreatment of lignocellulose materials is to break down the rigid structure and attack inter - and intramolecular bonds between cellulose, hemicellulose and lignin. Moreover, acids dissolve hemicellulose, making cellulose more accessible. This treatment can be conducted using diluted or concentrated acids, such as H₂SO₄ (Kumar, Dheeran, Singh, Mishra, & Adhikari, 2015; Maarten, Kootstraa, Beeftink, Scott, & Sanders, 2009; Sun, Tang, Iwanaga, Sho, & Kida, 2011), HCl (Hakansson & Ahlgren, 2005), H₃PO₄ (Yoon, Kim, Han, & Shin, 2015) or HNO₃ (Hendriks & Zeeman, 2009; Lee, Hamid, & Zain, 2014). The role of dilute and concentrated acids is hydrolysis of hemicellulose and cellulose to monomers (glucose, xylose, and other sugars). Monosaccharides originated from biomass are not stable end products and they are further converted into levulinic or formic acid and furans (Yoon et al., 2015).

The utilisation of concentrated acids to hydrolysis of biomass is associated with some disadvantages, such as toxic and corrosive character, difficult recovery after pretreatment processes, which makes this kind of hydrolysis costly (Kumar et al., 2009). Therefore, in order to minimize the problems mentioned the efforts involving the use of diluted acids are undertaken (Blanch, Simmons, & Klein-Marcuschamer, 2011).

Alkali Pretreatment

The main goal of alkali pretreatment of lignocellulosic materials is breaking down the structural linkages between carbohydrates and lignin by saponification of ester bonds, breaking of glycoside bonds due to dislocation of lignin, increasing specific surface of the material by swelling cellulose, which decreases the crystallinity of cellulose and reduces the degree of polymerization (Brodeur et al., 2011; Lee et al., 2014). In this method, NaOH (Zhu, Wan, & Li, 2010), Ca(OH)₂ (Xu & Cheng, 2011), and KOH (Sharma, Palled, Sharma-Shivappa, & Osborne, 2013) are used the most frequently.

Ionic Liquid (IL) Pretreatment

Ionic liquids are the most promising green solvents able to dissolve and separate different types of biomass. Ionic liquids are organic salts, which are the combination of organic cations and inorganic/organic anions (Vancov, Alston, Brown, & McIntosh, 2012). They have many excellent properties such as: liquid state at low temperatures (melting points typically below 100°C), high thermal stability, immeasurably low vapor pressure, non-flammability and water stability (Pinkert, Marsh, Pang, & Staiger, 2009; Vancov et al., 2012).

Different ionic liquids and their combinations are able to dissolve lignocellulosic biomass samples, such as: wood (Kilpeläinen et al., 2007), corn stalk, rice straw, pine wood and sugarcane bagasse (Li, Wang, & Zhao, 2008), cotton stalk (Haykir, Bahcegul, Bicak, & Bakir, 2013), and wheat straw (Brodeur et al., 2011; Li et al., 2009).

The literature data (Wang, Zheng, & Zhang, 2010) demonstrates that imidazolium-based ILs possesses a greater ability for dissolution and separation of different lignocellulose components than other ionic liquids taking into account the same reaction conditions. It was explained by the lower melting point, lower viscosity, higher thermal stability and unique structure of the imidazolium-based ILs. The results of previous research revealed that ionic

liquids are highly efficient in dissolution and separation of different components of lignocellulose when they contain Cl^- (chloride), $[\text{HCO}_2]^-$ (formate), $[\text{CH}_3\text{CO}_2]^-$ (acetate, Ac^-), $[\text{NH}_2\text{CH}_2\text{CO}_2]^-$ (aminoethanic acid), $[\text{CH}_3\text{SO}_4]^-$ (methylsulfate), $[\text{RR}'\text{PO}_2]^-$ (phosphonate), $[\text{Me}_2\text{C}_6\text{H}_3\text{SO}_3]^-$ (xylenesulphonate) anions, among others (Wang et al., 2010).

Ionic liquids can dissolve both carbohydrates and lignin by disrupting the intricate network of noncovalent interactions between these polymers. This treatment can reduce lignin content and change crystalline cellulose into amorphous one (Lee et al., 2014).

Biomass pretreatment is an expensive process, but it is expected that further research can improve its efficiency and lower the overall cost of biomass conversion process.

4. STRATEGIES OF BIOMASS CONVERSION

Here, we are presenting two different strategies of biomass conversion:

1. Low temperature methods which convert biomass into valuable chemicals and fuel, referred to as “liquid phase catalytic processes.” These methods include wide range of reactions: hydrolysis, dehydration, isomeration, oxidation, hydrogenation, and hydrogenolysis. They are conducted in the presence of heterogeneous (metals, metal oxides, solid acids, zeolites, ion-exchange resins) or homogeneous (mineral acids) catalysts. Because conversion of biomass consists of variety of processes, it is desired to find multifunctional catalysts to make the conversion more economic (Chheda et al., 2007; Isikgor & Becer, 2015). Those processes are very crucial for today’s biorefinery schemes as they are leading to the formation of value added products so called platform molecules which was described earlier in this chapter. We decided to concentrate on three of them namely levulinic acid (LA), γ -valerolactone (GVL), and hydroxymethylfurfural (HMF) as we believe that they can play a pivotal role in present day chemical and energy sector. In our work, we focus on selected choice of molecules related to energy sector.
2. Higher temperature methods including pyrolysis, gasification, and various upgrading processes aimed at the increase in the value of the formed products. In this work we focus particularly on the production of high value bio-oil.

4.1. Value Added Chemicals Obtained from Biomass

a) Levulinic Acid (LA)

Levulinic acid (γ -ketovaleric acid, 4-oxopentanoic acid) contains two functional groups, carboxyl (COOH) and carbonyl (CO), which give this compound reactivity and functionality (Rackemann & Doherty, 2011; Ya’aini, Amin, & Asmadi, 2012). Levulinic acid is considered a platform molecule, i.e., biomass-derived precursor for production of many functional and valuable chemicals with industrial applications, such as solvents, polymers, pharmaceuticals, resins, plastics or antifreeze agents (Rackemann, & Doherty, 2011). Its derivatives (i.e., γ -valerolactone) can be converted into biofuels or fuel additives, called “valeric biofuels”, which can be safely blended with currently used gasoline or diesel thanks to their

compatibility with conventional fuels (De, Saha, & Luque, 2015; Lange et al., 2010). As Isikgor and Becer noticed, many industrial companies produce bio-polymers based on levulinic acid or its derivatives, because the production costs are competitive to those obtained by traditional methods. The recent levulinic ketals technology by Segetis uses levulinic acid to produce polyurethane and thermoplastics. Another example is diphenolic acid (DPA), also obtained from levulinic acid, which can replace petroleum based bisphenol A (BPA), used in consumer products and food containers. Many other applications of LA derivatives are shown in Figure 5 (Isikgor & Becer, 2015).

Levulinic acid can be obtained from various types of lignocellulosic biomass by using different acidic catalysts both homogenous (e.g., mineral acids, organic acids) or heterogeneous ones (e.g., polymeric resins, zeolites). LA can be obtained from cellulose or sugars in several steps that can be performed via cellulose hydrolysis and glucose dehydration to hydroxymethylfurfural (HMF) and then to levulinic acid (LA) in the presence of acidic catalysts. In this reaction formic acid is formed in equimolar amount to LA (Scheme 1).

Van de Vyver et al. suggested two approaches to cellulose conversion towards levulinic acid by using mineral acids. The first one requires concentrated acids and relatively low temperatures, and the second one is based on dilute acids, needing high temperatures (Van de Vyver et al., 2011).

Levulinic acid can be obtained not only from mono- and polysaccharides but also from different raw lignocellulosic materials. Theoretically we can produce it with 71.5 wt% yield from cellulose and 64.5 wt% from hexoses. However, in practice the yield is much lower, due to the possibility of the formation of undesired by-products such as humins and soluble polymers (Galletti, Antonetti, De Luise, Licursi, & Di Nasso, 2012).

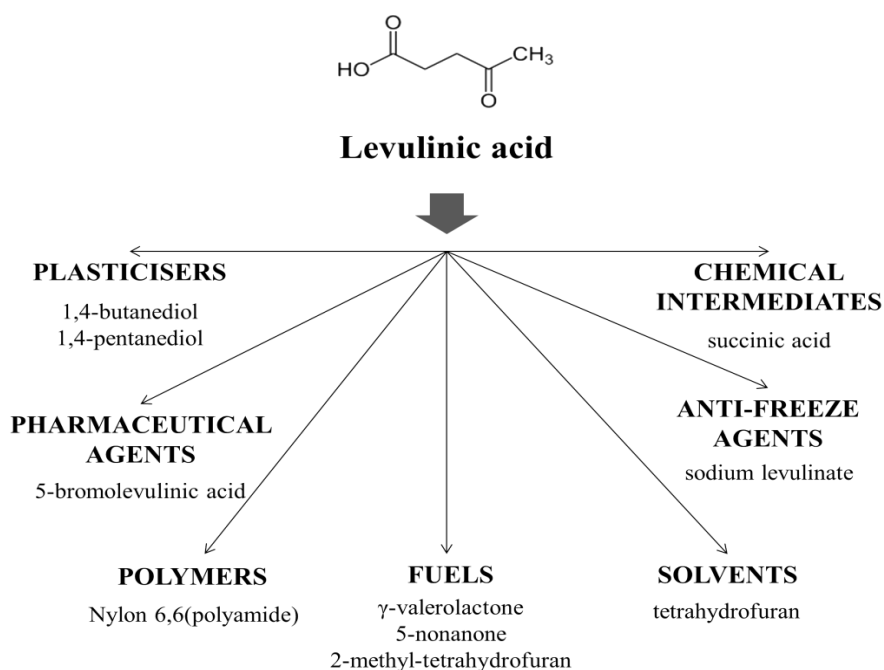
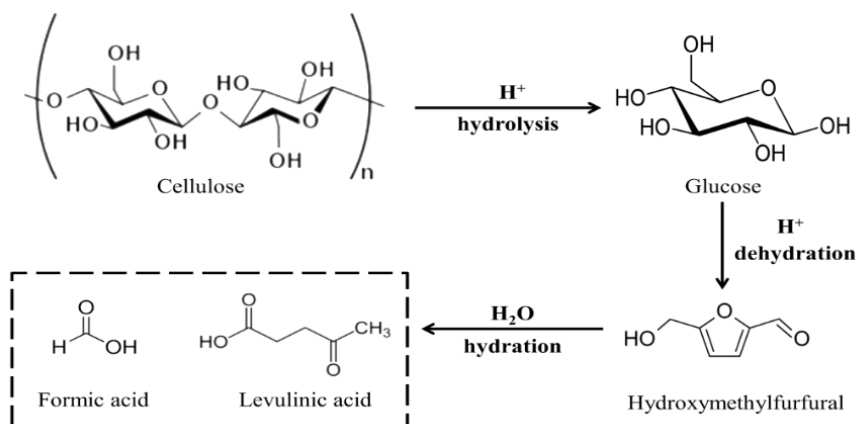


Figure 5. Example of possible applications of levulinic acid.



Scheme 1. Synthesis of levulinic acid from cellulose.

Taketuchi et al. investigated the hydrothermal conversion of glucose to levulinic acid, using HBr, HCl, H_2SO_4 , H_3PO_4 as catalysts. The highest levulinic acid yield was obtained in the presence of HCl, followed by H_2SO_4 and H_3PO_4 (Takeuchi, Jin, Tohji, & Enomoto, 2008). Moreover, Rackemann and Doherty describe the effectiveness of dilute acids in the conversion of sucrose to levulinic acid in the following order: HBr > HCl > H_2SO_4 (Rackemann & Doherty, 2011).

Galetti et al. studied the hydrothermal degradation of various waste biomass (poplar sawdust, paper mill sludge, tobacco chops, wheat straw, olive tree pruning) in the presence of homogenous acid catalysts (98% H_2SO_4 , 37% HCl). Higher yield of levulinic acid and lower amount of humins were observed for HCl (Galletti, Antonetti, De Luise, Licursi, et al., 2012).

The yield of LA can be improved by many different factors, e.g., adding NaCl, pre-hydrolysis of feedstock or using microwave irradiation, which is the most promising way to upgrade the production of LA from biomass. Galetti investigated the impact of microwave irradiation on yield of levulinic acid, finding that microwave heating at the same temperature improves the LA yield, shortening the time of reaction from 1 h to 0.25 h. The yield of levulinic acid was also improved by conducting conventional heating in two steps, with a pre-hydrolysis at lower temperature and further conversion (for poplar sawdust the yield of LA increased from 37% to 51%, yield based on cellulose content, and it was higher than after microwave heating for 15 minutes - 45,8%) (Galletti, Antonetti, De Luise, Licursi, et al., 2012). Two-step hydrolysis of cotton straw with dilute acid to obtain solution of sugars and levulinic acid was also investigated. Firstly, the hydrolysis was carried out in the presence of 0.2 mol/L H_2SO_4 at 120°C for 20 minutes. The second step was conducted at 180°C for 1 h in the same concentration of acid. The results of hydrolysis were unsatisfactory, with 4.2% yield of glucose and only 9.5% of levulinic acid (Yang et al., 2013). Homogenous acid catalysts are very effective in the conversion of biomass towards levulinic acid, however their disadvantages include corrosivity, problems with recycling and environmental pollution, so that heterogeneous catalysts can be an alternative for mineral acids. The solid catalysts include ion-exchange resins, zeolites, and solid superacids. Unfortunately, only minimal attention has been given to the use of solid acid catalyst for converting hexoses and other carbohydrates into LA. According to the Rackerman, the yield of levulinic acid obtained from

different materials by using heterogenous catalysts is very poor (Rackemann & Doherty, 2011). The yield of LA can be improved by various methods, such as pretreatment of biomass, or application of metal salts (Ramli & Amin, 2015).

According to Ramli and Amin, several factors influence the selectivity and yield of levulinic acid, such as the amount and strength of acid sites, their types, shape selectivity and porosity of zeolite materials. Lewis and Brønsted acid sites in the zeolite structure are required in the conversion of glucose towards levulinic acid. The isomerization of glucose to fructose needs Lewis acid sites, dehydration requires both types, and the rehydration of HMF to LA is catalyzed by Brønsted sites. Zeolites with surplus Lewis sites cause the transformation of glucose into humins (Ramli & Amin, 2015).

Insufficient acidity and porosity of the used materials could also decrease the activity of catalysts. The enhancement of the catalytic properties and increase in the levulinic acid yield can be achieved by the modification of zeolites with acidic metal halides. The modified materials raise LA yield more than other types of the catalysts and are more easily separated from the reaction mixture.

Ramli and Amin tested the performance of Fe/HY (HY zeolite was impregnated with FeCl_3) catalysts in the transformation of glucose to levulinic acid and found that the catalyst acidity influences the reaction yield. The best performance (yield of LA 62% at 180°C) was achieved for catalysts containing the highest number of reactive acid sites, which confirms that acid sites play a role in determining the catalytic activity. The reaction proceeds in the presence of a catalyst which is both microporous and mesoporous, as the dehydration to HMF is observed in mesopores, while rehydration HMF to LA takes place in micropores. It was shown that modification of zeolite catalysts with metals can improve their properties. After impregnation the catalyst was more active than the parent material, and both of them catalyze the dehydration of glucose to levulinic acid, which is strongly connected with acid properties of FeCl_3 and porosity of zeolite (Ramli & Amin, 2015). Ya'aini et al. also focused on the modification of HY zeolite. The catalyst was prepared by impregnation of HY with CrCl_3 . The highest yield of levulinic acid (62% at 160°C) was observed for catalysts with the highest number of acid sites per unit of the surface. Compared to Fe/HY the synthesised catalyst had smaller micropore size, and the reaction occurred at different active sites (Ya'aini, Amin, & Endud, 2013).

Peng et al. investigated the catalytic performance of a wide range of metal chlorides in the conversion of cellulose to levulinic acid in liquid water. High catalytic activity was exhibited by transition metal chlorides such as CrCl_3 , FeCl_3 , CuCl_2 and AlCl_3 , and the yields of levulinic acid increased in the order $\text{CuCl}_2 < \text{FeCl}_3 < \text{AlCl}_3 < \text{CrCl}_3$ under the same conditions. The highest yield of LA was 67 mol% for CrCl_3 . AlCl_3 showed a high yield of levulinic acid and better selectivity for conversion of glucose, which means that this compound promotes the process of isomerisation of glucose to fructose, whereas CrCl_3 favors the depolymerization of cellulose to glucose and then to LA to a higher extent. The catalytic performance was correlated with the acidity of the reaction system due to addition of the metal chlorides (Peng et al., 2010).

Zeolites are not the only catalysts used for the synthesis of levulinic acid. Chen et al. focused on solid superacid $\text{S}_2\text{O}_8^{2-}/\text{ZrO}_2\text{-SiO}_2\text{-Sm}_2\text{O}_3$, which could be used as a catalyst in the LA production from steam exploded rice straw due to high catalytic activity. The feedstock before reaction was pretreated by different methods: steam explosion, mechanical grinding and superfine grinding. Steam explosion combined with superfine grinding

improved the yield of levulinic acid formation from 7.3 to 22.8% (70% of the theoretical value) at 200°C after 10 minutes. The results of solid superacid-catalyzed decomposition of rice straw to LA were comparable to liquid acid-catalyzed production of LA from biomass resources (Chen, Yu, & Jin, 2011).

The ion-exchange resins with strongly acidic sulfonic groups were also investigated in the production of LA from fructose, under mild conditions. The use of Amberlyst 15 for this process gave 52% yield of levulinic acid (120°C, 24 h). Moreover, the high activity was reduced only by 30% after 5 runs recycling. Due to its high exchange capacity the conversion of fructose and yield of LA was the highest for Amberlyst 15 in comparison with other solid catalysts (Nafion NR50 and SBA-SO₃H) (Son, Nishimura, & Ebitani, 2012).

Table 2. Chosen examples of the application of the catalysts to the LA production processes

No.	Feedstock	Final product	Reaction conditions	Catalyst	Yield [%]	Conversion [%]	Reference
1	Poplar sawdust	LA	200°C, 1 h	37% HCl	37*	-	(Galletti, Antonetti, De Luise, Licursi, et al., 2012)
	Poplar sawdust (pre-hydrolysis: 120 °C for 2h)		200°C °C, 1 h	37% HCl	51*	-	
	Poplar sawdust		MW irr.** 200°C, 0.25 h	37% HCl	45.8*	-	
2	Cotton straw (two step process)	LA	first step- 120°C, 20 min; second step- 180°C, 1 h	0.2 M H ₂ SO ₄	9.5	-	(Yang et al., 2013)
3	Glucose	LA	180°C, 3 h	10%Fe/HY	62	100	(Ramli, & Amin, 2015)
4	Glucose	LA	160°C, 3 h	Hybrid catalysts containing CrCl ₃ and HY zeolite	62	100	(Ya'aini et al., 2013)
5	Cellulose	LA	200°C, 3 h	CrCl ₃	67	100	(Peng et al., 2010)
	Glucose	LA	180°C, 2 h	AlCl ₃	66	100	
6	Rice straw after pretreatment (mechanical grinding)	LA	200°C, 10 min	Solid superacid S ₂ O ₈ ²⁻ /ZrO ₂ -SiO ₂ -Sm ₂ O ₃	7.3	-	(Chen et al., 2011)
	Rice straw after pretreatment (superfine grinding, steam exploded)	LA	200°C, 10 min	solid superacid S ₂ O ₈ ²⁻ /ZrO ₂ -SiO ₂ -Sm ₂ O ₃	22.9	-	
7	Fructose	LA	120°C, 24 h	Amberlyst 15	52	93	(Son et al., 2012)
				Nafion NR50	41	78	
				SBA-SO ₃ H	29	84	

* Yield based on cellulose content (%).

** Microwave irradiation.

In summary, LA can be obtained from cellulose with the use of acidic catalysts both homogeneous and heterogeneous (Table 2). As homogeneous one mostly mineral acids are

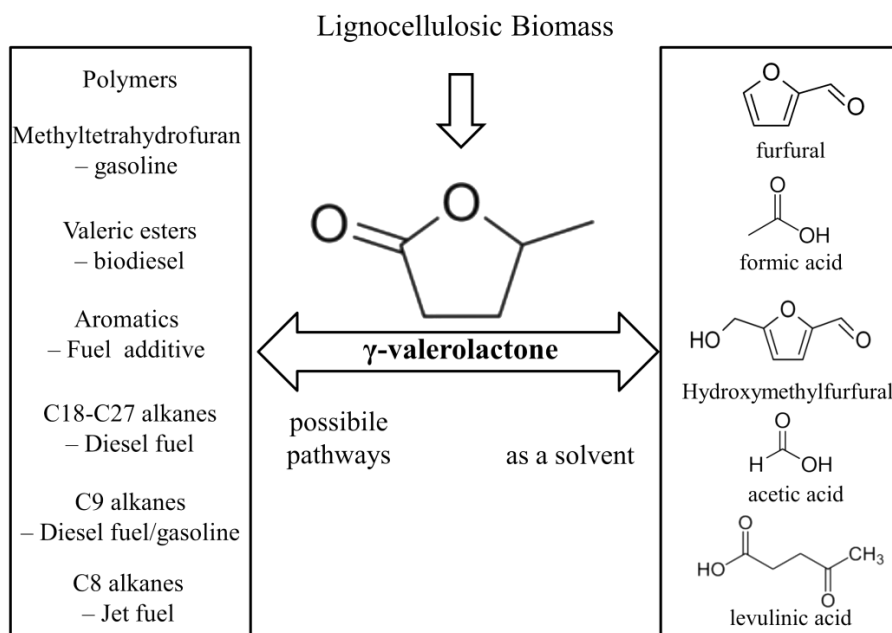
applied, however due to typical problems associated with the use of diluted acids (like corrosion and difficulty of separation from reaction mixture) intensive search is observed for heterogeneous counterparts. Among them zeolites, heteropolyacids or commercial catalysts were often applied. In the later case successful results were mainly obtained when as a feedstock sugars or pretreated cellulose was used.

Levulinic acid can be converted to many valuable derivatives (Figure 5), among which γ -valerolactone is of the greatest interest.

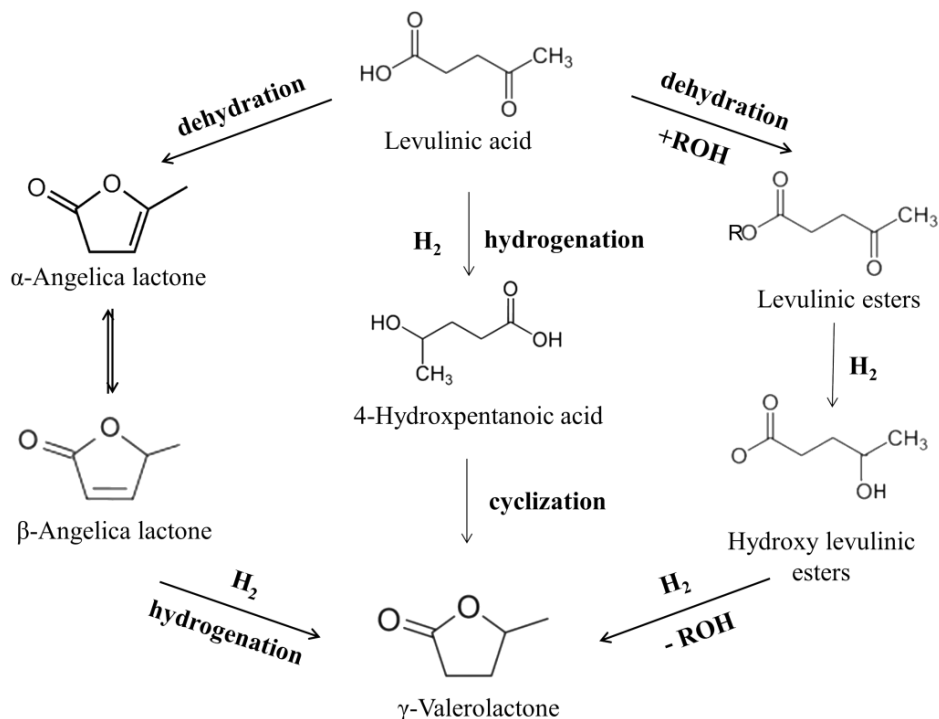
b) γ -Valerolactone (GVL)

GVL is a valero-cyclic ester containing four carbon atoms in the ring (γ -lactone). In normal conditions it is a liquid, its boiling point is high and it is non-toxic. GVL is a biomass-derived valuable compound. Although, GVL is not considered a platform molecule, but its wide range of applications makes it an important chemical. GVL molecule gained an increasing attention recently which was highlighted in some excellent reviews (Alonso, Wettstein, & Dumesic, 2013; Climent et al., 2014; Wright, & Palkovits, 2012).

GVL can be used not only as a solvent, but also as a precursor for other green solvents for the production of valuable chemicals and fuels from biomass. Moreover, it can be used as an additive to conventional fuels or biofuels. It can potentially replace ethanol, as it has higher energy density and similar combustion energy. GVL is a crucial compound in the production of valeric biofuels, which have a great potential to be blended with currently used fuels. It can also be applied to produce polymers, perfumes or food additives (Scheme 2) (Alonso et al., 2013; Climent et al., 2014).



Scheme 2. Reaction pathways for the conversion of GVL into fuels and chemicals (right) and products obtained by using GVL as a solvent (left).



Scheme 3. Possible pathways together with intermediates showing possibility of GVL synthesis from levulinic acid.

There are several probable selective pathways to produce GVL. The first is by cyclization of 4-hydroxypentanoic acid (γ -hydroxyvaleric acid) - an unstable intermediate, another one is based on dehydration of levulinic acid to α - or β -angelica lactone followed by its hydrogenation to GVL. The third one contains the hydrogenation of levulinic esters to hydroxy levulinic esters, the ring of which closes by intramolecular transesterification to produce GVL and the corresponding alcohol (Scheme 3) (Alonso et al., 2013; Ruppert, Grams, Matras-Michalska, Chełmicka, & Przybysz, 2014; Tang et al., 2014).

Several different metals like Ir, Ru, Ni, Pt, Au, Pd or Cu were investigated as catalysts for production of GVL from levulinic acid with external H_2 (Manzer, 2004; Obregón, Corro, Izquierdo, Requies, & Arias, 2014; Upare et al., 2011; Yan et al., 2013). Among them ruthenium and platinum are often considered as catalysts of choice for this process. There are several successful examples in the literature in which both Pt and Ru, mainly supported on carbon or metal oxides were used in the hydrogenation of levulinic acid towards γ -valerolactone (Upare et al., 2011; Z. P. Yan, Lin, & Liu, 2009). These studies mostly focused on the choice of proper catalysts, but also on the influence of the reaction medium, e.g. vapor vs. liquid phase, batch vs. flow reactor, various temperatures and pressures or solvent effect. The choice of catalysts is however directly connected with reaction conditions. In a protic solvent, Ru is very often a metal of choice, which we recently explained by combining the experimental and theoretical investigations (Michel et al., 2014). We analyzed three noble metal catalysts (Ru, Pt, Pd) supported on titania in two different environments (water and tetrahydrofuran) under mild reaction conditions (70°C, 50 bar of H_2). Interestingly, the

performance of Ru was strongly dependent on the reaction media. While not active in THF, this metal exhibited a very high activity in water (99% LA conversion, 95% GVL yield). The Pt and Pd activities were however not sensitive to the solvent: around 15-20% of GVL yield together with a 20-30% conversion of LA were achieved using the former, while the latter only showed a negligible activity. These phenomena were possible to explain with the help of DFT calculations which allowed us to conclude that the presence of an H-bonded water molecule significantly reduces the energetic span of the reaction pathway, consequently enhancing the catalytic activity. Additionally we predict that this activation can be generalized to other oxophilic metals such as Co or Ni while Pt and Pd are insensitive to their aqueous environment.

Ru was therefore very often the metal of choice when liquid phase reactions were performed. Also bimetallic systems like Ru–Re were investigated, in which the addition of a second metal was beneficial for increasing the activity (Braden, Henao, Heltzel, Maravelias, & Dumesic, 2011; Corbel-Demaiilly et al., 2013).

Very recently the group of Weckhuysen presented their work on bimetallic catalysts (Luo et al., 2015). They studied gold-palladium and ruthenium-palladium systems supported on titanium dioxide in the hydrogenation of levulinic acid. In their study they claimed that Ru-Pd/TiO₂ was both exceptionally active and selective towards γ -valerolactone (99%). The dilution and isolation of ruthenium by palladium is thought to be responsible for this superior catalytic performance. Additionally, it was shown that alloy formation greatly improves the stability of these supported nano-alloy catalysts.

On the other hand, in gas or vapor phase the choice of active metal might be very different. Lange et al. in their study showed results concerning levulinic acid hydrogenation in vapor phase on a very active platinum catalyst supported on zirconia. Furthermore, among many tested materials Pt/TiO₂ and Pt/ZrO₂ exhibited the best performance in levulinic acid hydrogenation, especially with respect to the support stability during extended reaction times (Lange et al., 2010).

Large part of work on this topic was dedicated to the effect of support. The group of Weckhuysen showed that the support acidity can enhance the conversion of levulinic acid (Luo et al., 2013) and exhibited that strong acidic sites present in zeolite-supported catalysts can even push the reaction course towards pentanoic acid (PA). The same for the first time they showed possibility to convert in a one pot the LA to pentanoic acid. In their work they tested 1 wt% Ru catalysts supported on H-ZSM-5 and H- β , which are strongly acidic, and compared with Nb₂O₅ and TiO₂ which do not possess strong acidic sites. Additionally they investigated the influence of several solvents like dioxane, 2-ethylhexanoic acid (EHA) and neat levulinic acid. They found out that both factors as well as solvent choice and acidity of the support have strong influence on catalytic performance. The non-acidic supports gave high selectivities to GVL and the highest GVL yield was observed for Ru/TiO₂ both in net LA and in dioxane (e.g., in dioxane the yield of GVL for Ru/TiO₂ was 92.3% (selectivity 95.8%), with a minor presence of MTHF (2.3%)). In the presence of EHA, the hydrogenation of levulinic acid to GVL was carried out with high selectivity over ruthenium catalysts supported on Nb₂O₅ and TiO₂, where only <1 mol% of by-products was formed. In the case of acidic catalysts it was possible to convert LA to PA as strong acid sites were pushing the conversion of LA forward and were crucial for the most difficult step which was the GVL ring opening. It was shown that zeolite-supported highly acidic catalyst allowed for the direct

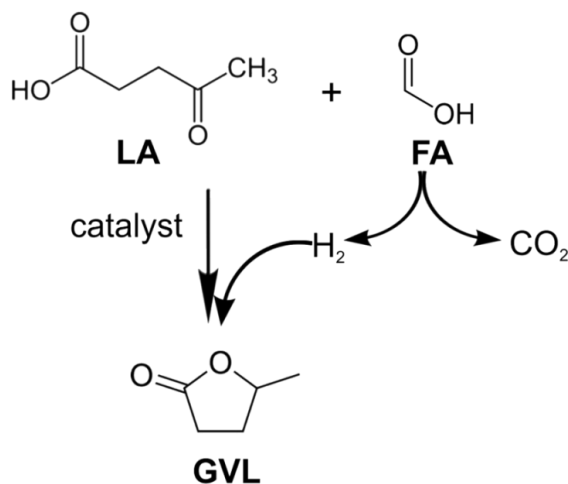
conversion of levulinic acid to pentanoic acid (PA) under relatively mild conditions when dioxane was used as a solvent.

Galletti et al. described the hydrogenation of aqueous solutions of levulinic acid to GVL over commercial ruthenium catalysts (5%Ru/Al₂O₃; 5%Ru/C) in combination with heterogeneous acid co-catalysts Amberlyst A70 and A15, niobium oxide and phosphate. The processes were conducted at low hydrogen pressure and 50-70°C. The most effective co-catalyst was A70 (99 mol% GVL after 3 h reaction at 70°C). This high efficiency was strongly connected with the strength of acid sites of the applied catalysts (Galletti, Antonetti, De Luise, & Martinelli, 2012).

In our work, we explored different titania supports and their influence on the Pt and Ru activity in levulinic acid hydrogenation towards GVL in mild conditions in water (Ruppert et al., 2015). A strong influence of the choice of the support on the catalyst activity in the reaction was found. Surprisingly this behaviour was different for Ru and Pt catalysts. For Ru based catalysts the highest activity was reached when mixed-phase anatase-rutile support was used. Pure anatase of large surface area did not allow to reach good dispersion of Ru, whereas on rutile with large surface area the crystallites were too small. In contrast, for platinum the situation was more predictable - large surface materials allowed better dispersion independently of the crystalline phase.

The groups of Weckhuysen (Luo et al., 2013) and Palkovits (Al-Shaal, Wright, & Palkovits, 2012) demonstrated that the solvent choice can have a strong influence on the ruthenium catalytic performance and reaction yield as well.

Most of the studies presented earlier were concerned with hydrogenation processes of levulinic acid to GVL using external hydrogen source. However more recently transfer hydrogenation has also been examined, especially with formic acid as an alternative source of hydrogen. The use of formic acid is especially convenient as it is produced in equimolar amount together with levulinic acid during the hydrolysis of carbohydrates (Ortiz-Cervantes, & García, 2013). Selective decomposition of FA can lead to the formation of carbon dioxide and hydrogen which can be directly used for LA hydrogenation (Scheme 4).



Scheme 4. GVL production from LA with the FA as a hydrogen source.

There are some examples of such process in the literature, large part of them concerns homogeneous catalysts. Recently, group of Horváth and co-workers tested $[(\eta^6\text{-C}_6\text{Me}_6)\text{Ru}(\text{bpy})(\text{H}_2\text{O})][\text{SO}_4]$ which gave 25% GVL yield at 70°C after 18 h reaction (Mehdi et al., 2008).

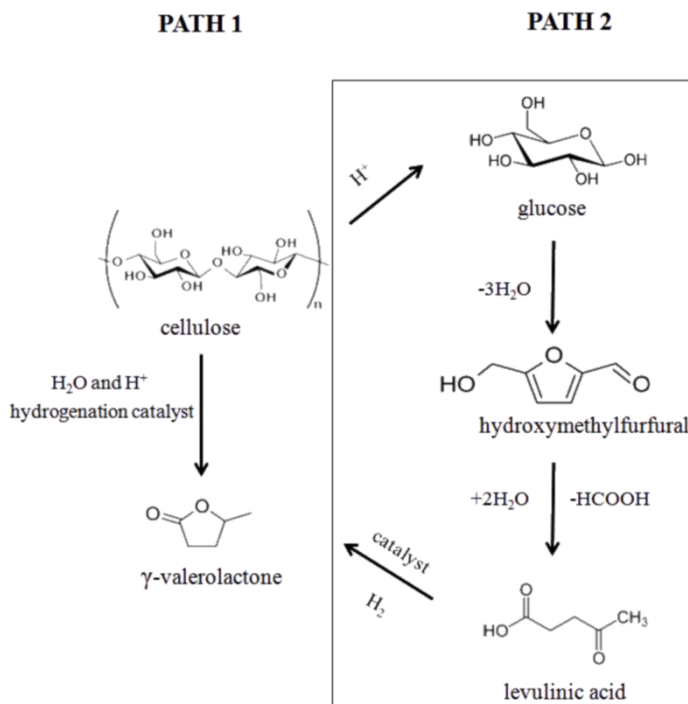
In another work, Deng et al. tested homogeneous catalyst $\text{RuCl}_3/\text{PPh}_3$ together with bases used as co-catalysts. The great advantage of their work lies in performing the reaction directly from biomass delivered LA/FA mixture. The activity of the investigated catalysts was directly associated with the basicity strength of the co-catalysts. The overall GVL yield of 48% based on glucose was obtained at 150°C with $\text{RuCl}_3/\text{PPh}_3$ and pyridine, as a catalyst (Deng, Li, Lai, Fu, & Guo, 2009). The studies of Tang et al. showed that Ru-NP formed in situ gave a completely quantitative conversion of LA at 130°C in 24 h with the assistance of Et_3N (Tang et al., 2014). However, poor catalyst stability was observed already after the 3rd run in this case.

The weak points of homogeneous catalysts such as difficulties in separation, lack of stability or poor water resistance are pushing scientists towards development of more stable heterogeneous ones.

In this field also some interesting examples were present. Son et al. tested 5% Ru/C, 5% Ru/SBA-15, 5% Ru/ Al_2O_3 , 5% Ru/ TiO_2 and 5% Ru/ ZrO_2 catalysts in water as a solvent and formic acid as a hydrogen source. The highest yield of GVL was achieved over 5% Ru/C (21%, with GVL selectivity 73%) and 5% Ru/SBA-15 (22%, with 71% GVL selectivity). The researchers observed that temperature of reaction strongly influences the GVL yield, which was dramatically decreased below 150°C (for Ru/C the yield of GVL at 150°C was 90%, but at 130-140°C it dropped to 32-22% (selectivity 63-62%), and only 2% at 100°C) (Son, Nishimura, & Ebitani, 2014).

Besides Ru, Pd and Au were also studied with very promising result. Du et al. tested Au/ ZrO_2 catalyst which showed an excellent performance in comparison to Ru and Pd catalyst. After 6 hours of reaction in 150°C with equimolar FA to LA ratio they reached 99% of GVL (Du, Bi, Liu, Cao, & Fan, 2011; Du, He, et al., 2011). Also Ag and Ag-Ni catalytic systems were analysed (Hengne, Malawadkar, Biradar, & Rode, 2014). A very interesting phenomena were noticed for 10%Ag-20%Ni catalysts supported on zirconia at 220°C after 5h of the reaction when almost full conversion of LA and full GVL yield was reached. Additionally, this catalysts benefit from its magnetic properties and therefore facile separation from reaction media.

The next studies were focused on the GVL synthesis directly from biomass. Generally, two different ways were discussed; one involving one-pot hydrolysis together with hydrogenation and the second consisting of two disconnected steps: hydrolysis of cellulose followed by hydrogenation (one pot procedure vs. two steps path) which are illustrated on scheme 5. Reactions with Ru/ TiO_2 (Ruppert et al., 2014) have been carried out using both procedures. The catalytic activity results together with catalyst surface studies showed that one-pot reaction was ineffective due to deactivation of catalysts by carbon deposit formation on the catalyst surface. The yield of GVL was only 6% for 1%Ru/ TiO_2 at 170°C after 5 h under 50 bar of H_2 . The two-step process resulted in much higher yield of GVL (31%).



Scheme 5. Two different paths of hydrolytic hydrogenation of cellulose to GVL

The problems connected with one pot procedure are related to hydrolysis process itself and the feedstock source. Hydrolysis of biomass can be done efficiently in the presence of sulfuric acid, which however creates waste disposal and causes reactor corrosion and additionally can poison the metal catalysts (because of adsorption of sulfur) that are often used for further upgrading of hydrolysis products toward other value added chemicals. Furthermore another issue is related to selectivity of biomass hydrolysis, as formed hydrolytic products can undergo hydrogenation, e.g., to hydroxymethylfurfural, and in consequence form a carbon deposit and also deactivate the catalyst. Gaining a deeper insight into the catalyst deactivation issues and finding ways to prevent them would therefore enable us to greatly improve the efficiency of lignocellulosic biomass valorization (Ruppert et al., 2014).

Although most of the examples described in the literature involved prior separation of LA from biomass hydrolytic mixture, Galetti et al. attempted to convert biomass directly to GVL without separation of LA. The one-pot system included acid-catalyzed dehydration and catalytic hydrogenation of giant reed. Hydrogenation was carried out in the presence of 5% Ru/C with niobium phosphate (NBP) or niobium oxide (NBO) as an acidic co-catalyst. The direct conversion of giant reed water slurries to GVL conducted in the presence of bifunctional catalytic system (5% Ru/C with NBP) at mild hydrogenation conditions (70°C and 0.5 MPa of H_2) gave 16.3% GVL yield based on dry giant reed starting weight (81.2% GVL calculated from the molar amount of LA) (Galetti et al., 2013). A niobium-based solid acid was also used with 5% Ru/C in the direct catalytic conversion of cellulose to GVL. In the first step niobium phosphate was used for hydrolysis of cellulose towards levulinic acid with the presence of 5% Ru/C for 24 h under N_2 pressure of about 8 bar (used as a protective gas). Then the reaction was quenched with cool water, N_2 gas in the autoclave was replaced

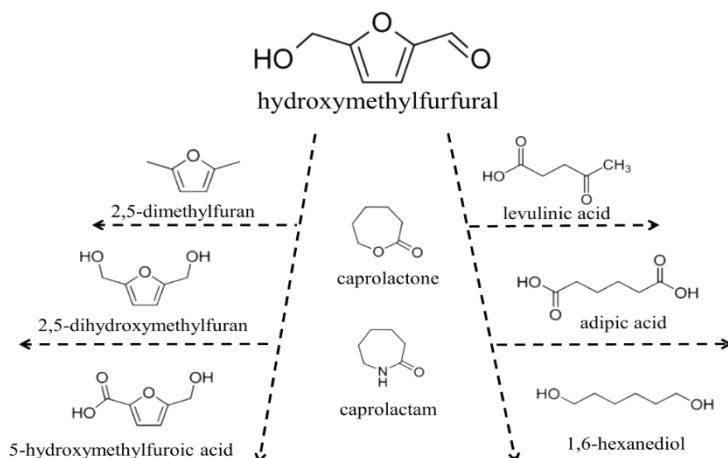
with H₂ and the reaction was restarted without separation. Hydrogenation was conducted for 12 h under 50 bar at 180°C. The yield of GVL (56.9%) was higher than LA (52.3%), due to the adsorption of LA on the catalyst surface, most of which would be released back into the solution once converted to GVL by hydrogenation (Ding et al., 2014).

Summarizing many parameters were investigated for these reactions like the role of the solvent, reaction temperature, hydrogen pressure and last but not least catalysts properties (Table 3). Mostly, the reactions were conducted in liquid phase from commercial levulinic acid with external hydrogen source. Often Ru was investigated as a metal of choice, beneficial effect of the dopands like Re or Pd was highlighted and strong effect of support was studied. Biomass was also considered as feedstock and some problems associated with this reaction like necessity of prior LA separation were discussed.

5-Hydroxymethylfurfural (HMF)

HMF (5-(hydroxymethyl)-2-furaldehyde, hydroxymethyl furfuraldehyde, 5-hydroxymethyl-2-formylfuran, oxymethylfurfurole) is a heterocyclic molecule with a hydroxyl and aldehyde group in 2- and 5- positions, respectively. This compound is considered a platform molecule which means it can be transformed into a wide range of chemicals and added-value products, such as fuels, solvents and pharmaceuticals. Moreover, HMF derivatives become potential building blocks for polymers. HMF can be converted to 2,5-diformylfuran (DFF), which is an intermediate in the production of antifungal agents and pharmaceuticals, and also to 2,5-furandicarboxylic acid, a key bioderived platform chemical transformed into useful products. HMF is also used as a substrate for the production of liquid hydrocarbon fuels (Scheme 6) (van Putten et al., 2013; Wang, Noltea, & Shanks, 2014).

The production of hydroxymethylfurfural is associated with numerous challenges that should be overcome, i.e., formation of LA and FA in presence of water, arising of humins and solid acid or low selectivity towards HMF. The role of the catalyst, solvent (water, DMSO, MIBK, ionic liquids) and reaction conditions (single, biphasic systems) are also important. It appears that an application of heterogeneous catalysts to the HMF production can be very attractive solution due to easy separation of the catalyst from the reaction mixture, its reusability and regeneration.



Scheme 6. Possible applications of HMF.

Table 3. Chosen examples of the application of the catalysts to the GVL production processes

No.	Feedstock	Final product	Reaction conditions	Catalyst	Yield [%]	Conversion [%]	Reference
1	LA	GVL	70°C, 1 h, 50 bar H ₂	1%Ru/TiO ₂	95	99	(Michel et al., 2014)
			70°C, 1 h, 50 bar H ₂	1%Pt/TiO ₂ 1%Pd/TiO ₂	15-20	20-30	
2	LA	GVL	200°C, 0.5 h, 40 bar H ₂	1%Ru-Pd/TiO ₂	98.6	>99	(Luo et al., 2015)
3	LA	GVL	200°C, 4 h, 40 bar H ₂	1%Ru/TiO ₂	92.3	1	(Luo et al., 2013)
4	LA	GVL	70°C, 3 h, 5 bar H ₂	5%Ru/C Amberlyst A70	99	98	(Galletti, Antonetti, De Luise, & Martinelli, 2012)
5	LA	GVL	70°C, 18 h, N ₂ autogenic pressure	[(η ⁶ -C ₆ Me ₆)Ru(bpy)(H ₂ O)][SO ₄]	25	-	(Mehdi et al., 2008)
6	Glucose (two step process)	GVL	First step: 220°C, 0.8 M HCl; second step: 150°C	RuCl ₃ / PPh ₃ and pyridine	48	-	(Deng et al., 2009)
7	LA	GVL	150°C, 5 h, 2 mmol FA	5%Ru/C	21	29	(Son et al., 2014)
			100°C, 5 h, 6 mmol FA	5%Ru/C	2	7	
			130°C, 5 h, 6 mmol FA	5%Ru/C	22	35	
			140°C, 5 h, 6 mmol FA	5%Ru/C	32	50	
			150°C, 5 h, 6 mmol FA	5%Ru/C	90	100	
8	LA	GVL	150°C, 6 h	1%Au/ZrO ₂	99	-	(Du, He, et al., 2011)
9	LA	GVL	220°C, 5 h, ratio LA:FA [mol] = 1:1	10%Ag-20%Ni/ZrO ₂	99	-	(Hengne et al., 2014)
10	Delignified pine wood in sheets	GVL	“one pot,” 170°C, 5 h, 50 bar of H ₂	1%Ru/TiO ₂	6	94	(Ruppert et al., 2014)
			“two steps path,” first step: 170°C, 5 h, 0.9% H ₂ SO ₄ , second step: 170°C, 1 h, 50 bar H ₂	1%Ru/TiO ₂	31	87	
11	Giant reed (pre-treatment at 80 °C for 2h, 0.4 HCl)	GVL	First step: 180°C, 1 h, 0.4 HCl; second step: 70°C, 5 h, 5 bar of H ₂	5%Ru/C with niobium phosphate (NBP)	16.3	-	(Galletti et al., 2013)
12	Cellulose (two step process)	GVL	First step: 180°C, 24 h, Al-NbOPO ₄ ; second step: 180°C, 12 h, 50 bar of H ₂	5%Ru/C	56.9	-	(Ding et al., 2014)

The investigations of the conversion of fructose towards HMF conducted in the presence of solid heteropolyacid $\text{Cs}_{2.5}\text{H}_{0.5}\text{PW}$ (a very strong acid) in a biphasic system (water – methylisobutylketone (MIBK)) exhibited a high selectivity towards the desired product. The yield of HMF was 74% and selectivity 94.7% at 115°C after 60 min. The use of MIBK as a solvent was supported by the fact that it suppresses unwanted side reactions accompanying dehydration of fructose in water in the presence of solid catalysts. The activity of $\text{Cs}_{2.5}\text{H}_{0.5}\text{PW}$ was compared with Amberlyst 15, zeolite and $\text{SO}_4^{2-}/\text{ZrO}_2$ and the highest selectivity to HMF was observed for the heteropolyacid (Q. A. Zhao, Wang, Zhao, Wang, & Wang, 2011). Another tests aimed at studying the effectiveness of a biphasic system, solvent and modified heterogenous catalysts - zeolites. Zeolites due to their unique shape selectivity have a great potential to be used for the conversion of fructose towards HMF. Several zeolite catalysts and silica modified zeolites, such as: MOR, ZSM5 and BEA were investigated in the formation of HMF from fructose in a biphasic system (water - MIBK). The addition of MIBK to the reaction mixture increased the selectivity of HMF. MIBK including ketone group fulfilled the pores of zeolite and interacted with Brönsted acid sites in zeolite by hydrogen bond. Its presence in the zeolite pores prohibited the oligomerization of HMF by displacement of hydroxymethylfurfural molecules from acid sites into the liquid phase and dilution of fructose and HMF present inside the pores by the organic solvent. HMF molecule cannot return into pores of zeolite, as it is absorbed by MIBK. The main role of modification of zeolite by silylation was the deactivation of its external surface. Moreover, it was used to determine reasons of the HMF selectivity changes. The experiment consisting of a deactivation of external acid sites of the catalysts revealed that the external surface was also involved in the fructose dehydration. Its contribution in the reaction depended on the pore size and acid strength of different zeolites. It was also showed that the presence of an organic solvent could suppress the performance of the catalyst external acid sites leading to the increase of HMF selectivity even at high degree of fructose conversion. The mentioned effect of organic solvent on the HMF selectivity changed as follows: MOR > ZSM-5 > BEA > aluminosilicate. This phenomenon corresponded with the change of acid sites strength of the analyzed catalysts. It was suggested that in the presence of strong acid sites fast dehydration of fructose without the formation of intermediates took place. A decrease in the rate of humins formation in the presence of organic solvent resulted in a growth of the zeolite stability in the dehydration process (Ordonsky, van der Schaaf, Schouten, & Nijhuis, 2012).

Dornath and Fan investigated the dehydration of fructose in aqueous phase in presence of zeolite catalyst using carbon black as the adsorbent. They compared the obtained results with the data achieved for the biphasic system (water MIBK). The carbon black adsorbed the formed HMF, thus preventing the formation of LA and FA and a decrease in the selectivity towards hydroxymethylfurfural. The used material (Carbon black BP2000) exhibited a high selectivity and adsorption capacity of HMF from water in a wide range of process temperatures. The adsorbed HMF was desorbed from the sorbent using ethanol. The results showed that in contrast to LA and FA more than 98% of HMF and furfural were adsorbed on the BP2000 and only a small amount of them remained in the aqueous phase. It allowed for the improvement of HMF overall selectivity from 20% to 38%, which was similar to that observed in the case of the biphasic system. Summarizing, the use of organic solvent MIBK and black carbon as an adsorbent improved the selectivity of HMF, prevented the oligomerization of HMF, but did not eliminate the formation of undesired humin by-products (Dornath & Fan, 2014).

Further studies were devoted to the investigation of a selective route of HMF synthesis from glucose. Yan et al. tested $\text{SO}_4^{2-}/\text{ZrO}_2$ and $\text{SO}_4^{2-}/\text{ZrO}_2\text{-Al}_2\text{O}_3$ catalysts, which exhibited a high activity and strong surface acidity. The obtained results revealed that in the presence of $\text{SO}_4^{2-}/\text{ZrO}_2\text{-Al}_2\text{O}_3$ the conversion of glucose and the yield of HMF were 97.2% and 47.6%, respectively. The reaction was conducted at 130°C for 4 h under N_2 atmosphere and in the presence of DMSO as a solvent, what could prevent undesirable reactions. The high yield of HMF could result from an integrated effect of suitable amounts of acidic and basic sites present on the catalyst surface (H. P. Yan, Yang, Tong, Xiang, & Hu, 2009).

Hu et al. focused on the conversion of glucose toward HMF using zeolite catalysts, such as HY-zeolite, H-mordenite, H β -zeolite, and H-ZSM-5 in presence of an ionic liquid. The investigations showed the highest activity of H β -zeolite, which possessed BEA pore structure and suitable balance between the density and strength of the acidic sites. The authors suggested that HMF formation occurred mainly on the outer surface of the catalyst, because the glucose molecule is larger than the zeolite pore sizes. Moreover, it was proved that the presence of 1-butyl-3-methylimidazolium chloride ([BMIM]Cl) influenced the conversion of glucose leading to the increase in HMF yield (Hu et al., 2014).

Cellulose is one of the fractions of lignocellulosic biomass. Its specific structure and chemical properties make the conversion of cellulose into HMF a great challenge. The main problem of this process is associated with the insolubility of cellulose in the conventional solvents.

Moreover, the hydrolysis of cellulose requires the use of acid catalysts (mineral acids are the most popular), but their corrosive character and the need for recovery from the reaction mixture necessitate finding alternative solutions. Therefore, an application of various solid catalysts (such as: zeolite, ion resins, solid acids) is proposed.

The catalytic systems consisted of H-form zeolite (CBV-400) and single alkali metal chloride (LiCl, NaCl, and KCl) were used in the conversion of cellulose into furan derivatives, HMF with 1-ethyl-3-methylimidazolium chloride [EMIM]Cl as a solvent. The results demonstrated that an addition of LiCl to the zeolite significantly improved its performance in the HMF formation. It was strongly associated with the higher Lewis acidity of lithium salts than NaCl or KCl. However, all employed systems (zeolite/LiCl, zeolite/NaCl and zeolite KCl) exhibited a higher catalytic performance than H-form zeolite in the conversion of cellulose towards HMF (Abou-Yousef & Hassan, 2014).

The next study focused on the one pot conversion of cellulose to HMF conducted with the use of Brönsted-Lewis-surfactant-combined heteropolyacid (HPA) $\text{Cr}[(\text{DS})\text{H}_2\text{PW}_{12}\text{O}_{40}]_3$ as a heterogenous catalysts. It allowed to obtain 52.7% yield of HMF at 150°C after 2 hours. The high activity of the studied catalysts was associated with micelles assembling in the aqueous solutions. The presence of both Brönsted and Lewis acid sites allows for the conversion of cellulose into sugars and their dehydration to hydroxymethylfurfural in the subsequent reactions. The use of such catalyst facilitated the diffusion of reactants in the solid-solid reaction and increased the reaction rate. Moreover, the micellar HPA catalyst provided a hydrophobic environment which protected HMF against further decomposition (S. Zhao, Cheng, Li, Tian, & Wang, 2011).

In summary, similarly to LA, in the synthesis of HMF analogous types of heterogeneous acidic catalysts are used (Table 4). The main difference lays in the solvent choice here usually DMSO, MIBK are used as solvent as it suppresses unwanted side reactions.

Table 4. Chosen examples of the application of the catalysts to the HMF production processes

No.	Feedstock	Final product	Reaction conditions	Catalyst	Yield [%]	Conversion [%]	Reference
1	Fructose	HMF	115°C, 1 h	Cs _{2.5} H _{0.5} PW ₁₂ O ₄₀	74	78.2	(Q. A. Zhao et al., 2011)
2	Glucose	HMF	130°C, 4 h, under autogenic atmosphere	SO ₄ ²⁻ /ZrO ₂ -Al ₂ O ₃	47.6	97.2	(H. P. Yan et al., 2009)
3	Glucose	HMF	140°C, 30 min	H-Y-zeolite	11.8	24.6	(Hu et al., 2014)
			140°C, 30 min	H-mordenite	13.1	27.2	
			140°C, 30 min	H-β-zeolite	23.7	48.1	
			140°C, 30 min	H-ZSM-5	20.5	42.7	
4	Cellulose	HMF	160°C, 30 min	zeolite (CBV 400) / LiCl*	70.3	-	(Abou-Yousef, & Hassan, 2014)
			120°C, 2 h	zeolite (CBV 400) / NaCl-KCl	58.2	-	
5	Cellulose	HMF	150°C, 2 h	Cr[(DS)H ₂ PW ₁₂ O ₄₀] ₃ *	52.7	77.1	(S. Zhao et al., 2011, 2011)

*Brønsted-Lewis-surfactant-combined HPA catalyst Cr[(DS)H₂PW₁₂O₄₀]₃ (DS represents OSO₃C₁₂H₂₅ dodecyl sulfate).

4.2. Upgrading of the Products of High Temperature Treatment of Lignocellulosic Biomass

High temperature treatment of lignocellulosic biomass leads to the formation of a wide range of valuable products which can be obtained by pyrolysis or gasification (Carlson, Vispute, & Huber, 2008; Ruddy et al., 2014; Yaman, 2004). The literature data shows numerous examples of such processes (Brown, & Brown, 2013; Huber, & Corma, 2007; Xue, Zhou, Brown, Kelkar, & Bai, 2015; Zhang, Brown, Hu, & Brown, 2013). Depending on the type of the process and reaction conditions different composition of gaseous and liquid phase is achieved (Collard, & Blin, 2014). In the case of the pyrolysis, three modes of operation can be applied - slow, intermediate or fast. The literature data demonstrates that an application of fast pyrolysis of lignocellulosic biomass (which becomes more and more popular in recent years) allows for increasing the amount of the liquid products (to about 75%). A very short reaction time and separation of the arising products limit secondary reactions resulting in cracking of bigger intermediates and formation of permanent gases (Bridgwater, 2012). The obtained mixture of products consists of several groups of organic compounds such as acids, ketones, aldehydes, alcohols, esters, ethers, hydrocarbons and sugars. Unfortunately, this mixture cannot be directly supplied to automotive engines due to its lower heating value and higher corrosiveness and chemical, and thermal instability in comparison with petroleum fuels. Therefore, it should be upgraded before the use. This can be realized by the upgrading

of vapors arising in fast pyrolysis of biomass in presence of heterogeneous catalyst leading to a decrease in the yield of undesirable compounds (Figure 6). The most commonly used catalysts in this process were zeolites, mesoporous materials and metal oxides. Moreover, it was found that introduction of noble or transition metals on their surface noticeably improves the properties of obtained bio-oil (Liao, Ye, Lu, & Dong, 2014; Stefanidis, Kalogiannis, Iliopoulou, Lappas, & Pilavachi, 2011). The examples of the performance of the heterogeneous catalysts in a high temperature treatment of different kinds of lignocellulosic biomass are presented in Table 5. The mechanism of the occurring reactions of bio-oil upgrading was described in (Isahak, Hisham, Yarmo, & Hin, 2012; Ruddy et al., 2014; Wang, Male, & Wang, 2013) among others.

4.2.1. Influence of Zeolites and Mesoporous Materials as Catalysts

The influence of the catalyst type on the yield of products of in-situ upgrading of biomass pyrolysis vapors was investigated by Stefanidis et al. (Stefanidis et al., 2011). They tested different commercially available materials, such as: FCC catalyst, ZSM-5, magnesium oxide, nickel oxide, alumina, zirconia, titania, zirconia/titania, and silica/alumina. It was demonstrated that high surface ZSM-5 and zirconia/titania samples were most promising in upgrading of biomass pyrolysis vapours due to their ability to formation of liquid fraction of organic products with reduced oxygen content and higher amount of aromatics. Despite the highest selectivity towards aromatics observed for pure alumina this system limited the production of liquid organic compounds. The worst material among the investigated samples seemed to be FCC catalysts which gave the lowest carbon to oxygen ratio in the upgraded mixture due to very fast carbon deposition on its surface.

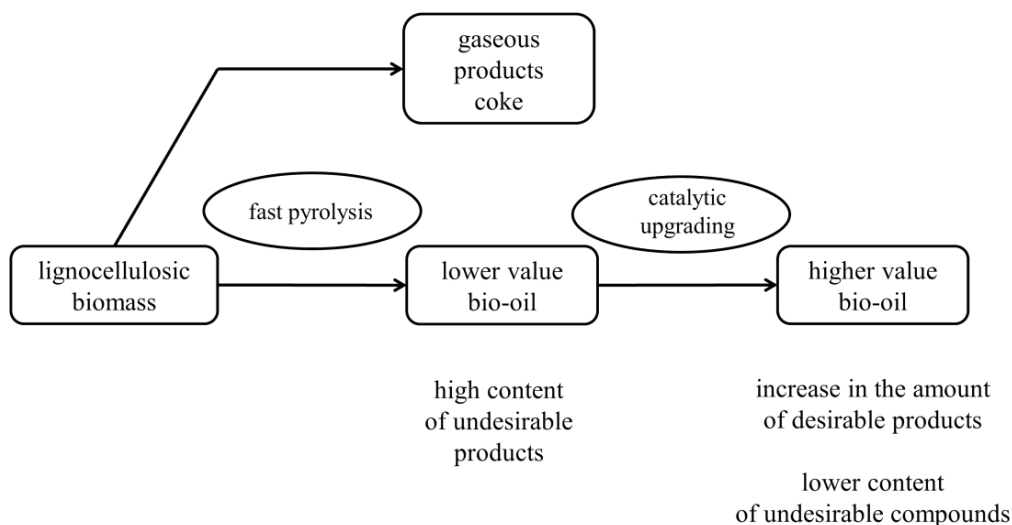


Figure 6. Bio-oil upgrading process.

Table 5. Catalysts and processes of the production and upgrading of bio-oil

No.	Catalyst	Feedstock	Process and products, influence of the catalyst	Reference
1	ZSM-5, MgO, NiO, Al ₂ O ₃ , ZrO ₂ , TiO ₂ , ZrO ₂ /TiO ₂ , and SiO ₂ /Al ₂ O ₃	Beech wood	In-situ upgrading of fast pyrolysis vapors in a fixed bed bench-scale reactor, ZSM-5 and zirconia/titania catalysts the most promising in upgrading of biomass pyrolysis vapours due to their ability to form liquid fraction of organic products with reduced oxygen content and higher amount of aromatics.	(Stefanidis et al., 2011)
2	Zeolites including ZSM-5 (modified by Co, Fe, Ni, Ce, Ga, Cu, Na), other silica and alumina materials	Cellulose, straw lignin, aspen wood	Upgrading of pyrolysis vapors in a tubular quartz micro-reactor, the best catalytic performance among the studied materials - acidic ZSM-5 catalysts modified by nickel, cobalt, iron or gallium.	(French, & Czernik, 2010)
3	ZSM-5, silicate, beta, Y-zeolite, silica-alumina	Glucose, cellobiose, cellulose and xylitol	Fast pyrolysis in a pyroprobe pyrolyzer, presence of ZSM-5 led to the production of the highest amount of aromatics (30% carbon yield).	(Carlson, Tompsett, Conner, & Huber, 2009)
4	Spray-dried ZSM-5	Eastern pine sawdust	Fast pyrolysis in a bubbling fluidized bed reactor with on-stream particle input and output, constant yield of aromatics over 6h with continuous catalyst circulation.	(Jae, Coolman, Mountziaris, & Huber, 2014)
5	Spray-dried ZSM-5	Cellulose	Fast pyrolysis in a bubbling fluidized bed reactor – the effect of steam, steam caused a loss of the acidity and growth in the zeolite-crystal size, the yield of aromatics dropped from about 17.5% to 11%.	(Yang et al., 2015)
6	H-ZSM-5	Hybrid poplar wood	In-situ and ex-situ pyrolysis in a micro-reactor, selectivity shifted from aromatics to olefins with the increase in the catalyst temperature, in-situ pyrolysis more aromatics (26%) and less olefins (5.4%), ex-situ pyrolysis less aromatics (18.5%) and more olefins (17.4%).	(Wang, Johnston & Brown, 2014)
7	H-ZSM-5	Duckweed	Fast pyrolysis in micro-reactor, production of aromatic hydrocarbons including benzene, toluene and xylene.	(Liu, Wright, Zhao, & Brown, 2015)
8	ZSM-5 modified by the addition of Ni and Co	Beech wood	In-situ upgrading of fast pyrolysis vapors performed on a bench-scale fixed bed tubular reactor, enhancement in the production of aromatics and phenols in the presence of ZSM-5 modified by transition metals.	(Iliopoulou et al., 2012)
9	ZSM-5, LOSA-1, gamma-Al ₂ O ₃ and FCC catalysts	Rice stalk	Fast pyrolysis in an internally interconnected fluidized reactor, ZSM-5 allowed to obtain the highest yield of aromatics (12.8%) and olefins (10.5%)	(Zhang et al., 2013)

No.	Catalyst	Feedstock	Process and products, influence of the catalyst	Reference
10	ZSM-5	Pine, corncob and straw cellulose, hemicellulose and lignin	Fast pyrolysis in Pyroprobe analyzer, the highest yield of aromatics (38.4% for cellulose and 25.4% for pine) was obtained in the presence of catalyst.	(Zheng et al., 2014)
11	desilicated ZSM-5	Beech wood	Fast pyrolysis in Pyroprobe analyzer, desilicated ZSM-5 more active towards production of aromatics than unmodified material (26.2% and 30.2%, respectively) and slightly limits coke formation (from 41.2% to 39.9%).	(Li et al., 2014)
12	FCC catalyst based on Y-zeolite with ZSM-5	Hybrid poplar wood	Pyrolysis in a bench scale unit, addition of ZSM-5 decreased cracking and carbon deposition rate leading to arising of higher amount of liquid products, presence of ZSM-5 increased the amount of aromatics, while Y-zeolite favored production of aliphatics.	(Mante, Agblevor, Oyama, & McClung, 2014)
13	ZSM-5, Ni/ZSM-5, MCM-41, Ni/MCM-41	Miscanthus, Scots pine, and mahogany	Fast pyrolysis in Pyroprobe analyzer, the presence of catalysts increased content of aromatics and lighter phenols.	(Melligan, Hayes, Kwapinski, & Leahy, 2012).
14	Ni/ZSM-5	Miscanthus	Hydropyrolysis in Pyroprobe analyzer, both hydrogen pressure and the presence of catalyst led to the increase in the amount of saturated hydrocarbons.	(Melligan, Hayes, Kwapinski, & Leahy, 2013)
15	MCM-41, Al-MCM-41, Cu-Al-MCM-41, SBA-15, Al-SBA-15, commercial FCC	Spruce wood, Miscanthus	Upgrading of biomass derived fast pyrolysis vapours in a fixed bed reactor, in the presence of the catalysts hydrocarbon and acid yields increased, while the carbonyl and acid yields decreased, all catalysts reduced the amount of undesirable product, while the desirable product yield remained on the same level or increased.	(Adam et al., 2006)
16	SBA-15, Pt/SBA-15, AISBA-15, Pt/AISBA-15	Cellulose, hemicellulose and lignin	Fast pyrolysis in Pyroprobe analyzer, the use of catalyst led to a growth in the amount of acids, hydrocarbons, phenolics, aromatics and polycyclic aromatic hydrocarbons in comparison to non-catalytic process, in the case of Pt/AISBA-15 the amount of phenolics and aromatics was even larger and the slight reduction of polycyclic aromatic hydrocarbons content was observed simultaneously.	(Jeon et al., 2013)
17	amorphous silica alumina containing alkali metal or alkaline earth metals including Na, K, Cs, Mg and Ca	Canadian pinewood	Fixed-bed reactor, the catalysts allowed for the deoxygenation of the obtained bio-oil in the range of 73%-85%.	(Zabeti, Nguyen, Lefferts, Heeres, & Seshan, 2012)

Table 5. (Continued)

No.	Catalyst	Feedstock	Process and products, influence of the catalyst	Reference
18	TiO ₂ (rutile), TiO ₂ (anatase) and ZrO ₂ /TiO ₂ modified with Ce, Ru and Pd	Poplar wood	Fast pyrolysis in Pyroprobe analyzer, the presence of the catalyst limited the amount of sugars and aldehydes. At the same time the content of furans, ketones, hydrocarbons and cyclopentanones was increased. In the case of phenols and acids, their concentration depended on the type of the applied catalysts.	(Q. Lu, Zhang, Tang, Li, & Zhu, 2010)
19	MgO, CaO, TiO ₂ , Fe ₂ O ₃ , NiO and ZnO nano metal oxides	Poplar wood	Fast pyrolysis in Pyroprobe analyzer, CaO was the most effective catalyst. Its presence allowed for the reduction of anhydrosugars and phenols content, elimination of carboxylic acids and increase in the amount of hydrocarbons, cyclopentanones, ketones and aldehydes, the production of hydrocarbons was also enhanced by Fe ₂ O ₃ (but in this case polycyclic aromatic hydrocarbons were also formed)	(Q.A. Lu, Zhang, Dong, & Zhu, 2010)
20	Ni supported on Al ₂ O ₃ , SiO ₂ , MgO, CeO ₂ , and ZrO ₂ (prepared by different methods)	Cellulose	Fast pyrolysis in Pyroprobe analyzer, Ni/Al ₂ O ₃ and Ni/ZrO ₂ appeared the most effective in the production of hydrocarbon fraction, while Ni/CeO ₂ and Ni/SiO ₂ were not so active. Moreover, in the last two cases the highest content of carboxylic acids was noticed.	(Grams, Niewiadomski, Ruppert, & Kwapinski, 2015, in press)

French and Czernik studied catalytic upgrading of pyrolysis vapors arising from different biomass samples using series of zeolites (French, & Czernik, 2010). The upgrading process was conducted in a semi-continuous flow reactor. They supposed that the presence of the catalyst should facilitate cracking reaction leading to deoxygenation of pyrolysis intermediates through simultaneous dehydration, decarbonylation and decarboxylation, and owing to that a bigger amount of hydrocarbon fraction can be produced. The obtained results revealed that the best catalytic performance among the studied materials demonstrated acidic ZSM-5 catalysts modified by nickel, cobalt, iron or gallium. However, their activity dropped in a few minutes due to carbon deposit formation. The investigations of catalytic fast pyrolysis of biomass showed that ZSM-5 is able to increase the yield of aromatics and limit the coke formation. However, the product selectivity is influenced by both the size of pores and acidity of the catalyst (Carlson et al., 2009). The literature data demonstrated that ZSM-5 catalyst was applied to the catalytic fast pyrolysis of lignocellulosic biomass conducted in a bubbling fluidized bed reactor with on-stream particle input and output (Jae et al., 2014). It was also showed that an addition of steam to the reactor can influence the properties of the used catalysts, which was manifested by a loss of the acidity and growth in the zeolite-crystal size (Yang et al., 2015). The comparison of in-situ and ex-situ pyrolysis of hybrid poplar carried out in the presence of HZSM-5 exhibited that in the case of in-situ process larger

amount of aromatics was produced while during ex-situ catalytic pyrolysis more olefin was formed (Wang, Johnston, & Brown, 2014).

An analysis of the product composition of the catalytic fast pyrolysis of duckweed revealed that the use of ZSM-5 allowed to obtain more aromatic hydrocarbons (Liu et al., 2015). Further research performed by Iliopoulou et al. confirmed an enhancement in the production of aromatics and phenols (which increases the quality of the obtained bio-oil) in the presence of ZSM-5 modified by transition metals (Ni, Co) (Iliopoulou et al., 2012). However, it was observed that the modified catalysts decrease the amount of the organic phase and increase a formation of gaseous products. A slight increase in the relative abundance of aromatics noticed in the case of modified ZSM-5 in comparison to unmodified material was ascribed to the facilitation of dehydrogenation pathway of pyrolysis products via oligomerization and cyclization of light alkenes in the presence of transition metals, whereas a growth in the amount of phenols was attributed to a decrease in Brønsted acidity due to the deposition of metal ions on the catalyst surface. The researchers noticed also in situ reduction of the metal oxides supported on the ZSM-5 during the reaction. They suggested that the presence of reduced metallic species can favor hydrogen transfer reactions leading to the formation of the enhanced amount of aromatics.

The results of the catalytic fast pyrolysis of straw biomass conducted in an internally interconnected fluidized bed revealed that the use of ZSM-5 led to the formation of the largest fraction of aromatics (12.8%) and C2-C4 olefins (10.5%). Although, it was simultaneously noticed that the catalyst was responsible for the highest amount of coke (32.2%). The opposite phenomenon was observed for γ -Al₂O₃ which produced considerably lower amount of coke and char (22.7%) but also gave the highest yield of oxygenated compounds (43.9%) (Zhang et al., 2013). The investigation by Zheng et al. showed that the selectivity and yield of aromatics in the bio-oil can be controlled by the choice of the optimal physicochemical properties of the ZSM-5 catalyst (Zheng et al., 2014). The fast pyrolysis of different lignocellulosic biomass (pine, corncob, and straw) and reference (cellulose, hemicellulose and lignin) samples conducted using a Pyroprobe pyrolyzer exhibited that the highest yield of aromatics (38.4% for cellulose and 25.4% for pine) was obtained in the presence of ZSM-5 material possessing highest micropore surface area and volume, highest amount of weak acid sites and Brønsted to Lewis acid sites ratio. Moreover, a slightly lower amount of coke was observed in this case. According to the authors the results suggested that weak acid sites facilitate the formation of aromatics while medium and strong Brønsted acid sites can be responsible for the production of coke. A decrease in the aromatic yield observed for the ZSM-5 with small crystal size (50 nm) may be associated with too small length of channels hindering the contact of enough acid sites in the catalyst by the reactants.

Although, the structure of ZSM-5 can favor the conversion of lignocellulosic biomass into aromatics it was indicated that this material cannot efficiently convert some larger oxygenates because of their higher molecular size than the pore size of the catalyst. Due to that the mentioned compounds are unable to enter inside ZSM-5 structure and can only be converted on its surface which limits the yield of the process. In order to improve the efficiency of production of aromatics in fast pyrolysis of beech wood, Li et al. decided to apply the catalyst prepared by desilication of ZSM-5 with sodium hydroxide solutions (Li et al., 2014). It was demonstrated that desilicated ZSM-5 was more active towards production of aromatics than unmodified material (the yield raised from 26.2% to 30.2%, respectively) and slightly limited the formation of coke (from 39.9% to 41.2%). The authors suggested that in

spite of a decrease in the density of Brønsted acid sites during desilication the growth in the amount of aromatics was associated with an increase in their accessibility due to the formation of mesoporous structure. This way the acid sites could be more efficiently used in the conversion of oxygenates. The formation of mesopores facilitated cracking of larger oxygenates to smaller molecules that could diffuse into ZSM-5 micropores.

On the other hand, Mante et al. applied ZSM-5 as co-catalyst to Y-zeolite in the catalytic pyrolysis of poplar (Mante et al., 2014). It is known that Y-zeolite is highly acidic and possesses large pore size. This catalyst is effective in deoxygenation of lignocellulosic biomass derived compounds, however its strong acidity facilitates dehydration reaction which results in a decrease of liquid fraction. In the case of Y-zeolite very efficient cracking of a higher amount of primary vapors into light gases with simultaneous formation of coke can be observed. An addition of ZSM-5 decreased cracking and carbon deposition rate leading to higher amount of liquid products. Smaller pore size of ZSM-5 hinders penetration of larger molecules and formation of polyaromatics being coke precursors. Moreover, the presence of ZSM-5 increased the amount of aromatics, while Y-zeolite favored production of aliphatics. It was suggested that the Y-zeolite facilitates formation of aliphatic hydrocarbons via hydrogen transfer reactions and ZSM-5 leads to formation of a higher yield of aromatics by isomerization, Diels-Alder and aldol condensation.

Another way of the bio-oil upgrading is hydrotreatment. The principles of the process are similar to that applied in the case of the hydrotreatment of conventional fuels. Jacobson et al. showed several examples of the catalyst which can be used for this process (Jacobson, Maheria, & Dalai, 2013). They described both zeolites and supported metallic (NiMo, CoMo, and noble metals) systems. Melligan et al. presented the results of the investigations of hydrolysis of different kinds of lignocellulosic biomass samples and catalytic vapor upgradation using Ni/ZSM-5 and Ni/MCM-41 catalysts (Melligan, Hayes, Kwapinski, & Leahy, 2012, 2013). The results of the investigations demonstrated that the presence of both hydrogen and catalyst led to significant improvement of the bio-oil properties. The most important change observed during the upgrading process was an increase in the amount of aromatic hydrocarbons. The Ni catalyst supported on ZSM-5 appeared the most efficient in the formation of aromatics. It was suggested that a growth in the amount of hydrocarbons was promoted by dehydration, decarboxylation and decarbonylation reactions. The experimental data also showed an increase in the yield of the lighter phenols. The authors indicated that the presence of metal on the support surfaces led to the destruction of high molecular weight phenols and production of smaller molecules and was more important in this case than the existence of acid sites on ZSM-5. Moreover, it was exhibited that an introduction of hydrogen decreased ethanoic acid content which was further reduced by the catalyst indicating that metallic sites of the catalysts facilitated degradation of the carboxylic acids.

The literature data showed that not only ZSM-5 based catalysts were investigated. Adam et al. performed proof of principle study of series of mesoporous catalysts (Al-MCM-41, SBA-15 and aluminum incorporated SBA-15 among others) used in the catalytic upgrading of biomass derived fast pyrolysis vapors of spruce wood (Adam et al., 2006). Before an analysis the upgrading products were divided into eight groups: hydrocarbons, phenols, furans, acids, alcohols, carbonyls, polycyclic aromatic hydrocarbons and heavy compounds. Hydrocarbons, phenols and alcohols were ascribed to desirable compounds, while acids, carbonyls and polycyclic aromatic hydrocarbons were assigned to undesirable ones. The interpretation of the obtained results revealed that all the investigated catalysts reduced the

yield of undesirable substances and increased the amount of desirable products. The most favorable ratio between desirable and undesirable compounds was obtained with the use of SBA-15 material. An incorporation of aluminum into SBA-15 framework resulted in further increase in the content of eligible compounds, but this phenomenon was also accompanied by a growth of undesirable products. In spite of that an increase in the pore size in the case of Al-MCM-41 catalysts led to the raise in the amount of desirable compounds, the yield of non favorable substances grew even faster and the ratio between desirable and undesirable compounds dropped. The comparison of two Al-MCM-41 samples (unmodified and modified by Cu) demonstrated that the presence of metal resulted in the increase in the amount of desirable products, however undesirable substances were formed in a greater amount as well. On the other hand the researchers noticed that one of the most significant drawbacks of the application of the catalysts to the upgrading of biomass fast pyrolysis vapors can be an increase in the content of polycyclic aromatic hydrocarbons.

Jeon et al. continued the study of the catalytic upgrading of bio-oil over mesoporous catalysts (Jeon et al., 2013). They used SBA-15 and AISBA-15 catalysts modified by platinum. As a feedstock three main biomass constituents – cellulose, hemicellulose and lignin were applied. In general, the presence of the catalyst improved the bio-oil quality for all biomass components. In the case of the pyrolysis of cellulose the use of AISBA-15 mesoporous material resulted in a growth in the amount of acids, hydrocarbons, phenolics, aromatics and polycyclic aromatic hydrocarbons in comparison to non-catalytic process. In the presence of Pt/AISBA-15, the amount of phenolics and aromatics was even larger and at the same time the slight reduction in the content of polycyclic aromatic hydrocarbons was observed. An increase in the amount of acids noticed for catalytic process can be associated with secondary decomposition of primary pyrolytic products. The carboxylic acids are usually decomposed in the presence of strong acid catalysts (i.e., H-ZSM-5), but the authors supposed that the acid strength of AISBA-15 catalyst is not sufficient for that. An application of SBA-15 to the pyrolysis of lignin enhanced the production of phenolics, but when AISBA-15 was used the content of aromatics also increased. The authors suggested that the presence of AISBA-15 facilitated depolymerization and oligomerization of lignin leading to the formation of a larger amount of aromatics. It was showed that the concentration of aromatic compounds could be further increased in the presence of platinum. This metal raised the rate of cracking and dehydrogenation reactions. Due to that a transformation of reaction intermediates to aromatics was facilitated.

Lignocellulosic biomass was also pyrolysed in the presence of amorphous silica alumina (Zabeti et al., 2012). This material was modified with alkali or alkaline earth metals, such as Na, K, Cs, Mg and Ca. The catalysts were prepared using dry impregnation method to give 10wt.% of the metal on the catalyst surface. All the investigated samples allowed for the deoxygenation of the obtained bio-oil in the range of 73%-85% (deoxygenation degree in comparison to the untreated biomass). The obtained results indicated that silica alumina modified by K and Na eliminated oxygen via decarboxylation route while the catalyst modified by Cs was more active in the removal of oxygen via decarbonylation. Moreover, it was observed that the last sample facilitated selective conversion of undesired phenols to hydrocarbons. Owing to that the catalyst modified by Cs was considered the most promising candidate for the production of bio-oil from biomass among the investigated materials.

4.2.2. Influence of Metal Oxides as Catalysts

The next part of the investigations of catalytic upgrading of lignocellulosic biomass pyrolysis vapors was devoted to the use of different metal oxides and their application as catalysts' supports. Lu et al. studied the influence of TiO₂ (rutile), TiO₂ (anatase), and ZrO₂/TiO₂ modified with Ce, Ru and Pd on the composition of bio-oil formed in fast pyrolysis of poplar wood (Q. Lu et al., 2010). Generally, it was noticed that the presence of the catalyst limited the amount of sugars and aldehydes. At the same time the content of furans, ketones, hydrocarbons and cyclopentanones increased. In the case of phenols and acids, their content depended on the type of the applied catalysts. Although, the authors did not provide detailed mechanism of the process it could be observed that the composition of the obtained bio-oil was influenced more strongly by different types of supports than their modification with noble metals.

The next work concerned the comparison of the catalytic activity of MgO, CaO, TiO₂, Fe₂O₃, NiO and ZnO nano metal oxides (Q.A. Lu et al., 2010). The same feedstock as was used in a previous case. The authors demonstrated that CaO was the most effective material in a described process. Its presence allowed for the reduction of anhydrosugars and phenols content, elimination of carboxylic acids and increase in the amount of hydrocarbons, cyclopentanones, ketones and aldehydes. It was observed that CaO facilitated production of acetaldehyde, acetone, 2-butanone and methanol, among others. The formation of hydrocarbons was also enhanced by Fe₂O₃. Unfortunately, the presence of this oxide facilitated the formation of polycyclic aromatic hydrocarbons.

The studies performed by our group (Grams, Niewiadomski, Ruppert, & Kwapinski, 2015) aimed at the determination of the activity of Ni catalysts supported on different metal oxides (Al₂O₃, SiO₂, MgO, CeO₂, and ZrO₂). Nickel was introduced on the support surface in the form of NiO which underwent reduction to the metallic nickel in the initial step of the reaction. The effects of the surface acidity, type of the support and its preparation method, crystalline phase of the support, interactions between active phase and the support, surface area of the catalyst and NiO crystalline size on the formation of cellulose fast pyrolysis vapors upgrading were investigated (Figure 7). The results of the measurements performed for unsupported NiO exhibited that the presence of this oxide can significantly change the composition of the obtained products. An increase in the content of hydrocarbons and esters, and slight reduction of the amount of alcohols, aldehydes and acids in comparison to non-catalytic process was observed. The further investigations revealed that an introduction of Ni on the support could enhance its catalytic properties. Taking into account the amount of hydrocarbon fraction produced, Ni/Al₂O₃ and Ni/ZrO₂ appeared the most interesting, while Ni/CeO₂ and Ni/SiO₂ exhibited at most moderate activity. Moreover, in the last two cases the highest content of carboxylic acids was noticed. The studies performed by Wang et al. suggested that the formation of hydrocarbons from oxygenates arising in the first step of the pyrolysis underwent rather via decarbonylation route (Wang, Kim, & Brown, 2014). The comparison of the composition of bio-oil obtained in the presence of Ni supported on different oxides with physicochemical properties of the catalysts showed that not only surface acidity can play an important role in the product distribution in the upgrading process (i.e., Ni/ZrO₂ catalysts prepared by three different methods showed diverse behavior in the investigated reaction). The results confirmed also a positive impact of CaO on reduction of carboxylic acids, however, this effect was not as strong as that described in (Q.A. Lu et al., 2010).

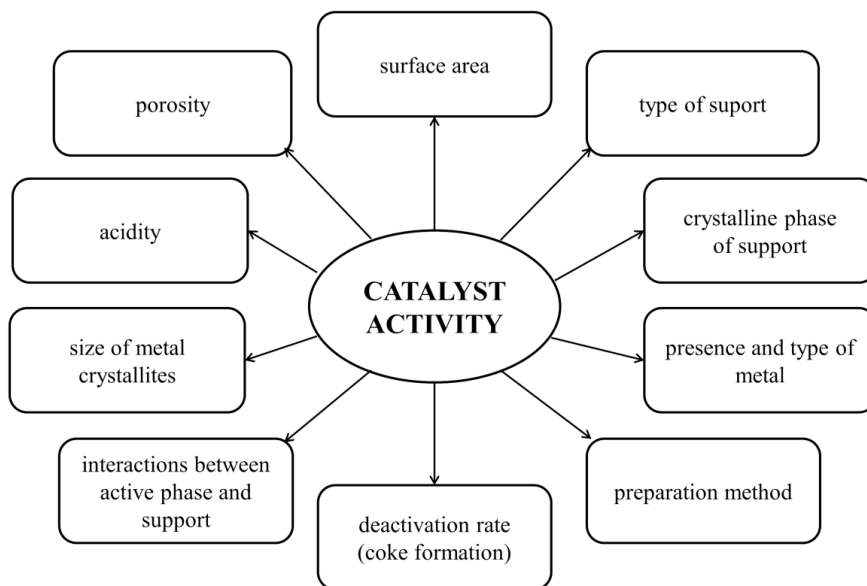


Figure 7. Factors affecting the activity of the catalyst.

As it was demonstrated the upgrading of the quality of bio-oil is a complex process. The main problems with the use of heterogeneous catalysts are associated with their relatively fast deactivation by formation of carbon deposit and selectivity leading to the production of both desirable and undesirable compounds. The activity of the catalysts not only depends on the surface acidity, but can also be controlled by the choice of appropriate method of preparation or catalyst modification by different dopants. The noble and transition metals were applied as an active phase of the supported catalysts, however the use of Ni seems to be more and more popular due to relatively low price and high activity of this metal.

5. POSSIBILITY OF THE INDUSTRIALIZATION OF BIOMASS CONVERSION PROCESSES

It was demonstrated in the previous part of this chapter that the researchers are still interested in developing the most efficient method of the conversion of lignocellulosic biomass and this problem has not been completely solved. However, it should be noted that several companies invented and implemented on a commercial scale various technologies of the production of fuels and fuel additives based on the conversion of the lignocellulosic biomass. One of them was developed by KiOR company which applied biomass to produce hydrocarbon-based mixture later processed to gasoline and diesel. In this process, the solid biomass particles are pretreated below 200°C to form a biomass-catalyst mixture. Then the deoxygenation and cracking processes take place and obtained intermediates are converted with steam at 450°C to produce fuel additives or biorafinery products (Yanik, Bartek, O'Connor, Stamires, & Brady, 2011). The other technology concerns pyrolysis of biomass performed in order to obtain bio-oil, olefins, methane, and carbon monoxide with further conversion of CO and CH₄ to generate H₂ for hydrotreating of the bio-oil (Ditsch, 2014).

It was also reported that Shell company patented the process of hydrocarbons transformation based on the conversion of a renewable feedstock. In this case, zeolites (with pore diameter from 0.5 nm to 0.7 nm) are used. The reaction is conducted at 480°C for 10 seconds. These conditions ensure cracking of paraffins to yield lighter products that contained a large amount of olefins (Maxwell, & Minderhoud, 1989). One of the latest solutions proposed by Shell to produce fuel blends is to mix the bio-based carbohydrates directly with hydrogen in the presence of a hydrogenolysis catalyst. In this way, alcohols, light polyols, and higher polyols can be obtained (Chheda, Johnson, & Powell, 2011).

Anellotech is one of the companies which focuses on the production of the substitutes of petroleum from non-food biomass by catalytic fast pyrolysis. In this process, the biomass is rapidly heated in the presence of zeolite catalyst which leads to the formation of hydrocarbons. One of the inventions of this company is related to the method of olefins separation from the mixture of the products. There are some advantages of this process, such as turning back a part of the by-products to the pyrolysis reactor for further conversion to more valuable substances or reducing char formation (Mazanec, Whiting, Pesa, & Norenberg, 2014).

CONCLUSION

In this chapter, we presented different aspects of the application of heterogeneous catalysts to the production of fuels and fuel additives from biomass. HMF as an example of fuel additive can be formed in the presence of acidic catalysts (i.e., different zeolites, Amberlyst, Nafion, heteropolyacid, etc.). GVL, product of the hydrogenation of levulinic acid, is produced with the use of metal base catalysts (depends on the reaction conditions in water phase mostly ruthenium based whereas in a gas phase also other metals were investigated like platinum). On the other hand, the literature data demonstrates that the upgrading of bio-oil was performed in the presence of zeolites (mainly ZSM-5), mesoporous materials like SBA-15, etc. However, an addition of metals (among which nickel was the most popular) in the case of supported catalysts resulted in substantial increase of the reaction yield. In all cases, an improvement of susceptibility to coke formation and thermal stability was key issue for the potential application of the studied catalysts to the industrial processes.

Perspectives on Biomass Valorization

Research involving lignocellulosic biomass utilization has significantly developed during last decade. This topic has been present in numerous areas (e.g., transport, energy, chemicals sectors). Various studies have been done on every step of biomass utilization, starting from the choice and cultivation of biomass feedstocks, biomass treatment, as well as their catalytic conversion. Based on this research two emerge areas has been chosen, one related to small number of selected chemicals called platform molecules, expected to have pivotal role in future biorafinery schemes, and second deals with production of bio-oil very important for energy sector.

The important question is what is next and if this is still promising direction of research for next decades.

Nowadays, there are contradictory opinions related to the use of biomass. On one hand, the governments across the world are stimulating the processes related to biomass valorization, and we are aware about the great potential of this feedstock, while, on the other hand, we are facing problems related with the biomass utilization such as high cost of transportations, availability issues, lack of feedstock's reproducibility, and complex way of valorization.

In our opinion, however, biomass research will still be important direction in the future, but could be limited to some areas such as, transportation and chemical sector where it is impossible to fulfill the growing demand with other renewable sources.

We should, however, concentrate our research on emerging targets and direct our investigations towards minimizing the drawbacks of biomass valorization. This would involve the improvement of technology and materials particularly heterogeneous catalysts.

ACKNOWLEDGMENTS

The authors gratefully acknowledge that part of this work was financially supported by the National Science Center (Poland) - project 2011/03/B/ST5/03270. A.M.R. acknowledges the support of the Polonium project "Hydrogen transfer reactions for biomass transformation."

REFERENCES

- Abou-Yousef, H., & Hassan, E. B. (2014). A novel approach to enhance the activity of H-form zeolite catalyst for production of hydroxymethylfurfural from cellulose. *Journal of Industrial and Engineering Chemistry*, 20, 1952-1957.
- Adam, J., Antonakou, E., Lappas, A., Stöcker, M., Nilsen, M. H., Bouzga, A., Hustad, J. E., & Øye, G. (2006). In situ catalytic upgrading of biomass derived fast pyrolysis vapours in a fixed bed reactor using mesoporous materials. *Microporous and Mesoporous Materials*, 96(1), 93-101.
- Alonso, D. M., Bond, J. Q., & Dumesic, J. A. (2010). Catalytic conversion of biomass to biofuels. *Green Chemistry*, 12, 1493-1513.
- Alonso, D. M., Wettstein, S. G., & Dumesic, J. A. (2013). Gamma-valerolactone, a sustainable platform molecule derived from lignocellulosic biomass. *Green Chemistry*, 15, 584-595.
- Al-Shaal, M. G., Wright, W. R. H., & Palkovits, R. (2012). Exploring the ruthenium catalysed synthesis of γ -valerolactone in alcohols and utilisation of mild solvent-free reaction conditions. *Green Chemistry*, 14, 1260-1263.
- Blanch, H. W., Simmons, B. A., & Klein-Marcuschamer, D. (2011). Biomass deconstruction to sugars. *Biotechnology Journal*, 6(9), 1086-1102.

- Braden, D. J., Henao, C. A., Heltzel, J., Maravelias, C. T., & Dumesic, J. A. (2011). Production of liquid hydrocarbon fuels by catalytic conversion of biomass-derived levulinic acid. *Green Chemistry*, *13*, 1755-1765.
- Brandt, A., Gräsvik, J., Hallett, J. P., & Welton, T. (2013). Deconstruction of lignocellulosic biomass with ionic liquids. *Green Chemistry*, *15*, 550-583.
- Bridgwater, A.V. (2012). Review of fast pyrolysis of biomass and product upgrading. *Biomass and Bioenergy*, *38*, 68-94.
- Brodeur, G., Yau, E., Badal, K., Collier, J., Ramachandran, K. B., & Ramakrishnan, S. (2011). Chemical and physicochemical pretreatment of lignocellulosic biomass: A review. *Enzyme Research*, *2011*, 1-17.
- Brown, T. R., & Brown, R. C. (2013). A review of cellulosic biofuel commercial-scale projects in the United States. *Biofuels, Bioproducts and Biorefining*, *7*(3), 235-245.
- Carlson, T. R., Tompsett, G. A., Conner, W. C., & Huber, G. W. (2009). Aromatic production from catalytic fast pyrolysis of biomass-derived feedstocks. *Topics in Catalysis*, *52*(3), 241-252.
- Carlson, T. R., Vispute, T. P., & Huber, G. W. (2008). Green gasoline by catalytic fast pyrolysis of solid biomass derived compounds. *ChemSusChem*, *1*(5), 397-400.
- Chatterjee, C., Pong, F., & Sen, A. (2015). Chemical conversion pathways for carbohydrates. *Green Chemistry*, *17*, 40-71.
- Chen, H. Z., Yu, B., & Jin, S. Y. (2011). Production of levulinic acid from steam exploded rice straw via solid superacid, S2O82-/ZrO2-SiO2-Sm2O3. *Bioresource Technology*, *102*(3), 3568-3570.
- Chheda, J. N., Huber, G. W., & Dumesic, J. A. (2007). Liquid-phase catalytic processing of biomass-derived oxygenated hydrocarbons to fuels and chemicals. *Angewandte Chemie International Edition*, *46*(38), 7164-7183.
- Chheda, J. N., Johnson, K. A., & Powell, J. B. (2011). Biofuels via hydrogenolysis-condensation. WO 2011082001 A1.
- Climent, M. J., Corma, A., & Iborra, S. (2014). Conversion of biomass platform molecules into fuel additives and liquid hydrocarbon fuels. *Green Chemistry*, *16*, 516-547.
- Collard, F. X., & Blin, J. (2014). A review on pyrolysis of biomass constituents: Mechanisms and composition of the products obtained from the conversion of cellulose, hemicellulose and lignin. *Renewable and Sustainable Energy Reviews*, *38*, 594-608.
- Corbel-Demilly, L., Ly, B. K., Minh, D. P., Tapin, B., Especel, C., Epron, F., . . . Pinel, C. (2013). Heterogeneous catalytic hydrogenation of biobased levulinic and succinic acids in aqueous solutions. *ChemSusChem*, *6*(12), 2388-2395.
- De, S., Saha, B., & Luque, R. (2015). Hydrodeoxygenation processes: Advances on catalytic transformations of biomass-derived platform chemicals into hydrocarbon fuels. *Bioresource Technology*, *178*, 108-118.
- Deng, L., Li, J., Lai, D. M., Fu, Y., & Guo, Q. X. (2009). Catalytic conversion of biomass-derived carbohydrates into γ -valerolactone without using an external H₂ supply. *Angewandte Chemie International Edition*, *48*(35), 6529-6532.
- Ding, D., Wang, J., Xi, J., Liu, X., Lu, G., & Wang, Y. (2014). High-yield production of levulinic acid from cellulose and its upgrading to gamma-valerolactone. *Green Chemistry*, *16*(8), 3846-3853.

- Ditsch, A. (2014). Bio-oil production with optimal byproduct processing. U. S. Patent No. 8,772,556 B2.
- Dornath, P. & Fan, W. (2014). Dehydration of fructose into furans over zeolite catalyst using carbon black as adsorbent. *Microporous and Mesoporous Materials*, 191, 10-17.
- Du, X. L., Bi, Q. Y., Liu, Y. M., Cao, Y., & Fan, K. N. (2011). Conversion of biomass-derived levulinate and formate esters into γ -valerolactone over supported gold catalysts. *ChemSusChem*, 4(12), 1838-1843.
- Du, X. L., He, L., Zhao, S., Liu, Y. M., Cao, Y., & He, H. Y. (2011). Hydrogen-independent reductive transformation of carbohydrate biomass into γ -valerolactone and pyrrolidone derivatives with supported gold catalysts. *Angewandte Chemie International Edition*, 50(34), 7815-7819.
- French, R., & Czernik, S. (2010). Catalytic pyrolysis of biomass for biofuels production. *Fuel Processing Technology*, 91(1), 25-32.
- Galletti, A. M. R., Antonetti, C., De Luise, V., & Martinelli, M. (2012). A sustainable process for the production of γ -valerolactone by hydrogenation of biomass-derived levulinic acid. *Green Chemistry*, 14, 688-694.
- Galletti, A. M. R., Antonetti, C., De Luise, V., Licursi, D., & Nassi, N. (2012). Levulinic acid production from waste biomass. *Bioresources*, 7(2), 1824-1835.
- Galletti, A. M. R., Antonetti, C., Ribechini, E., Colombini, M. P., Nassi, N., & Bonari, E. (2013). From giant reed to levulinic acid and gamma-valerolactone: A high yield catalytic route to valeric biofuels. *Applied Energy*, 102(C), 157-162.
- Grams, J., Niewiadomski, M., Ruppert, A. M. & Kwapinski, W. (2015). Influence of Ni catalyst support on the product distribution of cellulose fast pyrolysis vapors upgrading. *Journal of Analytical and Applied Pyrolysis*, 113, 557-563.
- Grams, J., Niewiadomski, M., Ruppert, A. M., & Kwapinski, W. (2015). Catalytic performance of a Ni catalyst supported on CeO₂, ZrO₂ and CeO₂-ZrO₂ in the upgrading of cellulose fast pyrolysis vapors. *Comptes Rendus Chimie*, 18, 1223-1228.
- Guo, F., Fang, Z., Charles, C., & Smith Jr., R. L. (2012). Solid acid mediated hydrolysis of biomass for producing biofuels. *Progress in Energy and Combustion Science*, 38(5), 672-690.
- Hakansson, H., & Ahlgren, P. (2005). Acid hydrolysis of some industrial pulps: effect of hydrolysis conditions and raw material. *Cellulose*, 12(2), 177-183.
- Haykir, N. I., Bahcegul, E., Bicak, N., & Bakir, U. (2013). Pretreatment of cotton stalk with ionic liquids including 2-hydroxy ethyl ammonium formate to enhance biomass digestibility. *Industrial Crops and Products*, 41, 430-436.
- Hendriks, A. T. W. M. & Zeeman, G. (2009). Pretreatments to enhance the digestibility of lignocellulosic biomass. *Bioresource Technology*, 100(1), 10-18.
- Hengne, A. M., Malawadkar, A. V., Biradar, N. S., & Rode, C. V. (2014). Surface synergism of an Ag-Ni/ZrO₂ nanocomposite for the catalytic transfer hydrogenation of bio-derived platform molecules. *RSC Advances*, 4, 9730-9736.
- Hu, L., Wu, Z., Xu, J., Sun, Y., Lin, L., & Liu, S. (2014). Zeolite-promoted transformation of glucose into 5-hydroxymethylfurfural in ionic liquid. *Chemical Engineering Journal*, 244, 137-144.
- Huber, G. W., & Corma, A. (2007). Synergies between bio- and oil refineries for the production of fuels from biomass. *Angewandte Chemie International Edition*, 46(38), 7184-7201.

- Iliopoulou, E. F., Stefanidis, S. D., Kalogiannis, K. G., Delimitis, A., Lappas, A. A., & Triantafyllidis, K. S. (2012). Catalytic upgrading of biomass pyrolysis vapors using transition metal-modified ZSM-5 zeolite. *Applied Catalysis B: Environmental*, *127*, 281-290.
- Isahak, W. N. R. W., Hisham, M. W. M., Yarmo, M. A., & Hin, T. Y. (2012). A review on bio-oil production from biomass by using pyrolysis method. *Renewable and Sustainable Energy Reviews*, *16*(8), 5910-5923.
- Isikgor, F. H., & Becer, C. R. (2015). Lignocellulosic biomass: a sustainable platform for the production of bio-based chemicals and polymers. *Polymer Chemistry*, *6*, 4497-4559.
- Jacobson, K., Maheria, K. C., & Dalai, A. K. (2013). Bio-oil valorization: A review. *Renewable and Sustainable Energy*, *23*, 91-106.
- Jae, J., Coolman, R., Mountziaris, T. J., & Huber, G. W. (2014). Catalytic fast pyrolysis of lignocellulosic biomass in a process development unit with continual catalyst addition and removal. *Chemical Engineering Science*, *108*, 33-46.
- Jeon, M. J., Jeon, J. K., Suh, D. J., Park, S. H., Sa, Y. J., Joo, S. H., & Park, Y. K. (2013). Catalytic pyrolysis of biomass components over mesoporous catalysts using Py-GC/MS. *Catalysis Today*, *204*, 170-178.
- Wang, J., Zheng, Y., & Zhang, S. (2010). The application of ionic liquids in dissolution and separation of lignocellulose. *Clean Energy Systems and Experiences Kei Eguchi* (2010), ISBN 978-953-307-147-3
- Kilpeläinen, I., Xie, H., King, A., Granstrom, M., Heikkinen, S., & Argyropoulos, D. S. (2007). Dissolution of wood in ionic liquids. *Journal of Agricultural and Food Chemistry*, *55*(22), 9142-9148.
- Kumar, P., Barrett, D. M., Delwiche, M. J., & Stroeve, P. (2009). Methods for pretreatment of lignocellulosic biomass for efficient hydrolysis and biofuel production. *Industrial and Engineering Chemistry Research*, *48*(8), 3713-3729.
- Kumar, S., Dheeran, P., Singh, S. P., Mishra, I. M., & Adhikari, D. K. (2015). Kinetic studies of two-stage sulphuric acid hydrolysis of sugarcane bagasse. *Renewable Energy*, *83*, 850-858.
- Lange, J. P., Price, R., Ayoub, P. M., Louis, J., Petrus, L., Clarke, L. & Gosselink, H. (2010). Valeric biofuels: A platform of cellulosic transportation fuels. *Angewandte Chemie International Edition*, *49*(26), 4479-4483.
- Lee, H. V., Hamid, S. B. A., & Zain, S. K. (2014). Conversion of lignocellulosic biomass to nanocellulose: Structure and chemical process. *The Scientific World Journal*, *2014*, 1-20.
- Li, C. Z., Wang, Q., & Zhao, Z. K. (2008). Acid in ionic liquid: An efficient system for hydrolysis of lignocellulose. *Green Chemistry*, *10*(2), 177-182.
- Li, J., Li, X., Zhou, G., Wang, W., Wang, C., Komarneni, S., & Wang, Y. (2014). Catalytic fast pyrolysis of biomass with mesoporous ZSM-5 zeolites prepared by desilication with NaOH solutions. *Applied Catalysis A: General*, *470*, 115-122.
- Li, Q., He, Y. C., Xian, M., Jun, G., Xu, X., Yang, J. M., & Li, L. Z. (2009). Improving enzymatic hydrolysis of wheat straw using ionic liquid 1-ethyl-3-methyl imidazolium diethyl phosphate pretreatment. *Bioresource Technology*, *100*(14), 3570-3575.
- Liao, H. T., Ye, X. N., Lu, Q., & Dong, C. Q. (2014). Overview of bio-oil upgrading via catalytic cracking. *Advanced Materials Research*, *827*, 25-29.

- Liu, G., Wright, M. M., Zhao, Q., & Brown, R. C. (2015). Catalytic fast pyrolysis of duckweed: Effects of pyrolysis parameters and optimization of aromatic production. *Journal of Analytical and Applied Pyrolysis*, *112*, 29-36.
- Lu, Q., Zhang, Y., Tang, Z., Li, W. Z., & Zhu, X. F. (2010). Catalytic upgrading of biomass fast pyrolysis vapors with titania and zirconia/titania based catalysts. *Fuel*, *89*(8), 2096-2103.
- Lu, Q., Zhang, Z. F., Dong, C. Q., & Zhu, X. F. (2010). Catalytic upgrading of biomass fast pyrolysis vapors with nano metal oxides: An analytical Py-GC/MS study. *Energies*, *3*(11), 1805-1820.
- Luo, W., Deka, U., Beale, A. M., van Eck, E. R. H., Bruijninx, P. C. A., & Weckhuysen, B. M. (2013). Ruthenium-catalyzed hydrogenation of levulinic acid: Influence of the support and solvent on catalyst selectivity and stability. *Journal of Catalysis*, *301*, 175-186.
- Luo, W., Sankar, M., Beale, A. M., He, Q., Kiely, C. J., Bruijninx, P. C. A., & Weckhuysen, B. M. (2015). High performing and stable supported nano-alloys for the catalytic hydrogenation of levulinic acid to γ -valerolactone. *Nature Communications*, *6*, 6540-6549.
- Luque, R., Herrero-Davila, L., Campelo, J. M., Clark, J. H., Hidalgo, J. M., Luna, D., Marinas, J. M., & Romero, A. A. (2008). Biofuels: A technological perspective. *Energy and Environmental Science*, *1*, 542-564.
- Maarten, A., Kootstra, J., Beeftink, H. H., Scott, E. L., & Sanders, J. P. M. (2009). Comparison of dilute mineral and organic acid pretreatment for enzymatic hydrolysis of wheat straw. *Biochemical Engineering Journal*, *46*, 126-131.
- Mante, O. D., Agblevor, F. A., Oyama, S. T., & McClung, R. (2014). Catalytic pyrolysis with ZSM-5 based additive as co-catalyst to Y-zeolite in two reactor configurations. *Fuel*, *117*, 649-659.
- Manzer, L. E. (2004). Catalytic synthesis of α -methylene- γ -valerolactone: a biomass-derived acrylic monomer. *Applied Catalysis A: General*, *272*(1-2), 249-256.
- Maxwell, I. E., & Minderhoud, J. K. (1989). Process for the conversion of a hydrocarbonaceous feedstock. U. S. Patent No. 4,886,934.
- Mazanec, T., Whiting, J., Pesa, F., & Norenberg, G. (2014). Olefin conditioning in a fast catalytic pyrolysis recycle process. U. S. Patent No. 2014/0031583 A1.
- Mehdi, H., Fábos, V., Tuba, R., Bodor, A., Mika, L. T., & Horváth, I. T. (2008). Integration of homogeneous and heterogeneous catalytic processes for a multi-step conversion of biomass: From sucrose to levulinic acid, γ -valerolactone, 1,4-pentanediol, 2-methyl-tetrahydrofuran, and alkanes. *Topics in Catalysis*, *48*(1-4), 49-54.
- Melligan, F., Hayes, M. H. B., Kwapinski, W., & Leahy, J. J. (2012). Hydro-pyrolysis of biomass and online catalytic vapor upgrading with Ni-ZSM-5 and Ni-MCM-41. *Energy and Fuels*, *26*(10), 6080-6090.
- Melligan, F., Hayes, M. H. B., Kwapinski, W., & Leahy, J. J. (2013). A study of hydrogen pressure during hydro-pyrolysis of *Miscanthus x giganteus* and online catalytic vapour upgrading with Ni on ZSM-5. *Journal of Analytical and Applied Pyrolysis*, *103*, 369-377.
- Michel, C., Zaffran, J., Ruppert, A. M., Matras-Michalska, J., Jędrzejczyk, M., Grams, J., & Sautet, P. (2014). Role of water in metal catalyst performance for ketone hydrogenation: a joint experimental and theoretical study on levulinic acid conversion into γ -valerolactone. *Chemical Communications*, *50*, 12450-12453.

- Mushrif, S. H., Vasudevan, V., Krishnamurthy, C. B., & Venkatesh, B. (2015). Multiscale molecular modeling can be an effective tool to aid the development of biomass conversion technology: A perspective. *Chemical Engineering Science*, *121*, 217-235.
- Obregón, I., Corro, E., Izquierdo, U., Reques, J., & Arias, P. L. (2014). Levulinic acid hydrogenolysis on Al₂O₃-based Ni-Cu bimetallic catalysts. *Chinese Journal of Catalysis*, *35*(5), 656-662.
- Ordonsky, V. V., van der Schaaf, J., Schouten, J. C., & Nijhuis, T. A. (2012). The effect of solvent addition on fructose dehydration to 5-hydroxymethylfurfural in biphasic system over zeolites. *Journal of Catalysis*, *287*, 68-75.
- Ortiz-Cervantes, C., & García, J. J. (2013). Hydrogenation of levulinic acid to γ -valerolactone using ruthenium nanoparticles. *Inorganica Chimica Acta*, *397*, 124-128.
- Peng, L., Lin, L., Zhang, J., Zhuang, J., Zhang, B., & Gong, Y. (2010). Catalytic conversion of cellulose to levulinic acid by metal chlorides. *Molecules*, *15*(8), 5258-5272.
- Pinkert, A., Marsh, K. N., Pang, S., & Staiger, M. P. (2009). Ionic liquids and their interaction with cellulose. *Chemical Reviews*, *109*(12), 6712-6728.
- van Putten, R. J., van der Waal, J. C., de Jong, E., Rasrendra, C. B., Heeres, H. J., & de Vries, J. G. (2013). Hydroxymethylfurfural, a versatile platform chemical made from renewable resources. *Chemical Reviews*, *113*(3), 1499-1597.
- Rackemann, D. W., & Doherty, W. O. (2011). The conversion of lignocellulosics to levulinic acid. *Biofuels, Bioproducts and Biorefining*, *5*(2), 198-214.
- Ramli, N. A. S., & Amin, N. A. S. (2015). Fe/HY zeolite as an effective catalyst for levulinic acid production from glucose: Characterization and catalytic performance. *Applied Catalysis B: Environmental*, *163*, 487-498.
- Ruddy, D. A., Schaidle, J. A., Ferrell III, J. R., Wang, J., Moens, L., & Hensley, J. E. (2014). Recent advances in heterogeneous catalysts for bio-oil upgrading via “ex situ catalytic fast pyrolysis”: Catalyst development through the study of model compounds. *Green Chemistry*, *16*, 454-490.
- Ruppert, A. M., Grams, J., Jędrzejczyk, M., Matras-Michalska, J., Keller, N., Ostojka K., & Sautet, P. (2015). Titania-supported catalysts for levulinic acid hydrogenation: influence of support and its impact on γ -valerolactone yield. *ChemSusChem*, *8*(9), 1538-1547.
- Ruppert, A. M., Grams, J., Matras-Michalska, J., Chełmicka M., & Przybysz, P. (2014). ToF-SIMS study of the surface of catalysts used in biomass valorization. *Surface and Interface Analysis*, *46*(10-11), 726-730.
- Serrano-Ruiz, J. C., & Dumesic, J. A. (2011). Catalytic routes for the conversion of biomass into liquid hydrocarbon transportation fuels. *Energy and Environmental Science*, *4*, 83-99.
- Serrano-Ruiz, J. C., Luque, R., & Sepulveda-Escribano, A. (2011). Transformations of biomass-derived platform molecules: from high added-value chemicals to fuels via aqueous-phase processing. *Chemical Society Reviews*, *40*, 5266-5281.
- Sharma, R., Palled, V., Sharma-Shivappa, R. R., & Osborne, J. (2013). Potential of potassium hydroxide pretreatment of switchgrass for fermentable sugar production. *Applied Biochemistry and Biotechnology*, *169*, 761-772.
- Shuttleworth, P. S., De Bruyn, M., Parker, H. L., Hunt, A. J., Budarin, V. L., Matharu, A. S., & Clark, J. H. (2014). Applications of nanoparticles in biomass conversion to chemicals and fuels. *Green Chemistry*, *16*, 573-584.

- Son, P. A., Nishimura, S., & Ebitani, K. (2012). Synthesis of levulinic acid from fructose using Amberlyst-15 as a solid acid catalyst. *Reaction Kinetics, Mechanisms and Catalysis*, 106(1), 185-192.
- Son, P. A., Nishimura, S., & Ebitani, K. (2014). Production of γ -valerolactone from biomass-derived compounds using formic acid as a hydrogen source over supported metal catalysts in water solvent. *RSC Advances*, 4(21), 10525-10530.
- Stefanidis, S. D., Kalogiannis, K. G., Iliopoulou, E. F., Lappas, A. A., & Pilavachi, P. (2011). In-situ upgrading of biomass pyrolysis vapors: Catalyst screening on a fixed bed reactor. *Bioresource Technology*, 102(17), 8261-8267.
- Sun, Y., & Cheng, J. (2002). Hydrolysis of lignocellulosic materials for ethanol production: a review. *Bioresource Technology*, 83(1), 1-11.
- Sun, Z. Y., Tang, Y. Q., Iwanaga, T., Sho, T., & Kida, K. (2011). Production of fuel ethanol from bamboo by concentrated sulfuric acid hydrolysis followed by continuous ethanol fermentation. *Bioresource Technology*, 102(23), 10929-10935.
- Takeuchi, Y., Jin, F., Tohji, K., & Enomoto, H. (2008). Acid catalytic hydrothermal conversion of carbohydrate biomass into useful substances. *Journal of Materials Science*, 43(7), 2472-2475.
- Tang, X., Zeng, X., Li, Z., Hu, L., Sun, Y., Liu, S., Lei, T., & Lin, L. (2014). Production of γ -valerolactone from lignocellulosic biomass for sustainable fuels and chemicals supply. *Renewable and Sustainable Energy Reviews*, 40, 608-620.
- Upare, P. P., Lee, J. M., Hwang, D. W., Halligudi, S. B., Hwang, Y. K., & Chang, J. S. (2011). Selective hydrogenation of levulinic acid to γ -valerolactone over carbon-supported noble metal catalysts. *Journal of Industrial and Engineering Chemistry*, 17(2), 287-292.
- Van de Vyver, S., Thomas, J., Geboers, J., Keyzer, S., Smet, M., Dehaen, W., Jacobs, P. A., & Sels, B. F. (2011). Catalytic production of levulinic acid from cellulose and other biomass-derived carbohydrates with sulfonated hyperbranched poly(arylene oxindole)s. *Energy & Environmental Science*, 4, 3601-3610.
- Vancov, T., Alston, A. S., Brown, T., & McIntosh, S. (2012). Use of ionic liquids in converting lignocellulosic material to biofuels. *Renewable Energy*, 45, 1-6.
- Wang, H., Male, J., & Wang, Y. (2013). Recent advances in hydrotreating of pyrolysis bio-oil and its oxygen-containing model compounds. *ACS Catalysis*, 3(5), 1047-1070.
- Wang, K., Johnston, P. A., & Brown, R. C. (2014). Comparison of in-situ and ex-situ catalytic pyrolysis in a micro-reactor system. *Bioresource Technology*, 173, 124-131.
- Wang, K., Kim, K. H., & Brown, R. C. (2014). Catalytic pyrolysis of individual components of lignocellulosic biomass. *Green Chemistry*, 16, 727-735.
- Wang, T., Nolte, M. W., & Shanks, B. H. (2014). Catalytic dehydration of C6 carbohydrates for the production of hydroxymethylfurfural (HMF) as a versatile platform chemical. *Green Chemistry*, 16, 548-572.
- Wang, W., Wang, S., Ma, X., & Gong, J. (2011). Recent advances in catalytic hydrogenation of carbon dioxide. *Chemical Society Reviews*, 40(7), 3703-3727.
- Wright, W. R. H., & Palkovits, R. (2012). Development of heterogeneous catalysts for the conversion of levulinic acid to γ -valerolactone. *Chem Sus Chem*, 5(9), 1657-1667.
- Xu, J.; Cheng, J. J.; (2011). Pretreatment of switchgrass for sugar production with the combination of sodium hydroxide and lime. *Bioresource Technology*, 102(4), 3861-3868.

- Xue, Y., Zhou, S., Brown, R. C., Kelkar, A., & Bai, X. (2015). Fast pyrolysis of biomass and waste plastic in a fluidized bed reactor. *Fuel*, *156*, 40-46.
- Ya'aini, N., Amin, N. A. S., & Asmadi, M. (2012). Optimization of levulinic acid from lignocellulosic biomass using a new hybrid catalyst. *Bioresource Technology*, *116*, 58-65.
- Ya'aini, N., Amin, N. A. S., & Endud, S. (2013). Characterization and performance of hybrid catalysts for levulinic acid production from glucose. *Microporous and Mesoporous Materials*, *171*, 14-23.
- Yaman, S. (2004). Pyrolysis of biomass to produce fuels and chemical feedstocks. *Energy Conversion and Management*, *45*(5), 651-671.
- Yan, H., Yang, Y., Tong, D., Xiang, X., & Hu, C. (2009). Catalytic conversion of glucose to 5-hydroxymethylfurfural over SO₄²⁻/ZrO₂ and SO₄²⁻/ZrO₂-Al₂O₃ solid acid catalysts. *Catalysis Communications*, *10*, 1558-1563.
- Yan, K., Lafleur, T., Wu, G., Liao, J., Ceng, C., & Xie, X. (2013). Highly selective production of value-added γ -valerolactone from biomass-derived levulinic acid using the robust Pd nanoparticles. *Applied Catalysis A: General*, *468*, 52-58.
- Yan, Z. P., Lin, L., & Liu, S. (2009). Synthesis of γ -valerolactone by hydrogenation of biomass-derived levulinic acid over Ru/C catalyst. *Energy and Fuels*, *23*(8), 3853-3858.
- Yang, H., Coolman, R. J., Karanjkar, P., Wang, H., Xu, Z., Chen, H., Moutziaris, T. J., & Huber, G. W. (2015). The effect of steam on the catalytic fast pyrolysis of cellulose. *Green Chemistry*, *17*(5), 2912-2923.
- Yang, Z., Kang, H., Guo, Y., Zhuang, G., Bai, Z., Zhang, H., Feng, C., & Dong, Y. (2013). Dilute-acid conversion of cotton straw to sugars and levulinic acid via 2-stage hydrolysis. *Industrial Crops and Products*, *46*, 205-209.
- Yanik, S., Bartek, R., O'Connor, P., Stamires, D., & Brady, M. (2011). Biomass conversion process. U. S. Patent No. 8, 003,835 B2.
- Yoon, S. Y., Kim, B. R., Han, S. H., & Shin, S. J. (2015). Different response between woody core and bark of goat willow (*Salix caprea* L.) to concentrated phosphoric acid pretreatment followed by enzymatic saccharification. *Energy*, *81*, 21-26.
- Zabeti, M., Nguyen, T. S., Lefferts, L., Heeres, H. J., & Seshan, K. (2012). In situ catalytic pyrolysis of lignocellulose using alkali-modified amorphous silica alumina. *Bioresource Technology*, *118*, 374-381.
- Zhang, H., Xiao, R., Jin, B., Shen, D., Chen, R., & Xiao, G. (2013). Catalytic fast pyrolysis of straw biomass in an internally interconnected fluidized bed to produce aromatics and olefins: Effect of different catalysts. *Bioresource Technology*, *137*, 82-87.
- Zhang, Y., Brown, T. R., Hu, G., & Brown, R. C. (2013). Techno-economic analysis of two bio-oil upgrading pathways. *Chemical Engineering Journal*, *225*, 895-904.
- Zhao, H., Kwak, J. H., Wang, Y., Franz, J. A., White, J. M., & Holladay, J. E. (2006). Effects of crystallinity on dilute acid hydrolysis of cellulose by cellulose ball-milling study. *Energy and Fuels*, *20*(2), 807-811.
- Zhao, Q., Wang, L., Zhao, S., Wang, X., & Wang, S. (2011). High selective production of 5-hydroxymethylfurfural from fructose by a solid heteropolyacid catalyst. *Fuel*, *90*(6), 2289-2293.
- Zhao, S., Cheng, M., Li, J., Tian, J., & Wang, X. (2011). One pot production of 5-hydroxymethylfurfural with high yield from cellulose by a Brønsted-Lewis-surfactant-combined heteropolyacid catalyst. *Chemical Communications*, *47*, 2176-2178.

-
- Zheng, A., Zhao, Z., Chang, S., Huang, Z., Wu, H., Wang, X., He, F., & Li, H. (2014). Effect of crystal size of ZSM-5 on the aromatic yield and selectivity from catalytic fast pyrolysis of biomass. *Journal of Molecular Catalysis A: Chemical*, 383-384, 23-30.
- Zhu, J., Wan, C., & Li, Y. (2010). Enhanced solid-state anaerobic digestion of corn stover by alkaline pretreatment. *Bioresource Technology*, 101(19), 7523-7528.

*Chapter 8***LIGNIN CONVERSION TO FUELS AND CHEMICALS**

Yu Gao, Merima Beganovic and Marcus B. Foston*

Department of Energy, Environmental and Chemical Engineering,
Washington University in St. Louis, Saint Louis, MO, US

ABSTRACT

The rapid worldwide increase in the consumption of fuels and chemicals has led to concern over the depletion of non-renewable resources and the environmental impact of their processing and utilization. The structure of lignin, the second most abundant biopolymer on earth after cellulose, suggests that its deconstruction via various conversion technologies (e.g., gasification, pyrolysis, etc.) can be a renewable alternative for the production of fuels and chemicals. However, commercial conversion of lignin not only into transportation fuels but also commodity and value-added chemicals is currently limited by insufficient development in technologies that 1) overcome the recalcitrance and structural heterogeneity of lignin, 2) isolate and recover lignin as a co-product of and feedstock for fuel/chemical production, and 3) deconstruct lignin in a controlled manner such that product separations are tractable. This chapter introduces topics relevant to the conversion of lignin including the 1) structure and biosynthesis of lignin, 2) isolation and recovery of lignin, and 3) methods used to characterize lignin and its deconstruction products. Major technologies currently being developed with regards to lignin deconstruction and depolymerization are reviewed, focusing on conversion 1) mechanisms, 2) processing factors, and 3) products. Lastly, a future perspective is presented, detailing the potential intersection of lignin genetic engineering with the conversion of lignin into desired products.

Keywords: lignin, depolymerization, biorefinery, conversion, structure, isolation

* Corresponding Author address; Email: mfonton@wustl.edu.

INTRODUCTION

One of the great challenges that societies face in the 21st century is the development of sustainable technologies that can accommodate increasing worldwide demand for fuels, chemicals, and materials (Bentley, 2002; Qu, Zhu, Liu, Bao, & Lin, 2006; Ragauskas et al., 2006). As the world's population increases and quality of life improves, the global demand for fuels, chemicals, and materials is projected to increase 50% by the year 2025 (Ragauskas et al., 2006). Currently, the world's energy and material supply mainly is derived from non-renewable, fossil resources (Renewable Energy Policy Network, 2010). More importantly, their processing and consumption greatly affects the environment (Bentley, 2002). Emissions, such as greenhouse gas, soot, and ash, resulting from fossil resource utilization can cause issues related to negative human health outcomes and environment impacts (e.g., global warming, acid rain, etc.) (Barbir, Veziroğlu, & Plass, 1990; Barreto, Makihira, & Riahi, 2003; Klass, 1998; Panwar, Kaushik, & Kothari, 2011; Von Blottnitz & Curran, 2007). Many estimates suggest irreparable damage to the climate can occur due to the release of carbon in the form of CO₂ and CH₄ that was once sequestered in the earth as coal, petroleum, and natural gas (Coumou & Rahmstorf, 2012). One recently developed concept, the biorefinery, has been considered as a promising direction for reliable energy, chemical, and material production from renewable and sustainable resources.

A biorefinery is analogous to current petroleum refineries, generating a wide-range of products by processing plant biomass as feedstock (Pandey & Kim, 2011; Ragauskas et al., 2014; Ragauskas et al., 2006). In a biorefinery, atmospheric CO₂, fixed by plants through photosynthesis can be efficiently converted to fuels, chemicals, and materials, thus establishing a sustainable carbon recycling pathway. Currently, bio-based ethanol has been introduced on a demonstration-scale in several countries (Hahn-Hägerdal, Galbe, Gorwa-Grauslund, Lidén, & Zacchi, 2006). Even though bio-ethanol can be produced at competitive prices, much of this production relies on raw materials like corn, sugar cane, or sugar beet, which has limited utilization because large-scale conversion can threaten food supplies and biodiversity (Hahn-Hägerdal et al., 2006). Efforts have shifted towards production of second generation biofuels obtained from abundant and relatively cheap lignocellulose feedstock, such as agricultural and forest residues (Hahn-Hägerdal et al., 2006). Lignocellulosic biomass is mainly comprised of cellulose, hemicellulose, and lignin. Thus, the biorefinery concept requires the efficient utilization for all three of these lignocellulosic cell wall components to increase biorefinery product diversity, value, and yield. Most biorefinery schemes emphasize fermentation of sugars derived from cellulose and hemicellulose to generate fuels and chemicals (Pandey & Kim, 2011; Ragauskas et al., 2014); however, under this scheme lignin remains relatively underutilized (Pandey & Kim, 2011).

Lignin, the second most abundant terrestrial polymer after cellulose, constitutes approximately 15-30% of the dry weight of lignocellulosic materials. Currently, lignin is considered as waste (Argyropoulos & Menachem, 1997; Boerjan, Ralph, & Baucher, 2003). However, lignin is a very abundant and potentially useful renewable resource. There are approximately 3×10^{11} metric tons of lignin on the planet, being biosynthesized at an annual rate of approximately 2×10^{10} metric tons (Argyropoulos & Menachem, 1997). Each year, approximately 4×10^7 to 5×10^7 metric tons of lignin are generated worldwide as industrial waste, mainly as a result of paper manufacturing and bio-ethanol production (Kleinert &

Barth, 2008). Moreover, as the bio-economy grows and second generation biofuel production increases, even more lignin will be available in the future. For example, in the US, annual lignin production only from commercial bio-ethanol biorefineries (14 billion gal/year) is projected to be about 5×10^7 metric tons by 2022 (Kaparaju, Serrano, Thomsen, Kongjan, & Angelidaki, 2009; Regalbuto, 2009). As a result, the biorefinery concept, economical biomass processing, and large-scale biofuel production, in part, relies of the efficient conversion of lignin into valuable products.

Due to the complex and heterogeneous nature of lignin, it is extremely challenging to depolymerize or deconstruct in a controlled fashion for the production of valuable products. Most lignin is currently used in low value commercial applications, such as a low-grade fuel that provides on-site process heat and power generation (Doherty, Mousavioun, & Fellows, 2011; Gasser, Hommes, Schäffer, & Corvini, 2012; Huber, Iborra, & Corma, 2006; Vishtal & Kraslawski, 2011). Lignosulfonates have been used as road binders, soil neutralizers, and drilling mud viscosity control agents (Gargulak & Lebo, 1999; Harkin, 1969; Liu, Jiang, & Yu, 2015). However, the abundant aromatic substructures that comprise lignin's molecular structure are similar to many value-added chemicals derived from petroleum. The natural abundance, high carbon-to-oxygen ratio (compared to cell wall carbohydrates), high energy density, and aromatic substructure of lignin make it a highly attractive potential source for the production of diverse types of renewable fuels, chemicals, and materials.

This chapter provides an overview of the current understanding of lignin including the 1) physical and chemical properties of lignin, 2) methods used to isolate and recover lignin, 3) techniques used to characterize lignin and lignin deconstruction products, and 4) technologies being developed to convert lignin into fuels and chemicals. These conversion technologies will be categorized and discussed as thermal, biological, and hybrid conversion platforms.

LIGNIN

What Is Lignin?

Lignin is synthesized as a major plant secondary cell wall component, providing structural integrity, facilitating vascular water transport, and protecting plants from pathogens (Boerjan et al., 2003; Campbell & Sederoff, 1996; Freudenberg, 1959). Lignin contributes to the stiffness and hydrophobicity of xylem cell walls, which allows the xylem to resist the compressive stresses caused by water transport and to support the mass of the plant itself (Campbell & Sederoff, 1996). Lignin content, composition, and distribution are critical factors affecting the growth and development of plants. While the inherent recalcitrance, rigidity, and insolubility of lignin make it naturally resistant to biological or environmental mediated degradation (advantageous properties for the plant), those same properties also make lignin difficult and expensive to industrially convert into value-added products (Campbell & Sederoff, 1996). In addition, the molecular structure of lignin is comprised of randomly positioned phenolic subunits and subunit linkages. This structural heterogeneity can lead to a wide distribution of deconstruction products, making the conversion and purification of desired products from lignin even more challenging.

Lignin Structure

Lignin is described as a random, racemic, and three-dimensional polymer comprised of variously linked hydroxycinnamyl alcohol monomers or monolignols, differing mainly in their degree of methoxylation (e.g., coniferyl, sinapyl, and *p*-coumaryl alcohol) as shown in Figure 1. Lignification of the plant cell wall is mediated through radical coupling reactions. Following the transport of monolignols into the plant cell wall, enzymes (e.g., peroxidases, laccases, polyphenol oxidases, and coniferyl alcohol oxidase) catalyze dehydrogenation of phenolic moieties to generate monolignol radicals. These relatively stable monolignol radicals undergo radical-coupling reactions in a combinatorial fashion to polymerize a three-dimensional lignin polymer (Boerjan et al., 2003). Typically, coniferyl, sinapyl, and *p*-coumaryl alcohol monolignols are incorporated into lignin as guaiacyl (G), syringyl (S), and *p*-hydroxyphenyl (H) units (i.e., phenylpropanoids units). Coupling between monolignols and/or pre-formed lignin oligomers can result in a number of inter-unit linkages. Common types of lignin inter-unit linkages are illustrated in Figure 2. Nevertheless, after many years of study, the exact molecular structure of native lignin still remains unclear. However, as methods for lignin substructure identification have improved, both common and rare monomer and substructures in lignin have been elucidated. The results from these studies have yielded, what is believed to be, an approximate representation of the structure of lignin (shown in Figure 3).

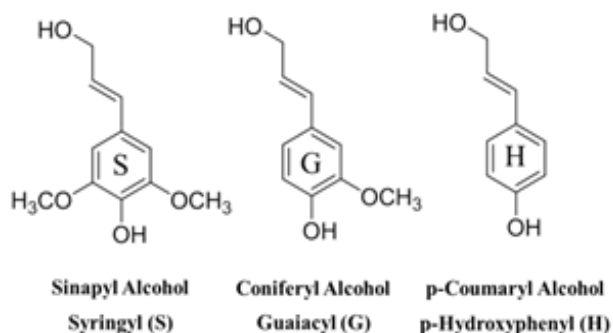


Figure 1. Hydroxycinnamyl alcohol monomers in the biosynthesis of lignin.

The composition and quantity of lignin varies from species-to-species, within a species (i.e., genotype-to-genotype), or even within a single genotype (i.e., plant clone-to-plant clone), influenced by genetic, developmental, and environmental factors (Boerjan et al., 2003; Campbell & Sederoff, 1996). For example, the cell walls from gymnosperm plants (softwood) are known to contain a greater amount of lignin, followed by the cell walls from dicot (hardwood) and monocot (grasses) angiosperm plants (Boerjan et al., 2003). Moreover, hardwood lignin has higher methoxyl content because it consists of roughly equal amounts of guaiacyl and syringyl units, while softwood lignin is mainly guaiacyl units. Grass lignin is composed of similar amounts of guaiacyl and syringyl units along with some *p*-hydroxyphenyl units (Boerjan et al., 2003).

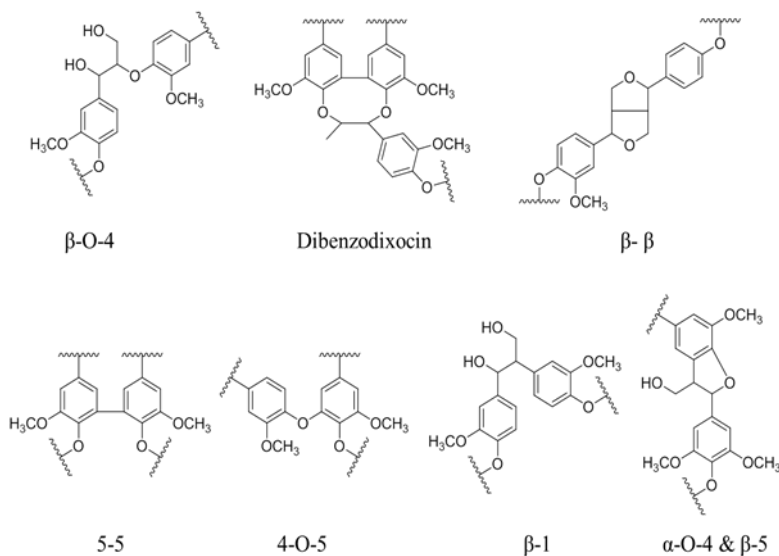


Figure 2. Types of lignin inter-unit linkages.

The variation in monolignol and monolignol inter-unit linkage distributions is, in part, due to changes that can occur in the expression of monolignol biosynthesis genes in response to developmental and environmental factors, but also due to the random nature of monolignol radical coupling reactions which have no apparent biochemical control (Boerjan et al., 2003; Campbell & Sederoff, 1996; Freudenberg, 1959). Major monolignol inter-unit linkage distributions in the lignin of softwoods and hardwoods are shown in Table 1 (Boerjan et al., 2003). The most frequent monolignol inter-unit linkage is the β -O-4 (β -aryl ether) linkage, which composes about half of the total linkages in both softwood and hardwood lignin (Boerjan et al., 2003). During cell wall lignification, monolignol coupling of lignin oligomers (as opposed to dimerization) is less likely to form β - β linkages, thus affording a higher proportions of β -O-4 and β -5 linkages (Boerjan et al., 2003). Similarly, the formation C-O bonds are energetically favored over the formation of C-C bond, thus the β -O-4 linkage is the most prevalent linkage formed. Hardwood lignin has a slightly higher percentage of β -O-4 linkages than softwood lignin, due to the greater amount of syringyl units which have a lower chance of forming β -5, 5-5, and 4-O-5 linkages during lignification. The resulting functional groups associated with the various lignin substructures, inter-unit linkages, and terminal sites, mainly methoxyl, phenolic and aliphatic hydroxyl, benzyl alcohol, non-cyclic benzyl ether, and carbonyl groups, have major influence on the reactivity and deconstruction of lignin (Pandey & Kim, 2011). For example, the β -O-4 linkage is one of the most easily cleaved chemically, whereas other monolignol linkages, such as β -5, β - β , 5-5, 4-O-5, and β -1 linkages, are more relatively stable to chemical degradation. As a result, most chemical routes targeting the selective depolymerization (without secondary or side reactions occurring) of lignin into its constituent phenolic subunits are based on selective cleavage of β -O-4 linkages. The goal of these selective lignin depolymerization efforts focus on narrowing downstream product distributions, making product separation and purification more practicable, and affording more tractable chemical production.

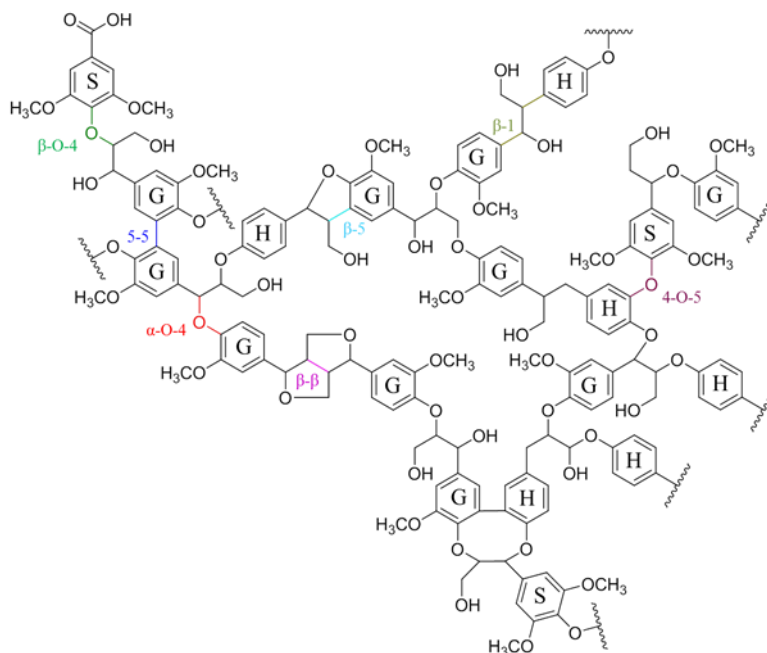


Figure 3. A representative structure of a lignin.

The overall structure and structural subunits of lignin (including their heterogeneity) evolved in plants over millions of years, in part, as a defensive structure to protect cell wall carbohydrates from fungal and microbial attack and/or the plant from chemical degradation from the environment. Fungi and microbes utilize the carbohydrate component of biomass as a source of carbon and energy, secreting various enzymes and compounds to disrupt lignin and to depolymerize cell wall carbohydrates. In this case, lignin acts as a physical barrier coating and protecting the cell wall carbohydrates. In response, lignin has evolved in plants to resist chemical and biochemical degradation. This evolved recalcitrance, inherent structural heterogeneity, and plant-to-plant variability represents a major obstacle to harnessing lignin efficiently for the production of desired and specific chemicals (Argyropoulos & Menachem, 1997; Gosselink et al., 2012).

Table 1. Percent of inter-unit linkages in softwood and hardwood lignin (Pandey & Kim, 2011)

Linkages	Softwood (spruce)	Hardwood (birch)
β -O-4, Aryl ether	46%	60%
α -O-4, Aryl ether	6-8%	6-8%
4-O-5, Diaryl ether	3.5-4%	6.5%
β -5, Phenylcoumaran	9-12%	6%
5-5, Biphenyl	9.5-11%	4.5%
β -1, 1,2-Diarylpropane	7%	7%
β - β , Resinol	2%	3%
Others	13%	5%

Lignin Isolation and Type

Lignin for production of renewable fuels and chemicals can be obtained directly from fractionation or isolation methods, or as a by-product of biomass processing to generate some other primary product. In either case, the processes used are generally very similar and broadly overlapping, differing at times only in process name and/or severity of condition. Lignin isolation from lignocellulosic feedstock can be conducted in a variety of ways involving different mechanical, chemical, and biochemical processes. These isolation or biomass processing methods invariably alter the native structure of lignin, thus further increasing the structural variability observed in industrial lignin and complicating efforts to design processes to use lignin as feedstock for chemical production. Depending on the type of isolation methods and the conditions used, lignin obtained from the same biomass feedstock can have very different structure and properties (furthering issues related to natural structural variation). Generally, these lignin isolation methods can be divided into two major categories, those that: 1) depolymerize cell wall carbohydrates into their soluble components, leaving the lignin as an insoluble solid residue, or 2) isolate lignin by fragmenting and solubilizing lignin, leaving cell wall carbohydrates as an insoluble solid residue.

In the pulp and paper industry, lignin is removed as a by-product from the desired product (i.e., cellulosic pulp) using various pulping methods. In these processes, conditions have been optimized for the isolation of cellulose (rather than the isolation or co-utilization of lignin) and belong to the latter category of lignin isolation. Kraft pulping is the most commonly used chemical pulping process, accounting for 98% of chemical pulp production in the US and 92% of chemical pulp production in the world (DeKing, 2004). During kraft pulping, wood chips are soaked in a sodium sulfide and sodium hydroxide mixture at an elevated temperature (e.g., 170°C) for roughly two hours (Ntziachristos & Samaras, 2009; Obst & Kirk, 1988; Smook, 1992). During delignification in kraft pulping, hydroxide and hydrosulfide anions cleave the β -O-4 and α -O-4 linkages in lignin. Cleavage at aryl ether linkages serves to fragment the lignin into small oligomers and increase ligno-oligomeric hydroxyl group content thus forming alkali/water soluble lignin fragments (Sjostrom, 2013). Lignin can be recovered by precipitation after acidification, typically with acetic acid (Obst & Kirk, 1988). Kraft lignin normally contains contamination from the cell wall carbohydrates.

Soda pulping is another type of alkaline process similar to kraft pulping, which generates alkaline lignin. The soda process uses aqueous sodium hydroxide, sometime with anthraquinone, on annual plants (e.g., rice and wheat straw, flax, and bagasse) to generate cellulosic pulp. Anthraquinone may be used as a pulping additive to decrease the carbohydrate degradation. Soda pulping can be operated in temperature range from 85 to 150°C and ambient pressure for a residence time between 1-6 h (Mosier et al., 2005). The lignin can be recovered by a solid/liquid separation process, followed by precipitation at a lower pH.

Sulfite pulping, an acidic pulping process, employs the addition of a mixture of sulfurous acid and bisulfite ions in the form of calcium, magnesium, sodium, or ammonium bisulfate (Brady et al., 1998). Delignification is usually carried out at around 175°C for more than 1.5 hours (Obst & Kirk, 1988). The bisulfite ions stabilize electrophilic carbocations formed either by protonation of C-C double bonds or by acidic cleavage of ether bonds through resonance intermediates to give sulfonates during the delignification (Sjostrom, 2013).

Lignosulfonate can be recovered from precipitation by adding excess lime, forming insoluble calcium lignosulfonates (Yu, Wang, Liu, & Ruhan, 2012). Since the process is conducted under acidic conditions, more contamination from degraded cell wall carbohydrates will be present than in kraft lignin (Brady et al., 1998). More importantly, the lignin isolated from sulfite pulping is highly contaminated by an external element, sulfur. Sulfur contamination is a large issue for the production of chemicals and materials from lignin because 1) sulfur is incorporated in an uncontrolled manner into the product stream, thus increasing purification requirements and lowering product quality, and/or 2) sulfur is known to poison many catalysts.

Organosolv pulping was developed as an alternative to kraft or sulfite pulping in an effort to generate a lignin by-product more amenable for co-utilization, and is considered more of a biomass fractionation process. Organosolv pulping uses organic solvents to dissolve lignin instead of reacting with inorganic chemicals. The dissolved lignin can be recovered in a less degraded and altered form than in kraft and sulfite pulping (Johansson, Aaltonen, & Ylinen, 1987). Organosolv pulping is conducted by using a wide range of pure organic solvents or organic/water solutions at elevated temperatures, typically ranging from 70 to 250°C. The process fragments lignin at aryl ether linkages via either acid- or auto-catalyzed hydrolysis, increasing the solubility of the lignin in the organic solvent (Johansson et al., 1987).

Steam explosion, another biomass fractionation process, is generally used to separate plant cell wall components and prepare cellulose pulp (Avellar & Glasser, 1998). The process involves treating biomass at temperatures from 180-240°C and high pressures of steam (from 1 to 3.5 MPa) for a short residence time (Kokta & Ahmed, 1998). Hydrolysis occurs during this short residence time. Subsequently, the pressure is rapidly released causing explosive decompression. Acetic acid generated from the hydrolysis of acetyl groups associated with hemicellulose degradation further catalyzes the hydrolysis (Mosier et al., 2005). The explosive decompression blows the biomass apart, facilitating more than 90% lignin recovery once the treated biomass is washed with alkali or organic solvents (Holladay, Bozell, White, & Johnson, 2007).

Oxidative delignification is also an effective process in separating lignin from lignocellulosic biomass. This process is performed under milder conditions, at a temperature from 70-130°C and atmospheric pressure in a medium of hydrogen peroxide (2-4%), acetic acid (25%), sulfuric acid (< 2%), and water for 1 to 4 h (Kuznetsov, Kuznetsova, Danilov, Yatsenkova, & Petrov, 2011; Kuznetsov, Sudakova, Garyntseva, Djakovitch, & Pinel, 2013). Optimal delignification occurs at different conditions depending on the origin of the biomass. However, in general at higher temperatures and concentrations of acetic acid and sulfuric acid, polysaccharides hydrolysis increases (Kuznetsov et al., 2013). During oxidative delignification, the decomposition of hydrogen peroxide and peroxy acid forms hydroxyl and peroxy radicals, which oxidize, fragment, and solubilize lignin into an aqueous medium (Kuznetsov et al., 2013). More than 99% of lignin can be separated from cellulose by this process. However, during oxidative delignification, the isolated lignin is highly fragmented and oxidized containing high percentages of carbonyl and carboxylic groups, and much reduced proportion of β -O-4 linkages (Li, Bansal, et al., 2015; Prinsen et al., 2013). Oxidative isolated lignins exhibited a more than threefold increase in the oxidation of benzyl alcohols that comprise β -O-4 linkages relative to native lignin (Li, Bansal, et al., 2015).

In the above pulping methods the structural features (functional groups and molecular weight) of the recovered lignins are strongly dependent on the process conditions (Johansson et al., 1987). The process conditions (e.g., pH value, temperature, solvent, etc.) control not only the rate and extent of delignification, but also the chemical and molecular modifications to the recovered lignin that occur. For example, severe organosolv pulping conditions can effectively isolate lignin from the cell wall. However, the recovered lignin typically has a low molecular weight and high polydispersity (Jääskeläinen, Sun, Argyropoulos, Tamminen, & Hortling, 2003; Obst & Kirk, 1988). In addition, those severe conditions cause the formation of condensed C-C bonds in the lignin (Holtman, Chang, Jameel, & Kadla, 2006; Jääskeläinen et al., 2003; Obst & Kirk, 1988), which make chemical routes targeting selective cleavage of β -O-4 linkages less effective. In summary, lignins resulting from chemical pulping and fractionation methods can generate poor feedstocks for conversion to chemicals primarily due to contamination, severe reduction in aryl-ether linkages, reduced solubility in organic solvents, and other unadvantageous chemical, molecular, and physical modifications.

Post-fermentation lignin (similar to cellulolytic enzyme lignin) refers to the solids isolated after enzymatic hydrolysis and fermentation of cell wall carbohydrates in bio-ethanol production. During enzymatic hydrolysis, most of the polysaccharides in biomass are broken down into small soluble sugar fragments by cellulases. After fermentation, the insoluble solid residue is lignin enriched also containing significant amounts of 1) proteins from hydrolytic enzymes due to strong non-specific bindings and 2) carbohydrates due to steric inaccessibility to the hydrolytic enzymes. Thus, post-fermentation lignin requires additional purification for higher value purposes and potential chemical production. The enzymes used in biomass saccharification, prior to the fermentation of the monosaccharides released as a result of enzymatic hydrolysis of cell wall carbohydrates, are not very effective due to biomass's inherent recalcitrance. Typically, a pretreatment is employed prior to biomass saccharification to increase the enzymatic hydrolysis rate and yields. The structure of post-fermentation lignin is highly dependent on the type pretreatment method used and the conditions of that pretreatment. For example, alkaline pretreatments produce higher molecular weight post-fermentation lignin with fewer condensed linkages than when acid pretreatment is employed (Samuel, Foston, Jiang, Allison, & Ragauskas, 2011). Many of these pretreatments are similar to the biomass fractionation processes discussed above. For example, organosolv and steam explosion are also popular pretreatment methods, but in this case are optimized not for delignification or biomass fractionation but for increasing enzymatic hydrolysis rates and yields. Lignin removal is highly correlated with increased enzymatic hydrolysis rates and yields. Therefore, the same mechanisms that make many biomass fractionation methods effective also apply to their role as an effective pretreatment method. Lignin for chemical production can also often be recovered from the pretreatment effluents or liquors in bio-ethanol production.

Milled wood lignin (MWL) is isolated using the Bjorkman method that mainly relies on mechanical degradation of cell wall components instead of a chemical pathway (Pandey & Kim, 2011). In the Bjorkman process, biomass is milled for long residence times, usually for 7 to 14 days, to disrupt the crystallinity of the cell wall cellulose and fragment lignin (Holtman, 2004). Solvents are then used to penetrate the cell wall and dissolve the lowered molecular weight lignin. The changes observed in the structural characteristics of the MWL in comparison to the native lignin strongly depend on the milling time and the type of mechanical milling tool being used. The long residence times and significant power

consumption required, make the Bjorkman method unattractive in an industrial setting; however, it has long been used as a method to isolated lignin (representing native lignin) for analytical purposes. In many cases, selective depolymerization methods are tested successfully on MWL, but are shown to be ineffective on lignins resulting from chemical pulping and fractionation methods.

During lignin isolation (i.e., fractionation, pulping, recovery, and pretreatment), the native lignin structures can be altered significantly by fragmentation and condensation reactions. This additional source of structural heterogeneity presents a significant challenge to the utilization of lignin for chemical production (Cui, Sun, & Argyropoulos, 2014). Lignin solubility in various organic solvents is highly dependent on the lignin chemical properties such as molecular weight distribution, monolignol distribution, monolignol linkage distribution, and terminal functional group distribution. As a result, solvent-based extraction or fractionation processes can be applied to isolated lignin. In this case, a solvent is used to further isolate fractions of lignin with specific chemical and physical properties with less structural variability. For example, the terminal phenolic content of lignin decreases with increasing polarity of the extraction solvent. This trend is opposite for the amount of aliphatic hydroxyl groups (van de Pas et al., 2011). Narrowing the diversity of the structural heterogeneity of isolated lignin can be beneficial to downstream processing of lignin into fuels, chemicals, and materials.

CHARACTERIZATION OF LIGNIN AND LIGNIN CONVERSION PRODUCTS

As mentioned before, lignin is a complex and heterogeneous macromolecule with various substructures and chemical moieties. Lignin within the plant cell wall displays significant plant-to-plant structural variation further exacerbated by biomass processing and lignin isolation methods. This structural variation not only affects the physical and chemical properties of lignin, but also influences the performance of lignin conversion technologies. As a result, understanding the characteristics of both the 1) original lignin feedstock and 2) lignin-derived product distributions is crucial in the research and development of lignin conversion technologies. Different types of analytical methods have been developed to study lignin conversion pathways, kinetics, and product distributions as well as the structure of lignin as a feedstock, providing knowledge to improve the efficacy of lignin conversion. Generally, the complexity of the lignin and lignin conversion products is such that the required information cannot be obtained by a single analytical tool. Many times, multiple analysis tools (see Table 2) must be employed to profile major chemical, molecular, and morphological features. The integration of these analysis is then used to reveal information about lignin 1) biosynthesis (Humphreys, Hemm, & Chapple, 1999; Vanholme, Demedts, Morreel, Ralph, & Boerjan, 2010), 2) native structure (Villaverde, Li, Ek, Ligerio, & de Vega, 2009), 3) fractionation/isolation (Garcia-Perez, Chaala, Pakdel, Kretschmer, & Roy, 2007; Jääskeläinen et al., 2003), 4) depolymerization/deconstruction (Nagy, David, Britovsek, & Ragauskas, 2009; Torr, van de Pas, Cazeils, & Suckling, 2011), and 5) conversion (Ben & Ragauskas, 2011b; Ben & Ragauskas, 2011c).

The most basic and common class of lignin analytical methods determines the lignin content within the cell wall of bulk biomass samples. A two-stage acid-hydrolysis procedure yields a combination of acid-insoluble lignin (the residual solids after two stage acid-hydrolysis, measured by mass) and acid-soluble lignin (measured by UV-Vis spectroscopy) content (Lin & Dence, 1992). This procedure has been standardized as the Technical Association of the Pulp and Paper Industry (TAPPI) methods 222-om and UM-250, and delivers results in mg of lignin per g of dry biomass (TAPPI, 1991, 2002). There are also other wet chemistry methods that determine lignin content in intact biomass (Lin & Dence, 1992). For example, an acetyl bromide assay can be used to rapidly quantify the lignin content in biomass by spectrophotometry. This method has been modified and extended to a rapid, micro-scale, and high-throughput determination of lignin content (Fukushima & Hatfield, 2001).

Spectroscopy

Analytical spectroscopy is the study of the interaction of electromagnetic radiation with matter. Spectroscopy can be used to identify, probe, and quantify atomic, molecular, and morphological features that define and comprise lignin and lignin-based products. Spectroscopy techniques generally include: infrared (IR), ultraviolet-visible (UV/Vis), and nuclear magnetic resonance (NMR) spectroscopy. These techniques have been shown effective at characterizing lignin and lignin substructures.

One technique in particular, solution-state NMR spectroscopy, can provide a high level of detailed chemical and structural information. It is especially useful in the analysis of lignin, lignin following isolation, and lignin conversion products. Specifically for the characterization of isolated lignin, a number of important chemical functional groups can be quantitatively profiled using 1D ^1H NMR, such as the relative proportion of protons associated with carboxylic acids, aldehydes, phenolic hydroxyls, β -5 phenolic hydroxyls, syringyl C_5 phenolic hydroxyls, aromatics, and aliphatics (Lundquist, 1979, 1981, 1992; Lundquist & Olsson, 1977). Improving the solubility of isolated lignin by acetylation can also increase the resolution of key chemical shifts used to identify and quantify the above chemical functionality. Although some lignin substructural information can be elucidated from ^1H NMR, due to its highly overlapping spectral appearance, it's most useful as a functional group profiling tool.

The increased chemical shift dispersion of ^{13}C NMR makes 1D ^{13}C NMR of isolated or acetylated lignin is ideal for profiling both lignin functional groups and lignin substructural moieties. 1D ^{13}C NMR is used for the analysis and quantification of aromatic (e.g., C-O, C-C, and C-H) and aliphatic carbons. It is ultimately capable of substructural analysis, determining monolignol distributions (i.e., S/G/H) and quantifying certain key monolignol inter-unit linkages (i.e., β -O-4, β - β , and β -5) (Gellerstedt & Robert, 1987; Robert, 1992; Samuel, Pu, Raman, & Ragauskas, 2010). Quantitative ^{13}C NMR is particularly useful in the analysis of specific features important to lignin isolation, conversion, and properties, such as methoxyl content, carboxyl content, and degree of aromatic condensation (Hallac, Pu, & Ragauskas, 2010).

NMR techniques observing nuclei in derivatized lignin other than protons and carbons can also provide quantitative data on the concentration of a variety of other functionalities.

For example, using ^{19}F NMR and a procedure that derivatizes lignin with 4-(trifluoromethyl)phenylhydrazine, the quantitative analysis of carbonyl functional groups in lignin can be performed (Sevillano, Mortha, Barrelle, & Lachenal, 2001). ^{31}P NMR following the derivatization of lignin with trimethyl phosphite has been used to measure the combined *ortho*- and *para*-quinone contents (Zawadzki, 1999). However, one of the most useful techniques has included the phosphorylation of lignin with 2-chloro-4,4,5,5-tetramethyl-1,3,2-dioxaphospholane or other hydroxyl phosphorylating agents to determine and profile the aliphatic and phenolic hydroxyl distribution and content with ^{31}P NMR (Ben & Ragauskas, 2011c; Pu, Cao, & Ragauskas, 2011). The phenolic hydroxyl distribution is indicative of the lignin polymer chain terminal monomer unit profile (i.e., S, G, H, and condensed terminal units).

Barta et al. used quantitative ^1H NMR to perform functional group profiling (which was also called “holistic ^1H NMR”) on organosolv lignin transformed using supercritical methanol and a Cu-doped porous metal oxide as the catalyst (Barta et al., 2010). The relative percentage of aromatic, aliphatic, and O-aliphatic protons were determined for the lignin as a feedstock and its breakdown products to understand the effect supercritical methanol and catalyst had. There are several other examples of ^1H NMR of oils generated from lignin by various thermochemical conversion methods (Capanema, Balakshin, & Kadla, 2004; Kirk & Jeffries, 1996; Marchessault, Coulombe, Morikawa, & Robert, 1982). Similarly, quantitative ^{13}C NMR can be used for functional group profiling of lignin conversion products. For example, Ben et al. studied the pyrolysis of softwood kraft lignin by 1D ^{13}C NMR detailing carboxyl, aromatic C-O, aromatic C-C, aromatic C-H, aliphatic C-O, aliphatic C-C, and methoxyl carbons for the feedstock lignin and the different lignin pyrolysis oils generated as a function of temperature (Ben & Ragauskas, 2011c). Edited ^{13}C techniques, such as distortionless enhancement by polarization transfer (DEPT) or attached proton test (APT), have been used to sort carbon signals by multiplicity, giving further information on the types of molecules found in pyrolysis oil (Mullen, Strahan, & Boateng, 2009).

Because many of the ^{13}C NMR chemical shifts for lignin were determined using native lignin and lignin model compounds, depending on the conversion technology utilized and the extent of chemical modification occurring during conversion, ^{13}C NMR substructural analysis based on lignin chemical shifts can only be performed on lignin conversion products in limited cases. Instead, a more basic functional group analysis must be employed. However, when 1) knowledge of the conversion technology suggest native lignin substructures exist in the lignin conversions products and/or 2) a number of corresponding and corroborating native lignin chemical shifts are unaltered, then ^{13}C NMR substructural analysis can be used. Similar to ^{13}C NMR, ^{31}P NMR following phosphorylation of lignin conversion product can detail changes in hydroxyl distribution and content. This analysis is particularly powerful in developing an understanding of lignin chain scission. Typically, hydrolysis of aryl ether linkages in lignin leads to a reduction in aliphatic hydroxyl content and increase in phenolic content. ^{31}P NMR can also be used to detect C-C condensation at terminal monolignols, C-O condensation at phenolic hydroxyls, or selective cleavage at, or the release of, a particular monolignol.

2D ^1H - ^{13}C heteronuclear single quantum coherence (HSQC) NMR experiments are even more useful in resolving a variety of overlapping spectral features by spreading complex spectral information over both a proton and carbon dimension. Thus, 2D ^1H - ^{13}C HSQC NMR has been applied to lignin, and is established as effective method for the semi-quantitative

determination of lignin monomer distribution (i.e., %H, %G, and %S), monomer linkage distribution (e.g., % β -O-4, % β - β , % β -5, and etc.), and functional group distribution (e.g., methoxyl or acetyl contents). In particular, 2D ^1H - ^{13}C HSQC NMR is very useful in profiling the presence of monolignol inter-unit linkages which are not easily detectable or resolvable by 1D ^{13}C NMR. In work by Ragauskas et al. (Ben & Ragauskas, 2011a) and similar work by Ralph et al. (Kim & Ralph, 2010), a pyridine- d_5 /DMSO- d_6 or a perdeuterated pyridinium chloride/DMSO- d_6 solvent system has been used to swell, or even dissolve, intact biomass samples for 2D ^1H - ^{13}C HSQC NMR. These electrolytic solvent or ionic liquid system facilitate the analysis of lignin without employing time-consuming lignin extraction and purification techniques that may alter the innate chemical structure of the lignin.

Similar to the 1D NMR methods discussed above, 2D ^1H - ^{13}C HSQC NMR can not only be applied to lignin but also to lignin conversions products. 2D ^1H - ^{13}C HSQC NMR has been applied to pyrolysis oil generated from softwood kraft lignin. Chemical-shift databases of model compounds in lignin pyrolysis oil were used to analyze the differences in pyrolysis oils generated at different temperatures. Lignin conversions in which the basic monomeric substructure is not greatly altered, substructural analysis by 2D ^1H - ^{13}C HSQC NMR can be employed to identify which native substructures are disrupted or remain. For instance, the β -carbon of β -O-4 linkages has a specific proton and carbon chemical shift and HSQC cross-peaks. When a β -O-4 linkage is broken, the proton and carbon chemical shifts change significantly, and the well-annotated HSQC cross-peak disappear and/or move to a different location in the spectrum.

The usefulness of solid-state NMR analysis, such as ^{13}C cross polarization magic angle spinning (CP/MAS), on isolated lignin is limited by reduced resolution, overlapping resonances, and difficult quantification. Nonetheless, a variety of studies has shown that solid-state NMR can provide useful information about functional groups in lignin (Hatfield, Maciel, Erbatur, & Erbatur, 1987; Mao, Holtman, Scott, Kadla, & Schmidt-Rohr, 2006), especially for lignin or lignin conversion products that have poor or no solubility even in electrolytic solvents or ionic liquids. For example, ^{13}C solid-state NMR techniques have been used to analyze and study lignin-based carbon fiber (Foston et al., 2013) and bio-char (Brewer, Schmidt-Rohr, Satrio, & Brown, 2009; Cao et al., 2012; Cheng, Wartelle, Klasson, & Edwards, 2010) formation.

Moreover, chemical fingerprinting involves the use of spectroscopy to produce a unique spectral pattern that is indicative of a specific lignin substructure or chemical moiety. Near infrared (NIR) (Robinson & Mansfield, 2009), and Fourier transform infrared spectroscopy (FTIR) (Chen et al., 1998; Lin & Dence, 1992; Mouille, Robin, Lecomte, Pagant, & Höfte, 2003) are generally employed in chemical fingerprinting. However, without the proper models or standards these spectroscopy-based chemical fingerprinting methods can be difficult to quantify or even correctly assign adsorption bands to the proper lignin substructure or chemical moiety. Conversely though, given the proper models or standards, NIR (Kelley, Rowell, Davis, Jurich, & Ibach, 2004; Malkavaara & Alen, 1998) and FTIR (Boeriu, Bravo, Gosselink, & van Dam, 2004; Cotrim, Ferraz, Gonçalves, Silva, & Bruns, 1999; Malkavaara & Alen, 1998) spectroscopy has been used in conjunction with multivariate analysis, such as principal component analysis (PCA) and projection to latent structures (PLS), for rapid lignin analysis, including grouping samples based on their chemical similarities and differences. Similarly, spectroscopy-based chemical fingerprinting methods have been used on lignin conversion products. Ye et al. used FTIR to confirm that isolated

lignin can be depolymerized in ethanol-water to form low molecular weight phenolics at mild conditions (Ye, Zhang, Fan, & Chang, 2011).

In summary, these above characterization methods can be applied to lignin as a function of 1) genetic or growth factors to understand biosynthesis, 2) isolation or fractionation method and conditions to understand the effect of isolation on lignin structure, and 3) conversion method and conditions to understand the effect of the conversion processes have on lignin conversion products. With respect to the latter two applications, these characterization methods can also help to understand the effect that feedstock lignin structure has on mechanisms of and optimization for lignin isolation and conversion to desired products.

Molecular Weight Analysis

Spectroscopy is very useful at assessing chemical structure and the changes occurring as a result of conversion. However, spectroscopy lacks the capability to directly assess changes occurring in molecular features that can indicate the rate, extent, and pattern of depolymerization or deconstruction. A variety of molecular weight analysis techniques can be used to determine key parameters that describe the molecular weight distribution of lignin and lignin conversion products. The average molecular weight of polydispersed lignin distributions is typically expressed as an ordinary arithmetic mean or weighted mean, denoted as the number average molar mass (M_n) and weight average molar mass (M_w), respectively. The polydispersity index (PDI) is a measure of the spread of the molecular weight distribution, and is calculated as the ratio of M_w to M_n . A variety of methods for measuring either M_n or M_w can be used to determine the molecular weight of lignin, including vapor pressure osmometry (Brunow, 2005; Lin & Dence, 1992), terminal hydroxyl group to lignin monomer ratio, cryoscopy (Gross, Sarkanen, & Schuerch, 1958), light scattering (Brunow, 2005; Fredheim, Braaten, & Christensen, 2002; Gidh, Decker, See, Himmel, & Williford, 2006; Gidh, Decker, Vinzant, Himmel, & Williford, 2006; Woerner & McCarthy, 1988), ultrafiltration (Brunow, 2005; Lage, Sant'Anna Jr, & Nobrega, 1999; Toledano, García, Mondragon, & Labidi, 2010; Woerner & McCarthy, 1988), isopiestic methods (Gross et al., 1958), sedimentation equilibrium (Himmel, Tatsumoto, Grohmann, Johnson, & Chum, 1990), gel permeation chromatography (GPC) (Brunow, 2005; Himmel et al., 1990; Lage et al., 1999), matrix-assisted laser desorption/ionization mass spectrometry (MADLI-MS) (Banoub & Delmas, 2003; Metzger et al., 1992), and intrinsic viscosity (Dong & Fricke, 1995).

The molecular weight of lignin is highly dependent on the molecular weight analysis technique applied. Thus, the apparent molecular weight for the same sample of lignin can be different depending on the molecular weight analysis technique used. Gel permeation chromatography (GPC), one of the more important and most widely applied methods, is sensitive to the determination of relative average molecular weights (Brunow, 2005). Furthermore, most of the techniques listed above for lignin molecular weight analysis are solution-based techniques. Due to the lack of good solvents for lignin, typically lignin needs to be derivatized to improve its solubility (Brunow, 2005; Himmel et al., 1990). A commonly utilized technique generates acetylated lignin by treating isolated lignin with acetic anhydride to facilitate dissolution in tetrahydrofuran (THF) and elution in a GPC system (typically with UV and/or refractive index detection). However, using GPC for lignin molecular weight analysis is

fundamentally problematic because size exclusion columns separate polymer distributions based on hydrodynamic volume rather than molecular weight, and rely on external standards to correlate retention times to the average molecular weight. In more traditional polymer systems, using external standard calibration curves to calculate relative average molecular weights is sufficient to compare the molecular weight of systems of consistent composition and geometric arrangement, followed by applying Mark–Houwink constants to calculate absolute average molecular weights. However, when analyzing lignin, its inherently random monomer sequence and geometric arrangement make it difficult to determine Mark–Houwink constants and to apply external standard calibration curves consistently from sample to sample. Nevertheless, most researchers simply accept this random bias as inherent to lignin molecular weight determination when applying GPC and external standard calibration curves. Besides acetylated lignin, aqueous-soluble lignins (e.g., kraft lignin) (Lage et al., 1999), or lignosulfonates (Fredheim et al., 2002), can be analyzed via GPC using special aqueous size exclusion columns. GPC techniques have been coupled with quasi-elastic and multi-angle light scattering to also detect changes in molecular size, structure, and configuration (Gidh, Decker, See, et al., 2006; Gidh, Decker, Vinzant, et al., 2006).

GPC has also been applied to lignin conversion products. According to Ben et al., GPC analysis indicated that an increase in molecular weight and polydispersity values of pyrolysis oil products from softwood kraft lignin was correlated with an increase in pyrolysis operating temperature (Ben & Ragauskas, 2011b). Ye et al. suggested that decreases in lignin molecular weight confirmed that hydrothermal depolymerization of lignin occurs in an aqueous ethanol solution at 523 K, detecting the presence of oligomeric products by GPC (Ye et al., 2011). Moreover, based on the changes in molecular weights of lignin conversion products, the degree of oligomeric condensation was correlated with ethanol concentration, operating temperature, reaction time, and lignin concentration (Ye et al., 2011).

Pyrolysis gas chromatography mass spectrometry (py-GC-MS) and pyrolysis molecular beam mass spectrometry (py-MBMS) techniques can be used directly on organic solids (i.e., biomass) and produce a mass spectral fingerprint for biomass or lignin, determining the lignin content and monolignol distribution. Pyrolysis GC-MS and py-MBMS analyses are based on the fact that components within the plant cell wall and lignin depolymerize and degrade during pyrolysis differently and in specific, repeatable pathways, resulting in a distinct fragmentation pattern upon MS analysis. These fragmentation patterns contain prominent mass peaks that can be associated with the presence of lignin or even lignin monomer units. During pyrolysis the thermal decomposition pathways and resulting mass spectra can be particularly complex, and similar to spectroscopy-based chemical fingerprinting methods, standards are required to calculate the absolute concentration of lignin or H, G, and S contents. For example, py-MBMS analysis was used for the rapid analysis of the chemical composition of agricultural fibers (Kelley et al., 2004), a QTL analysis of Loblolly pine for cell wall compositional phenotypes (Tuskan et al., 1999), and an investigation into within-tree lignin content variation (Sykes, Kodrzycki, Tuskan, Foutz, & Davis, 2008).

Because gas chromatography mass spectrometry (GC-MS) requires volatilization of an analyte, it is not useful for the analysis of polymeric lignin. However, GC-MS and gas chromatography-electrospray ionization-mass spectroscopy (GC-ESI-MS) are powerful tools in the chemical analysis of low molecular weight compounds in lignin conversion products. This combined chromatographic separation and mass spectroscopy detection can be used to identify and profile both gaseous and volatile conversion products of lignin (Busetto et al.,

2011; Zhao, Deng, Liao, Fu, & Guo, 2010). Both internal and external standards can be used to relatively and absolutely quantify the compounds that are made during the conversion of lignin. Traditional mass spectroscopy detection is based on the generation of a mass fragmentation pattern, which when compared with the mass fragmentation patterns in a database can be used for the determination of the structure of unknown compounds. ESI-MS detection represents a soft ionization technique which allows observation of only the molecular ion peak (rather than causing fragmentation). When available fragmentation libraries do not exist, unknown compound identification can be facilitated with high-resolution GC-ESI-MS by matching the isotope distribution for a molecular ion to the simulated isotope distribution of a suspected compound. Lee et al. used negative-ion mode GC-ESI-MS to characterize over 800 chemical compositions from pyrolysis oil, only 40 of which had been previously detected by GC-MS (Smith, Park, Klein, & Lee, 2012).

In contrast to GC-MS analysis, liquid chromatography-electrospray ionization-mass spectroscopy (LC-ESI-MS) and liquid chromatography-time of flight-mass spectroscopy (LC-TOF-MS) can be used to identify and quantify higher molecular weight compounds, especially oligomeric and condensation conversion products. Similar to GC-ESI-MS, LC-ESI-MS can be used to observe molecular ion peaks, but it extends the range of detectable compounds to 3,000 g/mol. A LC-TOF-MS system provides accurate mass analysis for a variety of analytical applications, including profiling, identification, characterization, and quantification of molecules up to ~20,000 g/mol. LC-TOF-MS structural identification of these high molecular weight products is limited. However, the mass spectra can be used in a qualitative fashion to understand the evolution of lignin fragment molecular weight during conversion.

Table 2. Summary of major characterization techniques for lignin and lignin conversion products

Major Characterization Techniques	Information Provided
UV-Vis	Determination of soluble lignin content
NIR/FTIR	Determination of lignin content and lignin monomer distribution Functional group analysis
¹ H NMR	Functional group analysis
¹³ C NMR	Functional group analysis Quantification of lignin monomers and certain key monolignol inter-unit linkages
³¹ P NMR	Quantification of aliphatic and phenolic hydroxyls
HSQC NMR	Functional group analysis Semi-quantification of lignin monomers and certain key monolignol inter-unit linkages
Solid-state NMR	Functional group analysis of insoluble substrates
GPC	Determination of molecular weight distribution
GC-MS and LC-MS	Quantification of compounds in lignin conversion products

LIGNIN CONVERSION

Since lignin is a renewable and under-utilized resource, extensive research has been conducted to develop conversion technologies that efficiently degrade lignin into high value products (Kang, Li, Fan, & Chang, 2013; Pandey & Kim, 2011). The remainder of this chapter briefly introduces these technologies, which are classified as thermal, biological, and hybrid conversion methods. Herein, these technologies are summarized, detailing their application toward the production of lignin-based products, primarily fuels and chemicals.

Thermal Conversion

Thermal conversion defines a broad class of technologies that rely on thermal energy to convert lignin into other forms (i.e., fuels and chemicals). This section presents thermal conversion techniques of lignin, which include pyrolysis, hydrothermal liquefaction (HTL), gasification, oxidative cracking, hydrogenolysis, and solvolysis as shown in Figure 4 and 5. Most thermal conversion methods used to transform lignin (or more broadly lignocellulosic biomass) result in the generation of three products: 1) gaseous, 2) liquid, and 3) solid. These methods typically involve numerous complex reactions, occurring both in series and parallel to one another. Due to differing conditions (temperature, environment, catalyst, etc.) certain reaction pathways are favored in specific thermal conversion methods altering the yield and composition of the gaseous, liquid, and solid products.

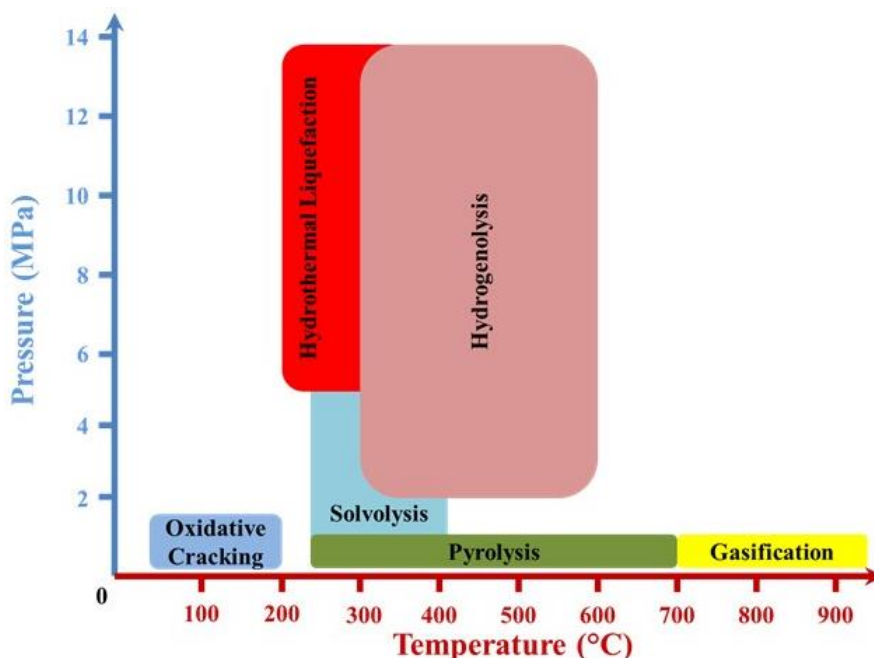


Figure 4. Pressure and temperature parameters range for thermochemical conversions of lignin.

Gasification

Gasification is defined as the thermal conversion of organic materials to combustible gases. Gasification is performed under high temperatures (greater than 700°C) in a controlled atmosphere with sub-stoichiometric levels of an oxidant usually air, oxygen, or steam (Huber et al., 2006; Kirkels & Verbong, 2011; Pereira, da Silva, de Oliveira, & Machado, 2012; TwE, 2014). The heat required for gasification is usually supplied in two ways: 1) indirect gasification, heat is generated by an outside source, and 2) direct gasification, heat is generated by exothermic combustion within the gasifier (Huber et al., 2006; Kumar, Jones, & Hanna, 2009). The primary product from the gasification of lignin is a gaseous product, called syngas, which is generally composed of hydrogen, carbon monoxide, carbon dioxide, and methane (Huber et al., 2006; Kirkels & Verbong, 2011; Pereira et al., 2012; TwE, 2014). Syngas typically is used to generate heat or electricity via combustion. Syngas can also be used to produce fuels and chemicals via the Fischer-Tropsch process (Pandey & Kim, 2011). Char (the solid product), tar (the liquid product), and ash are considered unwanted by-products from the incomplete gasification of lignin.

The three major reactions that take place in the gasification of lignin are 1) steam reforming, which involves the reaction of water with the lignin to produce carbon monoxide, carbon dioxide, and hydrogen; 2) water-gas shift reaction, which involves the reaction of water and carbon monoxide forming hydrogen and carbon dioxide; and 3) methanation, forming methane and water following the reaction between carbon monoxide and hydrogen. During the gasification process, thermal degradation of lignin occurs in three general stages (Kumar et al., 2009). The first stage, the loss of water by dehydration, occurs at temperatures below 125°C. The second stage involves the active pyrolysis of lignin at temperature between 125-500°C in which lignin is partially depolymerized. The residual lignin continues to degrade in the third stage of passive pyrolysis, at temperatures above 500°C (Huber et al., 2006; Kumar et al., 2009). The kinetics of lignin degradation in gasification mainly depends on the rate of heat transfer affected primarily by the lignin particle size, moisture content, and reactivity (Kumar et al., 2009; Pereira et al., 2012).

Hydrogasification

Gasification of lignin can also be accomplished in supercritical or near supercritical water, a process referred to as hydrogasification (or supercritical gasification). Hydrogasification uses steam as the oxidizing agent instead of air, producing a syngas with a higher heating value (Huber et al., 2006). Under supercritical conditions, the additional water favors the water-gas shift and methane reforming reactions that lead to higher hydrogen production and greater heating value (Kumar et al., 2009). Less unwanted tar is formed in hydrogasification as a result of increased steam reforming (Kumar et al., 2009). One advantage of hydrogasification, is that the water in the lignin feedstock is not vaporized, improving the thermal efficiency of the process. Wet lignin feedstock from isolation processes can efficiently be gasified with super/subcritical water (Huber et al., 2006). For example, the black liquor from kraft pulping can be used directly as feedstock, which has been shown to be a promising feedstock for syngas production via hydrogasification (Kang et al., 2013). When the moisture content of lignin is more than 30%, hydrogasification

is more attractive than the conventional gasification methods for lignin conversion (Kang et al., 2013).

Catalytic Gasification

The major purpose of using catalysts in the gasification process is either to improve the energy content of the resulting syngas or to reduce tar formation. To improve hydrogen production, three types of catalysts have been used, 1) alkali and alkali salts (NaOH, KOH, CaO, and Na₂CO₃), 2) transition metal catalysts (Ni, Pt, Ru, and Rh), and 3) metal oxide catalysts, such as ZrO₂ (Kang et al., 2013). Alkali and alkali salts can promote water-gas shift reactions, eventually increasing hydrogen production. Alkali and alkali salts can also neutralize organic acids formed as a result of lignin decomposition, shifting the equilibrium of lignin decomposition and promoting greater conversion to syngas. Alkali and alkali salts have been found to reduce tar formation; however, can also simultaneously enhance char formation. Transition metal catalysts improve depolymerization of lignin by accelerating the cleavage of C-O and C-C bonds during gasification. Some metal and metal oxide catalysts can favor the steam reforming and methanation reactions. For example, Rh/CeO₂/SiO₂ catalysts have been shown to be one of the most effective in regards of the reduction in tar formation (Huber et al., 2006). Sato et al. reported hydrogen production through gasification of lignin could be improved by using magnesium oxide supported nickel catalyst (Sato et al., 2006). Similarly, Yamaguchi et al. used titania and activated carbon supported metal catalysts to increase the hydrogen production from lignin gasification (Yamaguchi et al., 2009).

Lignin Gasification Products

Lignin-derived syngas can be used to synthesize a variety of fuels and chemicals with wide application. The products produced from syngas of lignin include 1) hydrogen, 2) methanol by methanol synthesis, 3) alkanes by Fischer-Tropsch synthesis, 4) isobutane by isosynthesis, 5) ethanol by fermentation or with catalysts, and 6) aldehydes or alcohols by oxosynthesis (Huber et al., 2006). Hydrogen formed from the water-gas shift reaction can be used as fuel directly in fuel cells, or to produce heat and electricity via combustion. Hydrogen can also be used to produce chemicals or intermediate products that ultimately yield ammonia, hydrocarbons, and methanol (Kumar et al., 2009). According to Yang et al., lignin gasification produces four times more hydrogen than cellulose and almost three times more than hemicellulose (Yang, Yan, Chen, Lee, & Zheng, 2007). Additionally, lignin gasification produces significantly less char than the gasification of cellulose (Osada, Sato, Watanabe, Adschiri, & Arai, 2004). Methanol, which is a platform chemical used to produce a range of other chemicals and fuels (e.g., formaldehyde, dimethyl ether, methyl tert-butyl ether, and acetic acid), can be produced from lignin-derived syngas by the methanol synthesis reaction. Lignin-derived syngas can also be upgraded by Fischer-Tropsch synthesis to generate alkanes by using Co-, Fe-, or Ru-based catalysts. The alkanes produced from syngas usually are linear alkanes with a carbon range from 1 to 50 (Kang et al., 2013), and are generally used as a transportation fuel. Many types of catalysts have been researched to selectively narrow the hydrocarbon range of alkanes produced. For example, Cr₂O₃-ZnO promotes high carbon monoxide conversion, generating mostly a gasoline range alkane fraction (Kumar et al., 2009).

Parameters Affecting Gasification of Lignin

The lignin- or biomass-derived syngas yield and composition can be substantially influenced by several gasification parameters, such as temperature, moisture content, operating pressure, oxidizing agent, particle size, and the presence of catalyst. In the gasification of lignin on a dry basis, lignin needs to be ground into appropriate particle sizes to provide greater surface area for faster heat transfer rates and more efficient conversion. Reduction of particle size can lead to higher gas yields, gas energy content, and carbon conversion efficiency (Kumar et al., 2009). Moreover, the moisture content of lignin affects both the operation of the gasifier and the composition of syngas, because higher moisture contents reduce both the molar fractions of the combustible components and the thermal efficiency of the process (Pereira et al., 2012). The type of feedstock has little effect on the composition of products from gasification. The major product of lignin gasification is syngas. However, the yield of hydrogen in gasification depends on the level of carbohydrate contamination (Yang et al., 2007). For example, hydrogen is more readily produced as a result of aromatic C-C and C-H bond cracking than cracking of sugars (Yang et al., 2007). Meanwhile, the abundant methoxyl functionality specific to lignin produces more methane upon cracking than sugar, which can favor the gas reforming reaction to subsequently generate hydrogen. In addition, the heating rate of lignin can effect hydrogen production (Barneto, Carmona, Galvez, & Conesa, 2008; Crocker, 2010). A decreased heating rate can diminish char reactivity, making its rapid oxidation more difficult and favoring other relatively important reactions that produce hydrogen (Barneto et al., 2008). Different oxidizing environments have various effects on the yield and composition of products from gasification of lignin. The equivalence ratio (ER) of the air supply is the ratio of the airflow rate used in the process to the airflow rate required for stoichiometric combustion. For example, a higher ER can lead either to a higher gas yield due to higher combustion temperature or to lower conversion due to the shortened residence time. Also, a high ER results in a higher degree of combustion, which increases the oxygen content of the gas produced because portions of the organic carbons are completely oxidized (Kumar et al., 2009; Pereira et al., 2012).

Pyrolysis

Pyrolysis thermally converts lignin in the absence of oxygen. The primary product from the pyrolysis of lignin is a liquid product called bio-oil or pyrolysis oil, though a gaseous and solid product (bio-char) is also generated. Generally, pyrolysis of lignin is optimized to maximize bio-oil yield and/or to produce a desired bio-oil composition. Pyrolysis of lignin operates at a wide range of temperatures, from 250-700°C (Brownsort, 2009; Pandey & Kim, 2011). However, lignin pyrolysis typically occurs from 200-450°C, with the highest decomposition rates observed at temperatures between 360-400°C (Collard & Blin, 2014). During pyrolysis of lignin, the decomposition of monolignol inter-unit linkages at hydroxyl groups can generate formic acid, formaldehyde, carbon dioxide, carbon monoxide, and water (Collard & Blin, 2014; Pandey & Kim, 2011). Lignin α -O-4 and β -O-4 linkages cleave at 200°C and 245°C, respectively (Collard & Blin, 2014). When the temperature of pyrolysis is greater than 300°C, most of the aliphatic C-C bonds within those inter-unit linkage also

become unstable and readily break (Collard & Blin, 2014), thus phenol production maximizes at 360-400°C (Collard & Blin, 2014). Even though the ether bonds at methoxyl groups are resistant to thermal degradation, different types of fragmentations still occur at 380°C, causing substitution or removal of those methoxyl groups (Collard & Blin, 2014; Pandey & Kim, 2011). As a result, methanol is produced at lower pyrolysis temperatures (Collard & Blin, 2014). At higher pyrolysis temperatures, these methoxyl groups also are the major source of methane production (~430°C) (Collard & Blin, 2014). At temperatures higher than 450°C, most of the aryl ether inter-unit linkages are gone, but 5-5 and 4-O-5 linkages are still present (Collard & Blin, 2014). At 500°C and higher, carbon monoxide is produced from aromatic ring substituent removal, while the remaining stable chemical moieties undergo secondary re-polymerization and condensation into the polycyclic aromatic hydrocarbons that comprise bio-char (Collard & Blin, 2014). Generally, higher pyrolysis temperatures promote the formation of more condensed bio-char with greater aromatic rings units per cluster and less oxygen content. Although the general trend of depolymerization is similar, the yield of particular products and the specific temperature for bond breakage vary according to the lignin type and structure (Pandey & Kim, 2011).

Fast Pyrolysis

In the pyrolysis of lignin, longer residence times for vapor products in the reactor result in more bio-char formation through secondary re-polymerizations (Bridgwater, 2012; Goyal, Seal, & Saxena, 2008; Jahirul, Rasul, Chowdhury, & Ashwath, 2012). Fast pyrolysis occurs typically in less than 2 seconds, reducing the vapor residence time and minimizing re-polymerizations (Bridgwater, 2012; Jahirul et al., 2012). The heating rate for fast pyrolysis is about 300°C/min, which is much higher than for slow pyrolysis with a heating rate of 5-7°C/min (Goyal et al., 2008). The pyrolysis temperature is typically set at 500°C to maximize bio-oil production (Goyal et al., 2008). In fast pyrolysis, not only can the yield of bio-char be significantly reduced, but also the quality of lignin pyrolysis oil produced can be improved (Goyal et al., 2008). Patwardhan et al. reported the primary products of lignin pyrolysis are volatile monomeric compounds, but these compounds further transform to lignin-derived oligomeric species through re-oligomerization prior to the condensation of bio-oil (Patwardhan, Brown, & Shanks, 2011). Short residence time and rapid quenching of the product vapor in fast pyrolysis can reduce the occurrence of re-oligomerization, and produce a lighter bio-oil. According to Ma et al., a very high yield of liquid and selectivity to aromatic hydrocarbons can be obtained by catalytic fast pyrolysis of lignin using zeolites, due to the stabilization of depolymerized intermediates and the suppression of re-polymerization (Ma, Troussard, & van Bokhoven, 2012).

Hydrothermal Liquefaction

Hydrothermal liquefaction (HTL) is a thermal degradation technique similar to pyrolysis. HTL was designed to convert high-moisture content lignin into bio-oil that can be used for direct combustion or refined for transportation fuels (Zhang, 2010). This process is operated under medium temperatures from 250-400°C and pressures from 5-20 MPa (Zhang, 2010). This temperatures and pressure profile forms supercritical water, which has an unusually high dielectric constant that enables the dissolution of significant amounts of lignin. Moreover, the supercritical water splits into H⁺ and OH⁻ ions that can hydrolyze linkages of the lignin into a

liquid bio-oil product similar to that of pyrolysis, but with a higher content of aromatic compounds. Kanetake et al. reported the main products from the hydrothermal liquefaction of lignin were catechol, phenols, and cresols, which indicated removal of methoxyl groups occurred (Kanetake, Sasaki, & Goto, 2007) and that aromatic rings are stable (Toor, Rosendahl, & Rudolf, 2011). The bio-oil generated from HTL has an advantageously lower oxygen content than fast pyrolysis (Kang et al., 2013; Zhang, 2010). Hydrothermal liquefaction of lignin may also produce significant amounts of bio-char (Toor et al., 2011).

Lignin Pyrolysis Products

In the pyrolysis of lignin, three primary products: permanent gases, bio-oil, and bio-char, are obtained. Lignin pyrolysis generates ~60-80% bio-oil, which is a dark brown, free flowing liquid with a smoky odor (Babu, 2008; Effendi, Gerhauser, & Bridgwater, 2008; Oasmaa & Czernik, 1999; Pandey & Kim, 2011) produced by condensing the organic vapor formed from pyrolysis. Generally, lignin-derived bio-oil is considered as a potential fuel oil substitute, which has heating values 40-50% that of hydrocarbon fuels (Jahirul et al., 2012). Lignin pyrolysis oil is a complex, unresolved, and multi-component mixture of different sized molecules derived from the depolymerization and fragmentation of lignin. Lignin pyrolysis oil can be fractionated into light, middle, and heavy oil fractions according to its physical and chemical properties, such as molecular weight, solubility, polarity, and volatility (Lindfors, Kuoppala, Oasmaa, Solantausta, & Arpiainen, 2014). The light bio-oil fraction is composed of mostly water and has strong acidity, poor stability, and good fluidity (Lindfors et al., 2014). The middle fraction is more viscous and has a lower water content (Lindfors et al., 2014). Whereas, the heavy fraction contains a small percentage of volatile substances and has a relatively high heating value (Lindfors et al., 2014). It contains 300-400 different compounds, which can be categorized as acids, alcohols, ethers, ketones, aldehydes, phenolics, and esters (Bu et al., 2012; Jahirul et al., 2012; Zhang, Chang, Wang, & Xu, 2007). This wide distribution of compounds makes lignin pyrolysis bio-oil difficult to use for chemical production. However, catalytic upgrading can make lignin pyrolysis bio-oil very useful as a transportation fuel.

There are other challenges for the application of lignin pyrolysis oils (Jahirul et al., 2012). First, the water content in bio-oil is as high as 15-30%, decreasing its heating value and flame temperature. The relatively high oxygen content of lignin bio-oil reduces its energy density with respect to hydrocarbon fuels (Zhang et al., 2007). The acidity and alkali metal content of lignin pyrolysis oil can cause erosion and corrosion problems in engines, storage containers, or reactors (Zhang et al., 2007). Moreover, the compounds, responsible for the low pH of bio-oil, also cause instability in which bio-oil properties change due to aging reactions and re-polymerizations. For instance, aldehydes in bio-oil can react with other compounds, such as water, phenolics, and alcohols, affecting its viscosity and average molecular weight (Bu et al., 2012). In short, bio-oil presents many challenges as a direct replacement for petroleum fuels. Ultimately, it requires catalytic stabilization for effective storage and transportation, and further catalytic upgrading to be used as a gasoline substitute (Bridgwater, 2012; Bu et al., 2012; Jahirul et al., 2012; Mu, Ben, Ragauskas, & Deng, 2013).

Lignin bio-oil can be upgraded via two major routes: catalytic hydrodeoxygenation (HDO) and deoxygenation (Bu et al., 2012). The HDO of bio-oil can be accomplished with Co-Mo, Ni-Mo, and their oxides, supported on alumina, as catalysts under a high pressure of hydrogen or carbon monoxide as a reducing agent to remove the oxygen in

the form of water (300-600°C) (Bu et al., 2012; Mu et al., 2013; Zhang et al., 2007). The six mechanisms involved in the HDO process are 1) water separation, 2) dehydration due to condensation polymerization, 3) decarboxylation, 4) hydrogenation, 5) hydrogenolysis, and 6) hydrocracking (Bu et al., 2012). In deoxygenation of bio-oil, zeolites are typically used to catalytically crack or decompose oxygenated compounds into hydrocarbons removing oxygen in form of water and carbon oxides. Other upgrading methods include 1) emulsification, where bio-oil is mixed with diesel fuel directly to generate a transportation fuel or 2) steam reforming to produce hydrogen (Zhang et al., 2007).

The gaseous products of lignin pyrolysis are composed of mainly of carbon monoxide, carbon dioxide, methane, and volatile organic liquids (Mu et al., 2013; Pandey & Kim, 2011). Similar to the syngas generated from gasification, the gaseous products of lignin pyrolysis are a renewable alternative source of heat, power generation, and transportation fuel (Jahirul et al., 2012; Mu et al., 2013).

Bio-char is the remaining solid (similar to polycyclic aromatic hydrocarbons) after thermal degradation of lignin via pyrolysis. Bio-char comprises 10-35% of the total products of lignin pyrolysis, depending on the operating condition (Jahirul et al., 2012). Bio-char is mainly composed of carbon, hydrogen, and various inorganic species in two structures: condensed aromatic structures and stacked crystalline graphene sheets (Jahirul et al., 2012; Mu et al., 2013). The physical and chemical properties of bio-char are greatly affected by the heteroatoms in its structure (H, O, N, P, and S) (Jahirul et al., 2012). The composition, distribution, and proportion of these heteroatoms strongly depend on the lignin source and the pyrolysis conditions used (Jahirul et al., 2012). Depending on the composition and physical properties of bio-char, it can be used in various industrial processes: as solid fuel in boilers, in the production of activated carbon, in soil amendment, in making carbon nanotubes, and in producing hydrogen-rich gas (Jahirul et al., 2012).

Parameters Affecting Pyrolysis of Lignin

Pyrolysis operating conditions, such as residence time, temperature, catalyst, and inert gas flow rate, have strong effects on the yield and chemical composition of bio-oil from lignin (Effendi et al., 2008; Pandey & Kim, 2011). Moreover, the type, composition, and structure of the feedstock lignin will also affect the yield and chemical composition of generated bio-oil (Lin et al., 2015). Pyrolysis of lignins from hardwood release more methanol due to the higher methoxyl group content from the syringyl units (Wang et al., 2009). Lin et al. reported that pyrolysis of sulfite lignin produced furans as the major products and large amounts of sulfur-containing compounds, while pyrolysis of alkaline lignin, milled wood lignin, and enzymatic hydrolysis lignin generated phenols as the predominant products (Lin et al., 2015).

The yield of bio-char is maximized at low temperatures and heating rates, while the production of bio-oil is maximized at low to mid temperatures (i.e., 350-500°C) and high heating rate. Lastly, the yield of the gaseous fractions of products can be maximized at a high temperature and a low heating rate (Jahirul et al., 2012).

Depending on the pyrolysis reactor design, the particle size of the feed lignin can limit the effectiveness of heat transfer during the process. To achieve a smoothly continuous process, the particle size of lignin needs to be reduced by cutting and grinding. Moreover, the moisture content of the lignin feedstock can affect the behavior of lignin during pyrolysis and the composition and properties of the resulting pyrolysis oil (Akhtar & Amin, 2012). High

moisture contents lower the pyrolysis temperature and slows the heating rate for pyrolysis (Akhtar & Amin, 2012; Jahirul et al., 2012).

Catalysts can be added directly to the lignin to improve the conversion efficiency, reduce the severity of the reaction conditions, and increase the yield of bio-oil during the pyrolysis of lignin. This process is called in-situ catalytic pyrolysis. In the presence of catalysts, pyrolysis kinetics can be enhanced by cracking higher molecular weight compounds into lighter hydrocarbon products (Jahirul et al., 2012). These pyrolysis catalysts include dolomite, Ni-based catalysts, alkali metal catalysts, and noble metal catalysts (Jahirul et al., 2012). For example, although calcined dolomite improves the yield of syngas and decreases the yield of bio-oil and bio-char, calcined dolomite is unstable under high pyrolysis temperatures and less effective than other catalysts in cracking heavy tar (Jahirul et al., 2012).

Oxidative Cracking

The wide distribution of products generated from pyrolysis or HTL of lignin limits the commercial potential of lignin for chemical production, because of the expensive upgrading, separation, and purification required. Thus, in order to valorize lignin for chemical production rather than just fuel production, a more facile and selective lignin depolymerization method is needed. Oxidative cracking is one such method. Oxidative cracking processes cleave the linkages in lignin with an oxidant, such as air or hydrogen peroxide (Pandey & Kim, 2011; Taraban'ko, Fomova, Kuznetsov, Ivanchenko, & Kudryashev, 1995; Zakzeski, Bruijninx, Jongerius, & Weckhuysen, 2010). These oxidants also target hydroxyl groups, converting them into moieties such as aldehyde, ketones, and carboxylic acids. This process has been used to produce vanillin or syringaldehyde from lignosulfonate (Fargues, Mathias, & Rodrigues, 1996; Taraban'ko, Koropatchinskaya, Kudryashev, & Kuznetsov, 1995).

Oxidative cracking of lignin takes place at moderate temperatures in the range of 60-160°C with hydrogen peroxide as the oxidizing agent (Pandey & Kim, 2011; Wu, Heitz, & Chornet, 1994; Xiang & Lee, 2000), which primarily generate aromatic aldehydes and carboxylic acids. The yields of these products are in the range of 10-11% of the initial lignin mass (Xu, Arancon, Labidi, & Luque, 2014). The reaction mechanism and the product distribution are strongly dependent on the pH value of the reaction (Pandey & Kim, 2011; Xiang & Lee, 2000). Under alkali conditions, hydrogen peroxide dissociates and forms molecular oxygen and other radical species that can react with lignin in various ways (Hu, Pan, Zhou, & Zhang, 2011). The reaction proceeds well under strong alkaline conditions, even at the low reaction temperatures of 80-90°C (Xiang & Lee, 2000). Under acidic conditions, due to the increasing stability of hydrogen peroxide, a higher reaction severity at temperatures of 130-160°C is required to achieve the same degree of cracking (Xiang & Lee, 2000). Instead of forming aromatic compounds as under alkaline conditions, acetic and formic acid constitutes about 90% of the products formed under acidic condition (Xiang & Lee, 2000).

Lignin Oxidation Products

Oxidative cracking of lignin seeks to maximize the yield of and selectivity for aromatic aldehydes, ketones, and carboxylic acids. Many of these chemicals are either commodity chemicals or serve as platform chemicals for subsequent organic synthesis of target fine chemicals (Das, Kolar, & Sharma-Shivappa, 2012; Pandey & Kim, 2011; Zakzeski et al., 2010). For example, alkaline oxidation of softwood lignin produces vanillin and vanillic acid, while syringaldehyde and syringic acid can be obtained from hardwood lignin (Pandey & Kim, 2011). Though, the highest reported yields of such oxidative products from lignin are 10-11% (Das et al., 2012), the average yields of vanillin is in the 3-5% range (Das et al., 2012). This difference signals that significant technical difficulties needing to be addressed (Xu et al., 2014).

Parameters Affecting Oxidation of Lignin

According to many recent studies on the oxidative cracking of lignin, the yields of products strongly depends on the reaction conditions (i.e., temperature, pH value, oxygen partial pressure, reaction time, types of oxidizing agents, and catalysts). Also, the type, composition, and structure of lignin can have significant effects on the performance of the oxidation process, especially on the structure of the aldehydes that is produced. For example, softwood lignin consists of mainly guaiacyl units, which means vanillin is the main product (Kang et al., 2013). Vanillin, syringaldehyde, and *p*-hydroxybenzaldehyde can all be obtained from herbaceous lignin, while higher levels of syringaldehyde can be obtained from hardwood lignin (Kang et al., 2013). On the other hand, the altered properties of lignin from different isolation methods can also influence the performance of oxidative processing. For example, organosolv lignin has poor solubility in aqueous solution, which can lead to low conversion and yield of products. Since oxidative cracking processes cleave the linkages in lignin, the prevalence of specific types of linkages (e.g., aryl ether), which may be altered by different isolation methods, can affect the yield and rate of depolymerization during oxidative cracking. Taraban'ko et al. found that oxidative cracking performance of lignin with molecular oxygen was close to that of the oxidation of lignin with nitrobenzene. Thus, the vanillin yield from lignin following oxidative cracking is related to the stability of lignins toward oxidation with nitrobenzene which seemed to be correlated with the severity of pretreatment or isolation conditions. For example, aldehyde yields from organosolv lignin and lignosulfonates were smaller than less condensed MWL (Taraban'ko, Koropatchinskaya, et al., 1995).

The rate of decomposition of lignin by oxidative cracking increases with temperature and pH value (Xiang & Lee, 2000). However, the yields of desired products may not always increase as temperature and reaction time increase. For example, an increased time/temperature profile can cause further oxidation of desired aldehyde products (e.g., vanillin) to carboxylic acids. The concentration of the oxidant can affect the oxidative cracking of lignin. For example, a higher rate of oxygen transfer into the liquid phase can enhance the rate of the ionic pathways that facilitate oxidative cracking. High oxygen pressure increases the conversion of lignin and yields of aldehydes, but can also induce syringaldehyde degradation (Wu et al., 1994).

Different types of oxidizing agents used in oxidative cracking of lignin can highly affect the product yield and distribution. When oxidative cracking of lignin is performed with hydrogen peroxide, the major products identified include mono- and di-carboxylic acids

(Pandey & Kim, 2011). Xiang et al. reported that in the oxidative cracking of lignin by hydrogen peroxide at 160°C for 10 min. The products detected were dominated by oxalic, formic, and acetic acids (Xiang & Lee, 2000). Only trace amounts of vanillin, syringaldehyde, or other aromatic aldehydes and acids were found, because of degradation due to secondary oxidation by hydrogen peroxide (Pandey & Kim, 2011). However, milder oxidizing agents, such as nitrobenzene, metal oxides, and molecular oxygen, can be used to preserve the aromatic rings and maximize the yields of aldehydes (Pandey & Kim, 2011).

Catalysts in oxidative cracking of lignin can improve the quality of products and reduce the severity of reaction conditions required. In oxidative cracking of lignin with air, copper (II) sulfate has been shown to improve the production of vanillin by fast and selective fragmentation of the hydrogen peroxide (Taraban'ko, Fomova, et al., 1995). For example, in comparison to oxidative cracking without catalyst, Cu^{2+} increases the yield of total aldehydes from 8.5% to 12.1% and the conversion of lignin from 58.0% to 71.8% (Fargues et al., 1996; Wu et al., 1994). Oxidative cracking catalysts can be designed specifically to break targeted linkages or to oxidize specific functionalities on lignin (Zakzeski et al., 2010). For example, heterogeneous perovskite-type oxide catalysts have been developed for oxidative cracking of lignin into aromatic aldehydes (Deng, Lin, & Liu, 2010; Zhang, Deng, & Lin, 2009). More recent efforts, have used catalysts to facilitate the selective oxidation of secondary benzylic alcohols, accomplishing depolymerization with a subsequent step to achieve C–C or C–O bond cleavage (Rahimi, Azarpira, Kim, Ralph, & Stahl, 2013; Rahimi, Ulbrich, Coon, & Stahl, 2014). Rahimi et al. depolymerized oxidized lignin under mild conditions with aqueous formic acid, resulting in more than 60% yield of aromatic compounds (Rahimi et al., 2014).

Hydrogenolysis

Hydrogenolysis is another method that selectively depolymerizes and valorizes lignin for chemical production. Typically, hydrogen gas is used to reduce and disrupt the linkages of lignin (Gasser et al., 2012; Pandey & Kim, 2011). In this case, hydrogenolysis can be performed on lignin with suitable solvents and catalysts, cleaving aryl ether linkages to generate phenolic monomers and dimers. Because ~55-60% of total inter-unit linkages in lignin are aryl ether linkages, commercially viable hydrogenolysis methods must selectively cleave aryl ethers, suppressing not only 1) competing side reactions such as aromatic ring hydrogenation, aliphatic ether cleavage, or carbon-carbon bond cleavage, but also 2) secondary reactions which convert lignin fragments and phenolic/aromatic products into other compounds that further broaden the product distribution. Significant research has been conducted on the performance of different catalysts for the selective hydrogenolysis of lignin under mild conditions to improve the yield and selectivity of monomeric phenol production (Sergeev & Hartwig, 2011; Ye, Zhang, Fan, & Chang, 2012; Zhang, Asakura, et al., 2014).

Hydropyrolysis

Hydropyrolysis employs elevated temperatures and a high hydrogen partial pressure to hydrodeoxygenate lignin pyrolysis vapors, producing a low-oxygen-containing hydrocarbon-rich liquid product (Meier, Ante, & Faix, 1992). During hydropyrolysis, lignin depolymerization is facilitated by hydrogenolysis or hydrocracking. Due to higher yields of

phenolics and lower char formation, hydrolysis of lignin is a more promising method for phenol production than pyrolysis (Pandey & Kim, 2011). Typical operating conditions are temperatures in the range of 300-600°C and hydrogen pressure in the range of 1-15 MPa (Joffres et al., 2013; Pandey & Kim, 2011). The conditions at which hydrolysis is performed results in a thermal deconstruction that is very similar to pyrolysis with regards to lack of depolymerization control, thus producing a product similar to pyrolysis bio-oil.

Solvolytic

Solvolytic utilizes solvents to convert lignin into soluble fragments with high yields. Lignin solvolytic can be categorized into two general categories, base-catalyzed depolymerization or hydrogenolysis in supercritical solvents (Azadi, Inderwildi, Farnood, & King, 2013). Hydrogenolysis processes in solvolytic receive hydrogen in three ways: 1) hydrogen gas can be directly pressurized into the reaction system; 2) hydrogen can be produced in-situ from a hydrogen-donating solvent, such as formic acid; and 3) partial reforming of the solvent, such as methanol, can also generate hydrogen for lignin depolymerization in the presence of metal catalysts (Azadi et al., 2013).

Supercritical Hydrogenolysis

The operating conditions for solvolytic in supercritical solvents usually depend on the properties of the solvent. For example, water has supercritical condition at 374.15°C and 22.1 MPa. The decomposition of lignin in supercritical solvents occurs by breaking β -O-4 linkages and dealkylation at weak C-C bonds, yielding low molecular weight fragments (Pandey & Kim, 2011). The formation of an insoluble char fraction (higher molecular weight fragments) is due to cross-linking reactions among those low molecular weight fragments (Pandey & Kim, 2011). One of the benefits of solvolytic in supercritical solvents is that it overcomes issues related to lignin insolubility and transport. The supercritical conditions facilitate thermal fragmentation at the surface of lignin particles while also increasing the solubility of lignin and lignin fragments due to changes in the solvent properties. The molecular weight of the dissolved lignin during solvolytic ranges from about 150 to 2,500 g/mol, corresponding to degrees of polymerization ranging from 1 to 15 (Azadi et al., 2013). The liquid fraction following solvolytic contains these fragments in addition to monomeric and dimeric compounds. The solid fraction contains larger oligomers, re-polymerized products, and unreacted lignin (Azadi et al., 2013). Supercritical solvents during solvolytic of lignin also advantageously stabilize radicals and limit the formation of condensed products and chars with respect to pyrolysis (Joffres et al., 2013; Pandey & Kim, 2011). A mixture of solvents can have a beneficial effect on the conversion. For instance, Saisu et al. reported that adding phenol to water as a supercritical solvent mixture decreased the fraction of insoluble products (Saisu, Sato, Watanabe, Adschiri, & Arai, 2003). Phenol reacts with the depolymerized fragments at the reactive sites and prevents cross-linking reaction during the process (Pandey & Kim, 2011). Similarly, solvolytic of lignin with *p*-cresol and water in the supercritical condition generates almost no insoluble products, and the molecular weights of fragments are significantly lower than that of the lignin feedstock (Matsumura et al., 2006).

Base Catalyzed Depolymerization

Base catalyzed depolymerization (BCD) is performed by using a solid base and a supercritical alcohol (e.g., methanol) to depolymerize lignin, generating phenols and phenol derivatives (Shabtai, Zmierczak, & Chornet, 1999). BCD is typically carried out at temperatures ranging from 250 to 310°C and pressures from 11 to 17 MPa (Shabtai et al., 1999). During BCD, aryl ether linkages in lignin are mainly cleaved and produce with high yield, phenolic compounds (Beauchet, Monteil-Rivera, & Lavoie, 2012). The products obtained from BCD include: a minor gaseous product (mostly CO₂), small organic compounds, lignin monomeric phenol derivatives (usually up to 10%), ligno-oligomers (45-70%), and a solid residue (Beauchet et al., 2012). In the monomeric fraction, Lavoie et al. detected and identified 26 compounds after the reaction of softwood and hemp lignin with a dilute NaOH solution at temperatures between 300 and 330°C under pressures ranging from 9 to 13 MPa. Among the identified compounds, guaiacol, catechol, and vanillin were the most abundant (Lavoie, Baré, & Bilodeau, 2011). The monomeric fraction can be valorized directly by HDO or hydrogenation to produce liquid transportation fuels. The oligomer-rich fraction is mainly composed of dimeric and trimeric compounds, which are hard to separate via industrially convenient methods (distillation or flash chromatography) (Beauchet et al., 2012). To further increase the commercialization opportunities for the oligomer-rich fraction, Shabtai et al. proposed the hydrocracking of this fraction into fuel additives (Shabtai et al., 1999).

The yield and selectivity of depolymerized lignin-derived compounds are dependent on the temperature, time, type of catalyst, and lignin/solvent ratio (Shabtai et al., 1999). At lower operating temperatures (230-250°C), the products from BCD of lignin are mainly methoxyl-substituted alkylphenols (Shabtai et al., 1999). As the temperature increases to 270-290°C, the products become mainly mono-, di-, tri-, and polymethylated phenols, due to direct ring alkylation or deoxygenative rearrangement of the methoxyl substitutes (Shabtai et al., 1999). Longer reaction times may negatively affect the performance of BCD due to the formation of acidic molecules, which over time, deactivate the catalyst via acid/base neutralization (Pandey & Kim, 2011).

Acid Catalyzed Depolymerization

Acid catalyzed depolymerization (ACD) is practiced by using different types of mineral or organic acids; Lewis acids; zeolites or other solid acids; or acidic ionic liquids in supercritical solvents or solvent mixtures to depolymerize lignin (Li, Zhao, Wang, Huber, & Zhang, 2015). The resulting organic phase consists of a wide range of aliphatic and aromatic hydrocarbons (Güvenatam, Heeres, Pidko, & Hensen, 2015). ACD is generally performed at temperatures ranging from 250 to 400°C for 1 to 4 h (Deepa & Dhepe, 2014; Güvenatam et al., 2015; Wang, Tucker, & Ji, 2013). ACD focuses on the cleavage of aryl ether linkages in lignin (Li, Zhao, et al., 2015; Wang et al., 2013). Acids serve as effective hydrogen-donators, forming H₃O⁺ and cleaving aryl ether linkages via hydrolysis (Wang et al., 2013). Güvenatam et al. reported that ACD of soda lignin at 400°C with Lewis acidic metal triflates generated aliphatic hydrocarbons (e.g., paraffins and olefins), aromatic hydrocarbons (i.e., alkylated non-oxygenated mono-aromatics, alkylbenzenes, and mono-aromatic oxygenates, mainly phenolics), condensed aromatics (e.g., naphthalenes), and saturated oxygenates (e.g., ketones and carboxylic acids) (Güvenatam et al., 2015). The most of lignin was converted

into lignin monomeric phenol derivatives; however, a small fraction of the lignin generated higher molecular weight (up to 650 g/mol) products (Güvenatam et al., 2015).

Similar to BCD, the reaction parameters have a remarkable effect on improving the yield of depolymerized lignin-derived compounds. The product yield is dependent on the temperature (Wang et al., 2013), reaction time (Wang et al., 2013), type of catalyst (Deepa & Dhepe, 2014), and lignin to solvent ratio (Forchheim, Gasson, Hornung, Kruse, & Barth, 2012; Gasson et al., 2012). At lower operating temperatures (78-200°C), the complex lignin structure cannot be efficiently converted into monomeric compounds (Wang et al., 2013); however, methoxyphenol, catechol, and phenol were the major components when the reaction temperature was raised from 360 to 400°C (Wang et al., 2013). Deepa et al. reported that solid acid catalysts gave a higher yield of THF soluble aromatic monomers (87%) than mineral acid catalysts like sulfuric acid (39%) and hydrochloride acid (29%) (Deepa & Dhepe, 2014).

Hydrogenolysis Products

The solid product of lignin hydrogenolysis is mainly composed of macromolecular lignin and re-polymerized phenolics and aromatics. The liquid product of lignin hydrogenolysis will have a non-volatile and volatile fraction. The non-volatile fraction is comprised of oligomeric fragments of lignin. Breaking of aryl ether linkages during hydrogenolysis decreases molecular weight and increases the number of aromatic hydroxyl groups, which can improve its solubility of these oligomeric fragments in the reaction solvent. The volatile fraction is primarily phenolic or aromatic ethers, which resemble the monomeric units of lignin. Short chain alcohols from side chain cleavage and small cyclic aliphatic compounds resulting from aromatic hydrogenation can also be generated.

Parameters Affecting Hydrogenolysis of Lignin

Product yield and distribution resulting from the hydrogenolysis of lignin strongly depends on reaction parameters, such as temperature, pressure, reaction time, catalyst, and solvent. These parameters are typically optimized to promote hydrogenolysis over hydrogenation. Severe reaction temperature enhances lignin conversion, but consequently decreases selectivity. Ye et al. reported that as the reaction temperature increased from 200 to 312°C, the yield of 4-ethylphenolics increased by three-fold (Ye et al., 2012). Meanwhile, more compounds were generated at higher temperatures than at a lower temperatures (Ye et al., 2012). The yield of phenolics during hydrogenolysis of lignin can be correlated with reaction time. According to Ye et al., the yield of 4-ethylphenolics increased with the reaction time increasing from 90 to 180 min at 250°C and from 60 to 90 min at 275°C (Ye et al., 2012). However, the yield of phenolics decreases when reaction times are significantly longer (Meier et al., 1992). This may be due to the re-polymerization and/or hydrogenation. The partial pressure of hydrogen remarkably influences the hydrogenolysis of lignin. A high pressure of hydrogen not only improves the yield of monomeric products, but also suppresses the formation of char (Meier et al., 1992). However, the high hydrogen pressure may also enhance hydrogenation, increasing the formation of cyclic aliphatic compounds (Pandey & Kim, 2011).

The physical and chemical properties of solvents have significant influences on the performance of lignin hydrogenolysis. The solubility of lignin during hydrogenolysis

can strongly affect the transport, and thus, the conversion of lignin. Solvents which can dissolve lignin or large lignin oligomers during hydrogenolysis increase the interactions between lignin and catalyst. Ionic liquids are excellent solvents to dissolve lignin for depolymerization. Binder et al. investigated hydrogenolysis of lignin model compounds in ionic liquids and found significantly high yields of products (Binder, Gray, White, Zhang, & Holladay, 2009). Moreover, phenolic products can be remarkably affected by the hydrogen donation ability of the reaction solvent, because the solubility of hydrogen in reaction medium can be limited. The mass transfer of hydrogen to the catalyst can control the absorption rate of hydrogen onto the catalyst, effecting the rate of catalytic hydrogenolysis (Pandey & Kim, 2011). Toledano et al. reported that hydrogenolysis of lignin using hydrogen-donating solvents combined with Ni-based catalyst could generate promising quantities of monomeric phenolic products and minimize the production of char (Toledano et al., 2013).

Catalysts play a crucial role in the hydrogenolysis of lignin. Catalysts have been developed to improve lignin conversion, selectivity for hydrogenolysis over hydrogenation, and specificity for aryl ether cleavage. There are two types of hydrogenolysis catalysts: homogenous and heterogeneous. Lignin is insoluble in most solvents, thus homogenous catalysts advantageously overcome issues related to mass transfer. However, homogenous catalysts tend to be unstable, degrading easily (especially at high temperatures) and have strict requirements for dry, anaerobic conditions. Homogenous catalysts are also difficult to separate and recover in an industrial product streams. On the other hand, heterogeneous catalysts are more robust and easily recovered. The major obstacle of using heterogeneous catalysts for the hydrogenolysis of lignin is related to the transport of an insoluble lignin to the surface of solid catalyst. Many homogenous catalysts have single-site active centers that facilitate more catalytic specificity than the multiple active-sites typical of heterogeneous catalysts.

Several homogeneous catalysts have been researched specifically targeting the selective cleavage of the β -O-4 linkages. Wu et al. illustrated the hydrogenolysis of lignin model dimers using a Ru-xantphos catalyst, observing a 95% C-O cleavage (Wu, Patrick, Chung, & James, 2012). Sergeev et al. used a soluble nickel carbene complex to selectively cleave the aromatic C-O bonds in the alkyl aryl and diaryl ethers, forming exclusively arenes and alcohols under mild conditions (Sergeev & Hartwig, 2011). In addition, Zhang et al. reported that a colloidal bimetallic catalyst composed of nickel and another noble metal (Ru, Rh, or Pd) was effective at hydrogenolysis of lignin model compounds (Zhang, Teo, et al., 2014). On the other hand, many heterogeneous noble metals catalysts have been studied. Song et al. stated that nickel-catalyzed hydrogenolysis of lignin model dimers with aryl ether linkages (e.g., benzylphenyl ether) gave a conversion of 62% and aromatic products selectivity between 42-58% (Song, Wang, & Xu, 2012). Furthermore, copper particles supported on γ -alumina catalyze the cleavage of β -O-4 linkages under HDO conditions, yielding phenol and ethylbenzene in substantial amounts (Strassberger, Alberts, Louwerse, Tanase, & Rothenberg, 2013).

Bioconversion and Hybrid Conversion of Lignin

Bioconversion

Bioconversion of biomass employs biological processes or systems, such as microorganisms, to generate fuels and chemicals. Millions of years of evolution have shaped the features of lignin to resist biological depolymerization and protect cell wall carbohydrates. Thus, the biological depolymerization of lignin is characterized by slow kinetics and low yields (Gasser et al., 2012). With the exception of a few bacteria and brown-/white-rot fungi (Bugg, Ahmad, Hardiman, & Singh, 2011), most natural biological systems do not have a significant ability to depolymerize lignin (Gasser et al., 2012). The few examples of the bioconversion of lignin with fungi can require several days, if not months (Van Soest, 1994). With that said, bioconversion, particularly with microbial systems, have several main advantages over thermal conversion systems (Lynd, Van Zyl, McBride, & Laser, 2005): 1) microbes can selectively produce chemical products, minimizing waste generation and required separations, 2) microbes usually have rapid growth rates, serving as cheap catalytic systems, and 3) microbial fermentation is performed under mild conditions, avoiding cost associated with the use of high temperatures, high pressures, and synthetic catalysts. This section briefly discusses specific biological routes of lignin processing.

Enzymes

Similar to cellulosic enzymatic hydrolysis for bio-ethanol production, enzymes that depolymerize lignin have been studied. There are two families of enzymes known to play a role in aerobic lignin degradation: peroxidases and laccases. These enzymes are used by biological systems, such as white-rot fungi, to degrade lignin (Pérez, Munoz-Dorado, de la Rubia, & Martinez, 2002), and some cases require an additional mediator like hydrogen peroxide. Two particular types of peroxidases are well characterized, lignin peroxidases (LiPs) and manganese-dependent peroxidases (MnPs) (Pérez et al., 2002). LiPs are glycoproteins with a heme group in their active center and have a molecular weight that ranges from 38-43 kDa (Pérez et al., 2002). They are described as the most effective peroxidases for oxidizing phenolics, amines, aromatic ethers, and polycyclic aromatics (Pérez et al., 2002; Sánchez, 2009). Like LiPs, MnPs are glycosylated proteins, but MnPs have slightly higher molecular weights, 45-60 kDa (Pérez et al., 2002). MnPs can oxidize Mn(II) to Mn(III), which is a strong oxidant that can leave the active center and oxidize phenolic compounds, but does not affect non-phenolic units of lignin (Pérez et al., 2002; Sánchez, 2009). However, the phenoxy-radicals generated from the oxidation and a variety of other reactions result in both depolymerization and re-polymerization. The re-polymerization reaction pathway occurs faster than depolymerization, thus treatment of lignin with peroxidases and hydrogen peroxide generally lead to mostly a lignin product with increased molecular weight. Laccases are copper-containing phenoloxidases that can catalyze the one-electron oxidation of phenolic and non-phenolic compounds in lignin in the presence of mediators (van de Pas et al., 2011). During oxidation catalyzed by laccases, phenoxy-radicals can form by the loss of an electron from the phenolic unit of lignin, which can lead to side chain cleavage (Pérez et al., 2002). However, these enzymes are also prone to re-polymerization of phenolics through a dehydrogenation pathway (Boerjan et al., 2003).

Microorganisms

White-rot fungi are one of the best degraders of lignin, and are the only known organisms that can completely break down lignin, producing carbon dioxide and water (ten Have & Teunissen, 2001). In 1975, a study suggested that the cleavage of aromatic rings from oxidation could degrade lignin into fragments using the extracellular extracts (ligninolytic peroxidases) of white-rot fungi (ten Have & Teunissen, 2001). As a result of the extensive research on lignin degradation by white-rot fungi, lignin bio-degradation is known to be affected by many parameters. The major factor is the oxygen level in the growth culture. According to studies with *P. chrysosporium*, lignin degradation occurs when nutrients, nitrogen, carbon, or sulfur are depleted (ten Have & Teunissen, 2001). Hence, nitrogen-limited conditions favor lignin degradation. Increasing the oxygen concentration in the culture can reduce the nitrogen content, which can enhance lignin degradation. Furthermore, the oxygen level of the culture can elevate hydrogen peroxide production, and hydrogen peroxide is essential for the activity of peroxidases that catalyze aromatic oxidation (ten Have & Teunissen, 2001). Moreover, agitation can effect lignin degradation. Agitation of the growth culture can limit oxygen availability and inhibit lignin oxidation (ten Have & Teunissen, 2001). Other factors, such as the pH value of the culture and the concentration of certain minerals (e.g., calcium and manganese), can also affect the performance of white-rot fungi in lignin degradation (ten Have & Teunissen, 2001). Besides white-rot fungi, brown-rot fungi also can convert lignin, but instead of significantly degrading lignin, brown-rot fungi alters the structure of lignin (Gasser et al., 2012). The modified lignin has a lower methoxyl content and higher content of phenolic hydroxyl, conjugated carbonyl, and carboxyl groups (Yelle, Ralph, Lu, & Hammel, 2008). Although lignin modified by brown-rot lignin is still polymeric and retains most of its aromatic residues (Jin, Schultz, & Nicholas, 1990), brown-rot fungi does initially depolymerize lignin (Gasser et al., 2012).

There are some literature reports that lignin can be degraded by bacteria (Bugg et al., 2011). Although the enzymology of bacterial lignin degradation is still not understood, types of extracellular enzymes (e.g., ligninolytic peroxidases) that are similar to fungi may be used to degrade lignin (Gasser et al., 2012). For example, Mercer et al. found several actinomycetes exhibiting extracellular peroxidase activity (Mercer, Iqbal, Miller, & McCarthy, 1996). Ahmad et al. identified a dye decolorizing peroxidase (DyP) in the actinomycete *Rhodococcus jostii* sp. RHA1, which was able to catalyze the cleavage of the C α -C β bond in a lignin model compound (Ahmad et al., 2011). Laccase produced by bacteria was reported to degrade lignin (Miyazaki, 2005). A summary of current lignin conversion techniques including their major products and advantages and disadvantages is provided in Table 3.

Hybrid Conversion

Hybrid conversion is an integrated process that employs both biological and thermochemical conversion routes to produce fuels and chemicals from lignin. Efficiently overcoming the inherent recalcitrance of lignin, lignin can be treated and depolymerized by a thermal process. Taking advantage of the specificity of biology, depolymerized lignin can undergo further biological conversion, acting as a biological “funnel” and overcoming issues related to the wide distribution of products generally associated with thermal conversion. For

example, the syngas produced from gasification of lignin can be upgraded to higher quality fuels and chemicals by using microbial fermentation. This process is known as syngas fermentation, and uses genetically developed microorganisms to rely on syngas as a source of carbon and energy to produce commercially valuable metabolites. These syngas fermentation microorganisms include autotrophs (e.g., *Clostridium ljungdahlii*), which use C₁ compounds (e.g., carbon monoxide, carbon dioxide, methane, and methanol) as their sole carbon source and hydrogen as their energy source or unicarbonotrophs (e.g., *Rhodospseudomonas gelatinosa*), which use C₁ compounds as their only source of carbon and energy (Brown & Wright, 2008; Hayes, 2009). For example, Heiskanen et al. investigated the effect of syngas composition on the growth and product formation of *Butyribacterium methylotrophicum*, and found that more butyric acid formed as the hydrogen composition in the syngas increased (Heiskanen, Virkajärvi, & Viikari, 2007).

Table 3. Summary of conversion techniques and their advantages and disadvantages

Conversion Techniques	Major Products	Advantages and Disadvantages
Gasification	Syngas	Advantages: production of hydrogen; direct use for heat and power supply Disadvantages: low heating value; tar formation; further upgrading is required; high capital and maintenance cost
Pyrolysis	Bio-oil	Advantages: significant bio-oil production Disadvantages: wide distribution compounds generated; bio-char formation
Oxidative Cracking	Aromatic aldehydes, ketones, and carboxylic acids	Advantages: generation of oxidized aromatic Disadvantages: low yield
Hydrogenolysis	Monomeric phenolics Short chain alcohols, and alkanes Large lignin fragments	Advantages: higher content of phenolic compounds Disadvantages: low yield; limited solubility of lignin
Bioconversion	Lignin monomeric compounds	Advantages: convenient process; high selectivity Disadvantages: low yield; slow kinetics; limited solubility of lignin in cell growth culture

Similarly, lignin can be effectively broken down to phenolic compounds by thermal conversion. These phenolic products can be used to generate industrial important chemicals through a bioconversion. Sainsbury et al. reported that a gene deletion mutant of *Rhodococcus jostii* RHA1 can convert thermally degraded lignin to high value chemicals

(e.g., vanillin) (Kosa & Ragauskas, 2012; Sainsbury et al., 2013; Wei, Zeng, Huang, et al., 2015; Wei, Zeng, Kosa, Huang, & Ragauskas, 2015). Wells et al. reported *Rhodococcus opacus* DSM 1069 used carbohydrates and aromatics to accumulate oils composed of oleic, palmitic, and stearic fatty acids (Wells, Wei, & Ragauskas, 2015). Similarly, Wei et al. used light oil from pyrolysis as sole carbon source to support the growth of *Rhodococcus opacus* and produce triacylglycerols (Wei, Zeng, Kosa, et al., 2015). Lignin fragments within the effluent of organosolv pretreatments for lignocellulosic biomass has been used to grow *Rhodococcus opacus* and produce lipids (Kosa & Ragauskas, 2013; Wei, Zeng, Huang, et al., 2015).

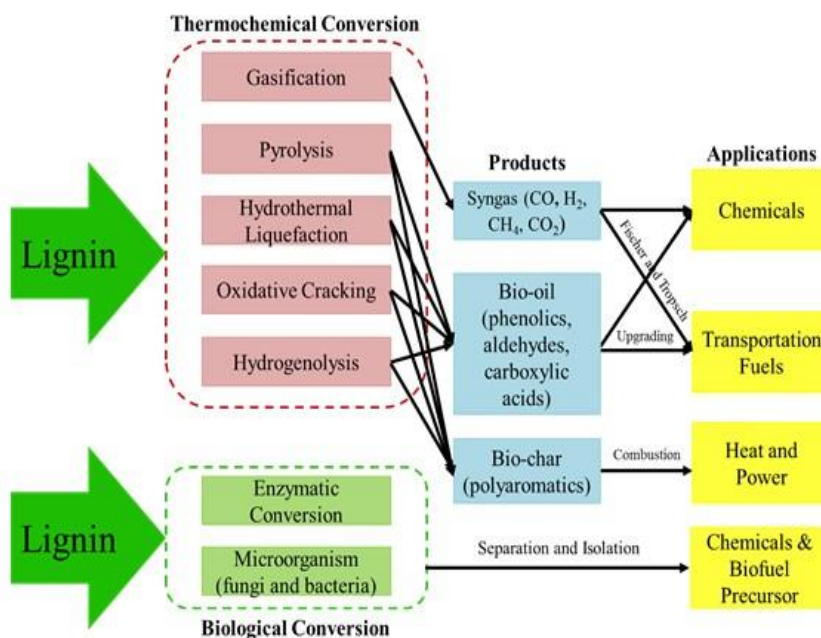


Figure 5. Lignin conversion processes and their potential products.

FUTURE PERSPECTIVE

Genetic Engineering of Lignin

Lignin has an immense potential in industry as a feedstock for the production of fuels and chemicals. Because of its importance, great effort has been put into understanding the biosynthetic pathways of lignin. Hence, recently genetic engineering of lignin has become a notable division of lignin research (Baucher, Monties, Montagu, & Boerjan, 1998). Using lignocellulosic biomass for the production of value-added chemicals and fuels requires decreasing plant cell wall recalcitrance, the inherent ability of the cell wall to resist deconstruction (Ragauskas et al., 2014). To address issues related to plant cell wall recalcitrance, plants that produce genetically altered lignin have been developed. Second generation bio-ethanol (and co-products) is produced via the fermentation of monosaccharides generated from lignocellulosic biomass via enzymatic hydrolysis. However,

the plant cell wall recalcitrance of most biomass, in part due to the presence and structure of lignin, causes enzymatic hydrolysis to be inefficient and costly. As a result, genetic engineering of lignin has primarily focused on: 1) decreasing lignin content and/or 2) modifying the monolignol distributions, in order to establish biomass with lower recalcitrance (Ragauskas et al., 2014).

Lignin monomers are biosynthesized through several multi-step pathways including the shikimate and phenylpropanoid pathways, and a final pathway that is specific to the plant (Baucher et al., 1998; Boudet & Grima-Pettenati, 1996). A few enzymes studied in these pathways include phenylalanine ammonia-lyase (PAL), and caffeic acid O-methyltransferase (COMT), ferulate-5-hydroxylase (F5H), and cinnamoyl-CoA reductase (CCR) (Baucher et al., 1998; Boudet & Grima-Pettenati, 1996; Fu et al., 2011; Whetten & Sederoff, 1995). Genetic engineering of lignin mainly involves down-regulation of various enzymes in the lignin biosynthesis pathway (Boudet & Grima-Pettenati, 1996). By altering the gene expression of these lignin biosynthesis enzymes, the monomer flux for lignin radical polymerization can be altered, thus altering the resulting lignin content and/or monolignol distributions. Moreover, because the monolignol distributions affect the types of inter-unit linkage formed, altering gene expression of these lignin biosynthesis enzymes can alter not only the size and structure of lignin, but also its physical and chemical properties.

For example, in studies involving the down-regulation of PAL in *Nicotiana tabacum*, the enzyme involved in the first step in the phenylpropanoid pathway, the amount of total lignin decreased, the S/G ratio increased, and the amount of G units decreased (Baucher et al., 1998). COMT was down-regulated in tobacco, switchgrass, poplar and alfalfa; and was shown to reduce the S/G lignin ratio in all four plant species (Baucher et al., 1998; Boerjan et al., 2003; Fu et al., 2011; Guo, Chen, Inoue, Blount, & Dixon, 2001). In switchgrass (*Panicum virgatum* L.), down-regulation of the COMT gene resulted in phenotypically normal plants with decreased lignin and changed lignin composition, which made the switchgrass more suitable for pretreatment (Fu et al., 2011). The ethanol yield from these transgenic switchgrass was also increased relative to the wild type plants with milder pretreatments necessary (Fu et al., 2011).

Lignin with more S units and fewer G units is easier to depolymerize, and is thus more favorable for processing (Boerjan et al., 2003; Boudet & Grima-Pettenati, 1996; Ragauskas et al., 2014; Ralph et al., 2004; Whetten & Sederoff, 1995). The S units of lignin primarily form β -O-4 linkages. The β -O-4 linkage is more easily chemically cleaved than other monolignol linkages, such as β -5, β - β , 5-5, 4-O-5, and β -1 linkages. Therefore, a lignin mutant with a high S/G ratio or only S units would be ideal for conversion technologies that selectively cleave aryl ether linkages. Genetically controlling monolignol distributions, inter-unit linkages distributions, and methoxylation could also be employed to manipulate lignin chain flexibility, molecular weight, fractal shape, and solubility.

These examples of engineered lignin show that lignification can be altered in plants drastically (Boerjan et al., 2003). The implications of the genetic engineering of lignin naturally extend to the generation of plants designed for specific lignin conversion technologies or even depolymerization catalyst. Currently, genetic engineering of lignin has only been researched in the context of bio-ethanol production and pulping. However, the ability to decrease the recalcitrance of lignin for those purposes, makes it highly likely that in the near future lignin will be genetically modified for the thermal or hybrid conversion of lignin into renewable fuels and chemicals (Ragauskas et al., 2014).

CONCLUSION

This chapter provides an overview of current technologies for lignin conversion into fuels and chemicals. Although these technologies have been researched for more than a decade and have shown the capability to convert lignin into value-added products, the product yield and selectivity of these processes are not sufficient to facilitate economical, large-scale production. Currently, there are several challenges facing the efficient depolymerization or deconstruction of lignin. First, thermal conversion methods for lignin utilize severe conditions, requiring significant energy input and investment in infrastructure for safe operation. These severe conditions are required to overcome the inherent recalcitrance of lignin, but also promote uncontrolled deconstruction and secondary reactions that reduce selectivity and broaden the product distribution. Thus, most of these conversion techniques have low yields of and selectivity for desired products. A significant portion of the carbon and energy of lignin is wasted in the production of undesired products. In addition, the required separations and purifications for chemical production from lignin using current conversion methods is expensive and unpractical. As far as fuel production, in order to generate quality bio-fuel, current lignin-based liquid products need further upgrading to reduce their oxygen content, which consumes additional energy and increases the cost of that bio-fuel. Hence, the development of catalysts and methods for lignin selective depolymerization and deconstruction that can greatly increase lignin conversion while also increasing product yield and selectively is therefore required. To accomplish this, a deeper understanding of 1) lignin structure and its effect on depolymerization, 2) lignin depolymerization catalyst structure–activity relationships, and 3) lignin depolymerization mechanisms and kinetics must be established.

REFERENCES

- Ahmad, M., Roberts, J. N., Hardiman, E. M., Singh, R., Eltis, L. D., & Bugg, T. D. (2011). Identification of DypB from *Rhodococcus jostii* RHA1 as a lignin peroxidase. *Biochemistry*, *50*(23), 5096-5107.
- Akhtar, J., & Amin, N. S. (2012). A review on operating parameters for optimum liquid oil yield in biomass pyrolysis. *Renewable and Sustainable Energy Reviews*, *16*(7), 5101-5109.
- Argyropoulos, D. S., & Menachem, S. B. (1997). Lignin. *Biotechnology in the Pulp and Paper Industry* (pp. 127-158): Springer.
- Avellar, B. K., & Glasser, W. G. (1998). Steam-assisted biomass fractionation. I. Process considerations and economic evaluation. *Biomass and Bioenergy*, *14*(3), 205-218.
- Azadi, P., Inderwildi, O. R., Farnood, R., & King, D. A. (2013). Liquid fuels, hydrogen and chemicals from lignin: a critical review. *Renewable and Sustainable Energy Reviews*, *21*, 506-523.
- Babu, B. (2008). Biomass pyrolysis: a state-of-the-art review. *Biofuels, Bioproducts and Biorefining*, *2*(5), 393-414.
- Banoub, J. H., & Delmas, M. (2003). Structural elucidation of the wheat straw lignin polymer by atmospheric pressure chemical ionization tandem mass spectrometry and matrix-

- assisted laser desorption/ionization time-of-flight mass spectrometry. *Journal of Mass Spectrometry*, 38(8), 900-903.
- Barbir, F., Veziroğlu, T., & Plass, H. (1990). Environmental damage due to fossil fuels use. *International Journal of Hydrogen Energy*, 15(10), 739-749.
- Barneto, A. G., Carmona, J. A., Galvez, A., & Conesa, J. A. (2008). Effects of the composting and the heating rate on biomass gasification. *Energy & Fuels*, 23(2), 951-957.
- Barreto, L., Makihira, A., & Riahi, K. (2003). The hydrogen economy in the 21st century: a sustainable development scenario. *International Journal of Hydrogen Energy*, 28(3), 267-284.
- Barta, K., Matson, T. D., Fetting, M. L., Scott, S. L., Iretskii, A. V., & Ford, P. C. (2010). Catalytic disassembly of an organosolv lignin via hydrogen transfer from supercritical methanol. *Green Chemistry*, 12(9), 1640-1647.
- Baucher, M., Monties, B., Montagu, M. V., & Boerjan, W. (1998). Biosynthesis and genetic engineering of lignin. *Critical Reviews in Plant Sciences*, 17(2), 125-197.
- Beauchet, R., Monteil-Rivera, F., & Lavoie, J. (2012). Conversion of lignin to aromatic-based chemicals (L-chems) and biofuels (L-fuels). *Bioresource Technology*, 121, 328-334.
- Ben, H., & Ragauskas, A. J. (2011a). Heteronuclear Single-Quantum Correlation-Nuclear Magnetic Resonance (HSQC-NMR) Fingerprint Analysis of Pyrolysis Oils. *Energy & Fuels*, 25(12), 5791-5801.
- Ben, H., & Ragauskas, A. J. (2011b). NMR characterization of pyrolysis oils from kraft lignin. *Energy & Fuels*, 25(5), 2322-2332.
- Ben, H., & Ragauskas, A. J. (2011c). Pyrolysis of Kraft lignin with additives. *Energy & Fuels*, 25(10), 4662-4668.
- Bentley, R. W. (2002). Global oil & gas depletion: an overview. *Energy Policy*, 30(3), 189-205.
- Binder, J. B., Gray, M. J., White, J. F., Zhang, Z. C., & Holladay, J. E. (2009). Reactions of lignin model compounds in ionic liquids. *Biomass and Bioenergy*, 33(9), 1122-1130.
- Boeriu, C. G., Bravo, D., Gosselink, R. J., & van Dam, J. E. (2004). Characterisation of structure-dependent functional properties of lignin with infrared spectroscopy. *Industrial Crops and Products*, 20(2), 205-218.
- Boerjan, W., Ralph, J., & Baucher, M. (2003). Lignin biosynthesis. *Annual Review of Plant Biology*, 54(1), 519-546.
- Boudet, A. M., & Grima-Pettenati, J. (1996). Lignin genetic engineering. *Molecular Breeding*, 2(1), 25-39.
- Brady, B., Brush, S., Burmark, B., Corbin, M., Demay, J., Drabek, J., Figueroakaminsky, C., Hibbard, R., Keel, L., Newman, A., Otterson, S., Schweiters, J., Dahlgren, T., Das, T., Keill, L., & Piening, C. (1998). *Washington State Air Toxic Sources and Emission Estimation Methods*. Washington State Department of Ecology.
- Brewer, C. E., Schmidt-Rohr, K., Satrio, J. A., & Brown, R. C. (2009). Characterization of biochar from fast pyrolysis and gasification systems. *Environmental Progress & Sustainable Energy*, 28(3), 386-396.
- Bridgwater, A. V. (2012). Review of fast pyrolysis of biomass and product upgrading. *Biomass and Bioenergy*, 38, 68-94.
- Brown, R. C., & Wright, M. (2008). Biomass conversion to fuels and electric power. *Biofuels: Environmental Consequences and Interactions with Changing Land Use*.

- Proceedings of the Scientific Committee on Problems of the Environment (SCOPE) International Biofuels Project Rapid Assessment, 22-25.*
- Brownsort, P. (2009). Biomass pyrolysis processes: review of scope, control and variability. *Edinburgh: UK Biochar Research Center.*
- Brunow, G. (2005). Methods to Reveal the Structure of Lignin. *Biopolymers Online: Wiley-VCH Verlag GmbH & Co. KGaA.*
- Bu, Q., Lei, H., Zacher, A. H., Wang, L., Ren, S., Liang, J., Wei, Y., Liu, Y., Tang, J., Zhang, Q., & Ruan, R. (2012). A review of catalytic hydrodeoxygenation of lignin-derived phenols from biomass pyrolysis. *Bioresource Technology, 124*, 470-477..
- Bugg, T. D., Ahmad, M., Hardiman, E. M., & Singh, R. (2011). The emerging role for bacteria in lignin degradation and bio-product formation. *Current Opinion in Biotechnology, 22*(3), 394-400.
- Busetto, L., Fabbri, D., Mazzoni, R., Salmi, M., Torri, C., & Zanotti, V. (2011). Application of the Shvo catalyst in homogeneous hydrogenation of bio-oil obtained from pyrolysis of white poplar: New mild upgrading conditions. *Fuel, 90*(3), 1197-1207.
- Campbell, M. M., & Sederoff, R. R. (1996). Variation in lignin content and composition. *Plant Physiology, 110*, 3-13.
- Cao, X., Pignatello, J. J., Li, Y., Latta, C., Chappell, M. A., Chen, N., Miller, L. F., & Mao, J. (2012). Characterization of wood chars produced at different temperatures using advanced solid-state ¹³C NMR spectroscopic techniques. *Energy & Fuels, 26*(9), 5983-5991.
- Capanema, E. A., Balakshin, M. Y., & Kadla, J. F. (2004). A comprehensive approach for quantitative lignin characterization by NMR spectroscopy. *Journal of Agricultural and Food Chemistry, 52*(7), 1850-1860.
- Chen, L., Carpita, N. C., Reiter, W. D., Wilson, R. H., Jeffries, C., & McCann, M. C. (1998). A rapid method to screen for cell-wall mutants using discriminant analysis of Fourier transform infrared spectra. *The Plant Journal, 16*(3), 385-392.
- Cheng, H., Wartelle, L. H., Klasson, K. T., & Edwards, J. C. (2010). Solid-state NMR and ESR studies of activated carbons produced from pecan shells. *Carbon, 48*(9), 2455-2469.
- Collard, F. X., & Blin, J. (2014). A review on pyrolysis of biomass constituents: mechanisms and composition of the products obtained from the conversion of cellulose, hemicelluloses and lignin. *Renewable and Sustainable Energy Reviews, 38*, 594-608.
- Cotrim, A. R., Ferraz, A., Gonçalves, A. R., Silva, F. T., & Bruns, R. E. (1999). Identifying the origin of lignins and monitoring their structural changes by means of FTIR-PCA and SIMCA. *Bioresource Technology, 68*(1), 29-34.
- Coumou, D., & Rahmstorf, S. (2012). A decade of weather extremes. *Nature Climate Change, 2*(7), 491-496.
- Crocker, M. (2010). *Thermochemical conversion of biomass to liquid fuels and chemicals*: Royal Society of Chemistry.
- Cui, C., Sun, R., & Argyropoulos, D. S. (2014). Fractional Precipitation of Softwood Kraft Lignin: Isolation of Narrow Fractions Common to a Variety of Lignins. *ACS Sustainable Chemistry & Engineering, 2*(4), 959-968.
- Das, L., Kolar, P., & Sharma-Shivappa, R. (2012). Heterogeneous catalytic oxidation of lignin into value-added chemicals. *Biofuels, 3*(2), 155-166.

- Deepa, A. K., & Dhepe, P. L. (2014). Solid acid catalyzed depolymerization of lignin into value added aromatic monomers. *Royal Society of Chemistry Advances*, 4(25), 12625-12629.
- DeKing, N. (2004). Pulp and paper global fact and price book: 2003-2004. *Paperloop, San Fransisco*.
- Deng, H., Lin, L., & Liu, S. (2010). Catalysis of Cu-doped Co-based perovskite-type oxide in wet oxidation of lignin to produce aromatic aldehydes. *Energy & Fuels*, 24(9), 4797-4802.
- Doherty, W. O., Mousavioun, P., & Fellows, C. M. (2011). Value-adding to cellulosic ethanol: Lignin polymers. *Industrial Crops and Products*, 33(2), 259-276.
- Dong, D., & Fricke, A. L. (1995). Intrinsic viscosity and the molecular weight of kraft lignin. *Polymer*, 36(10), 2075-2078.
- Effendi, A., Gerhauser, H., & Bridgwater, A. V. (2008). Production of renewable phenolic resins by thermochemical conversion of biomass: a review. *Renewable and Sustainable Energy Reviews*, 12(8), 2092-2116.
- Fargues, C., Mathias, Á., & Rodrigues, A. (1996). Kinetics of vanillin production from kraft lignin oxidation. *Industrial & Engineering Chemistry Research*, 35(1), 28-36.
- Fengel, D., & Wegener, G. (1983). *Wood: chemistry, ultrastructure, reactions*: Walter de Gruyter.
- Forchheim, D., Gasson, J. R., Hornung, U., Kruse, A., & Barth, T. (2012). Modeling the Lignin Degradation Kinetics in a Ethanol/Formic Acid Solvolysis Approach. Part 2. Validation and Transfer to Variable Conditions. *Industrial & Engineering Chemistry Research*, 51(46), 15053-15063.
- Foston, M., Nunnery, G. A., Meng, X., Sun, Q., Baker, F. S., & Ragauskas, A. (2013). NMR a critical tool to study the production of carbon fiber from lignin. *Carbon*, 52, 65-73.
- Fredheim, G. E., Braaten, S. M., & Christensen, B. E. (2002). Molecular weight determination of liginosulfonates by size-exclusion chromatography and multi-angle laser light scattering. *Journal of Chromatography A*, 942(1), 191-199.
- Freudenberg, K. (1959). Biosynthesis and Constitution of Lignin. *Nature*, 183(4669), 1152-1155.
- Fu, C., Mielenz, J. R., Xiao, X., Ge, Y., Hamilton, C. Y., Rodriguez, M., Chen, F., Foston, M., Ragauskas, A., Bouton, J., Dixon, R. A., & Wang, Z. Y. (2011). Genetic manipulation of lignin reduces recalcitrance and improves ethanol production from switchgrass. *Proceedings of the National Academy of Sciences*, 108(9), 3803-3808.
- Fukushima, R. S., & Hatfield, R. D. (2001). Extraction and isolation of lignin for utilization as a standard to determine lignin concentration using the acetyl bromide spectrophotometric method. *Journal of Agricultural and Food Chemistry*, 49(7), 3133-3139.
- Garcia-Perez, M., Chaala, A., Pakdel, H., Kretschmer, D., & Roy, C. (2007). Characterization of bio-oils in chemical families. *Biomass and Bioenergy*, 31(4), 222-242.
- Gargulak, J. D., & Lebo, S. E. (1999). Commercial Use of Lignin-Based Materials. *Lignin: Historical, Biological, and Materials Perspectives* (Vol. 742, pp. 304-320): American Chemical Society.
- Gasser, C. A., Hommes, G., Schäffer, A., & Corvini, P. F. X. (2012). Multi-catalysis reactions: new prospects and challenges of biotechnology to valorize lignin. *Applied Microbiology and Biotechnology*, 95(5), 1115-1134.

- Gasson, J. R., Forchheim, D., Sutter, T., Hornung, U., Kruse, A., & Barth, T. (2012). Modeling the lignin degradation kinetics in an ethanol/formic acid solvolysis approach. Part 1. Kinetic model development. *Industrial & Engineering Chemistry Research*, 51(32), 10595-10606.
- Gellerstedt, G., & Robert, D. (1987). Quantitative ^{13}C NMR analysis of kraft lignins. *Acta Chemica Scandinavica*, 41b(7), 541-546. doi: 10.3891/acta.chem.scand.41b-0541.
- Gidh, A. V., Decker, S. R., See, C. H., Himmel, M. E., & Williford, C. W. (2006). Characterization of lignin using multi-angle laser light scattering and atomic force microscopy. *Analytica Chimica Acta*, 555(2), 250-258.
- Gidh, A. V., Decker, S. R., Vinzant, T. B., Himmel, M. E., & Williford, C. (2006). Determination of lignin by size exclusion chromatography using multi angle laser light scattering. *Journal of Chromatography A*, 1114(1), 102-110.
- Gosselink, R. J., Teunissen, W., Van Dam, J. E., De Jong, E., Gellerstedt, G., Scott, E. L., & Sanders, J. P. (2012). Lignin depolymerisation in supercritical carbon dioxide/acetone/water fluid for the production of aromatic chemicals. *Bioresource Technology*, 106, 173-177.
- Goyal, H., Seal, D., & Saxena, R. (2008). Bio-fuels from thermochemical conversion of renewable resources: a review. *Renewable and Sustainable Energy Reviews*, 12(2), 504-517.
- Gross, S. K., Sarkanen, K., & Schuerch, C. (1958). Determinations of Molecular Weight of Lignin Degradation Products by Three Methods. *Analytical Chemistry*, 30(4), 518-521.
- Guo, D., Chen, F., Inoue, K., Blount, J. W., & Dixon, R. A. (2001). Downregulation of caffeic acid 3-O-methyltransferase and caffeoyl CoA 3-O-methyltransferase in transgenic alfalfa: impacts on lignin structure and implications for the biosynthesis of G and S lignin. *The Plant Cell*, 13(1), 73-88.
- Güvenatam, B., Heeres, E. H., Pidko, E. A., & Hensen, E. J. (2015). Lewis acid-catalyzed depolymerization of soda lignin in supercritical ethanol/water mixtures. *Catalysis Today*, 269(2016), 9-20.
- Hahn-Hägerdal, B., Galbe, M., Gorwa-Grauslund, M.-F., Lidén, G., & Zacchi, G. (2006). Bio-ethanol—the fuel of tomorrow from the residues of today. *Trends in Biotechnology*, 24(12), 549-556.
- Hallac, B. B., Pu, Y., & Ragauskas, A. J. (2010). Chemical transformations of *Buddleja davidii* lignin during ethanol organosolv pretreatment. *Energy & Fuels*, 24(4), 2723-2732.
- Harkin, J. M. (1969). *Lignin and its uses* (No. FSRN-FPL-0206). FOREST PRODUCTS LAB MADISON WIS.
- Hatfield, G. R., Maciel, G. E., Erbatur, O., & Erbatur, G. (1987). Qualitative and quantitative analysis of solid lignin samples by carbon-13 nuclear magnetic resonance spectrometry. *Analytical Chemistry*, 59(1), 172-179.
- Hayes, D. J. (2009). An examination of biorefining processes, catalysts and challenges. *Catalysis Today*, 145(1), 138-151.
- Heiskanen, H., Virkajärvi, I., & Viikari, L. (2007). The effect of syngas composition on the growth and product formation of *Butyribacterium methylotrophicum*. *Enzyme and Microbial Technology*, 41(3), 362-367.
- Himmel, M. E., Tatsumoto, K., Grohmann, K., Johnson, D. K., & Chum, H. L. (1990). Molecular weight distribution of aspen lignins from conventional gel permeation

- chromatography, universal calibration and sedimentation equilibrium. *Journal of Chromatography A*, 498, 93-104.
- Holladay, J. E., Bozell, J. J., White, J. F., & Johnson, D. (2007). *Top Value-Added Chemicals from Biomass-Volume II—Results of Screening for Potential Candidates from Biorefinery Lignin* (No. PNNL-16983). Pacific Northwest National Laboratory (PNNL), Richland, WA (US).
- Holtman, K. M. (2004). *An Investigation of the Milled Wood Lignin Isolation Procedure by Solution-and Solid-State NMR Spectroscopy*. Ph.D, North Carolina State University, Wood and Paper Science.
- Holtman, K. M., Chang, H. m., Jameel, H., & Kadla, J. F. (2006). Quantitative ^{13}C NMR characterization of milled wood lignins isolated by different milling techniques. *Journal of Wood Chemistry and Technology*, 26(1), 21-34.
- Hu, L., Pan, H., Zhou, Y., & Zhang, M. (2011). Methods to improve lignin's reactivity as a phenol substitute and as replacement for other phenolic compounds: A brief review. *BioResources*, 6(3), 3515-3525.
- Huber, G. W., Iborra, S., & Corma, A. (2006). Synthesis of transportation fuels from biomass: chemistry, catalysts, and engineering. *Chemical Reviews*, 106(9), 4044-4098.
- Humphreys, J. M., Hemm, M. R., & Chapple, C. (1999). New routes for lignin biosynthesis defined by biochemical characterization of recombinant ferulate 5-hydroxylase, a multifunctional cytochrome P450-dependent monooxygenase. *Proceedings of the National Academy of Sciences*, 96(18), 10045-10050.
- Jääskeläinen, A., Sun, Y., Argyropoulos, D., Tamminen, T., & Hortling, B. (2003). The effect of isolation method on the chemical structure of residual lignin. *Wood Science and Technology*, 37(2), 91-102.
- Jahirul, M. I., Rasul, M. G., Chowdhury, A. A., & Ashwath, N. (2012). Biofuels production through biomass pyrolysis—a technological review. *Energies*, 5(12), 4952-5001.
- Jin, L., Schultz, T. P., & Nicholas, D. D. (1990). Structural characterization of brown-rotted lignin. *Holzforschung-International Journal of the Biology, Chemistry, Physics and Technology of Wood*, 44(2), 133-138.
- Joffres, B., Laurenti, D., Charon, N., Daudin, A., Quignard, A., & Geantet, C. (2013). Thermochemical conversion of lignin for fuels and chemicals: a review. *Oil & Gas Science and Technology—Revue d'IFP Energies nouvelles*, 68(4), 753-763.
- Johansson, A., Aaltonen, O., & Ylinen, P. (1987). Organosolv pulping—methods and pulp properties. *Biomass*, 13(1), 45-65.
- Kanetake, T., Sasaki, M., & Goto, M. (2007). Decomposition of a lignin model compound under hydrothermal conditions. *Chemical Engineering & Technology*, 30(8), 1113-1122.
- Kang, S., Li, X., Fan, J., & Chang, J. (2013). Hydrothermal conversion of lignin: a review. *Renewable and Sustainable Energy Reviews*, 27, 546-558.
- Kaparaju, P., Serrano, M., Thomsen, A. B., Kongjan, P., & Angelidaki, I. (2009). Bioethanol, biohydrogen and biogas production from wheat straw in a biorefinery concept. *Bioresource Technology*, 100(9), 2562-2568.
- Kelley, S. S., Rowell, R. M., Davis, M., Jurich, C. K., & Ibach, R. (2004). Rapid analysis of the chemical composition of agricultural fibers using near infrared spectroscopy and pyrolysis molecular beam mass spectrometry. *Biomass and Bioenergy*, 27(1), 77-88.
- Kim, H., & Ralph, J. (2010). Solution-state 2D NMR of ball-milled plant cell wall gels in DMSO-d₆/pyridine-d₅. *Organic & Biomolecular Chemistry*, 8, 576-591.

- Kirk, T. K., & Jeffries, T. W. (1996). Roles for Microbial Enzymes in Pulp and Paper Processing. *Enzymes for Pulp and Paper Processing* (Vol. 655, pp. 2-14): American Chemical Society.
- Kirkels, A. F., & Verbong, G. P. (2011). Biomass gasification: Still promising? A 30-year global overview. *Renewable and Sustainable Energy Reviews*, *15*(1), 471-481.
- Klass, D. L. (1998). *Biomass for renewable energy, fuels, and chemicals*: Academic Press.
- Kleinert, M., & Barth, T. (2008). Phenols from lignin. *Chemical Engineering & Technology*, *31*(5), 736-745.
- Kokta, B., & Ahmed, A. (1998). *Steam explosion pulping*: John Wiley and Sons, Inc., Madison.
- Kosa, M., & Ragauskas, A. J. (2012). Bioconversion of lignin model compounds with oleaginous Rhodococci. *Applied Microbiology and Biotechnology*, *93*(2), 891-900.
- Kosa, M., & Ragauskas, A. J. (2013). Lignin to lipid bioconversion by oleaginous Rhodococci. *Green Chemistry*, *15*(8), 2070-2074.
- Kumar, A., Jones, D. D., & Hanna, M. A. (2009). Thermochemical biomass gasification: a review of the current status of the technology. *Energies*, *2*(3), 556-581.
- Kuznetsov, B. N., Kuznetsova, S. A., Danilov, V. G., Yatsenkova, O. V., & Petrov, A. V. (2011). A green one-step process of obtaining microcrystalline cellulose by catalytic oxidation of wood. *Reaction Kinetics, Mechanisms and Catalysis*, *104*(2), 337-343.
- Kuznetsov, B. N., Sudakova, I. G., Garyntseva, N. V., Djakovitch, L., & Pinel, C. (2013). Kinetic study of aspen-wood sawdust delignification by H₂O₂ with sulfuric acid catalyst under mild conditions. *Reaction Kinetics, Mechanisms and Catalysis*, *110*(2), 271-280.
- Lage, L. E. C., Sant'Anna Jr, G. L., & Nobrega, R. (1999). Molecular weight distribution of chlorolignin in bleached Kraft effluent by GPC and ultrafiltration. *Bioresource Technology*, *68*(1), 63-70.
- Lavoie, J.-M., Baré, W., & Bilodeau, M. (2011). Depolymerization of steam-treated lignin for the production of green chemicals. *Bioresource Technology*, *102*(7), 4917-4920.
- Li, C., Zhao, X., Wang, A., Huber, G. W., & Zhang, T. (2015). Catalytic Transformation of Lignin for the Production of Chemicals and Fuels. *Chemical Reviews*, *115*(21), 11559-11624.
- Li, Z., Bansal, N., Azarpira, A., Bhalla, A., Chen, C. H., Ralph, J., Hegg, E., & Hodge, D. B. (2015). Chemical and structural changes associated with Cu-catalyzed alkaline-oxidative delignification of hybrid poplar. *Biotechnology for Biofuels*, *8*(1), 1-12.
- Lin, S. Y., & Dence, C. W. (1992). *Methods in lignin chemistry*: Springer Science & Business Media..
- Lin, X., Sui, S., Tan, S., Pittman, C. U., Sun, J., & Zhang, Z. (2015). Fast Pyrolysis of Four Lignins from Different Isolation Processes Using Py-GC/MS. *Energies*, *8*(6), 5107-5121.
- Lindfors, C., Kuoppala, E., Oasmaa, A., Solantausta, Y., & Arpiainen, V. (2014). Fractionation of bio-oil. *Energy & Fuels*, *28*(9), 5785-5791.
- Liu, W. J., Jiang, H., & Yu, H. Q. (2015). Thermochemical conversion of lignin to functional materials: a review and future directions. [10.1039/C5GC01054C]. *Green Chemistry*, *17*(11), 4888-4907.
- Lundquist, K. (1979). NMR studies of lignins. 3. ¹H NMR spectroscopic data for lignin model compounds. *Acta Chemica Scandinavica*, *33b*, 418-420.
- Lundquist, K. (1981). NMR studies of lignins. 5. Investigation of non-derivatized spruce and birch lignin by ¹HNMR spectroscopy. *Acta Chemica Scandinavica*, *35b*, 497-501.

- Lundquist, K. (1992). Proton (^1H) NMR spectroscopy *Methods in Lignin Chemistry* (pp. 242-249): Springer.
- Lundquist, K., & Olsson, T. (1977). NMR studies of lignins. 1. Signals due to protons in formyl groups. *Acta Chemica Scandinavica*, *31b*(9), 788-792..
- Lynd, L. R., Van Zyl, W. H., McBride, J. E., & Laser, M. (2005). Consolidated bioprocessing of cellulosic biomass: an update. *Current Opinion in Biotechnology*, *16*(5), 577-583..
- Ma, Z., Troussard, E., & van Bokhoven, J. A. (2012). Controlling the selectivity to chemicals from lignin via catalytic fast pyrolysis. *Applied Catalysis A: General*, *423*, 130-136.
- Malkavaara, P., & Alen, R. (1998). A spectroscopic method for determining lignin content of softwood and hardwood kraft pulps. *Chemometrics and Intelligent Laboratory Systems*, *44*(1), 287-292.
- Mao, J., Holtman, K. M., Scott, J. T., Kadla, J. F., & Schmidt-Rohr, K. (2006). Differences between lignin in unprocessed wood, milled wood, mutant wood, and extracted lignin detected by ^{13}C solid-state NMR. *Journal of Agricultural and Food Chemistry*, *54*(26), 9677-9686.
- Marchessault, R., Coulombe, S., Morikawa, H., & Robert, D. (1982). Characterization of aspen exploded wood lignin. *Canadian Journal of Chemistry*, *60*(18), 2372-2382.
- Matsumura, Y., Sasaki, M., Okuda, K., Takami, S., Ohara, S., Umetsu, M., & Adschiri, T. (2006). Supercritical water treatment of biomass for energy and material recovery. *Combustion Science and Technology*, *178*(1-3), 509-536.
- Meier, D., Ante, R., & Faix, O. (1992). Catalytic hydrolysis of lignin: influence of reaction conditions on the formation and composition of liquid products. *Bioresource Technology*, *40*(2), 171-177.
- Mercer, D. K., Iqbal, M., Miller, P., & McCarthy, A. (1996). Screening actinomycetes for extracellular peroxidase activity. *Applied and Environmental Microbiology*, *62*(6), 2186-2190.
- Metzger, J. O., Bicke, C., Faix, O., Tuszynski, W., Angermann, R., Karas, M., & Strupat, K. (1992). Matrix-Assisted Laser Desorption Mass Spectrometry of Lignins**. *Angewandte Chemie International Edition in English*, *31*(6), 762-764.
- Miyazaki, K. (2005). A hyperthermophilic laccase from *Thermus thermophilus* HB27. *Extremophiles*, *9*(6), 415-425.
- Mosier, N., Wyman, C., Dale, B., Elander, R., Lee, Y., Holtzapple, M., & Ladisch, M. (2005). Features of promising technologies for pretreatment of lignocellulosic biomass. *Bioresource Technology*, *96*(6), 673-686.
- Mouille, G., Robin, S., Lecomte, M., Pagant, S., & Höfte, H. (2003). Classification and identification of *Arabidopsis* cell wall mutants using Fourier-Transform InfraRed (FT-IR) microspectroscopy. *The Plant Journal*, *35*(3), 393-404.
- Mu, W., Ben, H., Ragauskas, A., & Deng, Y. (2013). Lignin Pyrolysis Components and Upgrading—Technology Review. *BioEnergy Research*, *6*(4), 1183-1204.
- Mullen, C. A., Strahan, G. D., & Boateng, A. A. (2009). Characterization of Various Fast-Pyrolysis Bio-Oils by NMR Spectroscopy†. *Energy & Fuels*, *23*(5), 2707-2718.
- Nagy, M., David, K., Britovsek, G. J., & Ragauskas, A. J. (2009). Catalytic hydrogenolysis of ethanol organosolv lignin. *Holzforschung*, *63*(5), 513-520.
- Ntziachristos, L., & Samaras, Z. (2009). EMEP/EEA emission inventory guidebook. *European Environment Agency, Copenhagen*.

- Oasmaa, A., & Czernik, S. (1999). Fuel oil quality of biomass pyrolysis oils state of the art for the end users. *Energy & Fuels*, *13*(4), 914-921.
- Obst, J. R., & Kirk, T. K. (1988). Isolation of lignin. *Methods Enzymol*, *161*(Biomass, Pt. B), 3-12.
- Osada, M., Sato, T., Watanabe, M., Adschiri, T., & Arai, K. (2004). Low-temperature catalytic gasification of lignin and cellulose with a ruthenium catalyst in supercritical water. *Energy & Fuels*, *18*(2), 327-333.
- Pandey, M. P., & Kim, C. S. (2011). Lignin depolymerization and conversion: a review of thermochemical methods. *Chemical Engineering & Technology*, *34*(1), 29-41.
- Panwar, N., Kaushik, S., & Kothari, S. (2011). Role of renewable energy sources in environmental protection: a review. *Renewable and Sustainable Energy Reviews*, *15*(3), 1513-1524.
- Patwardhan, P. R., Brown, R. C., & Shanks, B. H. (2011). Understanding the fast pyrolysis of lignin. *ChemSusChem*, *4*(11), 1629-1636.
- Pereira, E. G., da Silva, J. N., de Oliveira, J. L., & Machado, C. S. (2012). Sustainable energy: a review of gasification technologies. *Renewable and Sustainable Energy Reviews*, *16*(7), 4753-4762.
- Pérez, J., Munoz-Dorado, J., de la Rubia, T., & Martinez, J. (2002). Biodegradation and biological treatments of cellulose, hemicellulose and lignin: an overview. *International Microbiology*, *5*(2), 53-63.
- Prinsen, P., Rencoret, J., Gutiérrez, A., Liitiä, T., Tamminen, T., Colodette, J. L., Berbis, M. A., Jiménez-Barbero, J., Martínez, Á. T., & del Río, J. C. (2013). Modification of the Lignin Structure during Alkaline Delignification of Eucalyptus Wood by Kraft, Soda-AQ, and Soda-O₂ Cooking. *Industrial & Engineering Chemistry Research*, *52*(45), 15702-15712.
- Pu, Y., Cao, S., & Ragauskas, A. J. (2011). Application of quantitative ³¹P NMR in biomass lignin and biofuel precursors characterization. *Energy & Environmental Science*, *4*(9), 3154-3166.
- Qu, Y., Zhu, M., Liu, K., Bao, X., & Lin, J. (2006). Studies on cellulosic ethanol production for sustainable supply of liquid fuel in China. *Biotechnology Journal*, *1*(11), 1235-1240.
- Ragauskas, A. J., Beckham, G. T., Bidy, M. J., Chandra, R., Chen, F., Davis, M. F., Davison, B. H., Dixon, R. A., Gilna, P., Keller, M., Langan, P., Naskar, A. K., Saddler, J. N., Tschaplinski, T. J., Tuskan, G. A., & Wyman, C. E. (2014). Lignin valorization: improving lignin processing in the biorefinery. *Science*, *344*(6185), 1246843.
- Ragauskas, A. J., Williams, C. K., Davison, B. H., Britovsek, G., Cairney, J., Eckert, C. A., Frederick, W. J., Hallett, J. P., Leak, D. J., Liotta, C. L., Mielenz, J. R., Murphy, R., Templer, R., & Tschaplinski, T. (2006). The path forward for biofuels and biomaterials. *Science*, *311*(5760), 484-489.
- Rahimi, A., Azarpira, A., Kim, H., Ralph, J., & Stahl, S. S. (2013). Chemoselective Metal-Free Aerobic Alcohol Oxidation in Lignin. *Journal of the American Chemical Society*, *135*(17), 6415-6418.
- Rahimi, A., Ulbrich, A., Coon, J. J., & Stahl, S. S. (2014). Formic-acid-induced depolymerization of oxidized lignin to aromatics. *Nature*, *515*(7526), 249-252.
- Ralph, J., Lundquist, K., Brunow, G., Lu, F., Kim, H., Schatz, P. F., Marita, J. M., Hatfield, R. D., Ralph, S. A., Christensen, J. H., & Boerjan, W. (2004). Lignins: natural polymers

- from oxidative coupling of 4-hydroxyphenyl-propanoids. *Phytochemistry Reviews*, 3(1-2), 29-60.
- Regalbuto, J. R. (2009). Cellulosic biofuels—got gasoline. *Science*, 325(5942), 822-824.
- Renewable Energy Policy Network for the 21st Century (2010). Global status report. *Renewable Energy Policy Network for the 21st Century, Paris, France*.
- Robert, D. (1992). Carbon-13 nuclear magnetic resonance spectrometry *Methods in lignin chemistry* (pp. 250-273): Springer.
- Robinson, A. R., & Mansfield, S. D. (2009). Rapid analysis of poplar lignin monomer composition by a streamlined thioacidolysis procedure and near-infrared reflectance-based prediction modeling. *The Plant Journal*, 58(4), 706-714.
- Sainsbury, P. D., Hardiman, E. M., Ahmad, M., Otani, H., Seghezzi, N., Eltis, L. D., & Bugg, T. D. (2013). Breaking down lignin to high-value chemicals: The conversion of lignocellulose to vanillin in a gene deletion mutant of *Rhodococcus jostii* RHA1. *ACS Chemical Biology*, 8(10), 2151-2156.
- Saisu, M., Sato, T., Watanabe, M., Adschiri, T., & Arai, K. (2003). Conversion of lignin with supercritical water-phenol mixtures. *Energy & Fuels*, 17(4), 922-928.
- Samuel, R., Foston, M., Jiang, N., Allison, L., & Ragauskas, A. J. (2011). Structural changes in switchgrass lignin and hemicelluloses during pretreatments by NMR analysis. *Polymer Degradation and Stability*, 96(11), 2002-2009.
- Samuel, R., Pu, Y., Raman, B., & Ragauskas, A. J. (2010). Structural characterization and comparison of switchgrass ball-milled lignin before and after dilute acid pretreatment. *Applied Biochemistry and Biotechnology*, 162(1), 62-74.
- Sánchez, C. (2009). Lignocellulosic residues: biodegradation and bioconversion by fungi. *Biotechnology Advances*, 27(2), 185-194.
- Sato, T., Furusawa, T., Ishiyama, Y., Sugito, H., Miura, Y., Sato, M., Suzuki, N., & Itoh, N. (2006). *Hydrogen production from lignin with supported nickel catalysts through supercritical water gasification*. Paper presented at the HEC16: 16 World Hydrogen Energy Conference, France.
- Sergeev, A. G., & Hartwig, J. F. (2011). Selective, nickel-catalyzed hydrogenolysis of aryl ethers. *Science*, 332(6028), 439-443.
- Sevillano, R. M., Mortha, G., Barrelle, M., & Lachenal, D. (2001). ¹⁹F NMR spectroscopy for the quantitative analysis of carbonyl groups in lignins. *Holzforschung*, 55(3), 286-295.
- Shabtai, J. S., Zmierczak, W. W., & Chornet, E. (1999). *U.S. Patent No. 5,959,167*. Washington, DC: U.S. Patent and Trademark Office.
- Sjostrom, E. (2013). *Wood chemistry: fundamentals and applications*: Elsevier.
- Smith, E. A., Park, S., Klein, A. T., & Lee, Y. J. (2012). Bio-oil analysis using negative electrospray ionization: comparative study of high-resolution mass spectrometers and phenolic versus sugarc components. *Energy & Fuels*, 26(6), 3796-3802.
- Smook, G. A. (1992). *Handbook for Pulp & Paper Technologists*. TAPPI and Canadian Pulp and Paper Association, 106.
- Song, Q., Wang, F., & Xu, J. (2012). Hydrogenolysis of lignosulfonate into phenols over heterogeneous nickel catalysts. *Chemical Communications*, 48(56), 7019-7021.
- Strassberger, Z., Alberts, A. H., Louwse, M. J., Tanase, S., & Rothenberg, G. (2013). Catalytic cleavage of lignin β -O-4 link mimics using copper on alumina and magnesia-alumina. *Green Chemistry*, 15(3), 768-774.

- Sykes, R., Kodrzycki, B., Tuskan, G., Foutz, K., & Davis, M. (2008). Within tree variability of lignin composition in *Populus*. *Wood Science and Technology*, 42(8), 649-661. doi: 10.1007/s00226-008-0199-0.
- Technical Association of the Pulp and Paper Industry. (1991). *UM-250: Acid-soluble lignin in wood and pulp*. TAPPI Test Methods.
- Technical Association of the Pulp and Paper Industry. (2002). 222 om-02: Acid-insoluble lignin in wood and pulp. 2002–2003 TAPPI Test Methods.
- Taraban'ko, V. E., Fomova, N. A., Kuznetsov, B. N., Ivanchenko, N. M., & Kudryashev, A. V. (1995). On the mechanism of vanillin formation in the catalytic oxidation of lignin with oxygen. *Reaction Kinetics and Catalysis Letters*, 55(1), 161-170.
- Taraban'ko, V. E., Koropatchinskaya, N. V., Kudryashev, A. V., & Kuznetsov, B. N. (1995). Influence of lignin origin on the efficiency of the catalytic oxidation of lignin into vanillin and syringaldehyde. *Russian Chemical Bulletin*, 44(2), 367-371.
- ten Have, R., & Teunissen, P. J. (2001). Oxidative mechanisms involved in lignin degradation by white-rot fungi. *Chemical Reviews*, 101(11), 3397-3414.
- Toledano, A., García, A., Mondragon, I., & Labidi, J. (2010). Lignin separation and fractionation by ultrafiltration. *Separation and Purification Technology*, 71(1), 38-43.
- Toledano, A., Serrano, L., Labidi, J., Pineda, A., Balu, A. M., & Luque, R. (2013). Heterogeneously Catalysed Mild Hydrogenolytic Depolymerisation of Lignin Under Microwave Irradiation with Hydrogen-Donating Solvents. *Chem Cat Chem*, 5(4), 977-985.
- Toor, S. S., Rosendahl, L., & Rudolf, A. (2011). Hydrothermal liquefaction of biomass: a review of subcritical water technologies. *Energy*, 36(5), 2328-2342.
- Torr, K. M., van de Pas, D. J., Cazeils, E., & Suckling, I. D. (2011). Mild hydrogenolysis of in-situ and isolated *Pinus radiata* lignins. *Bioresource Technology*, 102(16), 7608-7611.
- Tuskan, G., West, D., Bradshaw, H., Neale, D., Sewell, M., Wheeler, N., Megraw, B., Jech, K., Wiseloge, A., Evans, R., Elam, C., Davis, M., & Dinus, R. (1999). Two high-throughput techniques for determining wood properties as part of a molecular genetics analysis of hybrid poplar and loblolly pine. *Applied Biochemistry and Biotechnology*, 77(1-3), 55-65.
- Talent with Energy. (2014). Gasification Technologies Review – Technology, Resources and Implementation Scenarios. Talent with Energy for the City of Sydney's Advanced Waste Treatment Master Plan.
- van de Pas, D., Hickson, A., Donaldson, L., Lloyd-Jones, G., Tamminen, T., Fernyhough, A., & Mattinen, M. L. (2011). Characterization of fractionated lignins polymerized by fungal laccases. *BioResources*, 6(2), 1105-1121.
- Van Soest, P. J. (1994). *Nutritional ecology of the ruminant*: Cornell University Press.
- Vanholme, R., Demedts, B., Morreel, K., Ralph, J., & Boerjan, W. (2010). Lignin biosynthesis and structure. *Plant Physiology*, 153(3), 895-905.
- Villaverde, J. J., Li, J., Ek, M., Ligeró, P., & de Vega, A. (2009). Native lignin structure of *Miscanthus x giganteus* and its changes during acetic and formic acid fractionation. *Journal of Agricultural and Food Chemistry*, 57(14), 6262-6270.
- Vishtal, A. G., & Kraslawski, A. (2011). Challenges in industrial applications of technical lignins. *BioResources*, 6(3), 3547-3568.

- Von Blottnitz, H., & Curran, M. A. (2007). A review of assessments conducted on bio-ethanol as a transportation fuel from a net energy, greenhouse gas, and environmental life cycle perspective. *Journal of Cleaner Production*, 15(7), 607-619.
- Wang, H., Tucker, M., & Ji, Y. (2013). Recent development in chemical depolymerization of lignin: a review. *Journal of Applied Chemistry*, 2013, 9.
- Wang, S., Wang, K., Liu, Q., Gu, Y., Luo, Z., Cen, K., & Fransson, T. (2009). Comparison of the pyrolysis behavior of lignins from different tree species. *Biotechnology Advances*, 27(5), 562-567.
- Wei, Z., Zeng, G., Huang, F., Kosa, M., Sun, Q., Meng, X., Huang, D., & Ragauskas, A. J. (2015). Microbial lipid production by oleaginous Rhodococci cultured in lignocellulosic autohydrolysates. *Applied Microbiology and Biotechnology*, 99(17), 7369-7377.
- Wei, Z., Zeng, G., Kosa, M., Huang, D., & Ragauskas, A. J. (2015). Pyrolysis Oil-Based Lipid Production as Biodiesel Feedstock by *Rhodococcus opacus*. *Applied Biochemistry and Biotechnology*, 175(2), 1234-1246.
- Wells, T., Wei, Z., & Ragauskas, A. (2015). Bioconversion of lignocellulosic pretreatment effluent via oleaginous *Rhodococcus opacus* DSM 1069. *Biomass and Bioenergy*, 72, 200-205.

Chapter 9

NANOCELLULOSES FROM LIGNOCELLULOSIC BIOMASS

*G. Siqueira and V. Arantes**

Department of Biotechnology, Lorena School of Engineering
University of São Paulo, Brazil

ABSTRACT

Nanocellulose is a bio-based material with outstanding physicochemical properties and with innumerable possible applications. It is defined as cellulose particles in which one of the dimensions (e.g., diameter) is less than 100 nm. Such nanoparticles have gained attention not only due to their impressive properties, but also because they are produced from the most abundant natural polymer on Earth, cellulose. Two types of nanocellulose can be produced from lignocellulosic materials: cellulose nanofibrils and nanocrystals. The former is produced through mechanical (or chemical) separation of the cellulose fibrils and the latter, through catalyzed hydrolysis of the more disorganized cellulosic domains, resulting in the release of nanocrystals. Several techniques can be used to produce both types of nanoparticles and the physicochemical properties of nanocellulose may change, depending on the production method. This chapter reviews the methods to obtain cellulose-rich pulps from lignocellulosic materials and the following top-down deconstructing strategies to release the nanoparticles. A discussion of the physicochemical properties of nanocelluloses is also provided.

Keywords: nanocellulose, nanocellulose production, cellulose nanofibrils, cellulose microfibrils, cellulose nanocrystals

INTRODUCTION

Plant cell wall is known to be a strong load-bearing structure, allowing plants to grow vertically, up to several meters (Aulin et al., 2009; Wang et al., 2012). This impressive

* Correspondence to: valdeir.arantes@usp.br.

capacity is a result of the combination of the three main components of cell wall matrix, namely cellulose, hemicelluloses and lignin, and their organization in a hierarchical structure. Of these components, cellulose typically represents almost 50% of the lignocellulosic materials (on dry basis) and, although the others are essential to maintain both the structure and function of the cell wall, it is the most important strengthening agent (Aulin et al., 2009).

The isolation of cellulose from wood or other lignocellulosic materials, which generally involves chemithermomechanical treatments, followed by a top-down deconstructing strategy, chemical or mechanical, results in the release of nanocellulose, a fibrillar organization of cellulose molecules, in which the width is less than 100 nm. Nanocelluloses have been studied over the past few decades due to their wide range of potential applications, including reinforcement agents in composites, drug delivery, cosmetic industry, photonic films and others (Shatkin, Wegner, Bilek, & Cowie, 2014). Basically, two types of nanocellulose can be produced from lignocellulosic biomass: cellulose nanofibrils (CNF) and cellulose nanocrystals (CNC). The differences between them start with the production methods, which reflect the physicochemical properties of the nanomaterials.

Cellulose nanofibrils are produced by intensive mechanical defibrillation treatment of cellulose fibers, resulting in the separation of cellulose microfibrils. The less organized regions, often termed amorphous, are kept in the CNF as transversal cuts are not aimed by defibrillation strategies. Also, considering the applications and properties of CNF, high purity is typically not required, and small amounts of residual hemicelluloses and lignin may be present. As a nanomaterial, the width is in the nanometer scale, but the length can reach several micrometers, reason why it is often also referred to as microfibrillated cellulose (Khalil et al., 2014).

The production of cellulose nanocrystals involves the breakage of the glycosidic ether bonds of cellulose, achieved with a hydrolysis step. During the hydrolysis, the amorphous regions are preferentially hydrolyzed, as the less organized cellulose molecules in these domains leads to higher accessibility to the catalyst. As a result, the highly organized crystalline regions are released, material known as cellulose nanocrystals, or cellulose whiskers (Habibi, Lucia, & Rojas, 2010). Since cellulosic fibrils are cut transversally during hydrolysis, CNC is shorter in length than CNF. Also, due to the severe hydrolysis conditions normally applied, residual hemicellulosic polymers are solubilized, leading to a high purity material.

Prior to the mechanical and/or chemical treatments to produce nanocellulose, the other components of lignocellulosic materials (hemicellulose and lignin) need to be removed, at least partially, resulting in cellulose-rich pulps. Although it is still not clear, the methods to produce cellulose pulps are thought to influence the properties of the nanocellulose particles (Klemm, Heublein, Fink, & Bohn, 2005).

In this chapter, we review the most often used techniques for isolating cellulose from biomass, as well the following traditional and novel processes to produce cellulose nanofibrils and nanocrystals. Finally, differences in the physicochemical aspects of the nanocelluloses due the processing strategies are also discussed.

STRUCTURE OF CELLULOSE

Cellulose is a ubiquitous polymer, found both in eukaryotic – plants, algae, and some animals (tunicates), and in prokaryotic organisms, as in *Gluconoacetobacter* family. In wood and other lignocellulosic materials, cellulose represents 40-45% of the dry mass, and it is located predominantly in the secondary wall. In the case of plants, the presence of cellulose as a strengthening component is of major importance, since cell wall must be strong enough to support osmotic pressure and weight (Samir, Alloin, & Dufresne, 2005; Sjöström, 1993).

A cellulose chain is an unbranched homopolysaccharide with anhydro β -D-glucopyranoses as monomeric units, which are three-dimensionally arranged in a chair conformation. The hydroxyl groups are distributed in equatorial position, linked to each other by (1 \rightarrow 4) glycosidic bonds (Figure 1).

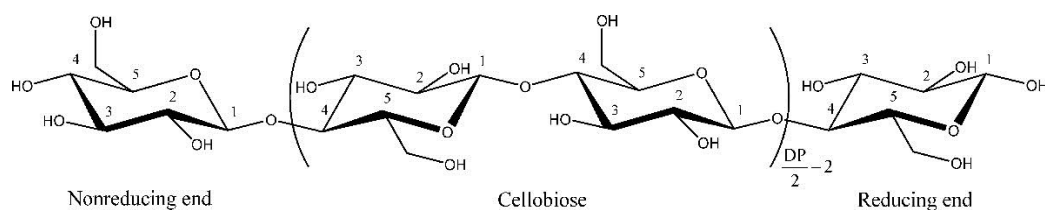


Figure 1. Chemical structure of a cellulose chain. Reprinted with permission from ref. (Habibi et al., 2010). Copyright 2010, American Chemical Society.

The polarity of the glycosidic bond reflects an important difference in the two chain ends. In one of the terminals, the carbon 1 is not linked to another monomeric unit, and in aqueous media, equilibrium between the cyclic and opened structures is established. The acyclic carbohydrates are reducing agents and this chain end is called reducing end, and the other, non-reducing end (Fengel & Wegener, 1989). This is an important difference when considering cellulose isolation techniques (i.e., pulping) and enzymatic deconstruction of the polymer. In alkaline pulping conditions, for instance, endwise peeling depolymerization at the reducing end results in a considerable decrease in pulp yield. The number of glucose residues in a single cellulose chain (degree of polymerization – DP) varies, depending on the source, and even in the cell wall layer. DP values of 10,000 are generally attributed to wood cellulose and 15,000 to cotton cellulose. Nevertheless, extraction methods may affect the DP, as discussed later in this chapter, making it difficult to precisely measure the size of native cellulosic chains (Fengel & Wegener, 1989; O’Sullivan, 1997; Payne et al., 2015; Sjöström, 1993).

Despite the simple molecular structure of cellulose, its ultrastructural organization is particularly complex and still not completely understood. Cellulosic chains bind laterally to each other by hydrogen bonds, forming a sheet of cellulose molecules. These sheets can organize on top of each other, forming a more complex structure. Considering the intersheet bonding pattern and the orientation of the chains, cellulose can assume different crystalline forms, or polymorphs (Nishiyama, 2009). Cellulose I is the natural crystalline arrangement of the chains, formed of stacked cellulose sheets in a parallel orientation (reducing ends in the same direction), with van der Waals interactions playing the major role stabilizing the structure. Variations in the displacement of the sheets results in different cellulose I crystal lattices. Cellulose I α , mainly found in bacteria and algae, has a one-chain triclinic unit cell,

whereas cellulose I β , the major cellulose crystalline structure in cotton, wood, and tunicates, has a two-chain monoclinic unit cell (Atalla & Vanderhart, 1984; Koyama, Helbert, Imai, Sugiyama, & Henrissat, 1997; Nishiyama, Langan, & Chanzy, 2002; Nishiyama, Sugiyama, Chanzy, & Langan, 2003). Cellulose I can be converted into other crystalline forms by chemical treatment. Cellulose chains assume anti-parallel orientation when treated with sodium hydroxide, a process known as mercerization, assuming the cellulose II polymorph. Cellulose III is formed upon treatment of cellulose I or II with ammonia, resulting in cellulose III_I and cellulose III_{II}, respectively. As in cellulose I, the sheets in cellulose III are parallel oriented. Both cellulose II and III are less organized than cellulose I, which reflects in their greater digestibility. Another possible cellulose polymorph is cellulose IV, which is very similar to cellulose I β (Atalla & Vanderhart, 1984; Koyama et al., 1997; Nishiyama et al., 2002, 2003; Nishiyama, 2009; Payne et al., 2015; Sugiyama, Vuong, & Chanzy, 1991).

Cellulose in wood and other lignocellulosic materials exhibit a hierarchical organization. Single chains interact with each other, forming the elementary fibril. It was well accepted that 36 cellulosic chains form an elementary fibril (Ding & Himmel, 2006; Herth, 1983; Mueller & Brown, 1980), but recent findings suggest that 18-24 might be more correct (Fernandes et al., 2011; Newman, Hill, & Harris, 2013; Thomas et al., 2013). The latter is based on the consideration that a square cross section of the elementary fibril is 2.4-3.2 nm (Kennedy et al., 2007). However, it is still not clear how many chains compose each sheet in the elementary fibril. Elementary fibrils, also termed microfibrils, can reach micrometers in length, and 5-50 nm in width (Moon, Martini, Nairn, Simonsen, & Youngblood, 2011). Microfibrils form aggregates and these are embedded in a lignin/hemicellulose matrix, within the cell wall layers.

The fibrils are organized in crystalline structures, but probably due to tilts and twists resulted from internal strains, some domains are less organized (Rowland & Roberts, 1972). These regions, often called amorphous, are more accessible to catalysts (chemicals and enzymes), which results in higher reaction rates. During the production of nanocrystalline cellulose, the amorphous regions must be hydrolyzed, in order to release the nanocrystals (Figure 2).

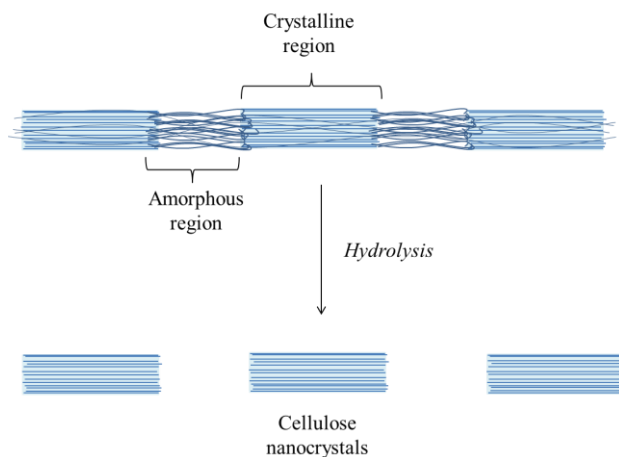


Figure 2. Schematic representation of amorphous and crystalline regions of cellulose and the production of nanocrystals through hydrolysis.

METHODS FOR ISOLATING CELLULOSE

Lignocellulosic biomass is a mixture of macromolecules and low molecular weight compounds interacting with each other through covalent and non-covalent bonds, which creates a complex matrix that is very difficult to fractionate into its individual components (Alvira, Tomás-Pejó, Ballesteros, & Negro, 2010; Iiyama, Lam, & Stone, 1994). Therefore, an important first step for nanocellulose production is the isolation of cellulose from a lignocellulosic material. Industrially, the most common technology for isolation of cellulose is based on pulp and paper processes. However, with the emerging biorefinery concept, considerable efforts have also been directed to other thermochemical technologies to isolate cellulose while also recovering the hemicellulose and lignin in usable forms.

Kraft Pulping

The commercial production of isolated cellulose, with reduced amounts of other lignocellulosic components, is mainly through chemical pulping, which corresponds to more than 75% of all the global pulp production. The sulfate process, generally referred to as kraft pulping, accounts for more than 90% of the production of chemical pulps (Brännvall, 2009; Sixta, 2006).

In the kraft process, the combined action of hydroxide and bisulfide ions efficiently removes more than 90% of the lignin due to a series of depolymerization reactions. A considerable fraction of the hemicelluloses is solubilized (40-65%, depending on the feedstock), resulting in a cellulose-rich solids (65-80%, on dry weight). This enrichment is due to the higher stability of cellulose compared to hemicelluloses. The most expressive polysaccharides loss is due to endwise depolymerization (*peeling* reactions), with less frequent chains breakage due to hydrolysis and, because of that, the decrease in the degree of polymerization (DP) of cellulose is not much higher than 30% after kraft pulping, reaching an approximated value of 6,000 (DP_w) (Brännvall, 2009; Sixta, 2006).

Sulfite Pulping

The sulfite pulping process generates a very high purity cellulose pulp (>90%) with very low content of hemicellulose and lignin. Although sulfite pulping can be conducted over a wide pH range, the most applied conditions are acidic. The ionic species involved in lignin solubilization are protons and bisulfite. The main polysaccharide reaction is acid catalyzed hydrolysis, which promotes a higher decrease in the degree of polymerization of cellulose and generates pulps with inferior strength properties as compared to the kraft process. For example, for paper-grade pulp, sulfite pulping is less suitable than kraft pulping. Consequently, the latter became the dominant chemical pulping process (sulfite pulping corresponds to only about 5% of the chemical pulping processes) (Sixta, 2006).

Organosolv Pulping

Contrarily to the other major chemical pulping processes, the organosolv process is based on organic solvents and therefore, a sulfur-free pulping technology. The process can be concisely described as a treatment of biomass with water, an organic solvent (e.g., ethanol, methanol or acetone), and a catalyst (generally acid). Expected results are solubilization of lignin (breakage of lignin-carbohydrates and lignin-lignin bonds) and hemicelluloses (especially in acid catalyzed organosolv treatment), producing a cellulosic-rich residue (Del Rio, Chandra, & Saddler, 2010; McDonough, 1992). As hydrolysis is enhanced by the presence of organic solvents (Fengel & Wegener, 1989), cellulose degree of polymerization is significantly decreased (Cateto, Hu, & Ragauskas, 2011; Hallac & Ragauskas, 2011). Despite generating a high-content cellulose pulp, organosolv pulp was not adopted in the pulp and paper sector. However, it has been investigated as an attractive pretreatment step in the bioconversion of biomass-to-fuels process, with some environmental advantages, as the organic solvent can be directly recovered after the cooking step by distillation and the process results in less emissions and less toxic effluents, compared to the dominant kraft pulping (Bajpai, 2010).

Other Thermochemical Treatments

In addition to the pulping technologies, other chemical treatments, also combined with high temperature and pressure, have been extensively studied over the past few decades for fractionation of lignocellulosic biomass. By choosing the proper chemical and operating conditions, biomass can be partially deconstructed to preserve most of the cellulose in the solid fraction while producing a liquid stream rich in hemicellulosic sugars and/or solubilized lignin (depending on the chemical environment), that can also be recovered and used for the production of a range of bioproducts (Alvira et al., 2010; Hu & Ragauskas, 2012). Currently, the primary goal of these chemical treatments is not the production of cellulosic pulp for applications that relies on the macromolecular properties (i.e., mechanical properties) of cellulose but rather in its glucose residues for production of biofuels and biochemicals. However, it should be pointed out that in a near future these pretreatment technologies might also be considered for production of cellulose pulps for application based on cellulose polymeric properties, as process integration is required in the modern biorefinery concept. For example, steam pretreatment and dilute acid pretreatment, processes that already have been employed at commercial plants for biofuels production, can efficiently depolymerize hemicelluloses (in oligomeric and monomeric sugars) via disruption of the plant cell wall structure and acid hydrolysis, resulting in a substrate mainly composed of cellulose and modified lignin (Mosier et al., 2005). A subsequent delignification set can be used to remove the remaining lignin, therefore, producing a cellulosic pulp that could be suitable for nanocellulose production.

Alkaline based pretreatments can be combined with a physical disruption of biomass, such as in ammonia fiber expansion. However, as it is an alkaline treatment, lignin is preferentially removed, and only partial solubilization of hemicellulose occurs. Moreover, cellulose swelling may result in a decrease of cellulose crystallinity, an effect undesirable for a nanocellulose production process (Hu & Ragauskas, 2012).

Ionic liquids are a relative new class of chemicals for biomass deconstruction. Often referred to as “green solvents,” they are high-boiling temperature salts able to solubilize the major components of lignocellulosic materials, and with selectivity dependent on the cationic and anionic species (Abushammala, Krossing, & Laborie, 2015; Anugwom et al., 2012; Pinkert, Goeke, Marsh, & Pang, 2011). Using the appropriate salt, lignin can be selectively removed without dissolving or impacting cellulose crystallinity (Pinkert et al., 2011). This is an important feature to be considered for the production of cellulose-rich pulp.

NANOCELLULOSE PRODUCTION

The term nanocellulose defines cellulose molecules arranged in fibrillar structures, in which one of the dimensions is smaller than 100 nm. Two types of nanocelluloses can be produced from cellulosic pulp, depending on the extraction technique. Separation of fibrils using mechanical disintegration without hydrolysis (or with a mild hydrolysis as a pretreatment) results in the release of cellulose nanofibrils. Chemical treatments that aim cellulose hydrolysis, generally with concentrated strong mineral acids, are used to produce CNCs (Figure 3).

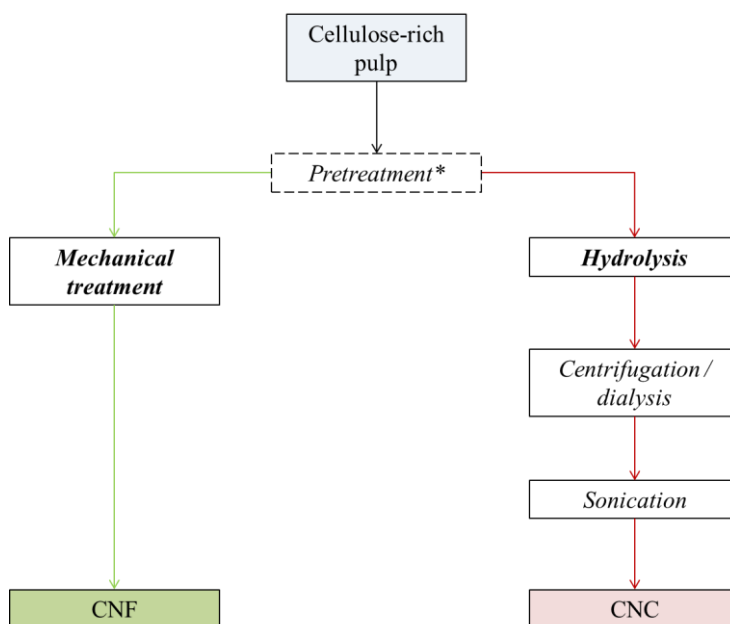


Figure 3. Simplified flowchart of cellulose nanofibrils (CNF) and cellulose nanocrystals (CNC) production. *Hydrolysis and mechanical treatment (for CNC and CNF, respectively) may be preceded by a pretreatment step.

Cellulose Nanofibrils

Cellulose nanofibrils, also termed microfibrillated cellulose, are the fundamental structural unit of cellulose. The microfibrils are formed during cellulose synthesis and

grouped in bundles in the cell walls. To disrupt this supramolecular organization, high energy demanding mechanical treatments are required to break the hydrogen bonds that hold the microfibrils together. The separation of microfibrils is followed by a substantial increase in the specific area, which results in its extensive hydrogen-bonding ability, desirable in several applications (Lavoine, Desloges, Dufresne, & Bras, 2012; Moon et al., 2011).

The most used feedstock for production of cellulose nanofibrils is kraft pulp, followed by sulfite pulp, as it is the most available cellulose feedstock. A brief description of the leading techniques to prepare cellulose nanofibrils is presented below.

High Pressure Homogenization

In this treatment, the disruption of cellulose structure is reached by a combination of high shearing forces and large pressure drop, promoting a high defibrillation of the cellulosic fibers. A very dilute suspension of pulp fibers (typically 1-2 wt%) is pumped at high pressure through a thin slit where the fibers are subjected to high shear forces. Also, a spring-loaded valve assembly opens and closes in rapid succession as the suspension is fed in the homogenizer, causing a pressure drop (Figure 4). However, passing the suspension through the slit only once does not release the nanofibrils. Thus, several more passes in the homogenizer are required and the suspension is pumped back into the system. Generally after 5-10 passes through the homogenizer, the visual aspect of the suspension changes; it becomes creamy, more viscous and translucent, indicating the separation of the microfibrils. This procedure is considered an efficient and simple technique to produce nanofibrillated cellulose. However, the high-energy demand for the several passes through the homogenizer represents a bottleneck, and current efforts are aimed to develop technologies to overcome this costly limitation. Another challenge associated to the high pressure homogenization is clogging, as long fibers suspension passes through the slit. This is a reason why sometimes the process is preceded by a pretreatment step. (Dufresne, 2012; Lavoine et al., 2012; Nakagaito & Yano, 2004)

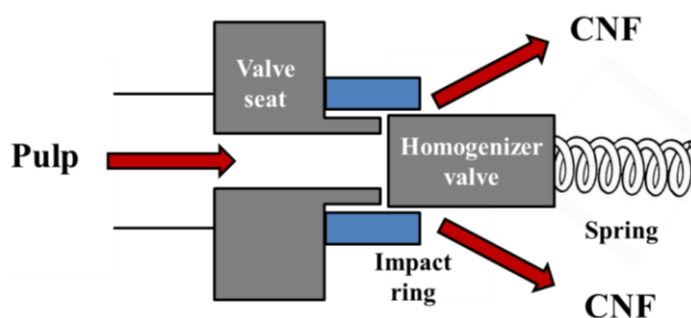


Figure 4. Schematic design of a high pressure homogenizer.

Microfluidization

An alternative to high pressure homogenization is the microfluidization. It is also based on forcing the pulp suspension through a thin orifice applying high pressure, which causes shear forces (Khalil et al., 2014). The sample passes through a z-shaped chamber with channel dimensions between 200 and 400 μm (Figure 5). The fibrils are more uniformly sized, compared to the ones produced in a homogenizer. More passes are generally required,

compared to high pressure homogenization, and values between 10 and 30 are common. Clogging is also a problem, and size reduction of the fibers prior to microfluidization is often considered. An economical and environmental disadvantage of the process is the high energy consumed due to the pressure applied in the system and to the number of passes required (Khalil et al., 2014; Aulin et al., 2009; Dufresne, 2012; Siqueira, Bras, & Dufresne, 2010).

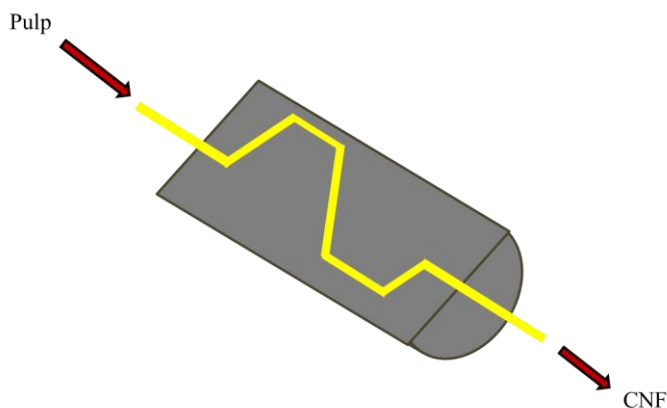


Figure 5. Representation of a z-shaped microfluidizer chamber.

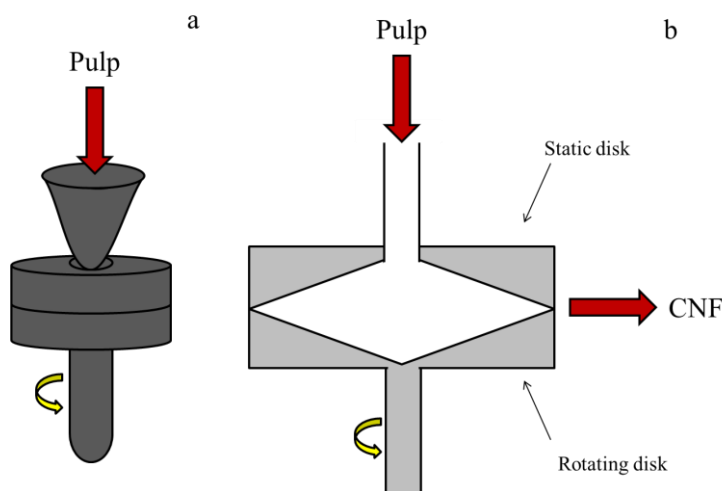


Figure 6. Scheme of a grinder (a) outside view and (b) inside chamber view. The upper disk is static and the lower rotates, driving the fibrillated cellulose out to the edges of the disks, due to centrifugal forces.

Grinding

Cellulose nanofibrils can be also produced using a grinder (Figure 6). The process is similar to the production of mechanical pulps that makes use of two grinding disks to separate cellulose fibers. For the separation of the fibrils in nanoscale, two non-porous ceramic disks with adjustable space between them are used. The upper disk is fixed and the lower rotates (≈ 1500 rpm), creating shearing and friction forces that isolate fibrils 20-90 nm wide. The pulp is fed into a hopper and dispersed to the disk border by centrifugal force, where the shear

stress is more intense. Grinding requires fewer passes to individualize the fibrils, but may result in length decrease thus compromising the reinforcement and physical properties of the nanocellulose. This technique can be used as a pretreatment step, passing the pulp suspension through the grinder before submitting it to high pressure homogenization process (Khalil et al., 2014; Dufresne, 2012; Iwamoto, Nakagaito, & Yano, 2007; Lavoine et al., 2012; Stelte & Sanadi, 2009; Wang et al., 2012).

Cryocrushing

Cryocrushing is a less common method for producing nanofibrils. The pulp immersed in liquid nitrogen causes the water in the fibers to freeze consequently forming ice crystals. Frozen pulp is then crushed with a cast iron mortar and pestle. The ice crystals exert pressure on the fibers, destroying the structure and releasing fiber fragments. These fragments have hundreds of micrometers in length and form large bundles of fibrils, generally between 0.1 and 1 μm in width. These lateral dimensions are still large for a nanomaterial (less than 100 nm), but considerable shorter than original pulp fibers (20 to 50 μm wide). Because of that, cryocrushing can be used rather as a pretreatment step, followed by defibrillation of the crushed fibers through high pressure homogenization or microfluidization (Khalil et al., 2014; Dufresne, 2012; Lavoine et al., 2012; Moon et al., 2011).

Pretreatments

Mechanical processes to disrupt the fiber structure of cellulose are high energy demanding. This is due to the high number of passes through the homogenizer or microfluidizer. Energy consumption over 30,000 kWh/ton of pulp are typical, and values as high as 70,000 kWh/ton have also been reported (Nakagaito & Yano, 2004). Pretreatments that involve partial breakage of glycosidic bonds (acidic and enzymatic hydrolysis) or introduction of charged groups (oxidation) have been studied. With a pretreatment step, the energy required to separate the fibrils can be as low as the energy typically required to produce mechanical pulp from wood (using disk refiner), making the process more economically viable. Moreover, clogging problems are reduced (Dufresne, 2012; Spence, Venditti, Rojas, Habibi, & Pawlak, 2011).

Enzymatic Pretreatment

Cellulose is a naturally recalcitrant material as a result of its organized structure maintained by intensive hydrogen bonding. The enzymatic deconstruction of cellulose is performed by a complex mixture of enzymes, generally categorized in three major groups of hydrolytic proteins. All of them catalyze the hydrolysis of β -(1 \rightarrow 4) glycosidic bonds, but differences in the enzymes tridimensional structure result in different sites of action and specificity towards cellulose domains. Endoglucanases (EC 3.2.1.4) randomly hydrolyze glycosidic bonds in the middle of cellulose chains, creating two new chain terminals. Cellobiohydrolases (exoglucanases, EC 3.2.1.91) catalyze the hydrolysis of glycosidic bonds close to the terminals, releasing cellobiose or glucose. The third group that takes part in complete depolymerization is composed by β -glucosidases (EC 3.2.1.21), enzymes that break the glycosidic bond in cellobiose releasing glucose molecules (Zhang & Lynd, 2004).

The most studied type of cellulase in CNF production is endoglucanase. This is because endoglucanases are more selective to catalyze the hydrolysis of amorphous regions of

cellulosic fibers (Teixeira et al., 2015). Generally, the nanofibrils obtained have lower aspect ratio (ratio between length and diameter), but this property may be controlled by adjusting the enzyme concentration in the pretreatment. Fibril aggregates with diameter around 10-20 nm can be obtained combining endoglucanase pretreatment with microfluidization (Dufresne, 2012; Henriksson, Berglund, Isaksson, Lindström, & Nishino, 2008; Pääkkö et al., 2007; Wang et al., 2012). Besides the decrease in energy consumption, pretreatment with cellulases reduces process problems such as clogging during homogenization or microfluidization and result in more homogeneous nanofibrils.

Another approach to enzymatic pretreatment is process integration, in which the production of nanofibrillated cellulose can be associated with sugar-based biorefinery platform (i.e., cellulosic ethanol production). In this context, a fraction of the cellulosic fibers are hydrolyzed to soluble sugars (oligo and monomeric) during the enzymatic pretreatment. Subsequently, sugars can be separated and the residual solid (structurally modified by the enzymes) can be submitted to mechanical treatments to produce nanofibrils (Zhu, Sabo, & Luo, 2011).

TEMPO Oxidation

Oxidation of glucose residues in cellulose chains is also beneficial to produce cellulose nanofibrils. Treating pulp suspension with sodium hypochlorite (NaClO) and catalytic amounts of 2,2,6,6-tetramethyl-1-piperidinyloxy (TEMPO), in the presence of sodium bromide, causes the oxidation of C6 in the glucose residues to carboxylate groups (Isogai, Saito, & Fukuzumi, 2011). Negative charges in the cellulose surface result in repulsive forces and, consequently, the separation of the fibrils is facilitated. TEMPO-mediated oxidation is the most studied pretreatment aiming the release of nanofibrils, and up to 90% of the energy used in subsequent mechanical treatments can be reduced (A. Isogai, 2013). Another advantageous consequence is that oxidation of cellulose prevents clogging problems (Dufresne, 2012; A. Isogai et al., 2011; T. Isogai, Saito, & Isogai, 2011; Kalia, Boufi, Celli, & Kango, 2014; Lavoine et al., 2012; Saito & Isogai, 2004; Saito, Kimura, Nishiyama, & Isogai, 2007). However, TEMPO-mediated oxidation of cellulose has some disadvantages. Cellulose is a natural biodegradable polymer. TEMPO-oxidized cellulose, on the other hand, is not easily digested by cellulases (Szczena-Antczak, Kazimierczak, & Antczak, 2012), which may compromise its biodegradability. In addition, TEMPO is a toxic and expensive chemical, and economic viability of the pretreatment depends on effective recovery methods, still to be developed (Brinchi, Cotana, Fortunati, & Kenny, 2013; Zhu et al., 2011).

Cellulose Nanocrystals

Nanocrystals were first produced in the late 40's by Rånby (Rånby, Banderet, & Sillén, 1949; Rånby, 1951), when he obtained cellulose suspensions after treating wood cellulose and cotton with concentrated sulfuric acid. After that, transmission electronic microscopic analyses of dried suspensions showed that cellulose fibrils were grouped to form needle shaped particles. These particles had the same crystalline structure as original fibers (Mukherjee & Woods, 1953).

As mentioned earlier, it is hypothesized that cellulose has two main structural domains, amorphous and crystalline, that exhibit different behavior when submitted to hydrolysis reactions. The less organized amorphous regions are more accessible and, as a consequence, the hydrolysis rates are higher when compared to the crystalline fractions (Gehlen, 2010).

Because of that, amorphous cellulose is preferentially hydrolyzed and after the hydrolysis, the less accessible crystalline regions are preserved, and cellulose rod-like crystals are released (Gehlen, 2010; Habibi et al., 2010).

During hydrolysis, cellulose degree of polymerization decreases substantially and then stabilizes at a value called level-off degree of polymerization (LODP) (Battista, Coppick, Howsmon, Morehead, & Sisson, 1956). This value correlates with the crystals size, and it depends on the source of lignocellulosic biomass and also on the method for cellulose isolation (e.g., kraft and sulfite pulping) (Battista et al., 1956; Håkansson & Ahlgren, 2005). Although the hydrolysis time required to reach the LODP is shorter when hydrolyzing pulps with concentrated acids, the value itself seems to be independent of the catalyst concentration (Battista et al., 1956; Habibi et al., 2010; Håkansson & Ahlgren, 2005).

After the hydrolysis step, the dispersed crystals are then exhaustively dialyzed (4-days dialysis are reported in the literature) to remove residual acid from the suspension (Habibi et al., 2010). It is generally accepted the importance of an ultrasonication treatment to further disperse and release the nanocrystals in suspension. However, the conditions differ substantially in the literature, and no consensus was achieved so far.

The most commonly used catalysts in the hydrolysis stage and the main characteristics of the crystals produced are described below.

Acid Hydrolysis

Sulfuric acid is the most used catalyst to release the nanocrystals from cellulosic pulps. Besides being a strong acid that efficiently hydrolyzes amorphous cellulose, in the hydrolysis conditions sulfate ester bonds are formed, creating negative surface charges along the crystals. The repulsive forces due to negative charges make the crystal aggregation more difficult, thus enhancing the stability of the suspension. On the other hand, the thermostability of the sulfated nanocrystals is reduced, compared to crystals with unmodified surface (Revol, Bradford, Giasson, Marchessault, & Gray, 1992; Roman & Winter, 2004).

Distinct conditions for sulfuric acid hydrolysis have been reported in the literature, and the divergence is mainly in the temperature and time of hydrolysis. Sulfuric acid concentration is conventionally around 65% (w/w), and optimization studies pointed 63.5% as the acid concentration that yielded nanocrystals with length between 200 and 400 nm, less than 10 nm wide, after 2-hour hydrolysis at 45 °C. The nanocrystals yield was 30% (based on the initial mass) (Bondeson, Mathew, & Oksman, 2006). Nevertheless, a recent work by Chen et al. questioned the traditional statistical experimental design for nanocrystals production, showing that there is a sharp increase in nanocrystals yields between 56 and 58% sulfuric acid, followed by a significant decrease at higher concentrations (e.g., 64%). In this case, optimum acid concentration is close to 58%, not to 65%, as it has been previously thought. Also, they showed that it is possible to tailor the crystal properties (e.g., surface sulfation, crystal length) by slightly adjusting the reaction conditions such as temperature, time, and acid concentration (Chen et al., 2015).

Another important catalyst is hydrochloric acid. Differently from nanocrystals produced through sulfuric acid hydrolysis, surface is not charged. Therefore, the stability of the suspension is compromised as interactions between crystals and particle aggregation are favored. To increase stability, sulfate groups can be esterified to crystal surfaces through a post treatment of the suspension with sulfuric acid. However, production of nanocrystals with unmodified surfaces has some advantages, since particles are more thermostable and other

chemical groups can be promptly added, increasing possible applications. The acid concentration ranges from 2.5 to 4.0 N and the reaction is normally conducted under reflux, time depending on the feedstock. (Araki, Wada, Kuga, & Okano, 1999; Habibi et al., 2010; Peng, Dhar, Liu, & Tam, 2011; Roman & Winter, 2004; Sacui et al., 2014).

Enzymatic Hydrolysis

Conventional, acid-based hydrolysis has crucial technical and environmental drawbacks. Because of the large amount of corrosive acid used for the production of nanocrystals, acid-resistant equipment is required (Song, Winter, Bujanovic, & Amidon, 2014). Additionally, undesirable byproducts are formed during hydrolysis (sugar degradation products), demanding downstream purification steps. Crystalline regions are partially hydrolyzed, as acid hydrolysis is not specific towards amorphous domains (although rates are higher), contributing to low crystals yields (20-30%, based on initial mass). Finally, substantial amounts of water are used to remove the residual acid from nanocrystal suspension in the centrifugation and dialysis steps. Combined, these disadvantages increase capital investment and operational costs (Song et al., 2014).

Enzymatic hydrolysis is a promising and attractive alternative strategy to produce cellulose nanocrystals. As mentioned above, cellulases are a complex mixture of enzymes, evolved to efficiently deconstruct cellulose. However, differences in hydrolysis mechanism and specificity of different cellulases can be explored aiming to release crystals from cellulosic materials. Endoglucanases are known to preferentially hydrolyze less organized amorphous regions of cellulose, and have recently attracted attention as possible catalyst to produce nanocrystals. With the more selective hydrolysis of amorphous cellulose, higher nanocrystal yields can be ideally achieved (Filson, Dawson-Andoh, & Schwegler-Berry, 2009). Nevertheless, yields reported in the literature are lower compared to the ones obtained through acid hydrolysis. This is probably a result of an inadequate use of enzyme mixtures, designed to completely deconstruct cellulosic biomasses, compromising the crystal yields (Meyabadi & Dadashian, 2012; Satyamurthy, Jain, Balasubramanya, & Vigneshwaran, 2011).

A few researchers have successfully demonstrated the release of rod-like nanocrystals with diameter between 4 and 80 nm, and length varying from 70 nm and 1.8 μm after enzymatic hydrolysis of different lignocellulosic materials, with crystal dimensions dependent on the biomass and on the enzyme used. As nanocrystals produced with hydrochloric acid, surface is not charged, resulting in less stable suspensions and more thermostable particles (Anderson et al., 2014; Chen, Deng, Shen, & Jiang, 2012; Filson et al., 2009; Meyabadi & Dadashian, 2012; Meyabadi, Dadashian, Sadeghi, & Asl, 2014; Teixeira et al., 2013, 2015; Xu et al., 2013).

CHARACTERISTICS OF NANOCELLULOSE

Cellulose is naturally a strengthening polymer in the cell wall matrix. Nanoparticles produced from this component show even more impressive structural and physicochemical characteristics that make them unique biobased materials. For example, increased specific surface area, aspect ratio, and crystallinity changes during the production process give the resulting material enhanced mechanical properties compared to natural cellulose (or cellulosic

pulps), and these properties are important parameters to be analyzed. However, data in the literature regarding to these features differ substantially, either to cellulose nanofibrils or to nanocrystals. The first cause of variation is the biomass source. Different plant materials have distinct chemical composition and structural organization, which may affect the cellulose production process, the second cause of variation. As discussed above, fractionation of lignocellulose components require thermochemical treatments that alter important characteristics of cellulose, such as crystallinity and degree of polymerization. Finally, different procedures to prepare cellulose nanofibrils and nanocrystals may also contribute to the wide variation observed in the literature. Since there is still no consensus about the treatment conditions, it is difficult to make fair comparisons among different materials. In this section, we compared some of the properties of cellulose nanoparticles based on data available in the literature, indicating the most common methodologies used in the measurements.

Morphology

Cellulosic nanoparticles morphology differs substantially when produced from different kingdom organisms (i.e., plants, bacteria and animals). However, plant nanocelluloses are morphologically similar, with the main differences being the dimensions (diameter and length). Difference in lengths and diameters is primarily a result of the cellulose source and production method. Cellulose nanofibrils are long entangled filaments and when isolated from lignocellulosic materials are generally 5-50 nm wide, but some researchers have reported higher diameters (Table 1). It is difficult to estimate the length of the nanofibrils because the dimensions are often measured by microscopic techniques and the fibrils are larger than the microscope reading section (Lavoine et al., 2012). Length is thus commonly reported as several micrometers. For cellulose nanocrystals, shorter needle-shaped particles, both dimensions are measured and the aspect ratio can be calculated. This important parameter represents the ratio between length and diameter, and it influences the mechanical properties of the crystals (in most cases, the higher the aspect ratio, the better the mechanical properties). (Eichhorn et al., 2009) Nanocrystals from lignocellulosic materials are 3-15 nm wide and 100-280 nm in length. Enzymatically-produced nanocrystals may be larger, and lengths of 1,000 nm were observed by (Teixeira et al., 2015). Crystal lengths are influenced by the hydrolysis conditions, and more severe hydrolysis result in shorter nanocrystals. Also, comparing crystals produced from different sources, length seems to correlate to the level-off degree of polymerization (discussed below). Reported aspect ratios vary from 20 to 60.

Although light scattering and nuclear magnetic resonance can also be used to measure dimensions, nanofibrils and nanocrystals dimensions are typically estimated using microscopic techniques. Most common analytical methods are scanning electron microscopy (SEM), transmission electron microscopy (TEM), and atomic force microscopy (AFM). This is another source of variation in the values available in the literature. AFM is a powerful analytical tool and gives a rapid indication of surface topography. However, it overestimates dimensions (especially the diameter) and displays perturbations in particles shapes, induced by tip-broadening effects (Kvien, Tanem, & Oksman, 2005). SEM sample preparation affects the measurement, since the particle surface must be covered with a conductive metallic layer, also overestimating dimensions (Fukuzumi, Saito, Iwata, Kumamoto, & Isogai, 2009). TEM

is recognized as the most suitable microscopic technique to analyze nanocellulose morphology because it is less affected by artefacts or sample preparation (Brinchi et al., 2013; Habibi et al., 2010). Nevertheless, drying the samples may cause particle aggregation, resulting in overestimated values similar to other analytical methods. This problem was overcome by cryo-TEM preparation, reported by (Elazzouzi-Hafraoui et al., 2008).

A compilation of diameters and length values from the literature regarding to cellulose nanofibrils and nanocrystals are displayed in Tables 1 and 2, respectively. Although it is widely discussed that cellulose source and isolation, as well as the nanocellulose production method, may influence the particles dimensions, it is not so easy to get to this conclusion based on the current knowledge. There are too many sources of variations in the production methodology and measurement techniques (discussed above). In addition, comparison of different particle dimensions is not a simple task. As it can be seen in Table 1, there is a wide range of nanofibrils diameters, and it seems to be independent from the biomass. However, it is clear that TEMPO oxidation results in narrower particles, which makes sense, since repulsive forces caused by the carboxylate groups on the fibrils surface contribute not only to defibrillation, but also prevents aggregation. Apart from this observation, the effect of the mechanical treatment or cellulose isolation method on fibrils diameter is still not conclusive.

Cellulose nanocrystals diameters are more uniform than of nanofibrils, with values ranging from 3 to 10 nm (Table 2). Variation in the length of crystals is bigger, ranging from 100 to 280 nm and 250 to 1,000 nm, for the acid and enzymatic catalysis, respectively. Apparently, shorter crystals are obtained if more concentrated acid is used in the hydrolysis step (Figure 7). This observation is supported by Battista et al. (Battista et al., 1956) and Håkansson and Ahlgren (Håkansson & Ahlgren, 2005) that showed that the more severe the hydrolysis conditions, the lower the degree of polymerization (up to the LODP). Since crystal length correlates with the degree of polymerization (Habibi et al., 2010), the variation can be explained.

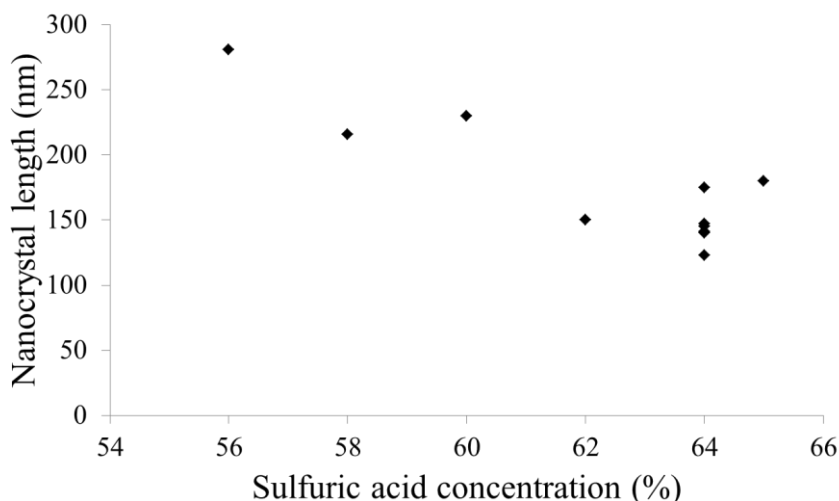


Figure 7. Decrease in nanocrystals length with increasing sulfuric acid concentration during hydrolysis step. Values extracted from the data presented in Table 2.

Table 1. Diameters of cellulose nanofibrils produced from various lignocellulosic biomasses

<i>Lignocellulosic material</i>	<i>Pretreatment</i>	<i>Mechanical treatment</i>	<i>Diameter (nm)</i>	<i>References</i>
Hardwood kraft pulp	Enzymatic	Microfluidization	20	(Zhu et al., 2011)
Hardwood kraft pulp	Enzymatic	Microfluidization	5 - 10	(Wang, Mozuch, et al., 2015)
Softwood sulfite pulp	Enzymatic	HPH*	5 - 20	(Pääkkö et al., 2007; Pääkkö et al., 2008)
Softwood sulfite pulp	Enzymatic	HPH	20 - 40	(Svagan, Samir, & Berglund, 2007)
Softwood sulfite pulp	Enzymatic	HPH	5 - 30	(Henriksson, Henriksson, Berglund, & Lindström, 2007)
Sugarcane bagasse (NaOH extracted)	Blender	HPH	30	(Bhattacharya, Germinario, & Winter, 2008)
Corn cob (NaOH extracted)	Blender	HPH	5 - 60	(Shogren, Peterson, Evans, & Kenar, 2011)
Hardwood kraft pulp	No pretreatment	Grinding	4 - 32	(Wang et al., 2012)
Softwood (ethanol, chlorite and NaOH extracted)	No pretreatment	Grinding	15	(Abe, Iwamoto, & Yano, 2007)
Hardwood kraft pulp	No pretreatment	Grinding	20 - 90	(Taniguchi & Okamura, 1998)
Softwood kraft pulp	No pretreatment	Grinding	20 - 90	(Taniguchi & Okamura, 1998)
Softwood (ethanol, chlorite and KOH extracted)	No pretreatment	Grinding	12 - 20	(Abe & Yano, 2009)
Rice straw (ethanol, chlorite and KOH extracted)	No pretreatment	Grinding	12 - 35	(Abe & Yano, 2009)
Wheat straw (NaOH extracted)	HCl	Cryocrushing	10 - 80	(Alemdar & Sain, 2008)
Soy hulls (NaOH extracted)	HCl	Cryocrushing	20 - 120	(Alemdar & Sain, 2008)
Hardwood kraft pulp	TEMPO	-	3 - 4	(Saito et al., 2007)
Softwood sulfite pulp	TEMPO	Blending	3 - 5	(Saito, Nishiyama, Putaux, Vignon, & Isogai, 2006)
Hardwood kraft pulp	TEMPO	Blending followed by sonication	5	(Saito et al., 2009)
Hardwood kraft pulp	TEMPO	Blending	3 - 4	(Fukuzumi et al., 2009)
Softwood kraft pulp	TEMPO	Blending	3 - 4	(Fukuzumi et al., 2009)

*HPH – high pressure homogenization.

Table 2. Dimensions of cellulose nanocrystals produced from lignocellulosic biomasses

<i>Lignocellulosic material</i>	<i>Pretreatment</i>	<i>Catalyst</i>	<i>Diameter (nm)</i>	<i>Length (nm)</i>	<i>References</i>
Hardwood kraft pulp	-	56% H ₂ SO ₄	-	281.2	(Chen et al., 2015)
Hardwood kraft pulp	-	58% H ₂ SO ₄	-	204.6 - 228.2	(Chen et al., 2015)
Softwood kraft pulp	-	60% H ₂ SO ₄	5	180 - 280	(Orts, Godbout, Marchessault, & Revol, 1998)
Hardwood kraft pulp	-	62% H ₂ SO ₄	-	143 - 177	(Chen et al., 2015)
Hardwood kraft pulp	-	64% H ₂ SO ₄	-	130 - 147	(Chen et al., 2015)
Softwood sulfite pulp	-	64% H ₂ SO ₄	5	141 ± 6	(Beck-Candanedo, Roman, & Gray, 2005)
Hardwood kraft pulp	-	64% H ₂ SO ₄	5	147 ± 7	(Beck-Candanedo et al., 2005)
Hardwood kraft pulp	-	64% H ₂ SO ₄	6 ± 1.5	145 ± 25	(de Mesquita, Donnici, & Pereira, 2010)
Softwood kraft pulp	-	64% H ₂ SO ₄	5 - 15	100 - 250	(Pu et al., 2007)
Soy hulls	-	64% H ₂ SO ₄	2.8 ± 0.67	122.7 ± 39.4	(Flauzino Neto, Silvério, Dantas, & Pasquini, 2013)
Softwood kraft pulp	-	65% H ₂ SO ₄	3.5	180 ± 75	(Araki, Wada, Kuga, & Okano, 1998)
Softwood kraft pulp	-	4N HCl	3.5	180 ± 75	(Araki et al., 1998)
Eucalyptus holocellulose	Grinding	Enzymatic treatment	4 - 6	500 - 1000	(Teixeira et al., 2015)
Unbleached softwood kraft pulp	Grinding	Enzymatic treatment	4 - 10	500 - 1500	(Teixeira et al., 2015)
Sugarcane bagasse	Grinding	Enzymatic treatment	4 - 8	250 - 1000	(Teixeira et al., 2015)

Degree of Polymerization

Degree of polymerization of cellulose is the number of glucose residues in single chains. It correlates with particle lengths, since more units in a chain lead to longer molecules (and consequently, longer nanofibrils/nanocrystals) (Battista et al., 1956). However, it is worth mentioning that the degree of polymerization is a property of single cellulose chains, whereas the length is a dimension of groups of cellulose molecules (nanoparticles). A common method to measure cellulose degree of polymerization is calculating the intrinsic viscosity value of a cellulose solution (dissolved in cupriethylenediamine) and converting it to degree of polymerization using the Mark-Houwink's equation (Lavoine et al., 2012). Another way to calculate degree of polymerization is through size exclusion chromatography, dissolving cellulose in dimethylacetamide/lithium chloride and running it through a column (Hallac & Ragauskas, 2011). The advantage of the latter is that it provides a distribution of the degrees of polymerization of a given nanocellulose sample.

As degree of polymerization correlates with particle lengths (Battista et al., 1956), the discussion presented in the previous section is also applied here. Production of nanofibrils and nanocrystals result in a decrease of degree of polymerization, and generally, cellulose molecules in nanocrystals are shorter than the ones in nanofibrils (Dufresne, 2012), because of the intentional chain breakage (hydrolysis) in the crystals production step.

The level-off degree of polymerization concept is based on the changes in the hydrolysis rates during the acid hydrolysis. It is hypothesized that cellulose has two distinct structural domains (crystalline and amorphous), differing in the intramolecular interactions and organization level of the molecules. The highly accessible amorphous cellulose is more reactive compared to the crystalline domains. Consequently, hydrolysis rates of the former are much higher than the latter, and once the amorphous cellulose is hydrolyzed, further depolymerization happens at slow rates. At this point, level-off degree of polymerization is reached and it is assumed to be the degree of polymerization of the crystals within the cellulosic material (Battista et al., 1956; Battista, 1950; Davidson, 1943; Håkansson & Ahlgren, 2005). Thus, it is dependent on the lignocellulosic biomass, since cellulose structural organization may vary between different species (see the topic "structure of cellulose").

Crystallinity

Crystallinity is an important parameter to be monitored during nanocellulose production, since it provides an indication of the organization level of cellulose and directly affects the physical and mechanical properties of the produced particles (Dufresne, 2012). As a matter of fact, it has been extensively used to follow changes in cellulose reactivity towards enzymes in enzymatic hydrolysis after submitting cellulosic materials through physicochemical treatments (Hall, Bansal, Lee, Reaff, & Bommarius, 2010). Especially in nanocrystals production, an increase in the crystallinity index would be expected if the amorphous regions were preferentially hydrolyzed. Nevertheless, there is a wide variation in the data available in the literature regarding to crystallinity measurements. Park et al., (Park, Baker, Himmel, Parilla, & Johnson, 2010) warned about this issue pointing out divergences in the crystallinity index of a commercial microcrystalline cellulose sample (Avicel PH101) presented in several

publications. Surprisingly, values ranging from close to 50% to above 90% have been reported for the same material. Variations were noticed not only for different analytical procedures, but also when the same technique was applied. Moreover, it has been reported that in the case of X-ray diffraction (XRD) methods, the crystallinity also depended upon the type of instrument used. This is an important consideration, as no comparisons are reliable with such variations until identical instruments and measuring conditions are used by the investigators (Agarwal, 2015).

The most used technique to measure crystallinity index is the XRD, and the diffractogram is widely analyzed by subtracting peak heights at different 2θ diffraction angles (around 18° and 22.5°) according to the method proposed by Segal et al. (Segal, Creely, Martin, & Conrad, 1959). Although the analysis is quite simple, it has been reported to overestimate the crystallinity index (Park et al., 2010). Crystallinity can also be measured by nuclear magnetic resonance, and one can refer to (Park et al., 2010) to appreciate a more detailed analysis on the advantages and disadvantages of each technique. Moreover, in 2010, after the work of Park et al. was published, a new technique based on Raman spectroscopy was published (now referred to as 380-Raman or Agarwal-Raman method) that uses the ratio of the intensities at 280 and 1096 cm^{-1} (Agarwal, Reiner, & Ralph, 2010). This method has been applied in the studies of nanocelluloses (Chen et al., 2015; Qing et al., 2013), pulps, agricultural residues and woods (Agarwal, Reiner, & Ralph, 2013), and it was reported that in the Raman estimated crystallinities, the effect of the presence of amorphous celluloses in a sample was much reduced (Agarwal et al., 2013).

Crystallinity change during nanofibrils production is also controversial. Some researchers reported a slight decrease in crystallinity index after homogenization (although the authors mentioned crystallinity was unchanged) (Agoda-Tandjawa et al., 2010) and others reported a decrease after grinding (Iwamoto et al., 2007). On the other hand, some authors have shown that crystallinity increased after high intensity ultrasonication (Cheng, Wang, Rials, & Lee, 2007) and after grinding (Abe & Yano, 2009). In the treatments that resulted in an increase in crystallinity, it is most likely that part of the amorphous regions was removed. TEMPO-oxidation apparently does not affect crystallinity, since oxidation occurs on the surface of fibrils (crystalline and amorphous) (A. Isogai et al., 2011).

Production of nanocrystals is expected to increase crystallinity. Amorphous fractions are preferentially hydrolyzed, and consequently the residual solid is enriched in crystalline structures. However, in some conditions, crystallinity does not change as shown recently by Chen et al. Under less severe hydrolysis conditions (58% H_2SO_4) crystals were released in yields higher (close to 70%) than what is normally reported in the literature (around 20-30%) and the crystallinity was similar to the initial pulp (Chen et al., 2015).

Mechanical Properties

Mechanical properties of nanocellulose materials are particularly important, since most of the applications are based on them. Methods to measure parameters related to these properties generally involve formation of films from nanocellulose suspensions and submitting them to elongation at constant rate, until failure. Elongation is recorded, as well as the force necessary to induce the elongation (Dufresne, 2012). From this test, information as tensile strength and tensile modulus (also known as Young's modulus) can be determined.

The reason why nanofibrils have better mechanical properties compared to original wood fiber (as in paper) is that the increase in surface area during the defibrillation process results in more possible hydrogen bonds formation in a sheet of fibrils (nanopaper), making it a stronger material (Brodin, Gregersen, & Syverud, 2014). Tensile modulus of nanofibrillated cellulose films have been reported between 6.2 to 17.5 GPa, and tensile strength from 129 to 250 MPa, depending on the feedstock and production method (Fukuzumi et al., 2009; Henriksson et al., 2008; Nogi, Iwamoto, Nakagaito, & Yano, 2009; Syverud & Stenius, 2009; Wang, Sabo, et al., 2015).

Mechanical properties of nanocrystals are even more impressive. At similar densities, its tensile modulus is higher than glass (70 GPa), comparable to Kevlar (60-125 GPa) and potentially stronger than steel (200-220 GPa) (Mariano, El Kissi, & Dufresne, 2014). The superior mechanical properties of nanocrystals is because it forms a continuous and rigid nanoparticles network, resulting from strong interactions between the particles (Dufresne, 2012). Although no good correlation was observed, Bras et al. (Bras, Viet, Bruzzese, & Dufresne, 2011) showed that the tensile modulus is higher in crystals with bigger aspect ratio (L/D).

CONCLUSION

Nanocellulose is a renewable bio-based material, with its source being almost inexhaustible. Associated with its fascinating properties, this nanomaterial is highlighted among the biopolymers. However, nanocellulose production is a relatively new technology and process improvements are still necessary. Moreover, better understanding on how the process steps influence the properties of the resulting nanocellulose needs to be achieved. With the increasing interest in the field, a rapid expansion of the knowledge is expected for the next years.

ACKNOWLEDGMENTS

The authors would like to thank the São Paulo Research Foundation FAPESP for financial support (Process No. 2015/00397-3 and 2015/02862-5).

REFERENCES

- Abe, K., & Yano, H. (2009). Comparison of the characteristics of cellulose microfibril aggregates of wood, rice straw and potato tuber. *Cellulose*, 16(6), 1017–1023.
- Abe, K., Iwamoto, S., & Yano, H. (2007). Obtaining cellulose nanofibers with a uniform width of 15 nm from wood. *Biomacromolecules*, 8(10), 3276–3278.
- Abushammala, H., Krossing, I., & Laborie, M.-P. (2015). Ionic liquid-mediated technology to produce cellulose nanocrystals directly from wood. *Carbohydrate Polymers*, 134, 609–616.

- Agarwal, U. P. (2015). Pros and cons of cellulose crystallinity estimation methods: 380-raman, 13C NMR, and Segal-WAXS. In *CELL Division Symposium, 249th American Chemical Society Meeting*. Denver, CO.
- Agarwal, U. P., Reiner, R. R., & Ralph, S. a. (2013). Estimation of cellulose crystallinity of lignocelluloses using near-ir ft-raman spectroscopy and comparison of the raman and segal-wax methods. *Journal of Agricultural and Food Chemistry*, *61*(1), 103–113.
- Agarwal, U. P., Reiner, R. S., & Ralph, S. A. (2010). Cellulose I crystallinity determination using FT-Raman spectroscopy: univariate and multivariate methods. *Cellulose*, *17*(4), 721–733.
- Agoda-Tandjawa, G., Durand, S., Berot, S., Blassel, C., Gaillard, C., Garnier, C., & Doublier, J.-L. (2010). Rheological characterization of microfibrillated cellulose suspensions after freezing. *Carbohydrate Polymers*, *80*(3), 677–686.
- Alemdar, A., & Sain, M. (2008). Isolation and characterization of nanofibers from agricultural residues – Wheat straw and soy hulls. *Bioresource Technology*, *99*(6), 1664–1671.
- Alvira, P., Tomás-Pejó, E., Ballesteros, M., & Negro, M. J. (2010). Pretreatment technologies for an efficient bioethanol production process based on enzymatic hydrolysis: A review. *Bioresource Technology*, *101*(13), 4851–61.
- Anderson, S. R., Esposito, D., Gillete, W., Zhu, J. Y., Baxa, U., & Mcneil, S. (2014). Enzymatic preparation of nanocrystalline and microcrystalline cellulose. *TAPPI Journal*, *13*(5), 35–42.
- Anugwom, I., Mäki-Arvela, P., Virtanen, P., Willför, S., Sjöholm, R., & Mikkola, J.-P. (2012). Selective extraction of hemicelluloses from spruce using switchable ionic liquids. *Carbohydrate Polymers*, *87*(3), 2005–2011.
- Araki, J., Wada, M., Kuga, S., & Okano, T. (1998). Flow properties of microcrystalline cellulose suspension prepared by acid treatment of native cellulose. *Colloids and Surfaces A: Physicochemical and Engineering Aspects*, *142*(1), 75–82.
- Araki, J., Wada, M., Kuga, S., & Okano, T. (1999). Influence of surface charge on viscosity behavior of cellulose microcrystal suspension. *Journal of Wood Science*, *45*(3), 258–261.
- Atalla, R. H., & Vanderhart, D. L. (1984). Native Cellulose: A Composite of Two Distinct Crystalline Forms. *Science*, *223*(4633), 283–285.
- Aulin, C., Ahola, S., Josefsson, P., Nishino, T., Hirose, Y., Österberg, M., & Wågberg, L. (2009). Nanoscale cellulose films with different crystallinities and mesostructures—their surface properties and interaction with water. *Langmuir*, *25*(13), 7675–7685.
- Bajpai, P. (2010). *Environmentally-friendly production of pulp and paper*. Hoboken, New Jersey: John Wiley & Sons.
- Battista, O. A. (1950). Hydrolysis and Crystallization of Cellulose. *Industrial & Engineering Chemistry*, *42*(3), 502–507.
- Battista, O. A., Coppick, S., Howsmon, J. A., Morehead, F. F., & Sisson, W. A. (1956). Level-Off Degree of Polymerization. *Industrial & Engineering Chemistry*, *48*(2), 333–335.
- Beck-Candanedo, S., Roman, M., & Gray, D. G. (2005). Effect of Reaction Conditions on the Properties and Behavior of Wood Cellulose Nanocrystal Suspensions. *Biomacromolecules*, *6*(2), 1048–1054.

- Bhattacharya, D., Germinario, L. T., & Winter, W. T. (2008). Isolation, preparation and characterization of cellulose microfibrils obtained from bagasse. *Carbohydrate Polymers*, *73*(3), 371–377.
- Bondeson, D., Mathew, A., & Oksman, K. (2006). Optimization of the isolation of nanocrystals from microcrystalline cellulose by acid hydrolysis. *Cellulose*, *13*(2), 171–180.
- Brännvall, E. (2009). Overview of pulp and paper processes. In M. Ek, G. Gellerstedt, & G. Henriksson (Eds.), *Pulp and paper chemistry and technology Volume 2* (pp. 1–11). Berlin: de Gruyter.
- Bras, J., Viet, D., Bruzzese, C., & Dufresne, A. (2011). Correlation between stiffness of sheets prepared from cellulose whiskers and nanoparticles dimensions. *Carbohydrate Polymers*, *84*(1), 211–215.
- Brinchi, L., Cotana, F., Fortunati, E., & Kenny, J. M. (2013). Production of nanocrystalline cellulose from lignocellulosic biomass: technology and applications. *Carbohydrate Polymers*, *94*(1), 154–69.
- Brodin, F., Gregersen, O. W., & Syverud, K. (2014). Cellulose nanofibrils: Challenges and possibilities as a paper additive or coating material-A review. *Nordic Pulp and Paper Research Journal*, *29*(01), 156–166.
- Cateto, C., Hu, G., & Ragauskas, A. (2011). Enzymatic hydrolysis of organosolv Kanlow switchgrass and its impact on cellulose crystallinity and degree of polymerization. *Energy & Environmental Science*, *4*(4), 1516.
- Chen, L., Wang, Q., Hirth, K., Baez, C., Agarwal, U. P., & Zhu, J. Y. (2015). Tailoring the yield and characteristics of wood cellulose nanocrystals (CNC) using concentrated acid hydrolysis. *Cellulose*, *22*(3), 1753–1762.
- Chen, X., Deng, X., Shen, W., & Jiang, L. (2012). Controlled enzymolysis preparation of nanocrystalline cellulose from pretreated cotton fibers. *BioResources*, *7*(3), 4237–4248.
- Cheng, Q., Wang, S., Rials, T. G., & Lee, S.-H. (2007). Physical and mechanical properties of polyvinyl alcohol and polypropylene composite materials reinforced with fibril aggregates isolated from regenerated cellulose fibers. *Cellulose*, *14*(6), 593–602.
- Davidson, G. F. (1943). The rate of change in the properties of cotton cellulose under the prolonged action of acids. *Journal of the Textile Institute Transactions*, *34*(10), T87–T96.
- de Mesquita, J. P., Donnici, C. L., & Pereira, F. V. (2010). Biobased Nanocomposites from Layer-by-Layer Assembly of Cellulose Nanowhiskers with Chitosan. *Biomacromolecules*, *11*(2), 473–480.
- Del Rio, L. F., Chandra, R. P., & Saddler, J. N. (2010). The effect of varying organosolv pretreatment chemicals on the physicochemical properties and cellulolytic hydrolysis of mountain pine beetle-killed lodgepole pine. *Applied Biochemistry and Biotechnology*, *161*(1-8), 1–21.
- Ding, S.-Y., & Himmel, M. E. (2006). The maize primary cell wall microfibril: a new model derived from direct visualization. *Journal of Agricultural and Food Chemistry*, *54*(3), 597–606.
- Dufresne, A. (2012). *Nanocellulose : From Nature to High Performance Tailored Materials*. Munchen: Walter de Gruyter.
- Eichhorn, S. J., Dufresne, A., Aranguren, M., Marcovich, N. E., Capadona, J. R., Rowan, S. J., Peijs, T. (2009). Review: current international research into cellulose nanofibres and nanocomposites. *Journal of Materials Science* (Vol. 45).

- Elazzouzi-Hafraoui, S., Nishiyama, Y., Putaux, J.-L., Heux, L., Dubreuil, F., & Rochas, C. (2008). The Shape and Size Distribution of Crystalline Nanoparticles Prepared by Acid Hydrolysis of Native Cellulose. *Biomacromolecules*, *9*(1), 57–65.
- Fengel, D., & Wegener, G. (1989). *Wood: Chemistry, Ultrastructure, Reactions*. (D. Fengel & G. Wegener, Eds.) (2nd ed.). Berlin: Walter de Gruyter.
- Fernandes, a N., Thomas, L. H., Altaner, C. M., Callow, P., Forsyth, V. T., Apperley, D. C., Jarvis, M. C. (2011). Nanostructure of cellulose microfibrils in spruce wood. *Proceedings of the National Academy of Sciences*, *108*(47), E1195–E1203.
- Filson, P. B., Dawson-Andoh, B. E., & Schwegler-Berry, D. (2009). Enzymatic-mediated production of cellulose nanocrystals from recycled pulp. *Green Chemistry*, *11*(11), 1808.
- Flauzino Neto, W. P., Silvério, H. A., Dantas, N. O., & Pasquini, D. (2013). Extraction and characterization of cellulose nanocrystals from agro-industrial residue – Soy hulls. *Industrial Crops and Products*, *42*, 480–488.
- Fukuzumi, H., Saito, T., Iwata, T., Kumamoto, Y., & Isogai, A. (2009). Transparent and High Gas Barrier Films of Cellulose Nanofibers Prepared by TEMPO-Mediated Oxidation. *Biomacromolecules*, *10*(1), 162–165.
- Gehlen, M. H. (2010). Kinetics of autocatalytic acid hydrolysis of cellulose with crystalline and amorphous fractions. *Cellulose*, *17*(2), 245–252.
- Habibi, Y., Lucia, L. A., & Rojas, O. J. (2010). Cellulose nanocrystals: chemistry, self-assembly, and applications. *Chemical Reviews*, *110*(6), 3479–500.
- Håkansson, H., & Ahlgren, P. (2005). Acid hydrolysis of some industrial pulps: effect of hydrolysis conditions and raw material. *Cellulose*, *12*(2), 177–183.
- Hall, M., Bansal, P., Lee, J. H., Reaff, M. J., & Bommarius, A. S. (2010). Cellulose crystallinity--a key predictor of the enzymatic hydrolysis rate. *The FEBS Journal*, *277*(6), 1571–82.
- Hallac, B. B., & Ragauskas, A. J. (2011). Analyzing cellulose degree of polymerization and its relevancy to cellulosic ethanol. *Biofuels, Bioproducts and Biorefining*, *5*(2), 215–225.
- Henriksson, M., Berglund, L. A., Isaksson, P., Lindström, T., & Nishino, T. (2008). Cellulose Nanopaper Structures of High Toughness. *Biomacromolecules*, *9*(6), 1579–1585.
- Henriksson, M., Henriksson, G., Berglund, L. a., & Lindström, T. (2007). An environmentally friendly method for enzyme-assisted preparation of microfibrillated cellulose (MFC) nanofibers. *European Polymer Journal*, *43*(8), 3434–3441.
- Herth, W. (1983). Arrays of plasma-membrane “rosettes” involved in cellulose microfibril formation of *Spirogyra*. *Planta*, *159*(4), 347–356.
- Hu, F., & Ragauskas, A. (2012). Pretreatment and Lignocellulosic Chemistry. *BioEnergy Research*, *5*(4), 1043–1066.
- Iiyama, K., Lam, T., & Stone, B. a. (1994). Covalent Cross-Links in the Cell Wall. *Plant Physiology*, *104*(2), 315–320. Retrieved from
- Isogai, A. (2013). Wood nanocelluloses: fundamentals and applications as new bio-based nanomaterials. *Journal of Wood Science*, *59*(6), 449–459.
- Isogai, A., Saito, T., & Fukuzumi, H. (2011). TEMPO-oxidized cellulose nanofibers. *Nanoscale*, *3*(1), 71–85.
- Isogai, T., Saito, T., & Isogai, A. (2011). Wood cellulose nanofibrils prepared by TEMPO electro-mediated oxidation. *Cellulose*, *18*(2), 421–431.
- Iwamoto, S., Nakagaito, A. N., & Yano, H. (2007). Nano-fibrillation of pulp fibers for the processing of transparent nanocomposites. *Applied Physics A*, *89*(2), 461–466.

- Kalia, S., Boufi, S., Celli, A., & Kango, S. (2014). Nanofibrillated cellulose: surface modification and potential applications. *Colloid and Polymer Science*, 292(1), 5–31.
- Kennedy, C. J., Cameron, G. J., Šturcová, A., Apperley, D. C., Altaner, C., Wess, T. J., & Jarvis, M. C. (2007). Microfibril diameter in celery collenchyma cellulose: X-ray scattering and NMR evidence. *Cellulose*, 14(3), 235–246.
- Khalil, H. P. S. A., Davoudpour, Y., Islam, M. N., Mustapha, A., Sudesh, K., Dungani, R., & Jawaid, M. (2014). Production and modification of nanofibrillated cellulose using various mechanical processes: A review. *Carbohydrate Polymers*, 99, 649–665.
- Klemm, D., Heublein, B., Fink, H.-P., & Bohn, A. (2005). Cellulose: fascinating biopolymer and sustainable raw material. *Angewandte Chemie (International Ed. in English)*, 44(22), 3358–93. 7.
- Koyama, M., Helbert, W., Imai, T., Sugiyama, J., & Henrissat, B. (1997). Parallel-up structure evidences the molecular directionality during biosynthesis of bacterial cellulose. *Proceedings of the National Academy of Sciences of the United States of America*, 94(17), 9091–9095.
- Kvien, I., Tanem, B. S., & Oksman, K. (2005). Characterization of Cellulose Whiskers and Their Nanocomposites by Atomic Force and Electron Microscopy. *Biomacromolecules*, 6(6), 3160–3165.
- Lavoine, N., Desloges, I., Dufresne, A., & Bras, J. (2012). Microfibrillated cellulose – Its barrier properties and applications in cellulosic materials: A review. *Carbohydrate Polymers*, 90(2), 735–764.
- Mariano, M., El Kissi, N., & Dufresne, A. (2014). Cellulose nanocrystals and related nanocomposites: Review of some properties and challenges. *Journal of Polymer Science Part B: Polymer Physics*, 52(12), 791–806.
- McDonough, T. (1992). The chemistry of organosolv delignification. *IPST Technical Paper Series*, 455, 1–17.
- Meyabadi, T. F., & Dadashian, F. (2012). Optimization of enzymatic hydrolysis of waste cotton fibers for nanoparticles production using response surface methodology. *Fibers and Polymers*, 13(3), 313–321.
- Meyabadi, T. F., Dadashian, F., Sadeghi, G. M. M., & Asl, H. E. Z. (2014). Spherical cellulose nanoparticles preparation from waste cotton using a green method. *Powder Technology*, 261, 232–240.
- Moon, R. J., Martini, A., Nairn, J., Simonsen, J., & Youngblood, J. (2011). Cellulose nanomaterials review: structure, properties and nanocomposites. *Chemical Society Reviews*, 40(7), 3941–94.
- Mosier, N., Wyman, C., Dale, B., Elander, R., Lee, Y. Y., Holtzapple, M., & Ladisch, M. (2005). Features of promising technologies for pretreatment of lignocellulosic biomass. *Bioresource Technology*, 96(6), 673–86.
- Mueller, S. C., & Brown, R. M. (1980). Evidence for an intramembrane component associated with a cellulose microfibril-synthesizing complex in higher plants. *Journal of Cell Biology*, 84(2), 315–326.
- Mukherjee, S. M., & Woods, H. J. (1953). X-ray and electron microscope studies of the degradation of cellulose by sulphuric acid. *Biochimica et Biophysica Acta*, 10, 499–511.
- Nakagaito, a. N., & Yano, H. (2004). The effect of morphological changes from pulp fiber towards nano-scale fibrillated cellulose on the mechanical properties of high-strength

- plant fiber based composites. *Applied Physics A: Materials Science & Processing*, 78(4), 547–552.
- Newman, R. H., Hill, S. J., & Harris, P. J. (2013). Wide-Angle X-Ray Scattering and Solid-State Nuclear Magnetic Resonance Data Combined to Test Models for Cellulose Microfibrils in Mung Bean Cell Walls. *Plant Physiology*, 163(4), 1558–1567.
- Nishiyama, Y. (2009). Structure and properties of the cellulose microfibril. *Journal of Wood Science*, 55(4), 241–249.
- Nishiyama, Y., Langan, P., & Chanzy, H. (2002). Crystal Structure and Hydrogen-Bonding System in Cellulose I β from Synchrotron X-ray and Neutron Fiber Diffraction. *Journal of the American Chemical Society*, 124(31), 9074–9082.
- Nishiyama, Y., Sugiyama, J., Chanzy, H., & Langan, P. (2003). Crystal Structure and Hydrogen Bonding System in Cellulose I α from Synchrotron X-ray and Neutron Fiber Diffraction. *Journal of the American Chemical Society*, 125(47), 14300–14306.
- Nogi, M., Iwamoto, S., Nakagaito, A. N., & Yano, H. (2009). Optically Transparent Nanofiber Paper. *Advanced Materials*, 21(16), 1595–1598.
- O’Sullivan, A. (1997). Cellulose : the structure slowly unravels. *Cellulose*, 4, 173–207.
- Orts, W. J., Godbout, L., Marchessault, R. H., & Revol, J.-F. (1998). Enhanced Ordering of Liquid Crystalline Suspensions of Cellulose Microfibrils: A Small Angle Neutron Scattering Study. *Macromolecules*, 31(17), 5717–5725.
- Pääkkö, M., Ankerfors, M., Kosonen, H., Nykänen, A., Ahola, S., Österberg, M., Lindström, T. (2007). Enzymatic Hydrolysis Combined with Mechanical Shearing and High-Pressure Homogenization for Nanoscale Cellulose Fibrils and Strong Gels. *Biomacromolecules*, 8(6), 1934–1941.
- Pääkkö, M., Vapaavuori, J., Silvennoinen, R., Kosonen, H., Ankerfors, M., Lindström, T., Ikkala, O. (2008). Long and entangled native cellulose I nanofibers allow flexible aerogels and hierarchically porous templates for functionalities. *Soft Matter*, 4(12), 2492.
- Park, S., Baker, J. O., Himmel, M. E., Parilla, P. a., & Johnson, D. K. (2010). Cellulose crystallinity index: measurement techniques and their impact on interpreting cellulase performance. *Biotechnology for Biofuels*, 3(1), 10.
- Payne, C. M., Knott, B. C., Mayes, H. B., Hansson, H., Himmel, M. E., Sandgren, M., Beckham, G. T. (2015). Fungal Cellulases. *Chemical Reviews*, 115(3), 1308–1448.
- Peng, B. L., Dhar, N., Liu, H. L., & Tam, K. C. (2011). Chemistry and applications of nanocrystalline cellulose and its derivatives: A nanotechnology perspective. *The Canadian Journal of Chemical Engineering*, 89(5), 1191–1206.
- Pinkert, A., Goeke, D. F., Marsh, K. N., & Pang, S. (2011). Extracting wood lignin without dissolving or degrading cellulose: investigations on the use of food additive-derived ionic liquids. *Green Chemistry*, 13(11), 3124.
- Pu, Y., Zhang, J., Elder, T., Deng, Y., Gatenholm, P., & Ragauskas, A. J. (2007). Investigation into nanocellulosics versus acacia reinforced acrylic films. *Composites Part B: Engineering*, 38(3), 360–366.
- Qing, Y., Sabo, R., Zhu, J. Y., Agarwal, U., Cai, Z., & Wu, Y. (2013). A comparative study of cellulose nanofibrils disintegrated via multiple processing approaches. *Carbohydrate Polymers*, 97(1), 226–234.
- Rånby, B. G. (1951). Fibrous macromolecular systems. Cellulose and muscle. The colloidal properties of cellulose micelles. *Discussions of the Faraday Society*, 11(111), 158.

- Rånby, B. G., Banderet, A., & Sillén, L. G. (1949). Aqueous Colloidal Solutions of Cellulose Micelles. *Acta Chemica Scandinavica*, 3, 649–650.
- Revol, J.-F., Bradford, H., Giasson, J., Marchessault, R. H., & Gray, D. G. (1992). Helicoidal self-ordering of cellulose microfibrils in aqueous suspension. *International Journal of Biological Macromolecules*, 14(3), 170–172.
- Roman, M., & Winter, W. T. (2004). Effect of sulfate groups from sulfuric acid hydrolysis on the thermal degradation behavior of bacterial cellulose. *Biomacromolecules*, 5(5), 1671–7.
- Rowland, S. P., & Roberts, E. J. (1972). The nature of accessible surfaces in the microstructure of cotton cellulose. *Journal of Polymer Science Part A-1: Polymer Chemistry*, 10(8), 2447–2461.
- Sacui, I. A., Nieuwendaal, R. C., Burnett, D. J., Stranick, S. J., Jor, M., Weder, C., Gilman, J. W. (2014). Comparison of the Properties of Cellulose Nanocrystals and Cellulose Nanofibrils Isolated from Bacteria, Tunicate, and Wood Processed Using Acid, Enzymatic, Mechanical, and Oxidative Methods. *Applied Materials & Interfaces*, 6, 6127–6138.
- Saito, T., & Isogai, A. (2004). TEMPO-Mediated Oxidation of Native Cellulose. The Effect of Oxidation Conditions on Chemical and Crystal Structures of the Water-Insoluble Fractions. *Biomacromolecules*, 5(5), 1983–1989.
- Saito, T., Hirota, M., Tamura, N., Kimura, S., Fukuzumi, H., Heux, L., & Isogai, A. (2009). Individualization of Nano-Sized Plant Cellulose Fibrils by Direct Surface Carboxylation Using TEMPO Catalyst under Neutral Conditions. *Biomacromolecules*, 10(7), 1992–1996. <http://doi.org/10.1021/bm900414t>.
- Saito, T., Kimura, S., Nishiyama, Y., & Isogai, A. (2007). Cellulose Nanofibers Prepared by TEMPO-Mediated Oxidation of Native Cellulose. *Biomacromolecules*, 8(8), 2485–2491.
- Saito, T., Nishiyama, Y., Putaux, J.-L., Vignon, M., & Isogai, A. (2006). Homogeneous Suspensions of Individualized Microfibrils from TEMPO-Catalyzed Oxidation of Native Cellulose. *Biomacromolecules*, 7(6), 1687–1691.
- Samir, M. A. S. A., Alloin, F., & Dufresne, A. (2005). Review of Recent Research into Cellulosic Whisker, Their Properties and Their Application in Nanocomposites Field. *Biomacromolecules*, 6, 612–626.
- Satyamurthy, P., Jain, P., Balasubramanya, R. H., & Vigneshwaran, N. (2011). Preparation and characterization of cellulose nanowhiskers from cotton fibres by controlled microbial hydrolysis. *Carbohydrate Polymers*, 83(1), 122–129.
- Segal, L., Creely, J. J., Martin, A. E., & Conrad, C. M. (1959). An Empirical Method for Estimating the Degree of Crystallinity of Native Cellulose Using the X-Ray Diffractometer. *Textile Research Journal*, 29(10), 786–794.
- Shatkin, J. A., Wegner, T. H., Bilek, E. M. T., & Cowie, J. (2014). Market projections of cellulose nanomaterial-enabled products - Part 1: Applications. *TAPPI Journal*, 13(5), 9–16.
- Shogren, R. L., Peterson, S. C., Evans, K. O., & Kenar, J. a. (2011). Preparation and characterization of cellulose gels from corn cobs. *Carbohydrate Polymers*, 86(3), 1351–1357.
- Siqueira, G., Bras, J., & Dufresne, A. (2010). Cellulosic Bionanocomposites: A Review of Preparation, Properties and Applications. *Polymers*, 2(4), 728–765.

- Sixta, H. (2006). *Handbook of Pulp*. (H. Sixta, Ed.). Weinheim, Germany: Wiley-VCH Verlag GmbH.
- Sjöström, E. (1993). Cellulose. In E. Sjöström (Ed.), *Wood Chemistry: fundamentals and applications* (2nd ed., pp. 51–70). Academic Press.
- Song, Q., Winter, W., Bujanovic, B., & Amidon, T. (2014). Nanofibrillated Cellulose (NFC): A High-Value Co-Product that Improves the Economics of Cellulosic Ethanol Production. *Energies*, 7(2), 607–618.
- Spence, K. L., Venditti, R. A., Rojas, O. J., Habibi, Y., & Pawlak, J. J. (2011). A comparative study of energy consumption and physical properties of microfibrillated cellulose produced by different processing methods. *Cellulose*, 18(4), 1097–1111.
- Stelte, W., & Sanadi, A. R. (2009). Preparation and Characterization of Cellulose Nanofibers from Two Commercial Hardwood and Softwood Pulp. *Industrial & Engineering Chemistry Research*, 48(24), 11211–11219.
- Sugiyama, J., Vuong, R., & Chanzy, H. (1991). Electron diffraction study on the two crystalline phase occurring in native cellulose from an algal cell wall. *Macromolecules*, 24, 4168–4175.
- Svagan, A. J., Azizi Samir, M. a S., & Berglund, L. a. (2007). Biomimetic Polysaccharide Nanocomposites of High Cellulose Content and High Toughness. *Biomacromolecules*, 8(8), 2556–2563.
- Syverud, K., & Stenius, P. (2009). Strength and barrier properties of MFC films. *Cellulose*, 16(1), 75–85.
- Szczesna-Antczak, M., Kazimierczak, J., & Antczak, T. (2012). Nanotechnology - methods of manufacturing cellulose nanofibres. *Fibres and Textiles in Eastern Europe*, 91(2), 8–12.
- Taniguchi, T., & Okamura, K. (1998). New films produced from microfibrillated natural fibres. *Polymer International*, 47(3), 291–294.
- Teixeira, R. S. S., da Silva, A. S., Kim, H.-W., Ishikawa, K., Endo, T., Lee, S.-H., & Bon, E. P. S. (2013). Use of cellobiohydrolase-free cellulase blends for the hydrolysis of microcrystalline cellulose and sugarcane bagasse pretreated by either ball milling or ionic liquid [Emim][Ac]. *Bioresource Technology*, 149, 551–5.
- Teixeira, R. S. S., Silva, A. S. Da, Jang, J.-H., Kim, H.-W., Ishikawa, K., Endo, T., Bon, E. P. S. (2015). Combining biomass wet disk milling and endoglucanase/ β -glucosidase hydrolysis for the production of cellulose nanocrystals. *Carbohydrate Polymers*, 128, 75–81.
- Thomas, L. H., Forsyth, V. T., Šturcová, A., Kennedy, C. J., May, R. P., Altaner, C. M., Jarvis, M. C. (2013). Structure of Cellulose Microfibrils in Primary Cell Walls from Collenchyma. *Plant Physiology*, 161(1), 465–476.
- Wang, Q. Q., Zhu, J. Y., Gleisner, R., Kuster, T. a., Baxa, U., & McNeil, S. E. (2012). Morphological development of cellulose fibrils of a bleached eucalyptus pulp by mechanical fibrillation. *Cellulose*, 19(5), 1631–1643.
- Wang, W., Mozuch, M. D., Sabo, R. C., Kersten, P., Zhu, J. Y., & Jin, Y. (2015). Production of cellulose nanofibrils from bleached eucalyptus fibers by hyperthermostable endoglucanase treatment and subsequent microfluidization. *Cellulose*, 22(1), 351–361.
- Wang, W., Sabo, R. C., Mozuch, M. D., Kersten, P., Zhu, J. Y., & Jin, Y. (2015). Physical and Mechanical Properties of Cellulose Nanofibril Films from Bleached Eucalyptus Pulp by Endoglucanase Treatment and Microfluidization. *Journal of Polymers and the Environment*, 23(4), 551–558.

- Xu, Y., Salmi, J., Kloser, E., Perrin, F., Grosse, S., Denault, J., & Lau, P. C. K. (2013). Feasibility of nanocrystalline cellulose production by endoglucanase treatment of natural bast fibers. *Industrial Crops and Products*, *51*, 381–384.
- Zhang, Y.-H. P., & Lynd, L. R. (2004). Toward an aggregated understanding of enzymatic hydrolysis of cellulose: noncomplexed cellulase systems. *Biotechnology and Bioengineering*, *88*(7), 797–824.
- Zhu, J. Y., Sabo, R., & Luo, X. (2011). Integrated production of nano-fibrillated cellulose and cellulosic biofuel (ethanol) by enzymatic fractionation of wood fibers. *Green Chemistry*, *13*(5), 1339.

*Chapter 10***TOWARDS ECONOMICALLY SUSTAINABLE
LIGNOCELLULOSIC BIOREFINERIES**

***N. V. S. N. Murthy Konda^{1,2,*},
Dominique Loqué^{1,2} and Corinne D. Scown^{1,3}***

¹Joint BioEnergy Institute,

Lawrence Berkeley National Laboratory, Berkeley, CA, US

²Biological Systems and Engineering Division,

Lawrence Berkeley National Laboratory, Berkeley, CA, US

³Energy Analysis and Environmental Impacts Division,

Lawrence Berkeley National Laboratory, Berkeley, CA, US

ABSTRACT

To succeed in the marketplace, cellulosic biorefineries must be both low-carbon and economically viable. Production of liquid fuels from lignocellulosic feedstocks has increased dramatically in recent years. Between 2014 and 2015, annual production grew from less than 1 million gallons to nearly 50 million gallons (EPA, 2015). Despite this impressive growth and the potential greenhouse gas (GHG) emissions reductions, total cellulosic fuel production is still dwarfed by the nearly 375 million gallons of gasoline consumed in the US each day (EIA, 2015). This shortfall underscores not only the underlying technological challenges that are yet to be overcome, but also highlights the unmet need for scalable and commercially viable lignocellulosic biomass conversion technologies. Techno-economic analysis (TEA) can be very helpful in guiding R&D activities and identifying opportunities to improve economic viability of cellulosic biorefineries. While it is important to maximize sugar and, ultimately, fuel yield, co-production of chemicals alongside fuels can provide additional revenue and potentially enable cellulosic biorefineries that would otherwise face challenging economics. In this study, we use TEA to evaluate the impact of co-product streams on the overall biorefinery economics. Specifically, the co-production of muconic acid – a precursor for both adipic acid and terephthalic acid - together with ethanol from engineered sweet sorghum is considered as a case study. Results indicate the direct impact of market price

* Correspondence to: MurthyKonda@lbl.gov.

– and thus the market demand - of the co-produced chemical(s) in determining the overall economic feasibility of the process.

1. INTRODUCTION

Within the next decade, the US has the potential to produce more than one billion dry tons of sustainable biomass annually for conversion to bioenergy and bioproducts (Perlack et al., 2011). This represents significant opportunity to replace gasoline (and other petroleum derived fuels and chemicals) with their renewable alternatives that are beneficial from an environmental standpoint. Using biomass availability projections, the US Environmental Protection Agency's (EPA) Renewable Fuel Standard (RFS2) mandate was established in 2007, requiring 36 billion gallons of annual renewable fuel production by 2022, 16 billion of which must be cellulosic biofuels (EPA). In contrast, the total nameplate production capacity of the current commercial scale cellulosic facilities (including facilities by INEOS, POET-DSM, and DuPont) is less than 100 million gallons per year. To comply with RFS2, with biorefineries producing only cellulosic liquid fuels, at least one to two commercial scale facilities (20-40 million gal/year) would need to be built per week between 2016 and 2022. This emphasizes the scale of the challenge that the cellulosic biofuel industry is confronted with, and the need for more economically sustainable pathways for converting biomass to fuels and co-products.

In rest of this chapter, we highlight key opportunities and potential barriers to improving the economic viability of cellulosic biorefineries. We use techno-economic analysis (TEA) to evaluate cellulosic biorefinery configurations and provide guidance for prioritizing future R&D efforts – this TEA section is based on a case study in which muconic acid is produced alongside ethanol in a cellulosic biorefinery, using engineered sweet sorghum as the feedstock.

2. OPPORTUNITIES TO IMPROVE ECONOMIC VIABILITY OF BIOREFINERIES AND CHALLENGES

Assuming fuel prices are fixed, there are two primary strategies for improving the economic viability of biorefineries: 1) Reducing production costs and 2) increasing revenue from co-products. These strategies and their associated challenges are discussed below.

2.1. Reducing Production Costs

This strategy refers to opportunities to optimize various aspects of biorefinery processes. A typical cellulosic biorefinery involves a complex process made up of multiple core sections (i.e., feedstock handling, pretreatment, enzymatic hydrolysis, fermentation, and downstream separation) as well as auxiliary sections (i.e., wastewater treatment and cogeneration facility to produce steam and electricity) (Humbird et al., 2011). Because of the complexity and relative immaturity of biorefinery technologies, there are numerous opportunities for

optimizing individual sections as well as the overall process. Some specific examples include reducing costs associated with the feedstock (e.g., improved yields), enzymes (e.g., reduced enzyme loading), and solvents (e.g., low loading and high recovery of expensive solvents such as ionic liquids). In addition, less water and energy intensive processes can improve both economic and environmental performance – this is particularly true in the context of cellulosic biorefineries. For instance, in a state of the art biorefinery designed by NREL (Humbird et al., 2011), the wastewater treatment (WWT) and cogeneration sections are two of the most capital intensive sections – combined, they make up approximately half of the total capital cost of the biorefinery. Reducing water and energy requirements can substantially impact capital costs by enabling reductions in WWT and cogeneration capacity. Furthermore, engineered feedstocks (e.g., lower lignin content, higher C6/C5 sugar ratio) can be utilized to reduce processing costs. For instance, it was previously shown that the engineered corn stover with reduced lignin content could potentially reduce the minimum ethanol selling price (MESPP) by around \$0.6-\$1.0/gal (Klein-Marcuschamer, Oleskowicz-Popiel, Simmons, & Blanch, 2010). Another strategy is to utilize mixed feedstocks, which can provide flexibility in selecting the lowest-cost available biomass, minimize transportation costs by reducing the feedstock collection radius, and reduce or eliminate seasonal impacts on the facility's ability to operate at full capacity.

Each of the aforementioned opportunities can be addressed through continued R&D and process improvements made during demonstration and scale-up. One challenge, however, is to ensure that advances in any individual section do not negatively affect costs elsewhere in the biorefinery. Conducting rigorous TEA can mitigate that risk by revealing such integration issues early and devising strategies to address them. At a more fundamental level, biorefineries that solely produce fuel face a competitive market with low profit margins in which the incumbent fossil fuel producers benefit from market dominance and extensive existing infrastructure (Demirbas, 2009; Werpy et al., 2004). Because of this inherent disadvantage, most – if not all – of the aforementioned opportunities may need to be realized simultaneously to ensure the long-term economic viability of cellulosic biofuel production.

Simple back-of-the-envelope calculations can be done to illustrate the economic challenge posed by converting lignocellulosic biomass to liquid fuels. For this analysis, a mature conversion technology (i.e., Nth plant) with an overall biomass-to-fuel yield of around 80 gal/ton is considered. In the case of corn stover¹, this would require pretreatment and hydrolysis technologies capable of >90% conversion of glucan and xylan to their respective monomeric sugars and a fermentation technology that is capable of co-utilizing glucose and xylose sugars with >90% conversion efficiency to produce fuel. With a delivered feedstock price of \$80/ton² (Davis et al., 2013), the feedstock cost contribution alone is around \$1/gal. Another key factor is the enzyme cost – again, a relatively mature technology is assumed that requires 20 mg protein per g of glucan to release monomeric sugars from both glucan and xylan with >90% conversion efficiency. With an estimated price range of \$5 to \$10/kg of protein (Liu, Zhang, & Bao, 2016), the enzyme cost contribution would be in the range of \$0.4 to \$0.8/gal. Furthermore, these biorefineries, as with most chemical plants, are capital-intensive. For example, pioneer plant estimates suggest that a 25 million gallon/year facility

¹ Even with other feedstocks, an yield of 80 gal/ton could be a good best case representation as long as the total sugar content is similar to that of corn stover.

² Estimated target price of feedstock delivered at plant-gate (i.e., includes logistics costs such as collection and transportation).

would require capital around \$10/annual-gallon³. Once the conversion technologies mature, however, the capital intensity is expected to be somewhat lower. For instance, a study by the National Renewable Energy Laboratory (NREL)(Humbird et al., 2011) estimated a capital intensity of around \$7/gal for an Nth plant. Depending on the requirements of the investment⁴, this could translate a capital cost contribution in the range of \$0.7 to \$2/gal. In other words, accounting only for the cost of the feedstock, enzyme, and capital contributions, the production cost sums to around \$2.1 to \$3.8/gal even with the matured technology (e.g., Nth plant with high yields). On top of this, there are other costs – e.g., chemical inputs (e.g., solvents, acids, and bases), waste disposal etc. - that are usually highly specific to the technology under consideration. In the case of drop-in biofuels, for which yields comparable to ethanol have not yet been achieved, these challenges are even more difficult to overcome. In a typical modeled cellulosic biorefineries, the only co-product is electricity exported to the grid, which is generated via combustion of lignin and biogas from the WWT anaerobic digester. However, at a selling price of 5.72 cents/kWh, this co-product only offsets approximately 10.8 cents/gal (Humbird et al., 2011). Producing a much higher-value co-product is a promising route to bringing the minimum selling price of cellulosic fuels within a range that is more competitive with conventional petroleum fuels.

2.2. Increasing Revenue from Co-Products

In contrast to strategies that center on reducing production costs, the co-production of chemicals alongside of the primary biofuel(s) aims to take advantage of markets with higher profit margins where, in some cases, biological production routes may be more efficient and cost-effective than conventional fossil-based routes. Co-production of these chemicals can be accomplished in multiple ways including:

- Conversion of a portion of cellulosic and/or hemicellulosic sugars to chemicals
- Valorization of lignin to produce chemicals such as aromatics, and
- Extraction of chemicals from natural or engineered plants (e.g., pinene from pine trees)

The three options outlined above can enable the development of advanced cellulosic biorefineries that mimic present-day petroleum refineries in that they will produce a suite of products. The biorefineries producing more than one product (i.e., at least one co-product other than the primary biofuel and heat/electricity) are referred to as *integrated biorefineries* in this chapter. A simplified representation is provided in Figure 1. As depicted in this representation, various components such as sugars, chemicals, and lignin can be extracted/recovered from different processing steps involved in a typical biorefinery, which can subsequently be converted and/or further purified in parallel processing steps to produce chemicals that can be utilized in a variety of applications. For instance, primary extraction may refer to processes as simple as washing (e.g., recovery of soluble sugars from sugarcane

³ Estimate based on the capital requirement for POET-DSM's biorefinery.

⁴ Corresponding to a capital recovery factor of around 10-20% (e.g., 10-20% interest rate over a project lifetime of around 30 years).

or sweet sorghum) or complex multi-step processes involving additional chemicals (e.g., recovery of alginate from macroalgae, (Konda, Singh, Simmons, & Klein-Marcusamer, 2015)). The secondary extraction step could refer to processes involving recovery of chemicals (e.g., α -pinene extraction from loblolly pine using chemical solvents such as hexane or dodecane, (N. Konda et al., 2015)) or lignin. These sugars, chemicals, and/or lignin extracted can be converted to value-added co-products.

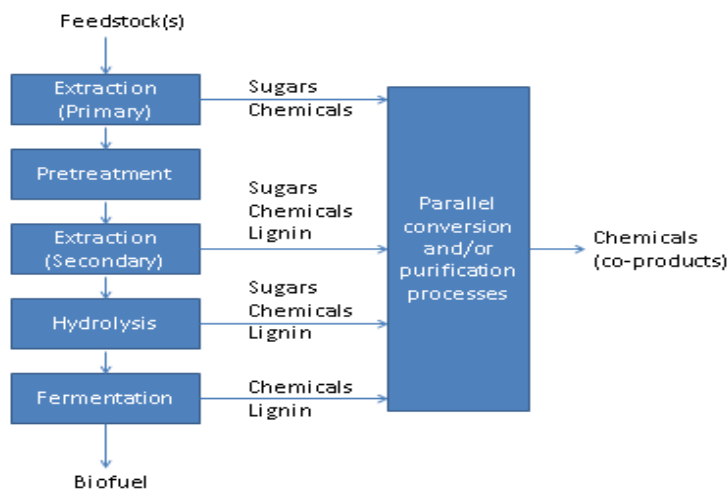


Figure 1. Simplified representation of envisioned integrated biorefinery complex.

The integrated biorefinery concept can provide a more promising business model relative to conventional biorefinery designs. Indeed, this concept has received increasing attention from the research community in recent years. However, as the research community invests more effort in the development of engineered feedstocks and conversion processes that enable integrated biorefineries, it is important to be mindful of the risks and practical challenges associated with this approach. Selection of target co-product(s) is an important first step, and requires background knowledge of the existing demand and price to ensure that the net value to the biorefinery is positive and significant. In many cases, the relationship between the market volume and price of chemicals (including commodity and specialty) is such that the market price is inversely proportional to market size. The deployment of commercial-scale biorefineries that co-produce a high-value specialty chemical runs the risk of quickly overwhelming the market for that chemical and causing the price to collapse (N. M. Konda et al., 2015). For instance, while the co-production of alginate in a macroalgae biorefinery was found to have positive impact on overall economics, the production capacity from a single biorefinery was found to far exceed the global market size for alginate – subsequently, it will not be a sustainable business model for macroalgae biorefineries to co-produce alginate (N. M. Konda et al., 2015). Conversely, many high volume chemicals are produced at low cost with minimal profit margins, meaning that co-production of these chemicals may yield minimal or even negative impacts on overall biorefinery economics. Thus, it is critical to ensure that target co-products are selected with careful consideration of the market volume and price.

Another consideration is the potential for additional co-product(s) to increase technological risk and therefore capital risk. Some molecules may be attractive targets based on market volume and price but require major scientific advancements before they can be produced at suitable yields, or produced at all if no known pathway exists. These are excellent opportunities for basic research, but may not be feasible for commercialization within the short- or medium-term. Lignin valorization presents an important opportunity to improve overall biorefinery economics. For instance, if the biorefinery can draw a net revenue of around \$1000 per metric tonne (MT) of lignin, it can potentially reduce minimum ethanol selling price (MESP) by around \$1/gal (Konda et al., 2014) considering that biomass contains approx. 15%-25% of lignin. In contrast, if lignin were to be used as a source of fuel in a boiler section to produce steam and electricity (i.e., current state of the art), lignin is effectively being valorized at a much lower price (i.e., ~\$50/MT). The challenge however is to ensure that the additional processing costs of lignin valorization are kept to a minimum so as to drive net value addition to a high level of around \$1000/MT.

3. ROLE OF TEA TOWARD DESIGNING ECONOMICALLY SUSTAINABLE BIOREFINERIES

Given the wide range of options for potential feedstocks, conversion technologies, and products – and the combinations thereof – there exist numerous possible configurations for future biorefineries. In a broad sense, TEA can be conducted to survey the landscape of possible configurations to develop a high-level understanding of the relative merits and challenges associated with each of the resulting pathways. As required, TEA can further be utilized to down select one or more options that meet certain predefined economic criteria. Even if a configuration is pre-selected, TEA can still be employed to identify the key cost-bottlenecks that are specific to that configuration to enable informed decisions around prioritizing future research.

Minimum selling price is a widely used economic metric in the context of biorefineries (Humbird et al., 2011; Konda et al., 2014). In the case of ethanol, this is usually referred to as minimum ethanol selling price (MESP). This is a high level metric that takes into account of various factors such as costs incurred (e.g., capital and operating expenses), revenues, financial assumptions (e.g., discount rate, project life time) and engineering aspects (e.g., construction and start-up time), resulting in a “plant gate” price. Downstream costs such as fuel distribution and retail operations are usually not included. Since MESP incorporates all the manufacturing costs (including raw materials, capital expenditure, utilities, labor, and waste disposal, etc.), one advantage with the MESP as a metric is that various stake-holders – including producers and policy makers – can easily compare it with the current or projected spot prices of fuel to determine the economic viability of their project(s). Since a large number of assumptions go into the computation of MESP, it is important to ensure that all the underlying assumptions are reasonable and, where possible, consistent across different project options so that a fair comparisons can be made across competing fuel pathways and/or process configurations. To this end, one of the important factors in determining MESP in a typical TEA study is the internal rate of return (IRR). The IRR is the discount rate in a multi-year cash flow analysis that results in a net present value (NPV) of zero for given price of

product(s). While the preferred IRR could vary significantly depending on the source of investment, a typical range is 10 to 25% in the case of TEA based on mature technology (i.e., Nth plant) within the context of cellulosic biorefineries.

4. CASE STUDY: ECONOMIC VIABILITY OF CO-PRODUCTION OF MUCONIC ACID (MA) FROM AN ENGINEERED SWEET SORGHUM (SS) FEEDSTOCK

In this section, we demonstrate TEA in the context of a novel application that involves co-production of muconic acid (MA) from engineered sweet sorghum (SS). We carried out a preliminary TEA to understand the economic impact of specific high-yield MA production pathways. The economic analysis was conducted consistent with the methods laid out by NREL (Humbird et al., 2011). The minimum ethanol selling price (MESP) was used as the key economic metric and was computed based on a detailed cash flow analysis with a 10% IRR. The base year for the economic analysis is 2014. Most of the key economic and financial assumptions in the cash flow analysis are based on the NREL study (Humbird et al., 2011) and these are provided in the table below. The current analysis is conducted using SuperPro Designer (a commercially available process modeling software package).

Table 1. Key economic and financial assumptions in the cash flow analysis (Humbird et al., 2011)

Plant life	30 years
Discount rate	10%
Depreciation method ^a (Humbird et al., 2011)	Straight-line (over 10 year period)
Federal taxes	35%
Financing	40% equity
Loan terms	10-year loan at 8% APR
Construction period	3 years
First 12 months expenditure	8%
Next 12 months expenditure	60%
Last 12 months expenditure	32%
Start-up time ^b	6 months
Revenues during start-up	50%

^abased on the method available in SuperPro Designer.

^bbased on a more recent NREL study (Davis et al., 2013).

4.1. Sweet Sorghum as a Potential Feedstock for Prospective Biorefineries

Sweet sorghum accumulates large quantities of soluble sugars (around 40 wt% on dry basis, Figure 2) that can be easily extracted. In addition to the bagasse (leftover biomass after sugar extraction), these sugars may be converted to biofuel or chemicals. Moreover, sweet sorghum offers a number of agronomic advantages (Regassa & Wortmann, 2014). It is an annual crop, has a fast growing season (three to four months), allowing it to be easily inserted in crop rotation programs and grown under wider latitudes than sugarcane that is perennial

and cold sensitive. It has a wide range of adaptability and can be grown in a wide series of environments (Ejeta & Knoll, 2007; Shoemaker & Bransby, 2010). It has very low water and fertilizer needs compared with sugarcane and corn. In addition, its abundant genetic resources have been poorly explored which offer outstanding potentials for biomass and sugar yield improvements and environmental adaptability (Stefaniak & Rooney, 2013). For example, corn originated from the tropics can now be grown up to 60° north latitude because of large genetic diversity and intensive breeding programs (Sood, Flint-Garcia, Willcox, & Holland, 2014).

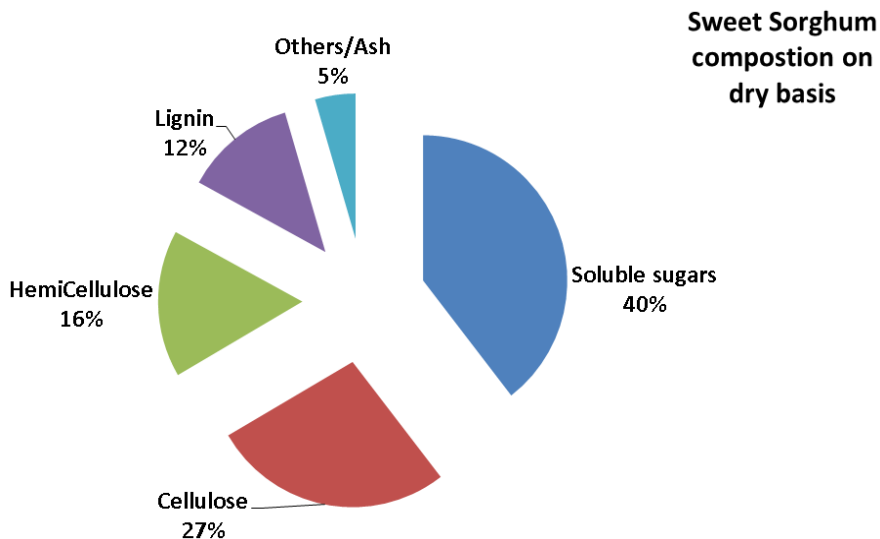


Figure 2. Representative sweet sorghum composition used in the model (Kim & Day, 2011).

4.2. Muconic Acid Co-Production Using Biosynthetic Pathways

- Muconic acid (MA), a dicarboxylic acid, is a platform chemical and a precursor for producing bio-plastics (Curran, Leavitt, Karim, & Alper, 2013). MA can be efficiently converted, via hydrogenation, into adipic acid, a chemical used to produce nylon-6,6 and polyurethanes (Curran et al., 2013). Muconic acid can also be converted, via Diels–Alder reaction with acetylene and oxidation, into terephthalic acid, which is one of the two primary constituents in the plastic polyethylene terephthalate (PET) (Curran et al., 2013). World production of adipic acid and terephthalic acid is over 2.8 and 71 million tonne, respectively (Curran et al., 2013). Currently, both of these chemicals are produced from petroleum and require the use of toxic intermediates, thus warranting a sustainable production platform. Current adipic acid production, from petroleum-derived chemicals, result in significant greenhouse gas emissions (NO_x) and bio-based approaches are highly desirable (Draths & Frost, 1994; Han et al., 2013; Niu, Draths, & Frost, 2002). Given the known production methods from MA to adipic acid and terephthalic acid, bio-derived MA enables the production of adipic acid and terephthalic acid from environmentally sustainable sources. In this study, we evaluated the economic

benefits of the MA co-production based on two biosynthetic pathways for the production of MA that are discussed below.

- *Sugars-to-MA biosynthetic pathway*: A traditional biosynthetic alternative is to produce MA from glucose. Known glucose-to-MA pathways, however, tend to suffer from low yields, e.g., the highest reported yields so-far are around 20-30 wt% (Xie, Liang, Huang, & Xu, 2014). The lower yields could be due to the low theoretical yield associated with glucose-to-MA pathways.
- *PCA-to-MA biosynthetic pathway*: One approach to improve the achievable yields in practice is by designing biosynthetic pathways with high theoretical yields. To accomplish this in our study, we take advantage of integrating plant engineering capabilities with novel biosynthetic pathways. For instance, aromatic molecules such as protocatechuate (PCA) is an intermediate precursor in many metabolic pathways. In particular, PCA is an intermediate in two of the three metabolic pathways used to produce muconic acid (Curran et al., 2013). Using plants to accumulate metabolic intermediates such as PCA allows for a reduction in the number of metabolic steps required to produce MA. PCA can be produced *in planta* directly from the aromatic amino acid pathway using a single enzyme (Eudes et al., 2014). Such pathways are also thermodynamically favorable, as they increase MA yield from sunlight (in contrast to pathways that start from glucose). Thus, plant engineering to accumulate and store PCA can potentially enable the utilization of PCA-to-MA pathways. Ensuring that the accumulated PCA can be easily extracted is key to realizing the potential of the PCA-to-MA pathway. Thus, choice of feedstock is critical. We chose sweet sorghum as our model feedstock in this study, as it offers the possibility of easy extraction of accumulated PCA, together with soluble sugars (e.g., sucrose), at no additional cost.

4.3. Base Case Scenario (S1)

To facilitate TEA, a biorefinery process model was built in commercially-available software, SuperPro Designer. To establish a basis, a base case model (S1) was constructed to represent an industrial scale facility capable of processing 1000 dry MT/day of sweet sorghum feedstock to produce ethanol from both the juice and bagasse (biomass stalk). A simplified representation of the modelled biorefinery is shown in Figure 3. The biorefinery has an on-site milling facility to extract juice (most of the soluble sugars) from sorghum. The bagasse is then pretreated (using dilute acid pretreatment technology (Humbird et al., 2011)) and hydrolyzed to produce fermentable sugars. In the base case (S1), both the soluble sugars from juice (mostly sucrose and glucose) and bagasse-derived-sugars (mostly glucose and xylose) were co-fermented to produce ethanol. Ethanol is then recovered from the fermentation broth (using distillation columns) and purified (using molecular sieve adsorption cycle) to industrial grade (~99.6 wt%). All process water is purified in a WWT section, consisting primarily of anaerobic and aerobic digesters, and subsequently recycled (or discharged). Solids residue from the distillation column bottoms (mostly lignin and unconverted glucan/xylan), together with biogas from anaerobic digester, is used as fuel in boiler to produce steam that is utilized in various processing steps. Excess steam is used to

drive a multi-stage turbine to produce electricity that can be used for processing needs. Excess electricity is sold to grid. In cases where steam production from on-site solids and biogas is not sufficient, supplementary natural gas is imported and combusted to meet steam demand in the biorefinery. All the main sections in the biorefinery (i.e., pretreatment, hydrolysis, co-fermentation, product recovery, wastewater treatment and co-generation) are modelled to represent mature technologies based on the National Renewable Energy Laboratory's (NREL) Nth plant assumptions (Humbird et al., 2011). The key process and economic data used to model the base case scenario are given in Table 1. Minimum ethanol selling price was used as a key economic performance indicator and was computed through a detailed cash flow analysis with 10% IRR.

Table 2. Key process and economic assumptions used in the TEA

Feedstock composition and price (Kim & Day, 2011)	
Soluble sugars (wt%, dry)	39%
Cellulose (wt%, dry)	27%
Hemicellulose (wt%, dry)	16%
Lignin (wt%, dry)	12%
Other/Ash (wt%, dry)	5%
Moisture content in the feedstock delivered (% total)	85%
Price of sweet sorghum (\$/dry ton, delivered at plant-gate)	120
Plant capacity (dry MT/day)	1000 ^a
Plant operation (days/year)	300 ^b
Milling	
Recovery of soluble sugars (and PCA)	95%
Pretreatment and hydrolysis (Humbird et al., 2011)	
Pretreatment technology	Dilute acid (DA)
Hydrolysis solids loading	
Hydrolysis enzyme loading (mg protein/g glucan)	20
Price of enzyme (\$/kg protein)	4.29 ^c
Glucan-to-glucose conversion	~93%
Xylan-to-xylose conversion	~92%
Fermentation	
Glucose/sucrose-to-ethanol conversion	95%
Xylose-to-ethanol conversion	85%
Plant construction period (years)	3
Start-up period (months)	3
Plant life-time for economic analysis (years)	30
Discount rate	10%

^a ~2 million wet MT/yr

^b Although SS is not perennial (growth/harvest season is typically 4 months in a year), given the possibilities to integrate with other crops, the plant is assumed to operate throughout the year except for planned shutdown for maintenance⁵.

^c (Humbird et al., 2011).

⁵ It should also be emphasized that the main purpose of this TEA is to understand any economic merit of co-production of MA and EtOH compared to a scenario with only EtOH production -- but not to evaluate economic potential of sweet sorghum or to compare sweet sorghum with other feedstocks. Therefore, the annual operational time is somewhat secondary.

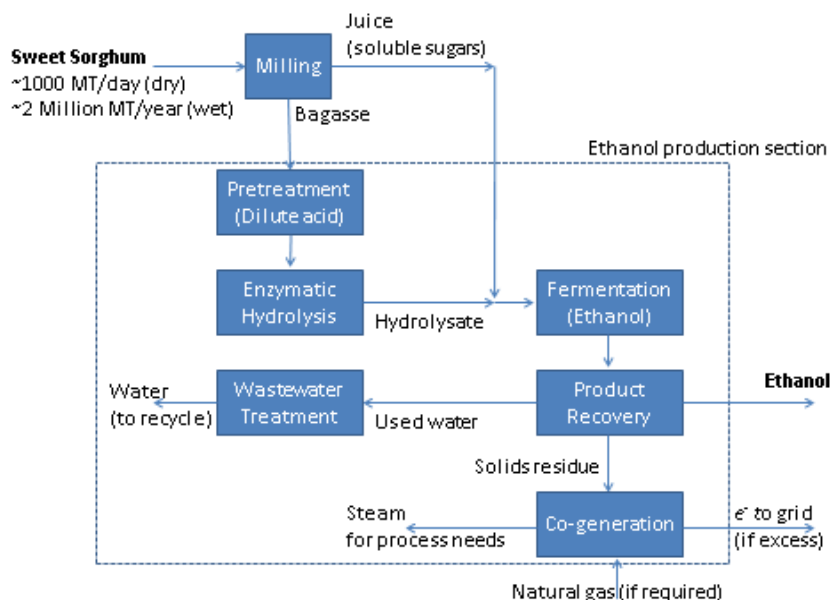


Figure 3. Simplified block flow diagram of the biorefinery modeled in the base case scenario S1 (the dotted rectangle represents the ethanol production section -- that encompasses several sub-sections including pretreatment, hydrolysis and fermentation – utilizing both the soluble sugars and bagasse fractions to produce ethanol).

4.4. Multiple Scenarios Studied

In contrast to the base case discussed in the previous section, where the only products were ethanol and excess electricity, we constructed additional scenarios in which MA is co-produced alongside ethanol (Figure 4 and Table 2). These scenarios serve as basis for an initial investigation of the economic feasibility of both MA production pathways discussed earlier (i.e., sugars-to-MA and PCA-to-MA). In addition to the base case (S1), four S2 scenarios (with sugars-to-MA pathway), four S3 scenarios (with PCA-to-MA pathway is superimposed on ‘current’ sugars-to-MA pathway), and four S4 scenarios (wherein PCA-to-MA pathway is superimposed on ‘projected’ sugars-to-MA pathway) were considered. In all these scenarios, as shown in Figure 4, a parallel fermentation line was assumed to co-produce MA from soluble sugars (i.e., S2 scenarios), PCA and soluble sugars (i.e., S3 and S4 scenarios). Compared to the ethanol-only scenario (S1, Figure 3), the MA co-production scenarios (S2, S3 and S4) require an additional parallel fermentation train to convert soluble sugars and, if available, PCA to muconic acid (MA). Muconic acid (MA) is produced in an aerobic fermenter. Aeration is electricity-intensive, with an estimated electricity requirement for aeration (and agitation) in the fermenter of 7 kW/m³ (Clark & Blanch, 1997). Since the MA is subsequently utilized to produce adipic acid (AA), MA recovery/purification may not be required, although this depends on the AA production method employed (Niu et al., 2002; Vardon et al., 2015). For the purposes of this preliminary TEA, it was assumed that further recovery/purification of MA from fermentation broth is not necessary. Due to the structural differences amongst all these scenarios, they span a wide range in terms of the yield of primary products (i.e., ethanol and MA) as shown in Table 3.

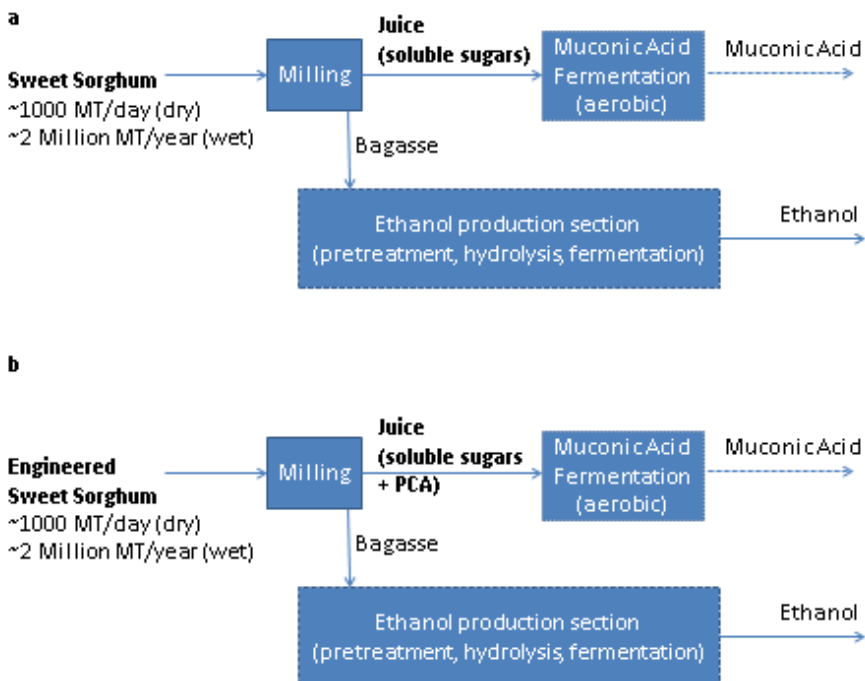


Figure 4. a) Co-production of muconic acid (MA) from soluble sugars fraction in a parallel fermentation section (while bagasse fraction is still utilized to produce ethanol); this configuration represents S2 scenarios. b) Co-production of muconic acid (MA) from soluble sugars and PCA derived from engineered sweet sorghum in a parallel fermentation train (while the bagasse fraction is still used to produce ethanol); this configuration represents S3 and S4 scenarios.

In total, we evaluated 13 scenarios: S1, S2 (a, b, c, d), S3 (a, b, c, d), and S4 (a, b, c, d). The general descriptions of S1, S2, S3, and S4 scenarios are as follows:

- S1 scenario: This is the base-case scenario where only ethanol is produced from the juice and bagasse.
- S2 scenarios: In the S2 scenarios, the soluble sugars in the extracted juice are fermented to produce MA using the known pathway. As in the S1 scenario, the bagasse is converted to ethanol. S2 sub-scenarios (a, b, c, d) are constructed to understand the impact of MA yield and price on MESP.
- S3 scenarios: The S3 scenarios (a, b, c, d) make use of a novel PCA-to-MA pathway with 75 wt% yield. It was assumed that the PCA was incorporated into the feedstock by replacing respective portion of soluble sugars. The remaining soluble sugars were assumed to be co-fermented to MA using the ‘current’ sugars-to-MA pathway employed in S2 (i.e., with 20% yield). The bagasse is converted to ethanol. The S3 sub-scenarios (a, b, c, d) are constructed to understand impact of PCA content and MA price on MESP.
- S4 scenarios: The S4 scenarios are designed to elucidate the cumulative benefits of advances in S2 and S3. Subsequently, as shown in Table 3, the ‘projected’ S2 scenarios (i.e., sugars-to-MA pathway with 50% yield) were superimposed on S3 (a, b, c, d) scenarios to generate respective S4(a, b, c, d) scenarios.

In scenarios that include the co-production of MA (S2, S3, and S4), the MA price is assumed to be fixed at the current estimated market price and the price of ethanol (i.e., MESP) is computed. This analysis allows us to compare all of the scenarios based on the resulting MESP values. However, the price of MA is volatile because its use as a platform chemical for production of fibers and plastics means that it is affected by fluctuations in oil prices. Thus, the muconic acid price is estimated to span a range of \$1000-1500/MT for the purposes of this study (i.e., scenarios suffixed with ‘a’ and ‘c’ considered a MA price of \$1000/MT, and scenarios suffixed with ‘b’ & ‘d’ considered a MA price of \$1500/MT).

Table 3. Scenarios studied in the TEA

Scenario		Description	EtOH yield (Mgal/yr) ^b	MA yield (MT/yr) ^c
S1: EtOH only	S1	Base case	39	0
S2: Sugars-to-MA pathway	S2a current	Low yield (20 wt%) and low price (\$1000/MT of MA)	21	22,500
	S2b current	Low yield (20 wt%) and high price (\$1500/MT of MA)	21	22,500
	S2c projected	High yield (50 wt%) and low price (\$1000/MT of MA)	21	55,800
	S2d projected	High yield (50 wt%) and high price (\$1500/MT of MA)	21	55,800
S3 ^a : PCA-to-MA pathway (75 wt% yield)	S3a	5 wt% (dry) PCA and low price (\$1000/MT of MA)	21	30,900
	S3b	5 wt% (dry) PCA and high price (\$1500/MT of MA)	21	30,900
	S3c	10 wt% (dry) PCA and low price (\$1000/MT of MA)	21	39,300
	S3d	10 wt% (dry) PCA and high price (\$1500/MT of MA)	21	39,300
S4: Cumulative S2 and S3 scenarios	S4a	S2 projected (S2c) + S3a	21	60,000
	S4b	S2 projected (S2d) + S3b	21	60,000
	S4c	S2 projected (S2c) + S3c	21	63,900
	S4d	S2 projected (S2d) + S3d	21	63,900

^a S3(a,b,c,d) are realized by assuming that PCA enhancement was possible by replacing soluble sugars and the remaining soluble sugars were converted to MA using the ‘current’ sugars-to-MA pathway (i.e., 20% yield) that is used in S2 scenarios.

^b Million gallon/year.

^c Metric tonne/year.

4.5. RESULTS AND DISCUSSION

In the basecase scenario (S1), the net operating cost was approximately \$65 Million and, as shown in Figure 5, the operating expenses are primarily driven by the feedstock costs indicating the importance of scenarios with the effective utilization of feedstock. In the Basecase (S1), the estimated MESP was ~\$3.4/gal.

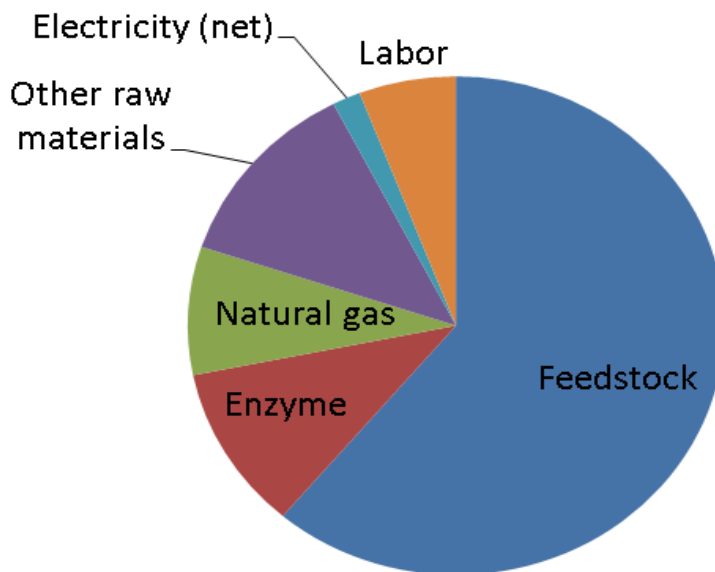


Figure 5. Cost-breakdown of operating expenses in the basecase scenario (S1).

The estimated MESP values for all the scenarios described above are shown in Figure 6.

- *S2 Scenarios (sugars-to-MA pathway)*: Comparing S2(a, b, c, d) with S1, it is clear that diverting all the soluble sugars in the juice to produce MA (instead of ethanol) is not economically viable, regardless of the price of MA. Given the low yield (20%) of current sugars-to-MA pathway, S2(a,b) scenarios are particularly expensive (with MESP >\$5/gal). Though S2(c, d) are relatively more economical (compared to S2(a, b)), due to higher yields (50% vs 20%), they remain more expensive compared to the basecase S1, mainly due to the significant energy requirement in the aerobic fermenters for the production of MA.
- *S3 Scenarios (PCA-to-MA pathway)*: Similar to the S2 scenarios, all the S3 scenarios suffered from the significant energy required in the aerobic fermenters for the production of MA. Thus, all the S3 scenarios remain more expensive than the basecase S1, calling for even more efficient pathways if MA co-production were to be economically feasible.
- *S4 Scenarios (combination of S2 'projected' and S3 scenarios)*: Maximizing MA production by combining the S3 scenarios (i.e., PCA-to-MA pathways) with the advanced/projected S2 scenarios (i.e., with high yield sugar-to-MA pathway) proves to be a more optimal strategy among the options evaluated. The respective MESP values are lowest in the S4 scenarios. With favorable market conditions (i.e., \$1500/MT of MA; as is the case in S4(b, d)), the co-production of MA could be economically favorable. In the best case scenario studied (i.e., S4d), this could translate to about 10% reduction in the MESP compared to the basecase S1.

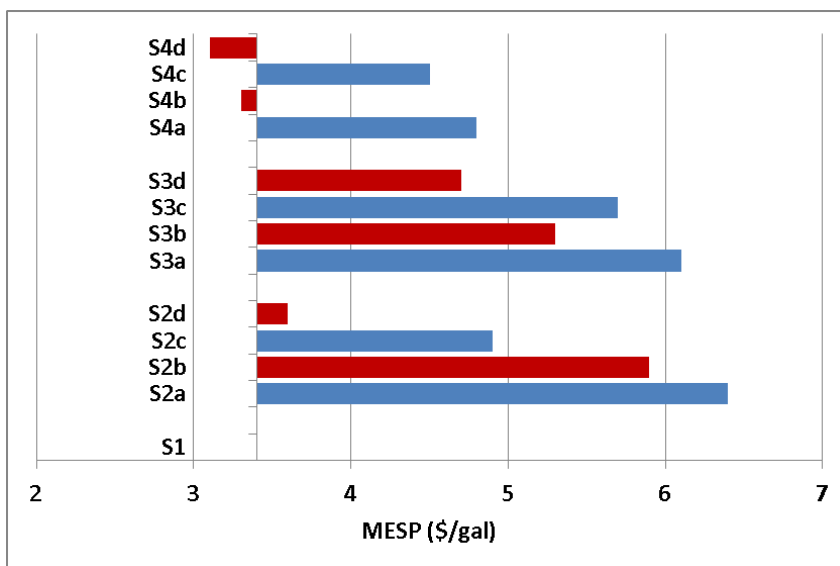


Figure 6. Estimated MESP values based on the preliminary TEA of the scenarios investigated in this study. The ‘blue’ and ‘red’ bars represent different market scenarios with regards to MA selling price (i.e., \$1000/MT and \$1500/MT, respectively).

Comparing the favorable market scenarios (i.e., S2(b, d), S3(b, d) and S4(b, d)) with the respective less favorable market scenarios (i.e., S2(a, c), S3(a, c), and S4(a, c)), it is evident that the value of the target molecule is key to significantly improving biorefinery economics – this emphasizes the importance of high value-added molecules in this context. Our preliminary results indicate that increasing PCA accumulation in the feedstock beyond the 5-10 wt% (dry) analyzed here could yield further reductions in MESP. However, it is important to note that excessive accumulation of secondary metabolites could cause serious toxicity damage that would be detrimental for plant productivity (Farré et al., 2014; Kristensen et al., 2005). While strategies exist to minimize this damage, further research to understand PCA accumulation potential in sweet sorghum is necessary. Furthermore, the aerobic nature of the MA production required significant amount of energy (~58 MW to facilitate aeration and agitation in MA production fermenters) thus making the MA co-production scenarios less favorable except in the best case scenarios studied (i.e., S4(b,d)). Nonetheless, the preliminary TEA presented in this study (based on MA co-production from engineered sweet sorghum) is successful in evaluating the relative economic merits of potential scenarios under consideration and in identifying the targets for important metrics such as yield.

CONCLUSION

Cellulosic biorefineries producing only biofuel as the major product are likely to face challenging economics. Co-production of chemicals (e.g., from sugars, lignin or extractable chemicals present in the feedstock) can help improving the overall process economics. To this end, as discussed in this chapter, tools such as TEA can be used to evaluate multiple pathways - involving different feedstocks, conversion technologies and/or products – to carry out comparative assessment of different pathways as well as to identify key cost bottlenecks in a

given pathway. Based on the specific TEA case-study presented (the co-production of muconic acid from engineered sweet sorghum), it was shown that the price -- and thus the market size -- of the co-produced chemical(s) is important to ensure the net impact of the co-production on the overall economics is favorable and significant. Continued R&D is necessary on this front to identify right chemicals that can enable the deployment of a large number of cellulosic biorefineries towards realizing a sustainable bioenergy industry.

ACKNOWLEDGMENTS

This work was part of the DOE Joint BioEnergy Institute (<http://www.jbei.org>) supported by the U. S. Department of Energy, Office of Science, Office of Biological and Environmental Research, through contract DE-AC02-05CH11231 between Lawrence Berkeley National Laboratory and the U. S. Department of Energy. The United States Government retains and the publisher, by accepting the article for publication, acknowledges that the United States Government retains a non-exclusive, paid-up, irrevocable, world-wide license to publish or reproduce the published form of this manuscript, or allow others to do so, for United States Government purposes.

REFERENCES

- Clark, D. S., & Blanch, H. W. (1997). *Biochemical engineering*: CRC Press.
- Curran, K. A., Leavitt, J. M., Karim, A. S., & Alper, H. S. (2013). Metabolic engineering of muconic acid production in *Saccharomyces cerevisiae*. *Metabolic Engineering*, *15*, 55-66.
- Davis, R., Tao, L., Tan, E., Bidy, M., Beckham, G., Scarlata, C., . . . Lukas, J. (2013). Process design and economics for the conversion of lignocellulosic biomass to hydrocarbons: Dilute-acid and enzymatic Deconstruction of biomass to sugars and biological conversion of Sugars to Hydrocarbons: National Renewable Energy Laboratory (NREL), Golden, CO.
- Demirbas, M. F. (2009). Biorefineries for biofuel upgrading: a critical review. *Applied Energy*, *86*, S151-S161.
- Draths, K. M., & Frost, J. W. (1994). Environmentally compatible synthesis of adipic acid from D-glucose. *Journal of the American Chemical Society*, *116*(1), 399-400. doi: 10.1021/ja00080a057.
- EIA. (2015). <https://www.eia.gov/tools/faqs/faq.cfm?id=23&t=10>.
- Ejeta, G., & Knoll, J. E. (2007). Marker-assisted selection in sorghum *Genomics-assisted crop improvement* (pp. 187-205): Springer.
- EPA. Program Overview for Renewable Fuel Standard Program.
- EPA. (2015). <http://www.epa.gov/fuels-registration-reporting-and-compliance-help/2015-renewable-fuel-standard-data>].
- Eudes, A., Sathitsuksanoh, N., Baidoo, E. E. K., George, A., Liang, Y., Yang, F., . . . Loque, D. (2015). Expression of a bacterial 3-dehydroshikimate dehydratase reduces lignin content and improves biomass saccharification efficiency. *Plant Biotechnology Journal*,

- 13(9), 1241-1250. Farré, G., Blancquaert, D., Capell, T., Van Der Straeten, D., Christou, P., & Zhu, C. (2014). Engineering complex metabolic pathways in plants. *Annual Review Of Plant Biology*, 65, 187-223.
- Han, L., Chen, W., Yuan, F., Zhang, Y., Wang, Q., & Ma, Y. (2013). [Biosynthesis of adipic acid]. *Sheng wu gong cheng xue bao= Chinese journal of biotechnology*, 29(10), 1374-1385.
- Humbird, D., Davis, R., Tao, L., Kinchin, C., Hsu, D., David, D., & Aden, A. (2011). Process design and economics for biochemical conversion of lignocellulosic biomass to ethanol. *National Renewable Energy Technology*, 275-3000.
- Kim, M., & Day, D. F. (2011). Composition of sugar cane, energy cane, and sweet sorghum suitable for ethanol production at Louisiana sugar mills. *Journal Of Industrial Microbiology & Biotechnology*, 38(7), 803-807.
- Klein-Marcuschamer, D., Oleskiewicz-Popiel, P., Simmons, B. A., & Blanch, H. W. (2010). Technoeconomic analysis of biofuels: A wiki-based platform for lignocellulosic biorefineries. *Biomass and Bioenergy*, 34(12), 1914-1921. doi: <http://dx.doi.org/10.1016/j.biombioe.2010.07.033>.
- Konda, N., Papa, G., Kirby, J., Keasling, J., Peter, G., Simmons, B. A., & Klein-Marcuschamer, D. (2015). *Integrated biorefinery for the production of biofuels and terpenes from loblolly pine: A technoeconomic assessment*. Paper presented at the 37th Symposium on Biotechnology for Fuels and Chemicals.
- Konda, N. M., Shi, J., Singh, S., Blanch, H. W., Simmons, B. A., & Klein-Marcuschamer, D. (2014). Understanding cost drivers and economic potential of two variants of ionic liquid pretreatment for cellulosic biofuel production. *Biotechnology for biofuels*, 7(1), 86.
- Konda, N. M., Singh, S., Simmons, B. A., & Klein-Marcuschamer, D. (2015). An Investigation on the Economic Feasibility of Macroalgae as a Potential Feedstock for Biorefineries. *Bioenergy Research*, 1-11.
- Kristensen, C., Morant, M., Olsen, C. E., Ekstrøm, C. T., Galbraith, D. W., Møller, B. L., & Bak, S. (2005). Metabolic engineering of dhurrin in transgenic Arabidopsis plants with marginal inadvertent effects on the metabolome and transcriptome. *Proceedings of the National Academy of Sciences of the United States of America*, 102(5), 1779-1784.
- Liu, G., Zhang, J., & Bao, J. (2016). Cost evaluation of cellulase enzyme for industrial-scale cellulosic ethanol production based on rigorous Aspen Plus modeling. *Bioprocess And Biosystems Engineering*, 39(1), 133-140.
- Niu, W., Draths, K., & Frost, J. (2002). Benzene-Free Synthesis of Adipic Acid. *Biotechnology Progress*, 18(2), 201-211.
- Perlack, R. D., Eaton, L. M., Turhollow Jr, A. F., Langholtz, M. H., Brandt, C. C., Downing, M. E., . . . Shamey, A. M. (2011). US billion-ton update: biomass supply for a bioenergy and bioproducts industry.
- Regassa, T. H., & Wortmann, C. S. (2014). Sweet sorghum as a bioenergy crop: Literature review. *Biomass and Bioenergy*, 64, 348-355.
- Shoemaker, C. E., & Bransby, D. I. (2010). *The role of sorghum as a bioenergy feedstock*. Paper presented at the Sustainable alternative fuel feedstock opportunities, challenges and roadmaps for six US regions, Proceedings of the Sustainable Feedstocks for Advance Biofuels Workshop, Atlanta, GA.

- Sood, S., Flint-Garcia, S., Willcox, M. C., & Holland, J. B. (2014). Mining natural variation for maize improvement: Selection on phenotypes and genes *Genomics of Plant Genetic Resources* (pp. 615-649): Springer.
- Stefaniak, T., & Rooney, W. (2013). Breeding sorghum as a bioenergy crop. *Bioenergy Feedstocks: Breeding and Genetics*, 83-116.
- Vardon, D. R., Franden, M. A., Johnson, C. W., Karp, E. M., Guarnieri, M. T., Linger, J. G., Beckham, G. T. (2015). Adipic acid production from lignin. *Energy & Environmental Science*, 8(2), 617-628.
- Werpy, T., Petersen, G., Aden, A., Bozell, J., Holladay, J., White, J., Jones, S. (2004). Top Value Added Chemicals From Biomass. Volume 1-Results of Screening for Potential Candidates From Sugars and Synthesis Gas: DTIC Document.
- Xie, N.-Z., Liang, H., Huang, R.-B., & Xu, P. (2014). Biotechnological production of muconic acid: current status and future prospects. *Biotechnology Advances*, 32(3), 615-622.

Chapter 11

ENVIRONMENTAL AND PERFORMANCE IMPACTS OF ALTERNATIVE FUELS IN TRANSPORTATION APPLICATIONS

Thomas D. Durbin, Georgios Karavalakis
and Kent C. Johnson*

College of Engineering - Center for Environmental Research and Technology,
University of California, Riverside, California, US

ABSTRACT

The market for renewable fuels for transportation applications has grown significantly in recent years due to governmental regulations at the local, regional, and national levels throughout the world. One of the most important requirements for expanding the use of alternative fuels in transportation applications is to understand how these fuels might impact vehicle performance and emissions, and to understand their compatibility with different vehicle/engine technologies. Some fuels such as ethanol and biodiesel have been extensively studied in this regard and are used widely in the current marketplace. Other fuels such as butanol, dimethyl ether (DME), and renewable diesel and jet fuel, or new potential fuels such as pentanol, dimethyl carbonate (DMC), 2,5-Dimethylfuran (DMF), and P-series fuels have either not been studied extensively or have not been extensively used in the transportation fuel marketplace.

The purpose of this chapter is to provide an overview of how the use of alternative fuels impacts the transportation sector, in terms of how the fuels are utilized and their emissions/performance impacts. This includes a brief introduction to how each of the fuels is commonly produced, a subsection on the unique characteristics of each fuel and how that impacts how the fuel is or could be utilized in motor vehicles, and finally a subsection on emissions, performance, and other potential environmental impacts of the different fuels. This chapter includes ethanol and biodiesel, other alcohols and ethers, such as butanol, methanol, pentanol, and DME, Fischer-Tropsch (F-T), gas-to-liquid (GTL), and renewable diesels, and some newer alternative fuel options, such as DMC,

* Corresponding author: durbin@cert.ucr.edu.

DMF, and P-series fuel. A list of fuel properties for the fuels covered in this chapter is provided in Table 1.

Keywords: engine, fuels, renewable, combustion, emission, ethanol, butanol, biodiesel

ETHANOL AS A TRANSPORTATION FUEL

Ethanol is the most widely used renewable fuel in the United States. Ethanol is produced from starch- or sugar-based feedstocks, with corn being the predominant source in the US. Ethanol production in the US has expanded considerably over the past decade due in part to production incentives from federal and state governments. The U.S. production capacity expanded from 3.64 billion gallons to 15.08 billion gallons from January 2005 through January 2015, which is about a 300% increase (RFA, 2015a). The main drivers of increased ethanol use at the national level is the US Energy and Security Independence Act (U.S. DOE, 2007), which established the Renewable Fuel Standard (RFS). This legislation had mandated production of 36.0 billion gallons of renewable fuel by 2022, with requirements that emphasized the development of cellulosic ethanol. More recent EPA action has reduced the interim targets for ethanol use based on limitations on the use of ethanol in vehicles and on the production of cellulosic ethanol.

Ethanol Production

Ethanol produced via fermentation is currently the most widely used biofuel in the world including the US. Ethanol is primarily made from feedstock crops such as corn, barley and sugarcane, all which contain significant amounts of sugar or starches that can be converted into sugar. Starch molecules are made up of long chains of glucose groups that can be broken up into simple glucose molecules. Starchy materials require a reaction of starch with water (hydrolysis) to break down the starch into fermentable sugars (saccharification). Typically, hydrolysis is performed by mixing the starch with water to form a slurry which is then stirred and heated to rupture the cell walls. Specific enzymes that will break the chemical bonds are added at various times during the heating cycle.

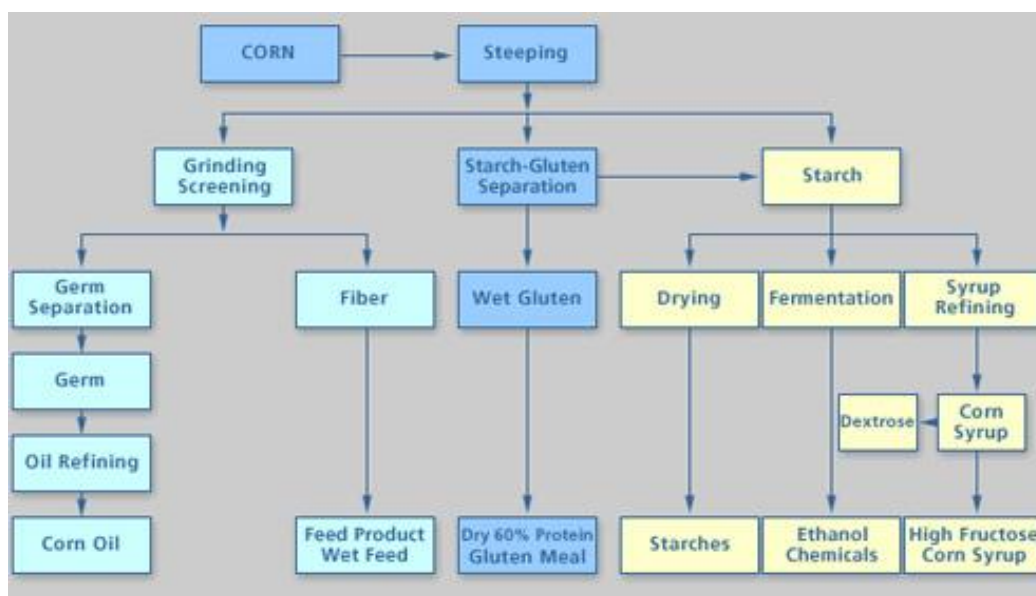
Conventional Ethanol production from corn and sugarcane technologies is a mature process that is widely used both in the U.S. and elsewhere. There are two predominant types of processes currently employed in the United States for corn-based ethanol production: wet mill processes and dry mill processes. Schematics for wet mill and dry mill processes are provided in Figures 1 and 2, respectively. In the wet mill process, the corn kernels are first “steeped” by soaking in a mixture of water and H_2SO_2 and then separated into their basic components, i.e., starch, protein, germ, and fiber. These components are then processed to produce corn oil, corn gluten, corn syrups, and ethanol.

Table 1. Table of Fuel Properties

	Gasoline	Methanol	Ethanol	t-Butanol	DMF	Diesel	Biodiesel	F-T Diesel	HVO Diesel	DMF	DME	DMC
Chemical Formula	C ₄ -C ₁₂	CH ₄ O	C ₂ H ₆ O	C ₄ H ₁₀ O	C ₆ H ₈ O	C ₃ -C ₂₅	C ₁₉ H ₃₆ O ₂		C ₁₆ H ₃₂	C ₃ H ₈ O ₂	C ₂ H ₆ O	C ₃ H ₆ O ₃
Molecular weight (g/mol)	100-105	32	46	74	96	200	296		224	76	46	90
Density at (g/cm ³)	0.71-0.77	0.79	0.79	0.81	0.89	0.848	0.878	0.7838	0.778	0.85	0.688	1.07
Cetane Number						40-50	47-51	>74	80-99	30	55-60	35
Octane Number (RON)	91-92	108.7	108.6	103	101.3							
Octane Number (MON)	82-83	88.6	89.7	91	88.1							
Octane Number (AKI)	87	98.65	99.15	97	94.7							
Kinematic viscosity (mm ² /s)	0.37-0.44	0.64	1.52	3.64	0.73	2.77	1.9-4.1	3.276	3.087	0.3642	0.185	0.63
Latent heat of vaporization (kJ/kg)	350	1104	841	585	332	250	236-245			318.6	410	369
Lower heat value (MJ/kg)	43.2-44.4	19.9	26.9	34.4	33.7	45.4	37.53	43.9	43.64	23.4	28.88	13.5
Carbon content (% by weight)	85-88	37.5	52.2	64.9	49.3	87	77	85.6	85.3	47.4	52.1	40
Oxygen content (% by weight)	0	50	34.7	21.6	21.9	0	11	15.4	0	42.1	34.8	53.33
Boiling point (°C)	27-225	64.7	78.37	117.4	92	180-360	315-350	150-350	313	43	-24	90.9

Dry mill technology is the most prevalent production process for ethanol production, due to its lower capital costs, and represents more than 80% of the ethanol plants in the U.S. (U.S. DOE, 2015a). The dry mill process produces just two main coproducts, ethanol and distiller co-products. The dry mill process begins by grinding the entire corn kernel into flour. The flour is combined with water and processed with enzymes to convert the starch into fermentable sugars (saccharification). Yeast is added to convert the sugars into ethanol and other alcohols (fermentation). Following distillation, the pure ethanol stream is denatured with a small amount of gasoline or other chemicals for tax purposes and to deter human consumption.

One of the limitations of conventional ethanol production is that it makes use of land and crops that could be otherwise be used for human or animal food consumption, so there is a limit to the extent at which starch or sugar-based ethanol production can expand. One bushel of corn produces approximately 2.8 gallons of ethanol and 18 pounds of distillers dried grains with solubles (DDGS) that can be used as animal feed. For 2013, about 40% of the U.S. corn crop went to ethanol production, representing about 10% of gasoline used in the country on a volumetric basis.

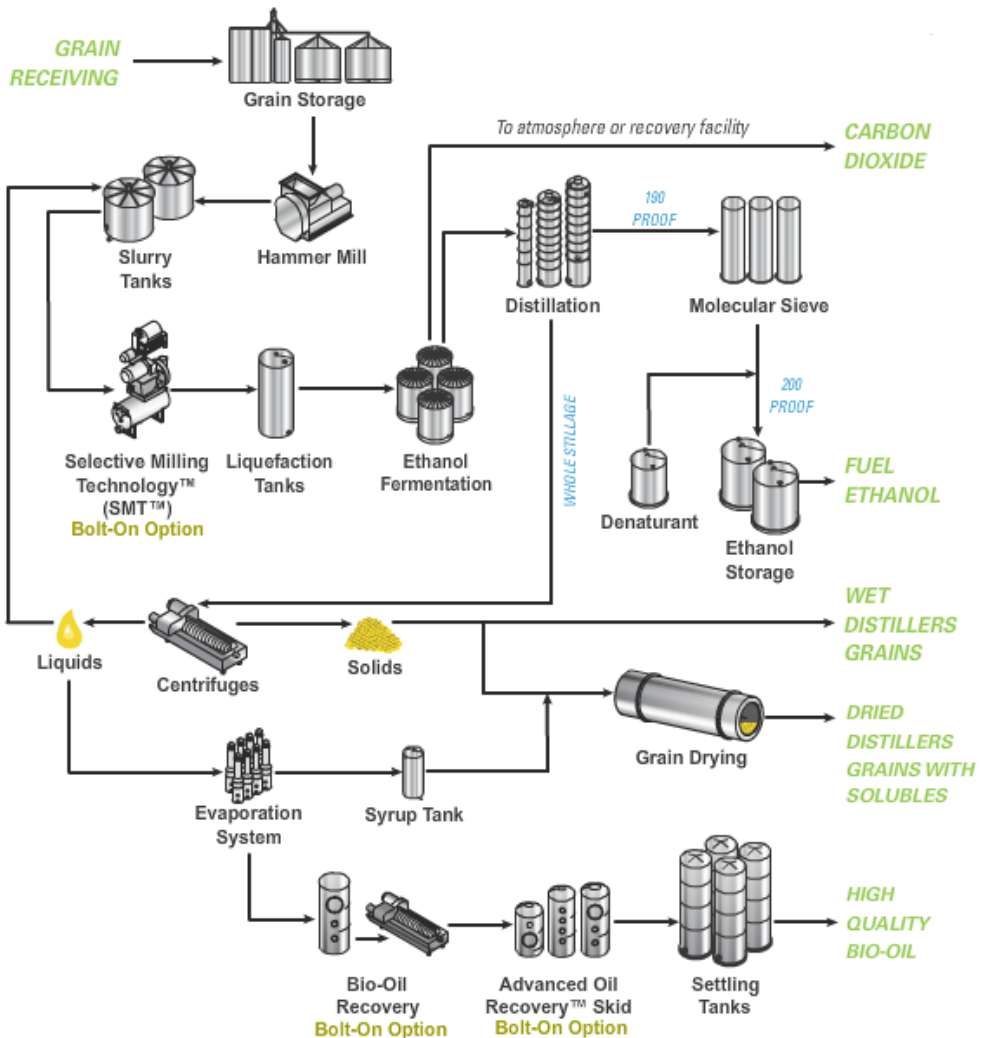


Source: Renewable Fuels Association, 2015b.

Figure 1. Wet Mill Ethanol Process Schematic.

Processes also exist to produce ethanol from cellulosic feedstocks, which are the fibrous and generally inedible portions of plant material, such as woody biomass and agricultural residues like corn stover and wheat straw. There is still significant research ongoing to work to achieve lower costs and higher yields with these processes. Although the production levels of cellulosic ethanol have fallen short of the initial expectations, a number of cellulosic ethanol plants have come on line in the last several years. This includes a production facility from Ineos, a chemical company based in Switzerland, in Vero Beach, Florida; a commercial plant in Edmonton from Enerkem, a Canadian waste to energy company; a commercial plant in Emmetsburg, Iowa from POET, one of the world's largest ethanol producers; and a

commercial plant in Hugoton, Kansas from Abengoa, a Spanish based company. Other commercial cellulosic ethanol plants around the world include a plant in Crescentino, Italy from Beta Renewables and a plant in Alagoas, Brazil from GranBio.



Source: ICM, Inc. (www.icminc.com).

Figure 2. Dry Mill Ethanol Process Schematic.

Utilization of Ethanol as a Transportation Fuel

Ethanol has some important characteristics that impact its use as a transportation fuel. Ethanol has a higher octane rating than gasoline, and as such provides a relatively cheap blendstock for improving octane number. This allows petroleum refiners to utilize a lower octane rating base gasoline while still meeting octane requirements at the pump. The use of domestic ethanol as a transportation fuel has also previously been supported by tax credits and tariffs. A \$0.54 per gallon tariff was placed on imported ethanol in the 1980s, primarily to

reduce the import of Brazilian sugarcane ethanol. In 2004, a tax credit was also put in place for blenders for each gallon of ethanol that was mixed with gasoline. Both the tariff and tax credit were not extended by the U.S. Congress as of the end of 2011, so these incentives no longer have an impact on the fuels market.

The use of ethanol in vehicles is limited by its compatibility with conventional vehicle technology. Currently, the use of ethanol in conventional gasoline vehicles is limited to 10-15% by regulatory limits and potential impacts on vehicle operation and durability. Although the U.S. EPA has extended the blend limit for 2001 and newer model vehicles has been extended from 10 to 15% based on an extensive series of studies (U.S. EPA, 2011; McCormick, Yanowitz, Ratcliff, & Zigler, 2013; Hochhauser & Schleyer, 2014), the continued restriction of the use of ethanol blends greater than 10% for vehicles older than 2001 will make it difficult to implement E15 on a retail level. In particular, as of the end of 2014, only 65% of the registered gasoline vehicles are 2001 and newer (Polk, 2014). For this reason, a national average of 10% ethanol is considered to be the “blend wall,” above which is it hard to expand ethanol use in the marketplace. Higher level blends, up to E85, can only be utilized in specially designed flexible fuel vehicles (FFVs). Currently, there are more than 17.4 million FFVs on the road in the U.S. (U.S. DOE, 2014).

While ethanol is already used extensively in blending with gasoline, there are a number of issues with the utilization of ethanol within the traditional petroleum infrastructure and with conventional gasoline vehicles. Ethanol is not shipped by pipeline due to ethanol’s special chemical properties. First, ethanol has material incompatibility issues with current existing petroleum pipelines, which will corrode and crack with long time ethanol exposure. Second, ethanol is extremely soluble in water, and thus it will dissolve any water it comes in contact with in the pipeline distribution system. If gasoline/ethanol blends are transported via pipelines, the ethanol can be removed from the gasoline/ethanol blend by dissolving in the water in the pipeline distribution system. The number of gasoline fuel stations that provide higher blend levels, up to E85, is very limited. For E15, a tremendous amount of work by refueling equipment manufacturers, industry groups, and federal agencies has resulted in a long list of equipment that can be used with E15 (Moriarity & Yanowitz, 2015). There are a number of obstacles to the expanded use of E15 in the marketplace, however, beside the compatibility with older vehicles. These include additional federal and state regulations and misfueling liability. E15 also has a similar vapor pressure to E10, but does not receive the same 1 pound per square inch (psi) EPA waiver on increased Reid Vapor Pressure that E10 does during the summer, making E15 less favorable to produce compared to E10 (Moriarity & Yanowitz, 2015). Similar to E10, E15 also has a lower energy density than gasoline and can not practically be used in a traditional pipeline system.

State of Minnesota and the Renewable Fuels Association (RFA) conducted a yearlong feasibility study of E20 as a motor fuel to study the effects and performance of E20 on engines and engine components, drivability, and material compatibility (Mankato, 2009; Mead, Jones, Stevens, Hanson, & Harrenstein, 2009; Jones et al., 2008a, 2008b, 2008c; Kittelson, Tan, Zarling, & Evans, 2007). These studies were done in response to a 2005 state legislative bill requiring that the state’s total consumption of gasoline fuel should include at least 20 percent ethanol by 2013. For the durability study, 40 pairs of 2000 to 2006 vehicles were evaluated over a one calendar year road test by the University of Minnesota (Kittelson, et al., 2007). The results showed that E20 provided similar power and performance compared to E10, including for fuel economy. More controlled drivability tests under cold start, warm

up, and hot fuel drivability conditions did not show statistically significant drivability issues for ethanol blends from E10 to E20 (CRC 2004, 2007, 2008, 2010, 2011a). Minnesota State University also conducted some associated material compatibility studies with E20, E10 and E0 on plastics, metals, and elastomers in gasoline vehicles. The results showed greater impacts with ethanol blends than gasoline, but that the ethanol blends were generally compatible with most materials (Jones et al., 2008a, 2008b, 2008c). The materials that were found to be incompatible included one of 19 metals and 3 of 8 plastics that were not commonly found in vehicles. Minnesota State University also evaluated the impacts of E10 and E20 on fuel pumps and sending units over a 4000-hour durability period, and did not find any significant differences between the different fuels (Mead et al., 2009). Studies of fuel pumps and senders by CRC did find some failure of fuel pumps for E15 compared to E10 and E0 and some problems with fuel level senders with E15 (CRC, 2011b, 2013), although McCormick et al. (2013) noted that these studies did not reach statistically significant conclusions and could be misleading.

Several studies by the National Renewable Energy Laboratory (NREL) (Knoll et al., 2009), The Transportation Research Center Inc. (TRC, 2009; West, Sluder, Knoll, Orban, & Feng, 2012), and the Orbital Engine Company in Australia (2004) were conducted to evaluate the potential impact of ethanol use on the durability of emission control systems. While most modern vehicles use an oxygen sensor in a closed loop configuration to maintain stoichiometric air-fuel mixture and thus adjust for alcohol content, one observation from these studies is that some vehicles do not adjust open-loop fueling to compensate for ethanol in the fuel, while others use learned fuel trim (LFT) to correct open loop air-fuel ratios with ethanol blends. For the vehicles without LFT, ethanol fuel blends will be leaner under open loop conditions, resulting in higher catalyst temperatures that could damage the catalyst. Both CRC and DOE conducted screening tests to identify the types of vehicles that use or don't use LFT (Knoll et al., 2009; TRC, 2009). DOE subsequently conducted a long term durability test on 2000-2009 vehicles, including vehicles with and without LFT (West et al., 2012). This study did not find any impact for ethanol blends up to E20 on catalyst durability and emissions, and was part of the basis for EPA decision that E15 would not contribute to Tier 2 motor vehicles exceeding their emission standards over their fuel useful life.

An important limitation with ethanol blends is the low energy density of ethanol compared to gasoline, and the corresponding reduction in volumetric fuel economy associated with this. There is also the possibility of running neat ethanol or other alcohol fuels in port fuel injection (PFI) SI engines, which can provide benefits in higher efficiency and specific power and lower emissions, but also has some challenges. Several technology developers and manufacturers such as AVL Powertrain, Ricardo, MAHLE Powertrain, Sturman Industries, John Deere, Nissan, HP2G, AHL-TECH, and MCE-5 have worked to develop engine technology to permit optimized operation on ethanol, while still being able to run on gasoline.

It is also important to understand how on-board diagnostic (OBD) systems work and adapt with ethanol in aged production vehicles. One of the main concerns was whether vehicles operating near their lean-limit on E0 or E10 might experience an OBD malfunction if operated on E15 or E20, even if within design tolerances. This is the objective of the CRC E-90 program series (McClement & Austin, 2011; Shoffner & Whitney, 2013), as well as some testing by DOE (Sluder and West, 2012). Screening studies indicated that a small number of vehicle models (ranging from 1 to 4%) would have a greater tendency for malfunction indicator lamp (MIL) illuminations when the ethanol content of the fuel increased

(McClement & Austin, 2011). Laboratory testing indicated that the thresholds for MIL illumination were above E20 at warm temperatures, but could show greater sensitivity at lower temperatures (Shoffner & Whitney, 2013). The DOE suggested that this phenomenon would be even less prevalent in the in-use fleet, ranging from 0.1 to 0.2% (Sluder & West, 2012).

Researchers at ORNL (Kass et al., 2011, 2012a, 2012b, 2014a, 2014b, 2015a) and the University of California at Riverside (UCR) (Durbin et al., 2015a, 2015b) have also conducted studies of the potential impacts of ethanol blends on infrastructure materials. In these studies, elastomer, plastic, and metal materials used in various parts of the petroleum infrastructure were exposed to blends with varying percentages of ethanol along with contaminants that could potentially be found in the liquid fuel infrastructure system at varying levels based SAE J1681 protocols (Society of Automotive Engineers, 2000). These studies showed that the elastomer materials showed the most significant fuel impacts followed by the plastic materials, with the metals showing the smallest impacts. The elastomers and plastics generally increased in volume and mass immediately following the exposures, indicating the adsorption of the liquid fuels into the elastomer and plastic material. Following drying, the most elastomers shrank to volume/mass values below that of the original sample, indicating that the liquid fuel and some of the associated elastomer components were removed from the sample, while plastics retained some of this volume swell/mass gain after drying, indicating that the liquid fuel was retained in the plastic structure. The volume expansion of a given elastomer or plastic material upon exposure to a given fuel can be understood in terms of the mutual solubility between the material and the fluid or fuel, with materials and fuels having similar solubility parameters having a greater affinity for permeation and dissolution than those with dissimilar values. Kass and coworkers have performed a series of solubility potential calculations using a Flory-Huggins model with Hansen solubility parameters methodology (Hansen, 2007), which have shown that this is a good correlation between the calculated results and the experimental results (Kass et al., 2012a, 2012b, 2014a, 2014b). For elastomers and plastics, volume expansion for most materials in going from E0 to E85 generally showed a maximum around E10 to E25 and then decreased as ethanol concentration increased to E85 (Kass et al., 2012a, 2012b, 2015a). In general, these studies did not show high levels of metal corrosion for metals with ethanol blends (Kass et al., 2011, 2012a; Durbin et al., 2015a, 2015b).

Environmental Considerations with the Use of Ethanol as a Transportation Fuel

The impact of ethanol content on exhaust emissions has been one of the most extensively studied fuel properties over time. Extensive studies of ethanol emissions impacts were conducted in the early 1990s by the Coordinating Research Council (CRC) under the Auto/Oil Air Quality Improvement Research Program (AQIRP) and by the U.S. EPA (Hochhauser et al., 1991; Reuter et al., 1992; Knepper et al., 1993; Mayotte et al., 1994a, 1994b). This included studies of E10 and lower blends, as well as higher ethanol blends in flexible fuel vehicles (FFVs). These earlier studies generally found that ethanol blends of 10% or less tended to decrease HC and CO emissions while increasing acetaldehyde emissions, especially for older vehicles. There were also some trends in toxic emissions of

decreasing benzene emissions and increasing NO_x emissions with ethanol use, although these trends are less consistent over a wide range of studies (Hochhauser, 2008). These studies also showed consistent increases in acetaldehyde emissions and decreasing benzene emissions with increasing ethanol content. Trends of lower CO emissions were also seen in newer vehicles in a study by Durbin et al. (2006, 2007), although NMHC and toxic emissions showed more varied results with the fuel distillation properties. For E85, emissions trends found in these earlier studies included reductions in NMHCs, NO_x, CO, along with increases in formaldehyde and acetaldehyde (Yanowitz & McCormick, 2009a).

CRC, the Department of Energy (DOE) National Renewable Laboratory (NREL) and Oakridge National Laboratory (ORNL), and the U.S. EPA conducted an additional series of studies of ethanol exhaust emission impacts designed to better understand the impacts of intermediate ethanol blends (51% > x > 10%), as it was anticipated that higher ethanol blends would be needed to meet the RFS regulation. Crawford et al. (2009) evaluated E0, E10, and E20 blends for 1994 to 2006 vehicles at two temperatures. The results showed some similar trends to earlier studies with Emissions of HC and CO being decreased for E10 and E20 relative to E0, while NO_x emissions increased for E10 and E20. A DOE study of intermediate blends evaluated E0, E10, E15, and E20 in 1999-2007 vehicles (Knoll et al., 2009). This study showed reductions in CO and NMHC for E10, E15, and E20 relative to E0, increases in acetaldehyde emissions with increasing ethanol, and no statistically significant NO_x effects. The EPA/DOE/CEC EPAct study (U.S. EPA, 2013a, 2013b) included one of the most comprehensive fuel matrices for emissions studies on modern vehicles, with testing conducted on a fleet of 2008 model year vehicles with 27 fuel test matrix, including fuels blended at E0, E10, E15, and E20 levels. The EPA developed a regression model based on the full fuel matrix to calculate the emissions changes for different fuel properties. The model showed that E10 and E15 generally decreased HC and CO and increased NO_x relative to E0.

The EPAct and subsequent studies by the U.S. EPA and others have also focused on the potential impacts of ethanol on PM mass emissions. Initial analysis of the EPAct data by the U.S. EPA (2013b) suggested increasing ethanol content, as well as increasing total aromatic content, T50, and T90, was associated with increasing PM mass emissions. Subsequent to the design and launch of the EPAct program, several other studies investigated further the formation of PM in gasoline engines. Honda introduced a model that is being more widely used that computes a PM Index (PMI) parameter that predicts the relative potential of a given gasoline formulation to produce PM (Aikawa, Sakuri, & Jetter, 2010). This method combines detailed compositional information about the fuel with the volatility and structural characteristics of its constituent compounds, and asserts that a small proportion of low-volatility hydrocarbons (especially aromatics) in gasoline are responsible for a large share of PM emissions. The index assigned to ethanol with this method is zero. In a further study by Anderson et al. (2014), these researchers suggested that the initial finding that increasing ethanol content leads to higher PM emissions could instead be due to the higher hydrocarbons that are added to fuels containing ethanol to match the T50 and T90 values with the fuels that do not contain ethanol. The U.S. EPA conducted subsequent studies to evaluate this issue in greater detail that suggested reinforcing interaction between the PM index and ethanol similar to that observed in the original EPAct study (Butler, Sobotowski, Hoffman, & Machiele, 2015; Sobotowski, Butler, & Guerra, 2015). They suggested that while ethanol may chemically suppress the formation of soot precursors, it may impede evaporation of the fuel

(through the impact of its high heat of vaporization), exacerbating heterogeneity of the cylinder charge and increasing PM emissions.

Several more recent studies have also included gasoline direct injection (GDI) model vehicles, which were not in production at the time of these earlier studies. GDI engines/vehicles provide improved fuel economy, so it is anticipated that these vehicles will become the predominant technology in the light-duty vehicle market in coming years as automobile manufacturers strive to meet increasing more stringent standards for CO₂ emissions. GDI engines can use either a wall-guided injection strategy, in which the fuel spray is directed from a side-mounted fuel injector towards a contoured piston and then deflected upward toward the spark plug, or a spray guided injection strategy, where the fuel injector and spark are in close proximity which confines the fuel spray such that it does not contact the cylinder walls, improving mixing and reducing soot formation and THC emissions. An important consideration for GDI vehicles, is that they typically produce more PM than more conventional gasoline technologies, particularly for wall-guided GDI engines. Karavalakis et al. (2015) evaluated the effects of different alcohol blends on a fleet of 9 2007-2014 vehicles, including five GDI vehicles and two FFVs. The test fuels included E10, E15, E51, E83, and Bu16 (a 16% butanol blends), Bu24, Bu32, and Bu55. The results showed some clear trends with increasing levels of alcohol in the blends for some pollutants, but not for others. There was a trend for lower CO, CO₂, PM mass, and particle number, and lower fuel economy with higher alcohol content fuels. For other pollutants, such as THC, NMHC, CH₄, and NO_x, there were not strong fuel trends, while some carbonyl species showed some trends towards higher emissions for higher alcohol blends. The U.S. EPA (Sobotowski et al., 2015) also conducted a study with four 2007-2009 vehicles, including one GDI vehicle, with fuels having varying PM indices and ethanol contents from 0 to 15%. The spray-guided GDI vehicle generally produced higher PM emissions than the PFI vehicles during operation on the lower-PM-Index fuels over the LA92 test cycle, but comparable PM emissions over the US06. Mamakos et al. (2013) and colleagues found large reductions in particle number and PM mass emissions from a Euro 5 GDI-FFV with the use of 75-85% ethanol/gasoline blends over the New European Driving Cycle (NEDC) and the Artemis cycles. Storey et al. (2010) analyzed the effect of E10 and E20 blends on a 2007 model year GDI vehicle and found that NO_x, CO, formaldehyde, and benzaldehyde emissions decreased with higher ethanol blends, while acetaldehyde emissions showed increases. They also showed decreased PM mass and particle number emissions with ethanol blends. Maricq et al. (2012) showed small benefits in PM mass and particle number emissions as the ethanol level in gasoline increased from 0 to 20% when they tested a GDI turbocharged vehicle with two engine calibrations over the Federal Test Procedure (FTP); while particle size was unaffected by ethanol level. Chen et al. (2012) investigated the effect of ethanol blending on the characteristics of PM and particle number emissions from a spray-guided GDI engine. They found increases in particulate emissions as the ethanol content increased. Clairotte et al. (2013) showed that a flex fuel vehicle fitted with a GDI engine reduced CO, CO₂, and NO_x emissions with higher ethanol blends. However, the same study showed higher emissions of THC, NMHC, formaldehyde, and acetaldehyde with increasing ethanol content.

Evaporative emissions are one of the more important environmental considerations for ethanol blends. Evaporative emissions are the result of ethanol and gasoline vapors escaping from the vehicle's fuel system, as opposed to tailpipe emissions. The sources of evaporative emissions from vehicles are fuel permeation, liquid and vapor leaks, and fuel tank venting

(canister losses) (Haskew, Liberty, & McClement, 2006), with tank venting and fuel permeation generally considered to be the most important sources. This is due to the formation of minimum-boiling azeotropes (by ethanol and some hydrocarbons in gasoline) whose boiling points are lower than either component. This increase in Reid Vapor Pressure (RVP) with gasoline-ethanol blends peaks at relatively low ethanol blend levels (5-10% ethanol), and decreases steadily for higher ethanol blends above this (Andersen, Anderson, Wallington, Mueller, & Nielsen, 2010).

A number of earlier studies have shown that low level-blends of ethanol increase evaporative emissions (CARB, 1999; CARB, 1998; Reuter et al., 1992). CRC carried out a series of studies to better understand evaporative emissions as a function of ethanol content, including vehicles designed to meet the newest and most stringent evaporative emissions standards. This included the CRC E-65 program (Haskew, Liberty, & McClement, 2004; Haskew et al., 2006), where only the evaporative control systems of the vehicles were tested, and the CRC E-77 (Haskew and Liberty, 2010a), E-77-2c (Haskew and Liberty, 2010b), and E-80 (Haskew and Liberty, 2011) studies where tests were conducted on full vehicles. These studies as a whole found that permeation emissions increase for low-level ethanol blends (i.e., E6, E10, and E20) compared to E0. It was also found that evaporative emissions as a whole decreased as the evaporative control systems became more advanced, with the most advanced systems showing the smallest increase due to ethanol in comparison with the older technology vehicles. In the CRC E-80 study, blends up to E85 were used, with the diurnal evaporative emissions (i.e., vapors emitted due during daily temperature variations) showing higher emissions for the E59 and E85 fuels, while running-loss evaporative emissions (i.e., vapors emitted while the vehicle is driving) and hot-soak evaporative emissions (i.e., vapors emitted after the vehicle is shut off, while the fuel system is still warm) did not show significant fuel trends.

Another important environmental consideration is the impact of ethanol use on greenhouse gas emissions (GHGs). Such assessments are generally done using a life-cycle analysis (LCA) technique that evaluates the GHG impacts of all stages of the of a fuels life from cradle to grave. This includes the extraction/growing of the raw material, its processing to a fuel, its distribution, and finally its use in a vehicle. The life cycle analyses impact of corn-based ethanol has been the subject of considerable debate over the years. In earlier research, some researchers, such as Fargione et al. (2008) and Searchinger et al. (2008), argued that ethanol use for fuel could have a negative impact on GHG emissions if native habitats are converted to support expanded growing of corn. The agro-economic models and associated databases used in some of these earlier studies have been further developed since these earlier studies to better predict the indirect land use change (ILUC) impacts for biofuels policy, and overall estimates of ILUC-induced GHG emissions have decreased (Broch, Hoekman, & Unnasch, 2013). More recent updates of the Greenhouse gases, Regulated Emissions, and Energy use in Transportation (GREET) model that was developed by the Argonne National Laboratory indicate GHG, indicate GHG benefits for ethanol for a wide range of feedstocks (Wang, Han, Dunn, Cai, & Elgowainy, 2012). Relative to petroleum diesel, Wang et al. (2012) found life-cycle GHGs for ethanol from corn in the U.S., sugarcane from Brazil for use in the U.S., corn stover via cellulosic production, switchgrass via cellulosic production, and miscanthus via cellulosic production to be reduced by 19-48%, 40-62%, 90-103%, 77-97%, and 101-115%, respectively. A summary of the environmental studies on ethanol as a transportation fuel are listed in the Table 2.

Table 2. References for Environmental Considerations with the Use of Ethanol as a Transportation Fuel

Author	Vehicle/Engine	Fuel	Notable Results
Aikawa et al., 2010	Gasoline engine	Indolene base fuel blended with various chemical species	1. A small proportion of low-volatility hydrocarbons (especially aromatics) in gasoline are responsible for a large share of PM emissions.
			2. High boiling point components with low double bond equivalent values displayed only a minor effect on PN.
			3. Low vapor pressure components correlated with high PN emissions.
Anderson et al., 2010		Alcohol-gasoline blends containing 5–85% by volume of methanol, ethanol, 1-propanol, 2-propanol, 1-butanol, 2-butanol, i-butanol (2-methyl-1-propanol), and t-butanol (2-methyl-2-propanol).	The increase in Reid Vapor Pressure (RVP) with gasoline-ethanol blends peaks at relatively low ethanol blend levels (5-10% ethanol), and decreases steadily for higher ethanol blends above this.
Anderson et al., 2014	Gasoline engine	Ethanol-gasoline blend	Increasing ethanol content leads to higher PM emissions possibly due to the higher hydrocarbons.
Butler et al., 2015	15 high-sales cars and light trucks from the 2008 model year	27 fuel test matrix, including fuels blended at E0, E10, E15, and E20 levels	1. Ethanol may chemically suppress the formation of soot precursors.
			2. Index fuel interacts in important ways with engine and vehicle design characteristics, calibrations, and control algorithms.
CARB, 1998;1999	12 light-duty vehicles	10 percent ethanol gasoline blend with 3.5 weight percent oxygen, a fully complying gasoline blended	A high RVP ethanol blend significantly increased overall emissions of NO _x , THC, NMOG, ozone forming potential, toxics, and potency weighted toxics, but decrease emissions of CO.
Chen et al., 2012	A single-cylinder optical access engine	Gasoline/ethanol blends in different blending proportions (E0, E10, E20, E50, E70, E85)	As the ethanol volumetric percentage increases, both the total PN and PM increased by a maximum of 16% and 11% for cold conditions and 7% and 8% for warm conditions.
Clairotte et al., 2013	A flex fuel vehicle fitted with a GDI engine	Gasoline/ethanol blends	1. CO, CO ₂ , and NO _x emissions decreased with higher ethanol blends.
			2. THC, NMHC, formaldehyde, and acetaldehyde decreased with increasing ethanol content.
Crawford et al., 2009	1994 to 2006 vehicles	E0, E10, and E20 blends	1. EPA MOBILE6.2 emission factor model currently overestimates CO emissions, underestimates the impact of increasing oxygenate content in reducing CO emissions, and overestimates the impact of increasing RVP in increasing CO emissions.
			2. Exhaust HC and CO decreased but NO _x increased for E10 and E20 relative to E0.

Author	Vehicle/Engine	Fuel	Notable Results
Durbin et al., 2006; 2007	12 2001-2003 light duty vehicles	12 gasoline with different ethanol content (0-10 vol %), T50 (195°F- 235°F), T90 (295°F-355°F) content	1. NMHC emissions increased with increasing ethanol content at the midpoint and high level of T90 but were unaffected at the low T90 level.
			2. CO emissions decreased as the ethanol content increased from the low to the midpoint level for all levels of T50, but between the 5.7 and 10% ethanol levels, CO showed only an increase for the high level of T50.
			3. NOx emissions increased with ethanol content for some conditions.
			4. Statistically significant interactions were found between ethanol and T90 for NMHC, ethanol, and T50 for CO and ethanol and T50 for NOx.
			5. Non-methane organic gases (NMOG) and toxic emissions were examined for only a subset of fuels with the highest T90 level, with NMOG, acetaldehyde, benzene, and 1-,3-butadiene all found to increase with increasing ethanol content.
Haskew, 2004;2006	10 1978-2001 model California vehicles	5 blend fuels includes: Non- oxygenated base fuel(E0), E6 – 5.7 Volume% ethanol fuel with 2 Weight% oxygen(E6), 5.7 Volume % ethanol fuel with increased aromatics content(E6Hi), 0 Volume% ethanol fuel(E10), 85 Volume% ethanol fuel(E85)	1. The low-level ethanol blends (E6, E6Hi and E10) showed increased permeation in all the vehicle systems and technologies tested, compared to the non-ethanol fuel (E0).
			2. The advanced technology LEV II and PZEV1 systems (2004 MY) had much lower permeation emissions than the MY 2000-2001 enhanced evaporative systems. The zero evaporative emissions system (PZEV) had the smallest increase due to ethanol of all the vehicles tested.
			3. The high-level ethanol blend (E85) tested in the flexible fuel vehicle system had lower permeation emissions than the non-ethanol (E0) fuel.
			4. Diurnal permeation rates do not appear to increase between E6 and E10.
			5. Diurnal permeation emissions were lower on all four rigs tested with the higher-level aromatics fuel (E6Hi) versus the lower aromatics fuel (E6).
			6. The average specific reactivities of permeates from the low-level ethanol blends were similar to one another and lower than those measured with the non-ethanol fuel (E0).
			7. The average permeation emissions with a 5.7 volume % ethanol gasoline were 1.40 grams/day higher than permeation emissions with the MTBE gasoline and 1.10 grams/day higher than permeation emissions with a non- oxygenated gasoline.
Haskew and Liberty, 2010a	8 1996-2004 model vehicles	5 gasoline fuel blends, including three levels of ethanol (0, 10, and 20 vol %)	1. Newer vehicle groups had lower emission levels.

Table 2. (Continued)

Author	Vehicle/Engine	Fuel	Notable Results
			2. Adding ethanol to the fuel increased permeation over the non-oxygenated levels.
			3. Increased volatility increased permeation levels on average, but produced mixed results on the individual vehicles.
Haskew and Liberty, 2010b	9 2000-2004 model vehicles	E20	1. Newer Tier 2 vehicles had lower permeation than Tier 1 vehicles on all fuels.
			2. Permeation is higher with E10 or E20 compared to an ethanol-free (E0) fuel.
Haskew and Liberty, 2011	8 2006-2007 model FFVs	Fuel blends of E6, E85 and intermediate blends of the two	1. Permeation emissions increase for low-level ethanol blends (i.e., E6, E10, and E20) compared to E0.
			2. Evaporative emissions as a whole decreased as the evaporative control systems became more advanced, with the most advanced systems showing the smallest increase due to ethanol in comparison with the older technology vehicles.
			3. Diurnal evaporative emissions showed higher emissions for the E59 and E85 fuels, while running-loss evaporative emissions and hot-soak evaporative emissions did not show significant fuel effects.
Hochhauser et al., 1991	14 1983-1989 vehicles	18 gasoline with different aromatic, olefin content, and MTBE blend in T90	1. HC and CO decreased by adding MTBE.
			2. NOx decreased and HC increased by adding olefins.
			3. Increased HC and decreased NOx in older vehicles, decreased HC and increased NOx in newer vehicles by reducing aromatics.
Hochhauser, 2008	Conventional vehicles	Gasoline with different ethanol content (>10%)	Summary of research on the use of intermediate ethanol blends in on-road vehicles including drivability, evaporative emissions, exhaust emissions, OBD, catalyst durability, materials compatibility, fuel system components, engine durability, and evaporative emissions control system durability.
Karavalakis et al., 2015	9 2007-2014 vehicles, including five GDI vehicles and two FFVs	Different alcohol blends included E10, E15, E51, E83, and Bu16 (a 16% butanol blends), Bu24, Bu32, and Bu55	1. There was a trend for lower CO, CO ₂ , PM mass, and particle number, and lower fuel economy with higher alcohol content fuels.
			2. For other pollutants, such as THC, NMHC, CH ₄ , and NOx, there were not strong fuel trends, while some carbonyl species showed some trends towards higher emissions for higher alcohol blends.
Knepper et al., 1993	7 high emitting 1986-1987 model year vehicles	Gasoline with different olefin, sulfur, fuel oxygen content	1. CO increased by reducing sulfur.
			2. HC and CO decreased in high emitters by reducing aromatic.
Knoll et al., 2009	1999-2007 vehicles	Intermediate blends evaluated E0, E10, E15, and E20	1. CO and NMHC decreased for E10, E15, and E20 relative to E0.
			2. Acetaldehyde emissions increased with increasing ethanol.
			3. No statistically significant NOx effects.

Author	Vehicle/Engine	Fuel	Notable Results
Mamakos et al., 2013	GDI (GPF, FFV and PFI) Vehicles	75-85% ethanol/gasoline blends	1. Study utilized the New Regulated European driving cycle and the common artemis driving cycle.
			2. The installation of a gasoline particulate filter with a filtration efficiency of more than 90% was found to effectively reduce the PN emissions below the legislated threshold of 6×10^{11} #/km, under all operating conditions examined.
			3. The use of 75–85% ethanol/gasoline blends on a flex-fuel vehicle resulted in large reductions in PN emissions, which spanned from approximately 20–35% under urban driving to an excess of 95% at motorway conditions.
Maricq et al., 2012	A GDI turbocharged vehicle with two engine calibrations	Ethanol and gasoline blends	1. Small benefits in PM mass and particle number emissions as the ethanol level in gasoline increased from 0 to 20%.
			2. Significant 30%-45% reduction in PM mass and particle number emissions as the ethanol level in gasoline increased to >30%.
			3. Engine-out hydrocarbon and NOx emissions exhibit 10%-20% decreases, consistent with oxygenated fuel additives.
Mayotte et al., 1994 a	20 1987-1990 normal emitters and 16 1986-1990 high emitters vehicles	8 gasoline with different oxygen concentration, RVP, and sulfur content	1. Sulfur concentration has the greatest effect on HC and NOx emissions.
			2. Increasing oxygen concentration and reducing RVP decreased HC emissions more for high-emitting than normal-emitting vehicles.
			3. Oxygenate concentration has a significant effect on aldehyde emissions.
Mayotte et al., 1994 b	27 1986-1991 normal emitters and 12 1986-1989 high emitters vehicles	12 gasoline with different oxygen concentration, T50, T90, RVP, aromatics, olefin, oxygenate type, and sulfur content	1. Oxygen, aromatics and olefins were found to have the greatest influence on THC emissions while sulfur and T90 were found to have the greatest influence on NOx emissions.
			2. Fuel aromatics and benzene content were found to be the key parameters for benzene emissions.
			3. No single fuel parameter was seen to stand out as being the key parameter in determining emissions performance for other measured exhaust emissions.
Reuter et al., 1992	20 1989 vehicles	11 gasoline fuels: four hydrocarbon only, four splash blended ethanol fuels (10 vol %), two MTBE blends (15 vol %) and one ETBE blend (17 vol %)	1. Exhaust emission results indicated that a reduction in fuel Reid vapor pressure of one psi decreased exhaust HC and CO. Adding oxygenates decreased exhaust HC and CO but increased NOx.
			1. A reduction in fuel RVP of one psi reduced exhaust HC and CO. Adding oxygenates reduced exhaust HC and CO but increased NOx.
			2. Evaporative emissions showed a reduction in diurnal emissions with reducing RVP in the non- oxygenated and ethanol blended fuels, but not with the MTBE fuel.

Table 2. (Continued)

Author	Vehicle/Engine	Fuel	Notable Results
			3. Adding ethanol or MTBE increased hot soak emissions. The ethanol increase was significantly larger than the MTBE effect. The effect of ETBE was similar to the MTBE effect in magnitude although not found to be statistically significant in itself.
Sobotowski et al., 2015	4 2007-2009 vehicles, including one GDI vehicle	7 fuels spanning PM Index values from 0.9 to 2.7, aromatic content from 14 to 38%, and ethanol content from 0 to 15%	1. Low volatility compounds have the strongest influence on PM emissions from gasoline vehicles.
			2. The presence of ethanol was found to have a reinforcing interaction with PM Index in PFI vehicles.
			3. The GDI vehicle generally produced higher PM emissions than the PFI vehicles.
Storey et al., 2010	A 2007 model year GDI vehicle	E10 and E20 blends	1. NOx, CO, formaldehyde, and benzaldehyde emissions decreased with higher ethanol blends, while acetaldehyde emissions showed increases.
			2. PM mass and particle number emissions decreased with ethanol blends.
U.S. EPA, 2013 a	15 new light duty cars and trucks of 2008 model year	27 fuel test matrix, including fuels blended at E0, E10, E15, and E20 levels	E10 and E15 generally decreased HC and CO and increased NOx relative to E0.
U.S. EPA, 2013 b	19 light-duty vehicles of 2008 model year	27 fuel test matrix, including fuels blended at E0, E10, E15, and E20 levels	Increasing ethanol content, as well as increasing total aromatic content, T50, and T90, were associated with increasing PM mass emissions.
Wang et al., 2012			1. Relative to petroleum gasoline, ethanol from corn, sugarcane, corn stover, switchgrass and miscanthus can reduce life-cycle GHG emissions by 19–48%, 40–62%, 90–103%, 77–97% and 101–115%, respectively.
			2. Estimated life-cycle energy consumption and GHG emissions from using ethanol produced from five feedstocks: corn, sugarcane, corn stover, switchgrass and miscanthus.
Yanowitz and McCormick, 2009a	Conventional FFVs	E85	1. Comparing Tier 1 FFVs running on E85 to similar non-FFVs running on gasoline showed, on average, significant reductions in emissions of NOx (54%), NMHCs (27%), and CO (18%) for E85.
			2. Comparing Tier 2 FFVs, there is a 28% reduction in NOx emissions and 28% reduction in NMOGs emissions compared to similar non-FFVs.
			3. E85 showed significant reductions in emissions of benzene and butadiene, and significant increases in emissions of formaldehyde and acetaldehyde, in comparison to emissions from gasoline in both FFVs and non-FFVs.

BIODIESEL AS A TRANSPORTATION FUEL

The second most prevalent liquid biofuel (after corn-ethanol) is biodiesel made from plant oils, waste cooking oils, and animal fats. Plant oils include soybean, rapeseed, canola (which is a genetic modification of rapeseed), palm, sunflower, and castor. In the US, the primary source of Fatty Acid Methyl Esters (FAMES), commonly known as biodiesel, is soy-oil, with other sources including yellow grease, canola oil, and distillers corn oil among others (U.S. EIA, 2015). Biodiesel has grown in popularity over the past decade from 2 million gallons per year in 2000 to 1.27 billion gallons per year in 2014 in the U.S. (U.S. EIA, 2015). More recently the U.S. EPA announced increases to the volume requirements for biomass-based diesel, which is expected to further augment the amount of biodiesel being used in the U.S. The required volumes range from 1.63 billion gallons in 2014 to 1.9 billion gallons in 2017. Worldwide biodiesel production has increased considerably over the last 15 years from 213 million gallons per year in 2000 to 4.95 billion gals per year in 2012 (U.S. EIA, 2015). Biodiesel production refers to the commercially mature process of converting oils, fats, and greases into FAMES via the transesterification process.

Biodiesel Production

The production process of biodiesel from triglycerides, the major components of plant oils and animal fats, is a very mature technology with a large number of commercial facilities in operation. As of 2012, United States, Germany, Argentina, and Brazil had the largest production capacities (U.S. EIA 2015). The vast majority of biodiesel produced in the world is through the transesterification or alcoholysis reaction of triglycerides. This process is illustrated below in Figure 3. The process involves a reaction between triglycerides and alcohol to form esters and glycerol. Different types of short-chain alcohols such as, methanol, ethanol, propanol, and butanol can be used. However, methanol and ethanol are the most widely used, particularly methanol due to its low cost and polar nature. The transesterification process consists of three sequential reversible reactions where one triglyceride molecule delivers one diglyceride molecule, from which one monoglyceride molecule is formed; in each step, one molecule of biodiesel is being produced. Different catalysts can be used for this reaction, including alkaline, acid, and enzyme catalysts, although sodium and potassium hydroxides are the most common catalysts being used in the biodiesel industry. The produced methyl ester and glycerol must be separated and purified to remove the remaining catalytic species and soaps, which create a wastewater product. The transesterification process is simple, with a relatively low capital cost compared to most other biofuel production routes. Transesterification can be performed with relatively short reaction times, in a low temperature and pressure environment, and with high conversion rates. The most significant cost of biodiesel production is the feedstock, which accounts about 60-80% of the total cost (Singh, 2014).

Feedstock availability is an important limitation to the expansion of biodiesel. There is enough virgin soy oil, recycled restaurant grease, and other feedstocks available in the US to produce ~1.7 billion gallons of biodiesel per year (AFAVDC, 2009c). This amount of biodiesel is ~5% of the US on-road diesel usage. Biodiesel is predominantly produced

soybeans in the U.S. Soy-oil is removed from the soybean by crushing and then pressing and solvent extraction. The soy-oil represents about 19% of the soybean, with the remainder of the residual used for soybean meal. Hence, soy-oil and soybean meal are co-products from soybean production. Soybean meal has an important use as animal feed for livestock and poultry, and represents the largest volume of soybean crushing and the main source of revenue for the soybean industry. Soy-oil is the mostly widely used edible vegetable oil in the U.S. that is used in cooking oil, almost all margarine and shortenings, mayonnaise, salad dressings, frozen foods, imitation dairy and meat products and commercially baked goods (AgMRC, 2015). Since the mid-2000s, when biodiesel began to be used in more appreciable amounts, greater fractions of soy-oil have been utilized for the production of biodiesel. As of 2012, biodiesel represents 25% of the market for soy-oil (Informa Economics, 2012). The use of soy-oil in food applications has declined over the same period, however, as a consequence of government policies that have reduced the use of trans-fats in food. As such, the overall production of soy-oil has only increased slightly even with the significant expansion of the biodiesel market.

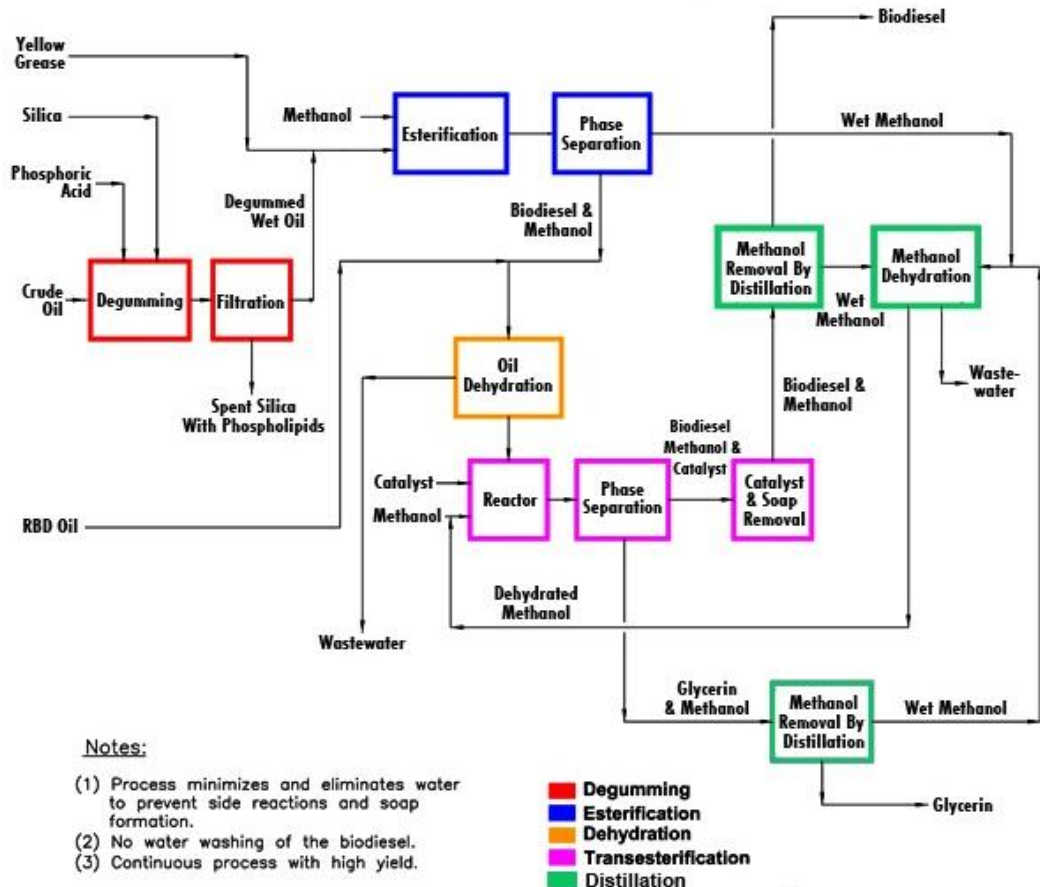


Figure 3. Biodiesel Process Technology by R.C. Costello & Assoc., Inc.

Utilization of Biodiesel as a Transportation Fuel

In general, biodiesel can be used in existing diesel engines and the refueling infrastructures without modification. While biodiesel is generally compatible with the diesel engines, it does have some physical and chemical properties that require some special housekeeping during its use and handling. Those properties include solvency, low temperature engine operability, stability, and materials incompatibility. The quality of biodiesel blend fuels in the market, and vehicle warranty coverage are important issues.

Another issue that merits discussion is how biodiesel could impact engine/vehicle warranties. Warranties are provided by engine and vehicle manufacturers are provided to cover the performance of the workmanship and materials used in the production of their product. If an engine experiences an issue that is attributable to an error in manufacturing and or a failure of a part, this failure must be corrected by the engine manufacturer, provided it is within the specified warranty period. Federal law prohibits the voiding of warranties strictly on the basis of the fuel that is used (15 U.S. Code § 2301). Rather, the warranty would only be voided if the fuel is determined to actually be the cause of the failure, and this applies regardless of whether the fuel is biodiesel, bad diesel fuel, or another external condition. In cases where the fuel is determined to be the cause of a failure, and it is determined that the fuel does not meet the applicable fuel specification, the fuel supplier may be required to cover the failure under its general liability insurance.

Most major engine and vehicle manufacturers have statements related to the use of biodiesel in their products. These statements are meant to define what fuel the engine is designed and what fuels are recommended fuel use in their products. A comprehensive listing of positions statements from engine and vehicle manufacturers is provided at the National Biodiesel Board (NBB) website at <http://biodiesel.org/using-biodiesel/oem-information/oem-statement-summary-chart>. Nearly original equipment manufacturers (OEMs) formally approve the use of up to B5 in their products, provided the biodiesel meets ASTM D6751 or the European biodiesel specification. The use of biodiesel up to B20 is also approved by many engine OEMs in large fractions of their product lines, particularly for heavy duty applications.

Methyl esters are commonly used in solvent products and cleaners. When using biodiesel, there is some tendency for it to dissolve accumulated sediments in diesel storage tanks and engine fuel tanks. These dissolved sediments can plug the filters at the fuel dispensers or travel through the system and clog fuel filters at the engine. In some cases, injector deposits can lead to injector failure, but this is a rare occurrence. Most users of B20 typically do not clean their fuel tanks prior to use since B20 is sufficiently diluted to mute the solvent effect. The effects of B100 are greater, so it is suggested that fuel tanks be cleaned and extra precautions be taken with the fuel system for B100 use (NREL, 2009). For B100, it has been suggested that extra fuel filters be kept on hand during initial use, since cases of filter plugging have been reported and are more likely in the first few tanks of fuel utilized.

Biodiesel can cause degradation, softening, or seeping through some hoses, gaskets, seals, elastomers, glues, and plastics with prolonged exposure. Concern about elastomer degradation is more critical for applications where B100 is used, as opposed to B20. Nitrile rubber compounds, polypropylene, polyvinyl, and Tygon are particularly vulnerable to B100. Materials such as Teflon, Viton, fluorinated plastics, and Nylon, on the other hand, are compatible with biodiesel. Older vehicles, manufactured before approximately 1993, are

more likely to contain materials that could be affected by B100 over longer periods of time (NREL, 2009). Engines newer than 1993 and modern repair kits should contain biodiesel-compatible materials, but do not always. For use at more standard B20 blend levels, fleet experience has shown that material compatibility issues are minimal, even for elastomers made of materials such as nitrile rubber that are not compatible with higher biodiesel blends.

It is also possible that residual metals from the biodiesel production process (Na, K) could also have an impact on metals of emission control catalysts. NREL, in conjunction with a range of collaborators such as ORNL, the Manufacturers of Emission Controls Association (MECA), and various catalyst and engine/vehicle manufacturers, has conducted several studies to look at the impact of fuel metal impurities on the durability of aftertreatment systems. In an initial study, Williams et al. (2011) used an accelerated aging method to expose aftertreatment systems consisting of a DOC/DPF/SCR to an equivalent of 435,000 miles of fuel metal and thermal exposure. This study showed that exposure to Na, K, and Ca resulted in reductions in thermal shock resistance, a loss of catalytic activity for HCs and NO oxidation, and a slight loss in NO_x conversion. In a second study, Williams et al. (2013) used electron probe microanalysis (EPMA), bench flow reactor testing, and vehicle testing to evaluate fuel metal impacts on aftertreatment systems. EPMA showed the penetration of Na and K into the washcoat of the DOC and SCR, while bench flow reactor experiments showed reduced NO_x conversion SCR catalyst performance for exposures to fuels with Na and K. When these partially deactivated catalysts were installed into a Ford F250 pickup truck, however, the vehicle emissions were below the 0.2 g/mi NO_x emission standard, indicating that even with the partial deactivation that there is sufficient catalyst volume to still provide adequate catalyst activity. Williams et al. (2014) conducted an additional study to evaluate how exposures to the same concentration of K over different periods of accelerated aging would impact catalyst deactivation. This study showed that increased levels of K in the catalyst correlated with reduced efficiency for the reduction of CO, HC, and NO, and NO_x, with the reductions primarily isolated to the inlet of the catalyst, whereas performance further down the length of the catalyst was mostly unaffected. The results also showed significantly higher level of K and reduced performance for the shortest exposure with higher K concentrations in the fuel, indicating that above a certain threshold the accelerated aging process can create an artificial mechanism for catalyst deactivation. NREL is evaluating this possibility in an ongoing study in collaboration with Cummins, ORNL, MECA, EMA (McCormick et al., 2015). This study includes aging a heavy-duty catalyst system for 100 hours.

Biodiesel has less favorable cold weather flow characteristics compared with conventional diesel fuel. Biodiesel fuels produced from feedstocks with highly saturated fatty acid structures (such as palm oil and tallow) have poorer cold weather operability than fuels generated from feedstocks with highly unsaturated fatty acid structures (such as rapeseed and safflower oil) (Hoekman, Gertler, Broch, & Robbins, 2009). Cold flow additives are available to mitigate these issues by inhibiting crystal formation, but they have varying degrees of success depending on the feedstock. NREL suggests that users specify to the blend supplier that the fuel remains crystal free at temperatures down to -14°F during the winter season (NREL, 2009). B20 has been used in cold temperature climates such as northern Minnesota and Wyoming, where temperatures regularly fall to below -30°F. Cold flow properties can be a limitation to the use of B100 in the wintertime. Some key properties in this regard are the cloud point and the pour point. The cloud point is the temperature at which wax formation

can begin to plug the fuel filter. The pour point is a measure of the temperature at which the fuel is no longer pourable. Cold filter plugging point, low temperature filterability, wax appearance point, and cold soak filterability are some other laboratory tests commonly used to define low temperature operability of biodiesel (Hoekman et al., 2009).

Fuel quality is very important to owners of diesel engines. Consumers expect all fuels to meet certain minimum quality, safety, and performance standards and engine manufacturers expect a fuel quality that does not affect engine performance and durability. The biodiesel industry continues to strive to improve product quality. The biodiesel industry has established a cooperative and voluntary program for the accreditation of producers and marketers of biodiesel fuel called BQ-9000 that has improved the quality level of in-use biodiesel. The program is a combination of the ASTM standard for biodiesel, ASTM D6751, and a systems quality program that includes storage, sampling, testing, blending, shipping, distribution, and fuel management practices. BQ-9000 helps companies improve their fuel testing and greatly reduce any chance of producing or distributing poor quality fuel. NREL has conducted several studies of the quality and stability of biodiesel and biodiesel blends in the US, dating back to 2004. Although some of the earlier studies found higher failure rates than expected (McCormick, Alleman, Ratcliff, Moens, & Lawrence, 2005; Alleman, McCormick, & Deutch, 2007), with many of the failures attributed to small and medium producers, more recent studies have shown a significant improvement in biodiesel quality. For the most recent study, where a sample was requested from each of the top 50 producers and every BQ-9000 producer, 95% of the samples surveyed met biodiesel specification ASTM 6751 for free and total glycerin, flash point, cloud point, oxidation stability, cold soak filterability, and metals. Earlier studies of B20 quality by NREL have also shown examples of poor blending and mislabeling of pumps (McCormick et al., 2005; Alleman and McCormick, 2009; Alleman, Fouts, & McCormick, 2010). The latest survey of B6 to B20 biodiesel blends showed 95% of the biodiesel blends were B20 or below, with 76% between B6 and B20, and only one sample greater than B20 (Alleman, Fouts, & McCormick, 2011).

Unlike petroleum diesel fuel, the nature of biodiesel makes it more susceptible to oxidation or autooxidation during long-term storage. Storage conditions, especially temperature, exposure to water, and exposure to oxygen, which is naturally present in the ambient air, influence the rate of oxidation. The biodiesel stability generally depends on the fatty acid composition of the parent feedstock. Therefore, biodiesels with high contents of unsaturated fatty acids, such as linoleic and linolenic, are especially prone to oxidation and autooxidation mechanisms (McCormick, Ratcliff, Moens, & Lawrence, 2007). Biodiesel degradation products such as hydroperoxides, cyclic acids, polymers, dimers, trimers, and free fatty acids may cause engine and injector problems. The presence of high molecular polymerization species can lead to deposit formation and higher viscosity, which may affect the fuel spray characteristics. Moreover, the formation of organic acids increases the total acidity and the risk of corrosion in the vehicle and distribution fuel handling systems. To overcome the major problem of biodiesel stability and to guarantee a specific fuel quality, the employment of antioxidation additives appears to represent the most viable solution. The most commonly used antioxidants for biodiesel include some additives developed for petroleum fuels, such as butylated hydroxytoluene (BHT), butylated hydroxyanisole (BHA), tert-butylhydroquinone (TBHQ), propyl gallate (PG), and pyrogallol (PA).

McCormick and Westbrook (2010) evaluated the oxidation storage stability of a range of B100 samples and B20 and B5 blends. They found that B100 samples with induction times of

3 hours or less on an EN14112 accelerated oxidation stability test, that were not additized with an antioxidant, will go out of specification within 4 months for B100 or B20, although B100 samples with induction times of 3 hours were stable in B5 blends for 12 months. The first studies on the oxidative stability of diesel/biodiesel blends with the use of the modified Rancimat method EN 15751, which requires that a blend of diesel fuel with biodiesel shall comply with a minimum induction period of 20 hours at 110°C, were conducted by Karavalakis et al. (2009a, 2010a, 2011). They showed that the oxidative stability of the finished blend was highly dependent on the biodiesel concentration, degree of unsaturation, presence and types of antioxidants, and the stage of oxidation of the methyl ester component itself. Both studies by McCormick and Westbrook (2010) and Karavalakis et al. (2010b, 2011) showed that the stability of biodiesel blends is dominated by the biodiesel stability and that antioxidant additives are very effective in stabilizing biodiesel blends. Christensen and McCormick (2014) evaluated longer term stability of 100% biodiesel and B5 and B20 blends. Samples were aged using an accelerated aging process (ASTM D4625) to simulate up to one year for the B100 samples and three years for the B5 and B20 samples. The B5 samples were stable for the entire storage time. Additionally, all but the most unstable B20 samples remained within specifications over the storage time, suggesting that long term storage of biodiesel blends is possible for biodiesels with high oxidative stability that are stored in clean conditions. In other studies, NREL is currently in the process of evaluating B20 oxidation stability on-board LD vehicles (McCormick et al., 2015). This is a collaborative effort with Volkswagen, Mercedes, GM, and the Engine Manufacturers Association (EMA). Four VW Passat were tested on a chassis dynamometer (hot test cell, hot fuel), and then were further aged at VW proving ground in Arizona for several months. CRC is also investigating the stability of biodiesel blends, including thermal, oxidative, and storage stability, and performing chassis dynamometer vehicle tests and test with test rigs, as part of their AVFL17c study.

Biodiesel is also very sensitive to microbial growth, and adding biocides to the biodiesel storage tank is a common method to control microbial contamination. Water contamination is another issue with biodiesel storage. Since water is more soluble in biodiesel than petroleum diesel, and water can promote microbial growth, water is undesired in the biodiesel (NREL, 2009). The use of a 10-micron filter at biodiesel fuel dispensers is an effective practice to prevent water entering the fuel tank and a 10-micron filter in the fueling system prevents water from entering the fuel injectors and engine system.

Biodiesel blends can be delivered and stored with the current diesel fuel delivery methods and refueling infrastructures with little or no modification. Biodiesel is not delivered in pipelines in the U.S., however, due to its potential impact on jet fuel, which cannot exceed 5 ppm in FAME content. Therefore, biodiesel is typically splash blended in the U.S. Some exceptions to this rule include the Kinder Morgan Plantation pipeline from Mississippi to Virginia, the Kinder Morgan Oregon pipeline, and the Colonial pipeline, which allow generally low-level biodiesel blends (i.e., B5 or less) (Gas Journal, 2009; Heating Oil News, 2011; Pipelines International, 2009). In Europe, however, B5 has been run in pipelines for years already. It is likely that more shipments of biodiesel blends would be made through the pipeline in the U.S. if an allowance for minimal amounts of biodiesel in jet fuel was developed. Boeing is looking to certify biodiesel in jet fuel around the world, and biodiesel is already being run with jet fuel in flight by Dutch airline KLM. The primary emphasis of the

aviation industry is more towards drop-in fuels, which are more hydrocarbon-like and similar to jet fuel (Hendricks, Bushnell, & Shouse, 2011).

Environmental Considerations with the Use of Biodiesel as a Transportation Fuel

Biodiesel is generally considered to provide emissions reductions compared to traditional diesel fuel. In particular, biodiesel has generally been shown to reduce many of the primary emissions of THC, CO, and PM (U.S. EPA, 2002; Yanowitz and McCormick, 2009b; Hajbabaei, Johnson, Okamoto, & Durbin, 2013a). The reduction of PM with biodiesel is due to its ability to lower soot formation during combustion, which can be attributed to a number of different factors. The presence of oxygen in the biodiesel can reduce local fuel-rich regions during combustion, limiting the formation of soot. Likewise, the reductions of THC and CO emissions with biodiesel can be attributed to the oxygen in the biodiesel fuel and more complete combustion and its impact on more complete combustion of the unburned fuel.

Another important pollutant is NO_x. NO_x emissions have shown a tendency to increase with biodiesel use, although this has been a subject of debate. Generally, the increases in NO_x are considerably smaller than the corresponding reductions in other pollutants; however, this remains an important issue in regions and cities when poor air quality is a persistent problem. The U.S. EPA conducted an analysis of the impacts of biodiesel on emissions in the 2002 and 2009 timeframes (US EPA, 2002, 2009), and found an increase in NO_x emissions based on a statistical analysis of a wide range of studies. Other reviews by Researchers at NREL (McCormick, Williams, Ireland, & Hayes, 2006) and Hoekman et al. (2009), suggested that the biodiesel did not have a significant impact on NO_x emissions, at least at the most commonly used B20 level. More recently, the California Air Resources Board (CARB) has conducted a series of studies in conjunction with the University of California at Riverside (UCR) to evaluate the issue of biodiesel NO_x emissions in California diesel fuels as part of the implementation of its Low Carbon Fuel Standard (LCFS) program. These results showed relatively strong trends in NO_x increases for biodiesel blends, even as low as the B5 level, suggesting that some increases in NO_x emissions are likely when biodiesel is blended with a “clean” diesel fuel (Durbin et al., 2011; Hajbabaei, Johnson, Okamoto, & Durbin, 2012; Karavalakis, Durbin, Johnson, & Hajbabaei, 2014).

The NO_x increase for biodiesel has been attributed to a variety of factors in the literature, including fuel density, cetane number, fuel chemical composition (carbon chain length and number of double bonds), and combustion chemistry and stoichiometry, as discussed in greater detail in the literature (Cheng, Upatnieks, & Mueller, 2006; Eckerle et al., 2008; Hoekman and Robbins, 2012; Mueller, Boehman, & Martin, 2009; Szybist, Kirby, & Boehman, 2005; Tat and Van Gerpen, 2003). The magnitude of the NO_x emissions increases can also change with the biodiesel feedstock, with more saturated feedstocks, such as animal tallow, often showing smaller or no increases (McCormick, Graboski, Alleman, Herring, & Tyson, 2001; Durbin et al., 2011; Hajbabaei et al., 2012; Hajbabaei et al., 2014; Karavalakis et al., 2014). In their work with CARB, Durbin et al. (2011) showed that a NO_x neutral B5 mixture could be made using a biodiesel made from a relatively saturated animal tallow-based feedstock, whereas NO_x increases were still seen at the B5 level for biodiesel produced from less saturated soy-based and yellow-grease-based biodiesel. One methodology to mitigate NO_x emissions is through the use of additives such as di-tertiary butyl peroxide (DTBP), as

shown in the California test program as well as other studies (Sharp, 1994; McCormick et al., 2002; Hajbabaei et al., 2012, 2014). Durbin et al. (2011) and Hajbabaei et al. (2012, 2014) also showed that NO_x increases with biodiesel blends could be mitigated using the additive and blending in combinations with a renewable diesel fuel, as discussed below. Several NO_x mitigation strategies were shown to be successful including additive formulations with about a 3 or 4 to 1 ratio of renewable or GTL diesel compared to the biodiesel. While these formulations are viable, the development of more cost-effective NO_x reduction strategies would provide a more economic pathway for the introduction of greater percentages of biodiesel in California.

The effects of biodiesel usage on vehicle emissions have been investigated by various groups within the academic, commercial and regulatory communities, with only a few studies being available on modern light-duty (LD) diesel vehicles, employing common-rail engine systems and aftertreatment technologies (Martini, Astorga, & Farfaletti, 2007; Bannister et al., 2010; Rose et al., 2010; Karavalakis et al., 2010a; Macor, Avella, & Faedo, 2011; Nikanjam, Rutherford, & Morgan, 2011). LD vehicle studies have not always documented decreases in PM mass emissions with the use of biodiesel blends that are generally found for test cell engines operating on steady-state conditions (Durbin et al., 2000; Martini et al., 2007; Fontaras et al., 2009; Karavalakis et al., 2009a; Bakeas, Karavalakis, & Stournas, 2011). Various reasons have been documented to explain the reductions in PM emissions with the use of biodiesel fuels, with the primary contributing factor for the PM decrease being the presence of oxygen in the methyl ester molecule. Oxygenated fuels, such as biodiesel blends, possess the ability to reduce locally fuel-rich regions and limit soot nucleation early in the formation process, thus reducing PM emissions. In addition, the absence of aromatic compounds in biodiesel fuels, which are generally considered to act as soot precursors, may also be a reason for the reductions in PM emissions compared to the baseline diesel fuels (Lapuerta, Armas, & Fernandez, 2008a). For studies that have shown increases in PM emissions for light-duty vehicles, where cold-start emissions are a significant portion of the overall PM emissions, it is possible that certain physical properties of biodiesel can prevail over its increased oxygen content (Fontaras et al. 2009; Bakeas et al. 2011; Karavalakis et al. 2009b; Martini et al. 2007). For example, the higher initial boiling point of biodiesel compared to regular petroleum ULSD, which leads to more difficult fuel evaporation at low temperatures, and the higher viscosity of biodiesel, which reduces the rate of spray atomization, could both contribute to increased PM emissions.

There also is a gap in the literature regarding the effect of biodiesel on unregulated pollutants in vehicles. Several studies have reported an increase in carbonyl emissions (aldehydes and ketones) with the use of biodiesel blends, as a consequence of the oxygen content in the methyl ester molecule (Correa and Arbilla, 2008; Fontaras et al., 2009; Fontaras et al., 2010a; Cahill and Okamoto, 2012). In addition, most authors have observed some decreases in emissions of polycyclic aromatic hydrocarbons (PAH) and their nitrated derivatives (nitro-PAH) when using biodiesel (Bagley, Gratz, Johnson, & McDonald, 1998; Yang et al., 2007; Macor et al., 2011; Surawski et al., 2011). However, the effect of biodiesel source material on PAH and nitro-PAH emissions is less clear, since there are a number of vehicle studies showing some increases in light molecular-weight PAH compounds with biodiesel (Karavalakis et al., 2010a; Karavalakis et al., 2010c). Similar to toxic PAH compounds, information in the literature on particle number (PN) emissions and particle size distributions (PSDs) from biodiesel vehicles is limited and inconsistent. Increased PN emissions and lower size particles are generally, but not always, observed for biodiesel, and

the reasons for such inconsistencies are not properly understood (Fontaras et al., 2009; Fontaras et al., 2010c).

Greenhouse gas emissions are another important environmental consideration for biodiesel. Hoekman et al. (2011) conducted an extensive review of LCA analyses of biodiesel from different sources. They reviewed over 40 LCA studies and found that biodiesel carbon intensities varied from 20 to 60 g CO₂e/MJ_{fuel} compared to reference petroleum diesel values of 80 to 100 g CO₂e/MJ_{fuel}. From this data, they estimated carbon intensity (CI) benefits of approximately 50-60% for biodistillates produced from virgin vegetable oil feedstocks, and a slightly larger benefit results from use of waste feedstocks. One complication noted in this review, however, was that few of these previous studies accounted for ILUC effects, which are more widely considered now in LCA modeling. CI estimates from CARB and the EPA were two that did include ILUC effects, and both estimates showed relatively large increases in CI values for soy-oil biodiesel from 21 to 83 g CO₂e/MJ_{fuel} in the CARB case, and from 8 to 40 g CO₂e/MJ_{fuel} in the EPA case. These values still represent reductions of 12% and 57%, respectively, for CARB and EPA soy-oil biodiesel in comparison with the base reference diesel fuel. CARB estimates for biodiesel produced from other sources are also significantly below those of the soy-oil, since they are assumed to not have ILUC impacts. This includes biodiesel produced from waste cooking oil, with a CI of 14 to 19 g CO₂e/MJ_{fuel} (CARB, 2012), and from corn oil, with a CI of 4 g CO₂e/MJ_{fuel} since the energy required to dry the distillers grains at the ethanol plant after the corn oil is extracted is considerably lower, and this energy savings is provided back as a credited (CARB, 2014a). Subsequent studies have reviewed various ILUC models, including the Forest and Agricultural Sector Optimization Model (FASOM), the Food and Agricultural Policy Research Institute (FAPRI) model, the Global Trade Analysis Project (GTAP), and the Modeling International Relationships in Applied General Equilibrium (MIRAGE BioFuel (BioF)) model (Broch, Hoekman, & Unnasch, 2012; Broch et al., 2013; Unnasch et al., 2014). These studies have indicated that there is much uncertainty and variability in modeling ILUC and in the associated agro-economic models, with some of the largest uncertainties attributable to the prediction of yields (Unnasch et al., 2014). A summary of the environmental studies on biodiesel as a transportation fuel are listed in the Table 3.

OTHER ALCOHOLS AND ETHERS AS TRANSPORTATION FUELS

Although ethanol is the most widely used biofuel in the world, other alcohols and ethers have either been used in the past or have the potential to be alternative fuels. These include higher alcohols such as butanol and pentanol that are alcohols, but are more hydrocarbon-like in nature than ethanol. Methanol was one of the more prominent fuels in the early development of alternative fuels, but interest in methanol waned as ethanol became more widely used. Dimethyl ether (DME) is being developed as an alternative fuel in other parts of the world, although it has not received much attention in the US. The potential of each of these fuels is discussed in section, along with the issues that would need to be addressed and environmental considerations with the implementation of these fuels.

Table 3. References for Environmental Considerations with the Use of Biodiesel as a Transportation Fuel

Author	Vehicle/Engine	Fuel	Notable Results
Bagley et al., 1998	An indirect injection diesel engine	Biodiesel	1. Use of an oxidation catalytic converter (OCC) with the biodiesel fuel showed generally similar or greater reductions in emissions than for use of the D2 fuel.
			2. Use of the biodiesel fuel should not increase any of the potentially toxic, health-related emissions that were studied.
Bakeas et al., 2011	A Euro 4 compliant common rail passenger car	4 biodiesels blended with a typical automotive diesel fuel at proportions of 10, 20, and 30% v/v	1. NOx emissions for the saturated blends were similar to those of diesel fuel.
			2. Higher NOx emissions were found for the unsaturated and oxidized biodiesel blends.
			3. The presence of oxidation products favors the formation of NOx.
			4. PM reductions were found for biodiesel blends due to the presence of oxygen.
			5. Some increases for PM, HC, and CO emissions were found during cold-start.
Bannister et al., 2010	A common-rail direct-injection diesel engine	Biodiesel blends	Reductions in engine-out CO and HC emissions did not always translate to lower tailpipe emissions as reduced exhaust gas temperatures at higher blend ratios lead to reduced catalyst conversion efficiencies and higher total cycle emissions.
Broch et al., 2012, 2013; Unnasch et al., 2014			There is much uncertainty and variability in modeling ILUC and in the associated agro-economic models, with some of the largest uncertainties attributable to the prediction of yields.
Cahill and Okamoto, 2012	2 heavy-duty trucks (2000 and 2008 model)	California ultralow sulfur diesel, soy biodiesel, animal biodiesel, and renewable diesel	1. Soy biodiesel had the highest acrolein emission rates, while the renewable diesel showed the lowest.
			2. The drive cycle also affected emission rates, with the cruise drive cycle having lower emissions than the urban drive cycle.
			3. The newer vehicle with the DPF had greatly reduced carbonyl emissions compared to the other vehicles.
CARB, 2012, 2014a			Biodiesel produced from waste cooking oil had a CI of 14 to 19 g CO ₂ e/MJfuel, and biodiesel produced from corn oil had a CI of 4 g CO ₂ e/MJfuel, since the energy required to dry the distillers grains at the ethanol plant after the corn oil is extracted is considerably lower, and this energy savings is provided back as a credit.
Cheng et al., 2006	An optically accessible diesel engine.	A soy-based biodiesel (B100) and three separate primary reference fuel (PRF) blends	1. A load-averaged NOx increase of ~10%t was observed for B100 relative to the PRF blend with matched premixed-burn fraction.
			2. Factors other than start of combustion and premixed-burn fraction affect the tendency for biodiesel to increase NOx.
			3. The effect of biodiesel on mixture stoichiometry at the lift-off length may also play an important role in increasing NOx emissions.

Author	Vehicle/Engine	Fuel	Notable Results
Correa and Arbillá, 2008	A heavy-duty diesel engine	Pure diesel (D) and biodiesel blends (v/v) of 2% (B2), 5% (B5), 10% (B10), and 20% (B20).	Reductions were found in benzaldehyde emissions (−3.4% for B2, −5.3% for B5, −5.7% for B10, and −6.9% for B20), while all other carbonyls showed a significant increase with biodiesel: 2.6, 7.3, 17.6, and 35.5% for formaldehyde; 1.4, 2.5, 5.4, and 15.8% for acetaldehyde; 2.1, 5.4, 11.1, and 22.0% for acrolein and acetone; 0.8, 2.7, 4.6, and 10.0% for propionaldehyde; 3.3, 7.8, 16.0, and 26.0% for butyraldehyde.
Durbin et al., 2000	4 light heavy-duty diesel trucks	Neat biodiesel, an 80% California diesel/20% biodiesel blend, and a synthetic diesel fuel	1. Biodiesel, the biodiesel blends, and the synthetic diesel produced generally lower THC and CO emissions than California diesel.
			2. NOx emissions were comparable over most of the fuel/vehicle combinations, with slightly higher NOx emissions found for the two noncatalyzed vehicles on 100% biodiesel.
			3. PM emissions were slightly higher for two test vehicles and significantly higher for a third test vehicle on the biodiesel fuels.
			4. PAH emissions for all fuel combinations were relatively low, probably due to the low fuel PAH levels.
Durbin et al., 2011	A 2006 Cummins ISM and 2007 MBE4000 engine	Many different biodiesel blend levels	1. For both two engines, average NOx emissions increased with increasing biodiesel blend level.
			2. The soy-based biodiesel blends showed a higher increase in NOx emissions for essentially all blend levels and test cycles in comparison with the animal-based biodiesel blends.
			3. For the 2006 Cummins engine, biodiesel provided reductions in THC and PM. CO emissions results on this engine showed consistent reductions for the animal-based biodiesel, but not for the soy-based biodiesel.
			4. For the 2007 MBE4000, the PM, THC, and CO emissions were all well below certification limits.
			5. CO ₂ emissions showed a slight increase of 1-5% for B100 and some B50 combinations.
Eckerle et al., 2008	Single cylinder diesel engine	20% blend of soy methyl ester biodiesel (B20)	1. Larger NOx increases are seen for duty cycles with higher average power.
			2. For biodiesel blends containing < 20% biodiesel, the NOx impact over the FTP cycle is proportional to the blend percentage of biodiesel.
			3. At B20, the difference in NOx emissions between a biodiesel blend and its base diesel fuel was relatively small.
Fontaras et al., 2009	A Euro 2 diesel passenger car	A neat soybean-oil derived biodiesel (B100) and its 50 vol.% blend with petroleum diesel (B50)	1. Biodiesel had a negative impact under cold start conditions on both regulated emissions and fuel consumption. Differentiations were limited and in several cases biodiesel had a beneficial effect on emissions and efficiency; however, in the case of warm start real-world cycles.

Table 3. (Continued)

Author	Vehicle/Engine	Fuel	Notable Results
			<p>2. Regarding particle number, solid particles decreased with biodiesel but total particles increased. Certain carbonyl compounds also increased with B100.</p> <p>3. Biodiesel at high blending ratios may strongly impact emissions, in a rather non-uniform manner, with the actual effect being dependent on driving conditions and blending ratio.</p>
Fontaras et al., 2010a	A Euro 3 common-rail passenger car	Low concentration biodiesel blends	<p>1. Generally, the use of biodiesel at low concentrations has a minor effect on carbonyl compound emissions.</p> <p>2. Certain biodiesels resulted in significant increases in carbonyl emissions while others led to decreases.</p> <p>3. Biodiesels associated with increases were those derived from rapeseed oil (approx. 200%) and palm oil (approx. 180%), with the highest average increases observed at formaldehyde and acrolein/acetone.</p>
Hajbabaee et al., 2012	2 2006-2007 heavy-duty engines	Soy-based and animal-based biodiesel, renewable diesel fuel, and gas-to-liquid (GTL) diesel fuel (blend levels 5 to 100%.)	<p>1. NOx emissions consistently increased with increasing biodiesel blend level, while increasing renewable diesel and GTL blends showed NOx emissions reductions with increasing blend level.</p> <p>2. NOx increases ranged from 1.5% to 6.9% for B20, 6.4% to 18.2% for B50, and 14.1% to 47.1% for B100.</p> <p>3. The soy-biodiesel showed higher NOx emissions increases compared to the animal-biodiesel.</p>
Hajbabaee et al., 2013a	2 heavy-duty diesel engines	Soy-based and animal-based biodiesel, renewable diesel fuel, and gas-to-liquid (GTL) diesel fuel (blend levels 5 to 100%.)	<p>1. PM, HC and CO emissions generally showed increasing reductions with increasing biodiesel and renewable/GTL diesel fuel blend levels for the non-DPF equipped engine.</p> <p>2. The DPF-equipped engine THC, CO, and PM emission levels were very low and did not show significant fuel impacts.</p> <p>3. Carbon dioxide (CO₂) emissions were slightly higher for biodiesel blends, and slightly lower for the renewable/GTL blends.</p>
Hajbabaee et al., 2014	Heavy-duty engine	3 B5 biodiesel fuels and six B20-soybean oil methyl ester (SME) with additive blends	<p>1. B5-soy and B5-Waste Vegetable Oil showed measurable increases in NOx emissions.</p> <p>2. B5-animal showed a slight reduction or no change in NOx emissions and passed the criteria of the CARB diesel certification test.</p> <p>3. One additive provided reductions in NOx emissions for the B20-soy blends. No additives reduced NOx enough for B20 to pass the CARB certification test.</p>

Author	Vehicle/Engine	Fuel	Notable Results
			4. Biodiesel blends generally showed either reductions or no significant changes in PM, THC, CO emissions.
Hoekman et al., 2009	HD, LD, and single-cylinder test engines	Many different biodiesel blend levels	1. Use of biodiesel, even at a B20 level, substantially decreases emissions of CO, HC, and PM generally by 10-20%. 2. NOx emissions impacts are much smaller, and more difficult to discern.
Hoekman et al., 2011			1. Biodiesel carbon intensities varied from 20 to 60 g CO ₂ e/MJ _{fuel} compared to reference petroleum diesel values of 80 to 100 g CO ₂ e/MJ _{fuel} . 2. CI estimates showed a relatively wide range in CI values for soy-oil biodiesel from 21 to 83 g CO ₂ e/MJ _{fuel} in the CARB case, and from 8 to 40 g CO ₂ e/MJ _{fuel} in the EPA case. This still represents reductions of 12% and 57%, respectively, for CARB and EPA soy-oil biodiesel in comparison with the base reference diesel fuel.
Hoekman and Robbins, 2012	Modern diesel engines	Biodiesel	1. Biodiesel is generally found to reduce emissions of HC, CO, and PM, but to increase NOx emissions. 2. There is evidence to suggest that effects on injection timing, ignition delay, adiabatic flame temperature, radiative heat loss, and other combustion phenomena all play some role on the biodiesel NOx effect
Karavalakis et al. 2009b	A Euro 3 compliant light duty vehicle	Diesel fuel and palm-based biodiesel blends at proportions of 5%, 20% and 40% (v/v)	1. The addition of biodiesel increased NOx emissions. This increase was more significant with the use of B20 over both cycles (13.7% and 23.2% over the NEDC and ADC, respectively). 2. Biodiesel addition resulted to increases in CO emissions with the highest increase being 11.78% for B20 over NEDC and 11.62% for B40 over ADC.
			3. HC emissions increased with biodiesel over the NEDC, while over the ADC biodiesel addition HC emissions with the highest reductions with the use of B40 (about 26.47%). The same observations hold for PM emissions. 4. CO ₂ emissions and fuel consumption followed similar patterns. B20 led to increases up to 6.16% and 2.94% in fuel consumption over NEDC and ADC, respectively. 5. Some PAH compounds demonstrated an increase with biodiesel, while nitro-PAHs decreased with most of them being almost undetectable. 6. Most carbonyl emissions decreased with biodiesel.

Table 3. (Continued)

Author	Vehicle/Engine	Fuel	Notable Results
Karavalakis et al., 2010a	A Euro 4 diesel passenger car	A soy-based biodiesel and an oxidized biodiesel, obtained from used frying oils, were blended with an ultra-low sulfur diesel at proportions of 20, 30, and 50% by volume	1. The results showed that the DPF had the ability to significantly reduce PM emissions over all driving conditions.
			2. CO and HC emissions were reduced with biodiesel; however, a notable increase in NOx emissions was observed with biodiesel blends.
			3. CO ₂ emissions and fuel consumption followed similar patterns, and increased with biodiesel.
			4. The influence of fuel type and properties was particularly noticeable on the unregulated pollutants. The use of the oxidized biodiesel blends led to significant increases in carbonyl emissions, such as formaldehyde, acetaldehyde, and acrolein. Sharp increases in most PAH compounds, and especially those which are known for their toxic and carcinogenic potency, were also observed with the oxidized blends.
Karavalakis et al., 2010c	A Euro 3 compliant common-rail diesel passenger car	5 different biodiesels was blended with EN590 diesel at a proportion of 10–90% v/v	1. The addition of biodiesel led to some increases in low molecular-weight PAHs (phenanthrene and anthracene) and to both increases and reductions in large PAHs which are characterized by their carcinogenic and mutagenic properties.
			2. Nitro-PAHs decreased with biodiesel, whereas oxy-PAH emissions showed increases with the biodiesel blends.
			3. Most PAH emissions decreased as the average load and speed of the driving cycle increased.
			4. In every case, PAH emissions (included high molecular-weight PAHs) were found in much higher levels during the cold-start UDC than the hot-start UDC and the EUDC.
Karavalakis et al., 2014	Heavy-Duty Engine	B5/B10 Biodiesel Blends	1. Soy biodiesel increases NOx emissions by ~1% on average at the B5 level and ~2% on average at the B10.
			2. Animal-based biodiesels have smaller NOx impacts than soy-based blends.
Lapuerta et al., 2008a	Diesel engine	Biodiesel fuels	1. Increase in fuel consumption were approximately proportion to the loss of heating value for a fuel.
			2. The majority of studies have found sharp reductions in particulate emissions with biodiesel as compared to diesel fuel.
Macor et al., 2011	2 Euro 3 commercial trucks	A 30% v/v biodiesel/diesel fuel blend (B30) and pure diesel fuel	1. Gaseous regulated emissions almost unchanged.
			2. PM, soot fraction and particle number showed a significant reduction with biodiesel.
			3. Formaldehyde emissions markedly increased for both vehicles, whereas acetaldehyde emissions showed ambiguous trends.

Author	Vehicle/Engine	Fuel	Notable Results
			<p>4. The lightest and most abundant PAHs species (3–4 benzene rings) showed increases to a different extent for the two different vehicles. The species with 4–5 rings (such as benzo(a)pyrene) showed a net reduction, often to under the instrumental detection limit.</p> <p>5. The B30 carcinogenic risk evaluation of PAHs exhibited a clear toxicity reduction compared to diesel, especially in the cold start cycle, when the catalytic converter's efficiency was not fully reached.</p>
Martini et al., 2007	2 light duty diesel passenger cars	3 different biodiesels	The vegetable oil used to produce the biodiesel, seems to have a very limited effect on emissions. Only in the case of palm oil, which had a higher cetane number, were some positive effects found for CO, HC and PAH.
McCormick et al., 2001	A heavy-duty truck engine	7 biodiesels produced from real-world feedstocks and 14 produced from pure fatty acids	<p>1. The molecular structure of biodiesel can have a substantial impact on emissions.</p> <p>2. The properties of density, cetane number, and iodine number were found to be highly correlated with one another.</p> <p>3. For neat biodiesels, PM emissions were essentially constant at about 0.07 g/bhp-hr for all biodiesels as long as fuel density was less than 0.89 g/cm³ or cetane number was greater than about 45. NOx emissions increased with increasing fuel density or decreasing fuel cetane number. Increasing the number of double bonds, quantified as iodine number, and correlated with increasing emissions of NOx.</p> <p>4. For fully saturated fatty acid chains, the NOx emission increased with decreasing chain length for tests using 18, 16 and 12 carbon chain molecules.</p> <p>5. There was no significant difference in NOx or PM emissions for the methyl and ethyl esters of identical fatty acids.</p>
McCormick et al., 2002	1991 DDC Series 60 truck engine	B20 blended with a nominally 10% aromatic diesel, zero aromatic Fisher-Tropsch (FT) diesel, and use of fuel additives	<p>1. Relative to certification diesel the B20 fuels exhibited 20% lower PM emissions but 3.3 and 1% higher NOx emissions for soy and yellow grease based blends, respectively.</p> <p>2. The 10% aromatic fuel exhibited 12% lower PM and 6% lower NOx.</p> <p>3. FT diesel had the lowest emissions with a 33% reduction in PM and 16% lower NOx.</p> <p>4. For B20, lowering of the base fuel aromatic content from 31.9 to 7.5% lowered NOx by 6.5%.</p>
McCormick et al., 2006	8 heavy-duty diesel vehicles	B20	<p>1. There does not appear to be discrepancy between engine and chassis testing studies for the effect of B20 and NOx emissions.</p> <p>2. Considering all of the data available, B20 has no net impact on NOx.</p>

Table 3. (Continued)

Author	Vehicle/Engine	Fuel	Notable Results
Mueller et al., 2009	A single cylinder version of a heavy-duty diesel engine	2 biodiesel fuels and two hydrocarbon reference fuels	1. The biodiesel NO _x increase is not quantitatively determined by a change in a single fuel property, but rather is the result of a number of coupled mechanisms whose effects may tend to reinforce or cancel one another under different conditions, depending on specific combustion and fuel characteristics.
			2. Charge-gas mixtures that are closer to stoichiometric at ignition and in the standing premixed auto ignition zone near the flame lift off length appear to be key factors in helping to explain the biodiesel NO _x increase under all conditions.
			3. Differences in prompt NO formation and species concentrations resulting from fuel and jet-structure changes also may play important roles.
Rose et al., 2010	3 light-duty diesel vehicles	4 fuels: a hydrocarbon-only diesel fuel and three FAME/diesel fuel blends containing up to 50% v/v FAME	1. As the RME content of the fuel increased, the PM and PN were generally found to decrease over the NEDC while the NO _x , CO, and HC emissions increased.
			2. The impact of RME on regulated tailpipe emissions is much smaller than the variations in emissions seen over the NEDC sub-cycles.
Sharp, 1994	A rebuilt, four-stroke 1991 Detroit Diesel Series 60 engine	5 different additized fuels and 2 “reference” fuels; an emissions grade, low-sulfur 2-D diesel fuel (R1), and a low sulfur, low aromatic diesel fuel	1. All the additized fuels had lower particulate and CO than either the low aromatic fuel or the 2-D reference fuel.
			2. None of the candidate blends produced NO _x emissions as low as the low aromatic fuel.
			3. B20 with a cetane improver had HC, CO, and PM emission levels below both reference fuels (R1, R2), and a NO _x level above that obtained with the low aromatic fuel (R2), but below the levels obtained with the other fuels.
Surawski et al., 2011	A single compression ignition engine	3 biodiesel fuels made from 3 different feedstocks at 4 different blend percentages (20%, 40%, 60%, and 80%)	1. Particle number size distributions showed a strong dependency on feedstock and blend level, with some fuel types showing increased particle number emissions, while others showed particle number reductions.
			2. The median particle diameter decreased as the blend percentage increased.
			3. Particle and vapor phase PAHs were generally reduced with biodiesel, with the results being relatively independent of the blend level.
			4. The ROS concentrations increased monotonically with biodiesel blend percentage, but did not exhibit strong feedstock variability.

Author	Vehicle/Engine	Fuel	Notable Results
Szybist et al., 2005	A single-cylinder DI diesel engine	Biodiesel, Fischer–Tropsch (FT) diesel, and their blends with a conventional diesel fuel	1. Compared to conventional diesel fuel at high load, biodiesel fuel blends produced increases in NOx emissions of 6–9% while FT fuels caused NOx emissions to decrease 21–22%.
			2. Shifts in fuel injection timing, caused by bulk modulus differences, were largely responsible for the NOx increases, but pure FT diesel produced lower NOx emissions than expected on the basis of start of ignition alone.
			4. The timing of the maximum cylinder temperature, did produce a relationship with NOx emissions that was not dependent on fuel type.
Tat and Van Gerpen, 2003	Diesel engines	Biodiesel	1. Fuel property changes could cause approximately a 1° of injection timing advance.
			2. Since NOx emissions increase with advanced timing, this effect may be partially responsible for the increase in NOx with biodiesel.
U.S. EPA, 2002	Heavy-duty highway engines	Biodiesel / conventional diesel blends	HC and CO decreased and NOx increased with increasing percentage of biodiesel in fuel blends.
U.S. EPA, 2009	Heavy-duty highway engines	Biodiesel / conventional diesel blends	An increase in NOx emissions for biodiesel blends was found based on a statistical analysis of a wide range of studies.
Yang et al., 2007	2 engines	Diesel and biodiesel	1. HC, CO and PM emissions did not increase significantly as the driving mileage accumulated.
			2. Total (gaseous and particulate phase) PAH emission levels for both B20 and diesel decreased as the driving mileage accumulated. However, for the engine using the B20 fuel, particulate PAH emissions increased as engine mileage increased.
Yanowitz and McCormick, 2009b	North American heavy-duty engine	Biodiesel blends	1. B20 consistently reduces emissions of PM, HC, and CO by 10–20%.
			2. Tests with B20 show varying effects on NOx emissions.

Development and Use of Butanol as a Transportation Fuel

Butanol Production

The commercial market for butanol is valued at more than \$6 billion and includes a variety of applications (Phytonics, 2012). Butanol can be used directly as solvent, but is also used for the production of acrylate, which is used in water-based paints, detergents, adhesives, and textiles; of acetate, which is used as a solvent in automotive coatings and in cosmetics and drugs; and of glycol ethers, which are used in water-based varnishes (Phytonic, 2012; Ceresana Technologiezentrum). Commercial butanol is primarily produced via the oxo-synthesis of propylene. Butanol can also be produced from biomass, starch or other related sources, and is termed biobutanol. Biobutanol production is being developed by a number of different domestic and international companies, including some producing n-butanol and other producing isobutanol (Nejame, 2010). Biobutanol production on a commercial basis has yet to be realized, however, as it is currently too expensive on a volumetric basis to produce. The overall production of biobutanol via the conventional acetone-butanol-ethanol (ABE) fermentation process is similar to that for ethanol. The difference from ethanol production is primarily in the fermentation process and minor changes in the distillation process. The butanol yields from this fermentation process are typically relatively low, however, because the accumulation of butanol in the fermentation broth exhibits strong toxicity toward the microorganisms. While it is more expensive to produce butanol than ethanol on a volumetric basis, Tao and Aden (2009) showed that the costs of butanol could be more comparable when the energy difference between ethanol and butanol is taken into account.

Gevo of Englewood, Colorado, and Butamax Advanced Biofuels, a joint venture of BP and DuPont based in Wilmington, Delaware, have both been working to develop commercial butanol production. Gevo is currently coproducing butanol with ethanol at its plant in Luverne, Minnesota. This plant did have issues in the 2012-2013 timeframe and had to shut down butanol production due to low yields from bacterial contamination. Butamax is producing butanol at a demonstration plant in Hull, England, and is retrofitting an existing ethanol plant from Highwater Ethanol in Lamberton, Minnesota, for butanol production. Butamax has also organized an alliance of ethanol producers in the U.S. who are considering making the shift. Green biologic, a United Kingdom based biotech company, has also purchased a ethanol plant in Minnesota that it is planning to retrofit for butanol production. Several other companies are also working to develop processes for butanol production from cellulosic materials.

Utilization of Butanol as a Transportation Fuel

In comparison with ethanol, butanol has several advantages as a transportation fuel (BP and Dupont, 2010). Butanol is more similar to gasoline than ethanol since it is a longer, fairly non-polar hydrocarbon. Its energy content is higher than that of ethanol (105,000 Btu per gallon versus 84,000 Btu per gallon in ethanol), although it is still less than that of gasoline. Thus, biobutanol would have less of an impact on fuel economy than ethanol and provide equivalent or better performance. Butanol, similar to ethanol, also has a higher octane rating than gasoline that could allow for greater compression ratios and higher efficiencies.

The compatibility of alcohol-based fuels with conventional fuel system components is also an important consideration. Butanol could potentially be more compatible at higher blend levels in conventional gasoline vehicles than ethanol, or offer co-blending synergies with

ethanol. Currently, biobutanol can be blended up to 11.5% in the US with the potential for this to increase up to 16% by volume, and up to 10% by volume in Europe. Gasoline containing butanol at 16% has about the same oxygen content as gasoline containing ethanol at 10%. Additional research is needed to determine if butanol use in gasoline should be limited to values only slightly higher than those applicable for ethanol or if much higher levels of butanol would be compatible with gasoline vehicles.

Butanol has a lower vapor pressure than ethanol. The Reid vapor pressure (RVP), or vapor pressure at 100°F using a specific protocol, is 2 psi for ethanol and 0.33 psi for butanol. Furthermore, butanol/gasoline blends have a lower vapor pressures than corresponding ethanol/gasoline blends. There are some vapor pressure co-blend synergies with butanol and gasoline containing ethanol that could facilitate ethanol blending (BP, 2008). Ratcliff et al. (2013) examined the effects of coblending of ethanol and butanol on gasoline RVP. These researchers found that coblending ethanol and butanol would provide refiners with increased flexibility in increasing the amount of volatile C₄-C₅ hydrocarbons in commercial gasoline blendstocks for oxygenate blending without exceeding RVP limits in the final blend.

Regarding the latent heat of vaporization, butanol is less attractive than gasoline and ethanol fuels. For PFI systems, when the fuel vaporizes in the inlet port it affects a temperature decrease of the intake charge. Therefore, fuels with higher latent heat of vaporizations have larger decreases in temperature in the intake charge with complete vaporization in the intake port. This increases the density of the combustible mixture and increases the charge mass (Szwaja & Naber, 2010). A recent study conducted by Irimescu (2011) investigated the real-world engine operation with 10, 30, and 50% butanol blends in a gasoline passenger car on chassis dynamometer. Results showed that the butanol blend exhibited a slight drop in fuel conversion efficiency. The author concluded that those differences were acceptable (a maximum of 12% drop efficiency at high load), and within close limits.

Butanol also has potential applications in diesel engines for both light- and heavy-duty applications. Due to its less hydrophilic nature, its higher heating value, higher cetane number, and higher miscibility than ethanol, butanol is a better alcohol candidate than ethanol for blending with conventional diesel fuel.

There is the possibility of transporting butanol by pipeline, unlike ethanol, but this issue has not been extensively studied (BP and Dupont, 2010). Thus, there is a potential to avoid the complication of terminal blending, as with ethanol. Butanol/gasoline blends are also less susceptible to separation due to water contamination than ethanol/gasoline blends. This makes butanol more compatible with the existing distribution infrastructure for petroleum fuels. Studies of the compatibility of infrastructure materials, including elastomers, plastics, and metals, with blends for butanol from 16 to 55% in gasoline has been conducted by Kass et al. (2013, 2014a, 2014b, 2015a) and Durbin et al. (2015a, 2015b). In general, the results for the butanol blends were similar to those seen for the ethanol blends, as discussed above. For elastomers, the butanol blends produced similar to or slightly lower volume swelling compared to the ethanol blends with an equivalent oxygen content (Kass et al., 2014a). For plastics, in comparing E10 and Bu16, most samples were affected in a similar way for both fuels in terms of volume swell and hardness change, although nylons and Novolac vinyl ester resin showed greater impacts for the E10 fuel than the Bu16 fuel (Kass et al., 2015a). Very little corrosion was seen for the metal samples exposed to the butanol blends, similar to the results seen for the ethanol blends (Kass et al., 2015; Durbin et al. 2015a, 2015b).

Environmental Considerations with the Use of Butanol as a Transportation Fuel

The emission characteristics of butanol blends have been studied in both conventional PFI gasoline engines and in GDI engines. In an earlier study carried out by Alasfour (1998), it was found that NO_x emissions were reduced with a 30% butanol blend (Bu30) compared to pure gasoline in a PFI engine. Xiaolong et al. (2009) found reduced CO and HC emissions, but higher NO_x emissions for a Bu30 blend compared to gasoline in a PFI gasoline engine due to higher combustion temperatures. They also found that the engine experienced a torque drop at high load for the Bu30 blend, but that it could be recovered by optimizing the spark advanced angle for the same engine and control strategy. Dernote et al. (2010) conducted tests using a Honda engine and found that, compared to pure gasoline, 20 and 40% n-butanol blends resulted in similar HC emissions, 60 and 80% n-butanol blends resulted in higher HC emissions, while NO_x emissions were similar for all blends, except the 80% n-butanol blend, which showed lower emission levels due to combustion deterioration (higher HC levels). A slight increase in specific fuel consumption with the n-butanol addition was also found, which was related to the blend's reduced combustion enthalpy. Ratcliff et al. (2013) evaluated the emissions impacts of blends of ethanol (16 vol%), n-butanol (17 vol%), i-butanol (21 vol%), and i-butanol (12 vol%)/ethanol (7 vol%) in a 2009 Tier 2 Bin 5 vehicle over the LA92 cycle. These results showed an increase in formaldehyde emissions for i-butanol, lower unburned alcohol and higher carbonyl emissions for the butanol blends compared to the ethanol blend, and that the i-butanol (12 vol%)/ethanol (7 vol%) showed the lowest total oxygenates and NMOG among the alcohol blends. The most significant carbonyls for the n-butanol blend were formaldehyde, acetaldehyde, and butyraldehyde, while those for the i-butanol were formaldehyde, acetone, and 2-methylpropanal.

Several recent studies have looked the impacts of butanol in GDI engines. Wallner et al. (2009) studied the combustion performance and exhaust emissions from a GDI 4-cylinder engine using pure gasoline, a 10% butanol blend (Bu10), and a E10 blend. They found relatively minor differences between the three fuels for different combustion characteristics, such as heat release rate for the 50% mass fraction burned and the coefficient of variation of indicated mean effective pressure at low and medium engine loads. The Bu10 blend had a lower volumetric fuel consumption compared to the ethanol blend, as expected based on energy density differences. The results showed little difference in regulated emissions between the E10 and Bu10, although the E10 produced the highest peak specific NO_x due to the high octane rating of ethanol and effective anti-knock characteristics. Wallner et al. (2010) tested ethanol and iso-butanol blends in a GDI engine and reported reduced NO_x and CO emissions with both blends, increased formaldehyde and acetaldehyde emissions for the iso-butanol, and increased acetaldehyde, but not formaldehyde emissions, for the ethanol blends. He et al. (2010) studied the influence of gasoline, two ethanol-blends (E10 and E20), and a 11.7% iso-butanol blend (Bu11.7) on particle size distributions and particle number concentrations using a turbocharged GDI engine. They found that E20 and Bu11.7 reduced particle emissions for all conditions studied and a higher reduction percentage for accumulation mode particles than nucleation mode particles, while the E10 exhibited almost the same particle emissions as gasoline. Karavalakis et al. (2015) included Bu16 (a 16% butanol blend), Bu24, Bu32, and Bu55 in their study of mixed alcohols with 9 2007-2014 vehicles. There was a trend of lower CO, CO₂, PM mass, and particle number, lower fuel economy, and higher emissions of some carbonyls for higher alcohol blends, as discussed above.

There is a large body of studies in the literature concerning the use of butanol-diesel blends in diesel engines, and its effects on performance and exhaust emissions. Rakopoulos et al. (2011) found that smoke opacity and NO_x emissions were reduced with increasing percentages of biofuels in E5, E10, and 8% and 16% n-butanol blends in a turbocharged heavy-duty, direct injection (DI), Mercedes Benz engine. In another study by Rakopoulos et al. (2010), they found that 8, 16, and 24% butanol blends reduced smoke density and CO emissions, slightly reduced NO_x emissions, and increased HC emissions compared to diesel fuel in a high-speed, DI diesel engine, with these changes being higher for higher percentages of butanol in the blend. Some increases in brake specific fuel consumption (BSFC) with butanol blends were also observed with a corresponding slight increase in brake thermal efficiency. Karabektas and Hosoz (2009) found that 5, 10, 15, and 20% isobutanol-diesel blends reduced CO and NO_x emissions, but increased HC emissions in a DI diesel engine. Based on these results, the authors suggested that 10% isobutanol was the optimum blend in terms of exhaust emissions. They also found that brake specific power decreased with all butanol blends, mainly due to the lower energy content of butanol compared to diesel fuel, and BSFC increased with butanol blends, with the increases roughly inversely proportional to the energy content of the blends. A summary of the environmental studies on butanol as a transportation fuel are listed in the Table 4.

Development and Use of Pentanol as a Transportation Fuel

Pentanol Production

Higher alcohols are used as feedstocks for manufacturing many product categories, such as cosmetics, perfumes, inks, solvents, and resins. Higher alcohols can be produced from coal-derived syngas or may be produced through integration of ethanol and methanol formation via fermentation and biomass gasification, respectively, with conversion of these simple alcohol intermediates into higher alcohols via the Guerbet reaction (Olson, Sharma, & Aulich, 2004).

Utilization of Pentanol as a Transportation Fuel

Higher alcohols, such as pentanol, are more favorable gasoline constituents than ethanol. Pentanol has a higher energy content than ethanol, which would significantly improve fuel economy over ethanol. One potential drawback could be the increased fuel reactivity with the longer chain which diminishes the potential for improved antiknock performance for SI combustion. With a longer alkyl chain, the polarity of alcohols rapidly decreases, and their physiochemical properties become more like those of the hydrocarbons in gasoline. Pentanol is less hydroscopic and less susceptible to separation in the presence of water when blending with hydrocarbon fuels. This is in sharp contrast with ethanol, and it makes pentanol more compatible with the existing fuel infrastructure. Material compatibility issues, such as elastomer swelling, are also less significant with pentanol and other higher alcohols.

Table 4. References for Environmental Considerations with the Use of Butanol as a Transportation Fuel

Author	Vehicle/Engine	Fuel	Notable Results
Alasfour, 1998	A hydra single-cylinder, spark-ignition, fuel-injection engine	30% Iso-butanol–gasoline blend	NOx emissions were reduced with a 30% butanol blend (Bu30) compared to pure gasoline.
Dernotte et al., 2000	A port fuel-injection, spark-ignition engine	Different butanol-gasoline blends	Compared to pure gasoline, 20 and 40% n-butanol blends produced similar HC emissions, 60 and 80% n-butanol blends produced higher HC emissions, while NOx emissions were similar for all blends, except the 80% n-butanol blend, which showed lower emission levels due to combustion deterioration (higher HC levels).
He et al., 2010	A turbocharged GDI engine	Gasoline, two ethanol-blends (E10 and E20), and a 11.7% iso-butanol blend (Bu11.7)	E20 and Bu11.7 reduced particle number emissions for all conditions studied, with the reductions being greater for accumulation mode particles than nucleation mode particles, while the E10 exhibited almost the same particle emissions as gasoline.
Karabektas & Hosoz, 2009	A DI diesel engine	5-20% isobutanol-diesel blends	<ol style="list-style-type: none"> 1. Isobutanol-diesel blends reduced CO and NOx emissions, but increased HC emissions. 2. The authors suggested that 10% isobutanol was the optimum blend in terms of exhaust emissions.
Karavalakis et al., 2015	9 2007-2014 vehicles	Mixed alcohols includes Bu16 (a 16% butanol blend), Bu24, Bu32, and Bu55	There was a trend of lower CO, CO ₂ , PM mass, and particle number, lower fuel economy, and higher emissions of some carbonyls for higher alcohol blends.
Ratcliff et al., 2013	A 2009 Honda Odyssey (a Tier 2 Bin 5 vehicle) over triplicate LA92 cycles	4 gasoline-alcohols blends (ethanol (16 vol%), n-butanol (17 vol%), i-butanol (21 vol%), and an i-butanol (12 vol%)/ethanol (7 vol%) mixture)	<ol style="list-style-type: none"> 1. Formaldehyde emissions increased for i-butanol, and lower unburned alcohol and higher carbonyl emissions were found for the butanol blends compared to the ethanol blend. 2. The i-butanol (12 vol %) /ethanol (7 vol %) showed the lowest total oxygenates and NMOG among the alcohol blends. 3. The most significant carbonyls for the n-butanol blend were formaldehyde, acetaldehyde, and butyraldehyde, while those for the i-butanol were formaldehyde, acetone, and 2-methylpropanal.
Rakopoulos et al., 2011	A turbocharged heavy-duty, direct injection (DI), Mercedes Benz engine	Ethanol or n-butanol diesel fuel blends (E5, E10, and 8% and 16% n-butanol)	Smoke opacity and NOx emissions were reduced with increasing percentages of biofuels.
Rakopoulos et al., 2010	A high-speed DI diesel engine	Butanol-diesel fuel blends (8%, 16% and 24% (by volume) n-butanol)	Butanol blends reduced smoke density and CO emissions, slightly reduced NOx emissions, and increased HC emissions compared to diesel fuel, with these changes being higher for higher butanol blend levels.

Author	Vehicle/Engine	Fuel	Notable Results
Wallner et al., 2009	A GDI 4-cylinder engine	Gasoline, a 10% butanol blend (Bu10), and a E10 blend	Little difference was seen in regulated emissions between E10 and Bu10, although E10 produced the highest peak specific NOx.
Wallner et al., 2010	A GDI engine	Ethanol and iso-butanol blends	<ol style="list-style-type: none"> 1. NOx and CO emissions decreased with both blends. 2. Formaldehyde and acetaldehyde emissions increased for the iso-butanol, and acetaldehyde, but not formaldehyde, emissions increased for the ethanol blends.
Xiaolong et al., 2009	A PFI gasoline engine	Bu30 blend	CO and HC emissions decreased, but NOx emissions increased for a Bu30 blend compared to gasoline.

Table 5. References for Environmental Considerations with the Use of Pentanol as a Transportation Fuel

Author	Vehicle/Engine	Fuel	Notable Results
Furey, 1985		Gasoline-Alcohol and Gasoline-Ether Fuel Blends	Higher alcohols as co-solvents in alcohol/gasoline blends could be a viable option for controlling the RVP and, consequently, for controlling evaporative emissions.
Gautam et al., 2000	Single cylinder Waukesha CFR engine	higher alcohol/gasoline blends	<ol style="list-style-type: none"> 1. The blends produced 12-16% higher NOx emissions at the higher power levels on a unit of time basis. 2. Brake specific emissions were significantly lower for the higher alcohol/gasoline blends than for neat gasoline (16-20% lower CO, 18-23% lower CO₂, 5-11% lower NOx, and 17-23% lower organic matter hydrocarbon equivalent). 3. The contribution of alcohols and aldehydes to the overall organic matter hydrocarbon equivalent emissions was found to be less than 1% for every blend tested.
Pumphrey et al., 2000		gasoline-alcohol (methanol, ethanol, isopropanol, and t-butanol) mixtures	<ol style="list-style-type: none"> 1. The vapor pressure of gasoline was initially elevated by the addition of the alcohols, then lowered as the proportion of alcohol was increased. 2. These solutions can be treated as pseudobinary solutions for prediction purposes.
Yacoub et al., 1998	Single cylinder SI engine	alcohol/gasoline blends with higher alcohols (C4 and C5)	Higher alcohols showed reductions in THC and CO emissions, increases in NOx emissions when operating at high compression ratios, and increases in aldehyde emissions.
Yang et al., 2010	HCCI engines	Isopentanol	Isopentanol has a good potential as a HCCI fuel, either in a neat form or in blend with gasoline.

Environmental Considerations with the Use of Pentanol as a Transportation Fuel

In general, there is very limited information available on pentanol emissions. Gautam et al. (2000) investigated the emission characteristics of higher alcohol/gasoline blends in a single-cylinder Waukesha CFR engine at steady state conditions, with the spark timing-compression ratio optimized for each fuel blend to produce the best mean indicated effective pressure. Under these conditions, the alcohol blends produced higher engine power, due, in part, to the fact that the blends have greater resistance to knock and allowed higher compression ratios. For all the emission species considered, the brake specific emissions were significantly lower for the higher alcohol/gasoline blends than for neat gasoline (16-20% lower CO, 18-23% lower CO₂, 5-11% lower NO_x, and 17-23% lower organic matter hydrocarbon equivalent), although the blends produced 12-16% higher NO_x emissions at the higher power levels on a unit time basis. The contribution of alcohols and aldehydes to the overall organic matter hydrocarbon equivalent emissions was found to be less than 1% for every blend tested. BSFC for the blends ranged from 15 to 19% lower than the BSFC of neat gasoline. Yacoub et al. (1998) found that blends with higher alcohols (C₄ and C₅) in a single cylinder SI engine showed reductions in THC and CO emissions, increases in NO_x emissions when operating at high compression ratios, which were attributed to their lower enthalpies of vaporization and higher flame temperatures, and increases in aldehyde emissions. They also found degraded knock resistance when compared with gasoline, with the pentanol/gasoline blends showing the highest knock tendency.

Evaporative emissions with alcohols are also an important consideration. In contrast with ethanol, the azeotropes formed by pentanol and other higher alcohols and gasoline compounds barely increase the mixture vapor pressure, but instead enhance the vaporization of these alcohols in engine operation since they usually have high boiling temperatures and high heats of vaporization. Pumphrey et al. (2000), Yang et al. (2010), and Furey (1985) investigated RVP changes in gasoline when methanol, ethanol, and higher alcohols were added. His findings showed that very small amounts of alcohol in the blend increased the RVP, with methanol having a more dramatic effect on RVP than the higher alcohols. When methanol was blended in gasoline together with higher alcohols, however, the increase in the RVP was lower compared with methanol alone. The authors reached the conclusion that higher alcohols as co-solvents in alcohol/gasoline blends could be a viable option for controlling the RVP and, consequently, for controlling evaporative emissions. A summary of the environmental studies on Pentanol as a transportation fuel are listed in the Table 5.

Development and Use of Methanol as a Transportation Fuel

Methanol Production

The production of methanol from syngas is a well understood, commercial process. Most of the world's industrial methanol is made from syngas derived from auto-thermal reforming of natural gas. While some other alcohols and chemicals are produced, the yield for this technology is more than 90 percent methanol. The reaction is very exothermic, and requires careful reactor design to remove the process heat. Methanol is often transformed into other chemicals/products, including formaldehyde, gasoline/fuel, dimethyl ether, MTBE/TAME, acetic acid, or olefins (Boyd, 2012), and it is used in plastics, adhesives, foams, plywood sub-floors, solvents, and windshield-washer fluid. Methanol production and demand have

continued to increase throughout the last decade. Worldwide methanol production reached about 21 billion gallons in 2013 (Methanol Institute, 2015a). China represents the largest demand for ethanol, and Asia as a whole is expected to represent 70% of the worldwide demand by 2016 (Boyd, 2012). Many of the production facilities are located in areas where there is access to cheap natural gas, such as Trinidad and Tobago, Chile, Venezuela, and Equatorial Guinea. Methanol can also be produced from coal, and coal-based methanol production has expanded considerably in China. Methanol production in the U.S. declined considerably with increases in natural gas prices between 1998 and 2012, when there were only four plants remained in the U.S., including facilities in Soperton, GA, Geismer, LA, Deer Park, TX, and Kingsport, TN (Methanol Institute, 2012). Methanol production in the U.S. is on an upsurge, however, sparked by increased demand for methanol in China. Methanol plants are being planned or reopened in Texas City, TX, by a Chinese company, in Beumont TX, by a Dutch fertilizer company, in Louisiana by Methanex, and in Channelview, TX, by LyondellBasell (Meyers, 2014). Currently most of the methanol consumed in the US is imported from the Caribbean and South America – with methanol representing almost 40% of our trade under the Caribbean Basin Economic Recovery Act (Methanol Institute, 2012).

Utilization of Methanol as a Transportation Fuel

Methanol can be used in either internal combustion engines or in fuel cells. This subsection focuses on the use of methanol in internal combustion engines. Methanol has characteristics similar to ethanol, in that it requires special vehicles and cannot be transported via pipeline. Methanol has a lower energy density than ethanol, with only about 51% of the BTU content of gasoline by volume. Methanol is even more corrosive than ethanol. Methanol is also less volatile than gasoline and burns at a lower temperature, making engine starting in cold weather more difficult. Some use of methanol in conventional vehicles has been permitted under waivers, such as those obtained for Oxynol-50 and a DuPont waiver. The European Fuel Quality Directive does, however, allow up to 3% methanol to be blended into gasoline with a cosolvent. It is reported that methanol is being used as a low-level blend agent in the United Kingdom. This is a blend of methanol and ethanol, in addition to other cosolvents and additives, to ensure compliance with vapor pressure and fuel stability criteria.

Similar to ethanol, the use of higher levels of methanol in vehicles requires the development of specialized FFVs. Some of the adjustments that are needed for methanol FFVs are similar to those needed for ethanol FFVs. These include larger fuel injectors, a larger fuel tank, a stainless steel fuel system, and other features for cold starts. Alcohol sensors were initially used to monitor the fuel mixture and adjust the fuel flow and timing, but alcohol sensors were phased out of many FFVs as ECUs became equipped with memory to retain prior A/F values. The methanol industry suggests that these changes add an incremental cost of only \$50-\$150 per vehicle or less (Dolan, 2008; Lynn, 2009).

It is possible to consider the use of methanol in existing ethanol FFVs. In this regard, it must be noted that automakers would most certainly object to this application since current E85 FFVs are not designed for use with M85. Material compatibility issues, especially over the long term, would be a major issue. Evaporative emissions would likely also increase due to increased permeability. Fuel injector capacity would also probably be an issue, given the differences in energy density between ethanol and methanol. Thus, methanol would have to be limited to lower levels, such as M67.5 or E42.5/M28.5/G29, to achieve the same air-fuel ratio as for E85. Given the limitations with potential use of methanol in E85 FFVs, it appears

unlikely that such an application would be practical for fleet wide use in the foreseeable future.

Interest in the use of methanol for a transportation fuel gained impetus in the 1970s in response to oil shortages. The State of California, as part of its Methanol Fuel and Vehicle Program, ran an experimental test program over the course of the 1980s and 1990s to evaluate the potential of methanol-fueled vehicles. This included dedicated methanol (M100) vehicles and flexible fuel vehicles designed to run on mixes of up to 85% methanol with gasoline. Some of the early M100-fueled light-duty vehicles initially used fuel with 5.5% isopentane. Subsequently, methanol with 10% gasoline, and still later methanol with 15% gasoline were used. M85, or the mixing of methanol with 15% gasoline, was eventually selected as the primary higher methanol blend ratio for several reasons, including safety considerations and considerations related to luminosity and vapor space flammability. M85 is also the blend level where the Reid Vapor Pressure was equal to that of gasoline, typically 7-9 psi at that time. This was also the limit that received a halving of California's gas tax. A summary of some early methanol demonstration programs is provided in Nichols (2003) and Ward and Teague (1996). The California program involved demonstrations with over 900 vehicles of 16 different models operated by 90 participating fleets, and led to the development of commercially available methanol/gasoline vehicles from Ford, General Motors, and Chrysler (MacDonald, 2005). Between 1987 and 1999, over 17,000 methanol FFVs and hundreds of transit buses and school buses were sold in California (Dolan, 2008).

These early programs had some success with the use of methanol-fueled vehicles, but over the years the use of methanol and deployment of methanol-fueled vehicles has declined significantly. A number of factors contributed to the significant decline in methanol fuel use, including a growth in interest in natural-gas-fueled vehicles for air quality improvement, increasingly cleaner gasoline vehicles, the discontinuation of the California's methanol program, declines in petroleum prices, a lack of methanol industry support, and a growth in the ethanol industry. The growth in the ethanol industry was supported by the farming community, government subsidies, and opportunities to take advantage of CAFE credits and nationwide marketing (Nichols, 2003; MacDonald, 2005). With the decline in interest in methanol, no methanol FFVs have been produced in the US since 1999. A network of 60 public retail stations and 45 private fleet stations was put in place in California during the time of its Methanol Fuel and Vehicle Program (Dolan, 2008). It is doubtful that any of these stations remain in use at this point, and the Alternative Fuels & Advanced Vehicle Data Center (AFAVDC, 2009) is not maintaining records relating to methanol stations, as it does for the other alternative fuels.

Methanol use has grown in China (Dolan, 2008; Lynn, 2009; Methanol Fuels, 2014). Nationwide in China, 160,000 vehicles have been modified already to run on methanol fuel blends. As of 2013, methanol represented 8% of China's fuel supply, and as of 2014, 15 Chinese provinces and cities have issued and implemented 29 local standards for methanol fuel, and a national M15 standard has been drafted. Many methanol fuel demonstrations have been conducted in coal producing provinces, such as Xinjian, Shanxi, Shaanxi, Henan, Inner Mongolia, Beijing Shi, Hebei, Anhui, Guangdong and Sichuan. M15 has been used at varying levels throughout the Shanxi Province since 2003. M100 has also been used in demonstrations in 200 buses and 1,000 taxis in Shanxi Province. China's Ministry of Industry & Information Technology (MIIT) conducted a two-year pilot program from 2012-2014 on methanol-fueled vehicle development in Eastern Shanghai, Shanxi and Shaanxi Provinces

(Methanol Fuels, 2014). MIIT plans to expand its pilot program from 435 vehicles in 2012-2014 to an additional 1,800 vehicles in 11 cities in Guizhou and Gansu provinces in the coming years. During the 2012-2014 pilot program, five automakers (Geely, Shaanxi Tongjia, Shanxi Victory, Zhengzhou Yutong and Shangxi Auto) released five categories of methanol-fueled vehicles, including M100 cars, M100 micro vans, M100 van trucks, M100 public buses, and methanol/diesel heavy trucks. At least 286 of 435 methanol vehicles produced have been put into circulation, including 168 taxis, 98 inter-city coaches, 15 light van trucks, and five dual-fuel trucks.

Environmental Considerations with the Use of Methanol as a Transportation Fuel

A number of studies have evaluated the emissions impacts of using methanol as a vehicle fuel. The vast majority of studies have shown that the use of methanol fuel generally results in lower CO, THC, and smoke emissions. However, methanol can produce more toxic pollutants such as formaldehyde and unburned methanol. A number of early studies were conducted in the 1990s as part of the Auto/Oil AQIRP program and as part of demonstration under the Alternative Motor Fuel Act of 1988 (Gorse, Benson, Burns, & Hochhauser, 1992; Burns, William, Benson, Gorse, & Rutherford, 1994; Kelly, 1994; Kelly et al., 1996). Zhao et al. (2010) studied the criteria and carbonyl compound emissions from two modern passenger cars equipped with three-way catalysts (TWCs) and fueled with pure methanol (M100) and 15% methanol-gasoline blend, over the New European Driving Cycle. They found reductions in THC and CO emissions, ranging from 9-21% and 1-55%, respectively, and increases in NO_x emissions ranging from 175-233%, with larger changes seen in the higher methanol fraction fuel blend. Compared to gasoline fuel, formaldehyde emissions with M15 and pure methanol were two and four times higher, respectively, while acetaldehyde emissions decreased with methanol. Shenghua et al. (2007) studied the performance and emissions of a PFI engine fueled with low-level blends of methanol in gasoline. They found that the engine power and torque decreased with an increasing fraction of methanol in the fuel blends under wide-open throttle conditions. They also found reductions in CO and THC emissions, increases in unburned methanol and formaldehyde emissions, and little changes in NO_x emissions upstream of the TWC with the methanol blends. A summary of the environmental studies on methanol as a transportation fuel are listed in the Table 6.

Development and Use of DME as a Transportation Fuel

DME Production

DME is the simplest ether and it is used as a precursor to other organic compounds and as an aerosol propellant. The Global Dimethyl Ether Market was valued at US\$ 4.46 Bn in 2013 and is likely to reach US\$ 8.37 Bn in 2020, expanding at a compound annual growth rate (CAGR) of 9.4% between 2014 and 2020. The DME industry in China has expanded considerably, since China has enormous coal reserves and coal is the primary feedstock used to produce DME. DME consumption in the China is predicted to grow at an average CAGR of around 10.6% from 2013 to 2023, with the potential for this growth to increase to over 20.0% after 2018 (Markets and Markets, 2013). Since 2006, the large Chinese investment program in methanol and dimethyl ether has created an installed capacity of 6,500,000 tons

per year (tpy), or about 85% of worldwide production. DME production in China has grown from an annual capacity of 22,000 tons in 2001 to 12 million tons in 2012, with production itself increasing from 10,000 tons to 4.25 million tons over the same time period (Taupy, 2012). DME is typically synthesized by the dehydrogenation of methanol. DME is typically synthesized by the dehydrogenation of methanol. This is usually a two-step process in which methanol is first produced from a synthesis gas and purified. This gas is then converted to DME in a second reactor using a catalyst that dehydrates the methanol into a mixture of DME, methanol, and water. An alternative to this two-step process for DME production (syngas to methanol, followed by methanol to DME) is a one-step process to convert syngas directly to DME using a “bifunctional” catalyst that can perform both the syngas to methanol and methanol to DME reactions in the same process vessel (Kang, Bae, Kim, Dhar, & Jun, 2010). A number of companies have been developing one-step DME production, including Haldor Topsoe (Denmark), JFE Holdings (Japan), Korea Gas Corporation (Korea), Air Products, NKK, Toyo, MGC, Lurgi and Udhe (Azizi, Rezaeimanesh, Tohidian, & Rahimpour, 2014). DME can also be made from renewable feedstocks. A demonstration gasification DME production plant by Chemrec began operation in Piteå, Sweden, that uses black liquor from pulp production as its main feedstock. In the U.S., Oberon (2015) has been producing DME at a small scale production plant in the Imperial Valley in California. The Oberon process has a nameplate capacity of 4,500 gallons per day and can use a variety of renewable and nonrenewable feedstocks, including shale gas and biogas from animal, food, and agricultural waste.

Utilization of DME as a Transportation Fuel

DME has a number of unique characteristics, so diesel vehicles must be designed or modified to use it as a transportation fuel. DME is a gas at ambient pressure and temperature (like LPG), and the liquefied DME fuel has extremely low lubricity and low viscosity. As a consequence, the fuel injection system for DME must be able to handle high vapor pressure, high compressibility, and low viscosity (Hansen & Mikkelsen, 2001). There are also lubrication issues with DME that will result in premature wear and eventual failure of pumps and fuel injectors if not addressed. In addition, DME is not compatible with most of the elastomers, and may dissolve the elastomers in the engine and fuel delivery system after prolonged exposure. DME is typically stored as a liquid, under conditions similar to LPG. Since the energy content of DME is about 65% of petroleum diesel, the size of fuel storage tanks in vehicles has to be enlarged for a DME vehicle to have a range comparable to a traditional diesel vehicle. The storage is typically done at pressure of 75 psi. Presently, DME vehicles have only been developed at a demonstration level, as discussed below, and currently no commercial DME vehicles are available.

Table 6. References for Environmental Considerations with the Use of Methanol as a Transportation Fuel

Author	Vehicle/Engine	Fuel	Notable Results
Burns et al., 1994	A fleet of 1993 production flexible/variable-fueled vehicles	Reformulated Gasoline and Methanol Blends	1. FTP exhaust and reactivity weighted emissions were lower by 18 to 32% with Phase 2 gasoline relative to industry average gasoline.
			2. With the exception of greater NMOG emissions with the M85 blends, and lower OMHCE emissions with M85 blended with industry average gasoline, exhaust organic emissions, CO and NOx with the methanol fuels were not significantly different than their base gasolines.
			3. M85 reactivity weighted emissions were lower by 25 to 32% than industry average gasoline, but were not significantly different from Phase 2 gasoline using both photochemical mechanisms and reactivity scales.
			4. Exhaust specific reactivity was lower by 50 to 55% for the M85 blends relative to gasoline, and by 6% to 8% for Phase 2 gasoline relative to industry average gasoline.
			5. Benzene and 1,3-butadiene were lower by 44 to 80% with Phase 2 gasoline relative to industry average and with the M85 blends relative to their base gasolines. Formaldehyde increased ten-fold with M85 fuels relative to base gasolines. Lower benzene and 1,3-butadiene emissions drove aggregate toxics lower by 40% with Phase 2 gasoline relative to industry average gasoline, while the increase in formaldehyde drove M85 aggregate toxics significantly greater by 57 to 146% relative to the gasolines.
			6. Hot soak evaporative organic emissions were marginally lower with Phase 2 gasoline relative to industry average, but were greater with the M10 and M85 blends relative to gasoline. Hot soak benzene tracked fuel benzene levels and was lower with Phase 2 gasoline and M85.
			7. Exhaust emissions and ozone-forming reactivity in the 1993 FFV/VFV fleet were nearly equivalent to the levels reported for the 1993 California Tier 1 gasoline fleet with Phase 2 gasoline.
Gorse et al., 1992	19 early prototype flexible/variable fueled vehicles (FFV/VFV)	Methanol/Gasoline Blends (industry average gasoline (M0), and 85% methanol-gasoline blend (M85), and a splash-blend of M85 with M0 (gasoline) giving 10% methanol (M10))	1. M0 and M10 emissions were very similar except for elevated M10 evaporative emissions resulting from the high M10 fuel vapor pressure.
			2. M85 showed lower exhaust emissions than M0 for NMHC (non- methane hydrocarbon), OMHCE (organic material hydrocarbon equivalent), CO and most species.
			3. M85 had higher exhaust emissions for NMOG (non- methane organic gases), NOx, methanol and formaldehyde.
			4. M85 had lower diurnal emissions, higher running loss emissions and higher hot soak OMHCE and NMOG than M0.

Table 6. (Continued)

Author	Vehicle/Engine	Fuel	Notable Results
			5. M85 showed 50% reductions in exhaust and evaporative ozone forming specific reactivities (grams ozone per gram NMOG) and also ozone forming potential (grams ozone per mile) relative to the M0 fuel.
Kelly, 1994	318 1991-1994 model alternative fuel vehicles	85% alcohol/15% gasoline, 50% alcohol/50% gasoline, and reformulated gasoline	The I/M240 test is not an appropriate comparison to the FTP. Further, the I/M240 test is not as reliable as the FTP in estimating the “real world” emissions of these relatively low-emission vehicles.
Kelly et al., 1996	71 flexible fuel M85 1993 Dodge Spirits, 16 flexible fuel 1994 M85	Fuels consisting of 85% methanol to 15% gasoline (M85), 50% methanol to 50% gasoline (M50), and	1. There appeared to be a small drop in NMHCs and CO, and an increase in NOx for M85 compared to the same vehicles tested on RFG.
			2. The OFP (expressed in grams of ozone per mile) from the M85 tests was 40% to 50% lower than the RFG tests performed on the Dodge Spirits and Ford Econoline vans.
			3. The M85 tests also showed lower levels of benzene and 1,3-butadiene, but increased formaldehyde.
	Ford Econoline Vans, and a similar number of standard gasoline Dodge Spirits and E150 Ford Econoline Vans	California Phase 2 reformulated gasoline (RFG)	
Shenghua et al., 2007	3-cylinder port fuel injection engine	Fuel of low fraction methanol in gasoline	Reductions in CO and THC emissions, increases in unburned methanol and formaldehyde emissions, and little changes in NOx emissions were found upstream of the TWC with the methanol blends.
Zhao et al., 2010	2 passenger cars	Methanol/gasoline blends (M15 and M100)	1. When cars were fueled with methanol/gasoline blends, CO and THC emissions decreased by 9–21% and 1–55% respectively, while NOx emissions increased by 175–233%
			2. Compared with gasoline vehicles, formaldehyde emissions with M15 and M100 were two and four times higher, respectively, and total carbonyls with M15 and M100 increased by 3% and 104%, respectively.
			3. With the use of the new TWC, both regulated gas-phase pollutants and formaldehyde decreased.

In the U.S., DME has obtained an official fuel specification and approvals to be sold as a fuel by the U.S. EPA. In February of 2014, an ASTM specification for DME was published under ASTM D7901 (Standard Specification for Dimethyl Ether for Fuel Purposes). The ASTM specification (see feature below) provides guidance for fuel producers, engine and component suppliers, and infrastructure developers on DME purity, testing, safety, and handling. In September of 2014, the U.S. EPA declared that DME produced from biogas and other renewable sources by Oberon Fuels qualifies for inclusion under the Renewable Fuel Standard (“RFS”). Oberon’s biogas-based DME is now eligible under the Clean Air Act for high value cellulosic biofuel (D-code 3) and advanced biofuel (D-code 5) renewable identification numbers (“RINs”) under the RFS. The California Department of Food and Agriculture’s (CDFA’s) Division of Measurement Standards (DMS) has approved DME’s use as a vehicle fuel. The regulation, Specifications for Dimethyl Ether Used in Compression Ignition Engines, proposed in July 2014, was approved and became effective in 2015. The California Air Resources Board (CARB) has also published its Multimedia Evaluation Tier I on DME, the first of three parts of the “multimedia risk assessment” required by the state before new fuel specifications can be adopted (McKone et al., 2015). DME is also subject to 13 CCR 2293, et seq., “Commercialization of Alternative Diesel Fuels.”

Since DME has similar properties to LPG, it can be handled and distributed using methods similar to those required for LPG, and with some of the LPG infrastructure. The distribution of DME can follow the platform of transporting LPG using ocean-based and land-based LPG infrastructures. Existing LPG refueling stations can be converted to DME refueling stations with minor modifications to the pumps, seals, and gaskets (Semelsberger, Borup, & Greene, 2006). Currently, there are 3,174 LPG refueling stations in the US and 353 stations in California (U.S. DOE, 2015b).

China has been running demonstrations with DME vehicles for over a decade and has also developed different specifications for DME fuel use. The fuel and associated specifications include a national DME fuel standard, different standards for engines and parts, and various local standards (Huang et al. 2010). Some of the first demonstrations of DME vehicles were done in China dating back to the mid-1990s (Taupy, 2012). Researchers from Shanghai Jiao Tong University (SJTU) and Xi’an Jiao Tong University (XJTU) have developed buses powered by DME. In Shanghai, a fleet of at least 10 buses has been demonstrated for a period of over 220,000 miles of operation (Huang, Zhang, Fang, & Qiao, 2010). In 2006, several DME bus demonstration projects were carried out in Shanghai and the Shandong province to evaluate the feasibility of DME as a transportation fuel. The world’s first commercial DME filling station was also built in Shanghai to supply the bus line. The demonstration was done in stages to ensure the buses would operate safely. The first bus was demonstrated on the SJTU campus. Then, two buses were demonstrated on the Shanghai No. 147 route. The demonstration was then increased to 4, 6, 8 and then 10 buses. The demonstration has been successful, as the vehicles did not experience any obvious technical troubles during the demonstration period. Researchers at SJTU have also been working on further development of a dedicated DME engine (Huang et al., 2010). The Shanghai Automobile Corporation has also been involved in the development of DME engines and vehicles (Taupy, 2012).

Japan has also been developing DME production and DME vehicles. Japan DME Ltd built a DME production pilot plant and carried out a feasibility study for production of 5,000 tons per day (tpd) in 2006. A group named DME Promotion Venture, including MGC,

ITOCHU, JAPEX, Taiyo Oil, Total, etc, established a joint-venture DME production plant with a capacity of 80,000 tpd that began operation in 2008 (Ishiwada, 2011). With financial support from the Japanese government, a number of diesel vehicle manufacturers, like Nissan Diesel, Hino Motors, Isuzu, and Mitsubishi Motors, were involved in developing DME-fueled, heavy-duty vehicles (Bourg, 2006). Demonstration vehicles have included a medium-size bus, a medium-duty crane truck, three other medium-duty trucks, and a couple of light-duty trucks developed by Isuzu; a microbus and a light-duty truck developed by the National Institute of Advanced Industrial Science and Technology and Iwatani Corporation, etc., in 2003; an 8-ton-GVW medium-duty truck developed by the DME Vehicle Practical Application Research and Development Group; and a 20-ton-GVW heavy-duty truck and a sprinkler truck developed jointly by National Traffic Safety and Environment Laboratory and Nissan Diesel Motor (now, UD Trucks Corporation) in 2004 (Japan DME Association, 2015).

Volvo in Sweden has been actively developing bio-DME vehicles. Volvo Trucks conducted multiple comprehensive customer-based field tests using bio-DME in 2007. Some of the earlier demonstrations ran into technical issues (Volvo Powertrain Sweden) that were resolved in the later demonstrations. Between 2010 and 2012, Volvo partnered with the EU, the Swedish Energy Agency, fuel companies and the transport industry to test Volvo FH trucks powered by bio-DME. Testing was done at four locations in different parts of Sweden to investigate the potential for full-scale investment in bio-DME as a transportation fuel. The demonstration included 10 trucks and accumulated at least 1.2 million kms (McLaughlin, 2013). Four DME refueling stations were built by a fuel company called Preem to support the demonstration project at various locations around Sweden. These demonstrations were tied to the Chemrec DME production plant in Piteå, Sweden, under the BioDME project. The goal of this project was to demonstrate the full range of technologies that would be used for bio-DME, from fuel production, distribution and refueling, to fuel utilization.

Some efforts for DME demonstrations are also ongoing in North America. In 2013, Volvo introduced 4 prototype DME trucks in the U.S. and announced plans to begin commercial offerings of DME trucks beginning in 2015 (Volvo, 2014). This included testing of one of the trucks by Oak Ridge National Laboratory (ORNL) and one by Pennsylvania State University (PSU) (Szybist, McLaughlin, & Iyer, 2014). PSU also conducted one of the first DME vehicle demonstrations with a shuttle bus in the early 2000s in collaboration with Air Products and Chemicals, Inc., and with support from the U.S. Department of Energy National Energy Technology Lab (Bhide et al., 2002; Eirich et al., 2003). Oberon has also received a grant to test two heavy-duty Volvo trucks powered by DME, in conjunction with Safeway. The trucks will be operated out of the Tracy, CA, Safeway distribution center located in the San Joaquin Valley. There is also a bio-DME demonstration project in Vancouver using a 2011 Ford F150 light-duty truck, which includes the City of Vancouver, Technocarb for the vehicle modifications, and NextGen Integrated Engineer for the fueling system.

Environmental Considerations with the Use of DME as a Transportation Fuel

DME fuel is advantageous in compression ignition engines, with an oxygenated molecular structure composed of an oxygen atom between two methyl radicals. Due to the absence of direct carbon-carbon (C-C) bonding, DME can drastically reduce or suppress the formation and development of soot during combustion, while still providing conventional diesel-like thermal efficiency. In addition, DME has good ignition capability in engines due

to its high cetane number (55-60), and the high latent heat of DME fuel leads to lower cylinder temperature of air-fuel mixtures early in the combustion phase. DME also has good atomization properties due to its low boiling point (248 K). DME is a volatile organic compound, but is non-carcinogenic, non-teratogenic, non-mutagenic, and non-toxic. NO_x emissions are generally lower with DME than with diesel fuel, which is attributed to the shorter ignition delay for DME than for diesel, the smaller amount of fuel injected during the ignition delay period, and the smaller amount of fuel burned during the pre-mixed burning phase. Moreover, the higher latent heat of evaporation of DME is beneficial to NO_x reduction, due to the larger temperature drop of the mixture in the cylinder. The low HC and CO emissions with DME are mainly due to the low C/H ratio, the lack of C-C bonds, and the high oxygen content of the fuel, which promotes faster and more effective oxidation of intermediate species (Arcoumanis, Bae, Crookes, & Kinoshita, 2008).

A number of researchers have worked in the development of DME engines. Researchers at SJTU have conducted a number of studies on DME engines. They have conducted studies of a Euro IV DME engine and implemented modifications such as on-line reforming and a DME De-NO_x control system with low-temperature catalyst (LTC), delaying the injection timing to 5°CA below top dead center (BTDC), and using exhaust gas recirculation (EGR) with a two-stage intercooler (Huang et al., 2010). Volvo has done a considerable amount of development of DME engines for commercial use (McLaughlin, 2013). Researchers at Chalmers University of Technology in Gothenburg, Sweden have done a number of studies of DME combustion in engines. Salsing (2011) found that combustion of DME in a diesel engine could be significantly improved by using a piston design that promotes flame spread, a nozzle configuration that improves mixing late during the diffusion combustion, and raising the injection pressure to promote faster mixing and combustion and lower CO emissions. Salsing and Denbratt (2007) showed that DME engines can utilize more aggressive measures to reduce NO_x emissions, such as retarding combustion phasing and high levels of EGR. Since DME does not produce PM, as such, there is no PM/NO_x tradeoff. Dr. Andre Boehman and his colleagues at PSU and the University of Michigan have also conducted considerable research in DME combustion, emissions and engine performance, and with DME vehicle demonstrations (Bhide et al., 2002, 2003; Boehman, 2008; Chapman, Boehman, Tijm, & Waller, 2003; Eirich et al., 2003).

Several studies have also evaluated the emissions and performance of DME vehicles. Researchers at ORNL and PSU conducted an evaluation of a DME-fueled, heavy-duty truck compared to a baseline diesel truck on a chassis dynamometer (Szybist et al., 2014). The DME truck was equipped with a 3-way catalyst, but was not equipped with a diesel particle filter (DPF) or lean NO_x aftertreatment. Emissions measurements for the prototype DME truck were below the expected level for vehicles meeting Euro V emissions for NO_x, PM, CO, and HC, consistent with the engine calibration. PM emissions were at least an order of magnitude below the 2010 U.S. emission standard and were near the measurement detection limits, without the use of a DPF. Some high spikes were observed during transient parts of the cruise cycle for unburned HC and CO emissions for the prototype DME truck. These emissions spikes did not lead to overall excessive emission levels, but suggest that further reductions in emissions and fuel consumption could be obtained with further hardware and controls development. The diesel-equivalent fuel economy of the prototype DME truck was 5.3 mpg, compared to 6.0 mpg for the baseline diesel truck. The authors suggested that this could be due to differences in the powertrains of the vehicles, with the diesel truck having a

single-drive axle compared to the DME truck with two drive axles, and that the engine efficiencies for the DME and diesel engines were similar. Nylund and Koponen (2012) conducted a study that included chassis dynamometer testing on a number of vehicle configurations at VVT in Finland and in Canada with collaboration between a number of different agencies. The test vehicles included a number of different conventional diesel technologies, diesel hybrids, alternative diesel fuels such as GTL, hydrotreated vegetable oil (HVO) renewable diesel, biodiesel, and a single prototype DME truck that was tested at VVT. The prototype DME truck showed NO_x emissions below Euro II and Euro III buses and comparable to the selective catalytic reduction (SCR)-equipped diesel vehicles. PM emissions were low for the DME truck compared to the diesel buses, as were PM emissions from a number of the other alternative technologies. Energy consumption and CO₂ emissions for the DME prototype were below those for most of the conventional-diesel and alternative-fuel technologies, but not those of a light weight bus and the hybrid buses. Additionally, on a LCA basis, GHGs for biomass-derived DME were near zero and considerably better than most of the other alternative technologies.

In other research, Xinling and Zhen (2009) studied the emission reduction potential from a medium-duty, direct injection, turbocharged diesel engine fueled with conventional diesel fuel, GTL, and DME. They found that DME significantly increased power and torque compared to diesel, as well as significantly reduced regulated emissions of HC by 40%, NO_x by 48%, and was smoke-free throughout all the engine conditions. However, particle-number emissions for DME were found close to that for diesel. Generally, the increased particle-number emissions with DME may be due to the fact that the number of accumulation-mode particles is very low due to the oxygen content and the absence of C-C bonds. This promotes the processes of nucleation and condensation of the semi-volatile compounds in the exhaust gas, and thus, more nucleation-mode particles are produced. Sidhu et al. (2001) conducted experiments with DME, CNG, biodiesel, and diesel fuels in a single-pulse shock tube, which was used to simulate CI combustion conditions. They found that DME yields a much lower particulate mass, but a higher soluble organic fraction (SOF) compared to diesel fuel. Jie et al. (2010) studied the effect of pure DME on a direct injection diesel engine and they found reduced CO and NO_x but increased formaldehyde emissions compared to diesel fuel, and almost no smoke emissions for DME.

GHG emissions from DME applications have also been evaluated. The EPA's analysis determined that biogas-based DME produced using the Oberon process resulted in an approximate 68% reduction in greenhouse gases when compared to baseline diesel fuel. The determination confirms that renewable DME produced using biogas from landfills, municipal wastewater treatment facility digesters, agricultural digesters, separated MSW digesters, and cellulosic components of biomass processed in other waste digesters, through the Oberon pathways, qualifies for cellulosic biofuel RINS. Renewable DME produced from biogas from waste digesters processing renewable biomass that is assumed to be non-cellulosic, through the Oberon pathways, qualifies for advanced biofuel RINs. Studies conducted using the CA-GREET model found a carbon intensity of $-5 \text{ gCO}_2\text{e/MJ}_{\text{fuel}}$ for the Oberon process, but DME produced from fossil fuel natural gas sources was found to have a carbon intensity of $91.1 \text{ gCO}_2\text{e/MJ}_{\text{fuel}}$, which is only slight below that of baseline diesel fuel (McKone et al., 2015). A summary of the environmental studies on DME as a transportation fuel are listed in the Table 7.

Table 7. References for Environmental Considerations with the Use of DME as a Transportation Fuel

Author	Vehicle/Engine	Fuel	Notable Results
Arcoumanis et al., 2008	Compression-ignition engines	DME	DME has comparable output performance to a diesel fuel engine, but with lower PM emissions.
Bhide et al., 2003		DME-diesel blend	<ol style="list-style-type: none"> 1. A methodology was developed to utilize a high-pressure capillary viscometer to measure the viscosity of pure DME and blends of DME and other compounds in varying proportions and at pressures up to 3500 psig. 2. While DME is miscible in diesel fuel at any mixture fraction, when the blend is held under pressures of 75 psi or above, the viscosity of the blends is below the ASTM diesel fuel specification for even a 25 wt % blend of DME in diesel fuel.
Chapman et al., 2003	Multi-cylinder Navistar 7.3L Turbodiesel engine	DME-diesel blend	DME can reduce the PM emissions from a compression ignition engine. However, the NOx emissions were not favorable for all conditions.
Eirich et al., 2003	7.3-liter turbodiesel engine in a campus shuttle bus	DME-diesel blend	<ol style="list-style-type: none"> 1. DME was blended with diesel fuel to provide sufficient viscosity and lubricity to permit operation of a 7.3-liter turbodiesel engine in a campus shuttle bus with minimal modification of the fuel injection system. 2. A significant challenge is posed by the rapid increase in DME vapor pressure with increasing fuel temperature.
Huang et al., 2010	Euro IV DME engine	DME	<ol style="list-style-type: none"> 1. Significant reductions in CO, HC, PM emissions and little reduction on NOx emissions. 2. Summary of recent progress of Shanghai DME bus demonstration.
Jie et al., 2010	A direct injection diesel engine	DME	Reduced CO and NOx but increased formaldehyde emissions were found for DME compared to diesel fuel, and almost no smoke emissions were seen for DME.
Nylund & Koponen, 2012	Different conventional diesel technologies, diesel hybrids, alternative diesel fuels such as GTL, Hydrotreated vegetable oil (HVO) renewable diesel, biodiesel, and a single prototype DME truck	DME	<ol style="list-style-type: none"> 1. A prototype DME truck showed NOx emissions below Euro II and Euro III buses and comparable to SCR-equipped diesel vehicles. 2. PM emissions were low for the DME truck compared to the diesel buses, as were PM emissions from other alternative technologies. 3. Energy consumption and CO₂ emissions for the DME prototype were below those for most of the conventional-diesel and alternative-fuel technologies, but not those of a light weight bus and the hybrid buses.

Table 7. (Continued)

Author	Vehicle/Engine	Fuel	Notable Results
Salsing & Denbratt, 2007	Single-cylinder heavy duty engine	DME	1. DME combustion does not produce soot and with the use of exhaust gas recirculation NO _x emissions can also be reduced to very low levels.
			2. High injection pressure and/or a DME-adopted combustion system is required to improve the mixing process and thus reduce the combustion duration and CO emissions.
Salsing, 2011	Single-cylinder heavy duty engine	DME	The combustion system for DME can be considerably improved by using a piston design or a nozzle configuration. These modifications result in significantly reduced exhaust emissions and increased engine efficiency.
Sidhu et al., 2001	A single-pulse shock tube	DME, CNG, biodiesel, and diesel fuels	DME yields much lower PM mass, but a higher soluble organic fraction (SOF) compared to diesel fuel.
Szybist et al., 2014	Prototype DME truck, Heavy Heavy-Duty Diesel Truck	DME	1. A prototype DME truck was calibrated to meet the Euro V emission standards, and the emission measurements confirmed that NO _x , PM, CO, and HC were below the expected level for vehicles meeting Euro V emissions.
			2. PM emissions were at least an order of magnitude below the 2010 U.S. emission standard, and were near the measurement detection limits, without the use of a DPF.
			3. NO _x emissions reductions are feasible with the use of NO _x aftertreatment, a pathway which could also enable higher efficiency combustion strategy.
Xinling & Zhen, 2009	Medium-duty, direct injection, turbocharged diesel engine	Conventional diesel fuel, GTL, and DME	1. DME significantly increased power and torque compared to diesel, as well as significantly reduced regulated emissions of HC by 40%, NO _x by 48%, and was smoke-free throughout all the engine conditions.
			2. PM emissions for DME were found close to those for the diesel fuel.

FISCHER-TROPSCH, GTL, AND RENEWABLE DIESELS AS TRANSPORTATION FUELS

Fischer-Tropsch, GTL, and Hydrogenated Renewable Diesel Fuel Production

The Fischer-Tropsch (FT) process is one technology that can be used to make diesel fuel from biomass. FT technology was originally developed in the 1920's, and has been commercialized in gas and coal to liquid facilities in Germany, Malaysia, South Africa, and Qatar. There are also a few projects either in-place or being developed for producing FT fuels from biomass (European Biomass Technology Platform, 2015). One active plant is the bioliq® pilot plant at Karlsruhe Institute of Technology (KIT), which is running successfully and has all stages of the process interconnected. Other projects are in various stages of planning or development. This includes Greensky in Thurrock, Essex; BioTfuel in France; the Air Liquide and CEA SYNDIÈSE-BtS project in Bure-Saudron; a 10-MMgy Sierra BioFuels facility with Fulcrum Bioenergy, Inc.; Cool Planet's 'Reformate' commercial facility in Louisiana, US; a facility by Red Rock Biofuels using Velocys Fischer-Tropsch technology; the UPM Stracel BTL project to develop a plant on UPM's Strasbourg site; and an AJos BtL project in northern Finland. Additionally, what was to be the world's first commercial BTL plant in Frieberg Saxony, utilizing the Choren Carbo-V ® Process, was discontinued when Choren filed for insolvency in 2011. A schematic of the BTL production process is shown in Figure 4.

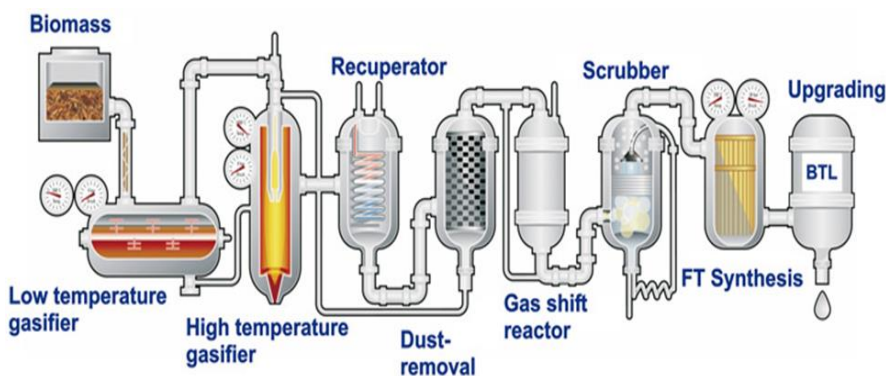


Figure 4. BTL Production Process Scheme.

Gasification can also be used to make renewable fuels. In the gasification process, high temperatures, with a controlled amount of oxygen, hydrogen, steam, and/or steam/hydrogen (termed partial oxidation, hydrogasification, steam gasification, and steam hydrogasification, respectively (Norbeck, Park, & Raju, 2008)) are used to convert carbonaceous materials to a synthesis gas. The synthesis gas from gasification can be utilized for the production of diesel or jet fuel via a Fischer-Tropsch (F-T) process; ethanol via catalysis or fermentation; or methanol, DME, or "green gasoline" from a methanol intermediate. The primary advantage of gasification is that it can utilize a very wide range of feedstocks compared to other processes. This includes a wide variety of biomass, coal or petroleum products, and a broader range of

MSW than biochemical processes. Gasification is a complex, expensive, and energy intensive process, so it is typically done in large scale applications, although some processes can be more optimized for small scale applications.

Renewable diesel fuels can also be produced via more traditional refinery approaches, such as hydrotreating. Hydrotreating is a process typically used to remove sulfur impurities from diesel fuel (as well as reduce unsaturates). Hydrogenated renewable diesel (HDRD) can be produced with a hydrotreating unit that is dedicated to the processing of only vegetable or animal oil feedstocks, or where oils or fats are coprocessed with the diesel distillate fractions derived from petroleum. A schematic of the HVO renewable diesel production process is shown in Figure 5.

The primary limitation for renewable diesel production is the cost. The coupling of high feedstock costs with production costs has not made the commercialization of hydrogenated renewable diesel cost competitive in the U.S. to date. There are currently several facilities producing renewable diesel fuels on a commercial basis around the world. The process has been commercialized in Europe, where economic considerations such, as higher fuel costs or government incentives, are more favorable. Neste Oil has one of the most advanced renewable diesel programs, with two production units having a capacity of 190,000 tpy in Porvoo, Finland, commissioned in 2007 and 2009, respectively; an 800,000-tpy facility in Singapore, commissioned in 2010; and an 800,000-tpy facility in Rotterdam, commissioned in 2011. Neste Oil is currently the largest producer of renewable fuels in the world, with an annual production output of over 2 million tons. Other manufacturers that are developing and testing HDRD refining processes include ConocoPhillips, Petrobras, UOP/ENI, REG Synthetic Fuels (who has acquired Syntroleum), Valero, UPM Biofuels, and Diamond Green Diesel.

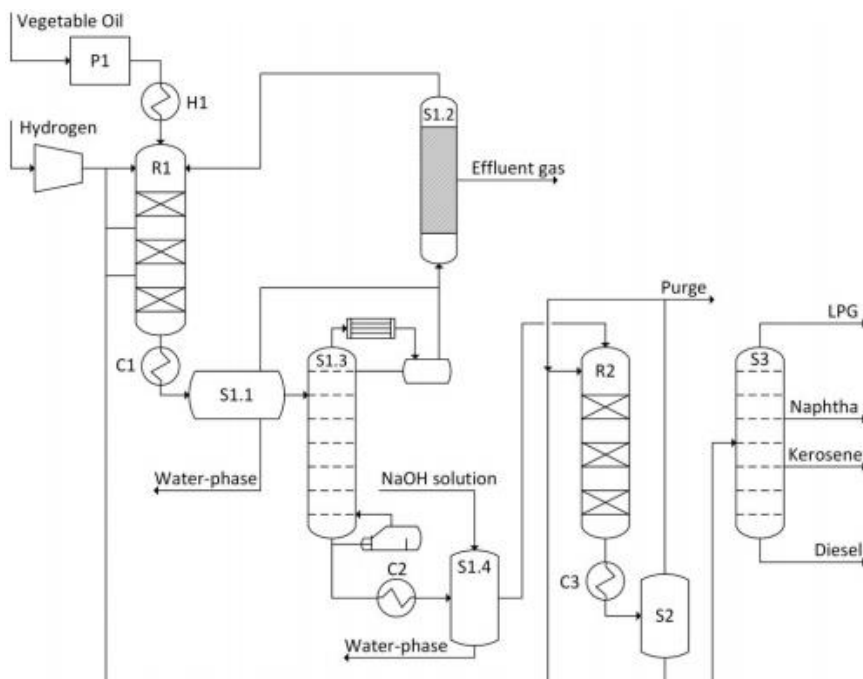


Figure 5. HVO Production Process Scheme.

Utilization of FT, GTL, and Hydrogenated Renewable Diesel Fuels for Transportation

An important issue with biomass to liquid fuels is that the final product fuels must meet the requirements for more traditional transportation fuels. These issues are specific to the particular type of fuel being produced.

F-T diesel is produced such that it can replace petroleum diesel without modification of the vehicles or refueling infrastructures. F-T diesel is predominantly normal and iso-paraffins, with low sulfur levels, a high cetane number, low density, and very good flow properties (Waterland, 2006). These characteristics provide good engine performance and generally reduced emissions. As it has similar properties to conventional diesel, the distribution of F-T diesel would not require new or modified pipelines or storage tanks. The lower density for the F-T diesel provides a slightly higher net heat of vaporization on a mass basis (2-3% higher), but a lower heat of combustion on a volume basis (3-7% lower) (Smagala et al., 2013). The very low aromatic content and near zero sulfur content of F-T diesel results in a low lubricity. A lubricity additive is typically used with F-T diesel to prevent excessive wear of fuel injectors and other related parts. The cold flow properties of F-T diesels can also be poor due to its paraffinic nature (Alleman & McCormick, 2003), but the cloud point can be lower by increasing the degree of isomerization for the paraffins, while still providing relatively high cetane numbers (Smagala et al., 2013). Currently, F-T diesel is usually used as blend stock for petroleum diesel. The cost of distribution of F-T diesel blends would be similar to that of petroleum diesel.

Hydrogenated renewable diesel can be produced with a hydrotreating unit that is dedicated to the processing of only vegetable or animal oil feedstocks or where oils or fats are coprocessed with diesel distillate fractions derived from petroleum. Hydrogenated renewable diesel has a chemical structure similar to petroleum-based diesel, in contrast to biodiesel that is derived by the transesterification processes. For a dedicated facility, the fuel properties of hydrogenated diesel are similar to those of a synthetic GTL or Fischer-Tropsch fuel, in that it is largely paraffinic in nature as discussed above. This includes a high cetane number, low aromatic content, and ultra-low sulfur content, which provide for better vehicle performance with lower emissions than traditional petroleum diesel fuels. Renewable diesel can have a more narrow carbon number distribution ($\sim C_{15}$ to C_{18}) compared to a broader carbon number distribution for F-T diesel ($\sim C_{10}$ to C_{25}) (Smagala et al., 2013). Subtle differences between different renewable diesel fuels can be attributed to differences in reaction conditions, particularly temperature and catalyst type, and feedstock characteristics. Hydrogenated renewable diesel can meet the ASTM-D975 specifications for diesel fuel, and hence could be used in the existing pipelines, refueling stations, and vehicles currently using conventional diesel. Hydrogenated renewable diesel can be used alone or blended with petroleum diesel.

Biofuels produced via the BTL, GTL, or HVO processes are also the most realistic biofuel options for providing renewable jet fuels, as the biofuel replacement must be as close to the existing petroleum-based jet fuel as possible. An important step in the development of renewable jet fuels was the establishment of ASTM 7566, which provides a specification for Aviation Turbine Fuel Containing Synthesized Hydrocarbons. This standard was first published in 2009 providing standards for biofuel components produced from a FT process. In July of 2011, this standard was amended to include requirements for synthetic fuel components manufactured from hydroprocessed esters and fatty acids produced from various renewable sources.

There are a number of companies engaged in the development of production facilities and commercial arrangements for renewable jet fuel. In September 2008, the Sustainable Aviation Fuel Users Group (SAFUG, 2015) was formed to accelerate the development and commercialization of sustainable aviation biofuels. SAFUG includes leading companies in the aviation industry, including airlines and airplane producers. The SAFUG website includes a number of case studies of the use of biofuel in aviation trials, including the world's most CO₂ efficient flight by Air France, the first commercial flight with renewable jet fuel in Australia by Qantas Airways in 2012, the first commercial flight with renewable jet fuel in the U.S. by United Airlines in 2011, and the first transpacific flight with renewable jet fuel by All Nippon Airlines (ANA) and Boeing in 2012. A number of companies are developing or have developed renewable jet fuel production facilities. UOP, a Honeywell subsidiary, has provided renewable fuel for testing in U.S. military aircraft, and its technology is being implemented in an AltAir Fuel refinery in Los Angeles and a planned refinery in the United Arab Emirates by Petrixo. The UOP Renewable Jet Fuel Process technology was originally developed under a contract from the U.S. Defense Advanced Research Projects Agency (DARPA). Gevo is also producing an alcohol-to-jet (ATJ) fuel at its Silsbee, TX, biorefinery using isobutanol (Lane, 2015).

Environmental Considerations with the Use of FT, GTL, and Hydrogenated Renewable Diesel as Transportation Fuels

Renewable and GTL diesel fuels generally provide emission benefits in comparison with petroleum diesel, including CARB-certified diesel, due to their favorable properties of high cetane number and low aromatics (Rothe et al. 2005; Kleinschek, 2005; Aatola, Larmi, Sarjovaara, & Mikkonen, 2008; Kuronen, Mikkonen, Aakko, & Murtonen, 2007). As part of the development of the LCFS, UCR evaluated the emissions of renewable diesel fuel and GTL compared with those of a CARB-certified diesel on a 2006 Cummins ISM 370 (Durbin et al., 2011; Hajbabaei et al., 2012). These results showed that NO_x emissions decreased with increasing levels of renewable diesel, with the emission reductions ranging from approximately 3 to 18%, depending on the testing condition and the blend level. Comparable emissions reductions were also found for the GTL fuel over a smaller subset of tests. Combinations of renewable diesel with biodiesel were found to be a viable strategy for mitigating the biodiesel NO_x increase, but generally a ratio of 3 or 4 parts renewable diesel to 1 part biodiesel was needed to achieve a NO_x-neutral blend.

Xinling & Zhen (2009) studied the emission-reduction potential from a medium-duty, direct-injection, turbocharged diesel engine fueled with conventional diesel fuel, GTL, and DME. They found the GTL exhibited almost the same power and torque output as diesel, with improved fuel economy. GTL significantly reduced regulated emissions with average reductions of 21.2% in CO, 15.7% in HC, 15.6% in NO_x and 22.1% in smoke in comparison to diesel, as well as average reductions in unregulated emissions of total ultrafine particle number and mass emissions by 85.3% and 43.9%, respectively.

Table 8. References for Environmental Considerations with the Use of FT, GTL, and Hydrogenated Renewable Diesel as a Transportation Fuel

Author	Vehicle/Engine	Fuel	Notable Results
Aatola et al., 2008	A heavy duty DI diesel engine	Sulfur free diesel fuel, neat HVO, and a 30% HVO + 70% diesel fuel blend	<ol style="list-style-type: none"> 1. HVO enables reductions in CO, THC, and NOx emission, and smoke without any changes to the engine or its controls. 2. With the default injection timing settings of the test engine, the use of 100% HVO led to 6% lower NOx and to 35% lower smoke compared with a sulfur-free EN 590 diesel fuel.
CARB, 2014b; CARB, 2012	Heavy Duty Diesel (HDD) truck, passenger vehicle	Crude oil, residual oil, diesel, gasoline, natural gas and electricity	<ol style="list-style-type: none"> 1. Renewable diesel produced from the conversion of tallow would provide significant reductions in carbon intensity values. 2. The current carbon intensity value used for California ULSD is 102.82 gCO₂e/MJ fuel in comparison with 39.33 gCO₂e/ MJ fuel and 19.65 gCO₂e/ MJ fuel for conversion of tallow to renewable diesel using higher and lower energy use for rendering, respectively. 3. The carbon intensity values for renewable diesel production from Midwest soybeans are higher than those from tallow at 82.16 gCO₂e/ MJ fuel, but still provide some benefits in carbon intensity relative to the baseline diesel.
Durbin et al., 2011	2 heavy-duty on-road engines, 2 non-road engines	Biodiesel, renewable diesel, and diesel fuel	<ol style="list-style-type: none"> 1. NOx emissions decreased with increasing levels of renewable diesel, with the emission reductions ranging from approximately 3 to 18%, depending on the testing condition and the blend level. 2. Comparable emissions reductions were also found for the GTL fuel over a smaller subset of tests.
Frank et al., 2013		Hydrothermal liquefaction (HTL) and lipid extraction (LE) pathways to renewable diesel from algae	The GHG contributions for HTL and LE of algae were found to be 31,000 gCO ₂ e per million BTU (MMBTU) and 21,500 gCO ₂ e MMBTU for renewable diesel, respectively, compared to a value of 100,000 gCO ₂ e MMBTU for diesel fuel.
Hajbabaee et al., 2012	2 heavy-duty engines	Soy- and animal-based biodiesels, a hydrotreated renewable diesel, GTL fuel (5%-100%)	<ol style="list-style-type: none"> 1. Increasing renewable diesel and GTL blends showed NOx emissions reductions with blend level. 2. NOx emissions neutrality with the CARB diesel was achieved by blending GTL or renewable diesel fuels with various levels of biodiesel or by using di-tert-butyl peroxide (DTBP).
Kuronen et al., 2007	2 heavy-duty engines, 2 city buses	HVO and sulfur-free EN 590 diesel fuel.	The effect of HVO on regulated emissions compared to EN 590 fuel was: NOx -7% ~-14%; PM -28% ~-46%; CO -5% ~-78%; and HC 0% ~-48%.
Xinling & Zhen, 2009	A medium-duty, direct-injection, turbocharged diesel engine	Conventional diesel fuel, GTL, and DME	<ol style="list-style-type: none"> 1. GTL exhibited almost the same power and torque output as diesel, with improved fuel economy. 2. GTL significantly reduced regulated emissions with average reductions of 21.2% in CO, 15.7% in HC, 15.6% in NOx and 22.1% in smoke in comparison to diesel, as well as average reductions in unregulated emissions of total ultrafine particle number and mass emissions by 85.3% and 43.9%, respectively.

It is expected that the production and use of renewable or BTL fuels will provide LCA reductions in GHGs. Well-to-wheel GHG emissions for various scenarios of renewable diesel production have been analyzed under the California LCFS program using the CA-GREET model. The results show that the renewable diesel produced from the conversion of tallow would provide significant reductions in carbon intensity values. Specifically, the current carbon intensity value used for California Ultra Low Sulfur Diesel fuel is 102.82 gCO_{2e}/MJ_{fuel} (CARB, 2014b) in comparison with 39.33 gCO_{2e}/ MJ_{fuel} and 19.65 gCO_{2e}/ MJ_{fuel} for conversion of tallow to renewable diesel using higher and lower energy use for rendering (CARB, 2012), respectively. The carbon intensity values for renewable diesel production from Midwest soybeans are higher than those from tallow at 82.16 gCO_{2e}/ MJ_{fuel}, but still provide some benefits in carbon intensity relative to the baseline diesel. This is primarily attributed to the contribution from land use effects used in CA-GREET, with is 62 gCO_{2e}/ MJ_{fuel} for renewable diesel production from Midwest soybeans. Researchers at Argonne National Laboratory have also studied the GHG impacts of renewable diesel made from algal sources (Frank et al., 2013). Based on the GREET model, Frank et al. (2013) found the GHG contributions for hydrothermal liquefaction and lipid extraction of algae to be 31,000 gCO_{2e} per million BTU (MMBTU) of renewable diesel and 21,500 gCO_{2e} MMBTU, respectively, compared to a value of 100,000 gCO_{2e} MMBTU for diesel fuel. A summary of the environmental studies on FT, GTL, and Hydrogenated Renewable Diesel as a transportation fuel are listed in the Table 8.

NATURAL GAS AS A TRANSPORTATION FUEL

Natural gas (NG) is now a vital component of the world's supply of energy and provides 27% of the marketable energy consumed in the United States (EIA). NG use is commonplace in applications including cooking, residential and commercial heating, industrial process feed stocks, electricity generation, and transportation. NG has been utilized in vehicle applications for over 30 years at various levels. Because NG is generally considered to be a cleaner fuel than gasoline or diesel, regulatory and other incentives have provided for the development of specifically-designed natural gas vehicles (NGVs). NG usage accounted for 3% of the total U.S. transportation sector's 31.53 quadrillion Btus of petroleum energy in 2014 (U.S. EIA, 2014a). NG can be derived from either fossil fuel sources or as a renewable source from waste streams or other processes. Renewable natural gas (RNG) is growing in usage due to its significantly lower GHG impact and its sustainability in comparison to fossil fuels.

Natural Gas and Renewable Natural Gas Production

NG is a naturally occurring gas mixture found in deep underground natural rock formations or associated with other hydrocarbon reservoirs. It is a complex mixture of hydrocarbon and non-hydrocarbon constituents and exists as a gas under atmospheric conditions. The NG used by consumers is composed mostly of methane (CH₄), with some other less significant species generally as listed in Table 9. The basic composition includes

CH₄, ethane, propane, and other hydrocarbons, as well as contaminants, such as nitrogen (N₂), carbon dioxide (CO₂), water, and hydrogen sulfides (H₂S).

United States is the world's largest NG producer, followed by Russia and Iran (U.S. EIA, 2011). U.S. NG annual production has increased steadily from 24,119 billion cubic feet per year (bcf/y) in 2003 to 30,005 bcf/y in 2013, resulting in a 24.4% increase in NG production over that period (U.S. EIA, 2015). Worldwide, NG production has increased approximately 27%, from 116,226 bcf/y in 2003 to 147,481 bcf/y in 2013 (U.S. EIA, 2015). In recent years, NG production in the U.S. has increased substantially due to technological advancements in NG extraction methods. This increased production has displaced traditional supply sources and resulted in reduced prices for NG consumers. These technological advancements have resulted in domestic production growth that has exceeded even the most optimistic forecasts of NG production from a decade ago. The prospect of NG supplies, continued low prices, and the favorable environmental and economic position of natural gas-fired electric generation plants are leading to expectations of growing U.S. demand for NG, especially in the electricity and industrial sectors, and potentially for export as liquefied natural gas (LNG). Besides the increase in NG production, the NG proven reserves have increased as well. U.S. NG reserves have increased from 189 trillion cubic feet (tcf) in 2004 to 338 tcf in 2014, resulting a 78.84% increase in NG reserves for the past decade. Worldwide, NG reserves have increased 14.7%, from 6,079 tcf in 2004 to 6,973 tcf in 2014 (U.S. EIA, 2015).

United States EIA expects that NG production will increase by 4 billion cubic feet per day (bcf/d) (5.4%) and 1.8 bcf/d (2.3%) in 2015 and 2016, respectively. EIA expects moderate growth through 2016, with increases in the lower 48 states expected to more than offset long-term production declines in the Gulf of Mexico. Increases in drilling efficiency will continue to support growing NG production in the forecast despite relatively low NG prices. Most of the growth is expected to come from the Marcellus Shale, as the backlog of uncompleted wells is reduced and as new pipelines come online to deliver Marcellus NG to markets in the Northeast (U.S. EIA, 2014b). EIA also projects LNG gross exports will increase to an average of 0.79 bcf/d in 2016, with the startup of a major LNG liquefaction plant in the lower 48 states. Greater replacement of petroleum-based fuels with NG could also contribute to reduced petroleum imports and increased national energy independence (C2ES, 2012).

Table 9. Typical Composition of Natural Gas¹

Name	Formula	Volume (%)
Methane	CH ₄	70-90
Ethane	C ₂ H ₆	0-20
Propane	C ₃ H ₈	
Butane	C ₄ H ₁₀	
Carbon dioxide	CO ₂	0-8
Hydrogen sulfide	H ₂ S	0-5
Nitrogen	N ₂	0-5
Oxygen	O ₂	0-0.2
Rare gases	Ar, He, Ne, Xe	trace

Source: http://www.naturalgas.org/naturalgas/processing_ng.asp.

Traditionally, NG comes from three types of vertically drilled wells: oil wells, gas wells, and condensate wells. NG that comes from oil wells is typically termed "associated gas." This

gas can exist separately from oil in a formation (free gas), or dissolved in the crude oil (dissolved gas). NG from gas and condensate wells, in which there is little or no crude oil, is termed “nonassociated gas.” Gas wells typically produce raw NG by itself, while condensate wells produce free NG along with a semi-liquid hydrocarbon condensate. Therefore, issues such as oil and condensate removal, water removal, separation of NG liquids, and sulfur and CO₂ removal are challenges to increasing traditional NG production. NG gas deposits can also occur in and be characterized by different rock formations. Tight gas is natural gas produced from reservoir rocks with low permeability. Shale gas is gas trapped in hard dense deposits. Figure 6 provides a breakdown of the different types of natural gas production for the period from 1990 to 2035.

Over the last several years there have been considerable increases in domestic NG production made possible by more advanced drilling and extraction processes that have increased the effectiveness of NG production and made it possible to tap shale gas formations that were once thought to be inaccessible. Horizontal drilling and hydraulic fracturing (also called fracking) are two of these techniques. Horizontal drilling involves drilling a vertical hole to specified depth and then branching out into several horizontal cuts. The horizontal drilling is an important development because it provides access to more of the NG formation underground from fewer above ground wells, as presented in Figure 7 (America’s Natural Gas Alliance).

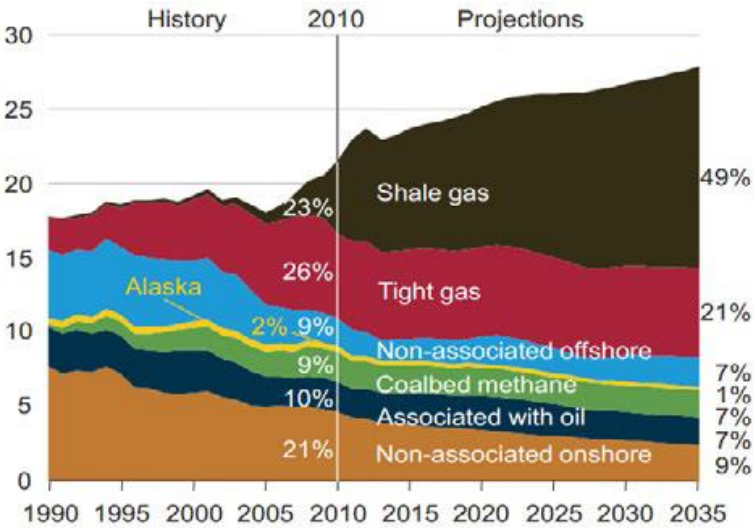
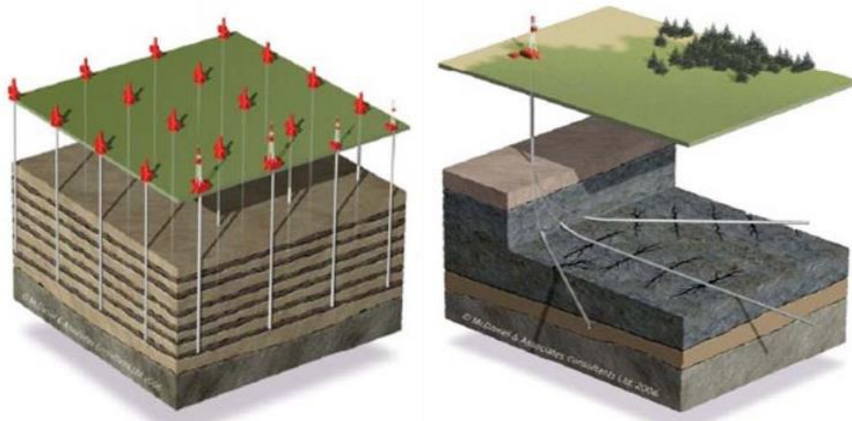


Figure 6. U.S. Natural Gas Production, 1990-2035 (Source: U.S. Energy Information Administration, Annual Energy Outlook 2012 Early Release Overview.

Once the horizontal holes have been prepared, the next step is fracturing the surrounding areas to access the NG, as shown in Figure 8. The fracturing step breaks apart the relatively impermeable shale with hydraulic fluids in the horizontal runs. From the 1940s to 2003 traditional (vertical) wells were the dominate method for NG production, then fracking increased and accounted for more than half of the NG production in 2006 and more than 90% of the NG production in 2010, see Figure 9. Currently, the fracking process is used in nearly all NG wells drilled in U.S. today and is spreading as the primary drilling method throughout

the world. Production from hydraulic fracturing shale gas wells has increased from 2.869 trillion cubic feet per year (tcf/y) in 2008 to 11.896 tcf/y in 2013.



Traditional Well

Horizontal Drilling

Source: U.S. America’s Natural Gas Alliance.

Figure 7. Conventional Oil and Gas Production from the Underground Resources.

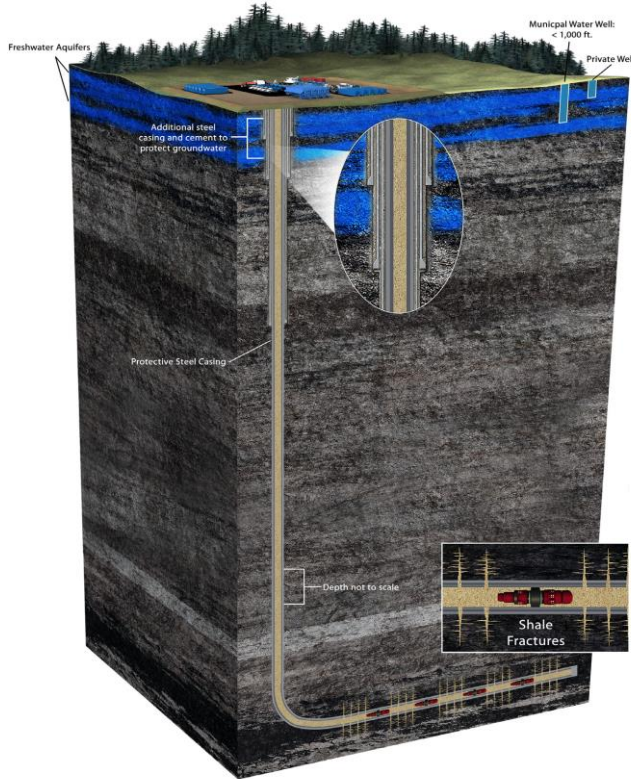


Figure 8. Horizontal well in an underground rock layer with multiple fracture stages created by hydraulic fracturing.

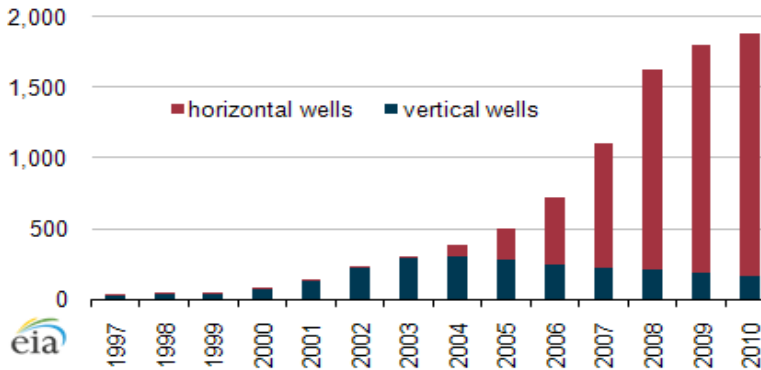


Figure 9. Horizontal compared with vertical (traditional) NG wells by year (bcf/y) (Source: U.S. Energy Information Administration based on HPDI, LLC).

RNG is produced from a variety of biomass and/or biogas sources, including landfill gas, solid waste, municipal wastewater, and agricultural manure via purpose-built anaerobic digesters (AD). It can also be produced from biomass sources such as forestry and agricultural waste via the process of thermal gasification (TG). The TG process includes gasifier, syngas clean up, and methanation. RNG is a pipeline quality gas that is fully interchangeable with fossil NG and can be used as a 100% substitute for, or blended with, conventional gas streams for use in vehicles. The use of RNG presents an opportunity to convert marginal and zero-value waste products into a useful transportation fuel. Estimates of the potential supply of RNG are dependent on various assumptions, including future waste streams, biomass availability, conversion technologies, and process yields. A review of the current literature indicates that the practical RNG potential is approximately 4.8 tcf/y or 40 billion gasoline gallon equivalents (GGE) per year. About 180 million dry tons per year (or approximately 12%) of total biomass resources is suitable for current AD conversion technologies. Also, it can be estimated that about 4.5 billion GGE or 0.5 tcf/y of RNG is the practical potential from feedstock sources for anaerobic digestion (Hamberg et al., 2012). Some of the considerations that were accounted for in estimating the practical resource potential of RNG include scale, operating practices, and other limitations, like production challenges such as H₂S, CO₂, water, and other contaminants removal, as well as odorization (Hamberg et al., 2012).

Utilization of Natural Gas as a Transportation Fuel

A variety of vehicle technologies available today allow NG to be used in light-, medium-, and heavy-duty vehicles, leading to the increasing use of NGVs. NGVs are considered to be as safe as or safer than traditional gasoline or diesel vehicles, and NGVs meet the strictest emission standards, including California's AT-PZEV standard. NG also provides advantages in terms of fuel costs, with NG currently costing from \$1.50 to \$2.00 less per gasoline gallon equivalent (GGE) than gasoline (NGV America, 2014), although the costs associated with the vehicles themselves and putting the infrastructure in place are higher.

Most commonly, NG is used in a highly pressurized form as CNG, or as LNG. CNG is NG compressed to less than 1 percent of its standard atmospheric pressure volume. As a

consequence of its highly pressurized state, CNG requires special handling and storage (altfueltrucks.com). In vehicles, CNG requires cylindrical storage tanks, which are significantly larger than conventional fuel tanks to keep the fuel at pressures of up to 3,600 pounds per square inch (Beach, Gonzales, & Butler, 2011). Given the size requirement of these tanks, their placement in passenger vehicles, can take up valuable passenger or trunk space.

LNG is NG chilled to -260 °F at normal pressures, at which point it condenses into a liquid with 0.0017 percent the volume of the gaseous form (NaturalGas.org). The conversion of NG to LNG removes compounds such as water, CO₂ and sulfur leaving a purer methane product (California Energy Commission, 2008). The stable, non-corrosive form of LNG makes it more readily transportable, so it can be moved by ocean tankers or trucks (Center for Liquefied Natural Gas, 2012). Large, heavy, and highly insulated fuel tanks are necessary to keep LNG at -260 °F, which adds a significant incremental cost to the vehicle (U.S. EIA, 2010). Today, LNG is mainly used as direct replacement for diesel in heavy-duty trucks because they are able to accommodate the storage system, can be refueled more quickly than CNG, and can use the LNG fueling infrastructure currently limited to trucking routes (Beach et al., 2011). Based on the energy density, LNG is more practical for long-haul, tractor-trailer rigs that can accommodate larger fuel tanks.

There are about 153,000 NGVs in the U.S. and more than 17.7 million worldwide. NGV Global, the international NGV association, estimates there will be more than 50 million NGVs worldwide within the next 10 years, account about 9 percent of the world's transportation fleets. The U.S. currently ranks 13th in the world, with less than 1.5 percent of the NGVs in use. However, North America is expected to see some of the fastest growth due to abundant proven reserves and the low cost of domestically produced NG (NGV America, 2014).

NG engine development for LDVs has been ongoing for a number of years (Ko et al. 1992; Ernst, Meacher, & Bascom, 1992; Varde, Patro, & Drouillard, 1995; Sulatisky et al. 1995; Bates & Germano, 1994; Kalam et al., 2004) and production NG vehicles are available. Honda produced a CNG light-duty vehicle from 2006 to 2015. This model sold approximately 10,000 vehicles between 2004 and 2014. In comparison, the Toyota Prius has sold over 1.56 million units since 2004 (Cobb, 2015). Honda announced in 2015 that it will stop selling the NG Honda Civic due to weak demand.

Heavy-duty (HD) NG engines have been made by a number of different OEMs over the past 15-20 years. Cummins, Cummins-Westport, John Deere, and Detroit Diesel are among the most prominent engine manufacturers that have produced heavy-duty NG engines. Currently, transit buses are the largest users of NG for HD vehicles. According to the American Public Transit Association, about one-fifth of all transit buses were run by CNG or LNG in 2012. The fastest growing NGV segment is waste collection and transfer vehicles, with almost 50 percent of the trash trucks purchased in 2012 powered by NG. More than 35 airports in the U.S. have NGVs in their own fleets or have policies that encourage NG use by private fleets operating on airport premises, making this sector the third largest in vehicular NG use. The successful Clean Port Initiative in Southern California is spurring adoption of similar policies in other ports on both coasts (NGV America, 2014). Heavy-duty NG vehicles sales were relatively robust from 2012 through 2014 in the U.S., but slowed down in late 2014 and 2015. This slowdown was due in large part to reductions in the price of crude,

which impacted some of the fuel-cost benefits of NGVs. This also led to the cancellation of a next-generation, heavy-duty NG engine that was being developed by Cummins, Inc.

One limitation for NGVs is that the infrastructure is not nearly as developed as it is for corresponding petroleum-fueled vehicles. A city-level NG transmission system is necessary to build up before NGVs can be utilized in a specific area. That should include pipe-coating materials, compressor stations, metering stations, city gate stations, and NG refueling infrastructure. For now, there are 1,564 CNG and 111 LNG fueling stations in the U.S., and refueling appliances are available for home use (NGV America, 2014). Of these, only about half are available for public use.¹ Another important consideration for NGV users is fuel quality. Different standards may be in place for different applications or different areas within a given region. Within California, for example, PG&E Rule 21 and SoCalGas Rule 30 are the gas quality standards for residential consumer use. These include parameters such as Wobbe Number and gross higher heating value (HHV), which are specified to be between 1279 and 1385 and between 970 and 1150 BTU/scf, respectively under SoCalGas Rule 30 (Rutledge, 2005). The specifications for CNG fuel for motor vehicles, on the other hand, are developed under the auspices of the California Air Resources Board (CARB).

While CNG and LNG are today the most common forms of NG fuels in vehicles, other technologies are available that could increase the use of NG in the broader transportation system. Gas-to-liquids (GTL) technology can be used to transform NG hydrocarbons into gasoline or diesel hydrocarbons. The resulting gasoline and diesel fuels have a similar energy density as traditionally-produced fuels and can be used in conventional vehicles.

Environmental Considerations with the Use of Natural Gas as a Transportation Fuel

A number of studies have already been conducted to evaluate NG's potential impact on engine and vehicle emissions and performance. Due to its simpler structure, NG has the potential to reduce emissions of PM, HCs, CO, and NO_x. These emissions benefits have become less significant, however, as the emission control and aftertreatment systems on gasoline and diesel vehicles have become more advanced. Nevertheless, NG engines and vehicles can still provide potential emissions advantages for both the light-duty and heavy-duty markets that could prove important to emissions control going into the future.

For light-duty vehicles over the years, NGVs have included an assortment of original equipment manufacturer (OEM) vehicles and retrofits. These vehicles have generally been able to provide emissions comparable to or better than the lowest emitting gasoline vehicles of similar vintages. The NG Honda Civic, for example, represented one of the earlier light-duty vehicles certified to the California Super Low Emissions Vehicle (SULEV) standards. Retrofit NG vehicles can also provide very low emission levels, with the provision that the systems must be shown to be sufficiently robust. It is also likely that NGVs will provide a distinct advantage in PM emissions for light-duty vehicles into the future, as the GDI vehicles that are becoming more predominant in the fleet tend to have higher PM emissions than more conventional gasoline technologies.

¹ http://www.afdc.energy.gov/fuels/stations_counts.html.

For heavy-duty vehicles, the emissions performance of NG engines and vehicles has been evaluated as the technology has changed and advanced over the years. The first generation of NG heavy-duty engines utilized a lean burn combustion strategy to take advantage of the characteristics of NG and provide lower emissions. The earliest production models of these engines in the early 1990s were open loop fuel control, with closed looped fuel control being implemented in the mid-1990s. West Virginia University (WVU) conducted many studies of the early generations heavy-duty NGV over the years to evaluate the emissions and performance. As early NG buses were being implemented in transit fleets throughout the 1990s, WVU conducted tests at many different fleet locations throughout the country using its transportable dynamometer. These studies included different generations of lean-burn NG engines as the engine technology became more advanced. These studies showed the effectiveness of NG engines in significantly reducing PM and CO emissions compared to diesel engines of the time. They also showed generally lower NO_x emissions, although these reductions were somewhat more modest; and, due to variations in cylinder to cylinder mixtures and straying of the air-fuel ratio from the design point, NO_x emissions were sometimes comparable to the level for diesel engines. In the early 2000s, WVU also did comparison studies between NG vehicles and diesel vehicles with DPFs, as part of a program conducted by ARCO/BP. These studies showed that diesel vehicles equipped with DPFs were able to provide PM emissions comparable to those of NG vehicles.

As emissions standards continued to be reduced, the heavy-duty NG engine technology transitioned from a lean-burn to a stoichiometric combustion strategy with EGR and a TWC to meet 2010 emissions standards. The Cummins ISL-G was the first production engine to utilize this technology, with additional other stoichiometric engines being developed over the past few years. Heavy-duty NGVs with stoichiometric NG engines have been studied by WVU, the University of California at Riverside (UCR), the California Air Resources Board (ARB), and others in a series of different studies (Thiruvengadam et al., 2015; Carder, Gautam, Thiruvengadam, & Besch, 2014; Miller, Johnson, Durbin, & Dixit, 2013; Yoon et al., 2013). One of the major recent studies of these later model heavy-duty NGVs was a study that was conducted in the South Coast Air Quality Management District, which represents the greater Los Angeles area. The study included 5 NG vehicles, 4 dual-fuel NG/diesel vehicles, 2 liquefied petroleum gas (LPG) vehicles, and 14 standard diesel vehicles, including drayage trucks, refuse haulers, and buses (Thiruvengadam et al., 2015; Carder et al., 2014; Miller et al., 2013). The results showed that both the NG and diesel vehicles were effective in reducing PM emissions to very low levels, but that the diesel vehicles emitted considerable higher NO_x emissions than the NG vehicles under lower temperature operating conditions when the SCR temperature was not high enough to activate. UCR has also conducted studies of drayage trucks, a transit bus, and a refuse hauler that were equipped with a ISL-G engine. These vehicles also showed significantly lower emissions of THC, NMHC, CH₄, NO_x, formaldehyde, and acetaldehyde emissions, and higher CO and ammonia (NH₃) emissions for the ISL-G engine compared to previous studies of lean-burn technology engines. Although the CO emissions were higher for the stoichiometric engine compared with the lean-burn engine, CO emissions were still considerably below the current engine certification values.

The increases in NH₃ emissions have been noted as an important change with the introduction of stoichiometric, TWC-equipped NGVs. In addition to the studies above, Bishop et al. (2012) also observed a 20-fold increase in ammonia emissions from trucks as a

result of new, stoichiometrically combusted, liquefied natural gas powered trucks in the Ports of Los Angeles and Long Beach. Ammonia is a secondary pollutant formed during the NO_x reduction process over the TWC, with the formation dependent on the presence of both nitrogen oxide (NO) and hydrogen (H₂) in the exhaust stream. For TWC-equipped stoichiometric natural gas engines, the production of NH₃ takes place in the presence of hydrogen molecules, which in turn are produced during periods of rich air-fuel mixtures. Hydrogen can also form from a water gas shift reaction involving CO and water or steam reforming reactions involving CH₄ and water in the exhaust (Mejia-Centeno, Martinez-Hernandez, & Fuentes, 2007; Huai et al., 2003; Gandhi, 1974).

Research has also been conducted to try to better understand the impacts of potentially changing NG composition on emissions from NGVs. Studies of the effects of NG composition have been conducted for small stationary source engines, such as compressors, and in heavy-duty engines and vehicles (Mejia-centeno et al., 2007; Huai et al, 2003; Gandhi, 1974; Gutierrez, 2003, 2006; Feist, 2006, 2009; Lee & Kim, 2000; Elder, Jones, & Taine, 1985; Matthews, Chiu, & Hilden, 1996; Malenshek & Olsen, 2009; Bach, 2008; Naber et al., 1994; McTaggart, Rogak, Munshi, Hill, & Bushe, 2010; Durbin et al. 2014). These studies showed that NG composition can have an impact on emissions. NO_x emissions, for example, were found to increase with increasing Wobbe number (WN) and/or decreasing methane number (MN) in several of these studies (Mejia-centeno et al., 2007; Huai et al., 2003; Gandhi, 1974; Gutierrez, 2003, 2006; Feist, 2006, 2009; Lee & Kim, 2000; Elder et al., 1985; Matthews et al., 1996; Malenshek & Olsen, 2009; Bach, 2008; Naber et al., 1994; McTaggart et al., 2010; Durbin et al., 2014). MN is a measure of the knock resistance of a gas, with the knock resistance of a gas increasing with increasing MN. WN is defined as the higher heating value (HHV) of a gas divided by the square root of the specific gravity of the gas with respect to air. The higher the WN of a gas, the greater the heat content of that gas will flow through a hole of a given size in a given amount of time. In terms of heavy-duty vehicles, the results have shown that fuel quality/composition can have important impacts on emissions for older lean-burn technology engines, but that the impacts of fuel composition for newer stoichiometric engines are relatively minor (Karavalakis et al., 2011, 2012a, 2012b, 2012c, 2013; Hajbabaei, Karavalakis, Johnson, Lee, & Durbin, 2013b).

Methane leaks have been another important environmental consideration for the use of NG as a transportation fuel. It is known that some percentage of gas is lost and can not be accounted for over the full lifecycle from the gas well to the end consumer, although there are considerable differences seen throughout the industry and in different studies (Ogburn, 2013). Given CH₄ is a greenhouse gas with a global warming potential 25 times higher than CO₂, methane leaks at too high a level could off-set or eliminate some of the other environmental benefits associated with NG as a fuel. Studies have suggested that CH₄ leak rates of less than 3 to 4% are needed to provide short-term climate benefits from substituting new coal fired power plants with new NG power plants (Alvarez, Pacala, Winebrake, Chameides, & Hamburg, 2012; Schweitzke, Griffin, Matthews, Bruhwiler, 2014). Other studies have suggested that leak rates of about 1% or less are needed to provide short term climate benefits from substituting heavy-duty diesel vehicles with NG (Alvarez et al., 2012; Camuzeaux, Alvarez, Brooks, Browne, & Sterner, 2015; Tong, Jaramillo, & Azevedo, 2015). EPA estimates a leakage rate of 1.16% for the full production to the end user process (U.S. EPA, 2014; Burnham, Han, Elgowainy, & Wang, 2014). The Environmental Defense Fund (EDF,

2015) has coordinated an extensive series of studies related to various aspects of methane leaks that has significantly enhanced the information available in this area. This includes studies of production, transmission, storage, and local distribution (Allen et al., 2013, 2015; Subramanian et al., 2015; Lamb et al., 2015; McCain et al., 2015; Zimmerle et al., 2015), including evaluations of pneumatic valves, liquid leaks, compressors, and equipment leaks as important sources of methane leaks. The studies showed a wide range of variability in different production, transmission, distribution, and other sites, with some facilities/locations having relatively low leak levels, while others had disproportionately higher emissions, including some “super emitting” sites (Allen et al., 2013, 2015; Mitchell et al., 2015; Zimmerle et al., 2015; Lamb et al., 2015; McKain et al., 2015). There were also studies conducted in a number of oil and gas fields/basins, including the Uintah basin in Utah (Karion et al., 2013), the Colorado Denver-Julesburg Basin (Pétron et al. 2014), the Haynesville, Fayetteville, and northeastern Marcellus shale gas production regions (Peischl et al., 2015), and the Barnett shale region in Texas (Harriss et al., 2015). Again the studies of oil and gas fields/basins showed differences with previous estimates, with some showing lower and some showing higher emission rates. Based on results of some of these more recent field studies, Marchese et al. (2015) estimated CH₄ emissions from NG gathering and processing plants using Mote Carlo modeling to be about 87% higher than those for the 2014 EPA Greenhouse Gas Inventory (GHGI), equivalent to about 30% of the total CH₄ emissions from NG systems. This represented a CH₄ loss rate of 0.47% for all U.S. gathering and processing operations when normalized by 2012 CH₄ production levels.

It should be noted that estimates of GHG emissions impacts for RNG tend to be much less than those from fossil fuel natural gas use. Studies using the CA-GREET model estimate carbon intensities for CNG and LNG to range anywhere from 68 to 93 gCO_{2e}/ MJ_{fuel} depending on if the gas is compressed or liquefied and whether it is from North America or overseas (CARB, 2012), while carbon intensities from biomethane from landfills sources, dairy digester biogas, high solid anaerobic digestion of organic food and green wastes, and wastewater sludge range from 11 to 33 gCO_{2e}/ MJ_{fuel} (CARB, 2012, 2013), 13 to 29 gCO_{2e}/ MJ_{fuel} (CARB, 2012), -15 to 35 gCO_{2e}/ MJ_{fuel} (CARB, 2014c), 8 to 30.5 gCO_{2e}/ MJ_{fuel} (CARB, 2014d), respectively. The CA-GREET values currently include credits in some cases for avoiding landfilling or composting, for surplus cogenerated electricity, and other credits. It should be noted that as of January 2016, CI values for biomethane for the LCFS will be computed based on information specific to a given production process for a given producer, or will require data from the production process to ensure that the process is operating within certain specifications if the more generalized values are used. A summary of the environmental studies on Natural Gas as a transportation fuel are listed in the Tables 9 and 10.

OTHER FUELS THAT COULD POTENTIALLY BE USED FOR TRANSPORTATION

As biofuels have continued to expand in the marketplace, interest has increased in developing new alternatives to provide a broader diversity of fuel options, to address some of

the limitations of existing commonly-used biofuels, and to evaluate biofuels that might provide additional benefits beyond those of the currently-used biofuels. Other oxygenates, such as carbonates like dimethyl carbonate (DMC), for example, could provide additional reductions in emissions compared to current biofuels. Different products of lignocellulosic biological conversions are also attracting attention as potential transportation fuels. This includes molecules that are hydrocarbons, as opposed to alcohols, that could be utilized as drop in fuels. Some of these are platform molecules, which can be produced from sugars via biological or chemical conversions and subsequently converted to a number of high-value, bio-based chemicals or materials, including furanic molecules such as DMF, ethoxymethylfurfural (EMF), or methyltetrahydrofuran (MeTHF), which can be used in fuels termed P-series fuels. These potential next-generation biofuels will be discussed in this section.

Development and Use of DMC as a Transportation Fuel

DMC Production

At present, the world dimethyl carbonate (DMC) annual production capacity is approximately 170,000 to 200,000 tons/year, with the actual annual DMC output being less than 100,000 tons/year, mainly in Western Europe, the U.S., Japan and other countries. Fifty-one percent of the global DMC consumption is for polycarbonate, and twenty-four percent is used as an electrolyte in lithium ion batteries (Coker, 2012).

Traditionally, DMC is formed by the reaction of methanol (MeOH) with phosgene or methyl chloroformate in the presence of a concentrated sodium hydroxide solution in a two-phase reaction that provides high yields and purity. Other alcohols can also be phosgenated. More recently, DMC is being produced via the direct oxidative carbonylation of MeOH, and phosgenation is losing its attractiveness in this application (Buysch, 2000). Varieties of metallic and nonmetallic materials have also been studied for an inexpensive and high-yield route to synthesize DMC nowadays, such as a polymer-complexed Cu(II) catalyst system with alkali addition to MeOH and a highly selective catalyst CuCl/MCM-41 for oxidative carbonylation of MeOH (Feng, Cao, Yi, Dai, & Fan, 2004; Li, Xie, & Slade 2001).

Utilization of DMC as a Transportation Fuel

DMC is another oxygenate choice. It is non-toxic and highly miscible with diesel fuel and gasoline. It also exists in liquid state at room temperature, which makes storage and transportation convenient. DMC can be used as an oxygenate to blend with diesel fuel to improve combustion and reduce pollutant emissions. It is difficult to fuel diesel engines directly with DMC, however, due to its low cetane number (CN) and high latent heat of vaporization. DMC could also be an option for meeting the oxygenate specifications for gasoline due to its high oxygen content (53 wt%, or about 1.5 times the oxygen content as ethanol), good blending octane, freedom from phase separation, low toxicity and rapid biodegradability. DMC is also a product of converting natural gas (NG) to a liquid transportation fuel. With reductions in production costs, DMC has also entered the energy market as a blend fuel in gasoline and diesel (Delledonne, Rivetti, & Romano, 2001; Arteconi, Mazzarini, & Nicola, 2011; Knifton & Duranleau, 1991).

Table 9. References for Environmental Considerations with the Use of Natural Gas as a Transportation Fuel

Author	Vehicle/Engine	Fuel	Notable Results
Bach, 2008	Advanced Methane Gas Vehicles	Methane	1. CH ₄ is a high temperature capable fuel that is well suited for turbo charged motor applications due to the high knock resistance.
			2. Dedicated CH ₄ gas engines have the potential for increased efficiency and reduced emissions.
			3. Propane should be limited in the NG grid or reduced/eliminated at the fueling station due to the potential of increasing knock.
Bishop et al., 2012	Heavy-duty diesel and LNG port trucks	Natural gas	1. Reductions in CO (30%), NO _x (48%) and infrared opacity (a measure of particulate matter, 54%) compared to diesel trucks.
			2. A 20-fold increase in NH ₃ emissions for the stoichiometric combustion, TWC LNG powered trucks compared to diesel trucks.
			3. Significant increases in NO _x emissions from new trucks equipped with DPFs; raising the mean CO ₂ to NO _x ratios from less than 10% to more than 30% at the Riverside freeway location.
Camuzeaux et al., 2015	Heavy-duty trucks with SI and HPDI natural gas engines	Natural gas	1. Converting heavy-duty trucks fleets to natural gas trucks leads to damages to the climate for several decades: around 70–90 years for the SI cases, and 50 years for the more efficient HPDI.
			2. These fuel switches have the potential to produce climate benefits on all time frames, but combinations of significant well-to-wheels CH ₄ emissions reductions and natural gas vehicle efficiency improvements would be required.
Durbin et al., 2014	A natural gas school bus, a natural gas waste hauler, a class 8 natural gas refuse truck, and two class 8 natural gas port trucks	3 to 7 different test natural gas fuels	1. The low methane fuels showed higher NO _x , NMHC, and aldehyde emissions, and lower THC and CH ₄ for the school bus engine.
			2. The stoichiometric engines showed considerably lower emissions compared to previous studies of lean burn technology engines for THC, NMHC, CH ₄ , NO _x , and formaldehyde emissions, and higher CO and NH ₃ emissions.
			3. For the low methane fuels, the waste hauler showed reduced NO _x emissions, and increased CO and NH ₃ emissions.
Elder et al., 1985	Vehicles have been run on a chassis dynamometer over the urban cycle of NZS 5420	2 LPG fuels(64% propane and 94% propane), 2 CNG fuels (81% methane/2.5% CO ₂ /2.3% N and 73% methane/12% CO ₂ /2.7% N ₂)	1. Little difference in vehicle power output and fuel consumption for the two LPG fuels.
			2. Significant differences in many aspects of vehicle performance for the two CNG fuels.

Table 9. (Continued)

Author	Vehicle/Engine	Fuel	Notable Results
Feist, 2006, 2009	Cummins, John Deere, and DDC Series 50G Natural Gas Engines	8 natural gas fuel blends with varying methane number (MN) and Wobbe Index	All lean burn engines showed increased NO _x and HC emissions with decreased MN and increased Wobbe level, while the stoichiometric engine showed no clear trend in NO _x or HC levels with the various fuels.
Gandhi, 1974			On base metal oxide catalysts, the extent of NH ₃ formation by hydrogen from the shift depends mainly on the activity of the catalyst in the water gas shift reaction. On Ru catalysts, the presence of CO increases NH ₃ formation. Thus, NH ₃ formation by the hydrogen from the shift is higher than that observed in NO-H ₂ system but less than in the NO-CO-H* system, where substantial amounts of CO are present, which makes pairing of N atoms a less probable event.
Gutierrez, 2003, 2006	a rich burn engine	Ventura Line Gas, Liquid Natural Gas, Pico Gas, Seal Beach Gas	1. Average CO and NO _x emissions were always below the requirements from Ventura Air Pollution Control District.
			2. With all the gases, there were some emissions spikes but the researchers were unable to conclude how they were generated.
Hajbabaie et al., 2013b	2 CNG buses equipped with lean burn combustion and OCs, and 1 stoichiometric CNG bus equipped with a TWC and EGR	6 natural gas compositions	1. For the lean burn buses, gases with low methane contents exhibited higher NO _x (19%–53%) and NMHC (39%–102%) emissions, but lower emissions of THC (9%–24%), CH ₄ (23%–33%), and formaldehyde emissions (14%–45%).
			2. The stoichiometric engine bus with a TWC showed significantly reduced NO _x and THC emissions compared to the lean burn buses, but did show higher levels of CO and NH ₃ .
			3. PM mass emissions did not show any fuel effects, while particle number emissions exhibited some reductions for the higher WN gases.
Huai et al., 2003	8 vehicles with low-emission vehicle (LEV) to super-ultralow-emission vehicle (SULEV)	California Phase 2 gasoline doped to 30 ppmw sulfur	1. NH ₃ emissions depend on driving mode and are primarily generated during acceleration events.
			2. High NH ₃ emissions were found for high vehicle specific power (VSP) events and rich operating conditions.
			3. For some vehicles, NH ₃ emissions formed immediately after catalyst light-off during a cold start.
Karavalakis et al., 2012a	A waste hauler truck equipped with a 2001 Cummins 8.3L C Gas Plus lean burn spark-ignited engine	7 Different Natural Gas Blends	1. Fuels with high energy contents and higher hydrocarbons gases exhibiting higher fuel economy and CO ₂ emissions.
			2. Emissions of NO _x increased for gases with higher levels of heavier hydrocarbons.
			3. With gases with higher levels of CH ₄ showed high THC and CH ₄ emissions and lower NMHC emissions.

Author	Vehicle/Engine	Fuel	Notable Results
			4. Decreases in PM mass, particle number, and, in some cases, CO emissions were also found for the gases with more heavy hydrocarbons, while fuel quality had a minimal impact on particle size distributions.
Karavalakis et al., 2012b	2 light-duty vehicles (a 2002 Ford Crown Victoria and a 2006 Honda Civic GX)	Various natural gas compositions	1. For modern light-duty NGVs, fuel properties have a clear and direct impact on fuel economy and some emissions components, such as CO ₂ and NMHC, but not for other emission components, such as THC, NO _x , and CO.
			2. Blends with heavier hydrocarbons and lower H/C ratios, had higher CO ₂ emissions.
			3. NMHC emissions did increase for the two fuels with the highest levels of heavier hydrocarbons for both vehicles.
			4. THC emissions showed higher emissions for the fuel with the higher levels of methane for the Crown Victoria, but no trends for the Honda.
			5. CO emissions were higher for the two fuels with the highest Wobbe numbers for the Honda under some test conditions, including the cold-start phases of the driving cycles, but did not show significant fuel differences for the Crown Victoria.
			6. Changing fuel compositions on this two vehicles showed limited impact on NO _x emissions.
Karavalakis et al., 2012c	A transit bus equipped with a 2003 Cummins C Gas Plus, lean burn, spark ignited natural gas engine	5 natural gas compositions	Natural gas composition had a strong influence on a number of emission components. Blends with higher methane contents showed lower NO _x , CO, and NMHC, but higher THC, CH ₄ , and formaldehyde emissions. PM, CO ₂ , and NH ₃ emissions and energy equivalent fuel economy did not show consistent trends between the fuels tested.
Karavalakis et al., 2013	A waste hauler equipped with a 2002 Cummins 8.3L, C Gas Plus, lean burn, spark ignited natural gas engine	7 natural gas compositions	1. Higher hydrocarbons gases exhibited higher fuel economy and CO ₂ emissions.
			2. NO _x increased for gases with higher levels of heavier hydrocarbons.
			3. THC, CH ₄ , CO, PM, and particle number emissions all showed some reductions for the gases with higher hydrocarbons, higher Wobbe numbers, and higher energy content.
			4. Formaldehyde and acetaldehyde were the most dominant aldehydes in the tailpipe, and decreased with the low methane number and high Wobbe number gases.
			5. NH ₃ emissions did not show consistent fuel trends, however, NH ₃ emission were higher for the higher speed and load phases of the cycle.
Lee & Kim, 2000	3 NGVs	6 different natural gas	1. There is no clear trends regarding the gas compositions to CO, NO _x , CH ₄ , and NMHC emissions.
			2. Gas composition variation has a negligible effect on vehicle drivability.

Table 9. (Continued)

Author	Vehicle/Engine	Fuel	Notable Results
Malenshek & Olsen, 2009	a Cooperative Fuel Research (CFR) F-2 engine	Eight alternative gaseous fuel compositions (ranged from 24 to 140 MN)	1. Extreme variation in the knock tendency of the different alternative gaseous fuels.
			2. The measured methane numbers for wood gas are below those of typical natural gas (61–70 MN).
			3. Maximizing the efficiency and reliability of engines operating on the alternative fuels tested would require fuel-specific engine designs due to the effect of MN on knock limited compression ratio.
Matthews et al., 1996	NGVs	CNG compositions	1. Relatively small changes in the fuel CH ₄ /HC percentage can have an important influence on the tailpipe NMHC emissions, the NMHC/THC ratio, and the HCHO/NMHC ratio.
			2. Substitution of CNG for gasoline should produce a greenhouse benefit of ~19%.
McTaggart et al., 2010	A heavy-duty natural-gas engine	Natural-gas composition (by adding ethane, propane, hydrogen, and nitrogen to the fuel)	1. Emissions of unburned fuel are reduced for all additives through either enhanced ignition or combustion processes.
			2. Black carbon PM emissions are increased by ethane and propane, but are virtually eliminated by including nitrogen or hydrogen in the fuel.
Mejia-Centeno et al., 2007	Commercial TWC	Low-sulfur fuel	Low-sulfur operation of commercial TWC favors formation of N ₂ O and NH ₃ as by products.
Miller et al., 2013	Drayage trucks, a transit bus, and a refuse hauler equipped with a ISL-G engine	Natural gas	Significantly lower emissions of THC, NMHC, CH ₄ , NO _x , formaldehyde, and acetaldehyde emissions, and higher CO and NH ₃ emissions for the ISL-G engine compared to previous studies of lean-burn technology engines.
Naber et al., 1994	A constant-volume combustion vessel	Natural gas compositions representative of variations observed across the U.S.	1. At temperatures < 1200 K, the ignition delay of NG under diesel combustion conditions has a dependence on temperature that is Arrhenius in character and a dependence on pressure that is close to first order.
			2. At higher temperatures > 1300 K, the ignition delays approached a limiting value that was consistent with physical delays associated with the injection system.
Thiruvengadam et al., 2015; Carder et al., 2014	11 heavy-duty goods movement vehicles	Diesel, natural gas, and dual-fuel	1. TWC equipped stoichiometric natural gas vehicles emit 96% lower NO _x emissions as compared to SCR equipped diesel vehicles.
			2. Diesel vehicles emitted considerably higher NO _x emissions than the NG vehicles under lower temperature operating conditions when the SCR temperature was not high enough to activate.

Author	Vehicle/Engine	Fuel	Notable Results
Tong et al., 2015	Medium and heavy-duty vehicles (MHDVs)	Natural gas	1. Compared to the petroleum-based fuels currently used in these vehicles, CNG and centrally produced LNG increase emissions by 0–3% and 2–13%, respectively, for Class 8 trucks.
			2. Compared to their diesel or gasoline counterparts, BEVs reduce emissions by 31–40% and 31%, respectively, for non-class and class 8 trucks.
			3. CNG and propane achieve relatively smaller emissions reductions 0–6% and 19% respectively compared to the petroleum-based fuels, while other NG pathways increase emissions for non-Class 8 MHDVs.
Yoon et al., 2013	2 CNG transit buses equipped with stoichiometric combustion engines and TWCs	Natural gas	1. Stoichiometric combustion with TWC was effective in reducing emissions of NO _x , PM, and NMHC by 87% to 98% depending on pollutants and test cycles, compared to lean combustion.
			2. Stoichiometric combustion with TWC produces higher CO emissions than lean combustion.
			3. Stoichiometric combustion with TWC produced higher GHG emissions including CO ₂ and CH ₄ than lean combustion during the UDSS cycle, but lower GHG emissions during the steady-state cruise cycle.

Table 10. References for Environmental Considerations with Natural Gas Fugitive Emissions

Author	Notable Results
Allen et al., 2013, 2015	This work reports direct measurements of methane emissions from 377 gas actuated (pneumatic) controllers at 190 onshore natural gas sites in the U.S. The measurements indicate that well completion emissions are lower than previously estimated; the data also show emissions from pneumatic controllers and equipment leaks are higher than EPA national emission projections. Estimates of total emissions are similar to the most recent EPA national inventory of methane emissions from natural gas production.
Alvarez et al., 2012	Compressed natural gas vehicles could produce climate benefits on all time frames if the well-to-wheels CH ₄ leakage were capped at a level 45–70% below current estimates. By contrast, using natural gas instead of coal for electric power plants can reduce radiative forcing immediately, and reducing CH ₄ losses from the production and transportation of natural gas would produce even greater benefits.
Burnham et al., 2014	1. The revised total fugitive CH ₄ emissions for shale and conventional NG pathways are now closer in magnitude than they were in our previous version due to the reduction in shale gas completion and workover emissions.
	2. The EPA’s estimates of NG system CH ₄ have decreased significantly since its 2011 inventory, while top-down analyses suggest these emissions should be higher.
Environmental Defense Fund, 2015	The 16 Study Series related to various aspects (like production, transmission, storage, and local distribution) of methane leaks that has significantly enhanced the information available in this area.
Harriss et al., 2015	Region-wide emission estimates can be efficiently obtained using airborne top-down methods, while source-specific measurements can provide insights about the contribution of specific source types.
Karion et al., 2013	Using atmospheric measurements in a mass balance approach to estimate CH ₄ emissions of $55 \pm 15 \times 10^3$ kg h ⁻¹ from a natural gas and oil production field in Uintah County, Utah, on 1 day: 3 February 2012. This emission rate corresponds to 6.2%–11.7% (1 σ) of the average hourly natural gas production in Uintah County in the month of February.
Lamb et al., 2015	Measured CH ₄ emissions from 13 urban distribution systems across the U.S. Emission factors were derived from direct measurements at 230 underground pipeline leaks and 229 metering and regulating facilities using stratified random sampling. When these new emission factors are combined with estimates for customer meters, maintenance, and upsets, and current pipeline miles and numbers of facilities, the total estimate is 393 Gg/Yr with a 95% upper confidence limit of 854 Gg/Yr, which is 36% to 70% less than the 2011 EPA inventory.
Marchese et al., 2015	Estimated CH ₄ emissions from NG gathering and processing plants using Mote Carlo modeling were estimated to be about 87% higher than those for the 2014 EPA Greenhouse Gas Inventory (GHGI), equivalent to about 30% of the total CH ₄ emissions from NG systems. This represented a CH ₄ loss rate of 0.47% for all U.S. gathering and processing operations when normalized by 2012 CH ₄ production levels.
McCain et al., 2015	This study quantifies the full seasonal cycle of CH ₄ emissions and the fractional contribution of NG for the urbanized region centered on Boston. Emissions from NG are found to be two to three times larger than predicted by existing inventory methodologies and industry reports. Our findings suggest that natural-gas-consuming regions may be larger sources of CH ₄ to the atmosphere than is currently estimated and represent areas of significant resource loss.

Author	Notable Results
Mitchell et al., 2015	1. At gathering facilities, the measured CH ₄ emission rates ranged from 0.7 to 700 kg per hour (kg/h) (0.6 to 600 standard cubic feet per minute (scfm)). Normalized emissions were less than 1% for 85 gathering facilities and 19 had normalized emissions less than 0.1%.
	2. The range of CH ₄ emissions rates for processing plants was 3 to 600 kg/h (3 to 524 scfm), corresponding to normalized CH ₄ emissions rates <1% in all cases.
Ogburn, 2013	Given CH ₄ is a greenhouse gas with a global warming potential 25 times higher than CO ₂ , methane leaks at too high a level could off-set or eliminate some of the other environmental benefits associated with NG as a fuel.
Pétron, et al., 2014	Total top-down CH ₄ emission estimates are 25.8 ± 8.4 and 26.2 ± 10.7 t CH ₄ /h for the 29 and 31 May flights, respectively. Using inventory data, total emissions of CH ₄ from non-O&G gas-related sources were estimate to be 7.1 ± 1.7 and 6.3 ± 1.0 t CH ₄ /h for these 2 days.
Burnham et al., 2014	The modeling suggests an upper bound global average fugitive emissions rates (FER) of 5% during 2006–2011, and a most likely FER of 2–4% since 2000, trending downward.
Subramanian et al., 2015	Equipment- and site-level methane emissions from 45 compressor stations in the transmission and storage (T&S) sector of the U.S. NG system were measured, including 25 sites required to report under the EPA greenhouse gas reporting program (GHGRP). The site-level CH ₄ emission rates were highly skewed; the highest emitting 10% of sites (including two superemitters) contributing 50% of the aggregate CH ₄ emissions, while the lowest emitting 50% of sites contributed less than 10% of the aggregate emissions.
U.S. EPA, 2014	1. Since the Industrial Revolution (i.e., about 1750), global atmospheric concentrations of CO ₂ have risen approximately 40 percent (IPCC 2007 and NOAA/ESLR 2013), principally due to the combustion of fossil fuels.
	2. Within the United States, fossil fuel combustion accounted for 94.2 percent of CO ₂ emissions in 2012. Globally, approximately 32,579 Tg of CO ₂ were added to the atmosphere through the combustion of fossil fuels in 2011, of which the United States accounted for about 17 percent.
	3. 13 Changes in land use and forestry practices can emit CO ₂ or can act as a sink for CO ₂ . In addition to fossil fuel combustion, several other sources emit significant quantities of CO ₂ .
Zimmerle et al., 2015	1. Estimated total CH ₄ emissions from the T&S sector at 1,503 [1,220 to 1,950] Gg/yr (95% confidence interval) compared to the 2012 EPA's Greenhouse Gas Inventory (GHGI) estimate of 2,071 [1,680 to 2,690] Gg/yr.
	2. For T&S stations that are required to report to the EPA's Greenhouse Gas Reporting Program (GHGRP), this study estimated total emissions to be 260% [215% to 330%] of the reportable emissions for these stations, primarily due to the inclusion of emission sources that are not reported under the GHGRP rules, updated emission factors, and super-emitter emissions.

DMC can be stored in a tight reservoir in a cool, dry, well-ventilated location away from moist air, plastics and resins. Metal containers used in the transfer of DMC should be grounded and bounded. Outside or detached storage is preferred. DMC can freeze at the same temperature as water. DMC and DMC-based coatings can be thawed out with no degradation of properties (U.S. EPA, 2009).

DMC is highly flammable, and is easily ignited by heat, sparks or flames. DMC vapors may form explosive mixtures with air. Vapors may travel to a source of ignition and flash back. Most vapors are heavier than air. They will spread along the ground and collect in low or confined areas (sewers, basements, tanks). Runoff to sewers may create a fire or explosion hazard. Containers may also explode when heated. Also, DMC needs to be separated from strong oxidants and stored in an area without drain or sewer access (International Program on Chemical Safety/Commission of the European Union 2005).

Environmental Considerations with DMC

DMC as an oxygenated fuel has been found to provide large reductions in PM emissions. There is a general consensus that fuel oxygen content provides reductions in soot formation and diesel PM emissions (Zhu, Cheung, & Huang, 2011; Ren et al., 2008; Mei, Hielscher, & Baar, 2013; Li, Chen, Zhe, & Huang, 2006). Zhu et al. (2011) indicated that PM mass as well as the total particulate number (PN) were both reduced by adding 4.5% to 18.6% DMC to diesel fuel by volume. Cheung et al. (2011) found a greater than 50% PM reduction by adding DMC to diesel at 18.6%. This is consistent with findings from researchers at the UCR, which showed a 75.6% reduction for a 20% DMC blend. Although some research on other oxygenated fuels has shown some slight trends of NO_x emissions reductions (Mei et al., 2013), the impact of DMC on NO_x emissions has generally shown varying results in different research studies. Some researchers have reported that oxygenated fuels can increase NO_x emissions (Singh, Kumar, Mahla, & Bath, 2013; Li et al., 2006; Mei et al., 2013), while others obtained different results (Cheung et al., 2011). Also, slight reductions of HC and CO emissions have been observed (Singh et al., 2013, Cheung et al., 2011, Ren et al., 2008), although researchers at UCR have found some increases in HC emissions.

The health risks of DMC are similar to those of a number of common industrial solvents (Toluene, methyl ethyl ketone). DMC has a recommended industrial exposure (REL) limit of 100 ppm by inhalation over an 8-hour work day. DMC is metabolized by the body to methanol and carbon dioxide, so accidental ingestion should be treated in the same manner as methanol poisoning. DMC is corrosive to the eyes and skin, and can cause serious or permanent injury (JECFA, 1990). It is generally considered to be non-corrosive to all metals. A summary of the environmental studies on DMC as a transportation fuel are listed in the Table 11.

Development and Use of Furans Fuels for Transportation

Furan Fuel Production from Biomass

Another potential fuel is 2,5-Dimethylfuran (DMF), which is a very flammable, water insoluble liquid. DMF serves as a scavenger for singlet oxygen, a property which has been exploited for the determination of singlet oxygen in natural waters. DMF also forms upon thermal degradation of some sugars and has been identified in trace amounts as a component

of caramelized sugars (Powrie, Wu, & Molund, 1986). DMF is commercially produced by a hydrogenolysis reaction. DMF can be synthesized from fructose in a catalytic biomass-to-liquid process via hydroxymethylfurfural (HMF). In 2007, Roman-Leshkov et al. (2007) first proposed a chemical reaction path for producing 2,5-Dimethylfuran from fructose with HCl used as the catalyst. Zhao et al. (2007) tested the efficiencies of a series of catalysts to convert sugars to HMF and found that chromium (II) chloride is the most efficient catalyst with a 70% yield. Besides Roman-Leshkov et al. (2007) and Zhao et al. (2007), a number of other studies have been done to improve the conversion efficiency of glucose to DMF (Chidambaram & Bell, 2010; Shimizu, Uozumi, & Satsuma, 2009; Yong, Zhang, & Ying, 2008). In addition to the conversion of fructose to DMF, DMF can also be made from cellulose (Binder & Raines, 2010; Li, Zhang, & Zhao, 2009; Su et al., 2009) and starch (Chun, Lee, Yi, Hong, & Chung, 2010; Bredihhin, Maorg, & Vares, 2013).

Similar to DMF, 2-Methylfuran (MF) is a flammable, water-insoluble liquid (Chemical Database) with a chocolate odor. MF is a chemical intermediate and is normally manufactured by catalytic hydrogenolysis of furfuryl alcohol or via a hydrogenation-hydrogenolysis sequence from furfural in the vapor phase (Burnette, Johns, Holdren, & Hixon, 1948). More recently, methods like the conversion of enol ether to furans and gold-catalyzed dehydrative cyclization of 1,4 diols and 3,4 diols in the presence of NaCl to form MF have been studied (Lauer, Henderson, Awad, & Stambuli, 2012; Minkler, Isley, Lippincott, Krause, & Lipshutz, 2014). Methoxymethylfurfural (MMF) can also be produced from hexoses (C-6 sugars), such as glucose and fructose, via the dehydration of the hexoses and subsequent etherification of HMF. DMF can also be produced basically through etherification of HMF in alcohols (Bing, Zhang, & Deng, 2012).

2-Methyl-tetrahydrofuran (2-MeTHF) is organic compound, which is a highly flammable mobile liquid and has a rare inversely solubility in water (Pace, Hoyos, Castoldi, Domínguez, & Alcántara, 2012). 2-MeTHF can be derived from renewable resources such as furfural and levulinic acid to be used as a biofuel (Huber, Iborra, & Corma, 2006; Corma, Iborra, & Velty, 2007; Palkovits, 2010) and is a promising alternative solvent. Its physical and chemical properties, such as its low miscibility with water, boiling point, remarkable stability compared to other cyclic-based solvents such as THF, and others make it appealing for applications in syntheses involving organometallics, organocatalysis, and biotransformations or for processing lignocellulosic materials (Pace et al., 2012). The chemical and physical properties of gasoline and alcohol are listed in Table 12.

Utilization of Furan Fuels for Transportation

DMF has the appropriate physicochemical properties to be used as a new type of biofuel in internal combustion (IC) engines. The application of DMF in internal combustion engines has been researched by a number of researchers in recent years (Tian, Xu, Daniel, Li, & Li, 2010; Thewes et al., 2011; Hu et al., 2012). DMF can be mixed with gasoline and diesel at any ratio without the help of additives. The spray characteristics of DMF (Tian et al., 2010) and 2-MF (Thewes et al., 2011) are similar to those of gasoline. Therefore, many researchers have studied the combustion and emission characteristics of pure DMF, DMF/gasoline mixtures, and DMF/diesel blends in gasoline and diesel engines, respectively.

Table 11. References for Environmental Considerations with the Use of DMC as a Transportation Fuel

Author	Vehicle/Engine	Fuel	Notable Results
Cheung et al., 2011	A 4-cylinder DI diesel engine	Euro V diesel blended with DMC in 4.48-18.6% vol	1. The ignition delay and the heat release rate in the premixed combustion phase increase, while the total combustion duration and the fuel consumed in the diffusion combustion phase decrease.
			2. Compared with diesel fuel, with an increase of DMC in the blended fuel, the brake thermal efficiency is slightly improved but the brake specific fuel consumption increases.
			3. CO increases significantly at low engine load but decreases at high engine load while HC decreases slightly for DMC blends.
			4. NOx decreases slightly but the reduction is not statistically significant, while NO ₂ increases slightly for DMC blends.
			5. PM mass and number concentrations decrease upon using the blended fuel while the geometric mean diameter of the particles shifts towards smaller size.
JECFA, 1990		DMC vapor	1. The health risks of DMC are similar to those of a number of common industrial solvents (Toluene, methyl ethyl ketone).
			2. DMC has a recommended industrial exposure (REL) limit of 100 ppm by inhalation over an 8-hour work day.
			3. DMC is metabolized by the body to methanol and CO ₂ , so accidental ingestion should be treated in the same manner as methanol poisoning.
Li et al., 2006	A two stroke single-cylinder diesel engine	Diesel, DMC	This DMC fueled engine has lower NOx emissions and 2–3% higher effective thermal efficiency than the engine operated with diesel fuel in moderate and high load zones.
Mei et al., 2013	A single-cylinder diesel engine	Diesel blended with DMC in 10% by vol	1. The heat release process is more concentrated because the addition of low boiling point DMC boosts the atomization and mixing with air of the blended fuel.
			2. The emissions of HCs and CO are apparently decreased for the 10% DMC blend.
			3. NOx emissions increase owing to the addition of oxygenated fuel DMC, but this is decreased with declining engine load.
Ren et al., 2008	A DI diesel engine	Diesel blended with oxygenated fuel (DMM, DGM, DMC, DEC, DEA, and ethanol) from 0%-20%	1. The smoke concentration decreases regardless of the types of oxygenate additives, and the smoke decreases with the increase of the oxygen mass fraction in the blends without increasing the NOx and engine thermal efficiency.
			2. CO and HC concentrations decrease with an increase in the oxygen mass fraction in the blends.
Singh et al., 2013	A 4-cylinder DI diesel engine	Diesel blend with DMC and DBM in 5-20% vol	1. The smoke content decreased by 35% at full load conditions using DMC20 blend, the oxygen content in the emission increases by 39% with DBM15, the decrease in the % of unburnt hydrocarbons and carbon monoxide is 19 and 21, respectively.

Author	Vehicle/Engine	Fuel	Notable Results
			2. The best fraction for reduction of smoke and CO emissions without significantly affecting the performance of the engine is 15% blends of DMC and DBM with diesel fuel.
Zhu et al., 2011	A 4-cylinder DI diesel engine	Euro V diesel blended with DMC in 4.48-18.6% vol	<p>1. The addition of DMC increases the ignition delay and the amount of heat release in the premixed combustion duration, but shortens both the diffusive burning duration and the total combustion duration.</p> <p>2. The smoke opacity, the PM mass concentration as well as the total number of particulates are all decreased, while the proportion of soluble organic fraction (SOF) in the particulate is increased, by using the DMC blends.</p> <p>3. The geometric mean diameter of the particles for DMC shifts towards smaller size in comparison with that of the diesel fuel.</p>

Table 12. Chemical and Physical Properties of Gasoline and Alcohols

Compound	Lower heating value (MJ/L)	Boiling point (°C)	Heat of vaporization (kJ/kg from 25°C)	Neat RON	Neat MON	Water solubility in oxygenate at 20°C, wt %	Solubility in water at 20°C, wt %	RVP (kPa)	Kinematic viscosity at 20°C (cSt)	Specific gravity @ 20°C
gasoline	30-33	27-225	~351	88-98	80-88	negligible	negligible	54-103	0.37-0.44	0.72-0.78
ethanol	21.4	78	919.6	109	90	miscible	miscible	16	1.5	0.794
1-propanol	24.7	97.2	792.1	104	89	miscible	miscible	6.2	2.7	0.804
2-propanol	24.1	82.3	756.6	106	99	miscible	miscible	12.4	3.1	0.789
1-butanol	26.9	117.7	707.9	98	85	20.1	7.7	2.2	3.6	0.81
2-butanol	26.7	99.6	671.1	105	93	60	12.5	5.3	4.7	0.808
2-methyl-1-propanol (i-butanol)	26.6	107.9	686.4	105	90	20	8.7	3.3	8.3	0.802
1-pentanol	28.5	137.8	647.1			10.6	2.2	0.83	5	0.816
3-methyl-1-butanol (i-pentanol)	28.3	132	617.1			9.8	2.5	1	5.5	0.8
2-methylfuran	27.6	64.7	389	103	86		0.3	18.5		0.913
2,5-dimethylfuran	30.1	94	389.1	119			0.26	13.4	0.57	0.888
2-methyl-tetrahydrofuran	28.2	78	375.3	86	73	5.1	12.1		1.52	0.855
methyl levulinate		196	332.5			miscible	miscible			1.0495
ethyl levulinate	24.8	206	306.7			8.5	15.2	2.1	2.2	1.02 at 25°C
butyl levulinate	27.1	237.5	277.5			2.6	1.3		3	0.97 at 25°C
ethyl pentanoate	25.9	126	371.5				<0.1	4	0.81	

The calorific value of liquid DMF is 33.7 MJ/kg, compared to 26.9 MJ/kg for ethanol and 43.2 MJ/kg for gasoline. DMF has a slightly lower yet comparable energy density (31.5 MJ/L) to gasoline and a higher research octane number (approximately 119), which means it provides better antiknock properties. Hu and his co-workers analyzed the lubricity of DMF and found that DMF had better anti-wear effects than gasoline (Hu et al., 2012). These characteristics suggest that pure DMF can be used directly as fuel in direct injection spark ignition (DISI) engines.

Daniel et al. (2012a) researched the ignition timing sensitivities of pure DMF compared to gasoline and ethanol. The conclusion was that DMF's ignition timing sensitivity was less than that of gasoline but more than that of ethanol. This means a smaller reduction in IMEP compared to gasoline when retarding the fuel injection timing at the same crank angle. Moreover, they also found that DMF has relatively high exhaust gas temperatures and would work well as a cold-start fuel.

Ethoxymethylfurfural (EMF) is a liquid with a boiling point of 235 °C and a energy density of 8.7 kWhL⁻¹, substantially higher than that of ethanol which is 6.1 kWhL⁻¹, and comparable to that of standard gasoline at 8.8 kWhL⁻¹ and diesel fuel at 9.7 kWhL⁻¹ (Gruter & Dautzenberg, 2007). EMF has been tested in blends with diesel fuel by Avantium Technologies, a spin-off of Royal Dutch Shell, which noted that the engine ran smoothly for several hours for all blends levels and the exhaust analysis also showed a significant reduction of soot (Avantium Technologies press).

2-MeTHF is a liquid with a lower heating value at 28.2 MJ/L, compared to 21.4 MJ/L for ethanol and 30-33 MJ/L for gasoline. 2-MeTHF also has advantage of low miscibility with water, less volatile, and high stability to other furan fuels, and thus is suitable for use as a motor fuel.

Environmental Considerations with Furan Fuels for Transportation

The effects of furan fuels on emissions have been studied for both diesel and gasoline engines (Zhang et al., 2013; Chen et al., 2013). The effects of DMF addition on combustion and emissions were investigated on single and multi-cylinder heavy-duty diesel engine in previous studies (Zhang et al., 2013; Chen et al., 2013). These results showed that DMF addition could effectively reduce soot emissions. As the DMF fraction reached up to 30% in volume, the trade-off relationship between NO_x and soot disappeared, and soot emissions were close to zero. The oxygen content studied was up to 16.7% by weight with DMF, which can inhibit soot formation. Zhang et al. (2013) studied DMF/diesel blend combustion properties in a diesel engine. The pressure rise rate with DMF addition was higher than that of diesel fuel and the addition of EHN (2-ethylhexyl nitrate) could shorten ignition delay and reduce the maximum pressure rise rate. The ignition delay of a fuel can be adjusted by mixing a high-octane-number fuel and a high-cetane-number fuel at a certain ratio. The ignition delay increase can drive the mixing of oil and gas, which significantly reduces the amount of soot generated during diffusion combustion.

There have also been some studies of the impact of furans in spark-ignition gasoline engines. Daniel et al. (2012b) studied the hydrocarbon and carbonyl emissions of DMF, which has a high octane number, in a spark-ignition gasoline engine. Of the 12 carbonyls measured in this study, many that were detected in the gasoline exhaust were not detected in the DMF exhaust, including formaldehyde, acetaldehyde, and benzaldehyde. The HC emissions from DMF were found to be governed by unburned DMF.

DMF's downstream environmental and human health impacts should also be evaluated (CDC, 2009; Luque et al., 2008; Mckone et al., 2011). DMF is one of many volatile organic compounds (VOCs) in cigarette smoke and coffee vapor, and it has been detected within exhaled air, systemic blood, and excreted urine of active and passive tobacco smokers (Alonso, Godayol, Antico, & Sanchez, 2010; CDC, 2009; Perbellini, Princivalle, Cerpelloni, Pasini, & Brugnone, 2003). In addition, DMF is one of the metabolites excreted in the urine of subjects exposed to hexane (Iwata, Takeuchi, Hisanaga, & Ono, 1983, 1984; CDC, 2009). Phuong et al. (2012) used a computational toxicology approach to assess the life-cycle impact of DMF. They identified potential adverse biological and environmental impacts of DMF, particularly for its combustion intermediates. Multiple potential associations with disease were predicted. Analysis of structural analogs of DMF revealed 21 genes that are altered by furan and may be potential targets of DMF, and play roles in its biological effects.

2-METHF has a less volatile and also has an environmental benefit. If accidentally spilled from a reaction container into the surrounding environment, 2-MeTHF can be idiotically degraded by sunlight and air, presumable via oxidation and right-opening. Hence, 2-MeTHF has a promising environmental footprint (biobased and easy to degrade). A summary of the environmental studies on furan fuels as a transportation fuel are listed in the Table 13.

Development and Use of P-series Fuels as Transportation Fuels

P-Series Fuels Production

The fuel group known as the P-series is a collection of gasoline additives developed by Dr. Stephen Paul of Princeton University. P-Series fuels are high-octane alternative fuels that can be used in FFVs. P-series can be generated from municipal and agricultural wastes. They are part of a larger family of liquid fuels that can be substituted for gasoline in FFVs. The P-series fuel is a blend of 45–50% ethanol, 15–20% methyltetrahydrofuran (MeTHF) and 30–35% pentanes-plus (C₅-C₉ natural gas liquids). MeTHF can be derived from feedstocks such as corn, waste paper, cellulosic biomass, agricultural waste, construction wood waste, and other wastes via a biochemical process. Lignocellulose (e.g., agricultural waste) is subjected to a dilute acid hydrolysis to obtain furfural from the xylose (C₅) fraction. The furfural is hydrogenated in a two-stage catalytic process to make MeTHF. The solids from the hydrolysis go through a second hydrolysis to liberate glucose (C₆), which is fermented to ethanol. One example, the Biofine Process, is a commercialized technology that uses two-step dilute mineral acid hydrolysis to break down biomass, containing lignocellulose, into intermediate chemicals that can be further transformed into MeTHF and other chemical products (IAGS). P-series fuels require no refining and contain essentially no undesirable olefins, sulfur or aromatics, such as benzene (Kar & Huseyin, 2006).

Table 13. References for Environmental Considerations with the Use of Furan and P-series Fuels as a Transportation Fuel

Author	Vehicle/Engine	Fuel	Notable Results
CDC, 2009; Alonso et al., 2010; Perbellini et al., 2003		DMF exposure	DMF is one of many volatile organic compounds (VOCs) in cigarette smoke and coffee vapor, and it has been detected within exhaled air, systemic blood, and excreted urine of active and passive tobacco smokers.
CDC, 2009; Iwata et al., 1983, 1984		DMF exposure	DMF is one of the metabolites excreted in the urine of subjects exposed to hexane.
Chen et al., 2013	a multi-cylinder CI engine	Diesel blended with DMF, n-butanol, and gasoline in 30% by vol	1. DMF and gasoline have similar fuel properties, but the combustion characteristics of D30 and G30 are greatly different.
			2. Extended ignition delay and fuel oxygen are two key factors to reduce soot emissions, and ignition delay has greater effects on soot reduction compared to fuel oxygen.
			3. As a diesel additive, DMF is superior to n-butanol and gasoline for reducing soot emissions.
Daniel et al., 2012b	A 4 stroke single-cylinder DISI engine	Methanol, ethanol, butanol, DMF, and gasoline	1. The results showed that unburned fuel (DMF) dominates the emissions.
			2. DMF produced the lowest overall carbonyl emissions compared with methanol, ethanol, n-butanol, and gasoline and, more importantly, the lowest emissions of formaldehyde.
Demirbas et al., 2003	2 Ford Tauruses (1996 and 1997 model year)	P-series fuels	Showed reductions in HC emissions (35%), CO emissions (40%), and ozone forming potential (50%), along with a 70% reduction in lifecycle CO ₂ emissions for P-series fuels.
Phuong et al., 2012			1. Assessed the life-cycle impact of DMF.
			2. Identified potential adverse biological and environmental impacts of DMF, particularly for its combustion intermediates.
			3. Analysis of structural analogs of DMF revealed 21 genes that are altered by furans that may be potential targets of DMF and play roles in its biological effects.
Zhang et al., 2013	A modified single cylinder heavy-duty diesel engine	Diesel blended with DMF in 20-40% by vol	1. When the DMF fraction is up to 40%, the trade-off relationship between NO _x and soot disappears and soot emissions are close to zero.
			2. DMF addition has little effect on CO and THC emissions.
			3. NO _x emissions increase for DMF-diesel blends.

Utilization of P-Series Fuels for Transportation

P-series fuels are clear, colorless, liquid blends with an octane between 89 and 93 that can be formulated specifically for winter or summer use in FFVs. In winter, 5% butane may be added for cold starts (Kar & Huseyin 2006). P-series are designed to be used alone or mixed with gasoline in any proportion inside the FFVs gas tank. The basic capability for utilizing P-series fuels in vehicles has already been incorporated into methanol/ethanol FFVs. However, P-series fuels are not gasoline, and cannot be used in a regular gasoline car.

Environmental Considerations with P-Series Fuels

Some limited studies have been conducted to evaluate the emissions impacts of P-series fuels. In an older study, Demirbas et al. (2003) conducted tests on P-series fuels with two Ford Tauruses (1996 and 1997 model year). These tests showed reduction in HC emissions (35%), CO emissions (40%), and ozone forming potential (50%), along with a 70% reduction in lifecycle CO₂ emissions. A summary of the environmental studies on P-series as a transportation fuel are listed in the Table 13.

CONCLUSION

The performance of renewable fuels in various transportation applications is likely to continue to be an important consideration, especially as these fuels become more prevalent in the transportation fuel marketplace. In the near term, the most important considerations will be how some of the more commonly used biofuels, such as ethanol and biodiesel, will impact existing technology vehicles, as well as technologies such as GDI vehicles that are rapidly expanding in production volume. As the biofuels industry advances into the future, it is likely that a broader range of fuels will be incorporated into the transportation fuel supply. This could include fuels like RNG, butanol, GTL fuels, or renewable jet fuels as their production becomes more cost competitive, or more exotic fuels such as DME, DMC, DMF, or P-series fuels that achieve technical breakthroughs. Alternatively, advanced vehicles or engines could be redesigned to take advantage of the unique properties of fuels such as ethanol. In the longer term, it is likely that biofuels will continue to grow in importance in conjunction with advanced technology vehicles with electric drivetrains in leading towards sustainability in the transportation sector.

ACKNOWLEDGMENT

The authors thank Mr. Jiacheng Yang of the University of California, Riverside for his contribution in preparing text, tables, and figures that were included in this chapter.

REFERENCES

Aatola, H., Larmi, M., Sarjoavaara, T., and Mikkonen, S. (2008). Hydrotreated Vegetable Oil (HVO) as Renewable Diesel Fuel; Trade-off between NO_x, Particulate Emission, and

- Fuel Consumption of a Heavy Engine. SAE Technical Paper No. 2008-01-2500. Warrendale, PA: Society for Automotive Engineers.
- AFAVDC. (2009). Alternative Fuels & Advanced Vehicles Data Center, Alternative Fueling Stations, See <http://www.afdc.energy.gov/afdc/fuels/stations.html>.
- AFAVDC. (2009c). Alternative Fuels & Advanced Vehicles Data Center, Biodiesel Production, http://www.afdc.energy.gov/afdc/fuels/biodiesel_production.html.
- AgMRC – Agricultural Marketing Resource Center. (2015). Soybean Oil and Biodiesel useage Projections and Balance Sheet. <http://www.extension.iastate.edu/agdm/crops/outlook/biodieselbalancesheet.pdf>.
- Aikawa, K., Sakuri, T., & Jetter, J. (2010). Development of a predictive model for gasoline vehicle particulate matter emissions. *SAE International Journal of Fuels and Lubrication*, 3(2):610-622.
- Alasfour, F. N. (1998). NOx emission from a spark ignition engine using 30% isobutanol-gasoline blend: Part 1-Preheating inlet air. *Applied Thermal Engineering*, 18, 245-256.
- Alleman, T. L., & McCormick, R. L. (2003). Fischer-Tropsch Diesel Fuels – Properties and Exhaust Emissions: A Literature Review, SAE Technical Paper No. 2003-01-0763. Warrendale, PA: Society for Automotive Engineers.
- Alleman, T. L., McCormick, R. L., & Deutch, S. (2007). 2006 B100 Quality Survey Results; NREL/TP-540-41549; National Renewable Energy Laboratory: Golden, CO, May; <http://www.nrel.gov/docs/fy07osti/41549.pdf>.
- Alleman, T. L. & McCormick, R.L. (2009). 2008 B20 Survey Results; NREL/PR-540-45184; National Renewable Energy Laboratory; Golden, CO, 2 February; <http://www.nrel.gov/vehiclesandfuels/npbf/pdfs/45184.pdf>.
- Alleman, T. L., Fouts, L., & McCormick, R. L. (2010). Analysis of Biodiesel Blend Samples Collected in the United States in 2008, NREL/TP-540-46592, March; <http://www.nrel.gov/vehiclesandfuels/npbf/pdfs/46592.pdf>.
- Alleman, T. L., Fouts, L., & McCormick, R. L. (2011). Quality Analysis of Wintertime B6-B20 Biodiesel Blend Samples Collected in the United States. *Fuel Processing Technology*, 92, 1297-1304.
- Allen, D. T., Torres, V. M., Thomas, J., Sullivan, D. W., Harrison, M., Hendler, A., ... & Seinfeld, J. H. (2013). Measurements of methane emissions at natural gas production sites in the United States. *Proceedings of the National Academy of Sciences*, 110, 17768-17773.
- Allen, D. T., Pacsi, A. P., Sullivan, D. W., Zavala-Araiza, D., Harrison, M., Keen, K., ... & Seinfeld, J. H. (2015). Methane emissions from process equipment at natural gas production sites in the United States: Pneumatic controllers. *Environmental Science & Technology*, 49, 633-640.
- Alonso, M., Godayol, A., Antico, E., Sanchez, J. M. (2010). Assessment of environmental tobacco smoke contamination in public premises: Significance of 2,5-dimethylfuran as an effective marker. *Environmental Science & Technology*, 44(21), 8289–8294.
- AltFuelTruck for a cleaner Fleet.com, CNG Fuel & Trucks, <http://altfueltrucks.com/cng-trucks.htm>.
- Alvarez, R. A., Pacala, S. W., Winebrake, J. J., Chameides, W. L., & Hamburg, S. P. (2012). Greater focus needed on methane leakage from natural gas infrastructure. *Proceedings of the National Academy of Sciences*, 109(7), 6435-6440.

- America's Natural Gas Alliance (ANGA), Safe & Responsible Development, <http://www.anga.us/media/content/F7CF8B54-E9E2-3459-33A250D1F38B3414/files/hydraulic-fracturing-101.pdf>.
- Andersen, V. F., Anderson, J. E., Wallington, T. J., Mueller, S. A., & Nielsen, O. J. (2010). Vapor pressures of alcohol– gasoline blends. *Energy & Fuels*, 24, 3647-3654.
- Anderson, J., Wallington, T., Stein, R., & Studzinski, W., (2014). Issues with T50 and T90 as Match Criteria for Ethanol-Gasoline Blends, *SAE International Journal of Fuels and Lubricants*, 7(3), 1027-1040,
- Arcoumanis, C., Bae, C., Crookes, R., & Kinoshita, E. (2008). The potential of di-methyl ether (DME) as an alternative fuel for compression-ignition engines: A review. *Fuel*, 87, 1014-1030.
- Arteconi, A., Mazzarini, A., & Nicola, G. D. (2011). Emissions from ethers and organic carbonate fuel additives: A review. *Water Air and Soil Pollution*, 221, 405–423.
- Avantium Technologies Press release: <http://www.avantium.com/index.php?p = 115&n = 2>.
- Azizi, Z., Rezaeimanesh, M., Tohidian, T., & Rahimpour, M. R. (2014). Dimethyl ether: A review of technologies and production challenges. *Chemical Engineering and Processing: Process Intensification*, 82, 150-172.
- Bach, C. (2008). Challenges and Potential of Advanced Methane Gas Vehicles. In: SATW Congress, August.
- Bagley, S. T., Gratz, L. D., Johnson, J. H., & McDonald, J. F. (1998). Effects of an oxidation catalytic converter and a biodiesel fuel on the chemical, mutagenic, and particle size characteristics of emissions from a diesel engine. *Environmental Science & Technology*, 32, 1183-1191.
- Bakeas, E., Karavalakis, G., & Stournas, S., (2011a). Biodiesel emissions profile in modern diesel vehicles. Part 1: Effect of biodiesel origin on the criteria emissions. *Science of the Total Environment*, 409, 1670-1676.
- Bannister, C. D., Hawley, J. G., Ali, H. M., Chuck, C. J., Price, P., Chrysafi, S. S., et al. (2010). The impact of biodiesel blend ratio on vehicle performance and emissions. *Proceedings of the Institution of Mechanical Engineers, Part D: Journal of Automobile Engineering*, 224, 405-421.
- Bates, G. J., & Germano, S. (1994). Vehicle Tail Pipe Emissions – A comparison of Natural Gas and Petrol Injection. SAE Technical Paper No. 942042. Warrendale, PA: Society for Automotive Engineers.
- Beach, F., Gonzales, M., & Butler, J. (2011). An Analysis of the Potential for Expanded Use of Natural Gas in Electric Power Generation, Transportation, and Direct Use: Texas as a Case Study, The University of Texas at Austin, October. Available at: <http://www.webberenergygroup.com/images/stories/NatGasFinalReport31712.pdf>.
- Bhide, S., Chapman, E., Stefanik, J., Glunt, H., Boehman, L.I., Boehman, A.L., & Waller, F.J. (2002). Development of a Dimethyl Ether-Fueled Shuttle Bus. *American Chemistry Society - Fuel Chemistry Division*, 47(2), 562-563.
- Bhide, S., Morris, D., Leroux, J., Wain, K.S., Perez, J. M., & Boehman, A.L. (2003). Characterization of the Viscosity of Blends of Dimethyl Ether with Various Fuels and Additives. *Energy and Fuels*, 17, 1126-1132.
- Binder, J. B., & Raines, R. T. (2009). Simple chemical transformation of lignocellulosic biomass into furans for fuels and chemicals. *Journal of the American Chemical Society*, 131(5), 1979–85.

- Bing, L., Zhang, Z., & Deng, K. (2012). Efficient one-pot synthesis of 5-(ethoxymethyl) furfural from fructose catalyzed by a novel solid catalyst. *Industrial & Engineering Chemistry Research*, 51, 15331-15336.
- Biodiesel Handling and Use Guide, forth edition. (2009). NREL/TP-540-43672, http://www.nrel.gov/vehiclesandfuels/npcf/feature_guidelines.html.
- Bishop, G. A., Schuchmann, B. G., & Stedman, D. H. (2012). Emission Changes Resulting from the San Pedro Bay, California Ports Truck Retirement Program. *Environmental Science & Technology*, 46(1), 551-558.
- Boehman, A.L. (2008). Developments in production and utilization of dimethyl ether for fuel applications, *Fuel Processing Technology*, 89, 1243.
- Bourg, H. (2006). Future Prospective of DME. 23rd World Gas Conference, Amsterdam.
- Boyd, B. (2012). Methanol Industry Presentation, Methanex.
- BP and Dupont (2010). Biobutanol Fact Sheet. http://www2.dupont.com/Production_Agriculture/en_US/assets/downloads/pdfs/BP_DuPont_Fact_Sheet_Biobutanol.pdf.
- BP (2008). 1-Butanol as a Gasoline Blending Biocomponent, presentation to the Mobile Source Technical Review Subcommittee, March.
- Brandt, A. R., Heath, G. A., Kort, E. A., O'Sullivan, F., Pétron, G., Jordaan, S. M., ... & Harriss, R. (2014). Methane leaks from North American natural gas systems. *Science*, 343, 733-735.
- Bredihhin, A., Maorg, U., & Vares, L. (2013). Evaluation of carbohydrates and lignocellulosic biomass from different wood species as raw material for the synthesis of 5-bromomethylfurfural. *Carbohydrate Research*, 375, 63-7.
- Broch, A., Hoekman, S. K., & Unnasch, S. (2012). Transportation Fuel Life Cycle Analysis: A Review of Indirect Land Use Change and Agricultural N2O Emissions. Final report for project E-88-2 by the Desert Research Institute for the Coordinating Research Council.
- Broch, A., Hoekman, S.K., & Unnasch, S. (2013). A review of variability in indirect land use change assessment and modeling in biofuel policy. *Environmental Science & Policy*, 29, 147-157.
- Burnette, L. W., Johns, I. B., Holdren, R. F., & Hixon, R. M. (1948). Production of 2-methylfuran by vapor-phase hydrogenation of furfural. *Industrial & Engineering Chemistry*, 40, 502-505.
- Burnham, A., Han, J., Elgowainy, A., & Wang, M. (2014). Updated Fugitive Greenhouse Gas Emissions for Natural Gas Pathways in the GREET1_2014 Model. Argonne National Laboratory.
- Burns, V. R., William J. K., Benson, J. D., Gorse, R. A., & Rutherford, J. A. (1994). Emissions with Reformulated Gasoline and Methanol Blends in 1992 and 1993 Model Year Vehicles, SAE Technical Paper No. 941969. Warrendale, PA: Society for Automotive Engineers.
- Butler, A. D., Sobotowski, R., Hoffman, G., & Machiele, P. (2015) Influence of fuel PM index and ethanol content on particulate emissions from light-duty gasoline vehicles, SAE Technical Paper 2015-01-1072.
- Byusch, H. Ullmann's Encyclopedia of Industrial Chemistry 7th ed. (1999-2012). NY, NY: John Wiley & Sons; Carbonic Esters. Online Posting Date: June 15, 2000.
- Cahill, T. M., & Okamoto, R. A. (2012). Emissions of acrolein and other aldehydes from biodiesel-fueled heavy-duty vehicles. *Environmental Science & Technology*, 46, 8382-8388.

- California Air Resources Board. (1998). Comparison of the Effects of a Fully-complying Gasoline Blend and a High RVP Ethanol Gasoline Blend on Exhaust and Evaporative Emissions. October.
- California Air Resources Board. (1999). Air Quality Impacts of the Use of Ethanol in California Reformulated Gasoline. December.
- California Air Resources Board. (2009a). Proposed Regulation to Implement the Low Carbon Fuel Standard. Volume I: Staff Report: Initial Statement of Reasons, <http://www.arb.ca.gov/regact/2009/lcfs09/lcfsisor1.pdf>.
- California Air Resources Board. (2012). LCFS lookup tables http://www.arb.ca.gov/fuels/lcfs/lu_tables_11282012.pdf.
- California Air Resources Board. (2013). North American Landfill Gas to CNG Method 1 Fuel Pathway, <http://www.arb.ca.gov/fuels/lcfs/2a2b/internal/nalfg-cng-031513.pdf>.
- California Air Resources Board. (2014a). California-Modified GREET Fuel Pathway: Biodiesel Produced in the Midwestern and the Western U.S. from Corn Oil Extracted at Dry Mill Ethanol Plants that Produce Wet Distiller's Grains with Solubles, http://www.arb.ca.gov/fuels/lcfs/2a2b/apps/co_bd_wdgs-rpt-102414.pdf.
- California Air Resources Board. (2014b). Detailed California-Modified GREET Pathway for Ultra Low Sulfur Diesel (ULSD) from Average Crude Refined in California, <http://www.arb.ca.gov/fuels/lcfs/121514ulsd.pdf>.
- California Air Resources Board. (2014c). Low Carbon Fuel Standard (LCFS) Pathway for the Production of Biomethane from High Solids Anaerobic Digestion (HSAD) of Organic (Food and Green) Wastes, 2014, <http://www.arb.ca.gov/fuels/lcfs/121514hsad.pdf>.
- California Air Resources Board. (2014d). Low Carbon Fuel Standard (LCFS) Pathway for the Production of Biomethane from the Mesophilic Anaerobic Digestion of Wastewater Sludge at a Publicly-Owned Treatment Works (POTW), 2014, <http://www.arb.ca.gov/fuels/lcfs/121514wastewater.pdf>.
- California Energy Commission. "Frequently Asked Questions About LNG." (2008). Available at <http://www.energy.ca.gov/lng/faq.html#100>.
- Camuzeaux, J. R., Alvarez, R. A., Brooks, S. A., Browne, J. R., & Sterner, T. (2015). Influence of methane emissions and vehicle efficiency on the climate implications of heavy-duty natural gas trucks. *Environmental Science & Technology*, 49(11), 6402-6410.
- Carder, D., Gautam, M., Thiruvengadam, A., & Besch, M. (2014). In-Use Emissions Testing and Demonstration of Retrofit Technology for Control of On-Road Heavy-Duty Engines, Final Report by West Virginia University for the South Coast Air Quality Management District.
- Center for Climate and Energy Solutions (C2ES). (2012). Natural gas use in the transportation sector, May.
- Center for Liquefied Natural Gas. (2012). Overview <http://www.lngfacts.org/About-LNG/Overview.asp>.
- Centers for Disease Control and Prevention. (CDC). (2009). Fourth National Report on Human Exposure to Environmental Chemicals. Available at: <http://www.cdc.gov/exposurereport/>.
- Ceresana Technologiezentrum, Market Study: Butanol. http://www.ceresana.com/upload/Marktstudien/brochueren/Ceresana-Brochure_Market_Study_Butanol.pdf.

- Chapman, E., Boehman, A., Tijm, P., & Waller, F., (2003). Emission Characteristics of a Navistar 7.3L Turbodiesel Fueled with Blends of Dimethyl Ether and Diesel Fuel, SAE Technical Paper 2001-01-3626. Warrendale, PA: Society for Automotive Engineers.
- Chen, G. S., Shen, Y. G., Zhang, Q. C., Yao, M. F., Zheng, Z., Q., & Liu, H. F. (2013). Experimental study on combustion and emission characteristics of a diesel engine fueled with 2,5-dimethylfuran-diesel, n-butanolediesel and gasolinediesel blends. *Energy*, *54*, 333-42.
- Chen, L., Stone, R., & Richardson, D. (2012). A study of mixture preparation and PM emissions using a direct injection engine with stoichiometric gasoline/ethanol blends. *Fuel*, *96*, 120-130.
- Cheng, A. S., Upatnieks, A., & Mueller, C. (2006). Investigation of the Impact of Biodiesel Fuelling on NO_x Emissions Using an Optical Direct Injection Diesel Engine. *International Journal of Engine Research*, *7*, 297-318.
- Cheung, C. S., Zhu, R. J., & Huang, Z. H. (2011). Investigation on the gaseous and particulate emissions of a compression ignition engine fueled with diesel-dimethyl carbonate blends. *Science of the Total Environment*, *409*, 523-529.
- Chidambaram, M., & Bell, A. T. (2010). A two-step approach for the catalytic conversion of glucose to 2,5-dimethylfuran in ionic liquids. *Green Chemistry*, *12*(7), 1253-62.
- Chun, J. A., Lee, J. W., Yi, Y. B., Hong, S. S., & Chung, C. H. (2010). Direct conversion of starch to hydroxymethylfurfural in the presence of an ionic liquid with metal chloride. *Starch/Stärke*, *62*(6), 326-30.
- Clairotte, M., Adam, T. W., Zardini, A. A., Manfredi, U., Martini, G., Krasenbrink, A., Vicet, A., Tournie, E., & Astorga, C. (2013). Effects of low temperature on the cold start gaseous emissions from light duty vehicles fuelled by ethanol-blended gasoline. *Applied Energy*, *102*, 44-54.
- Cobb, J. (2015). "December 2014 Dashboard." HybridCars.com and Baum & Associates. Retrieved 2015-08-25.
- Coker, A. (2012). Dimethyl Carbonate. Retrieved July 20, 2015, from http://thinking.nexant.com/sites/default/files/report/field_attachment_abstract/201212/2012S12_abs_R1.pdf.
- Coordinating Research Council. (2004). 2003 CRC Intermediate Temperature Volatility Program, CRC Report No. 638. <http://www.crcao.org/publications/performance/index.html>.
- Coordinating Research Council. (2007). 2006 CRC Hot-Fuel-Handling Program, Report No. 648. <http://www.crcao.org/publications/performance/index.html>.
- Coordinating Research Council. (2008). 2008 CRC Cold Start and Warm-Up E85 and E15/E20 Driveability Program, Report No. 652 <http://www.crcao.org/publications/performance/index.html>.
- Coordinating Research Council. (2010). 2009-2010 CRC/ASTM Hot-Fuel Handling Program, Report No. 658. <http://www.crcao.org>.
- Coordinating Research Council. (2011a). 2010 CRC Altitude Hot-Fuel Handling Program, CRC Report No. 659. <http://www.crcao.org/publications/performance/index.html>.
- Coordinating Research Council. (2011b). Durability of Automotive Fuel Components Exposed to E20, CRC Report No. 662, Project AVFL-15. <http://www.crcao.org/publications/advancedVehiclesFuelsLubricants/index.html>.

- Coordinating Research Council. (2013). Durability of Fuel Pumps and Fuel Level Sensors in Neat and Aggressive E15, CRC Report No. 664, AVFL-15a <http://www.crao.org/publications/advancedVehiclesFuelsLubricants/index.html>.
- Corma, A., Iborra, S., & Velty, A. (2007). Chemical routes for the transformation of biomass into chemicals. *Chemical Reviews*, 107(6), 2411-2502.
- Correa, S. M., & Arbilla, G., (2008). Carbonyl emissions in diesel and biodiesel exhaust. *Atmospheric Environment*, 42(4), 769-775.
- Crawford, R., Haskew, H., Heiken, J., McClement, D., & Lyons, J. (2009). Effects of Vapor Pressure, Oxygen Content and Temperature on CO Exhaust Emissions, CRC Report No. E-74b. <http://www.crao.org/publications/emissions/index.html>.
- Delledonne, D., Rivetti, F., & Romano, U. (2001). Developments in the production and application of dimethyl carbonate. *Applied Catalysis A - General*, 221(1-2), 241-251.
- Demirbas, A. (2003). Current advances in alternative motor fuels. *Energy Exploration & Exploitation*. No. 5 & 6, 21, 475-487.
- Daniel, R., Xu, H., Wang, C., Richardson, D., & Shuai, S. (2012a). Combustion performance of 2, 5-dimethylfuran blends using dual-injection compared to direct-injection in a SI engine. *Applied Energy*, 98, 59-68.
- Daniel, R., Wei, L. X., Mu, H. M., Wang, C. M., Wyszynski, M. L., & Shuai, S. (2012b). Speciation of hydrocarbon and carbonyl emissions of 2,5-dimethylfuran combustion in a DISI engine. *Energy & Fuels*, 26, 6661-8.
- Dernotte, J., Mounaim-Rousselle, C., Halter, F., & Seers, P. (2010). Evaluation of butanol-gasoline blends in a port fuel-injection, spark-ignition engine. *Oil & Gas Science and Technology - Revue d'IFP Energies nouvelles*, 65, 345-351.
- Dolan, G. (2008). Methanol Fuels: The Time has Come. presentation at the 17th ISAF conference, Taiyuan, China, October.
- Durbin, T. D., Collins, J. R., Norbeck, J. M., and Smith, M. R., (2000). Effects of biodiesel, biodiesel blends, and a synthetic diesel on emissions from light heavy-duty diesel vehicles. *Environmental Science & Technology*, 34, 349-355.
- Durbin, T. D., Miller, J. W., Younglove, T., Huai, T., & Cocker K. (2006). Effects of Ethanol and Volatility Parameters on Exhaust Emissions: CRC Project No. E-67. Final report for Coordinating Research Council, CRC Project No. E-67, January.
- Durbin, T. D., Miller, J. W., Younglove, T., Huai, T., & Cocker K. (2007). Effects of Fuel Ethanol and Volatility on Regulated and Unregulated Exhaust Emissions for the Latest Technology Gasoline Vehicles. *Environmental Science & Technology*, 41, 4059-4064.
- Durbin, T. D., Miller, J. W., Johnson, K., Hajbabaei, M., Kado, N. Y., Kobayashi, R., et al. (2011). Final Report for the CE-CERT Engine Testing Portion for the CARB Assessment of the Emissions from the Use of Biodiesel as a Motor Vehicle Fuel in California "Biodiesel Characterization and NOx Mitigation Study." Final Report Prepared for CARB, October.
- Durbin, T., Karavalakis, G., Johnson, K., Miller, J., & Hajbabaei, M. (2014). Evaluation of the Performance and Air Pollutant Emissions of Vehicles Operating on Various Natural Gas Blends – Heavy-Duty Vehicle Testing. Final Report submitted to California Energy Commission (CEC).
- Durbin, T. D., Karavalakis, G., Norbeck, J. M., Park, C. S., Castillo, J., Rheem, Y., Bumiller, K., Yang, J., Van, V., Hunter, K. (2015a). Material compatibility evaluation for

- elastomers, plastics, and metals exposed to ethanol and butanol blends. *Fuel*, 163, 248–259.
- Durbin, T. D., Karavalakis, G., Norbeck, J. M., Park, C. S., Castillo, J., Rheem, Y., Bumiller, K., Van, V., Hunter, K., Yang, J., Thanmongkhon, Y. (2015b). The RNG and Fungible Fuels Infrastructure Compatibility Study. Draft Final Report for the California Energy Commission under contract no. 500-11-015.
- Eckerle, W. A., Lyford-Pike, E. J., Stanton, D. W., LaPointe, L. A., Whitacre, S. D., & Wall, J. C. (2008). Effects of Methyl Ester Biodiesel Blends on NO_x Emissions. SAE Technical Paper 2008-01-0078. Warrendale, PA: Society for Automotive Engineers.
- Eirich, J., Chapman, E., Glunt, H., Klinikowski, D. et al., (2003). Development of a Dimethyl Ether (DME)-Fueled Shuttle Bus, SAE Technical Paper 2003-01-0756. Warrendale, PA: Society for Automotive Engineers.
- Elder, S. T., Jones, K., & Taine, R. R. (1985). Effects of Varying fuel Composition on the Performance of CNG and LPG Fuelled Vehicles. In: Professional Engineers of New Zealand Transcripts, 12, No. 3/EMCh, November.
- Environmental Defense Fund. (2015). Methane Research: The 16 Study Series an unprecedented look at methane from the natural gas system, http://www.edf.org/sites/default/files/methane_studies_fact_sheet.pdf.
- Ernst, W. D., Meacher, J. S., & Bascom, R. C. (1992). Status and Emissions Results for Natural-Gas-Fired Stirling Engine. SAE Technical Paper No. 920383.
- European Biomass Technology Platform, 24th European Biomass Conference and Exhibition. (n.d.). Retrieved July 29, 2015, from <http://www.eubce.com/home.html>.
- Evaporative Emissions Certified Vehicles, CRC Report No. E-77-2c. <http://www.crcao.org/publications/emissions/index.html>.
- Fargione, J., Hill, J., Tilman, D., Polasky, S., & Hawthorne, P. (2008). Land clearing and the biofuel carbon debt, *Science*, 319, 1235–3.
- Feist, M. D. (2006). Fuel Composition Testing using DDC Series 50G Natural Gas Engines. Final report prepared by Southwest Research Institute for the Southern California Gas Company, Report No. 11657, August.
- Feist, M. D. (2009). Fuel Composition Testing using Cummins, John Deere, and Detroit Diesel Natural Gas Engines. Final report prepared by Southwest Research Institute for the Southern California Gas Company, Report No. 03.13721, April.
- Feng, W. L., Cao, Y., Yi, N., Dai, W. L., & Fan, K. N. (2004). A remarkable effect of alkali addition in the oxidative carbonylation of methanol to dimethyl carbonate catalyzed by a polymer-complexed Cu (II) catalyst system. *Chemistry Letters*, 33, 958-959.
- Fontaras, G., Karavalakis, G., Kousoulidou, M., Tzamkiozis, T., Ntziachristos, L., Bakeas, E., Stournas, S., & Samaras, Z., (2009). Effects of biodiesel on passenger car fuel consumption, regulated and non-regulated pollutant emissions over legislated and real world driving cycles. *Fuel*, 88, 1608-1617.
- Fontaras, G., Karavalakis, G., Kousoulidou, M., Ntziachristos, L., Bakeas, E., Stournas, S., & Samaras, Z. (2010a). Effects of low concentration biodiesel blends application on modern passenger cars. Part 2: Impact on carbonyl compound emissions. *Environmental Pollution*, 158, 2496-2503.
- Frank, E. D., Elgowainy, A., Han, J., & Wang, Z. (2013). Life cycle comparison of hydrothermal liquefaction and lipid extraction pathways to renewable diesel from algae. *Mitigation & Adaption Strategies for Global Change*, 18, 137–158.

- Furey, R.L. (1985). Volatility characteristics of gasoline-alcohol and gasoline-ether fuel blends. SAE Technical Paper, 852116. Warrendale, PA: Society for Automotive Engineers.
- Gandhi, H. S. (1974). Ammonia Formation in the Catalytic Reduction of Nitric Oxide. III. The Role of Water Gas Shift, Reduction by Hydrocarbons, and Steam Reforming. *Industrial & Engineering Chemistry Product Research and Development*, 13, 80–5.
- Gas Journal. (2009). Kinder Morgan Begins Biodiesel Shipments on Oregon Pipeline, Sept. <http://www.pgjonline.com/kinder-morgan-begins-biodiesel-shipments-oregon-pipeline>.
- Gautam, M., Martin, II D. W., & Carder, D. (2000). Emissions characteristics of higher alcohol/gasoline blends. *Proceedings of the Institution of Mechanical Engineers, Part A: Journal of Power and Energy*, 214, 165-182.
- Gorse, R., Benson, J., Burns, V., Hochhauser, A. et al., (1992) The Effects of Methanol/Gasoline Blends on Automobile Emissions, SAE Technical Paper 920327. Warrendale, PA: Society for Automotive Engineers.
- Gruter, J. M., & Dautzenberg, F., (2007). European Patent Application, 1834950A1.
- Gutierrez, J. H., Saldivar, A. R., & Mora, J. R. (2003). LNG Research Study – Phase 1. Testing of a Natural Gas Compressor Engine. Report by the Southern California gas Company, October.
- Gutierrez, J., Hamze, F., & Mak, C. (2006). LNG Research Study [Internet]. April. Report by the Southern California gas Company. Available from: http://www.socalgas.com/documents/business/gasquality/Richburn_engine_report.pdf.
- Hajbabaei, M., Johnson, K., Okomoto, R., & Durbin, T. D. (2012). Evaluation of the Impacts of Biodiesel and Second Generation Biofuels on NOx Emissions for Clean Diesel Fuels. *Environmental Science & Technology*, 46(16):9163–73.
- Hajbabaei, M., Johnson, K. C., Okamoto, R., & Durbin, T. D. (2013a). Evaluation of the impacts of Biofuels on Emissions for a California-Certified Diesel Fuel from Heavy-Duty Engines. SAE Technical Paper 2013-01-1138. Warrendale, PA: Society for Automotive Engineers.
- Hajbabaei M., Karavalakis G., Johnson K. C., Lee L., & Durbin T. D. (2013b). Impact of natural gas fuel composition on criteria, toxic, and particle emissions from transit buses equipped with lean burn and stoichiometric engines. *Energy*, 62, 425-434.
- Hajbabaei, M., Karavalakis, G., Johnson, K. C., Guthrie, J., Mitchell, A., & Durbin, T. D. (2014). Impacts of Biodiesel Feedstock and Additives on Criteria Emissions from a Heavy-Duty Engine. *Fuel Processing Technology*, 126, 402-414.
- Hamberg, K., Furseth, D., Wegrzyn, J., LaRusso, A., Chahbazpour, D., Richardson, G., Carr, B., Clay, H., Cassidy, C., Ippoliti, M., Lewnard, J., Williams, G., & Chase, B. (2012). Renewable Natural Gas for Transportation: An overview of the Feedstock Capacity, Economics, and GHG Emission Reduction Benefits of RNG as a Low-Carbon Fuel, made available August 1.
- Hansen, C. (2007). Hansen Solubility Parameters: A User's Handbook, 2nd Edition, CRC Press, Boca Rotan, FL.
- Hansen, J.B., & Mikkelsen, S. (2001). DME as a Transportation Fuel. Prepared for the Danish Road Safety and Transport Agency and the Danish Environmental Protection Agency. Lyngby, Denmark.
- Harriss, R., Alvarez, R. A., Lyon, D., Zavala-Araiza, D., Nelson, D., & Hamburg, S. P. (2015). Using Multi-Scale Measurements to Improve Methane Emission Estimates from

- Oil and Gas Operations in the Barnett Shale Region, Texas. *Environmental Science & Technology*, 49, 7524-7526.
- Haskew, H. M., Liberty, T. F., & McClement, D. (2004). Fuel Permeation From Automotive Systems, CRC Project No. E-65. Report by Harold Haskew & Associates, Inc., Milford, MI, and Automotive Testing Laboratories, Inc. Mesa, Arizona.
- Haskew, H. M., Liberty, T. F., & McClement, D. (2006). Fuel Permeation From Automotive Systems: E0, E6, E10, E20 and E85, CRC Project No. E-65-3. <http://www.crcao.org/publications/emissions/index.html>.
- Haskew, H. M. & Liberty, T. F. (2010a). Enhanced Evaporative Emission Vehicles, CRC Report No, E-77-2. <http://www.crcao.org/publications/performance/index.html>.
- Haskew, H. M. & Liberty, T. F. (2010b). Study to Determine Evaporative Emission Breakdown, Including Permeation Effects and Diurnal Emissions, Using E20 Fuels on Aging Enhanced.
- Haskew, H., & Liberty, T. F. (2011). Exhaust and Evaporative Emissions Testing of Flex-Fuel Vehicles. CRC Project E-80. Final Report to the Coordinating Research Council.
- He, X., Ireland, J. C., Zigler, B. T., Ratcliff, M. A., Knoll, K. E., Alleman, T. L., ... & Tester, J. T. (2010, January). The impacts of mid-level alcohol content in gasoline on SIDI engine-out and tailpipe emissions. In ASME 2010 Internal Combustion Engine Division Fall Technical Conference (pp. 189-201). American Society of Mechanical Engineers.
- Heating Oil News. (2011). Colonial Okays Biodiesel Pipeline Shipments in Georgia. Nov. 9, <http://www.heatingnews.org/heatingoilnews.php?IID=50>.
- Hendricks, R. C., Bushnell, D. M., & Shouse, D. T. (2011). Aviation Fueling: A Cleaner, Greener Approach. *International Journal of Rotating Machinery*, (ID 782969), 13.
- Hochhauser, A. M., Benson, J. D., Burns, V. R., Gorse, R. A., Koehl, W. J., Painter, L. J., Rippon, B. H., Reuter, R. M., & Rutherford, J. A. (1991). The effect of Aromatics, MTBE, Olefins, and T90 on Mass Exhaust Emissions from Current and Older Vehicles – The Auto/Oil Air Quality Improvement Research Program. SAE Technical Paper No. 912322. Warrendale, PA: Society for Automotive Engineers.
- Hochhauser, A. M. (2008). Review of Prior Studies of Fuel Effects on Vehicle Emissions, CRC Report No. E-84. <http://www.crcao.org/publications/emissions/index.html>.
- Hochhauser, A. M., & Schleyer, C. H. (2014). Summary of Research on the Use of Intermediate Ethanol Blends in On-Road Vehicles. *Energy & Fuels*, 28, 3236-3247.
- Hoekman, S. K., Gertler, A., Broch, A., & Robbins C. (2009). Investigation of Biodistillates as Potential Blendstocks for Transportation Fuels. CRC Project No. AVFL-17 Final Report, June, <http://www.gasda.org/Lists/Announcements/DispForm.aspx?ID=33>.
- Hoekman, S. K., Broch, A., Robbins, C., Cenicerros, E. (2011). Investigation of Biodiesel Chemistry, Carbon Footprint and Regional Fuel Quality. Final report for project AVFL-17a by the Desert Research Institute for the Coordinating Research Council, January.
- Hoekman, S. K., & Robbins C. (2012). Review of the Effects of Biodiesel on NOx Emissions. *Fuel Processing Technology*, 96, 237–49.
- Honeywell. (2015). Honeywell's UOP Renewable Jet Fuel Technology to be Used for U.S. Military Testing and Certification, http://www51.honeywell.com/honeywell/news-events/case-studies-n3n4/jet_fuel_technology.html?c=.
- Hu, E., Hu, X., Wang, X., Xu, Y., Dearn, K. D., Xu, H. M. (2012). On the fundamental lubricity of 2,5-dimethylfuran as a synthetic engine fuel. *Tribology International*, 55, 119–25.

- Huai, T., Durbin, T., Miller, J., Pisano, J., Sauer, C., Rhee, S., et al. (2003). Investigation of NH₃ Emissions from New Technology Vehicles as a Function of Vehicle Operating Conditions. *Environmental Science & Technology*, 37, 4841–7.
- Huang, Z., Zhang, W., Fang, J., & Qiao, X. (2010). Shanghai DME Bus Demonstration: Recent Progress, 4th International DME Conference, Slussen, Stockholm, September.
- Huber, G. W., Iborra, S., & Corma, A. (2006). Synthesis of transportation fuels from biomass: chemistry, catalysts, and engineering. *Chemical reviews*, 106(9), 4044-4098.
- ICM (2009) Retrieved in 2009. From: <http://www.icminc.com/corporate/company-profile.html>.
- Informa Economics (2012). Impact of the Biodiesel Industry on the U.S. Soybean Complex. Presentation to the Minnesota Soybean Growers Association, December.
- Institute for Analysis of Global Security (IAGS), accessed July 15th, 2015, <http://www.iags.org/biofine.htm>.
- International Program on Chemical Safety/Commission of the European Union; International Chemical Safety Card on Dimethyl Carbonate (616-38-6) (April 20, 2005). Available from, as of February 14, 2013.
- Irimescu A. (2011). Fuel conversion efficiency of a port injection engine fueled with gasoline-isobutanol blends. *Energy*, 36, 3030-3035.
- Ishiwada, A. (2011) DME Promotion Project in Japan – As a Future Alternative Clean Energy, presented at the 7th Asian DME Conference, November.
- Iwata, M, Takeuchi, Y, Hisanaga, N, Ono, Y. (1984). Changes of n-hexane neurotoxicity and its urinary metabolites by long-term co-exposure with MEK or toluene. *International Archives of Occupational and Environmental Health*, 54(4), 273–281.
- Iwata, M, Takeuchi, Y, Hisanaga, N, Ono, Y. (1983). Changes of n-hexane metabolites in urine of rats exposed to various concentrations of n-hexane and to its mixture with toluene or MEK. *International Archives of Occupational and Environmental Health*, 53(1), 1–8.
- Japan DME Association. (2015). http://japan-dme.or.jp/english/dme/vehicle_fillingequipment.html.
- Joint FAO/WHO Expert Committee on Food Additives (JECFA), (1990). published in FNP 52.
- Jones, B., Mead, G., & Stevens, P. (2008a). The Effects of E20 on Plastic Automotive Fuel System Components, Minnesota Center for Automotive Research at Minnesota State University, Makato, MN. <http://www.mda.state.mn.us/news/publications/renewable/ethanol/e20onplastics.pdf>.
- Jones, B., Mead, G., Steevens, P., & Timanus, M. (2008b). The Effects of E20 on Metals Used in Automotive Fuel System Components, Minnesota Center for Automotive Research at Minnesota State University, Makato, MN <http://www.mda.state.mn.us/news/publications/renewable/ethanol/e20onmetals.pdf>.
- Jones, B., Mead, G., Steevens, P., & Connors, C. (2008c). The Effects of E20 on Elastomers Used in Automotive Fuel System Components, Minnesota Center for Automotive Research at Minnesota State University, Makato, MN <http://www.mda.state.mn.us/news/publications/renewable/ethanol/e20onelastomers.pdf>.
- Kalam, M. A., Masjuki, H. H., Maleque, M. A., Amalina, M. A., Abdesselam, H., & Mahlia, T.M.I. (2004). Air-Fuel Ratio Calculation for a Natural Gas Fueled Spark Ignition

- Engine. SAE Technical Paper No. 2004-01-0640. Warrendale, PA: Society for Automotive Engineers.
- Kang, S., Bae, J. K., Kim, H., Dhar, G. M., & Jun K. (2010). Enhanced Catalytic Performance for Dimethyl Ether Synthesis from Syngas with the Addition of Zr or Ga on a Biofunctional Catalyst. *Energy & Fuels*, 24, 804-510.
- Kar, Y., & Deveci, H. (2006). Importance of P-series fuels for flexible-fuel vehicles (FFVs) and alternative fuels. *Energy Sources Part a-Recovery Utilization and Environmental Effects*, 28(10), 909-921.
- Karabektas, M., & Hosoz, M. (2009). Performance and emission characteristics of a diesel engine using isobutanol–diesel fuel blends. *Renewable Energy*, 34, 1554-1559.
- Karavalakis G., Stournas S., & Karonis D. (2009a). Evaluation of the oxidation stability of diesel/biodiesel blends using the modified Rancimat method. *SAE International Journal of Fuels and Lubricants*, 2, 839-849.
- Karavalakis G., Alvanou F., Stournas S., & Bakeas E. (2009b). Regulated and unregulated emissions of a light duty vehicle operated on diesel/palm-based methyl ester blends over the NEDC and a non-legislated driving cycle. *Fuel*, 88, 1078-1085.
- Karavalakis G., Bakeas E., & Stournas S. (2010a). Influence of oxidized biodiesel blends on regulated and unregulated emissions from a diesel passenger car. *Environmental Science & Technology*, 44, 5306-5312.
- Karavalakis G., & Stournas S. (2010b). Impact of antioxidant additives on the oxidation stability of diesel/biodiesel blends. *Energy & Fuels*, 24, 3682-3686.
- Karavalakis, G., Fontaras, G., Ampatzoglou, D., Kousoulidou, M., Stournas, S., Samaras, Z., & Bakeas, E. (2010c). Effects of low concentration biodiesel blends application on modern passenger cars. Part 3: Impact on PAH, nitro-PAH, and oxy-PAH emissions. *Environmental Pollution*, 158, 1584-1594.
- Karavalakis, G., Hilari, D., Givalou, L., Karonis, D., & Stournas, S. (2011). Storage stability and ageing effect of biodiesel blends treated with different antioxidants. *Energy*, 36, 369-374.
- Karavalakis, G., Hajbabaei, M., Durbin, T. D., Zheng, Z., Johnson, K. C. (2012a). Influence of different Natural Gas Blends on the Regulated Emissions, Particle Number and Size Distribution Emissions from a Refuse Hauler Truck, SAE Technical Paper 2012-01-1583. Warrendale, PA: Society for Automotive Engineers.
- Karavalakis G., Durbin T. D., Villela M., Miller J. W. (2012b). Air pollutant emissions of light-duty vehicles operating on various natural gas compositions. *Journal of Natural Gas Science and Engineering*, 4, 8-16.
- Karavalakis, G., Gysel, N., Hajbabaei, M., Durbin, T. D., Johnson, K. C., Miller, J. W. (2012c). Influence of Different Natural Gas Compositions on the Regulated Emissions, Aldehydes, and Particle Emissions from a Transit Bus. *SAE International Journal of Fuels and Lubricants*, 5, 928-944.
- Karavalakis, G., Hajbabaei, M., Johnson, K. C., Durbin, T. D., Zheng, Z., Miller, J. W. (2013). The effect of natural gas composition on the regulated emissions, gaseous toxic pollutants, and ultrafine particle number emissions from a refuse hauler vehicle. *Energy*, 50, 280-291.
- Karavalakis, G., Durbin, T.D., Johnson, K., Hajbabaei, M. (2014). CARB Comprehensive B5/B10 Biodiesel Blends Heavy-Duty Engine Dynamometer Testing. Final Report Prepared for the California Air Resources Board under contract no. 11-413, June.

- Karavalakis, G., Short, D., Vu, D., Russell, R., Asa-Awuku, A., & Durbin, T. D. (2015). A Complete Assessment of the Emissions Performance of Ethanol Blends and Iso-Butanol Blends from a Fleet of Nine PFI and GDI Vehicles. *SAE International Journal of Fuels and Lubricants*, 8(2015-01-0957), 374-395.
- Karion, A., Sweeney, C., Pétron, G., Frost, G., Michael Hardesty, R., Kofler, J., ... & Conley, S. (2013). Methane emissions estimate from airborne measurements over a western United States natural gas field. *Geophysical Research Letters*, 40, 4393-4397.
- Kass, M. D., Theiss, T. J., Janke, C. J., Pawel, S. J., & Lewis, S. A. (2011). Intermediate Ethanol Blends Infrastructure Materials Compatibility Study: Elastomers, Metals, and Sealants, Final Report by Oak Ridge National Laboratory, Report No. ORNL/TM-2010/326.
- Kass, M. D., Theiss, T. J., Janke, C. J., & Pawel, S. J. (2012a) Compatibility Study for Plastic, Elastomeric, and Metallic Fueling Infrastructure Materials Exposed to Aggressive Formulations of ethanol-Blended Gasoline, Final Report by Oak Ridge National Laboratory, Report No. ORNL/TM-2012/88.
- Kass, M. D., Theiss, T., Janke, C., Pawel, S., Chapin, J.T., Yang, E., Boyce, K. (2012b). Compatibility of elastomers with test fuels of gasoline blended with ethanol. *Sealing Technology*, 12, 7-12.
- Kass, M. D., Janke, C. J., Pawel, S. J., Thomson, J. K., Meyer, H., Theiss, T. J. (2013). Compatibility Study for Plastic, Elastomeric, and Metallic Fueling Infrastructure Materials Exposed to Aggressive Formulations of Isobutanol-Blended Gasoline, Final Report by Oak Ridge National Laboratory; Report No. ORNL/TM-2013/243.
- Kass, M. D., Theiss, T., Pawel, S., Baustian, J., Wolf, L., Koch, W., Janke, C. (2014a). Compatibility Assessment of Elastomer Materials to Test Fuels Representing Gasoline Blends Containing Ethanol and Isobutanol. *SAE International Journal of Fuels and Lubricants*, 7(2), 445-456.
- Kass, M. D., Theiss, T., Pawel, S., Baustian, J., Wolf, L., Koch, W., Janke, C. (2014b). Compatibility Assessment of Plastic Materials to Test Fuels Representing Gasoline Blends Containing Ethanol and Isobutanol. *SAE International Journal of Fuels and Lubricants*, 7(2), 457-470.
- Kass, M., Janke, C., Theiss, T., Baustian, J., Wolf, L., & Koch, W. (2015a). Compatibility Assessment of Plastic Infrastructure Materials with Test Fuels Representing E10 and iBu16. *SAE International Journal of Fuels and Lubricants*, 8(1), 95-110.
- Kass, M. D., Janke, C., Connatser, R., Lewis, S., Keiser, J., & Theiss, T. (2015). Compatibility Assessment of Elastomeric Infrastructure Materials with Neat Diesel and a Diesel Blend Containing 20 Percent Fast Pyrolysis Bio-oil. *SAE International Journal of Fuels and Lubricants*, 8(1), 50-61.
- Kass, M. D., Janke, C. J., Connatser, R., Lewis, S., Keiser, J., Theiss, T. J., (2015) Compatibility Assessment of Elastomeric Infrastructure Materials with Off-Highway Diesel and a Diesel Blend Containing 20 Percent Fast Pyrolysis Bio-oil. *SAE International Journal of Fuels and Lubricants*, 8(1), 80-94.
- Kelly, K. J. (1994). Correlation of I/M240 and FTP Emissions for Alternative Motor Fuel Act Test Vehicles, SAE Special Publication 1053 - Progress in Emissions Control Technologies, SAE Technical Paper No. 941901. Warrendale, PA: Society for Automotive Engineers.

- Kelly, K. J., Bailey, B. K., Coburn, T. C., Clark, W., Eudy, L., & Lissiuk, P. (1996). FTP Emissions Test Results from Flexible-Fuel Methanol Dodge Spirits and Ford Econoline Vans, SAE Technical Paper No. 961090. Warrendale, PA: Society for Automotive Engineers.
- Kenneth Barbalace. "Chemical Database - 2-Methylfuran. Environmental Chemistry.com. 1995 - 2008. Accessed on-line: 8/26/2008."
- Kittelson, D., Tan, A., Zarling, D., & Evans, B. (2007). Demonstration and Driveability Project to Determine the Feasibility of Using E20 as a Motor Fuel; Submitted to Minnesota Department of Agriculture at St. Paul, MN.
- Kleinschek, G. (2005). Emission Tests with Synthetic Diesel Fuels (GTL & BTL) with a Modern Euor 4 (EGR) Engine. Kolloquium "Fuels" der Technischen Akademie Esslingen (TAE).
- Knepper, J. C., Koehl, W. J., Benson, J. D., Burns, V. R., Gorse, R. A., Hochhauser, A. M., Leppard, W. R., Rapp L. A., & Reuter, R. M. (1993). Fuel effects in Auto/Oil High Emitting Vehicles. SAE Technical Paper No. 930137. Warrendale, PA: Society for Automotive Engineers.
- Knifton, J. F., & Duranleau, R. G. (1991). Ethylene glycol-dimethyl carbonate cogeneration. *Journal of Molecular Catalysis*, 67, 389–399.
- Knoll, K., West, B., Clark, W., Graves, R., Orban, J., Przesmitzki, S., & Theiss, T. (2009). Effects of Intermediate Ethanol Blends on Legacy Vehicles and Small Non-Road Engines, Report 1 – Updated. (NREL/TP-540–43543, ORNL/TM-2008/117). www.nrel.gov.
- Ko, Y., Kurihara, K., Sakai, T., Osuga, R., Choi, B-C, Ayusawa, T., and Kim, E. (1992). Research and Development of LNG Vehicle for Practical Use. SAE Technical Paper No. 920594. Warrendale, PA: Society for Automotive Engineers.
- Kuronen, M., Mikkonen, S., Aakko, P., Murtonen, T. (2007). Hydrotreated Vegetable Oil as Fuel for Heavy-Duty Diesel Engines. SAE Technical Paper No. 2007-01-4031. Warrendale, PA: Society for Automotive Engineers.
- Lamb, B. K., Edburg, S. L., Ferrara, T. W., Howard, T., Harrison, M. R., Kolb, C. E., ... & Whetstone, J. R. (2015). Direct measurements show decreasing methane emissions from natural gas local distribution systems in the United States. *Environmental Science & Technology*, 49, 5161-5169.
- The UOP Renewable Jet Fuel Process technology was originally developed in 2007 under a contract from the U.S. Defense Advanced Research Projects Agency (DARPA) Lane, J. (2015). Alaska Airlines, Gevo To Demonstrate Renewable Alcohol-to-Jet Fuel, Biofuels digest. <http://www.renewableenergyworld.com/articles/2015/05/alaska-airlines-gevo-to-demonstrate-renewable-alcohol-to-jet-fuel.html>.
- Lapuerta M., Armas O., & Fernandez J.R., (2008). Effect of biodiesel fuels on diesel engine emissions. *Progress in Energy and Combustion Science*, 34, 198-223.
- Lauer, M. G., Henderson, W. H., Awad, A., & Stambuli, J. P. (2012). Palladium-Catalyzed Reactions of Enol Ethers: Access to Enals, Furans, and Dihydrofurans. *Organic Letters*, 14(23), 6000-6003.
- Lee Y-J, & Kim G-C. (2000). Effect of Gas Composition on NGV Performance. In: Seoul 2000 FISITA World Automotive Congress, June, Seoul, Korea.

- Li, C. Z., Zhang, Z. H., & Zhao, Z. K. (2009). Direct conversion of glucose and cellulose to 5-hydroxymethylfurfural in ionic liquid under microwave irradiation. *Tetrahedron Letters*, *50*, 5403–5.
- Li, X., Chen H., Zhe, Z., & Huang, Z. (2006). Study of combustion and emission characteristics of a diesel engine operated with dimethyl carbonate. *Energy conversion and Management*, *47*, 1438-1448.
- Li, X. L., & Huang, Z. (2009). Emission reduction potential of using gas-to-liquid and dimethyl ether fuels on a turbocharged diesel engine. *Science of the Total Environment*, *407*(7), 2234-2244.
- Li, Z., Xie, K., & Slade, R. C. (2001). High selective catalyst CuCl/MCM-41 for oxidative carbonylation of methanol to dimethyl carbonate. *Applied Catalysis A: General*, *205*, 85-92.
- Liu, J., Liu, S. H., Li, Y., Wei, Y. J., Li, G. L., & Zhu, Z. (2010). Regulated and nonregulated emissions from a dimethyl ether powered compression ignition engine. *Energy and Fuels*, *24*, 2465-2469.
- Luque, R., Herrero-Davila, L., Campelo, J.M., Clark, J.H., Hidalgo, J.M., Luna, D., Marinas, J.M., Romero, A.A. (2008). Biofuels: A technological perspective. *Energy & Environmental Science*, *1*, 542–564.
- Lynn, J. (2009). Can Methanol Really Make a Dent in US Oil Demand? Energy Tribune, July 29. <http://www.energytribune.com/articles.cfm?aid=2131>.
- MacDonald, T. (2005). Alcohol Fuel Flexibility: Progress and Prospects. Presented at the Fifteenth International Symposium on Alcohol Fuels, San Diego, CA.
- Macor A., Avella F., & Faedo D. (2011). Effects of 30% v/v biodiesel/diesel fuel blend on regulated and unregulated pollutant emissions from diesel engines. *Applied Energy*, *88*, 4989-5001.
- Malenshek, M. & Olsen D. (2009). Methane Number Testing of Alternative Gaseous Fuels. *Fuel*, *88*, 650–6.
- Mamakos, A., Martini, G., Marotta, A., & Manfredi, U. (2013). Assessment of different technical options in reducing particle emissions from gasoline direct injection vehicles. *Journal of Aerosol Science*, *63*, 115-125.
- Mankato, (2009). E20: The Feasibility of 20 Percent Ethanol Blends by Volume as a Motor Fuel, Executive Summary, Results of Materials Compatibility and Drivability Testing. http://www.growthenergy.org/images/reports/minnesota_e20execsumm.pdf.
- Marchese, A. J., Vaughn, T. L., Zimmerle, D.J., Martinez, D. M., Williams, L. L., Robinson, A. L., Michell, A. L., Subramanian, R., Tkacik, D. S., Roscioli, J. R., & Herndon, S. C. (2015). Methane emissions from United States natural gas gathering and processing. *Environmental Science & Technology*, *49*, 10718-10727.
- Maricq MM, Szente JJ, Jahr K. (2012). The impact of ethanol fuel blends on PM emissions from a light-duty GDI vehicle. *Aerosol Science & Technology*, *46*, 576-583.
- Markets and Markets. (2013). Dimethyl Ether (DME) Market By Applications (LPG Blending, Aerosol Propellant, Transportation Fuel & Others), By Raw Materials (Coal, Methanol, Natural Gas, Bio-based) & Geography - Global Trends & Forecasts to 2018 & 2023, <http://www.marketsandmarkets.com/Market-Reports/dimethyl-ether-market-1120.html>.

- Martini, G., Astorga, C., & Farfaletti, A. (2007). Effect of biodiesel fuels on pollutant emissions from EURO 3 LD diesel vehicles. Transport and Air Quality Unit; Institute for Environment and Sustainability, EC-Joint Research Centre.
- Matthews, R., Chiu, J., & Hilden, D. (1996). CNG Compositions in Texas and the Effects of Composition on Emissions, Fuel Economy, and Drivability of NGVs. SAE Technical Paper 962097. Warrendale, PA: Society for Automotive Engineers.
- Mayotte, S. C., Lindhjem, C. E., Rao, V., & Sklar, M. S., (1994a). Reformulated Gasoline Effects on Exhaust Emissions: Phase 1: Initial Investigation of Oxygenate, Volatility, Distillation, and Sulfur Effects. SAE Technical Paper No. 941973. Warrendale, PA: Society for Automotive Engineers.
- Mayotte, S. C., Rao, V., Lindhjem, C. E., & Sklar, M. S. (1994b). Reformulated Gasoline Effects on Exhaust Emissions: Phase 2: Continued Investigation of the Effects of Fuel Oxygenate Content, Oxygenate Type, Sulfur, Olefins, and Distillation Parameters. SAE Technical Paper No. 941974. Warrendale, PA: Society for Automotive Engineers.
- McClement, D., & Austin, T. C. (2011). Evaluation of Inspection and Maintenance OBD II Data to Identify Vehicles That May Be Sensitive to E10+ Blends. CRC Project No. E-90-2a.
- McCormick, R. L., Graboski, M. S., Alleman, T. L., Herring, A. M., & Tyson, K. S. (2001). Impact of Biodiesel Source Material and Chemical Structure on Emissions of Criteria Pollutants from a Heavy-Duty Engine. *Environmental Science & Technology*, 35, 1742–7.
- McCormick, R., Alvarez, J., Graboski, M., Tyson K et al. (2002). Fuel Additive and Blending Approaches to Reducing NOx Emissions from Biodiesel. SAE Technical Paper 2002–01–1658. Warrendale, PA: Society for Automotive Engineers.
- McCormick, R. L., Williams, A., Ireland, J., & Hayes R. R. (2006). Effects of Biodiesel Blends on Vehicle Emissions: Fiscal Year 2006 Annual Operating Plan Milestone 10.4. Milestone Report NREL/MP-540-40554.
- McCormick, R. L., Alleman, T. L., Ratcliff, M., Moens, L., & Lawrence, R. (2005) Survey of the Quality and Stability of Biodiesel and Biodiesel Blends in the United States in 2004; NREL/TP-540-38836; National Renewable Energy Laboratory: Golden, CO, October; <http://www.nrel.gov/docs/fy06osti/38836.pdf>.
- McCormick, R. L., Ratcliff, M., Moens, L., & Lawrence, L. (2007). Several factors affecting the stability of biodiesel in standard accelerated tests. *Fuel Processing Technology*, 88, 651–657.
- McCormick, R.L. & Westbrook, S.R. (2010). Storage stability of biodiesel and biodiesel blends, *Energy & Fuels*, 24, 690–698.
- McCormick, R., Yanowitz, J., Ratcliff, M., & Zigler, B. (2013). Review and Evaluation of Studies on the Use of E15 in Light-Duty Vehicles. Prepared by the National Renewable Energy Laboratory for the Renewable Fuels Association. October. <http://ethanolrfa.org/page/-/rfa-association-site/studies/RFA%20NREL%20Review%20and%20Evaluation%20of%20E15%20Studies.pdf?nocdn=1>.
- McCormick, R.L., Ratcliff, M., Christensen, E., Chupka, G., Burton, J., Alleman, T., Marchese, A., Olsen, D., & Tian, M. (2015). Performance of Biofuels and Biofuel Blends, presentation, June.
- McKain, K., Down, A., Raciti, S. M., Budney, J., Hutyra, L. R., Floerchinger, C., ... & Wofsy, S. C. (2015). Methane emissions from natural gas infrastructure and use in the

- urban region of Boston, Massachusetts. *Proceedings of the National Academy of Sciences*, 112, 1941-1946.
- McKone, T., Nazarov, W., Berck, P., Auffhammer, M., Lipman, T., Torn, M., Masanet, E., Lobscheid, A., Santero, N., & Mishra, U. (2011). Grand challenges for life-cycle assessment of biofuels. *Environmental Science & Technology*, 45, 1751–1756.
- McKone, T., Rice, D., Ginn, T., Bastani, M. Levy, A., Lenhart, A.,... & Boudreaux, R. (2015). Draft Final - California Dimethyl Ether Multimedia Evaluation Tier 1, February.
- McLaughlin, S. (2013). DME – Another Choice Alternative Fuel, SAE Presentation.
- McTaggart G. P., Rogak S. N., Munshi S. R., Hill P. G., & Bushe W. (2010). The Influence of Fuel Composition on a Heavy-duty, Natural-gas Direct-injection Engine. *Fuel*, 89, 752–9.
- Mead, G., Jones, B., Stevens, P., Hanson N., & Harrenstein, J. (2009). An Examination of Fuel Pumps and Sending Units During a 4000 Hour Endurance Test in E20, Minnesota Center for Automotive Research at Minnesota State University, Makato, MN.
- Mei, D., Hielscher, K., & Baar, R. (2013). Study on combustion process and emissions of a single-cylinder diesel engine fueled with DMC/diesel blend. *Journal of Energy Engineering*, 140, 04013004.
- Mejia-Centeno I., Martinez-Hernandez A., & Fuentes G. A. (2007). Effect of low-sulfur fuels upon NH₃ and N₂O emission during operation of commercial three-way catalytic converters. *Topics in Catalysis*, 42-43, 381-385.
- Methanol Fuels. (2014). Updates on China's Methanol Fuel and Vehicle Development Programs, September, <http://www.methanolfuels.org/updates-on-chinas-methanol-fuel-and-vehicle-development-programs/>.
- Methanol Institute. (2012). Methanol – The Clear Alternative for Transportation.
- Methanol Institute. (2015a). <http://www.methanol.org/Methanol-Basics/The-Methanol-Industry.aspx>.
- Meyers, R. (2014). Growing Chinese appetite ignites U.S. Methanol Renaissance. Fuelfix from the Houston Chronical, August. <http://fuelfix.com/blog/2014/08/29/growing-chinese-appetite-ignites-u-s-methanol-renaissance/>.
- Miller W., Johnson K., Durbin T., & Dixit P. (2013). In-Use Emissions Testing and Demonstration of Retrofit Technology for Control of On-Road Heavy-Duty Engines, Final Report for the South Coast Air Quality Management District under Contract No. 11612, September.
- Minkler, S., Isley, N., Lippincott, D., Krause, N., & Lipshutz, B. (2014). Leveraging the Micellar Effect: Gold-Catalyzed Dehydrative Cyclizations in Water at Room Temperature.
- Mitchell, A. L., Tkacik, D. S., Roscioli, J. R., Herndon, S. C., Yacovitch, T. I., Martinez, D. M., & Robinson, A. L. (2015). Measurements of methane emissions from natural gas gathering facilities and processing plants: measurement results. *Environmental Science & Technology*, 49, 3219–3227.
- Moriarty, K. & Yanowitz, J. (2015). E15 and Infrastructure, National Renewable Energy Laboratory (NREL) report NREL/TP-5400-64156, May.
- Mueller C, Boehman A, & Martin G. (2009). An Experimental Investigation of the Origin of Increased NO_x Emissions When Fueling a Heavy-Duty Compression-Ignition Engine with Soy Biodiesel. SAE Technical Paper 2009–01–1792. Warrendale, PA: Society for Automotive Engineers.

- Naber J. D., Siebers D. L., Caton J. A., Westbrook C. K., & Di Julio S. S. (1994). Natural Gas Autoignition under Diesel Conditions: Experiments and Kinetic Modeling. SAE Technical Paper 942034. Warrendale, PA: Society for Automotive Engineers.
- National Renewable Energy Laboratory. (2009). Biodiesel handling and Use Guide – fourth edition. Document No. NREL/TP-540-43672.
- National Renewable Energy Laboratory. (2015). Alternative Fuels Data Center. http://www.afdc.energy.gov/vehicles/flexible_fuel.html.
- Natural Gas Organization. <http://naturalgas.org/overview/>.
- Natural Gas Vehicles for America (NGV America). (2014). Vehicles for Fleet, <http://www.ngvamerica.org/vehicles/for-fleets/Nejame>, S. (2010). Butanol as A Fuel – View From The Field, Presentation at NREL, March.
- Nichols, R. J. (2003). The Methanol Story: A Sustainable Fuel for the Future. *Journal of Scientific & Industrial Research*, 62, 97-105.
- Nikanjam M., Rutherford J., & Morgan P. (2011). Performance and emissions of diesel and alternative diesel fuels in modern light-duty diesel vehicles. SAE Technical Paper 2011-01-0198. Warrendale, PA: Society for Automotive Engineers.
- Norbeck, J. M., C. S. Park, A. S. K. Raju, & C. Vo (2008). Suitability of the Steam Hydrogasification Process to Convert Biomass Materials Prevalent in Southern California into Synthetic Transportation Fuels. Final Report to the California Energy Commission from the University of California at Riverside under Contract No. 500-99-013, September.
- Nylund, N.-O., & Koponen, K. (2012). Fuel and Technology Alternatives for Buses Overall Energy Efficiency and Emission Performance. VTT Technology 46. IEA-AMF Annex 37. <http://www.vtt.fi/inf/pdf/technology/2012/T46.pdf>.
- Oberon Fuels Website, accessed July, (2015). <http://www.oberonfuels.com/2013/06/07/oberon-fuels-project-with-volvo-trucks-and-safeway-receives-grant-from-san-joaquin-valley-air-pollution-control-district-for-production-of-first-north-american-fuel-grade-dme/>.
- Ogburn S. & Wire C. (2013). How Much Natural Gas Leaks? Scientific American.com, August 1. <http://www.scientificamerican.com/article/how-much-natural-gas-leaks/>.
- Olson E. S., Sharma R. K., & Aulich T. R. (2004). Higher-Alcohols Biorefinery. Improvement of catalyst for ethanol conversion. *Applied Biochemistry and Biotechnology*, 113-114, 913-932.
- Orbital Engine Company. (2004). Market Barriers to the Uptake of Biofuels Study Testing Gasoline Containing 20% Ethanol (E20). Phase 2B Final Report to the Department of the Environment and Heritage, May.
- Pace, V., Hoyos, P., Castoldi, L., Domínguez de María, P., & Alcántara, A. R. (2012). 2-Methyltetrahydrofuran (2-MeTHF): A Biomass-Derived Solvent with Broad Application in Organic Chemistry. *ChemSusChem*, 5(8), 1369-1379.
- Palkovits, R. (2010). Pentensäure als Wegbereiter für cellulosebasierte Biotreibstoffe. *Angewandte Chemie*, 122(26), 4434-4436.
- Perbellini L., Princivalle A., Cerpelloni M., Pasini F., & Brugnone F. (2003). Comparison of breath, blood and urine concentrations in the biomonitoring of environmental exposure to 1, 3 butadiene, 2, 5-dimethylfuran, and benzene. *International Archives of Occupational and Environmental Health*, 76, 461–466.

- Peischl, J., Ryerson, T. B., Aikin, K. C., Gouw, J. A., Gilman, J. B., Holloway, J. S., ... & Parrish, D. D. (2015). Quantifying atmospheric methane emissions from the Haynesville, Fayetteville, and northeastern Marcellus shale gas production regions. *Journal of Geophysical Research: Atmospheres*, *120*, 2119-2139.
- Pétron, G., Karion, A., Sweeney, C., Miller, B. R., Montzka, S. A., Frost, G. J., ... & Schnell, R. (2014). A new look at methane and nonmethane hydrocarbon emissions from oil and natural gas operations in the Colorado Denver-Julesburg Basin. *Journal of Geophysical Research: Atmospheres*, *119*, 6836-6852.
- Phuong, J., Kim, S., Thomas, R., & Zhang, L. (2012). Predicted toxicity of the biofuel candidate 2, 5-dimethylfuran in environmental and biological systems. *Environmental and Molecular Mutagenesis*, *53*(6), 478-487.
- Pipelines International. (2009). Biodiesel via pipelines in US first, July 10, http://pipelinesinternational.com/news/biodiesel_via_pipelines_in_us_first/001583/#.
- Polk data. (2014). Based on a total U.S. gasoline light-duty vehicle registration of 228 million of which 149 million are model year 2001 and newer. From Moriarity and Yanowitz, NREL (2015).
- Powrie, W. D., Wu, C. H., & Molund, V. P. (1986). Browning reaction systems as sources of mutagens and antimutagens. *Environmental Health Perspectives*, *67*, 47.
- Pumphrey J. A., Brand J. I., & Scheller W. A. (2000). Vapour pressure measurements and predictions for alcohol-gasoline blends. *Fuel*, *79*, 1405-1411.
- Phytonics. (2012). Gen. 4 Production of Butanol & Pentanol for “Drop-in” Fuels and Renewable Chemicals. Biofuels Technology / Series A, presented at the NREL Industrial Growth Forum.
- Rakopoulos D. C., Rakopoulos C. D., Papagiannakis R. G., Kyritsis D. C. (2011). Combustion heat release analysis of ethanol or n-butanol diesel fuel blends in heavy-duty DI diesel engine. *Fuel*, *90*, 1855-1867.
- Rakopoulos D. C., Rakopoulos C. D., Giakoumis E. G., Dimaratos A. M., & Kyritsis D. C. (2010). Effects of butanol-diesel fuel blends on the performance and emissions of a high-speed DI diesel engine. *Energy Conversion and Management*, *51*, 1989-1997.
- Ratcliff, M. A., Luecke, J., Williams, A., Christensen, E., Yanowitz, J., Reek, A., & McCormick, R. L. (2013). Impact of Higher Alcohols Blended in Gasoline on Light-Duty Vehicle Exhaust Emissions. *Environmental Science & Technology*, *47*, 13865–13872.
- Ren, Y., Huang, Z., Miao, H., Di, Y., Jiang, D., Zeng, K., ... & Wang, X. (2008). Combustion and emissions of a DI diesel engine fuelled with diesel-oxygenate blends. *Fuel*, *87*, 2691-2697.
- Reuter, R. M., Hochhauser, A. M., Benson, J. D., Koehl, W. J., Burns, V. R., Painter, L. J., Gorse, Jr., R. A., Rippon, B. H., & Rutherford, J. A. (1992). Effects of Oxygenated Fuels on RVP on Automotive Emissions – Auto/Oil Air Quality Improvement Program. SAE Technical Paper No. 920326. Warrendale, PA: Society for Automotive Engineers.
- Renewable Fuels Association (RFA), (2015a) Statistics. (n.d.). Retrieved July 29, 2015, from <http://www.ethanolrfa.org/pages/statistics>.
- Renewable Fuels Association (RFA), (2015b) Retrieved November 24, 2015, from <http://www.ethanolrfa.org/how-ethanol-is-made/>.
- Roman-Leshkov Y., Barrett C. J., Liu Z. Y., & Dumesic J. A. (2007). Production of dimethylfuran for liquid fuels from biomass-derived carbohydrates. *Nature*, *447*, 982–6.

- Rothe, D., Lorenz, J., Lammermann, R., Jacobi, E., Rantanen, L., & Linnaila, R. (2005). New BTL Diesel Reduces Effectively Emissions of a Modern Heavy-Duty Engine. Kolloquium "Fuels" der Technischen Akademie Esslingen (TAE).
- Rose K. D., Samaras Z., Jansen L., Clark R., Elliott N., Fontaras G., et al., (2010). Impact of biodiesel blends on fuel consumption and emissions in Euro 4 Compliant vehicles. *SAE International Journal of Fuels and Lubricants*, 3, 142-164.
- Rutledge, B. (2005). California Biogas Industry Assessment, WestStart-CALSTART White paper, April.
- Salsing, H. & Denbratt, I. (2007). Performance of a Heavy Duty DME Diesel Engine - an Experimental Study. SAE Technical Paper 2007-01-4167. Warrendale, PA: Society for Automotive Engineers.
- Salsing, H. (2011). DME Combustion in Heavy Duty Diesel Engines, Chalmers University of Technology, Ph.D. Thesis.
- Schweitzke, S., Griffin, W. M., Matthews, H. S., Bruhwiler, L.M. P. (2014). Natural gas fugitive emissions rates constrained by global atmospheric methane and ethane. *Environmental Science & Technology*, 48(14), 7714-7722.
- Searchinger, T., Heimlich, R., Houghton, R. A., Dong, F. X., Elobeid, A., Fabiosa, J., . . . Yu, T. H. (2008). Use of US croplands for biofuels increases greenhouse gases through emissions from land-use change. *Science*, 319(5867), 1238-1240.
- Semelsberger, T. A., Borup, R. L., & Greene, H. L. (2006). Dimethyl ether (DME) as an alternative fuel. *Journal of Power Sources*, 156(2), 497-511.
- Sharp C. A. (1994). Transient Emissions Testing of Biodiesel and Other Additives in a DDC Series 60 Engine. Final Report to National Biodiesel Board, by Southwest Research Institute, December.
- Shenghua L., Clemente E.R.C., Tiegang H., & Yanju W. (2007). Study of spark ignition engine fueled with methanol/gasoline fuel blends. *Applied Thermal Engineering*, 27, 1904-1910.
- Shimizu, K., Uozumi, R., & Satsuma, A. (2009). Enhanced production of hydroxymethylfurfural from fructose with solid acid catalysts by simple water removal methods. *Catalysis Communications*, 10(14), 1849-1853.
- Shoffner, B., & Whitney, K. (2013). Impact of Ethanol Blends on the OBDII Systems of In-Use Vehicles, CRC Report No. E-90-2b. <http://www.crcao.org/publications/emissions/index.html>.
- Sidhu S., Graham J., & Striebich R. (2001). Semi-volatile and particulate emissions from the combustion of alternative diesel fuel. *Chemosphere*, 42, 681-690.
- Singh, B. (2014). Production of biodiesel from plant oils – an overview. *Journal of Biotechnology, Bioinformatics and Bioengineering*, 1(2), 33-42.
- Singh, S., Kumar, A., Mahla, S. K., & Bath, G. S. (2013). Experimental study on emission analysis of oxygenated fuels dimethyl carbonate (DMC) and dibutyl maleate (DBM) in a CI engine. *International Journal of Research in Engineering and Technology*, 2, 158-162.
- Sluder, C. S., & West, B. H. (2012). Investigating Malfunction Indicator Light Illumination Due to Increased Oxygenate Use in Gasoline, SAE Paper 2012-01-2305. Warrendale, PA: Society for Automotive Engineers.

- Smagala, T. G., Christensen, E., Christison, K. M., Mohler, R. E., Gjersing, E., & McCormick, R. L. (2013). Hydrocarbon Renewable and Synthetic Diesel Fuel Blendstocks: Composition and Properties. *Energy & Fuels*, 27, 237-246.
- Sobotowski, R., Butler, A., and Guerra, Z. (2015). A pilot study of fuel impacts on PM emissions from light-duty gasoline vehicles. *SAE International Journal of Fuels Lubricants*, 8(1):214-233.
- Society of Automotive Engineers (2000). Gasoline, Alcohol, and Diesel Fuel Surrogates for Materials Testing. SAE J1681, issued September, 1993, revised January 2000.
- Storey J. M., Barone T., Norman K., & Lewis S. (2010). Ethanol blend effects on direct injection spark-ignition gasoline vehicle particulate matter emissions. *SAE International Journal of Fuels Lubricants*, 3, 650-659.
- Su Y., Brown H. M., Huang X. W., Zhou X. D., Amonette J. E., & Zhang Z. C. (2009). Single-step conversion of cellulose to 5-hydroxymethylfurfural (HMF), a versatile platform chemical. *Applied Catalysis A: General*, 361, 117-22.
- Subramanian, R., Williams, L. L., Vaughn, T. L., Zimmerle, D., Roscioli, J. R., Herndon, S. C., ... & Robinson, A. L. (2015). Methane emissions from natural gas compressor stations in the transmission and storage sector: Measurements and comparisons with the EPA greenhouse gas reporting program protocol. *Environmental Science & Technology*, 49, 3252-3261.
- Sulatsky, M.T., Hill, S.G., Lychak, J.V., Nakamura, K., Matsui, T., & Rideout, G. (1995). Adapting a Geo Metro to Run on Natural Gas using Fuel-Injection Technology. SAE Technical Paper No. 951942. Warrendale, PA: Society for Automotive Engineers.
- Surawski, N. C., Miljevic, B., Ayoko, G. A., Elbagir, S., Stevanovic, S., Fairfull-Smith, K. E., ... & Ristovski, Z. D. (2011). Physicochemical Characterization of Particulate Emissions from a Compression Ignition Engine: The Influence of Biodiesel Feedstock. *Environmental Science & Technology*, 45(24), 10337-10343.
- Sustainable Aviation Fuel Users Group. (2015). website, <http://www.safug.org/>.
- Szybist, J.P., McLaughlin, S., & Iyer, S. (2014). Emissions and Performance of a Prototype Dimethyl Ether-Fueled Heavy-Duty Truck, Oak Ridge National Laboratory Report No. ORNL/TM-2014/59, February.
- Szwaja S., & Naber J.D. (2010). Combustion of n-butanol in a spark-ignition IC engine. *Fuel*, 89, 1573-1582.
- Szybist J., Kirby S. R., & Boehman A. L. (2005). NOx Emissions of Alternative Diesel Fuels: A Comparative Analysis of Biodiesel and FT Diesel. *Energy & Fuels*, 19, 1484-92.
- Tao, L., & Aden, A. (2009). The economics of current and future biofuels. *In Vitro Cellular & Developmental Biology-Plant*, 45(3), 199-217.
- Tat M. E., & Van Gerpen J. H. (2003). Measurement of Biodiesel Speed of Sound and Its Impact on Injection Timing. Final Subc. National Renewable Energy Laboratory.
- Taupy, J-A. (2012). Multi-Source: Multi-Purpose: Low Carbon: DME's Roles in the Energy Mix, presentation at International Conference on Energy and Automotive Technologies, Istanbul, Turkey, October.
- Thewes, M., Muether, M., Pischinger, S., Budde, M., Brunn, A., Sehr, A., ... & Klankermayer, J. (2011). Analysis of the impact of 2-methylfuran on mixture formation and combustion in a direct-injection spark-ignition engine. *Energy & Fuels*, 25, 5549-5561.

- Thiruvengadam, A., Besch, M. C., Thiruvengadam, P., Pradhan, S., Carder, D., Kappanna, H., ... & Miyasato, M. (2015). Emission Rates of Regulated Pollutants from Current Technology Heavy-Duty Diesel and Natural Gas Goods Movement Vehicles. *Environmental Science & Technology*, 49, 5236-5244.
- Tian G. H., Xu H. M., Daniel R., Li H. Y., & Li Y. F. (2010). Spray characteristics and engine adaptability of 2,5-dimethylfuran. *Journal of Automotive Safety and Energy*, 1, 132-40 (in Chinese).
- Tong, F., Jaramillo, P., & Azevedo, I. M. L. (2015). Comparison of life cycle greenhouse gases from natural gas pathways for medium and heavy-duty vehicles. *Environmental Science & Technology*, 49(12), 7123-7133.
- Transportation Research Center, Inc. (2009). CRC Report: E-87-1: Mid-Level Ethanol Blends Catalyst Durability Study Screening, Final Report to the Coordinating Research Council, July.
- Unnasch, S., Darlington, T., Dumortier, J., Tyner, W., Pont, J., & Broch, A. (2014) Study of Transportation Fuel Life Cycle Analysis: Review of Economic Models Used to Assess Land Use Effects. Final report for project E-88-3 by Life Cycle Associates LLC for the Coordinating Research Council.
- U.S. Code, Title 15, § 2301, Magnusson-Moss Warranty Act.
- U.S. Department of Energy. (U.S. DOE). (2007). Energy Independence and Security Act of 2007. Retrieved July 29, 2015, from <http://www.afdc.energy.gov/laws/eisa.html>.
- U.S. Department of Energy. (U.S. DOE). (2014). Flexible Fuel Vehicles. Retrieved July 29, 2015, from http://www.afdc.energy.gov/vehicles/flexible_fuel.html.
- U.S. Department of Energy (2015a) Ethanol Production and Distribution, Alternative Fuels Data Center, Retrieved November 24, 2015, http://www.afdc.energy.gov/fuels/ethanol_production.html.
- U.S. Department of Energy. (2015b). Alternative Fueling Station Counts by State. Retrieved July 20, 2015, from http://www.afdc.energy.gov/fuels/stations_counts.html.
- U.S. Energy Information Administration (EIA). <http://www.eia.gov/totalenergy/data/annual/index.cfm#summary>.
- U.S. Energy Information Administration (EIA). (2014a). Monthly Energy Review (March 2015), Table 2.5 and 3.8cm preliminary data.
- U.S. Energy Information Administration (EIA). (2010). Annual Energy Outlook 2010 with projection to 2035, Available at http://www.eia.gov/oiaf/aeo/otheranalysis/aeo_2010/analysispapers/natgas_fuel.html.
- U.S. Energy Information Administration (EIA). (2014b). Annual Energy Outlook 2014 with projection to 2040, [http://www.eia.gov/forecasts/archive/aeo14/pdf/0383\(2014\).pdf](http://www.eia.gov/forecasts/archive/aeo14/pdf/0383(2014).pdf).
- U.S. Energy Information Administration (EIA) Beta. (2011). International energy data and analysis, <http://www.eia.gov/beta/international/>.
- U.S. Energy Information Administration (EIA). (2015). International energy statistics, <http://www.eia.gov/cfapps/ipdbproject/iedindex3.cfm?tid=3&pid=3&aid=1&cid=regions&syid=2003&eyid=2013&unit=BCF>.
- U.S. Energy Information Administration - EIA - Independent Statistics and Analysis. (2015). June 30. Retrieved July 20, 2015, from <http://www.eia.gov/biofuels/biodiesel/production/>.
- U.S Environmental Protection Agency. (2002). A Comprehensive Analysis of Biodiesel Impacts on Exhaust Emissions. EPA Draft Final Report.

- U.S Environmental Protection Agency. (2009). Draft Regulatory Impact Analysis: Changes to Renewable Fuel Standard Program. Draft Final Report May.
- U.S. Environmental Protection Agency. (2009). Information about the EPA's action on exempting dimethyl carbonate as a VOC and petitioner's background information, public comments and other references are available electronically at <http://www.regulations.gov>, EPA's electronic public docket and comment system. The docket number for this action is Docket ID No. EPA-HQ-OAR-2006-0948. See <http://www.epa.gov/ttn/oarpg/t1pfpr.html> and scroll down to Jan 13, 2009 pdf for the rule.
- U.S Environmental Protection Agency. (2013a). Assessing the Effect of Five Gasoline Properties on Exhaust Emissions from Light Duty Vehicles Certified to Tier 2 Standards: Final Report on Program Design and Data Collection (EPA/V2/E-89, EPA-420-R-13-004); U. S. EPA: Washington, DC.
- U.S Environmental Protection Agency. (2013b). Assessing the Effect of Five Gasoline Properties on Exhaust Emissions from Light-Duty Vehicles Certified to Tier 2 Standards: Analysis of Data from EPA/V2/E-89), Final Report; EPA-420-R-13-002; U. S. EPA: Washington, DC.
- U.S. Environmental Protection Agency (U.S. EPA). (2014). Inventory of U.S. Greenhouse Gas Emissions and Sinks: 1990-2012. EPA 430-R-14-003; U.S. EPA: Washington, DC.
- U.S. Environmental Protection Agency (U.S. EPA). (2015a). E15: Notices & Regulations. (n.d.). Retrieved July 29, from <http://www.epa.gov/otaq/regs/fuels/additive/e15/e15-regs.htm>.
- U.S Environmental Protection Agency. (2015b). EPA Proposes Renewable Fuel Standards for 2014, 2015, and 2016 and the Biomass-Based Diesel Volume for 2017, EPA document No. EPA-420-F-15-028, May. <http://www.epa.gov/otaq/fuels/renewablefuels/documents/420f15028.pdf>.
- Varde, K.S., Patro, N., & Drouillard, K. (1995). Lean Burn Natural Gas Fueled S.I. Engine and Exhaust Emissions. SAE Technical Paper No. 952499. Warrendale, PA: Society for Automotive Engineers.
- Volvo website (2010). Volvo Bio-DME Unique Commercial Test Operations, 2010-2012, <http://www.volvotrucks.com/SiteCollectionDocuments/VTC/Corporate/News%20and%20Media/publications/Volvo%20BioDME.pdf>.
- Volvo Press Release, Accessed January, (2014). http://www.volvogroup.com/group/global/engb/volvo%20group/worldwide/Volvo-Group-North-America/_layouts/CWP.Internet.VolvoCom/NewsItem.aspx?News.ItemId=143305&News.Language=en-gb.
- Volvo Powertrain Sweden, DME Vehicle - Demonstration of DeMethyl Ether Vehicle for Sustainable Transport, Project No. LIFE05 ENV/S/000405.
- Wallner, T., Miers, S. A., & McConnell, S. (2009). A Comparison of Ethanol and Butanol as Oxygenates Using a Direct-Injection, Spark-Ignition Engine. *Journal of Engineering for Gas Turbines and Power-Transactions of the ASME*, 131(3), 032802.
- Wallner T., Shidore N., & Ickes A. (2010). Impact of ethanol and butanol as oxygenates on SIDI engine efficiency and emissions using steady-state and transient test procedures. 16th Directions in Engine-Efficiency and Emissions Research (DEER) Conference, Detroit, Michigan, September 27-30.
- Wang, M., Han, J., Dunn, J. B., Cai, H., & Elgowainy, A. (2012). Well-to-wheels energy use and greenhouse gas emissions of ethanol from corn, sugarcane and cellulosic biomass for US use. *Environmental Research Letters*, 7(4), 045905.

- Ward, P. & Teague, J.M. (1996). Fifteen Years of Fuel Methanol Distribution. California Energy Commission report No. CEC-999-1996-017.
- Waterland, L. (2006). California Alternative Fuels Market Assessment. CEC-600-2006-015-D.
- West, B. H., Sluder, C. S., Knoll, K. E., Orban, J. E., & Feng, J. (2012). Intermediate Ethanol Blends Catalyst Durability Program, ORNL/TM-2011/234; Oak Ridge National Laboratory: Oak Ridge, TN.
- Williams, A., McCormick, R., Luecke, J., Brezny, R., Geisselmann, A., Voss, K., Hallstrom, K., Leustek, M., Parsons, J., & Abi-Akar, H. (2011). Impact of Biodiesel Impurities on the Performance and Durability of DOC, DPF, and SCR Technologies. SAE Technical Paper 2011-01-1136. Warrendale, PA: Society for Automotive Engineers.
- Williams, A., Burton, J., McCormick, R. L., Toops, T., Wereszczak, A. A., Fox, E. E., Lance, M. J., Cavataio, G., Dobson, D., Warner, J., Brezny, R., Nguyen, K., & Brookshear, D. W. (2013). Impact of Fuel Metal Impurities on the Durability of Light-Duty Diesel Aftertreatment System. SAE Technical Paper 2013-01-0513. Warrendale, PA: Society for Automotive Engineers.
- Williams, A., McCormick, R., Lance, M., Xie, C., Toops, T., & Brezny, R. (2014). Effect of Accelerated Aging Rate on the Capture of Fuel-Borne Metal Impurities by Emissions Control Devices. SAE Technical Paper 2014-01-1500. Warrendale, PA: Society for Automotive Engineers.
- Xiaolong Y., Jing Y., & Tieping L. (2009). The effect of an SI engine using butanol-gasoline blended fuel on performance and environment. *ICEET Proceedings of the 2009 International Conference on Energy and Environment Technology*, October 16-18, pp 402-405.
- Yacoub Y., Bata R., & Gautam M. (1998). The performance and emissions characteristics of C1-C5 alcohol-gasoline blends with matched oxygen content in a single cylinder spark ignition engine. *Proceedings of the Institution of Mechanical Engineers, Part A: Journal of Power and Energy*, 212, 363-379.
- Yang Y., Dec J., Dronniou N., & Simmons B. (2010). Characteristics of isopentanol as a fuel for HCCI engines. SAE Technical Paper 2010-01-2164. Warrendale, PA: Society for Automotive Engineers.
- Yang H.H., Chien S.M., Lo M.Y., Lan J.C.W., Lu W.C., & Ku Y.Y. (2007). Effects of biodiesel on emissions of regulated air pollutants and polycyclic aromatic hydrocarbons under engine durability testing. *Atmospheric Environment*, 41, 7232-7240.
- Yanowitz, J., & McCormick, R. L. (2009a). Effect of E85 on tailpipe emissions from light-duty vehicles. *Journal of the Air & Waste Management Association*, 59, 172-182.
- Yanowitz, J., & McCormick, R. L. (2009b). Effect of biodiesel blends on North American heavy-duty diesel engine emissions. *European Journal of Lipid Science and Technology*, 111(8), 763-772.
- Yong, G., Zhang, Y. G., & Ying, J. Y. (2008). Efficient Catalytic System for the Selective Production of 5-Hydroxymethylfurfural from Glucose and Fructose. *Angewandte Chemie-International Edition*, 47(48), 9345-9348.
- Yoon, S., Collins, J., Thiruvengadam, A., Gautam, M., Herner, J., & Ayala, A. (2013). Criteria pollutant and greenhouse gas emissions from CNG transit buses equipped with three-way catalysts compared to lean-burn engines and oxidation catalyst technologies. *Journal of the Air & Waste Management Association*, 63(8), 926-933.

-
- Zhang Q. C., Chen G. S., Zheng Z. Q., Liu H. F., Xu J., & Yao M. F. (2013). Combustion and emissions of 2,5-dimethylfuran addition on a diesel engine with low temperature combustion. *Fuel*, *103*, 730-5.
- Zhao H., Ge Y., Hao C., Han X., Fu M., Yu L., Shah A.N. (2010). Carbonyl compounds emissions from passenger cars fueled with methanol/gasoline blends. *Science of the Total Environment*, *408*, 3607-3613.
- Zhao H. B., Holladay J. E., Brown H., Zhang Z. C. (2007). Metal chlorides in ionic liquid solvents convert sugars to 5-hydroxymethylfurfural. *Science*, *316*, 1597–600.
- Zhu, R., Cheung, C. S., & Huang, Z. (2011). Particulate emission characteristics of a compression ignition engine Fueled with diesel–DMC blends. *Aerosol Science and Technology*, *45*, 137-147.
- Zimmerle, D. J., Williams, L. L., Vaughn, T. L., Quinn, C., Subramanian, R., Duggan, G. P., & Robinson, A. L. (2015). Methane emissions from the natural gas transmission and storage system in the United States. *Environmental Science & Technology*, *49*, 9374-9383.

INDEX

#

2,5-Dimethylfuran, 339, 414, 417, 422, 426, 427, 430, 442, 445
2-methyl-tetrahydrofuran, 239, 417
5-Hydroxymethylfurfural, 82, 87, 88, 94, 107, 108, 128, 220, 237, 240, 242, 435, 441, 445

A

access, 4, 5, 48, 49, 52, 88, 350, 379, 398, 414
accessibility, 38, 46, 47, 48, 49, 51, 52, 68, 69, 71, 72, 73, 78, 79, 83, 84, 88, 90, 95, 120, 127, 230, 294
acetaldehyde, 99, 232, 346, 347, 348, 350, 351, 354, 365, 368, 374, 376, 377, 381, 403, 409, 410, 418
acetic acid, 53, 59, 85, 87, 94, 104, 106, 108, 110, 115, 117, 131, 136, 147, 178, 191, 251, 252, 263, 270, 378
acetone, 39, 53, 89, 113, 114, 116, 129, 191, 232, 284, 298, 365, 366, 372, 374, 376
acetylation, 44, 61, 62, 69, 84, 255
acidic, 87, 88, 94, 108, 187, 189, 210, 212, 213, 216, 219, 223, 226, 228, 230, 234, 251, 268, 272, 297, 302
acidity, 180, 212, 216, 223, 226, 228, 229, 230, 232, 233, 266, 359
acquisitions, 64
acrylate, 372
acrylic acid, 113
activated carbon, 263, 267, 282
active site, 212
active transport, 110
adaptability, 328, 442
adaptations, 2, 95, 99, 104, 105, 115, 128, 129

additives, 96, 127, 201, 202, 203, 209, 233, 234, 236, 272, 281, 353, 358, 359, 361, 366, 369, 379, 410, 415, 416, 419, 423
adhesives, 372, 378
adsorption, 41, 47, 48, 49, 50, 53, 73, 75, 77, 83, 88, 89, 93, 94, 95, 96, 129, 132, 219, 220, 222, 257, 329, 346
aerogels, 317
AFM, 306
age, 12, 28
agencies, 344, 388
aggregation, 31, 53, 156, 304, 307
aging process, 358, 360
agriculture, 2, 130, 160, 161, 162, 167
air pollutants, 444
air quality, 361, 380
alcohol oxidase, 248
alcohol production, 133, 175
alcohols, 59, 107, 109, 113, 123, 129, 137, 140, 147, 224, 230, 232, 234, 235, 252, 263, 266, 270, 273, 274, 277, 339, 342, 355, 363, 374, 375, 376, 377, 378, 406, 415
aldehydes, 106, 107, 108, 188, 224, 228, 232, 255, 263, 266, 268, 269, 270, 277, 283, 362, 377, 378, 409, 424
alfalfa, 33, 63, 75, 78, 279, 284
algae, 185, 191, 192, 193, 194, 197, 198, 199, 295, 395, 396, 429
aliphatic compounds, 273
alkaline earth metals, 227, 231
alkenes, 188, 229, 263
alkylation, 198, 272
alternative energy, 201
amines, 275
amino, 109, 128, 147, 329
amino acids, 109, 128, 147, 329

- ammonia, 26, 28, 31, 78, 85, 86, 88, 89, 115, 123, 125, 127, 145, 148, 155, 156, 163, 168, 206, 263, 279, 296, 298, 403
- ammonium, 109, 128, 237, 251
- anaerobic bacteria, 145, 165
- anaerobic digesters, 148, 155, 164, 400
- anaerobic digestion, 143, 144, 145, 150, 152, 162, 163, 164, 165, 166, 167, 168, 169, 175, 178, 243, 400, 405
- anatase, 217, 228, 232
- angiosperm, 248
- antioxidant, 360, 432
- antioxidant additives, 360, 432
- aquaculture, 191
- aqueous alkali solution, 49
- aqueous solutions, 83, 217, 223, 236
- aqueous suspension, 318
- Arabidopsis thaliana*, 74
- argon, 60
- aromatic compounds, 231, 266, 268, 270, 362
- aromatic hydrocarbons, 9, 32, 226, 227, 229, 230, 231, 265, 272
- aromatic rings, 62, 189, 265, 266, 270, 276
- aromatics, 42, 96, 188, 225, 226, 227, 228, 229, 230, 231, 242, 255, 272, 273, 275, 278, 290, 324, 347, 350, 351, 352, 353, 394, 419
- Asia, 379
- ASL, 40
- assessment, 31, 56, 125, 135, 136, 158, 183, 184, 185, 193, 197, 335, 337, 424, 437
- assets, 424
- atmosphere, 60, 172, 186, 202, 223, 224, 262, 412, 413
- atmospheric pressure, 252, 281, 400
- atomic force, 68, 71, 284, 306
- atoms, 56, 408
- ATP, 108, 134
- Automobile, 385, 423, 429
- automobiles, 112
- autooxidation, 359
- aviation industry, 361, 394
- base, 18, 53, 86, 144, 199, 234, 271, 272, 327, 329, 331, 332, 343, 350, 351, 363, 365, 367, 369, 383, 408
- basicity, 218
- beer, 99, 111, 112
- beneficial effect, 220, 271, 365
- benzene, 39, 191, 226, 347, 351, 353, 354, 369, 383, 384, 419, 439
- benzo(a)pyrene, 369
- bicarbonate, 61
- biocatalysts, 108, 109, 113, 114
- biochemical processes, 251, 392
- biochemistry, 138, 165
- bioconversion, 33, 37, 45, 75, 93, 95, 96, 133, 137, 275, 277, 286, 290, 298
- biocrude, 33, 185, 186, 188, 189, 190, 191, 192, 197, 198, 199, 200
- biodegradability, 144, 154, 158, 163, 166, 167, 303, 406
- biodegradable wastes, 151
- biodegradation, 86, 191, 290
- biodiesel, 2, 112, 135, 144, 164, 202, 339, 340, 355, 357, 358, 359, 360, 361, 362, 363, 364, 365, 366, 367, 368, 369, 370, 371, 388, 389, 390, 393, 394, 395, 421, 422, 423, 424, 427, 428, 429, 432, 434, 435, 436, 439, 440, 443, 444
- biodiversity, 246
- bioenergy, 1, 2, 3, 4, 6, 10, 23, 26, 30, 31, 32, 35, 144, 145, 153, 163, 164, 165, 322, 336, 337, 338
- biofuel, 5, 29, 32, 33, 71, 75, 79, 112, 113, 121, 122, 125, 126, 133, 135, 137, 184, 186, 187, 192, 193, 196, 197, 200, 201, 238, 247, 289, 322, 324, 327, 335, 336, 340, 355, 363, 385, 388, 393, 394, 415, 424, 428, 439
- biogas, 2, 80, 143, 144, 145, 147, 148, 149, 150, 151, 152, 153, 154, 155, 156, 157, 158, 159, 160, 161, 162, 163, 164, 165, 166, 167, 168, 286, 324, 329, 382, 385, 388, 400, 405, 440
- biological processes, 114, 150, 155, 173, 275
- biological stability, 151, 155, 168
- biological systems, 275, 439
- biomass characterization, 38, 44, 68, 71
- biomass growth, 94
- biomass materials, 21, 47
- biomass quality, 1, 16, 26, 28, 32
- biomaterials, 68, 161, 289
- biomonitoring, 439
- bio-oil, 26, 175, 179, 180, 184, 185, 186, 189, 192, 194, 196, 201, 203, 209, 225, 226, 227, 229, 230, 231, 232, 233, 234, 237, 238, 240, 241, 242, 264,

B

- bacteria, 82, 92, 99, 102, 104, 110, 113, 116, 123, 125, 129, 130, 138, 145, 147, 148, 150, 151, 157, 158, 275, 276, 282, 295, 306
- bacterial fermentation, 80
- bacteriophage, 125
- bacterium, 97

- 265, 266, 267, 268, 271, 277, 282, 284, 287, 291, 433, 434
- biopolymers, 37, 91, 245, 312, 316
- biopower, 24
- biorefinery, 1, 2, 4, 5, 6, 32, 121, 133, 137, 141, 161, 164, 165, 184, 209, 245, 246, 247, 285, 286, 289, 297, 298, 303, 321, 322, 323, 324, 325, 326, 329, 331, 335, 337, 394, 438
- bioremediation, 191
- biosynthesis, 38, 78, 117, 120, 123, 245, 248, 249, 254, 258, 279, 281, 284, 285, 292, 316
- biosynthetic pathways, 278, 329
- biotechnology, 122, 129, 138, 165, 168, 284, 336, 337
- bisphenol, 210
- black liquor, 139, 262, 382
- bleaching, 78
- blend wall, 112, 344
- blends, 112, 234, 319, 344, 345, 346, 347, 348, 349, 350, 351, 352, 353, 354, 358, 359, 360, 361, 362, 364, 365, 366, 367, 368, 369, 370, 371, 373, 374, 375, 376, 377, 378, 380, 381, 383, 384, 389, 393, 395, 408, 415, 416, 417, 418, 420, 421, 423, 426, 427, 428, 429, 431, 432, 435, 436, 439, 440, 444, 445
- blood, 419, 420, 439
- boilers, 27, 173, 181, 267
- bonds, 52, 59, 79, 81, 87, 89, 205, 206, 207, 208, 249, 251, 253, 263, 264, 271, 274, 294, 295, 298, 302, 387, 388
- branching, 81, 398
- breakdown, 52, 89, 96, 97, 98, 100, 106, 113, 124, 256, 334, 398
- break-even, 34
- breeding, 328
- BTU, 379, 395, 396, 402
- building blocks, 220
- burn, 364, 403, 404, 407, 408, 409, 410, 429, 445
- business model, 325
- butadiene, 351, 354, 383, 384, 439
- butanol, 2, 109, 113, 114, 115, 116, 117, 121, 126, 129, 133, 339, 340, 341, 348, 350, 352, 355, 363, 372, 373, 374, 375, 376, 377, 417, 420, 421, 424, 425, 427, 428, 433, 438, 439, 441, 443, 444
- butyl ether, 263
- calibration, 57, 61, 259, 285, 387
- capillary, 51, 52, 389
- capital expenditure, 326
- capital intensive, 21, 323
- carbohydrates, 1, 2, 4, 8, 15, 16, 26, 27, 28, 39, 42, 59, 60, 69, 72, 76, 77, 79, 82, 85, 87, 90, 91, 92, 97, 106, 111, 140, 152, 158, 169, 187, 190, 191, 192, 206, 208, 209, 211, 217, 234, 236, 237, 241, 247, 250, 251, 252, 253, 264, 275, 278, 295, 298, 424, 440
- carbon, 9, 26, 54, 59, 62, 65, 66, 74, 75, 79, 82, 94, 97, 109, 115, 119, 143, 144, 145, 147, 148, 152, 159, 164, 167, 171, 172, 173, 178, 180, 181, 182, 186, 187, 188, 189, 190, 191, 200, 201, 202, 214, 215, 217, 218, 219, 222, 225, 226, 227, 228, 230, 233, 237, 241, 246, 247, 250, 256, 257, 262, 263, 264, 266, 267, 270, 276, 277, 278, 280, 282, 283, 284, 285, 295, 321, 361, 363, 367, 369, 386, 388, 393, 395, 396, 397, 405, 410, 414, 416, 428
- carbon atoms, 62, 189, 191, 214
- carbon deposit, 218, 219, 225, 227, 228, 230, 233
- carbon dioxide, 74, 144, 145, 171, 180, 181, 186, 188, 201, 202, 217, 241, 262, 264, 267, 276, 277, 284, 397, 414
- carbon materials, 189
- carbon monoxide, 145, 147, 173, 178, 180, 181, 189, 233, 262, 263, 264, 266, 267, 277, 416
- carbon nanotubes, 267
- carbon neutral, 172
- carbonization, 26, 28, 33
- carbonyl groups, 249, 290
- carboxyl, 130, 209, 255, 256, 276
- carboxylic acids, 62, 107, 108, 110, 113, 199, 228, 230, 231, 232, 255, 268, 269, 272, 277
- carboxylic groups, 252
- catalysis, 284, 307, 391
- catalyst, 2, 69, 85, 89, 90, 175, 176, 189, 199, 200, 211, 212, 216, 217, 218, 219, 220, 222, 223, 224, 225, 226, 227, 228, 229, 230, 231, 232, 233, 234, 235, 237, 238, 239, 240, 241, 242, 256, 261, 263, 264, 267, 270, 272, 273, 274, 279, 280, 282, 287, 289, 294, 298, 304, 305, 345, 352, 358, 364, 382, 387, 393, 406, 408, 415, 424, 428, 435, 438, 445
- catalyst deactivation, 219, 358
- catalytic activity, 199, 212, 216, 218, 232, 358
- catalytic hydrogenation, 219, 236, 239, 241
- catalytic properties, 212, 232
- catalytic system, 218, 219, 223, 275
- CBP, 94
- cell death, 108, 109
- cell metabolism, 114

C

CAD, 152

cadmium, 149

calcium, 189, 200, 251, 276

- cellular energy, 97
- cellulase, 46, 47, 48, 49, 51, 53, 60, 69, 73, 74, 78, 79, 83, 89, 90, 91, 92, 93, 94, 95, 96, 107, 116, 117, 120, 122, 123, 125, 126, 127, 129, 136, 138, 140, 302, 317, 319, 320, 337
- cellulose, 2, 10, 16, 35, 38, 42, 43, 46, 47, 48, 49, 51, 53, 54, 55, 56, 61, 68, 69, 70, 71, 72, 73, 74, 75, 76, 77, 78, 79, 81, 82, 83, 84, 85, 86, 87, 88, 89, 90, 91, 92, 93, 94, 95, 96, 98, 99, 106, 107, 111, 114, 117, 118, 120, 122, 123, 124, 127, 129, 132, 136, 140, 141, 152, 174, 188, 189, 190, 191, 199, 200, 201, 204, 205, 206, 207, 208, 209, 210, 211, 212, 213, 218, 219, 223, 226, 227, 229, 231, 232, 235, 236, 237, 240, 241, 242, 245, 246, 251, 252, 253, 263, 282, 288, 293, 294, 295, 296, 297, 298, 299, 300, 301, 302, 303, 304, 305, 306, 307, 308, 309, 310, 312, 313, 314, 315, 316, 317, 318, 319, 320, 415, 435, 441
- cellulose microfibrils, 293, 294, 315, 318
- cellulose nanocrystals, 293, 294, 299, 305, 306, 307, 309, 312, 314, 315, 316, 319
- cellulose nanofibrils, 293, 294, 299, 300, 301, 303, 306, 307, 308, 314, 315, 317, 319
- cellulosic biofuel, 123, 236, 320, 322, 323, 337, 385, 388
- cellulosomes, 91, 92, 116
- cell wall, 8, 38, 44, 45, 46, 47, 50, 51, 59, 70, 72, 73, 75, 76, 77, 81, 82, 83, 88, 89, 94, 114, 118, 119, 121, 204, 246, 247, 248, 249, 250, 251, 252, 253, 254, 255, 259, 275, 278, 285, 287, 293, 295, 296, 298, 300, 305, 314, 315, 317, 319, 340
- ceramic, 301
- chain molecules, 369
- chain scission, 256
- chemical bonds, 340
- chemical degradation, 249, 250
- chemical pretreatments, 26
- chemical properties, 26, 38, 64, 68, 180, 203, 223, 247, 254, 266, 267, 273, 279, 344, 357, 415
- chemical reactions, 20, 187
- chemicals, 2, 37, 38, 68, 80, 113, 115, 122, 123, 137, 138, 141, 144, 172, 173, 174, 175, 178, 182, 186, 188, 201, 202, 203, 204, 209, 214, 219, 220, 234, 236, 238, 240, 241, 245, 246, 247, 250, 251, 252, 253, 254, 261, 262, 263, 269, 275, 276, 277, 278, 279, 280, 281, 283, 284, 286, 287, 288, 290, 296, 299, 314, 321, 322, 324, 325, 327, 328, 335, 342, 378, 406, 419, 423, 427
- chicken, 148, 163
- Chitosan, 314
- chloroform, 62, 64, 165, 190
- chlorophyll, 39, 191, 204
- cholesterol, 136
- chromatography, 40, 56, 69, 71, 258, 259, 260, 272, 283, 284, 310
- chromium, 63, 64, 415
- cigarette smoke, 419, 420
- clean energy, 4
- cleanup, 178
- cleavages, 45, 64, 78, 87, 88, 89, 249, 251, 253, 256, 263, 270, 272, 273, 274, 275, 276, 291
- climate change, 2, 202
- climates, 2, 202, 246, 358, 404, 407, 412, 425
- cloning, 129
- CO₂, 12, 85, 144, 147, 149, 151, 158, 173, 177, 186, 188, 190, 191, 198, 202, 246, 272, 348, 350, 352, 365, 367, 368, 374, 376, 377, 378, 388, 389, 394, 397, 398, 400, 401, 404, 407, 409, 411, 413, 416, 420, 421
- coal, 26, 27, 33, 34, 172, 173, 175, 179, 181, 183, 188, 199, 202, 246, 375, 379, 380, 381, 391, 404, 412
- coatings, 372, 414
- cobalt, 149, 226, 228
- Co-digestion, 143, 144, 155, 156, 157, 158, 159, 160, 161, 162, 163, 164, 166, 167, 168, 169
- coenzyme, 113, 132
- coffee, 419, 420
- cogeneration, 322, 434
- coherence, 58, 64, 75, 256
- coke, 189, 227, 228, 229, 230, 234
- coke formation, 189, 227, 228, 234
- collenchyma, 316
- combustion, 2, 11, 21, 30, 32, 131, 135, 163, 171, 172, 173, 174, 175, 178, 179, 181, 182, 183, 184, 187, 202, 203, 214, 237, 262, 263, 264, 265, 288, 324, 340, 361, 364, 367, 370, 374, 375, 376, 379, 386, 387, 388, 390, 393, 403, 406, 407, 408, 410, 411, 413, 415, 416, 417, 418, 419, 420, 426, 427, 430, 434, 435, 437, 439, 440, 441, 442, 445
- combustion processes, 202, 410
- commodity, 4, 11, 33, 245, 269, 325
- communities, 150, 362
- community, 164, 325, 380
- compatibility, 104, 135, 210, 339, 344, 352, 358, 372, 373, 375, 379, 427
- competition, 4, 118, 202
- composites, 133, 294, 317
- composition, 1, 2, 6, 8, 13, 14, 16, 26, 27, 28, 31, 32, 33, 34, 35, 39, 40, 41, 46, 65, 73, 75, 76, 77, 81, 91, 93, 97, 99, 108, 118, 122, 129, 136, 137, 151, 152, 153, 154, 156, 158, 159, 164, 166, 168, 173,

- 190, 191, 192, 197, 205, 224, 229, 232, 236, 247, 248, 259, 261, 264, 267, 269, 277, 279, 282, 285, 286, 288, 290, 291, 306, 328, 330, 359, 361, 396, 404, 409, 410, 429, 433
- compost, 168
- composting, 281, 405
- compound identification, 260
- compounds, 39, 70, 84, 85, 93, 94, 95, 96, 106, 107, 108, 120, 121, 138, 147, 148, 179, 180, 187, 188, 189, 191, 200, 202, 203, 225, 229, 230, 233, 236, 240, 241, 250, 256, 257, 259, 260, 265, 266, 267, 268, 270, 271, 272, 273, 274, 275, 277, 281, 286, 287, 297, 347, 354, 362, 366, 367, 368, 378, 388, 389, 401, 445
- compressibility, 382
- compression, 176, 370, 372, 377, 378, 386, 389, 410, 423, 426, 435, 445
- condensation, 49, 88, 188, 199, 230, 236, 254, 255, 256, 259, 260, 265, 267, 388
- conditioning, 72, 239
- conference, 167, 183, 200, 427
- configuration, 179, 259, 326, 332, 345, 387, 390
- constituents, 27, 41, 158, 231, 236, 282, 328, 375, 396
- construction, 2, 126, 326, 330, 419
- consumers, 396, 397
- consumption, 20, 85, 94, 97, 103, 104, 116, 122, 137, 148, 196, 202, 245, 246, 254, 302, 342, 344, 367, 381, 388, 389, 406
- containers, 210, 266, 414
- contaminant, 62, 110, 143
- contamination, 2, 8, 12, 13, 27, 97, 110, 116, 117, 124, 125, 251, 252, 253, 264, 360, 372, 373, 422
- controversial, 84, 311
- conversion rate, 182, 355
- COOH, 58, 65, 209
- cooking, 138, 298, 355, 356, 363, 364, 396
- cooling, 179, 181
- copper, 270, 274, 275, 291
- corn starch, 34, 80, 110
- corn stover, 7, 8, 13, 14, 15, 16, 18, 19, 23, 29, 30, 31, 32, 33, 34, 35, 46, 47, 72, 73, 78, 89, 100, 113, 119, 122, 125, 126, 127, 130, 134, 135, 139, 140, 166, 186, 187, 243, 323, 342, 349, 354
- corrosion, 8, 86, 90, 177, 214, 219, 266, 346, 359, 373
- corrosivity, 211
- cosmetic, 294
- cost, 1, 2, 4, 5, 6, 7, 11, 13, 21, 27, 28, 38, 82, 85, 90, 93, 95, 96, 110, 111, 113, 114, 123, 125, 136, 139, 140, 151, 153, 156, 174, 179, 181, 182, 194, 204, 207, 209, 235, 275, 277, 280, 323, 324, 325, 326, 329, 333, 335, 337, 355, 362, 379, 392, 393, 401, 402, 421
- cotton, 51, 74, 123, 154, 165, 208, 211, 237, 242, 295, 296, 303, 314, 316, 318
- covalent bond, 297
- crop residue, 2, 143, 144, 153, 154, 156, 186
- crops, 2, 4, 7, 12, 13, 17, 32, 81, 143, 144, 151, 153, 154, 155, 156, 159, 160, 161, 162, 163, 164, 166, 168, 185, 186, 187, 202, 327, 330, 336, 338, 340, 342, 422
- cross-linking reaction, 271
- crude oil, 175, 180, 398
- crystalline, 53, 54, 55, 81, 83, 89, 92, 205, 206, 207, 209, 217, 232, 267, 294, 295, 296, 303, 310, 311, 315, 319
- crystallinity, 38, 43, 53, 54, 55, 56, 68, 69, 74, 83, 85, 88, 92, 132, 207, 208, 242, 253, 298, 299, 305, 310, 311, 313, 314, 315, 317
- crystallites, 217
- crystals, 50, 302, 304, 305, 306, 307, 310, 311, 312
- cultivation, 193, 202, 234
- culture, 116, 128, 129, 136, 191, 276, 277
- cycles, 111, 348, 365, 367, 370, 376, 409, 411, 428
- cyclohexanol, 64
- cyclones, 179
- cytotoxicity, 114

D

- DDGS, 342
- DEA, 416
- deacetylation, 84, 88
- deactivation, 94, 96, 139, 197, 200, 218, 219, 222, 233, 358
- decay, 43, 74
- decomposition, 91, 203, 213, 217, 223, 231, 252, 263, 264, 269, 271
- deconstruction, 38, 74, 118, 127, 235, 245, 247, 249, 254, 258, 271, 278, 280, 295, 299, 302
- decoupling, 63
- defibrillation, 294, 300, 302, 307, 312
- deformation, 43, 58
- degradation, 14, 39, 44, 53, 64, 82, 84, 87, 88, 89, 91, 94, 95, 106, 107, 108, 122, 123, 125, 138, 145, 146, 148, 149, 150, 157, 167, 189, 190, 211, 230, 247, 250, 251, 252, 262, 269, 270, 275, 276, 282, 284, 291, 305, 316, 357, 359, 414
- degree of crystallinity, 53, 76, 90
- dehydration, 94, 137, 200, 209, 210, 212, 219, 222, 228, 230, 240, 241, 262, 267, 415

- delignification, 53, 72, 73, 86, 88, 128, 251, 252, 253, 287, 289, 298, 316
- density values, 22
- depolymerization, 46, 82, 87, 88, 98, 106, 128, 175, 188, 189, 204, 206, 212, 245, 249, 254, 258, 259, 263, 265, 266, 268, 269, 270, 271, 272, 274, 275, 279, 280, 283, 285, 287, 289, 290, 292, 295, 297, 302, 310
- deposition, 225, 227, 229, 230
- deposition rate, 227, 230
- deposits, 357, 398
- desorption, 109, 258, 281
- detoxification, 124, 127, 128, 131
- DFT, 216
- dialysis, 304, 305
- dielectric constant, 187, 265
- diesel engines, 357, 359, 366, 367, 373, 375, 388, 403, 406, 415, 435
- diesel fuel, 267, 357, 358, 359, 360, 361, 362, 363, 364, 365, 366, 367, 368, 370, 371, 373, 375, 376, 387, 388, 389, 390, 391, 392, 393, 394, 395, 396, 402, 406, 414, 416, 417, 418, 432, 435, 438, 439, 440
- differential scanning, 48
- differential scanning calorimetry (DSC), 48, 51
- diffraction, 54, 311, 319
- diffusion, 69, 102, 104, 223, 387, 416, 418
- digestibility, 35, 46, 53, 72, 83, 84, 88, 122, 127, 140, 141, 237, 296
- digestion, 83, 93, 143, 144, 149, 150, 151, 152, 155, 156, 157, 158, 159, 160, 161, 162, 163, 164, 166, 167, 168, 169, 175
- dimerization, 249
- Dimethyl carbonate, 339, 406, 426, 427, 428, 435, 440, 443
- Dimethyl ether, 200, 263, 339, 363, 378, 381, 423, 424, 435, 440
- dimethylsulfoxide, 70, 78
- direct measure, 412
- dispersion, 217, 255
- displacement, 222, 295
- dissolved oxygen, 148
- distillation, 79, 111, 112, 114, 124, 203, 272, 298, 329, 342, 347, 372, 436
- diversification, 186
- diversity, 135, 137, 166, 246, 254, 405
- DME, 200, 339, 341, 363, 381, 382, 385, 386, 387, 388, 389, 390, 391, 394, 395, 421, 423, 424, 428, 430, 431, 435, 437, 440, 441, 443
- DMF, 339, 340, 341, 406, 414, 415, 418, 419, 420, 421
- DNA, 130, 139
- DOC, 358, 444
- DOI, 287
- dopants, 233
- double bonds, 251, 361, 369
- down-regulation, 63, 64, 67, 75, 279
- drug delivery, 294
- dry matter, 12, 14, 16, 17, 27, 28, 30, 31, 52, 111
- drying, 5, 7, 11, 12, 14, 15, 17, 20, 21, 23, 26, 28, 31, 32, 39, 41, 47, 50, 52, 59, 60, 61, 73, 74, 94, 129, 174, 176, 192, 307, 346
- durability, 2, 23, 34, 344, 345, 352, 358, 359, 444
- dyes, 49, 72

E

- E. coli*, 104, 105, 106, 107, 114, 122
- E85, 344, 346, 347, 349, 350, 351, 352, 354, 379, 426, 430, 444
- ecology, 191, 292
- editors, 71, 73, 75
- EEA, 288
- effluents, 162, 167, 253, 278, 287, 292, 298
- Elam, 291
- elastomer material, 346
- elastomers, 345, 346, 357, 373, 382, 428, 433
- electricity, 2, 20, 161, 178, 181, 183, 187, 262, 263, 322, 324, 326, 330, 331, 395, 396, 397, 405
- electrolyte, 406
- electromagnetic, 255
- electron, 71, 275, 316, 358
- emission, 12, 21, 193, 194, 201, 202, 288, 340, 345, 347, 350, 351, 353, 358, 364, 366, 369, 370, 371, 374, 376, 378, 384, 387, 388, 390, 394, 395, 400, 402, 405, 408, 409, 412, 413, 415, 416, 422, 426, 432, 435, 437, 440, 445
- emitters, 352, 353
- endothermic, 180
- energy consumption, 11, 18, 19, 23, 34, 141, 144, 187, 193, 303, 319, 354
- energy density, 191, 214, 247, 266, 344, 345, 374, 379, 401, 402, 418
- Energy Independence and Security Act, 442
- energy input, 11, 21, 280
- energy security, 2, 186
- environment, 87, 94, 108, 146, 148, 150, 174, 178, 191, 216, 223, 246, 250, 261, 298, 355, 419, 444
- environmental conditions, 27, 149
- environmental effects, 152
- environmental factors, 13, 14, 248, 249
- environmental impact, 144, 245, 339, 419, 420

- environmental issues, 21
- environmental management, 163
- environmental protection, 289
- Environmental Protection Agency (EPA), 112, 168, 186, 198, 321, 322, 336, 340, 344, 345, 346, 347, 348, 350, 354, 355, 361, 363, 367, 371, 385, 388, 404, 412, 413, 414, 430, 441, 443
- environments, 33, 37, 99, 144, 164, 215, 264, 328
- enzyme interaction, 91
- enzymes, 38, 46, 47, 49, 52, 53, 59, 60, 68, 70, 72, 75, 79, 81, 82, 83, 84, 86, 89, 90, 91, 92, 93, 94, 95, 96, 99, 102, 103, 106, 107, 108, 111, 114, 115, 120, 122, 123, 125, 127, 129, 130, 132, 137, 138, 139, 146, 151, 156, 248, 250, 253, 275, 276, 279, 296, 302, 303, 305, 310, 315, 323, 329, 330, 337, 340, 342, 355
- equilibrium, 21, 51, 151, 173, 258, 263, 285, 295
- erosion, 27, 266
- ESI, 259, 260
- ESR, 282
- ester, 39, 42, 43, 57, 58, 88, 89, 121, 208, 214, 304, 355, 360, 362, 365, 366, 373, 432
- ester bonds, 88, 89, 208, 304
- Estonia, 166
- ethanol, 2, 29, 31, 35, 39, 56, 59, 61, 63, 64, 71, 72, 74, 76, 77, 78, 79, 80, 81, 82, 89, 93, 94, 95, 96, 97, 99, 101, 102, 103, 104, 105, 106, 107, 108, 109, 110, 111, 112, 113, 114, 115, 116, 117, 118, 119, 120, 121, 122, 123, 124, 125, 126, 128, 129, 130, 131, 132, 133, 134, 135, 136, 137, 138, 139, 140, 141, 178, 184, 203, 214, 222, 241, 246, 253, 258, 259, 263, 275, 278, 279, 283, 284, 287, 288, 291, 298, 303, 308, 315, 320, 321, 322, 323, 324, 326, 327, 329, 330, 331, 332, 333, 334, 337, 339, 340, 342, 343, 344, 345, 346, 347, 348, 349, 350, 351, 352, 353, 354, 355, 363, 364, 372, 373, 374, 375, 376, 377, 378, 379, 380, 391, 406, 416, 417, 418, 419, 420, 421, 424, 426, 428, 431, 433, 435, 438, 439, 442, 443
- etherification, 200, 415
- ethers, 62, 224, 266, 270, 273, 274, 275, 290, 339, 363, 372, 423
- ethyl acetate, 53, 191
- ethylene, 59, 89, 96, 173
- ethylene glycol, 89, 96
- eucalyptus, 319
- eukaryote, 96
- eukaryotic, 139, 295
- evaporation, 12, 61, 347, 362, 387
- evapotranspiration, 12
- evidence, 128, 316, 367
- evolution, 105, 110, 193, 260, 275
- exposure, 344, 346, 357, 358, 359, 382, 414, 416, 420, 431, 439
- extraction, 2, 39, 53, 56, 59, 60, 70, 90, 96, 97, 114, 121, 175, 187, 190, 199, 254, 257, 295, 299, 313, 324, 327, 329, 349, 356, 395, 396, 397, 398, 429
- extracts, 56, 59, 276
- extrusion, 106, 124, 132

F

- farmers, 27
- fast pyrolysis, 30, 31, 32, 74, 173, 175, 180, 181, 186, 194, 224, 226, 227, 228, 229, 230, 232, 234, 235, 236, 237, 238, 239, 240, 242, 243, 265, 266, 282, 288, 289
- fat, 158, 160
- fatty acids, 39, 110, 147, 150, 151, 164, 188, 278, 359, 369, 393
- fermentation, 2, 10, 38, 39, 73, 79, 80, 82, 84, 93, 94, 95, 96, 97, 98, 99, 101, 102, 103, 104, 105, 106, 108, 109, 110, 111, 113, 114, 115, 116, 117, 118, 119, 120, 121, 122, 124, 125, 126, 127, 128, 129, 131, 134, 135, 137, 138, 139, 151, 164, 166, 168, 169, 175, 186, 241, 246, 253, 263, 275, 277, 278, 322, 323, 329, 331, 332, 340, 342, 372, 375, 391
- fermentation technology, 323
- fertilization, 13, 14, 28, 31
- fertilizers, 186
- FFVs, 344, 348, 352, 354, 379, 380, 419, 421, 432
- fibers, 20, 26, 31, 46, 50, 51, 70, 73, 74, 75, 83, 85, 87, 89, 92, 115, 127, 129, 130, 135, 141, 206, 257, 259, 283, 286, 294, 298, 300, 301, 302, 303, 312, 314, 315, 316, 319, 320, 333, 340
- fibrillation, 315, 319
- field tests, 386
- films, 294, 311, 312, 317, 319
- filters, 357
- filtration, 39, 41, 190, 353
- financial, 29, 312, 326, 327, 386
- first generation, 110, 185, 403
- Fischer-Tropsch process, 262
- fission, 126
- fixation, 186
- flame, 266, 367, 370, 378, 387
- flammability, 208, 380
- flexible fuel vehicles (FFVs), 344, 346, 380
- flour, 342
- fluctuations, 6, 7, 150, 151, 333
- flue gas, 172, 181
- fluid, 51, 157, 163, 176, 181, 284, 346, 378

- fluidized bed, 179, 181, 183, 226, 228, 229, 242
- foams, 378
- food, 143, 147, 153, 154, 155, 156, 159, 160, 164, 166, 169, 185, 187, 201, 202, 210, 214, 234, 246, 317, 342, 356, 382
- food additives, 214, 317
- forage crops, 154
- force, 52, 301, 311
- formaldehyde, 263, 264, 347, 348, 350, 354, 365, 366, 368, 374, 376, 377, 378, 381, 383, 384, 388, 389, 403, 407, 408, 409, 410, 418, 420
- formation, 16, 44, 53, 67, 85, 86, 88, 99, 102, 105, 116, 120, 123, 137, 138, 157, 160, 176, 177, 179, 182, 189, 191, 202, 204, 209, 210, 213, 216, 217, 218, 220, 222, 223, 224, 225, 228, 229, 230, 231, 232, 233, 234, 249, 253, 257, 263, 265, 271, 272, 273, 277, 282, 285, 288, 291, 311, 312, 315, 347, 348, 349, 350, 358, 359, 361, 362, 364, 370, 375, 386, 398, 404, 408, 410, 414, 418, 442
- formula, 49, 50, 101
- fouling, 8, 177, 179, 181
- fragments, 251, 252, 253, 270, 271, 273, 276, 277, 278, 302
- France, 163, 165, 290, 391, 394
- freedom, 51, 406
- freezing, 313
- freshwater, 199
- friction, 301
- fructose, 98, 99, 212, 213, 222, 237, 240, 241, 242, 415, 424, 440
- fruits, 165
- FTIR, 38, 41, 42, 43, 54, 56, 57, 58, 74, 75, 76, 77, 137, 257, 260, 283
- FTIR spectroscopy, 42, 54, 74
- FTIR technique, 43
- fuel cell, 263, 379
- fuel consumption, 365, 367, 368, 374, 375, 387, 407, 416, 428, 429, 440
- fuel distribution, 326
- fuel management, 359
- fungi, 74, 86, 92, 94, 122, 123, 275, 276, 290, 291
- furan, 84, 94, 106, 107, 108, 223, 418, 419
- Furfural, 80, 82, 87, 88, 94, 106, 107, 108, 116, 128, 136, 138, 191, 222, 415, 419, 424
- 182, 183, 184, 186, 187, 198, 209, 224, 245, 261, 262, 263, 264, 267, 277, 281, 282, 286, 289, 290, 292, 375, 382, 391, 400
- gel, 38, 53, 61, 258, 285
- gel permeation chromatography, 38, 53, 61, 258, 285
- gene expression, 116, 123, 279
- General Motors, 380
- genes, 83, 102, 103, 104, 105, 114, 115, 116, 128, 138, 197, 249, 338, 419, 420
- genetic diversity, 328
- genetic engineering, 101, 108, 114, 245, 278, 279, 281
- genetics, 105, 138, 291
- genotype, 248
- genus, 97, 99, 110, 113
- geography, 186
- global climate change, 152
- global demand, 246
- global warming, 202, 246, 404, 413
- glucose, 17, 39, 40, 52, 56, 58, 79, 81, 82, 83, 90, 91, 92, 93, 94, 95, 96, 98, 99, 101, 102, 103, 104, 105, 107, 108, 109, 110, 114, 115, 116, 117, 120, 122, 123, 124, 126, 127, 128, 129, 130, 132, 134, 135, 138, 198, 199, 200, 205, 206, 207, 208, 210, 211, 212, 218, 223, 237, 240, 242, 295, 298, 302, 303, 310, 323, 329, 330, 336, 340, 415, 419, 426, 435
- glucosidases, 92, 95, 302
- glycerin, 359
- glycerol, 111, 202, 355
- glycol, 48, 89, 372, 434
- glycolysis, 96
- glycoproteins, 275
- glycoside, 208
- GPC, 38, 53, 56, 57, 59, 61, 258, 259, 260, 287
- graphene sheet, 267
- GRAS, 97
- grasses, 8, 9, 10, 12, 30, 31, 32, 33, 41, 100, 144, 148, 154, 155, 160, 248
- gravity, 110, 111, 117, 126, 139, 191, 417
- greenhouse, 30, 152, 181, 192, 202, 246, 292, 321, 328, 349, 388, 404, 410, 413, 440, 441, 442, 444, 445
- greenhouse gas (GHG), 30, 152, 181, 192, 193, 194, 202, 246, 292, 321, 328, 349, 354, 388, 395, 396, 404, 405, 411, 413, 429, 440, 441, 442, 444, 445
- greenhouse gas emissions, 30, 328, 349, 444, 445
- GVL, 201, 209, 214, 215, 216, 217, 218, 219, 221, 234
- gymnosperm, 248

G

- gallium, 226, 228
- garbage, 166
- gasification, 2, 8, 9, 11, 17, 21, 26, 30, 33, 35, 80, 119, 144, 171, 173, 175, 176, 177, 178, 179, 181,

H

habitats, 349
 hardness, 373
 hardwoods, 85, 249
 harmful effects, 114
 harvesting, 1, 4, 5, 6, 8, 12, 13, 14, 15, 16, 27, 28, 32, 33
 health, 364, 414, 416
 health risks, 414, 416
 heat loss, 367
 heat release, 174, 374, 416, 417, 439
 heat transfer, 176, 180, 262, 264, 267
 heating rate, 175, 180, 264, 265, 267, 268, 281
 heavy metals, 148, 149
 heavy oil, 194, 196, 266
 helium, 73
 hemicellulose, 2, 16, 35, 38, 42, 43, 46, 51, 53, 56, 57, 58, 68, 69, 70, 74, 78, 79, 81, 82, 83, 85, 86, 87, 88, 89, 90, 91, 93, 94, 95, 99, 101, 106, 107, 108, 132, 174, 201, 204, 205, 206, 208, 227, 229, 231, 236, 246, 252, 263, 289, 294, 296, 297, 298
 hemp, 73, 272
 heterogeneity, 61, 245, 247, 250, 254, 348
 heterogeneous catalysis, 201
 heterogeneous catalysts, 189, 192, 197, 201, 203, 211, 220, 225, 233, 234, 235, 240, 241, 274
 hexane, 190, 325, 419, 420, 431
 homogeneous catalyst, 189, 218, 274
 homopolymers, 206
 hybrid, 39, 76, 89, 186, 228, 242, 247, 261, 279, 287, 292, 388, 389
 hydraulic fluids, 398
 hydrocarbons, 39, 106, 177, 181, 186, 188, 191, 224, 227, 228, 230, 231, 232, 234, 236, 263, 267, 272, 336, 347, 349, 350, 373, 375, 397, 402, 406, 408, 409, 416
 hydrocracking, 31, 194, 196, 267, 270, 272
 hydrofluoric acid, 27
 hydrogen, 2, 26, 43, 53, 81, 90, 109, 135, 145, 147, 162, 164, 172, 173, 175, 177, 178, 180, 186, 188, 189, 190, 191, 196, 200, 205, 207, 217, 218, 220, 222, 227, 229, 230, 234, 239, 241, 252, 262, 263, 264, 266, 267, 268, 269, 270, 271, 272, 273, 274, 275, 276, 277, 280, 281, 295, 300, 302, 312, 391, 397, 404, 408, 410
 hydrogen bonds, 53, 90, 205, 207, 295, 300, 312
 hydrogen gas, 188, 270, 271
 hydrogen peroxide, 252, 268, 269, 270, 275, 276
 hydrogen sulfide, 397

hydrogenation, 175, 209, 215, 216, 217, 218, 219, 234, 237, 239, 240, 241, 242, 267, 270, 272, 273, 274, 282, 328, 415, 424
 hydroperoxides, 359
 hydrophobicity, 206, 247
 hydrothermal process, 188, 198
 hydrothermal treatment, 171, 175, 199
 hydroxide, 48, 49, 56, 240, 251, 297
 hydroxyl, 42, 49, 53, 57, 59, 64, 88, 220, 249, 251, 252, 254, 256, 258, 264, 268, 273, 276, 295
 hydroxyl groups, 49, 53, 59, 64, 88, 254, 264, 268, 273, 295

I

impregnation, 212, 231
 impurities, 60, 358, 392
 incompatibility, 344, 357
 incomplete combustion, 178
 infrared spectroscopy, 76, 77, 257, 281
 infrastructure, 2, 4, 33, 145, 180, 193, 280, 323, 344, 346, 373, 375, 385, 400, 401, 402, 422, 437
 ingestion, 414, 416
 inhibition, 92, 94, 95, 96, 104, 106, 109, 110, 115, 129, 131, 136, 137, 138, 148, 156, 163, 165, 166
 inhibitor, 108
 inhomogeneity, 51
 initial boiling point, 362
 inoculum, 164
 integration, 64, 66, 105, 114, 155, 254, 298, 303, 323, 375
 integrity, 23, 107, 129, 247
 intensity values, 395, 396
 interference, 70
 internal rate of return, 326
 International Energy Agency (IEA), 155, 161, 163, 165, 438
 intrinsic viscosity, 258, 310
 iodine, 369
 ion-exchange, 200, 209, 211, 213
 ionization, 187, 258, 259, 260, 281, 291
 ions, 117, 251, 265, 297
 IR spectra, 76
 IR spectroscopy, 41, 72, 75, 77
 iron, 9, 226, 228, 302
 irradiation, 211, 213, 435
 irrigation, 8, 12, 28
 isobutane, 263
 isolation, 53, 59, 60, 61, 62, 69, 70, 71, 73, 74, 77, 126, 140, 216, 245, 251, 254, 255, 258, 262, 269,

283, 284, 285, 287, 289, 294, 295, 297, 304, 307,
313, 314
isomerization, 102, 212, 230, 393
isomers, 102
isopentane, 380
isotope, 260

K

kerosene, 175
ketones, 188, 224, 228, 232, 266, 268, 269, 272, 277,
362
kinetic parameters, 130
kinetics, 17, 27, 116, 118, 126, 254, 262, 268, 275,
277, 280, 284
KOH, 88, 189, 208, 263, 308
Kraft, 50, 72, 78, 251, 252, 256, 257, 259, 262, 281,
283, 284, 287, 288, 289, 297, 298, 300, 304, 308,
309

L

lactate dehydrogenase, 122
lactic acid, 110, 116, 129, 131, 137
Lactobacillus, 110, 120, 125
lactose, 114, 133
landfills, 388, 405
landscape, 132, 326
lattices, 295
LC-MS, 260
leaching, 15, 27
lead, 8, 21, 33, 47, 80, 93, 110, 149, 151, 154, 179,
180, 194, 217, 247, 262, 264, 269, 275, 310, 357,
359, 364, 380, 387, 402
leakage, 404, 412, 422
leaks, 348, 404, 412, 413, 424, 438
Levulinic Acid, 94, 209, 210, 214, 237, 240
Lewis acids, 272
life cycle, 184, 185, 199, 292, 349, 442
light scattering, 61, 71, 258, 259, 283, 284, 306
light trucks, 350
Lignin, 2, 10, 16, 38, 39, 40, 41, 42, 43, 46, 51, 53,
57, 59, 60, 61, 62, 63, 64, 65, 66, 67, 68, 69, 70,
71, 72, 73, 74, 75, 76, 77, 78, 79, 81, 82, 83, 84,
85, 86, 87, 88, 89, 90, 91, 93, 94, 95, 96, 106,
107, 116, 117, 118, 119, 120, 121, 123, 124, 125,
127, 128, 130, 132, 133, 135, 140, 154, 158, 174,
184, 188, 190, 191, 199, 201, 204, 205, 206, 208,
209, 226, 227, 229, 231, 236, 245, 246, 247, 248,
249, 250, 251, 252, 253, 254, 255, 256, 257, 258,

259, 260, 261, 262, 263, 264, 265, 266, 267, 268,
269, 270, 271, 272, 273, 274, 275, 276, 277, 278,
279, 280, 281, 282, 283, 284, 285, 286, 287, 288,
289, 290, 291, 294, 296, 297, 298, 299, 317, 323,
324, 326, 329, 330, 335, 338
Lignocellulosic biomass, 2, 4, 8, 10, 26, 28, 31, 33,
37, 38, 41, 43, 49, 51, 53, 73, 78, 79, 81, 84, 87,
89, 116, 119, 122, 125, 126, 130, 137, 141, 184,
185, 186, 187, 188, 190, 201, 202, 203, 204, 205,
206, 207, 208, 210, 219, 223, 224, 228, 229, 230,
231, 232, 233, 234, 235, 236, 237, 238, 241, 242,
246, 252, 261, 278, 288, 294, 297, 298, 304, 308,
309, 310, 314, 316, 321, 323, 336, 337, 423, 424
linear polymers, 81
lipids, 42, 56, 107, 146, 191, 192, 197, 278
liquefied natural gas, 397, 404
liquid chromatography, 40, 260
liquid fuels, 144, 172, 173, 175, 185, 188, 190, 191,
202, 283, 321, 322, 323, 346, 393, 419, 440
liquid phase, 187, 209, 215, 216, 220, 222, 224, 269
liquids, 30, 89, 90, 111, 136, 141, 208, 209, 220,
236, 237, 238, 240, 241, 257, 267, 272, 274, 281,
299, 313, 317, 323, 398, 402, 419, 426
lithium, 223, 310, 406
lithium ion batteries, 406
livestock, 27, 150, 153, 155, 156, 162, 356
local mobility, 51
logging, 2
logistics, 1, 4, 6, 8, 27, 28, 31, 33, 185, 186, 323
low temperatures, 89, 208, 210, 267, 362
LPG, 382, 385, 403, 407, 428, 435
lumen, 46, 51
luminosity, 380

M

machinery, 6, 15, 16, 27, 108, 110
macroalgae, 199, 325
macromolecular systems, 317
macromolecules, 297
macronutrients, 151
magnesium, 110, 117, 138, 225, 251, 263
magnetic field, 51
magnetic properties, 218
magnetic resonance, 44, 74
magnetization, 50, 51
magnitude, 354, 361, 387, 390, 412
maltose, 98
manganese, 86, 275, 276
manipulation, 30, 284
mannitol, 111

- manufacturing, 97, 111, 246, 319, 326, 357, 375
- manure, 144, 148, 150, 152, 153, 155, 159, 160, 161, 163, 164, 166, 167, 168, 400
- MAS, 54, 55, 257
- mass, 26, 27, 61, 68, 69, 83, 91, 144, 152, 162, 172, 189, 247, 255, 258, 259, 260, 268, 274, 281, 286, 291, 295, 304, 305, 346, 347, 348, 352, 353, 354, 362, 373, 374, 376, 388, 390, 393, 394, 395, 408, 409, 412, 414, 416, 417
- mass spectrometry, 61, 68, 258, 259, 281, 286
- material handling, 82
- measurements, 40, 47, 48, 49, 50, 54, 148, 164, 232, 306, 307, 310, 317, 387, 390, 412, 433, 434, 437, 439
- mechanical degradation, 253
- mechanical properties, 46, 53, 298, 305, 306, 312, 314, 316
- MEK, 431
- melting, 50, 51, 87, 179, 208
- melting temperature, 50
- membranes, 135, 146, 198
- Mercury, 52, 71
- mesoporous materials, 198, 225, 234, 235, 237, 242
- Metabolic, 115, 116, 117, 118, 121, 127, 140, 141, 336, 337
- metabolic intermediates, 329
- metabolic pathways, 102, 329, 337
- metabolism, 97, 103, 105, 110, 115, 117, 122, 123, 132, 136, 150, 151
- metabolites, 277, 335, 419, 420, 431
- metabolome, 337
- metal ions, 229
- metal oxides, 209, 215, 225, 228, 229, 232, 239, 270
- metal salts, 189, 212
- metals, 149, 153, 209, 212, 215, 229, 234, 345, 346, 358, 359, 373, 414, 428
- methanol, 54, 89, 147, 178, 200, 232, 256, 263, 265, 267, 271, 272, 277, 281, 298, 339, 350, 355, 363, 375, 377, 378, 379, 380, 381, 383, 384, 391, 406, 414, 416, 420, 421, 428, 435, 437, 440, 445
- methanol poisoning, 414, 416
- methyl group, 58, 147
- methylation, 61
- microalgae, 164, 185, 186, 187, 188, 191, 192, 198, 199
- microbial cells, 108, 149
- microbial community, 149
- microcrystalline, 87, 287, 310, 313, 314, 319
- microcrystalline cellulose, 87, 287, 310, 313, 314, 319
- micronutrients, 151
- microorganisms, 38, 82, 87, 91, 92, 94, 111, 129, 146, 148, 150, 151, 169, 203, 275, 277, 372
- microscope, 306, 316
- microscopic analyses, 303
- microscopy, 43, 68, 71, 284, 306
- microstructure, 95, 318
- microwave heating, 211
- Miscanthus, 8, 9, 10, 31, 32, 46, 80, 200, 227, 239, 292
- mixing, 48, 157, 158, 160, 162, 181, 340, 348, 380, 387, 390, 416, 418
- modelling, 184
- models, 159, 257, 345, 349, 363, 364, 380, 403
- modifications, 56, 62, 87, 180, 253, 385, 386, 387, 390
- modulus, 311, 312, 371
- moisture, 1, 2, 4, 6, 7, 11, 12, 13, 14, 16, 17, 18, 19, 20, 21, 26, 28, 30, 33, 34, 39, 41, 87, 94, 154, 158, 174, 180, 182, 185, 187, 262, 264, 265, 267
- moisture content, 1, 4, 7, 11, 12, 13, 14, 18, 19, 20, 21, 26, 27, 28, 30, 39, 41, 94, 174, 180, 182, 185, 187, 262, 264, 265, 267
- molasses, 112, 113
- molecular beam, 259, 286
- molecular mass, 88
- molecular oxygen, 268, 269, 270
- molecular sensors, 72
- molecular structure, 247, 248, 295, 369, 386
- molecular weight, 38, 39, 54, 56, 57, 59, 61, 62, 68, 77, 180, 188, 206, 230, 253, 254, 258, 259, 260, 266, 268, 271, 273, 275, 279, 283, 285, 287, 297, 341
- molecular weight distribution, 188, 254, 258, 260
- molecules, 47, 48, 51, 65, 88, 91, 96, 107, 146, 179, 188, 201, 202, 203, 204, 209, 222, 230, 234, 236, 237, 240, 256, 260, 266, 272, 294, 295, 299, 302, 310, 326, 329, 335, 340, 404, 406
- monomers, 83, 91, 92, 95, 99, 106, 115, 190, 206, 208, 248, 260, 270, 273, 279, 283
- mordenite, 223, 224
- morphology, 30, 83, 133, 306, 307
- MSW, 153, 154, 168, 388, 392
- MTBE, 351, 352, 353, 354, 378, 430
- multivariate analysis, 77, 257
- municipal solid waste, 2, 81, 152, 153, 162, 166, 169
- mutagenesis, 105, 129
- mutant, 74, 123, 124, 277, 279, 288, 290
- mutations, 115

N

NaCl, 149, 164, 211, 223, 224, 415
 NAD, 103, 105
 NADH, 102, 103, 105, 128, 132
 nanocellulose, 238, 293, 294, 297, 298, 299, 302, 305, 307, 310, 311, 312, 314
 nanocellulose production, 293, 297, 298, 307, 310, 312
 nanocomposites, 314, 315, 316
 nanocrystals, 293, 294, 296, 299, 304, 305, 306, 307, 309, 310, 311, 312, 314, 315, 316, 319
 nanofibers, 313, 315, 317
 nanomaterials, 294, 315, 316
 nanoparticles, 240, 242, 293, 306, 310, 312, 314, 316
 nanotechnology, 317
 natural gas, 20, 144, 151, 152, 196, 202, 246, 330, 378, 388, 395, 396, 397, 398, 404, 405, 406, 407, 408, 409, 410, 412, 419, 422, 424, 425, 428, 429, 432, 433, 434, 435, 437, 439, 441, 442, 445
 natural polymers, 61, 290
 near infrared spectroscopy, 286
 neurotoxicity, 431
 neutral, 70, 102, 151, 361, 394
 Ni catalyst, 218, 230, 232, 237
 nickel, 225, 226, 228, 232, 234, 263, 274, 290, 291
 niobium, 217, 219, 221
 NIR, 257, 260
 nitrates, 53
 nitrile rubber, 358
 nitrobenzene, 269, 270
 nitrogen, 47, 48, 73, 110, 143, 145, 147, 148, 151, 164, 179, 181, 188, 190, 191, 276, 302, 397, 404, 410
 noble metals, 230, 232, 274
 non-polar, 372
 non-renewable resources, 245
 norbornene, 64, 65
 North America, 371, 386, 401, 405, 424, 425, 444
 Norway, 61, 75, 113
 Norway spruce, 75
 nuclear magnetic resonance (NMR), 38, 44, 45, 48, 50, 51, 54, 55, 56, 58, 59, 62, 63, 64, 65, 66, 69, 70, 72, 73, 74, 75, 77, 78, 255, 256, 257, 260, 281, 282, 283, 284, 285, 286, 287, 288, 289, 290, 306, 311, 313, 316, 317
 nucleation, 362, 374, 376, 388
 nuclei, 51, 63, 64, 255
 nucleic acid, 146
 nutrient concentrations, 149

nutrients, 13, 15, 31, 97, 99, 106, 110, 116, 127, 143, 144, 149, 155, 161, 180, 192, 276
 nylons, 373

O

octane, 343, 372, 374, 406, 418, 419, 421
 octane number, 343, 418
 oil, 13, 14, 26, 28, 30, 156, 175, 179, 180, 181, 184, 185, 186, 189, 191, 192, 194, 196, 198, 199, 201, 202, 203, 209, 225, 226, 227, 229, 230, 231, 232, 233, 234, 237, 238, 240, 241, 242, 256, 257, 259, 260, 264, 265, 266, 267, 268, 271, 277, 278, 280, 281, 282, 287, 289, 291, 333, 340, 355, 358, 363, 364, 365, 366, 367, 380, 392, 393, 395, 397, 405, 412, 418, 433, 434, 439
 oil production, 181, 192, 196, 237, 238, 265, 277, 412
 oilseed, 199
 olefins, 226, 229, 233, 234, 242, 272, 352, 353, 378, 419
 oligomerization, 222, 229, 231, 265
 oligomers, 106, 190, 248, 249, 251, 271, 272, 274
 oligosaccharide, 91
 opacity, 375, 376, 407, 417
 operating costs, 179, 181
 operations, 1, 4, 5, 6, 7, 8, 11, 13, 17, 20, 26, 28, 81, 113, 149, 193, 326, 405, 412, 439
 operon, 122
 optimization, 29, 74, 239, 258, 304
 organic compounds, 150, 152, 224, 225, 272, 381
 organic matter, 143, 144, 151, 168, 194, 196, 377, 378
 organic solvents, 61, 89, 189, 252, 253, 254, 298
 organism, 106, 107, 110
 osmotic pressure, 48, 295
 osmotic stress, 109, 111
 oxidation, 81, 85, 102, 148, 149, 178, 207, 209, 252, 264, 269, 270, 275, 276, 283, 287, 291, 302, 303, 307, 311, 315, 328, 358, 359, 364, 387, 391, 419, 423, 432, 445
 oxidation products, 364
 oxygen, 26, 83, 85, 97, 99, 143, 144, 145, 147, 148, 149, 165, 171, 172, 173, 174, 175, 176, 178, 179, 181, 184, 188, 194, 225, 226, 231, 241, 247, 262, 264, 266, 269, 270, 276, 280, 291, 345, 350, 351, 352, 353, 359, 361, 362, 364, 373, 386, 388, 391, 406, 414, 416, 418, 420, 444
 ozone, 85, 350, 383, 384, 420, 421

P

- palladium, 216
- palm oil, 167, 358, 366, 369
- pathogens, 155, 247
- pathways, 6, 10, 11, 13, 23, 26, 28, 38, 82, 98, 99, 100, 101, 102, 103, 104, 105, 113, 116, 122, 124, 130, 138, 141, 171, 173, 186, 193, 194, 203, 214, 215, 216, 229, 236, 242, 246, 253, 254, 259, 261, 269, 275, 279, 322, 326, 327, 329, 331, 332, 333, 334, 335, 336, 362, 388, 390, 395, 411, 412, 429, 442
- PCA, 257, 283, 329, 330, 331, 332, 333, 334, 335
- peat, 175
- pentanol, 339, 363, 375, 377, 378, 417, 439
- percolation, 125
- permeability, 379, 398
- permeation, 71, 258, 346, 348, 349, 351, 352
- peroxide, 43, 48, 134, 140, 252, 268, 270, 275, 276, 361, 395
- petroleum, 37, 112, 113, 178, 180, 187, 193, 194, 203, 210, 224, 234, 246, 247, 266, 322, 324, 328, 343, 344, 346, 349, 354, 359, 360, 362, 363, 365, 367, 373, 380, 382, 391, 392, 393, 394, 396, 397, 402, 403, 411
- pharmaceuticals, 209, 220
- phenol, 43, 94, 107, 265, 270, 271, 272, 273, 274, 285, 290
- phenolic compounds, 84, 94, 96, 107, 180, 191, 272, 275, 277, 285
- phenolic resins, 283
- phenotypes, 259, 338
- phenylalanine, 279
- phosphate, 13, 57, 98, 101, 102, 103, 130, 138, 141, 217, 219, 221, 238
- phosphatidylethanolamine, 122
- phosphorus, 53, 151, 191, 200
- phosphorylation, 64, 101, 256
- photosynthesis, 171, 202, 246
- physical properties, 6, 26, 31, 34, 46, 180, 254, 267, 302, 319, 362, 415
- physical structure, 84, 141
- physicochemical characteristics, 37, 78, 305
- physicochemical properties, 38, 61, 73, 229, 232, 293, 294, 314, 415
- pilot study, 441
- pipeline, 5, 344, 360, 373, 379, 400, 412, 429
- plant growth, 186
- plant type, 8, 81, 160
- plants, 16, 31, 59, 65, 70, 113, 122, 152, 153, 154, 155, 160, 163, 179, 186, 206, 246, 247, 248, 250, 251, 278, 279, 293, 295, 298, 306, 316, 323, 324, 329, 337, 342, 379, 397, 404, 412, 413, 437
- plasma membrane, 130
- plasmid, 104
- plastics, 113, 154, 209, 328, 333, 345, 346, 357, 373, 378, 414, 428
- platinum, 215, 216, 217, 231, 234
- playing, 295
- PLS, 257
- PM, 166, 181, 347, 348, 350, 352, 353, 354, 361, 362, 364, 365, 366, 367, 368, 369, 370, 371, 374, 376, 387, 389, 390, 395, 402, 403, 408, 409, 410, 411, 414, 416, 417, 424, 426, 435, 441
- polar, 83, 187, 355
- polarity, 109, 113, 114, 254, 266, 295, 375
- polarization, 54, 64, 256, 257
- policy, 5, 167, 169, 186, 326, 349, 424
- pollutants, 181, 348, 352, 361, 362, 368, 381, 384, 404, 406, 411, 428, 429, 432, 433, 435, 436, 445
- pollution, 152, 211, 438
- polyacrylamide, 156, 164
- polycarbonate, 406
- polycyclic aromatic hydrocarbon, 227, 228, 230, 231, 232, 265, 267, 362, 444
- polydispersity, 57, 61, 62, 253, 258, 259
- polyimide, 184
- polymer chain, 256
- polymer matrix, 82
- polymer systems, 259
- polymerization, 38, 53, 61, 71, 72, 81, 92, 132, 180, 207, 208, 265, 267, 271, 273, 275, 295, 297, 298, 304, 306, 307, 310, 314, 315, 359
- polymers, 52, 59, 74, 76, 79, 81, 82, 94, 99, 106, 107, 113, 158, 189, 198, 202, 204, 205, 206, 209, 210, 214, 220, 238, 246, 248, 256, 259, 281, 283, 293, 294, 295, 303, 305, 359, 406, 428
- polyphenols, 39
- polypropylene, 314, 357
- polysaccharides, 39, 56, 58, 73, 82, 88, 90, 98, 99, 114, 121, 135, 146, 210, 252, 253, 297
- polystyrene, 61
- polyurethane, 210
- polyurethanes, 328
- polyvinyl alcohol, 314
- population, 51, 148, 149, 246
- porosity, 46, 49, 50, 52, 73, 74, 84, 212
- porous materials, 48
- potassium, 9, 56, 179, 240, 355
- potato, 312
- poultry, 167, 356
- power generation, 181, 247, 267

power plants, 27, 33, 404, 412
 precipitation, 7, 12, 56, 78, 83, 149, 251, 252
 preparation, 41, 44, 60, 138, 174, 232, 233, 306, 313, 314, 315, 316, 426
 preprocessing, 1, 4, 5, 6, 7, 11, 12, 17, 20, 26, 27, 28
 pretreatment, 8, 10, 16, 17, 27, 29, 30, 32, 33, 34, 35, 37, 38, 43, 47, 48, 51, 52, 62, 63, 64, 67, 68, 70, 71, 72, 73, 74, 75, 76, 77, 78, 79, 80, 82, 83, 84, 85, 86, 87, 88, 89, 90, 93, 94, 95, 96, 104, 106, 107, 108, 110, 111, 114, 115, 118, 119, 120, 121, 123, 124, 125, 126, 127, 130, 131, 133, 134, 135, 136, 137, 138, 139, 140, 141, 161, 177, 186, 199, 203, 204, 206, 207, 208, 209, 212, 213, 236, 237, 238, 239, 240, 241, 242, 243, 253, 254, 269, 279, 285, 288, 290, 292, 298, 299, 300, 302, 303, 308, 309, 313, 314, 315, 316, 322, 323, 329, 330, 331, 337
 primary products, 265, 266, 331
 principal component analysis, 257
 probe, 48, 49, 50, 255, 358
 producers, 114, 323, 326, 342, 359, 372, 385, 394
 production costs, 210, 322, 324, 392, 406
 productivity rates, 99, 107
 profit, 323, 324, 325
 profit margin, 323, 324, 325
 profitability, 95
 promoter, 122
 propane, 397, 407, 410, 411
 propanol, 109, 113, 350, 355, 417
 propylene, 372
 proteins, 15, 91, 107, 110, 126, 146, 152, 158, 188, 191, 192, 204, 253, 275, 302
 protons, 58, 62, 64, 255, 256, 287, 297
 prototype, 18, 383, 386, 387, 389, 390
 PTFE, 61
 pulp, 39, 50, 74, 75, 77, 78, 251, 252, 286, 291, 295, 297, 298, 299, 300, 301, 302, 303, 308, 309, 311, 313, 314, 315, 316, 319, 382
 pulping, 53, 72, 131, 251, 252, 253, 254, 262, 279, 286, 295, 297, 298, 304
 purification, 59, 72, 91, 124, 203, 247, 249, 252, 253, 257, 268, 305, 331
 purity, 60, 78, 294, 297, 385, 406
 P-series fuels, 339, 406, 419, 420, 421, 432
 pyrolysis, 2, 9, 11, 17, 21, 26, 30, 31, 32, 35, 69, 74, 78, 171, 173, 175, 179, 180, 181, 182, 184, 186, 192, 194, 209, 224, 225, 226, 227, 228, 229, 230, 231, 232, 233, 234, 235, 236, 237, 238, 239, 240, 241, 242, 243, 245, 256, 257, 259, 260, 261, 262, 264, 265, 266, 267, 268, 270, 271, 277, 278, 280, 281, 282, 286, 287, 288, 289, 292, 433, 434

Q

quantification, 40, 43, 73, 255, 257, 260
 quartz, 226
 quinone, 78, 256

R

radiation, 41, 255
 radical polymerization, 279
 radical reactions, 187
 radicals, 248, 252, 271, 275, 386
 Raman spectroscopy, 56, 68, 76, 311, 313
 rate of change, 314
 raw materials, 246, 326
 reactants, 174, 177, 187, 205, 223, 229
 reaction mechanism, 268
 reaction medium, 93, 182, 187, 215, 274
 reaction rate, 9, 178, 192, 223, 296
 reaction temperature, 88, 89, 220, 268, 273
 reaction time, 216, 224, 259, 269, 272, 273, 355
 reactions, 9, 87, 90, 101, 102, 106, 107, 151, 180, 187, 197, 201, 209, 216, 220, 222, 223, 224, 229, 230, 231, 235, 248, 249, 254, 261, 262, 263, 264, 266, 270, 275, 280, 283, 284, 297, 303, 355, 382, 404
 reactive sites, 271
 reactivity, 16, 17, 64, 74, 82, 114, 118, 171, 209, 249, 262, 264, 285, 310, 375, 383
 reagents, 140
 receptors, 146
 recovery, 28, 82, 86, 91, 111, 137, 174, 187, 208, 223, 245, 252, 254, 288, 303, 323, 324, 330, 331
 recovery processes, 174
 recycling, 90, 93, 96, 112, 132, 211, 213, 246
 refractive index, 42, 48, 258
 regenerated cellulose, 90, 314
 regeneration, 90, 220
 regrowth, 202
 rehydration, 95, 212
 reinforcement, 294, 302
 relaxation, 51, 63, 64, 69
 reliability, 410
 renaissance, 437
 renewable energy, 32, 163, 168, 171, 182, 187, 202, 286, 289, 434
 renewable fuel, 112, 143, 247, 251, 279, 322, 339, 340, 391, 392, 394, 421
 Renewable Fuel Standard (RFS), 112, 322, 336, 340, 347, 385, 443

- Renewable Fuels Association, 80, 128, 133, 342, 344, 436, 440
- residues, 2, 9, 14, 32, 41, 45, 58, 59, 60, 80, 82, 84, 85, 92, 105, 106, 121, 129, 133, 147, 154, 161, 164, 178, 184, 186, 187, 189, 246, 251, 253, 272, 276, 285, 290, 295, 298, 303, 310, 311, 313, 315, 329, 342
- resins, 39, 189, 200, 202, 209, 210, 211, 213, 223, 375, 414
- resistance, 82, 105, 121, 126, 218, 358, 378, 404, 407
- resolution, 62, 63, 255, 257, 260, 291
- resource utilization, 246
- resources, 4, 5, 37, 121, 153, 161, 168, 172, 185, 187, 192, 201, 202, 213, 240, 246, 284, 328, 400, 415
- response, 110, 111, 128, 242, 249, 250, 316, 344, 380
- restaurants, 153, 154
- retail, 326, 344, 380
- reusability, 220
- revenue, 173, 321, 322, 326, 356
- ribose, 101
- rice husk, 148, 191, 199
- rings, 369
- risks, 148, 152, 192, 203, 323, 325, 326, 359, 369, 385
- room temperature, 39, 53, 56, 59, 61, 64, 86, 89, 406
- root, 13, 404
- routes, 111, 125, 136, 174, 240, 249, 253, 266, 275, 276, 285, 324, 355, 401, 427
- Ru catalysts, 216, 408
- rubber, 154, 357
- rubber compounds, 357
- ruthenium, 215, 216, 217, 234, 235, 240, 289
- scattering intensity, 54
- Scots pine, 227
- second generation, 29, 131, 202, 246, 247
- secrete, 92, 146
- sedimentation, 258, 285
- sediments, 357
- selectivity, 53, 73, 90, 212, 216, 218, 219, 220, 222, 225, 226, 228, 229, 233, 239, 243, 265, 269, 270, 272, 273, 274, 277, 280, 288, 299
- sensors, 345, 379
- severe stress, 107
- sewage, 144, 153, 155, 160, 164, 166, 167, 176
- shape, 6, 12, 17, 26, 46, 71, 76, 212, 222, 279
- shear, 11, 87, 97, 300, 301
- shelf life, 16
- shock, 110, 117, 163, 358, 388, 390
- shortfall, 321
- showing, 84, 99, 215, 304, 346, 349, 352, 361, 362, 370, 378, 405
- side chain, 56, 66, 81, 206, 273, 275
- side effects, 95
- signals, 44, 46, 54, 55, 58, 62, 63, 65, 66, 67, 256, 269
- silica, 13, 30, 189, 222, 225, 226, 227, 231, 242
- silver, 118
- SiO₂, 189, 212, 213, 226, 228, 232, 236, 263
- sludge, 150, 153, 155, 160, 163, 165, 166, 168, 176, 211, 405
- sodium, 53, 56, 57, 61, 74, 179, 229, 241, 251, 296, 303, 355, 406
- sodium hydroxide, 56, 74, 229, 241, 251, 296, 406
- softwoods, 84, 85, 130, 131, 249
- soil type, 13, 14, 28, 30
- solid matrix, 87
- solid waste, 147, 154, 157, 164, 165, 166, 400
- solubility, 53, 61, 77, 109, 124, 176, 252, 253, 254, 255, 257, 258, 266, 269, 271, 273, 277, 279, 346, 415, 417
- solution, 2, 32, 38, 40, 44, 48, 49, 59, 60, 61, 63, 65, 73, 78, 89, 90, 201, 211, 220, 255, 258, 259, 269, 272, 310, 359, 406
- solvents, 39, 56, 57, 61, 86, 89, 90, 189, 191, 202, 208, 209, 214, 216, 220, 223, 252, 257, 258, 270, 271, 272, 273, 274, 298, 299, 323, 324, 325, 375, 377, 378, 379, 414, 415, 416, 445
- soy-based, 361, 364, 365, 368
- soybeans, 356, 395, 396
- specialists, 186
- species, 1, 6, 8, 9, 34, 37, 38, 39, 44, 59, 61, 68, 75, 94, 97, 99, 102, 104, 105, 107, 113, 114, 153, 172, 173, 176, 178, 179, 180, 191, 204, 229, 248,

S

- Saccharomyces, 79, 97, 99, 102, 106, 107, 108, 109, 110, 114, 115, 116, 117, 118, 120, 121, 122, 123, 124, 125, 126, 127, 128, 129, 130, 131, 132, 134, 135, 136, 137, 138, 141, 336
- safety, 135, 359, 380, 385
- salts, 39, 86, 89, 208, 223, 263, 299
- saturated fat, 358, 369
- saturated hydrocarbons, 227
- savings, 181, 363, 364
- sawdust, 138, 191, 199, 211, 213, 226, 287
- scaling, 197
- scanning electron microscopy, 306
- scattering, 54, 316

- 265, 267, 268, 279, 292, 297, 299, 310, 348, 350, 352, 355, 359, 369, 370, 378, 383, 387, 396
- specific gravity, 404
- specific surface, 46, 47, 52, 87, 208, 305
- specifications, 1, 2, 4, 6, 8, 10, 17, 27, 34, 360, 385, 393, 402, 405, 406
- spectrophotometric method, 284
- spectrophotometry, 255
- spectroscopic techniques, 42
- spectroscopy, 38, 40, 41, 54, 56, 62, 63, 68, 69, 70, 73, 75, 255, 257, 258, 259, 260, 282, 287, 290
- spin, 50, 51, 52, 69, 418
- SSA, 87
- stability, 91, 109, 129, 150, 152, 159, 165, 189, 208, 216, 218, 222, 239, 266, 268, 269, 297, 304, 357, 359, 379, 415, 418, 432, 436
- stabilization, 155, 265, 266
- starch, 15, 98, 111, 113, 116, 128, 132, 200, 340, 342, 372, 415, 426
- steam hydrogasification, 171, 175, 177, 178, 182, 183, 184, 391
- steel, 312, 379
- sterols, 39, 126
- stoichiometry, 361, 364
- stress, 107, 108, 109, 110, 117, 136, 302
- stress response, 107, 109, 117
- stretching, 43, 58
- stroke, 370, 416, 420
- structural changes, 45, 283, 287
- structural characteristics, 37, 38, 64, 78, 253, 347
- structural variation, 251, 254
- structures, 33, 38, 44, 46, 49, 51, 52, 53, 56, 57, 58, 59, 62, 63, 67, 68, 70, 72, 73, 74, 75, 76, 77, 81, 82, 83, 84, 86, 87, 88, 89, 90, 94, 99, 107, 119, 121, 133, 141, 164, 188, 204, 205, 206, 207, 208, 212, 223, 229, 238, 245, 247, 248, 250, 251, 253, 254, 257, 258, 259, 260, 265, 267, 269, 273, 276, 279, 280, 281, 282, 284, 285, 289, 292, 293, 295, 296, 298, 299, 300, 302, 303, 310, 311, 315, 316, 317, 318, 319, 346, 358, 369, 370, 386, 393, 402, 436
- substitutes, 56, 234, 272
- substitution, 107, 155, 265
- substitutions, 88, 108
- substrates, 46, 47, 48, 49, 50, 69, 70, 71, 72, 73, 84, 89, 92, 93, 94, 95, 96, 97, 104, 105, 120, 121, 129, 132, 137, 139, 140, 143, 144, 146, 147, 148, 150, 152, 153, 155, 156, 157, 158, 159, 160, 161, 162, 163, 166, 167, 202, 220, 260, 298
- sucrose, 80, 98, 99, 211, 239, 329, 330
- sugar alcohols, 111
- sugar beet, 132, 164, 246
- sugar mills, 337
- sugarcane, 27, 30, 70, 111, 112, 113, 116, 121, 141, 208, 238, 319, 324, 327, 340, 344, 349, 354, 444
- sulfate, 224, 270, 297, 304, 318
- sulfur, 178, 200, 219, 252, 267, 276, 298, 352, 353, 364, 368, 370, 392, 393, 395, 398, 401, 408, 410, 419, 437
- sulfuric acid, 29, 39, 56, 72, 88, 89, 219, 241, 252, 273, 287, 303, 304, 307, 318
- sulphur, 71
- supplementation, 93, 97, 108, 110, 127
- supply chain, 4, 5, 6, 33, 191
- surface area, 46, 47, 48, 49, 51, 74, 82, 84, 85, 86, 89, 90, 93, 94, 165, 199, 217, 229, 232, 264, 312
- surface modification, 316
- surface properties, 38, 52, 68, 72, 201
- surface tension, 52
- surfactants, 96, 119, 202, 223, 224, 242
- surplus, 212, 405
- susceptibility, 191, 234
- suspensions, 303, 305, 311, 313
- sustainability, 121, 153, 161, 396, 421
- sustainable development, 166, 281
- sustainable energy, 165, 186
- swelling, 51, 83, 208, 298, 373, 375
- switchgrass, 8, 12, 14, 15, 16, 23, 26, 29, 30, 31, 32, 33, 35, 44, 45, 46, 47, 49, 55, 64, 67, 68, 69, 70, 72, 73, 75, 76, 89, 90, 93, 100, 115, 135, 139, 166, 186, 187, 189, 190, 200, 240, 241, 279, 284, 290, 314, 349, 354
- synergistic effect, 91, 156, 162
- synthesis, 34, 173, 178, 200, 201, 202, 212, 215, 218, 223, 235, 239, 263, 269, 299, 336, 372, 382, 391, 424

T

- tanks, 357, 382, 393, 401, 414
- tar, 8, 179, 182, 262, 263, 268, 277
- TEM, 306
- temperature, 12, 21, 32, 47, 50, 51, 54, 60, 64, 85, 86, 88, 89, 97, 99, 106, 122, 148, 149, 150, 157, 163, 165, 166, 167, 173, 176, 179, 180, 185, 186, 187, 190, 199, 201, 203, 209, 211, 218, 224, 226, 251, 252, 253, 256, 259, 261, 262, 264, 265, 266, 267, 268, 269, 272, 273, 289, 298, 299, 304, 349, 355, 357, 358, 359, 367, 371, 373, 379, 382, 387, 389, 393, 403, 407, 410, 414, 426, 445
- tensile strength, 311, 312
- terpenes, 191, 337

testing, 19, 156, 194, 345, 347, 358, 359, 369, 385, 386, 388, 392, 394, 395, 444

tetrahydrofuran, 215, 239, 258, 415, 417

textiles, 154, 202, 372

thermal decomposition, 179, 188, 259

thermal degradation, 69, 262, 265, 267, 318, 414

thermal energy, 172, 174, 180, 261

thermal properties, 72, 77

thermal stability, 208, 234

thermodynamic equilibrium, 173

thermoplastics, 210

thermostability, 304

tissue, 5, 83, 204

titania, 215, 217, 225, 226, 239, 263

titanium, 216

tobacco, 186, 187, 211, 279, 419, 420

tobacco smoke, 419, 420

toluene, 39, 77, 226, 431

top-down, 293, 294, 412, 413

total costs, 153

total energy, 21, 161, 442

total product, 114, 267

toxic substances, 149

toxicity, 107, 108, 109, 114, 116, 130, 139, 148, 156, 166, 335, 369, 372, 406, 439

toxicology, 419

transesterification, 215, 355, 393

transition metal, 212, 225, 226, 229, 233, 238, 263

transmission, 41, 303, 306, 402, 405, 412, 413, 441, 445

transmission electron microscopy, 306

transportation, 4, 5, 7, 11, 22, 23, 26, 27, 28, 34, 46, 59, 79, 83, 102, 109, 111, 119, 127, 128, 132, 134, 146, 152, 156, 173, 179, 180, 182, 183, 186, 187, 202, 234, 235, 238, 240, 245, 247, 248, 263, 265, 266, 267, 271, 272, 274, 285, 292, 323, 339, 343, 349, 363, 372, 375, 378, 380, 381, 382, 385, 386, 388, 393, 396, 400, 401, 402, 404, 405, 406, 412, 414, 419, 421, 425, 431

treatment, 10, 13, 26, 43, 51, 71, 74, 76, 88, 89, 108, 125, 133, 140, 147, 153, 155, 160, 162, 167, 168, 171, 175, 179, 194, 199, 207, 208, 209, 221, 224, 234, 275, 288, 294, 296, 298, 299, 300, 304, 306, 307, 308, 309, 313, 319, 320, 322, 330, 388

triglycerides, 355

turnover, 111, 112

U

ultrastructure, 38, 51, 68, 70, 71, 283

Upgrading, 176, 180, 182, 183, 190, 194, 196, 199, 200, 201, 203, 209, 219, 224, 225, 226, 227, 228, 230, 231, 232, 233, 234, 235, 236, 237, 238, 239, 240, 241, 242, 266, 267, 268, 277, 280, 282, 288, 336

upgrading of biomass fast pyrolysis vapors, 231, 239

upgrading of biomass pyrolysis vapors, 225, 238, 241

urban, 154, 155, 166, 353, 364, 407, 412, 437

urban areas, 154, 155

urine, 419, 420, 431, 439

V

vacuum, 59, 190

valence, 43

valorization, 133, 219, 235, 238, 240, 289, 326

vapor, 61, 176, 187, 208, 215, 216, 230, 239, 258, 265, 266, 344, 348, 350, 353, 370, 373, 377, 378, 379, 380, 382, 383, 389, 415, 416, 419, 420, 424

vegetable oil, 159, 175, 202, 356, 363, 369, 388, 389

vehicles, 339, 340, 344, 345, 346, 347, 348, 349, 350, 351, 352, 353, 354, 357, 360, 362, 364, 365, 368, 369, 370, 372, 374, 376, 379, 380, 382, 383, 384, 385, 386, 387, 389, 390, 393, 396, 400, 401, 402, 403, 404, 408, 409, 410, 411, 412, 421, 423, 424, 426, 427, 432, 435, 436, 438, 440, 441, 442, 444

velocity, 85

vibration, 41, 43, 58

viscosity, 180, 208, 247, 266, 283, 313, 341, 359, 362, 382, 389, 417

visualization, 118, 314

volatile organic compounds, 21, 419, 420

volatility, 191, 266, 347, 350, 352, 354

volatilization, 259

W

waste, 32, 85, 123, 144, 147, 151, 152, 153, 154, 155, 156, 159, 160, 161, 162, 163, 164, 165, 166, 167, 169, 171, 173, 174, 186, 202, 211, 219, 237, 242, 246, 275, 316, 324, 326, 342, 355, 363, 364, 382, 388, 396, 400, 401, 407, 408, 409, 419

waste disposal, 219, 324, 326

waste management, 152, 167

waste treatment, 161, 167

wastewater, 148, 155, 164, 168, 191, 195, 322, 330, 355, 388, 400, 405

water chemistry, 14

water evaporation, 175, 176
 water quality, 13, 28
 water resources, 135
 WAXS, 313
 wear, 27, 382, 393, 418
 wells, 397, 398, 400
 Western Europe, 406
 wetting, 52
 WHO, 431
 wild type, 64, 67, 279
 wood, 2, 9, 12, 22, 23, 24, 31, 34, 42, 57, 59, 62, 63,
 64, 69, 70, 71, 72, 74, 75, 76, 77, 80, 100, 104,
 113, 125, 128, 133, 137, 154, 172, 183, 184, 186,
 191, 208, 221, 226, 227, 228, 229, 230, 232, 238,
 251, 253, 267, 282, 285, 287, 288, 291, 294,
 295, 296, 302, 303, 312, 314, 315, 317, 320, 410,
 419, 424
 wood density, 12
 wood species, 71, 424
 wood waste, 80, 154, 419

X

X-ray diffraction (XRD), 54, 74, 311
 xylem, 247

Y

yeast, 82, 94, 97, 98, 99, 103, 106, 108, 109, 110,
 114, 115, 116, 117, 118, 119, 121, 122, 125, 126,
 128, 130, 131, 133, 135, 137
 yield, 5, 12, 13, 29, 30, 38, 46, 59, 60, 78, 82, 90, 93,
 94, 95, 96, 97, 103, 106, 111, 114, 121, 132, 144,
 147, 148, 150, 154, 156, 157, 158, 159, 160, 180,
 188, 189, 195, 196, 199, 201, 207, 210, 211, 212,
 213, 216, 217, 218, 219, 222, 223, 225, 226, 227,
 228, 229, 230, 231, 234, 236, 237, 240, 242, 243,
 246, 261, 263, 264, 265, 267, 268, 269, 270, 272,
 273, 277, 279, 280, 295, 304, 314, 321, 323, 325,
 327, 328, 329, 331, 332, 333, 334, 335, 378, 406,
 415

Z

zeolites, 189, 209, 210, 211, 212, 214, 222, 225, 228,
 230, 234, 238, 240, 265, 267, 272
 zinc, 149
 zirconia, 216, 218, 225, 226, 239
 zirconium, 44
 ZnO, 228, 232, 263

γ

γ -Valerolactone (GVL), 201, 209, 214, 215, 216,
 217, 218, 219, 221, 234